CONF-77[illegible]-202
(Abstr.)

[illegible] CRYSTALS

[illegible], U.S.A.

[illegible]

[illegible]

[illegible]

[illegible]

[illegible]

[illegible]

CONF-771002
(Absts.)

International Conference on

Defects in INSULATING CRYSTALS

Gatlinburg, Tennessee, U.S.A.
9-14 October 1977

sponsored by

Oak Ridge National Laboratory

Energy Research and Development Administration

National Science Foundation

Office of Naval Research

ORGANIZING COMMITTEE

R. F. Wood	Conference Chairman
E. Sonder	Program Chairman
Y. Chen	Conference Secretary
M. Mostoller	Editor, Abstract Book
M. M. Abraham	
J. B. Bates	
F. A. Modine	
G. S. Painter	
R. A. Weeks	
C. S. Yust	

DOMESTIC ADVISORY COMMITTEE

F. C. Brown	Illinois
J. H. Crawford, Jr.	North Carolina
M. N. Kabler	NRL
M. V. Klein	Illinois
F. Lüty	Utah
R. B. Murray	Delaware
W. A. Sibley	Oklahoma State
M. Sturge	Bell Labs
B. Wuensch	M.I.T.

FOREIGN ADVISORY COMMITTEE

M. Aegerter	Switzerland
R. Capelletti	Italy
B. Henderson	Ireland
A. E. Hughes	U.K.
N. Itoh	Japan
Y. Merle d'Aubigné	France
J. Rolfe	Canada
W. von der Osten	Germany

FOREWORD

This conference may be considered to be a member of the series of international symposia on the physics of color centers in ionic crystals which began in 1956. The 1977 conference, while maintaining the continuity and tradition of the series, departs substantially from the scope and emphasis of past color center conferences. Meetings in this series have been held at three year intervals to report and discuss results of studies of defects in ionic crystals. Traditionally, these studies have been heavily weighted toward the alkali halides as host crystals. However, over the years a slow but steady growth in the number of papers on defects in other insulating materials has occurred. An effort has been made by the Organizing Committee of the 1977 conference to encourage this growth and to emphasize research on materials of interest in newly evolving energy technologies. Although the committee judges this effort to have been only partially successful, the data for the conference abstracts show that the papers on alkali halides and those on all other materials are now roughly comparable in number. In order to stimulate discussion on a wider variety of materials and phenomena, the committee decided to introduce poster sessions. For the conference, 268 abstracts were received from scientists in 23 countries. Of these, approximately 80 percent were selected for oral or poster presentation. Assignment of papers to the two types of sessions in no way implied a judgement of the merit of the work reported. Without poster sessions only about 20 percent of the contributed papers could have been presented.

The planning and organization of any large conference involves the efforts of many people. The Organizing Committee would like to thank the members of the Advisory Committees for their advice over the past year. We would also like to acknowledge the help of Professors Ueta and Hirai of Tohoku University in the early stages of the conference planning. We wish to express our gratitude to our sponsoring agencies for their financial assistance and for their interest. Finally, we would like to add a special note of thanks to Velma Hendrix, who served as a one-person organizing committee for so many of the details of the conference.

R. F. Wood
Conference Chairman

PROGRAM OUTLINE

MONDAY, OCTOBER 10

Morning:	Session I.	*Transport*
	Session II.	*Defect Levels*
Afternoon:	Session III.	*Applications*
	Poster Session A.	*Transport, Applications, Superionic Conductors, Radiation Effects - Oxides, Aggregation, Electron-Lattice Interactions*

TUESDAY, OCTOBER 11

Morning:	Session IV.	*Superionic Conductors*
	Session V.	*Jahn-Teller Effect*
Evening:	Poster Session B.*	*Transport, Defect Levels, Superionic Conductors, Radiation Effects - Halides, Relaxed Excited States, Excitons, Mechanical Properties*

WEDNESDAY, OCTOBER 12

Morning:	Session VI.	*Radiation Effects - Oxides*
	Session VII.	*Radiation Effects - Halides*
Afternoon:	Session VIII.	*Aggregation*
	Poster Session C.	*Defect Levels, Jahn-Teller Effect, Radiation Effects - Oxides, Aggregation, Excitons, Impurities*

THURSDAY, OCTOBER 13

Morning:	Session IX.	*Relaxed Excited States*
	Session X.	*Excitons*
Afternoon:	Future of the Conference - an open discussion meeting	
Evening:	Poster Session D.*	*Transport, Defect Levels, Radiation Effects - Halides, Relaxed Excited States, Electron-Lattice Interactions, Impurities*

FRIDAY, OCTOBER 14

Morning:	Session XI.	*Electron-Lattice Interactions*
	Session XII.	*Electron-Lattice Interactions*
Afternoon:	Session XIII.	*Impurities*

**Invited papers will precede Poster Sessions B and D.*

CONTENTS

INVITED PAPERS

1 DEFECT-CONTROLLED METAL-INSULATOR TRANSITIONS, David Adler

85 RADIATION EFFECTS IN MgO, Yok Chen

109 THE JAHN-TELLER EFFECT IN IONIC CRYSTALS: RECENT DEVELOPMENTS, J. Duran

144 AgI-TYPE SOLID ELECTROLYTES, K. Funke

166 THE EXCITED STATES OF F CENTRES IN OXIDES, B. Henderson

224 ELECTRON-PHONON INTERACTION IN ALKALI AND SILVER HALIDES, H. Kanzaki

240 SEGREGATION PHENOMENA IN MAGNESIUM OXIDE, W. D. Kingery

290 BROADLY TUNABLE LASERS USING COLOR CENTERS IN THE ALKALI HALIDES, L. F. Mollenauer

391 THE ROLE OF FUNDAMENTAL RESEARCH IN DEVICE DEVELOPMENT, W. A. Sibley

396 ION TRANSPORT IN SIMPLE IONIC CRYSTALS, L. Slifkin

465 DISLOCATIONS AND MECHANICAL PROPERTIES OF IONIC CRYSTALS, R. W. Whitworth

469 PHOTOCHEMISTRY OF F-CENTER FORMATION IN SIMPLE HALIDE CRYSTALS, R. T. Williams

TRANSPORT

40 SELF-DIFFUSION AND IONIC CONDUCTIVITY IN NaI, F. Bénière, D. Kostopoulos, and K. V. Reddy

58 IONIC CONDUCTIVITY OF MIXED SILVER BROMIDE-SILVER CHLORIDE SINGLE CRYSTALS, L. S. Cain, H. Manning, and L. M. Slifkin

60 SOLUTION AND PRECIPITATION PHENOMENA OF TRIVALENT RARE-EARTH IMPURITIES IN DIVALENT METAL FLUORIDES, R. Capelletti, F. Fermi, and E. Okuno

62 DISSOLUTION PROCESSES OF Be AND Mg AND MAXWELL-WAGNER RELAXATIONS STUDIED BY MEANS OF ITC IN LiF CRYSTALS, R. Capelletti and A. Gainotti

75 DISORDER IN NON-CUBIC OXIDES, C. R. A. Catlow and R. James

79 DEFECT CHEMISTRY OF $SrTiO_3$, N.-H. Chan and D. M. Smyth

83 FIELD EFFECTS IN THE THERMAL DECOMPOSITION OF POTASSIUM AZIDE, H. Chaya and B. S. H. Royce

107 OXYGEN SELF-DIFFUSION IN NiO, C. Dubois, S. Barbezat, and C. Monty

117 THERMAL PROPERTIES AND ELECTRICAL RESISTIVITY OF OLIVINE AND PYROPHILLITE IN THE TEMPERATURE RANGE 400-2000°K, A. A. El-Sharkawy, M. A. Kenawy, and S. R. Atalla

118 CONCENTRATION DEPENDENT DIFFUSION IN STRONGLY IONIC CRYSTALS: A NEW METHOD OF ANALYSIS, Genghmun Eng and David Lazarus

130 NEUTRON-INDUCED DAMAGE INVESTIGATIONS IN ALKALI HALIDE CRYSTALS WITH RADIOACTIVE RARE GASES, F. W. Felix, B. Granéli, and M. Müller

132 IMPURITY DIFFUSION IN POTASSIUM AZIDE - A PSEUDOHALIDE, D. Foster and A. L. Laskar

136 ASPECTS OF DIFFUSION IN AN ELECTRIC FIELD, Robert J. Friauf

140 THERMALLY INCREASED RANGE AND NON-LINEAR EFFECTS IN PHOTOCONDUCTIVITY FROM F CENTERS IN KCl, Robert J. Friauf and Andrzek Radlinski

234 SURFACE CONDUCTANCE OF NH_4Cl CAUSED BY AN AMMONIUM ATMOSPHERE, A. Kessler and E. Bötz

242 RADIATION-INDUCED CONDUCTIVITY OF Al_2O_3: THEORY AND EXPERIMENT, R. W. Klaffky, B. H. Rose, and G. J. Dienes

253 PROPOSED CATALYTIC RECOMBINATION OF CLOSED CHARGED FRENKEL PAIRS IN ALKALI HALIDES, V. Krumins

256 NONLINEAR ARRHENIUS PLOTS IN IONIC TRANSPORT STUDIES IN SILVER HALIDES, A. L. Laskar, W. Mealing, and D. Foster

292 THERMAL CONDUCTIVITY OF DAMAGED MgO, A. R. Moodenbaugh, C. L. Tsai, H. Weinstock, and Yok Chen

297 THERMALLY STIMULATED DEPOLARIZATION CURRENTS IN THORIUM DIOXIDE, R. Muccillo and L. L. Campos

308 ELECTRICAL-CONDUCTION-INDUCED AGGREGATION OF DEFECTS AND THERMAL BREAKDOWN IN MgO, J. Narayan, R. A. Weeks, and E. Sonder

338 HIGH TEMPERATURE ELECTRICAL CONDUCTIVITY AND DEFECT CHEMISTRY OF IRON DOPED ALUMINA, T. M. Pollak, H. K. Bowen, and H. L. Tuller

346 POINT DEFECT PARAMETERS IN $NaNO_3$ CRYSTALS, C. Ramasastry and Y. S. Rao

369 OPTICAL AND ELECTRICAL PROPERTIES OF RbI:Pb, S. B. S. Sastry and K. Balasubramanyam

400 DETERMINATION OF THE Fe^{2+} AND Fe^{3+} CONCENTRATION IN MgO, E. Sonder, F. A. Modine, and R. A. Weeks

444 IONIC AND ELECTRONIC CONDUCTION IN THORIA OXIDE ELECTROLYTES, Harry L. Tuller

463 ELECTRIC FIELD INDUCED CHANGES IN CONDUCTIVITY OF MgO AT HIGH TEMPERATURE, R. A. Weeks, E. Sonder, J. C. Pigg, and K. F. Kelton

482 LATTICE DEFECT EQUILIBRIUM IN KCl:Eu, J. B. Wolfenstine and T. G. Stoebe

486 DIFFUSION OF IMPURITIES IN KI 1% KCl SINGLE CRYSTALS, S. C. Zilio, D. G. Pinatti, M. Siu Li, and Milton de Souza

DEFECT LEVELS

8 A NEW F_3-CENTER TYPE IN CaF_2, R. Alcalá, V. M. Orera, and J. Beamonte

10 POLARIZATION OF EXCITED STATE SPECTRA OF M CENTRES IN KCl CRYSTALS AT ROOM TEMPERATURE, A. O. H. Al-Chalabi

15 SOME NEW ASPECTS OF THE THERMAL F - Z_2 CENTER CONVERSION PROCESS IN KCl:Sr CRYSTALS, Ch. Anderson and H. J. Paus

48 ENDOR OF V_{OD} DEFECTS IN SrO, J. L. Boldu, H. J. Stapleton, Y. Chen, and M. M. Abraham

52 SODIUM-PERTURBED F_3-CENTRES (R_A-CENTRES) IN KCl, M. Buchanan and J. Rolfe

66 TWO PHOTON ABSORPTION OF COLOR CENTER IN NaF, M. Casalboni, G. Chiarotti, U. M. Grassano, and A. Tanga

98 ELECTRON AND HOLE TRAPPING CENTERS IN IONIC OXIDES, J. H. Crawford, Jr., K. H. Lee, and G. S. White

104 SPIN POLARIZATION QUENCHING OF TUNNELING RECOMBINATION LUMINESCENCE BETWEEN Ag° AND V_K CENTERS, C. J. Delbecq and P. H. Yuster

112 ELECTRON PARAMAGNETIC RESONANCE OF PHOSPHOROUS CENTERS IN PHENACITE, R. C. DuVarney and A. K. Garrison

121 OPTICAL PROPERTIES OF DEFECTS IN HEXAGONAL BORON NITRIDE, Koh Era, Takashi Kuzuba, Toshihiko Ishii, Tadao Sato, and Minoru Iwata

148 LASER SPECTROSCOPIC EXPERIMENTS WITH COLOR CENTERS IN KCl, M. Georgiev, Y. Vassilev, T. Todorov, and G. Todorov

158 RADIATION-INDUCED OXYGEN INTERSTITIALS IN MgO, L. E. Halliburton and L. A. Kappers

170 WHAT ABOUT THE Z_5 CENTER?, H. C. Hilber and H. J. Paus

182 EPR AND OPTICAL STUDIES OF γ-IRRADIATED MgO:Ga, G. E. Holmberg, K. H. Lee, and J. H. Crawford, Jr.

201 EPR STUDY OF V^{2+}-VACANCY DIPOLES IN ALKALI HALIDES, Takeo Iri and Takao Ito

207 THEORETICAL INVESTIGATION OF THE HYPERFINE-STRUCTURE CONSTANTS OF THE H-CENTER USING A VALENCE-BOND WAVE FUNCTION FOR THE HALOGEN-MOLECULE, A. N. Jette and F. J. Adrian

209 THERMOLUMINESCENCE IN KCl X-IRRADIATED AT 80K, M. Jiménez de Castro and J. L. Alvarez Rivas

258 LUMINESCENCE IN MgO: EVIDENCE FOR ELECTRON HOLE RECOMBINATION AT A MAGNESIUM ION VACANCY, K. H. Lee and J. H. Crawford, Jr.

260 EXPERIMENTAL AND THEORETICAL STUDY OF F CENTRES IN $SrCl_2$, BaClF AND SrClF, S. Lefrant, A. H. Harker, and L. Taurel

277 DISPERSION AND FARADAY ROTATION ASSOCIATED WITH POINT-IMPERFECTIONS, J. J. Markham and K. N. Vasudevan

288 OPTICAL DICHROISMS OF [Li]° DEFECTS IN MgO, F. A. Modine

295 ANISOTROPIC ELECTRIC FIELD EFFECTS ON THE SPIN RELAXATIONS OF THE $F_A(Li)$ CENTERS IN KCl, Yuzo Mori, Tohru Watanabe, and Hiroshi Ohkura

313 ENDOR INVESTIGATION OF F CENTRES IN BaClF, J. R. Niklas, G. Heder, M. Yuste, and J. M. Spaeth

333 THERMOLUMINESCENCE OF ORDERED AND DISORDERED $NaAlSi_3O_8$, E. S. Pasternack, A. M. Gaines, and P. W. Levy

354 RADIATION EFFECTS IN Al_2O_3, A. Rehavi and N. Kristianpoller

356 ABSORPTION SPECTRA OF O_2^- IN ALKALI HALIDE CRYSTALS, John Rolfe

358 RADIATION INDUCED DEFECTS IN THE OCTAHEDRAL COORDINATION SPHERE OF A_2MX_6-COMPOUNDS, K. Rössler and L. Pross

365 FURTHER EVIDENCE FOR THE DI-INTERSTITIAL MODEL FOR THE V_4 CENTRE, M. Saidoh and P. D. Townsend

371 OPTICAL AND THERMOLUMINESCENCE PROPERTIES OF UNDOPED AND TIN DOPED RbCl, S. B. S. Sastry and K. Balasubramanyam

373 THERMOLUMINESCENCE AND OTHER PROPERTIES OF UNDOPED AND TIN DOPED RbI CRYSTALS, S. B. S. Sastry and K. Balasubramanyam

381 MODULATED ABSORPTION OF $Z_2(Eu)$ CENTERS IN KCl, W. Scheu and H. J. Paus

410 PARAMAGNETIC RESONANCE OF THE OPTICALLY EXCITED TRIPLET STATE OF $Z_2(Sr)$ IN KCl, K. Strohm, L. Schwan, and H. J. Paus

448 PROBLEMS IN THE THEORY OF F- AND F_A-CENTRE STATES IN ALKALI HALIDES, John M. Vail

461 FIRST-SHELL ENDOR AND SPIN RELAXATION OF THE $F_A(Li)$ CENTERS IN KBr AT LHeT, Tohru Watanabe, Yuzo Mori, and Hiroshi Ohkura

477 ELECTRONIC STRUCTURE OF THE F^+ CENTER IN ALKALINE EARTH OXIDES, T. M. Wilson and R. F. Wood

488 CALCULATED PRESSURE SHIFTS OF F-CENTER HYPERFINE INTERACTION PARAMETERS IN ALKALI CHLORIDES, R. D. Zwicker

APPLICATIONS

35 COLOR CENTER CRYSTALS AS ACTIVE MATERIAL FOR CW INFRARED LASERS, R. Beigang, G. Litfin, and H. Welling

102 CATHODOLUMINESCENCE IN ZnS AND CdS CRYSTALS, S. Datta, D. B. Holt, and I. M. Boswarva

146 PHOTOINDUCED COLOR CENTER BANDS IN INSULATING CADMIUM SULPHIDE CRYSTALS, M. Georgiev, S. Kanev, K. Tsvetkova, and T. Todorov

191 DATING WITH LATTICE DEFECTS INDUCED BY NATURAL RADIATION: ESR AND THERMOLUMINESCENCE DATING OF CAVE DEPOSITS, Motoji Ikeya and Toshikatsu Miki

294 DEVELOPMENT OF HYDROGEN DOPED CRYSTALS FOR FAST NEUTRON DETECTION, S. P. Morato, B. M. Rzyski, and K. S. V. Nambi

389 DEFECTS AND PHOTOREFRACTION PROCESSES IN $LiNbO_3$ CRYSTALS, K. K. Shvarts, P. A. Augustov, and A. O. Ozols

398 FINITE-ENERGY SUM RULES FOR INFRARED REFLECTION SPECTROSCOPY: APPLICATION TO IONIC CRYSTALS AND SOLAR HEAT MIRRORS, David Y. Smith and Corinne A. Monague

412 CONTROLLED CRYSTAL GROWTH OF YTTRIA AND THE RARE EARTH SESQUIOXIDES, Sherman Susman and David Hinks

450 ABOUT RADIATION DAMAGE IN α-QUARTZ, A. Van den Bosch

481 LUMINESCENCE SITES FOR LiF DOSIMETRY, M. C. Wintersgill and P. D. Townsend

SUPERIONIC CONDUCTORS

27 SPECTROSCOPIC STUDIES OF CONDUCTION PLANE DEFECTS IN SODIUM β-ALUMINA, R. C. Barklie, K. P. O'Donnell, and B. Henderson

50 ELECTRONIC PROPERTIES AND DEFECTS OF THE SUPERIONIC CONDUCTOR LITHIUM NITRIDE, Hermann Brendecke and Elmar Wagner

77 SINGLE-CRYSTAL NEUTRON DIFFRACTION STUDY OF α-AgI BETWEEN 160° AND 300°C, R. J. Cava, F. Reidinger, and B. J. Wuensch

124 NEUTRON-DIFFRACTION STUDY OF STABILIZED ZrO_2: OBSERVATION OF OXYGEN SUBLATTICE SHEAR DISTORTIONS, J. Faber, Jr., M. H. Mueller, R. L. Hitterman, and T. H. Etsell

138 FURTHER RESULTS FOR THE CONDUCTIVITY ANOMALY IN AgCl AND AgBr, Robert J. Friauf and Ko-Jun Kao

162 LATTICE-DEFECT MODELS OF FAST ION CONDUCTORS, Y. Haven

165 FAST-ION BEHAVIOUR OF FLUORITE CRYSTALS AT HIGH TEMPERATURES, W. Hayes

236 IONIC TRANSPORT IN Na BETA-ALUMINA SINGLE CRYSTALS, K. K. Kim, J. N. Mundy, and W. K. Chen

266 GRAIN BOUNDARY CONDUCTIVITY IN BETA ALUMINA, E. Lilley and J. E. Strutt

299 COMPUTER SIMULATION OF CORRELATION EFFECTS IN SUPERIONIC CONDUCTIVITY AND DIFFUSION, G. E. Murch and R. J. Thorn

319 DEFECT INTERACTIONS IN CaO- AND Y_2O_3-DOPED CeO_2, A. S. Nowick, D. S. Park, J. Griffith, and M. P. Anderson

376 MICROSYNTACTIC INTERGROWTH AND DEFECTS OF β-ALUMINA TYPE COMPOUNDS, H. Sato, Y. Hirotsu, and Y. Tang

457 DIELECTRIC STUDY OF MOBILE IONS IN A SUPERIONIC CONDUCTOR, J. Wahl, U. Holland, and E. S. Koteles

459 LOCATIONS OF THE CONDUCTING-ION SITE NEAR THE MID-OXYGEN POSITION IN BETA-ALUMINAS, J. C. Wang

JAHN-TELLER EFFECT

41 JAHN-TELLER EFFECT IN TRIGONAL $4d^9$ CENTERS, B. D. Bhattacharyya

43 TUNNEL-SPLITTING IN TRANSITION-METAL OXIDES AND HALIDES ON QUASI-MOLECULAR JAHN-TELLER MODEL, B. D. Bhattacharyya

113 THERMALLY ACTIVATED ROTATION OF S^- IN KCl: A GROUND STATE JAHN-TELLER SYSTEM, B. Eilebrecht, G. Gelfert, and L. Schwan

149 JAHN-TELLER INDUCED MIXING OF MAGNETICALLY PERTURBED Tl^+-TYPE ENERGY LEVELS IN POTASSIUM BROMIDE, U. Giorgianni, G. Mondio, G. Saitta, and G. Vermiglio

275 THE ODD-PARITY JAHN-TELLER EFFECT FOR IMPURITY IONS IN ALKALI EARTH OXIDES, N. B. Manson

298 VIBRATIONAL RAMAN SCATTERING INDUCED BY JAHN-TELLER SYSTEMS IN POLAR CRYSTALS, E. Mulazzi and N. Terzi

310 LATTICE RELAXATION IN JAHN-TELLER SYSTEM AND POLARIZATION CORRELATION BETWEEN PHOTO-ABSORPTION AND LUMINESCENCE, Keiichiro Nasu and Tadanobu Kojima

342 A-P-E-S OF THE $|A_2>$ STATE OF Pb^{2+} IN CsBr, S. Radhakrishna and V. S. Sivasankar

344 AN EPR STUDY OF PALLADIUM AND PLATINUM GROUP IMPURITIES IN MgO AND CaO, A. Raizman and J. T. Suss

348 NON-RADIATIVE TRANSITIONS IN ALKALI-HALIDE PHOSPORS, A. Ranfagni, G. Viliani, M. Cetica, and G. Molesini

367 DYNAMIC JAHN-TELLER VIBRONIC COUPLING IN T x τ_2, N. Sakamoto and S. Muramatsu

383 SMALL POLARON VERSUS CRYSTAL FIELD TRANSITIONS IN A DEEP OXIDE ACCEPTOR, O. F. Schirmer

RADIATION EFFECTS

5 FORMATION AND ANNEALING OF HYDROGEN CENTERS IN IRRADIATED LiF CRYSTALS, Z. G. Akhvlediani

17 ION IMPLANTATION DAMAGE IN CRYSTALLINE QUARTZ AND FUSED SILICA, G. W. Arnold

34 FORMATION OF RADIATION DEFECTS IN LaF_3-TYPE CRYSTALS, S. Kh. Batygov, V. A. Myzina, and V. V. Osiko

106 DIFFERENCES INDUCED BY ENERGETIC IONS ON THE Ag^+ LATTICE IN AgCl ACCORDING TO THEIR ENERGY, Ch. Diaine, J. L. Gisclon, and J. Dupuy

115 KINETICS OF THE RADIATION DEFECTS FORMATION IN ALKALI HALIDE CRYSTALS, Y. A. Ekmanis

123 PARTICLE IRRADIATED CRYSTALLINE ALUMINA, B. D. Evans

142 THERMOLUMINESCENCE OF CRYSTALLINE QUARTZ, G. E. Fuller and P. W. Levy

174 THE F CENTRE STABILIZATION PROCESS IN THE FIRST COLOURING STAGE OF ALKALI HALIDE CRYSTALS, E. R. Hodgson, A. Delgado, and J. L. Alvarez Rivas

203 THE INITIAL PRODUCTION OF DEFECTS IN ALKALI HALIDES: F AND H CENTER PRODUCTION BY NON-RADIATIVE DECAY OF THE SELF-TRAPPED EXCITON, N. Itoh, A. M. Stoneham, and A. H. Harker

238 EFFECT OF Fe IONS ON THE EARLY STAGE COLORATION OF MgF_2, K. K. Kim, A. S. Nowick, and R. S. Title

246 UV RADIATION INDUCED ABSORPTION IN LITHIUM FLUORIDE, H.-J. Kos and R. Nink

247 TWO MODELS FOR EVALUATION OF TEMPERATURE DEPENDENCE OF F CENTRE ACCUMULATION EFFICIENCY IN DOPED ALKALI HALIDES, E. Kotomin, I. Tāle, and I. Fabrikant

249 F-CENTER FORMATION IN ION BOMBARDED MgO, G. B. Krefft and K. L. Brower

251 FORMATION OF HOLE CENTERS IN BaF_2 BY NON-IONIZING RADIATION, AND ANNIHILATION OF THESE CENTERS, N. Kristianpoller, B. Trieman, and Y. Kirsh

272 POSITIVE-ION BOMBARDMENT OF KCl: THE ROLE OF PARTICLE INFRATRACKS, M. Luntz, P. E. Thompson, and R. B. Murray

273 MECHANISMS OF CATION DEFECT CREATION IN ALKALI HALIDES, Ch. B. Lushchik, A. A. Elango, R. I. Gindina, A. Ch. Lushchik, A. A. Maaroos, T. N. Nurakhmetov, L. A. Ploom, L. A. Pung, J. V. Põllusaar, H. A. Soovik, and N. A. Jaanson

284 THE PART OF V_K CENTERS IN THE EQUILIBRIA BETWEEN CENTERS CREATED BY ELECTRON IRRADIATION AT LIQUID HELIUM TEMPERATURE IN KBr, E. Mercier, A. Nouailhat, and G. Guillot

286 RADIATION DEFECT BLEACHING IN ALKALI HALIDES AT HIGH TEMPERATURE AFTER PULSED ELECTRON BEAM IRRADIATION, D. K. Millers, E. A. Baumanis, A. E. Plaudis, J. J. Ābolinš, and P. Stučhka

301 POSITIVE ION DAMAGE AND RADIATION ANNEALING IN MAGNESIUM OXIDE, R. B. Murray, F. S. Uralil, C. M. Fou, and W. T. Franz

303 STUDIES ON C CENTER COLLOIDS AND ANNEALING OF RADIATION DAMAGE IN NaCl CRYSTALS, Y. V. G. S. Murti and N. Sucheta

335 PROTON-INDUCED X-RAY MEASUREMENTS IN ION IMPLANTED MgO, P. S. Peercy

352 RADIATION-INDUCED MICROSTRUCTURAL CHANGES IN YTTRIUM OXIDE AND ALUMINUM OXIDE, M. D. Rechtin, H. Wiedersich, and A. Taylor

360 DIELECTRIC MEASUREMENTS OF FRENKEL PAIRS IN K_2SnCl_6, K. Rössler and J. Winter

377 PULSE RADIOLYSIS STUDIES OF DEFECT FORMATION IN ALKALI HALIDES AT HIGH TEMPERATURES, R. D. Saxena, K. Tanimura, and N. Itoh

408 DIFFUSE X-RAY SCATTERING FROM NEUTRON IRRADIATED MgO, J. P. Stott, D. Grasse, B. von Guérard, and J. Peisl

414 F CENTER FORMATION IN PICO SECOND RANGE IN KI, Yoshiro Suzuki and Masamitsu Hirai

416 FORMATION OF SELF TRAPPED EXCITON IN PICO SECOND RANGE IN KI, Yoshiro Suzuki and Masamitsu Hirai

422 ENERGY TRANSFER BY THE PRECURSOR OF FRENKEL PAIRS IN ALKALI HALIDES, K. Tanimura

426 THE ELASTIC INTERACTION OF THE H CENTER WITH A Rb^+ ION DURING THE DYNAMIC MOTION AND THERMAL MIGRATION IN KBr, K. Tanimura

430 THE EFFECT OF HEATING RATE ON THE THERMOLUMINESCENCE SENSITIVITY OF LiF (TLD-100), G. C. Taylor and E. Lilley

434 DEFECT CREATION AND PRECIPITATION IN IMPLANTED MgO, P. Thévenard, A. Cachard, J. P. Dupin, M. Marichy, and M. Guermazi

442 OBSERVATION OF EXTRINSIC COLLOIDS OF POTASSIUM IMPLANTED IN MgO SINGLE CRYSTAL, M. Treilleux ard G. Chassagne

475 ELECTRON PULSE RADIOLYSIS OF MAGNESIUM FLUORIDE, R. T. Williams, C. L. Marquardt, J. W. Williams, and M. N. Kabler

484 TEMPERATURE AND RADIATION INDUCED PROCESSES IN SULPHATE DOPED ALKALI HALIDES, V. P. Zeikats

AGGREGATION

21 COLLOID CENTERS IN SILVER CHLORIDE INDUCED BY REACTOR IRRADIATION AT LOW TEMPERATURE, Kozo Atobe, Moritami Okada, and Masuo Nakagawa

86 PRODUCTION AND STABILITY OF [Li]° DEFECTS IN MgO SINGLE CRYSTALS, Y. Chen, H. T. Tohver, J. Narayan, and M. M. Abraham

110 ELECTRICAL CONDUCTIVITY OF ADDITIVELY COLOURED KCl CRYSTALS. INFLUENCE OF IMPURITIES, D. Durand, G. Chassagne, and J. Serughetti

128 HIGH TEMPERATURE ANNEALING OF RADIATION DEFECTS IN LiF, E. E. Feldmane, A. V. Podinsh, and K. K. Shvarts

151 THERMAL DECAY OF THE F^- CENTRE IN KCl, D. H. Goode and J. H. Simpson

156 INTERSTITIAL STABILIZATION MECHANISM IN ALKALI HALIDES IRRADIATED AT 77 K, G. Guillot and A. Nouailhat

168 POINT DEFECT EQUILIBRIA IN Al_2O_3 AS DEDUCED FROM TEM STUDIES OF Ti-DOPED CRYSTALS, A. H. Heuer, T. E. Mitchell, and D. S. Philips

172 VOID ANALOGUES IN IRRADIATED HALIDES, L. W. Hobbs, M. Saidoh, and V. M. Orera

178 THE EFFECT OF ANNEALING ON THE PROPERTIES OF COPPER-CALCIUM PHOSPHATE GLASSES, C. A. Hogarth and G. R. Moridi

187 DEFECT AGGREGATION IN IRRADIATED OXIDES, D. G. Howitt, R. S. Barnard, L. W. Hobbs, and T. E. Mitchell

193 TUNNELLING RECOMBINATION IN LiH IRRADIATED AT LOW TEMPERATURE, Motoji Ikeya and Toshikatsu Miki

219 ESR STUDY ON PHASE TRANSFORMATION OF Li METALS IN LiF, T. Kamikawa and S. Nagasaka

264 FORMATION OF M^{++}-VACANCY DEFECTS IN ALKALI HALIDE CRYSTALS, E. Lilley and J. E. Strutt

269 STUDY OF INTERSTITIAL CLUSTERS IN γ-IRRADIATED HIGH PURITY AND Mg DOPED LiF SINGLE CRYSTALS, BY THERMAL CONDUCTIVITY MEASUREMENTS BETWEEN 0.05 AND 70 K, M. Locatelli

306 TRANSMISSION ELECTRON MICROSCOPE STUDIES OF Li-DOPED MgO, J. Narayan, M. M. Abraham, Y. Chen, and H. T. Tohver

321 THE INFLUENCE OF IRRADIATION TEMPERATURE ON THE FORMATION OF F-AGGREGATE CENTERS IN LiF CRYSTALS, Moritami Okada, Kozo Atobe, and Masuo Nakagawa

420 THERMAL ANNEALING OF F AND V_2 CENTRES IN KCl CRYSTALS, I. Tāle and A. Nagornyi

432 ORDERING OF DEFECTS IN TiO_x, H. Tetsuchi and J. B. Cohen

440 ANNEALING STUDIES IN ERBIUM DOPED ALKALINE EARTH FLUORIDES, Donald Treacy, John Fontanella, and Carl Andeen

453 THE KINETICS OF BARIUM PRECIPITATION AT DISLOCATIONS IN NaCl MONOCRYSTALS, G. Vlasák and M. Hartmanová

467 PRODUCTION OF COLLOIDAL LEAD AND N_2 BY IRRADIATION OF $Pb(N_3)_2$, D. A. Wiegand and W. L. Garrett

RELAXED EXCITED STATES

23 MAGNETIC CIRCULAR DICHROIC EFFECTS IN [illegible] LUMINESCENCE AND ELECTRON-SPIN MEMORY IN THE OPTICAL-PUMPING CYCLE OF F CENTERS IN ALKALI HALIDES, G. Baldacchini, U. M. Grassano, and A. Tanga

25 F-CENTERS WITHOUT RELAXED EXCITED STATES? II) F-CENTER EMISSION IN NaI AND NaBr, Giuseppe Baldacchini and Fritz Lüty

28 VIBRATIONAL COUPLING IN THE RELAXED EXCITED STATE OF THE F CENTER IN KCl, R. H. Bartram and J. M. Dekle

100 JAHN-TELLER EFFECT IN THE $^3T_{1u}$ RELAXED EXCITED STATES OF Ga^+ IN KBr, Le Si Dang, R. Romestain, Y. Merle d'Aubigné, and A. Fukuda

189 VIBRONIC THEORY OF THE MAGNETIC PROPERTIES OF THE RELAXED EXCITED STATE OF THE F CENTERS, Takeshi Iida, Koichi Imanaka, and Hiroshi Ohkura

195 VIBRONIC THEORY OF THE STARK EFFECTS IN F CENTER EMISSION, Koichi Imanaka, Takeshi Iida, and Hiroshi Ohkura

211 LUMINESCENT CENTERS IN THALLIUM-DOPED ALKALI HALIDES, R. V. Joshi, L. H. H. Prasad, and P. W. Deshpande

232 AN APPROACH TO THE PROBLEM OF BOUND POLARON, Y. Kayanuma and Y. Kondo

282 RELAXED EXCITED STATES OF $(Tl^+)_2$-TYPE CENTERS IN ALKALI HALIDES, Akira Matsushima and Atsuo Fukuda

324 RADIATIVE DECAY OF THE TRIPLET STATE OF THE F_2 CENTER IN KCl AND KBr, J. M. Ortega, Y. Farge, and R. H. Silsbee

329 F-CENTERS WITHOUT RELAXED EXCITED STATES? I) ABSORPTION AND DOUBLE-LASER-BEAM RAMAN STUDIES OF F-AND F' CENTERS IN NaI, David S. Pan and Fritz Lüty

446 LUMINESCENCE IN MgO: TIME-RESOLVED SPECTROSCOPY WITH ELECTRON-PULSE EXCITATION, Thomas J. Turner, K. H. Lee, and Richard T. Williams

EXCITONS

3 EFFECT OF DIVALENT CATION IMPURITIES ON THE INTRINSIC LUMINESCENCE OF NaCl, M. Aguilar, F. Jaque, and F. Agulló-López

46 E.N.D.O.R. OF SELF-TRAPPED EXCITON IN KCl, D. Block, Y. Merle d'Aubigné, and A. Wasiela

81 Bi-EXCITON LUMINESCENCE FROM NaCl, P. J. Chandler, P. D. Townsend, and M. Aguilar

92 THE ABSORPTION EDGE SPECTRA OF PURE AND MIXED ALKALI HALIDES BELOW AND ABOVE THE MELTING POINT, C. D. Clark, A. H. Skull, and Jenifer S. Wells

126 MAGNETO-OPTICS STUDIES OF SELF-TRAPPED EXCITON LUMINESCENCE IN CsI, L. Falco, J. P. von der Weid, and M. A. Aegerter

163 EDGE LUMINESCENCE AND SELF-TRAPPING OF EXCITONS IN KI AND RbI, Tetsusuke Hayashi, Tokiko Ohata, and Shigeharu Koshino

215 VACANCY-INTERSTITIAL PAIR PRODUCTION BY ELECTRON-HOLE RECOMBINATION IN HALIDES, M. N. Kabler and R. T. Williams

222 LUMINESCENCE FROM KCl:I AT LOW TEMPERATURES, Ken-ichi Kan'no, Minoru Itoh, Eiji Yoshikawa, and Yoshio Nakai

304 RELAXED EXCITONIC STATES IN $CdBr_2$ AND $CdBr_2$:I, H. Nakagawa, K. Hayashi, and H. Matsumoto

317 DIFFUSION OF FREE EXCITONS IN KI, A. Nouailhat, E. Mercier, and G. Guillot

336 STUDIES OF SELF-TRAPPED EXCITON LUMINESCENCE IN CsI, J. P. Pellaux, T. Iida, and M. A. Aegerter

364 RECOMBINATION LUMINESCENCE BETWEEN TRAPPED ELECTRONS AND SELF-TRAPPED HOLES IN $SrCl_2$ DOPED WITH ALKALI CATIONS AFTER X-IRRADIATION, E. Rzepka, L. Taurel, and J. P. Chapelle

404 DIRECT-FORBIDDEN EXCITONS IN TETRAGONAL GeO_2, M. Stapelbroek and B. D. Evans

437 EXCITON DIFFUSION AND DEFECT FORMATION IN NaCl, P. D. Townsend and M. C. Wintersgill

438 LUMINESCENCE FROM SELF-TRAPPED EXCITONS IN KBr:Na, Koichi Toyoda, Kaizo Nakamura, and Yoshio Nakai

471 SHORT-PULSE LASER STUDIES OF EXCITON RELAXATION AND F-CENTER PRODUCTION IN ALKALI HALIDES, R. T. Williams, J. N. Bradford, and W. L. Faust

ELECTRON-LATTICE INTERACTIONS

19 EMISSION SPECTRA OF KI:Tl AT LOW TEMPERATURE UNDER HIGH PRESSURE, K. Asami, S. Masunaga, and M. Ishiguro

30 RESONANCE RAMAN SCATTERING FROM METASTABLE OXYGEN SPECIES IN IRRADIATED $NaClO_3$, J. B. Bates

32 RAMAN SCATTERING FROM F CENTERS IN CaO, J. B. Bates and R. F. Wood

37 ON THE ELECTRONIC EXCITED STATE OF THE MONOMER CENTRES IN ALKALI-HALIDE PHOSPHORS, S. Benci and M. Manfredi

39 RESONANT RAMAN SCATTERING FROM F-CENTRES IN CsF, Giorgio Benedek and E. Mulazzi

44 MAGNETIC VIBRATIONAL RAMAN SCATTERING OF KI DOPED WITH F CENTRES, M. Billardon, M. F. Russel, J. P. Buisson, and S. Lefrant

54 FIRST-ORDER RAMAN SCATTERING INDUCED BY F CENTERS IN CsCl, CsBr, and CsF, J. P. Buisson, S. Lefrant, M. Ghomi, L. Taurel, and J. P. Chapelle

56 E.P.R. INVESTIGATIONS OF THE DISPLACIVE STRUCTURAL PHASE CHANGE IN AMF_3 CRYSTALS ON USING PARAMAGNETIC PROBES: $|FeOF_5|^{4-}$, $|GdOF_5|^{4-}$ CLUSTERS, J. Y. Buzaré, J. J. Rousseau, and J. C. Fayet

59 ROLE OF THE ELECTRONIC EXCITED STATE OF Pb^{2+} ON THE ION REORIENTATION PROCESSES IN KCl, R. Capelletti, F. Fermi, and R. Fieschi

64 RAMAN SPECTRA IN KCl:Pb WITH SUZUKI-LIKE OCCLUSIONS, R. Capelletti, P. P. Lottici, and C. Razzetti

71 PHASE TRANSITIONS IN KCN, NaCN AND RbCN CRYSTALS. THE OCN^- VIBRATIONAL SPECTRUM, J. C. Castro, H. C. Basso, M. Siu Li, and Milton de Souza

119 INTENSITY OF POLARIZED RAMAN SCATTERING FROM METASTABLE O_2^* IN γ-IRRADIATED SODIUM CHLORATE, Herbert Engstrom

134 SPECTROSCOPY OF SMALL MOLECULAR IONS IN ALKALI HALIDE CRYSTALS, A. Freiberg and L. A. Rebane

160 LOCALIZED MODE OF LITHIUM IN AgBr-AgCl MIXED CRYSTALS, Takeshi Hattori and Akiyoshi Mitsuishi

180 OFF-CENTER DEFECTS UNDER HYDROSTATIC PRESSURE: "LOCALIZED MODEL CASES" FOR DISPLACIVE FERROELECTRICS AND SUPERIONIC CONDUCTORS, Ulrich Holland and Fritz Lüty

213 EVOLUTION OF MOLECULAR ORDER AND PHASE TRANSITIONS IN MIXED ALKALI-HALIDE-CYANIDE CRYSTALS. I. INFRARED ABSORPTION, DOMAIN SCATTERING AND CHRISTIANSEN EFFECT, Michael D. Julian and Fritz Lüty

217 REORIENTATIONAL DISORDER OF NO_3^- IN $CsNO_3$, R. Kamel, Y. A. Badr, and Z. I. Badawy

226 HYDROGEN IMPURITY MODES IN MONODOMAIN $SrTiO_3$ SINGLE CRYSTALS, S. Kapphan and J. Koppitz

228 VUV- AND NIR-ABSORPTION OF OH^--IMPURITIES IN ALKALI FLUORIDES, S. Kapphan and J. Koppitz

244 RES ABSORPTION SPECTRA OF F CENTER IN ALKALI HALIDES, Y. Kondo, Y. Kayanuma, and H. Kanzaki

255 EFFECT OF IMPURITY DOPING ON THE HIGH TEMPERATURE TRANSITION IN $(M_xV_{1-x})_2O_3$ ALLOYS, H. Kuwamoto, W. R. Robinson, and J. M. Honig

280 ANOMALOUS RELAXATION PROCESS OF THE OFF-CENTER Li^+ IONS IN KCl:Li AT ZERO ELECTRIC FIELD, Masao Matsuoka, Yuzo Mori, and Hiroshi Ohkura

312 THE TEMPERATURE DEPENDENCE OF PHONON-DEFECT MODE HYBRIDIZATION IN KCl(CN), R. M. Nicklow and W. P. Crummett

323 SPECTRAL DISTRIBUTION OF THE TRIPLET TO SINGLET LUMINESCENCE OF F_2 CENTER IN KCl, KBr AND KI, J. M. Ortega

326 PARAMAGNETIC DEFECTS AS PROBES OF STRUCTURAL PHASE TRANSITIONS, F. J. Owens

327 A NEW F-AGGREGATE CENTER: THE (F + U) - CENTER PAIR, David S. Pan and Fritz Lüty

340 MOLECULAR CHROMATE CENTERS IN CESIUM IODIDE, S. Radhakrishna, K. Hariharan, and S. Haridoss

379 EVOLUTION OF MOLECULAR ORDER AND PHASE-TRANSITIONS IN MIXED ALKALI-HALIDE-CYANIDE CRYSTALS. II. DEVELOPMENT OF FERROELASTICITY FROM PARAELASTIC DEFECT BEHAVIOR, Luiz Carlos Scavarda do Carmo and Fritz Lüty

385 TRANSIENT ABSORPTION FROM THE RELAXED EXCITED STATE OF THE F CENTER IN KF, Irwin Schneider

387 A FREELY LIBRATING ELASTIC DIPOLE IN KCl, Dirk Schoemaker and Ad Lagendijk

393 NON-RADIATIVE DECAY OF THE TRIPLET-SINGLET OF THE F_2 CENTER IN KCl AND KBr, R. H. Silsbee, Y. Farge, and J. M. Ortega

418 LUMINESCENCE OF THE F CENTERS IN LiCl, Ken Takiyama, Toshiaki Fujita, Atsuhiro Fujii, and Masato Nishi

424 NON-RADIATIVE RECOMBINATION PROCESS OF THE SELF-TRAPPED EXCITON IN ALKALI HALIDES, K. Tanimura

435 HYDROSTATIC PRESSURE TUNING OF MOLECULAR DEFECT ROTATION IN ALKALI-HALIDES, Klaus Thörmer and Fritz Lüty

455 F CENTERS PROPERTIES AND PHASE TRANSITIONS: KCN AND NaCN, J.-P. von der Weid and M. A. Aegerter

473 A SEARCH FOR INFRARED ABSORPTION BY SELF-TRAPPED EXCITONS IN SODIUM CHLORIDE, R. T. Williams, M. N. Kabler, and I. Schneider

479 EXCITON RELAXATION IN AgBr STUDIED BY RESONANT RAMAN SCATTERING, J. Windscheif, H. Stolz, and W. von der Osten

IMPURITIES

7 E.P.R. STUDIES OF RADIATION DAMAGE IN $CaSO_4 \cdot 2H_2O$ CRYSTALS, A. R. Albuquerque, S. Watanabe, and S. Isotani

13 DIELECTRIC RELAXATION IN RARE-EARTH AND ALKALI METAL DOPED ALKALINE EARTH FLUORIDES, Carl Andeen, Donald Schuele, John Fontanella, Richard L. Johnston, and Donald Treacy

68 OPTICAL PROPERTIES OF NaBr:Tl^+, M. Casalboni, U. M. Grassano, A. Scacco, and A. Tange

73 A THEORETICAL STUDY OF ALKALI HALIDE CRYSTALS CONTAINING UNIVALENT IMPURITY IONS, C. R. A. Catlow, J. Corish, K. M. Diller, P. W. M. Jacobs, M. J. Norgett, and B. M. C. Parker

88 OFF CENTER Cu^+ IN CsBr, B. V. R. Chowdari, S. Radhakrishna, and B. Ram Babu

90 OPTICAL PROPERTIES OF COBALT CENTERS IN NH_4Cl, B. V. R. Chowdari, S. Radhakrishna, and B. Ram Babu

94 EMISSION SPECTRA PRODUCED BY EXCITATION IN THE A, B, C AND D ABSORPTION BANDS OF KI:Sn^{2+}, Leighton L. Coatsworth, Patrick W. M. Jacobs, and Yoshio Kamishina

96 SPECTRAL BAND SHAPE FOR THE TRANSITION $a_{1g}^2 \rightarrow a_{1g}t_{1u}$ IN Sn^{2+}-DOPED ALKALI HALIDE CRYSTALS, Leighton L. Coatsworth, Patrick W. M. Jacobs, Yoshio Kamishina, and Mary Anne Millar

105 TUNNELING RECOMBINATION LUMINESCENCE BETWEEN Ag^{++} AND Ag°, Charles J. Delbecq, Philip H. Yuster, and David L. Dexter

153 ESR STUDY OF HEAVY METAL IMPURITIES WITH p^1 CONFIGURATION IN KCl, E. Goovaerts, A. Lagendijk, and D. Schoemaker

176 ENDOR STUDY OF THE VIBRATIONS OF HYDROGEN ATOMS IN KCl AND RbCl, Chr. Hoentzsch and J. M. Spaeth

184 DOUBLE QUANTUM EPR TRANSITION IN AgCl:Ni, G. E. Holmberg, L. M. Slifkin, and J. C. Hempel

197 ELECTROLYTIC COLOURATION OF KCl:Tl^+ CRYSTALS, A. Ioan and V. Topa

199 NEW CENTRES IN KCl:Tl^+ + Ca^{2+} AND KCl:Tl^+ + Sr^{2+} CRYSTALS, A. Ioan and V. Topa

205 Ag°-V_k TUNNELING RECOMBINATION IN ALKALI HALIDES, Noriaki Itoh, Shigeru Takeuchi, Takashi Tashiro, and M. Saidoh

230 ESR OF OFF CENTERED Eu^{2+} IN KCl:Eu CRYSTALS, K. Kawano, R. Nakata, M. Sumita, and E. Higuchi

262 VIBRONIC MODEL FOR AN ns^2 SYSTEM: KCl:Au^-, D. Lemoyne, J. Duran, and J. Badoz

270 THERMOLUMINESCENCE AND ELECTRON SPIN RESONANCE AFTER X-RAY IRRADIATION OF NaCl:Mn^{++}, F. J. López, F. Jaque, A. J. Fort, and F. Agulló-López

279 ELECTRON SPIN RESONANCE ABSORPTION SPECTROSCOPY INVESTIGATION OF MAGNETIC ION IMPURITIES IN SINGLE CRYSTAL YTTRIUM ALUMINUM GARNET, S. A. Marshall, T. Marshall, and R. A. Serway

315 ESR MEASUREMENTS ON Pb^{3+}- CENTER IN CUBIC PbF_2 CRYSTAL, Masato Nishi, Hideo Hara, Yoshifumi Ueda, and Yukio Kazumata

325 OPTICAL ABSORPTION, PHOSPHORESCENCE, PHOTOLUMINESCENCE AND THERMOLUMINESCENCE CORRELATION STUDIES IN CALCIUM FLUORIDE CRYSTALS DOPED WITH LANTHANIDES, Choyu Otani, R. Muccillo, K. S. V. Nambi, and S. M. D. Rao

331 OPTICAL SPECTROSCOPY OF LEAD IN ALKALI HALIDE CRYSTALS. EFFECT OF X-IRRADIATION, J. L. Pascual, L. Arizmendi, F. Jaque, and F. Agulló-López

350 EPR OBSERVATION OF SIZE EFFECTS IN SMALL DIELECTRIC PARTICLES OF $SrCl_2:Gd^{3+}$, M. Rappaz, C. Solliard, L. A. Boatner, and A. Châtelain

362 THE SIDE-BANDS IN ABSORPTION AND LUMINESCENCE EXCITATION SPECTRA OF KBr:Tl, M. Roth and A. Halperin

374 ESR, OPTICAL ABSORPTION AND THERMOLUMINESCENCE STUDIES ON IRRADIATED NaCl:Ni, S. B. S. Sastry, C. N. Subbanna, and A. Scharmann

394 SYSTEMATICS OF ENERGY LEVELS OF IONS IN HOST CRYSTALS, John Simonetti and Donald S. McClure

406 THE CALCULATION OF SURFACE AND BULK LATTICE DEFECTS IN ALKALINE-EARTH OXIDES AND NiO, R. F. Stewart and W. C. Mackrodt

451 ESR STUDY OF Sn^- DEFECTS IN ALKALI HALIDES, F. Van Steen, A. Lagendijk, and D. Schoemaker

MECHANICAL PROPERTIES

11 ON THE DISPARITY OF THE PARAMETERS OF VACANCIES OBTAINED FROM SPECIFIC HEATS AND OTHER METHODS, K. Alexopoulos and P. Varotsos

70 PLASTIC DEFORMATION OF NiO SINGLE CRYSTAL IN THE VICINITY OF THE NEEL TEMPERATURE, J. Castaing and M. Spendel

155 ATOMISTIC CALCULATIONS ON DISLOCATIONS AND POINT DEFECTS IN ALKALI AND SILVER HALIDES, F. Granzer, V. Belzner, M. Bücher, P. Petrasch, and H. Potstada

185 EFFECTS OF OSCILLATING DISLOCATIONS ON THE DISTRIBUTION OF SOLUTES IN AgBr, S. E. Horan and L. M. Slifkin

220 DIRECT OBSERVATION OF THE TRACE OF ULTRASOUND PROPAGATION IN AgCl CRYSTALS BY THE "PRINT-OUT EFFECT", Takuji Kaneda

402 OPTICAL PROPERTIES OF ADDITIVELY COLORED α-Al_2O_3 CRYSTALS, M. Springis and J. Valbis

428 DISLOCATION INTERACTION WITH RADIATION-INDUCED SINGLE HALOGEN INTERSTITIALS IN KBr, K. Tanimura, T. Hagihara, T. Okada, and M. Fujiwara

INVITED PAPER

DEFECT-CONTROLLED METAL-INSULATOR TRANSITIONS*

David Adler

Department of Electrical Engineering and Computer Science
Massachusetts Institute of Technology
Cambridge, Massachusetts 02139

A large class of crystals are insulating only because of the electrostatic repulsion between two electrons simultaneously located in the vicinity of the same atom. When this repulsion is larger than the bandwidth, the metallic state is unstable. Such crystals, which include NiO and MnF_2, are called Mott insulators.

The effective gap in Mott insulators is usually large (>1eV), and the electrical conduction at room temperature is defect-controlled. The relevant defects are ordinarily vacancies resulting from non-stoichiometry, although some materials are sufficiently dirty that impurity effects predominate.

At very low temperatures, excess electrons and holes are electrostatically bound near the defect centers. However, some of these are thermally excited as the temperature is increased. Once free, they are effective in screening the electrostatic forces which brought about the insulating state in the first place. This can result in a metal-insulator transition, known as a Mott transition, at a critical temperature.

Three specific cases will be discussed in detail, NiO, EuO, and NiS_2. In pure NiO, conduction is ordinarily dominated by Ni vacancies. Each vacancy leads to the creation of two Ni^{3+} ions, each of which produces a bound hole at low temperatures. The $3d^8$ band of the nickel ions is sufficiently narrow that hole conduction in the lower but much wider oxygen 2p band generally predominates. Conduction in the narrow $3d^8$ band takes place by the phonon-assisted hopping of small polarons, and is usually observed only in the ac conductivity. The difficulties in reconciling the electrical and optical properties of NiO, especially with regard to the location of the 2p band will be discussed in detail. The resolution involves the breakdown of the one-electron approximation in this highly cor-

related material.

EuO is a magnetic semiconductor, with a very striking metal-insulator transition at the Curie temperature when there is a stoichiometric excess of europium. The predominant defect in europium-rich samples is the oxygen vacancy, leading to the formation of two Eu^{+} ions, each containing an extra electron. These electrons are bound at room temperature, but the ferromagnetic splitting of the conduction band results in metallic conduction at low temperatures from simple band-overlap effects. Oxygen-rich samples of EuO are semiconducting at all temperatures, since the Fermi energy is then pinned by the $4f^{7}$ states.

It has recently been shown that NiS_2, like NiO, is a narrow-band Mott insulator, in which conduction occurs via phonon-assisted hopping. However, the energy gap is only 0.3 eV in NiS_2. Although screening leads to a collapse of the gap at high temperatures, the material does not become metallic, due to the persistence of an activation energy in the mobility. However, the addition of 15% or more Co substituting for Ni does produce an insulator-metal transition at a critical temperature. This system may be the best present example of a Mott transition.

*Research supported by the National Science Foundation Grant #DMR72-03027A05.

EFFECT OF DIVALENT CATION IMPURITIES ON THE INTRINSIC LUMINESCENCE OF NaCl

M. Aguilar, F. Jaque and F. Agulló-López

Sección de Optica y Estructura de Sólidos
Instituto de Física del Estado Sólido (C.S.I.C.)
Universidad Autónoma de Madrid (SPAIN)

An investigation of the x-ray induced luminescence in pure, Ca and Mn doped NaCl crystals has been carried out in the range from liquid nitrogen temperature (LNT) to 300° K (RT). The dependence of the luminescence yield on the concentration and the state of aggregation of the impurity has been studied for the various emission bands.

The more important features are the following.

The intensity of the σ and π bands decreases with the amount of impurity doping. The ratio between these bands is also function of impurity doping.

At low temperature a band at 415 nm has been observed in doped samples in addition to the typical σ and π emission. Fig. (1) shows the luminescence quenching of these bands. The information obtained suggestthat this band is not a perturbed pure crystal emission but is associated to a different intrinsic transition of the V_k+e system. This transition should be forbidden in the pure crystal, becoming allowed after divalent cation doping. One reasonable possibility is the singlet emission from the lowest excited level of the exciton.

At higher temperature the σ, π and 415 nm emission bands become quenched and two bands at 310 and 330 nm are observed in pure as well as doped crystals. They markedly decrease on increasing impurity concentration in quenched doped samples and reach maximum height in the nominally pure crystals. These

bands begin to be observed at the temperature corresponding to the onset of V_k-mobility.

The thermal evolution of the 310 nm emission band for pure and Ca-doped NaCl samples is shows in Fig. (2).

The experimental results suggest that radiative recombination between an electron and a mobile V_k seems to be involved. By considering the possible connection between mobile and excited V_k centers one might tentatively attribute the 310 and 330 nm emission bands to electron recombination with excited hole levels. The $B_{2g} - B_{1g}$ or $B_{1u} - B_{2u}$ doublets are the most attractive candidates for the two excited hole levels.

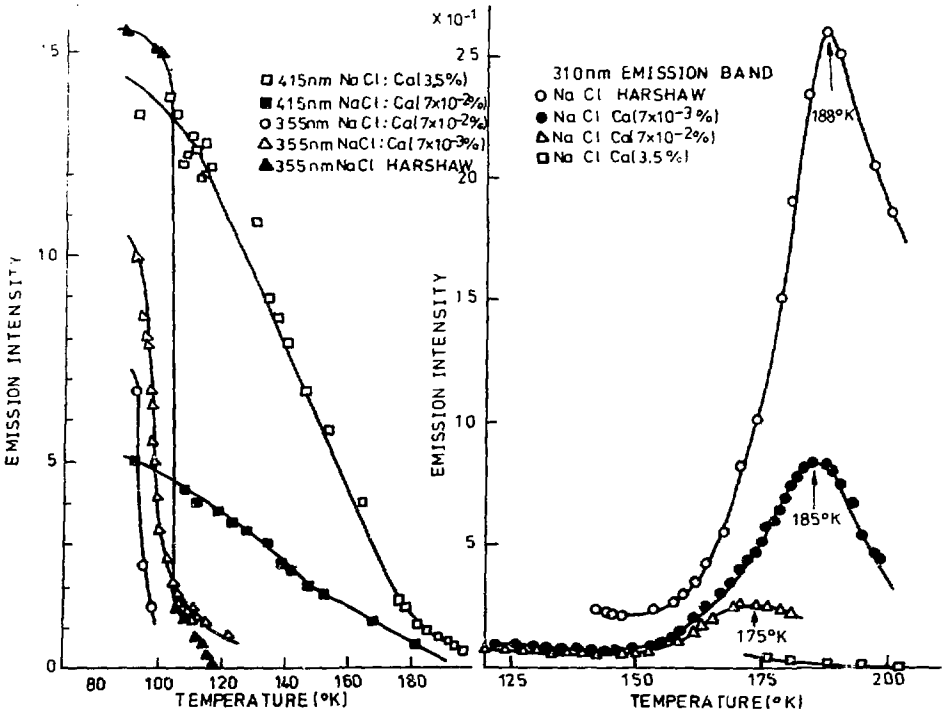

FORMATION AND ANNEALING OF HYDROGEN CENTERS IN IRRADIATED LiF CRYSTALS

Z. G. Akhvlediani
Institute of Physics, Academy of Sciences of the Georgian SSR, Tbilisi, USSR

In the early papers /1,2/ we had shown that as a result of irradiation of LiF molecular impurity OH^- decays with formation of interstitial hydrogen ions (U_1 - centers), due to infrared absorption bands in the region 2000 - 2200 cm^{-1}.

In this paper the accumulation of hydrogen as a result of irradiation of LiF at reactor temperature with thermal neutrons in the interval $5 \cdot 10^{15}$ - 10^{17} nvt (differential flux of irradiation is 1.3 10^{12} nv) is investigated.

Number of arising centers nonlinearly depends on the dose of irradiation. Fig. 1 shows that absorption coefficient at the maximum of U_1-band nonmonotonously changes with dose variation: at certain doses-1.4 10^{16} nvt and 2.2 10^{16} nvt favorable conditions for accumulation of maximum amount of hydrogen ions exist. At dose 10^{17} nvt the number of arising hydrogen centers is minimum in spite of the fact that all hydroxyl ions included in the crystal before the irradiation had been destroyed.

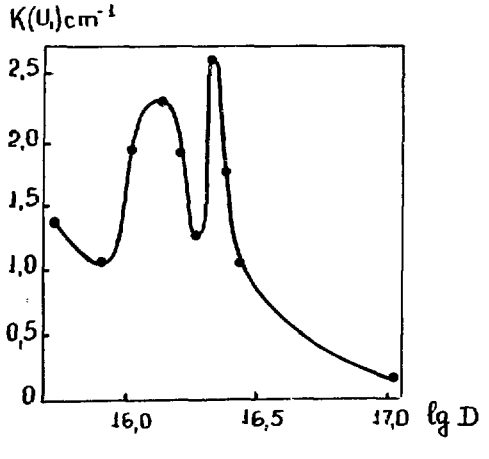

In the papers of Andronikashvili, Politov et al/3,4/ was shown, that accumulation curve of F-centers in alkali halide crystals by irradiation in reactor, has nonmonotonous character. This was explained by bleaching

effect of radiation on localized electrons during the irradiation. Results, obtained by us pointed that reactor irradiation in LiF leads to nonmonotonous dependence of OH^- ion radyolisis products on the dose. In the given case probably radiation produces bleaching effect on U_1-centers, since at dose $5 \cdot 10^{15}$ nvt all impurity OH^- ions, included in crystal are totally destroyed and the consequent effect of radiation can lead to transformation of radyolisis products themselves.

Thermal treatment of irradiated crystals causes decrease in intensity of IR bands, due to hydrogen centers: 250°C is an effective temperature for their distruction. Annealing of samples leads to restoration of hydroxyl ions, controlled by increasing of intensity of absorption band typical for stretching vibrations of OH^- group.

It must be noticed that restoration process of OH^- ions proceeds differently in crystals irradiated with different doses. At doses not more than $2 \cdot 10^{16}$ nvt crystal annealing at 300°C causes the restoration of 10-25% original quantity of hydroxyl. Almost total restoration of OH^- is observed as a result of four hour annealing of crystal at 400°C. In crystals, irradiated with higher doses, OH^- restoration process begins only at temperature 400°C. The restoration of initial amount of impurity is attained as a result of annealing at the same temperature.

References:

1. Z. G. Akhvlediani, N. G. Politov, Izvestia Akad. NauK SSSR, ser. fiz., 35, 1414, 1971.

2. N. G. Politov, Z. G. Akhvlediani, Proc. Int. Conf. Reading, 1971.

3. E. L. Andronikashvili, N. G. Politov, M. Sh.Getia, L. F. Vorozheikina, Izv. Akad. Nauk SSSR, ser. fiz., 29, 366, 1965.

4. E. L. Andronikashvili, N. G. Politov, M. G. Abramishvili, v sborn Elekt. i ionye proc. v tverd. telakh, 2, 14, 1965.

E. P. R. STUDIES OF RADIATION DAMAGE IN $CaSO_4 \cdot 2H_2O$ CRYSTALS*

A. R. Albuquerque, S. Watanabe and S. Isotani**
CPRD-AMD, Instituto de Energia Atômica, S. Paulo, Brazil

Paramagnetic resonance spectra of RT and LNT X-Ray induced free radicals have been studied in $CaSO_4 \cdot 2H_2O$ (gypsum). At room temperature four resonance lines are observed which can be grouped into two hyperfine doublets. Two magnetically equivalent complexes having different crystalline orientations have been found by angular variation studies and the paramagnetic species identified as hidroperoxy radical. At LNT the OH^- spectrum has been observed and the parameters of the effective spin Hamiltonian for the OH^- ion in gypsum have been determined.

*Research work sponsored by Comissão Nacional de Energia Nuclear.

**Instituto de Física, Universidade de São Paulo, Brazil.

A NEW F_3-CENTER TYPE IN CaF_2

R. Alcalá, V.M. Orera and J. Beamonte

Departamento de Física Fundamental. Universidad de Zaragoza.
Zaragoza (Spain).

Single crystals of additively colored CaF_2 show two absorption bands at about 375 nm and 520 nm which are due to F and F_2 centers [1], [2].

Optical bleaching in the 375 nm band at R.T. destroys some F and F_2 centers and creates some new centers with absorption bands at 680 nm and 600 nm.

The center that produces the 680 nm band has been identified by Beaumont et al. [3] as a linear F_3-center formed by three nearest neighbour F-center aligned along the <100> directions.

The 600 nm band has been sugested to be due to a square planar complex of four F-centers [4].

If the optical bleaching is performed at 160K the destruction of F and F_2 centers is accompanied by the growth of the F_4 centers and of a band at 450 nm and a shoulder at 320 nm. Warming up the sample to R.T. the 450 nm band and the 320 nm shoulder dissapear and we get the linear F_3 absorption spectrum together with the F, F_2 and F_4 bands.

The half width of the 450 nm band follows the equation $W = W_o[\coth(\hbar w_g/2kT)]^{1/2}$ with $w_g = 4.8 \times 10^{13}$ rads^{-1} and $W_o \simeq 0.12$ eV. The calculated Huang-Rish factor is $\sim$2.7, close to these found by Beaumont et al. [3] for the linear F_3-center in CaF_2 and SrF_2.

Optical bleaching with <110> polarized light in the 450 nm band at 180K induces some dichroism in this band but no dichroism is found in the 320 nm band.

If we bleach in the same conditions with <100> polarized light we find oposite dichroism in the 450 nm and 320 nm bands.

Optical bleaching with <110> polarized light in the 320 nm band at

180K does not induces any dichroism. Bleaching with <100> polarization induces oposite dichroism in the 320 nm and 450 nm bands.

From this and using the usual criteria [5] we conclude that the 450 nm band is due to a dipole oriented in the <110> direction (other posibilities are rejected after considering the possible models for the center). The 320 nm band is due to a <100> oriented dipole. The <100> and <110> dipoles are perpendicular and both transitions are due to the same center.

The <110> dichroism in the 450 nm band disapears by reorientation at 210K. On the other hand the dichroism in the <100> direction disappears at about 270K, both by reorientation and destruction of the center. Simultaneously the 680 nm band is created with a partial <100> dichroism corresponding to that of the previous 450 nm band.

All these results can be explained if we assume that the center responsible of the 450 nm and 320 nm bands is formed by three nearest-neighbour F-centers forming a rigth-angled triangle in a <100> plane.

Due to its symmetry this model of F_3-center can have transitions in the <100> and <110> directions which would explain the dichroic behaviour.

On the other hand assuming that the reorientation at 210K corresponds to vacancy jumps to a nearest-neighbour position in the <100> direction while the 270K disappearence and reorientation correspond to vacancy jumps in the <110> directions we can account both for the two diferent reorientation temperatures as well as for the appearence of a 680 nm band having the same dichroism as the 450 nm band when this is <100> oriented.

1) J. Arends. Phys. Stat. Sol. 7, 805 (1964).
2) J.H. Beaumont and W. Hayes. Proc. Roy. Soc.A 309, 41 (1969).
3) J.H. Beaumont, A.L. Harmer and W. Hayes. J. Phys. C 5, 257 (1972).
4) J.H. Beaumont, A.L. Harmer, W. Hayes and A.R.L. Spray. J. Phys. C. 5, 1489 (1972).
5) Hayes W.- "Crystals with the fluorite structure". p. 208. Clarendon Press - Oxford (1974).

POLARIZATION OF EXCITED STATE SPECTRA OF M CENTRES IN KCℓ CRYSTALS AT ROOM TEMPERATURE

A. O. H. Al-Chalabi
Physics Department, Faculty of Science
Kuwait University, Kuwait, Arabian Gulf

A very well resolved polarized excited state spectra of KCℓ crystals containing both F and M centres has been obtained using the method of modulation excitation spectrophotometry[1, 2].

Following the excitation of both F and M cnetres by an F light, chopped at low frequency (6 Hz), a temporary bleaching of the F and M bands was produced and, at the same time, new absorption bands appeared at 4400°A, 5000°A, 7100°A and 7660°A. The 7660°A band was found to disappear when the polarizer was rotated by 90°, which proves that this band belongs to a different transition. The first and second bands should belong to the triplet state of the F centre rather than to a singlet one, as they were proved to be paramagnetic[3]; and they decay with a long lifetime of the order of 50 s[4].

Due to the instantaneous excitation of both F and M centres, an interaction between these centres is expected. Accordingly, a metastable M' centres with a shorter lifetime of the order of 2.44×10^{-2} s[5], which decays, forming either centres in the triplet state or in the singlet state.

This conclusion is borne out from the model of the tunneling process[1] of an electron between two adjacent F centres or for an analogous process for the M centre. In this work it was found that the probability of the second tunneling process is proportional to the concentration of the centres.

1) A.O. Al-Chalabi, Second Europhysical Topical Conference on Lattice Defects in Ionic Crystals, (W. Berlin), Ausust 30 - September 3, 1976.
2) M.A. Slifkin and A.O. Al-Chalabi, Spectrochimica Acta, 32A, 661 (1976).
3) H. Seidel, Physics Letters 7, 27 (1963).
4) M. Ikezawa, J. Phys. Soc. Japan 19, 529 (1964).
5) F. Galluzi, U.M. Grassano and R. Rosei, Crystal Lattice Defects 1, 323 (1970).

ON THE DISPARITY OF THE PARAMETERS OF VACANCIES OBTAINED FROM SPECIFIC HEATS AND OTHER METHODS

K. Alexopoulos and P. Varotsos
Department of Physics, University of Athens, Solonos Str. 104,
Athens, Greece

The excess specific heat is usually attributed to the thermal creation of vacancies. At constant pressure it can be defined as

$$\Delta C_p = \frac{\partial(nh)}{\partial T} \quad , \tag{1}$$

where n is the concentration and h the formation enthalpy of the vacancies. Taking into account that $n = L \exp(-g/kT)$, where g is the Gibb's formation energy per vacancy, Eq (1) gives

$$\ell n\left(\frac{\Delta C_p}{L} T^2\right) = \ell n\left(\frac{h^2}{k} + T^2 \frac{\partial h}{\partial T}\right) + \frac{s}{k} - \frac{h}{kT} \tag{2}$$

It is usually assumed that $\partial h/\partial T = 0$ so that g falls linearly with T. In this case the slope of the plot of $\ell n(T^2 \Delta C_p)$ against $1/T$ gives the value of h and the intercept allows the calculation of the formation entropy s. The values of h and s determined in this way are larger than those obtained from other techniques.[1] Furthermore at very high temperatures the plot shows an upward curvature. It has been shown[2] that the temperature dependence of the elastic constants and the expansivity lead to an important increase of h and s at high temperatures, as a result of which g falls faster than linearly. One sees that methods based on the assumption that h and s are constants are valid only for restricted regions of temperature. Thus the parameters obtained from specific heats are in reality only mean values and cannot agree with values obtained from other methods at lower temperatures.

In the case of ionic crystals and at high concentrations of defects a further decrease, Δg_{LDH}, of g from linearity (and thus a further variation of h and s with the temperature) is produced by Lidiard-Debye-Hueckel interactions. In the case of silver halides Aboagye and Friauf[3] have found that a further decrease, Δg_{extra}, beyond Δg_{LDH} is necessary in order to describe

quantitatively the curvature of the conductivity plot. Batra and Slifkin[4] by comparing diffusion with conductivity data indicated that Δg_{extra} is mainly due to an excessive decrease of the formation free energy. One therefore can use the values h, s and $\Delta g_{LDH} + \Delta g_{extra}$ given in Ref. 3 in order to calculate the correct value of g at each temperature.

This allows the calculation of $s = -\partial g/\partial T$ and $h = g - T\,\partial g/\partial T$ as a function of temperature. Inserting these values into Eq. (2) one can calculate $\ell n(T^2 \Delta C_p)$ vs. $1/T$ and obtain a straight line with an upward curvature. The agreement between the experimental[5] and the calculated values of ΔC_p is within 2% in the higher temperature region while at lower temperatures the calculated values are too large by 20%. This difference can be attributed to experimental uncertainty resulting from the extrapolation of C_p^o of the vacancy-free lattice.

If the present method of calculating ΔC_p proves to be efficient, it can be used to determine C_p^o by subtracting ΔC_p from the experimental C_p.

References

1. D. M. Brudny, J. Phys. Chem. Sol. 37, 1109 (1976).
2. P. Varotsos and K. Alexopoulos, Phys. Rev. B 15, 4111 (1977); J. Phys. Chem. Sol. (to be published).
3. J. K. Aboagye and R. J. Friauf, Phys. Rev. B 11, 1654 (1975).
4. A. Batra and L. Slifkin, Phys. Rev. B 12, 3473 (1975).
5. K. Kobayashi, Phys. Rev. 85, 150 (1952).

DIELECTRIC RELAXATION IN RARE-EARTH AND ALKALI METAL DOPED ALKALINE EARTH FLUORIDES*+

CARL ANDEEN and DONALD SCHUELE, Case Western Reserve Univ., Cleveland, Ohio
JOHN FONTANELLA, RICHARD L. JOHNSTON, and DONALD TREACY, United States Naval Academy, Annapolis, Md.

The complex dielectric constant has been measured at five audio frequencies over the temperature range 5.5-400K for a variety of rare-earth and alkali metal doped alkaline earth fluorides.

Fourteen rare-earths and yttrium have been studied in calcium fluoride at a nominal concentration of 0.1 mol-%. Thirteen of the rare-earths have also been studied at 1.0 mol-%. Five independent relaxations are observed and it is concluded that at least three are cluster-associated. The activation energy for one of the three cluster-associated relaxations is found to depend strongly on the nature of the rare-earth ion and varies approximately linearly with the radius of the rare-earth ion between values of about 0.4 and 0.9 ev. The other two cluster-associated relaxations do not exist for rare-earths larger than europium in the as-received samples. Various cluster models such as dimer ions and trimers are proposed in an attempt to explain the results.

Four rare-earths in strontium fluoride in two concentrations 0.1 and 1.0 mol-% were also studied. Erbium was also studied at a nominal concentration of 0.1 mol-%. The usual Type I and Type II dipoles are found to continue increasing in strength up to the highest concentration studied. The relaxations are not very Debye-like. Consequently, the actual activation energies as determined in the present experiment are significantly higher (on the order of 0.1 ev) than those reported by other methods. A third relaxation is found only in the highest concentration samples and has a low activation energy similar to that for one of the cluster-associated relaxations observed in calcium fluoride. An analogous relaxation is not found in erbium doped barium fluoride to concentrations of 1.0 mol-%.

Finally, results for 0.1 mol-% of lithium, sodium, and potassium in calcium fluoride were obtained. The interesting feature of that work is

that the activation energy for the principal relaxation in these materials does not vary monotonically with the size of the alkali metal ion. In order of increasing activation energy, the dopants are potassium, lithium, and sodium. Further work on these materials is necessary, however, since the potassium doped sample was obtained from a source different from the other two.

†All of the rare-earth doped alkaline earth fluorides were obtained from Optovac, Inc., North Brookfield, Massachusetts. Lithium and sodium doped calcium fluoride were obtained from Research Crystals, Duncanville, Texas. Samples of potassium doped calcium fluoride were kindly provided by V. M. Carr and A. V. Chadwick of the University of Kent at Canterbury.

*Work supported by the Army Research Office.

SOME NEW ASPECTS OF THE THERMAL F - Z_2 CENTER CONVERSION process in KCl:Sr crystals

Ch. Anderson and H.J. Paus
Physikal. Institut Teil 2, Universität Stuttgart, Germany

Relying on the experimental results of several investigators /1,2/ one believes that F and Z_2 centers in Sr-doped KCl crystals find themselves in a thermal equilibrium. The usuable temperature range for this process (roughly 70°C to 200°C) is too small to get any decision from the Arrhenius-plot of the equilibrium reaction concerning the number of F centers used for the formation of one Z_2 center.

The diamagnetism of the Z_2 center favours the opinion that two F centers are combined with one Sr-complex to form a Z_2 center /3/. The process should proceed in two steps, the two F centers being incorporated successively forming some sort of intermediate center with only one F center. An absorption band between the F and the Z_2 bands, called Z_5, was tentatively attributed to this intermediate center. The Z_5 band, known since a long time /4/, was entirely ignored in the consideration of the F - Z_2 center equilibrium and in the interpretation of the experimental results. Fig. 1 shows the absorption spectrum of the F/Z_5/Z_2 center system in three stages during the thermal F - Z_2 conversion: The Z_5 band is clearly visible. Further experiments /5/ reveal however that this thermally created Z_5 center is another kind of Z_2 center. According to our present knowledge only the Z_1 center can serve as the wanted intermediate center: Z_1 is formed as the first reaction product in the optical F - Z_2 conversion /6/. The restricted resolution due to the broad bands prevents the detection of Z_1 in the thermal conversion process.

The existence of a thermal F - Z_2 center equilibrium as reported in the literature is not confirmed by our experiments. In crystals doped with various impurity concentrations such an equilibrium could never be established (fig. 2): in the quench-

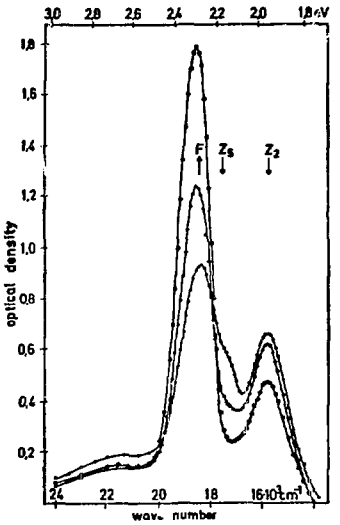

Fig. 1

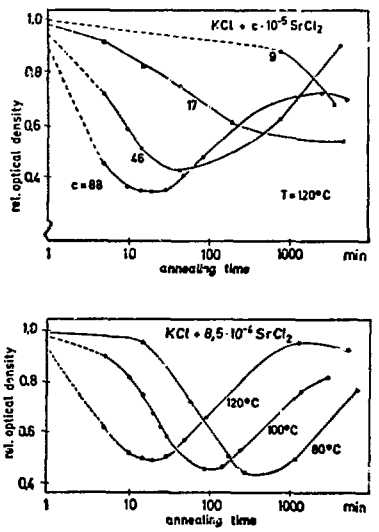

Fig. 2

ed crystals the F absorption first decreases during annealing due to the Z_2 formation. After passing through a minimum it increases again until almost all initial F centers are restored and almost all Z_2 centers are destroyed. The effect depends on the impurity concentration as well as on the annealing temperature. This throughs doubt on all activation energy data discussed so far for this process. The aggregation of the impurity vacancy complexes,can seemingly not be neglected any more and must be taken into consideration.

/1/P.Camagni, S.Ceresara, G.Chiarotti Phys.Rev.118,1226 (1960)
/2/G.Wolfram, V.Witt phys.stat.sol. 22, 245 (1967)
/3/K.H.Umbach, H.J.Paus 1974 Int.Col.Cent.Conf.Sendai,abstr. 154
/4/K.Kojima J.Phys.Soc.Jap.19, 868 (1964)
/5/ See abstract by H. C. Hilber and H. J. Paus, this conference.
/6/H.C.Hilber and H.J.Paus to be published

ION IMPLANTATION DAMAGE IN CRYSTALLINE QUARTZ AND FUSED SILICA*

G. W. Arnold
Sandia Laboratories, Albuquerque, New Mexico 87115

Controlled damage introduced in crystalline quartz and fused silica by ion implantation was studied through the use of UV-visible absorption spectroscopy and infrared reflection spectroscopy (IRS). Ion damage produces changes in the intensity, position, and number of the Si-O vibrational modes observed in the IRS spectra. Ion ranges in crystalline quartz were directly measured from transmission interference fringes.

The IRS spectra of quartz and fused silica are dominated by the Si-O stretching vibration at ~1130 cm^{-1}. Upon implantation this peak broadens and shifts to lower energy and a new peak develops at ~1000 cm^{-1} for both quartz and fused silica. For crystalline quartz we have also observed, for the first time, the growth of a second peak at about 830 cm^{-1} which is tentatively attributed to two nonbridging silicon-oxygen bonds in the SiO_4 tetrahedra. When two nonbridging silicon-oxygen bonds are present in the Si-O tetrahedron the local symmetry is expected[1] to change from T_d to C_{2V}, allowing the 830 cm^{-1} band to appear. The growth of both bands (1000 cm^{-1} and 830 cm^{-1}) correlates with energy into atomic processes. The Si-O band frequency shift in fused silica has been attributed[2] to a decrease in the average Si-O bond angle. For crystalline quartz, however, lattice expansion occurs upon implantation and the Si-O bond angle should increase.

Isochronal annealing of implanted fused silica demonstrated that the IRS spectrum was not affected until a temperature of 600°C was reached. For 900°C anneals the spectra were identical to those for unimplanted fused silica. For crystalline quartz, heavy-ion implantation gave IRS spectra similar

*This work was supported by the United States Energy Research and Development Administration (ERDA) under Contract AT(29-1)789.

to those of implanted fused silica. Annealing shifted the Si-O stretching peak back to its original position and removed the 830 cm^{-1} band at temperatures between 600°-900°C, but did not remove the implantation-induced change in the shape of the Si-O envelope or the 1000 cm^{-1} band.

The thickness of the modified layer in quartz was determined by measuring transmission interference fringes and using the known value[3] for the refractive index of ion-implanted quartz under saturation conditions. For 3.52×10^{16} 200 keV A^{++}/cm^2, the measured thickness of the expanded layer is ~6850 Å whereas calculations[4] give a projected range of R_p = 4110 Å and a spread of ΔR_p = 996 Å or $R_p + \Delta R_p$ = 5106 Å. The ranges measured for Xe^+, A^+, Al^+, and Kr^+ implants were also larger than predicted. Backscattering measurements[5] of the ion range for SiO_2 films showed a discrepancy between theory and experiment for those amorphous targets but not as large as for the present measurements on crystalline material. The interference fringe system for quartz was not altered by isochronal annealing to temperatures of 900°C. For both quartz and fused silica, however, the UV spectral features (E_1'- and B_2- absorption bands) annealed out in a stage near 500°C.

1. D. M. Sander, W. B. Person, and L. L. Hench, Appl. Spectroscopy 28, 247 (1974).
2. I. Simon in Modern Aspects of the Vitreous State, Vol. 1, edited by J. D. Mackenzie (Butterworths, London, 1960), p. 120.
3. W. Primak, Phys. Rev. 14B, 4679 (1976).
4. D. K. Brice (unpublished results).
5. W. K. Chu, B. L. Crowder, J. W. Mayer, and J. F. Ziegler, Appl. Phys. Lett. 22, 490 (1973).

EMISSION SPECTRA OF KI:Tl AT LOW TEMPERATURE UNDER HIGH PRESSURE

K. Asami, S. Masunaga* and M. Ishiguro
Institute of Scientific and Industrial Research,
Osaka University, Osaka Japan
*Kyushu Institute of Technology, Kitakyushu-shi

Most of the luminescence experiments under high pressure have been performed at room temperature, for the high pressure experiments at liquid helium temperature are accompanied with many technical difficulties. Recently, we made a high pressure cell for the optical measurements at liquid helium temperature and observed the absorption and emission spectra at liquid helium temperature under hydrostatic pressure (1~20000 bars).

Figure 1 shows emission spectra produced by the irradiation in the C absorption band. At atmospheric pressure, the emission spectra at 1.5 K consists of the A_T (A_X), B and C emission bands (we call the emission bands due to the reverse process of the A, B and C absorption A_T (A_X), B and C emission bands, respectively) and a small band peaking at 304 nm. As pressure rises, the C band and the band at 304 nm decrease, the B band remains almost unchanged, the A_T band drastically decreases, and the A_X band becomes broad and weak. The decrease of the total intensity of the A_T, A_X, B, C and 304 nm bands seems to be pressure effect of the oscillator strength of the C absorption band; the C absorption band decreases with increasing pressure. The coupling with T_{2g}= mode lattice vibration, which is enhanced by the applied pressure, causes a mixing of the C and B states, resulting in the decrease of the C absorption

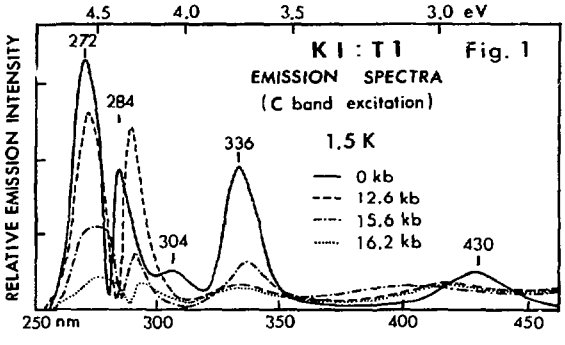

Fig. 1

and the increase of the B absorption band. No decrease of the B emission band contrary to the other bands will be attributed to the increase of the probability of the transition from the B state to the ground state, which is infered from the increase of the B absorption band by the applied pressure, and also to the decrease in the transition from the C- and B-APES (adiabatic potential energy surface) to the A-APES by the phonon process infered from the drastic decrease of the A_T band. The drastic decrease of the A_T emission will be due to the increase of the hump from the C- and B= APES to the A-APES similarly to the case of the $A_X \rightarrow A_T$ conversion by the applied pressure at room temperature. At 15.6 kbars where the phase transition NaCl→ CsCl begins to occure, the A_T emission recovers its intensity relatively to the other bands. It should be noticed that upon the phase transition a sapphire window of the pressure cell is cracked, resulting in the decrease of the emission light through the sapphire window, so we cannot compare mutually the emission intensity before and after the phase transition.

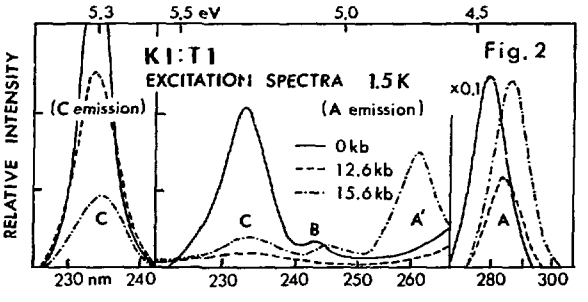

Figure 2 shows an excitation spectra for the C and A emission bands. From the former, we can find that the peak shift of the C absorption band with pressure is very small and besides there is no large shift before and after the phase transition, while, from the latter, the peak shift of the A absorption band is considerably large and upon the phase change there appears one more band (we call A′ band) at the shorter wavelength side of the A band ($\sim$ 260 nm). Moreover, we can observe that the excitation in the A′ band produces two emission bands near the A_T and A_X emission bands, respectively. These emission bands are very similar to those produced by the excitation in the A band. On the above emission we will report more details in the near future.

COLLOID CENTERS IN SILVER CHLORIDE INDUCED BY REACTOR IRRADIATION AT LOW TEMPERATURE

KOZO ATOBE, MORITAMI OKADA and MASUO NAKAGAWA

Research Reactor Institute, Kyoto University,
Kumatori-cho, Sennan-gun, Osaka, 590-04, Japan

Single crystals of undoped AgCl have been colored by reactor neutrons at 20K. The samples were irradiated with fast neutrons($E>0.1$MeV) in the range of $1.1 \times 10^{15} \sim 3.8 \times 10^{16}$ n/cm^2 and optical absorption measurements of these samples were carried out. In the temperature range from 77K to 710K, the isochronal changes of the optical absorption were investigated by the pulse-annealing method, where the samples were kept at desired temperatures for 3 min.

After irradiation, a broad absorption band(S-band) near the fundamental absorption edge was observed at 4.2K and 77K. The intensity and shape of the S-band are not changed by measured temperatures. No absorption band appeared in the region from 400 to 900 nm except the S-band. The intensity of the S-band changes during the thermal annealing process as shown in Fig.1. By warming the sample, the S-band continued to decrease as seen in the curve b~d. At the annealing stage of 500K, the S-band was disappeared almost completely, whereas a very intense band(L-band) was newly appeared at about 530 nm. It is also confirmed that the peak position and the half-width of the L-band are independent on temperatures lower than 500K. At higher temperatures than 500K, the L-band is broadend and the peak position of the band shifts to longer wavelength. In the process, it is interesting to notice that the L-band bleaches with the increase of annealing temperature, while a broad shoulder band(S-band) appears again at above 690K.

From these thermal properties and the analysis of the band shape, it is possible to attribute the S and L-band to two types of colloidal silver centers (S and L-colloids).[1] According to the calculation for some colloid bands corresponding to each diameter of the silver colloids[2], the diameter of the L-colloid are estimated as about 300Å. While, the minimum size of the stable S-colloid is not yet certain. The thermal annealing indicate the possibility that the coagulation of S-colloids results in a formation of L-colloid and also the decomposition of L-colloid produces again the dispersion of S-colloids with increasing temperature.

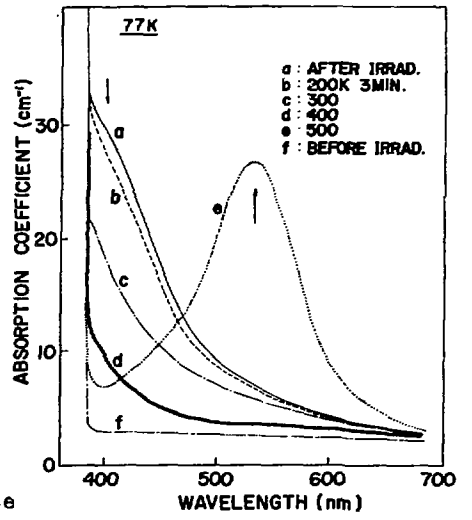

Fig.1 Absorption spectra of undoped AgCl before and just after the reactor irradiation are shown by curve f) and a). Behavior of the absorption spectra versus annealing temperatures; b)~e).

On the other hand, the effect of γ-ray irradiation was also studied at 77K to a dose of 2.3×10^7R, but any band was not observed by the same procedure of the annealing. It seems certainly that the reactor neutron irradiation enhances effectively to produce S-colloids in AgCl crystal at low temperature(20K).

(1) K.Atobe, M.Okada and M.Nakagawa, Annu.Rept.Res. Reactor Inst.Kyoto Univ. in the press.

(2) E.Rohloff, Z.Phys. Bd 132(1952)643.

MAGNETIC CIRCULAR DICHROIC EFFECTS IN THE LUMINESCENCE AND ELECTRON-SPIN MEMORY IN THE OPTICAL-PUMPING CYCLE OF F CENTERS IN ALKALI HALIDES

G. Baldacchini† (Laboratori Nazionali del CNEN, 00044 Frascati, Italy), U. M. Grassano and A. Tanga (Istituto di Fisica, Università di Roma and Gruppo Nazionale di Struttura della Materia del CNR, Roma, Italy).

Recently we have measured small but significant magnetic circular dichroic (MCD) effects in the luminescence of F centers in KI, KBr, and KCl.[1] The knowledge of such effects, especially the "paramagnetic" effect, so called because it is associated with a non-zero electron spin polarization in the relaxed excited state (RES), are of the uppermost interest in order to clarify the exact nature of the RES. However, the exact value of the spin polarization in the RES, P_ρ, has to be known a priori in order to calculate from the previous experimental data the parameters characterizing the RES. The value of P_ρ can be inferred by solving the rate equations which govern the optical-pumping cycle of the F center.[2] However, in the previous rate equations a central role is played by the spin mixing parameter, ε, which takes in account the slight loss of electron spin memory exibited by the F center during the whole optical cycle. Lately, it was suggested[3] that the choice of a unique value of ε can be justified only in special cases. In general, it is necessary to introduce two spin mixing parameters ε^+ and ε^- for the two Zeeman levels in absorption.

Disregarding higher harmonics we have solved the new rate equations obtained from the old ones[2] by introducing ε^+ and ε^- at the place of ε. The values found for P_ρ are slightly different in the region of interest from those given previously.[1] However, the new solutions clarify completely some experimental results, which we could not explain up to now using the old solutions. In addition, we have been able to measure the value of the differential spin mixing effect, more exactly the quantity $(\varepsilon^- - \varepsilon^+)/(\varepsilon^- + \varepsilon^+)$. The result in KBr agrees fairly well with that given by other authors.[3]

In conclusion the introduction of two spin mixing parameters in the optical cycle of the F center enables us to explain almost every aspect of the MCD experiments, which play an important role in the physics of the RES. The main results presented previously[1] are changed only so slightly that they don't need appreciable corrections. As a consequence, the values of the spin-lattice relaxation time calculated by the small variation of the "paramagnetic" effect at high magnetic fields are substantially valid. Indeed a confirmation of their validity was obtained[4] by using a different experimental method.

†Present address Physics Department, University of Utah, Salt Lake City, Utah 84112, where part of this work was done.

[1]G. Baldacchini, U.M. Grassano and A. Tanga, J. Phys. (Paris) C7-154 (1976), Sol. State Commun. 21, 225 (1977), and paper submitted to Phys. Rev.

[2]L. F. Mollenauer and S. Pan, Phys. Rev. B 6, 772 (1972).

[3]A. Winnacker, K. E. Mauser, and B. Niesent, Z. Phys. B 26, 97 (1977); Z. Phys. B 26, 107 (1977).

[4]G. Baldacchini, U.M. Grassano, and A. Tanga, not yet published.

F-CENTERS WITHOUT RELAXED EXCITED STATES ?

II) F-CENTER EMISSION IN NaI AND NaBr

Giuseppe Baldacchini* and Fritz Luty
Physics Department, University of Utah, Salt Lake City, Utah 84112

According to the Bartram-Stoneham criterion discussed in Part I,[1] F-centers in NaI and NaBr should not exhibit luminescence due to a radiationless cross-over transition in the optical cycle. It should be pointed out first, that this condition would not hold for an electron, retrapped by an ionized F-center (a process which works by capture into the RES, followed by the normal radiative transition into the ground state). Due to the very small energy difference ΔE between ionized and relaxed excited state, the cross-over point to the ground state curve would lie in this process at higher energies, so that F-luminescence under electron capture by an empty vacancy could occur.

We have studied the infrared emission of pure F center systems in NaI under variable laser excitation in the F band. (Here, again, it is important to eliminate the perturbed F-centers present in impure material as they give rise to different emission properties). Spurious emissions from F-aggregate centers are not a problem in NaI, because -- different from other alkali-halides -- light irradiation around RT does not produce any aggregates (tested in both absorption and emission), but only a slow F → U back-conversion.

Pure F-center systems in NaI give rise -- in a well reproducible way -- to weak IR luminescence, consisting of two components:

A) An emission at 2.2μ of 0.2eV width, with an excitation-spectrum following the F-band, and a low quantum efficiency ($<10^{-2}$), which decreases rapidly under temperature increase.

B) An emission at 1.63μ of 0.1eV width, with an excitation-spectrum following roughly the F' band. Its intensity is rather constant to ~100K, and decreases between 100 and 300K gradually by 2 orders of magnitude.

Both luminescence are intrinsically connected with the pure F and F'

system and depend on the dynamic equilibrium of both centers under irradiation. Double beam excitation experiments with a (DC) pump-beam shifting the F:F' equilibrium, and an (AC) probe-beam exciting the luminescence, are under way to sort out and definitely attribute the two emissions. It is highly likely that the component at 2.2μ is the F luminescence, while the narrow 1.63μ emission is due to F' center excitation. Clear results on this question are expected to be presented.

The main results from Part I and II of this work can be summarized and understood as follows:

1) The F → F' kinetics shows clearly, that essentially all optically excited F centers reach the RES, from which they can be ionized by thermal activation (up to full efficiency!) to form F' centers. The measured activation energy (0.04eV) fits well the value for the depth of the RES (0.048eV), predicted by Spinolo's ε^{-2} law. The measured pre-exponential factor of the F → F' kinetics indicates a low-temperature RES lifetime of about 10^{-9} sec.
2) The observation of an F luminescence shows again, that the excited centers reach the RES. The low quantum-efficiency of this emission ($<10^{-2}$) and the above mentioned short life-time give evidence for a strong non-radiative transfer from the RES to the ground-state with a rate of about 10^{9} sec^{-1}.

In conclusion: Strong radiationless de-excitation processes do occur in systems like NaI with very strong phonon-coupling -- however, not during relaxation by a rapid cross-over transition, but rather after relaxation in the RES by a rate-process, which competes with and strongly reduces the luminescence and shortens the RES lifetime.

Similar luminescence measurements are running on F-centers in NaBr, for which a low quantum efficiency emission has already been detected around 1.7μ. Results of this investigation will be reported.

*On leave from and partially supported by Laboratori Nazionali del CNEN, Frascati, Italy.

Work supported by NSF grant #DMR-74-13870-A02.

SPECTROSCOPIC STUDIES OF CONDUCTION PLANE DEFECTS IN SODIUM β-ALUMINA

R. C. Barklie, K. P. O'Donnell and B. Henderson
Physical Laboratory, Trinity College,
Dublin 2, Ireland.

E.S.R. and optical results are presented of measurements of defects produced in sodium β-alumina by irradiation with U.V. light, X-rays and electrons.

An E.S.R. spectrum showing hyperfine structure due to interaction with two equivalent ^{27}Al nuclei can be fitted to an axially symmetric spin Hamiltonian, the principal axis of which is parallel to the crystal c-axis. This spectrum strongly suggests a defect located at the bridging oxygen site in the conduction plane. The decay of this spectrum at room temperature has been compared with that of a strongly polarised optical band at 300 nm produced during irradiation to show that this band also originates at the bridging oxygen site. The ease of production of these centres suggests the presence of vacant oxygen sites in the conduction plane prior to irradiation.

VIBRATIONAL COUPLING IN THE RELAXED EXCITED STATE OF THE F CENTER IN KCl*

R. H. Bartram and J. M. Dekle
Physics Department and Institute of Materials Science,
University of Connecticut
Storrs, Conn. 06268, U.S.A.

Ham's vibronic model for the relaxed excited state of the F center involves the coupling of nearly degenerate 2s and 2p electronic states by odd-parity (Γ_4^-) vibrational modes.[1] By comparison with a variety of experiments, Ham and Grevsmühl[2] have established that the coupling is weak, and have inferred values of two parameters associated with the model: the 2s-2p coupling energy E_G and the energy separation of the uncoupled electronic states $|E_{sp}|$, where the 2s state is presumed to lie lower. In KCl, these parameters have the values $E_G \sim 0.014$ eV and $|E_{sp}| \sim 0.09$ eV.

The electron-lattice interaction actually involves very many modes, but it can be represented approximately in terms of a single set of modes with an effective coupling constant and effective frequency.[3] Values of the coupling energy E_G for KCl have been calculated with wave functions of the following form:

$$\psi_{1s} = A(1 + \alpha r)e^{-\alpha r} \quad ,$$
$$\psi_{2s} = B(1 + \alpha r)e^{-\alpha r} + Cr^2 e^{-\zeta r} \quad ,$$
$$\psi_{2p} = Dre^{-\zeta r} Y_1^m(\theta,\phi) \quad ,$$

where the coefficients A - D are determined by orthonormality. Several values of α were chosen, corresponding to a compact ground state. These wave functions were used to calculate the forces associated with coupling to the first two shells of ions surrounding the defect, which were then employed in conjunction with a Green's function matrix derived from an empirically-parametrized breathing-shell model of the lattice dynamics.[4] The contributions to E_G from forces on the remaining shells of ions were approximated by a continuum model based on the Fröhlich Hamiltonian, which involved coupling only to longitudinal optical modes.

The coupling energy E_G was calculated as a function of the exponential parameter ζ, which was assumed to have the same value in the 2s and 2p wavefunctions. For $\zeta \sim 0.4$ a.u., the value predicted by a rigid-lattice point-ion calculation, coupling to the first two shells of ions predominates, and one obtains a value $E_G \sim 0.2$ eV, an order of magnitude too large. Furthermore, the effective frequency of the Γ_4^- mode is about one-third of ω_{LO}, a value incompatible with the analysis of Ham and Grevsmühl.[2] A much more diffuse wavefunction with $\zeta \sim 0.07$ a.u., comparable to that inferred by Mollenauer and Baldacchini,[5] is required in order to obtain $E_G \sim 0.014$ eV. In this range of ζ, coupling to longitudinal optical modes via interactions beyond the first two shells of ions predominates.

Coupling of the 2p functions by modes of Γ_3^+ and Γ_5^+ symmetry was also calculated as a function of ζ. The possible role of this coupling in reducing the effective 2s - 2p coupling by Γ_4^- modes was investigated, but it does not appear to be significant. Preliminary point-ion and pseudopotential calculations which incorporate coupling to modes of Γ_1^+ symmetry also appear to support a diffuse wavefunction for the relaxed excited state, in agreement with the conclusions of prior investigators.[5,6]

*Supported by NSF Grant No. DMR 74-02604.

[1] F. S. Ham, Phys. Rev. B 8, 2926 (1973).
[2] F. S. Ham and U. Grevsmühl, Phys. Rev. B 8, 2945 (1973).
[3] M. C. M. O'Brien, J. Phys. C: Solid State Phys. 5, 2045 (1972).
[4] J. R. D. Copley, R. W. Macpherson and T. Timusk, Phys. Rev. 182, 965 (1969).
[5] L. F. Mollenauer and G. Baldacchini, Phys. Rev. Letters 29, 465 (1972).
[6] R. F. Wood and U. Öpik, Phys. Rev. 179, 783 (1969).

RESONANCE RAMAN SCATTERING FROM METASTABLE OXYGEN SPECIES IN IRRADIATED $NaClO_3$[1]

J. B. Bates
Solid State Division, Oak Ridge National Laboratory
Oak Ridge, Tennessee 37830

A variety of stable and metastable molecules and molecular ions are produced in alkali-metal chlorates by the action of ionizing radiation. In $NaClO_3$ irradiated at 300 K, these include the ozonide ion, O_3^-, and a recently discovered[2,3] molecular defect which has been identified by resonance Raman scattering as a metastable oxygen species, denoted by O_2^*. The resonance Raman effect observed with O_2^* implies that this species has an allowed electronic transition in the visible region. However, the lowest allowed transition of O_2, $^3\Sigma_g^- \rightarrow {}^3\Sigma_u^-$, is centered at about 200 nm. Although it appears to be stable idenfinitely at temperatures below 77 K, O_2^* decays at room temperature with a half-life of 1.4 days. A weakly bound complex, $[X,O_2]$, of oxygen with another molecule or molecular ion, X, has been proposed[3] as a model for O_2^*. The resonance Raman effect may occur from vibronic interaction between the O-O stretching motion of O_2 and an electronic transition of X. The decomposition of the complex, $[X,O_2] \rightarrow X + O_2$ could account for the apparent instability. The excitation profile determined for O_2^* indicates an optical band which is apparently coincident with the band[4] of O_3^-. In order to probe the possibility of complex formation with O_3^- and to further test the proposed model of O_2^*, the temperature dependence and the kinetic behavior of the resonance Raman scattering from O_2^* and O_3^- have been investigated.

Spectra of a freshly irradiated single crystal of $NaClO_3$ recorded at 15 K show that ozonide ions are produced on at least three non-equivalent lattice sites, as evidenced by the appearance of three components in the higher overtone regions ($n \geq 3$) of the symmetric stretching mode, ν_1. It was observed that the intensity of the lowest frequency member of each set of $n\nu_1$ components increased dramatically as the sample temperature increased from 35 to 55 K. For example, the intensity of the low frequency component of $2\nu_1$ increased by more than a factor of two over this interval. However, the $^2B_1 \rightarrow {}^2A_2$ transition of O_3^- to which ν_1 is coupled[4] showed no shift nor were any apparent changes observed in the position or width of the vibronic

fine structure lines of this transition between 10 and 70 K. The observed intensity change of $2\nu_1$ has been interpreted semi-quantitatively by using a recent theoretical development in the effects of line broadening on resonance Raman scattering.[5] Using the displaced oscillator model and the Condon approximation, an expression for the Raman scattering intensity for $2\nu_1$ of O_3^-, which included contributions from intramolecular broadening and damping from molecule-lattice interactions, was derived from this theory.

Virtually no changes were observed in the intensity of the bands due to the fundamental or overtones of O_2^* over the temperature interval investigated. It appears, therefore, that there is no association between oxygen and those ozonide ions which exhibit the temperature dependent Raman scattering. However, the intensity of the high frequency components of the O_3^- overtones, which show only a small temperature dependent intensity change, decays with time at 300 K according to a 1st order process, and a corresponding increase in the intensity of the low frequency components with time was also observed. These results provide some evidence that the O_3^- ions which produce the high frequency Raman components are associated with oxygen to form the complex, $[O_3^-, O_2]$.

---

1. Research sponsored by the Energy Research and Development Administration under contract with Union Carbide Corporation.

2. J. B. Bates and H. D. Stidham, Chem. Phys. Lett. 37, 20 (1976).

3. J. B. Bates and H. D. Stidham, J. Chem. Phys. 65, 3901 (1976).

4. J. B. Bates and J. C. Pigg, J. Chem. Phys. 62, 4227 (1975).

5. A. P. Penner and W. Siebrand, Chem. Phys. Lett. 39, 11 (1976).

RAMAN SCATTERING FROM F CENTERS IN CaO*

J. B. Bates and R. F. Wood
Solid State Division, Oak Ridge National Laboratory
Oak Ridge, Tennessee 37830, U.S.A.

First-order Raman scattering is formally forbidden in crystals with the rocksalt structure, such as the alkaline-earth oxides. However, the presence of substitutional impurities or defects destroys the translational symmetry, and first-order scattering from modes involving displacements of the ions of the host lattice in the vicinity of the defect can be observed. The F center in CaO consists of two electrons trapped at an O^{2-} ion vacancy. The optical properties and electronic structure of this defect have been well-characterized in previous experimental[1-3] and theoretical studies.[4,5] The absorption band is centered at 3.1 eV and has a half-width of approximately 0.5 eV; it arises from an allowed transition, $^1A_{1u} \rightarrow {}^1T_{1u}$.

Raman spectra of additively colored CaO crystals containing F centers were recorded at 10°K using exciting lines at 457.9, 488.0, and 514.5 nm. The relative intensities of the spectral features and especially sharp structure at 330 and 315 cm^{-1} are dependent on the wavelength of the exciting line. This dependence may arise from a resonance Raman effect, since the higher energy exciting lines fall well within the broad optical band of the $^1A_{1g} \rightarrow {}^1T_{1u}$ transition. Although the 514.5 nm line is within the wings of the optical band, the spectra obtained with this line are in agreement with the calculated spectra, which do not include resonance.

Theoretical calculations for the off-resonance case were carried out using methods described elsewhere.[6] The perfect crystal eigenfrequencies and eigenvectors were generated using the shell model data of Saunderson and Peckham.[7] Reasonably good agreement with the experimental data was achieved with the various symmetry projections of the perfect crystal density of states, thus suggesting that there are only small force constant changes when the F center replaces an O^{2-} ion. The calculations

showed that it is necessary to include polarizability derivatives for both first (Ca^{2+}) and second (O^{2-}) neighbor ions of the defect in order to fit the experimental data at all frequencies.

---

*Research sponsored by ERDA under contract with Union Carbide Corporation.

1. W. C. Ward and E. B. Hensley, Phys. Rev. 175, 1230 (1968).

2. B. Henderson, Y. Chen, and W. A. Sibley, Phys. Rev. B 6, 4060 (1972).

3. J. B. Bates and R. F. Wood, Phys. Letters 49A, 389 (1974); Solid State Commun. 17, 201 (1975).

4. R. F. Wood and T. M. Wilson, Solid State Commun. 16, 545 (1975).

5. R. F. Wood and T. M. Wilson, Phys. Rev. B 15, 3700 (1977).

6. R. F. Wood, *Methods in Computational Physics*, Vol. 15, (1976), p. 119.

7. D. H. Saunderson and G. E. Peckham, J. Phys. C: Solid State Phys. 4, 2009 (1971).

FORMATION OF RADIATION DEFECTS IN LaF_3-TYPE CRYSTALS

S.Kh.Batygov, V.A.Myzina, V.V.Osiko

Lebedev Institute of Physics, Moscow, USSR

In spite of having identical crystal lattices the single crystals of La F_3 homologous series (LaF_3, CeF_3, PrF_3, NdF_3) behave differently under γ-irradiation at room temperature. While undoped LaF_3 and NdF_3 readily form electron colour centres, that gives rise to intensive absorption in the 200-600 nm region, CeF_3 and, to a certain extent, PrF_3 are insensitive to γ-irradiation. Also, Eu^{3+}, Yb^{3+}, and Sm^{3+} impurity ions are reduced to divalent state at γ- irradiation in LaF_3 but are not reduced in CeF_3. These phenomena are explained by the lack of hole traps in CeF_3 and PrF_3. Because of low Ce^{3+} and Pr^{3+} ionization potentials these ions form high-lying valence bands that overlap the local levels at the bottom of the gap.

The study of mixed LaF_3-CeF_3 crystals doped with Sm^{3+} has shown that low CeF_3 concentration (up to 0.3-1.0%) increases the Sm^{2+} yield in LaF_3. This is in accord with our previous studies on the calcium fluoride crystals. It is concluded that Ce^{3+} and other ions with low ionisation potential, when added in small amounts, form deep hole traps favouring the formation of electron colour centres, and vice versa, when the concentration of these impurities becomes high enough for their levels to form the band they prevent from electron capture in defects.

COLOR CENTER CRYSTALS AS ACTIVE MATERIAL FOR CW INFRARED LASERS

R. Beigang, G. Litfin, H. Welling
Inst. f. Angew. Physik, TU Hannover
3000 Hannover, Fed. Rep. Germany

Certain color centers in alkali halide crystals have made possible tunable cw infrared lasers. Using $F_A(II)$, $F_B(II)$ and F_2^+ centers, it is expected that the wavelength range from 0.9 μm to 4 μm can be covered [1, 2]. For the first time we observed $F_B(II)$ center laser action with heavily Na doped KCl and RbCl crystals. The polarization behavior of $F_B(II)$ and $F_A(II)$ center lasers was investigated to determine the pump polarization and crystal orientation, which are best suited to achieve an efficient pump process. Differences between $F_A(II)$ and $F_B(II)$ centers have been measured. The lifetime of the relaxed excited state of $F_B(II)$ centers was measured as a function of the temperature. Further investigations of $F_A(II)$ and $F_B(II)$ center lasers were made to study in particular the output power, saturation effects and the frequency behavior. Due to the homogeneously broadened fluorescense line of color centers in alkali halide crystals at LN_2 temperature, the emission spectrum of the color center laser is remarkably clean. The linewidth of the single mode color center laser radiation is predominantly determined by the thermal conductivity, the temperature coefficient of the index of refraction and the specific heat of the crystal. Some results of our investigations with Na- and Li-doped KCl and RbCl crystals are given in the table below.

Crystal Type of Color Center	KCl : Li $F_A(II)$	RbCl : Li $F_A(II)$	KCl : Na $F_B(II)$	RbCl : Na $F_B(II)$
Pump Laser Pump Wavelength	Krypton;Argon 530,647,514nm	Krypton 647,676 nm	Argon;Krypton 470-530;568nm	Krypton 647,676nm
Pump Power at threshold	13 mW	100 mW	20 mW	26mW
Output Power	85 mW	6 mW	20mW	6mW
Slope Efficiency	7.7 %	2 %	2.3 %	2.1 %
Tuning Range	2.5 - 2.9 μm	2.75-3.05μm	2.25 -2.65 μm	2.5-2.9μm

There is a variety of other F aggregate centers which may be well suited for laser operation. Using the known spectroscopic data for the fluorescense quantum efficiency, the lifetime in the relaxed excited state and the width of the fluorescense line and considering the different loss mechanisms we calculated the pump power at threshold. Some ot these systems are under preparation. A review of M, M_A, M_A^+, Z, F_2^+, $F_A(I)$ and $F_B(I)$ centers is given including available pump sources and loss mechanisms due to competing absorptions of other aggregate centers which are present in the crystals.

1 L. F. Mollenauer and D. H. Olson, J. Appl. Phys. 46, 3109 (1975)

2 G. Litfin, R. Beigang and H. Welling submitted to Appl. Phys. Lett.

ON THE ELECTRONIC EXCITED STATE OF THE MONOMER CENTRES IN ALKALI-HALIDE PHOSPHORS.

S. Benci and M. Manfredi

Istituto di Fisica dell'Università - 43100 Parma
Gruppo Nazionale di Struttura della Materia del CNR.

Previous lifetime measurements of the A_x emission in systems such as $KI:Tl^+$ (1), $NaI:Tl^+$ (2), $KCl:Pb^{2+}$ (3) and $KCl:Tl^+$ (4) slightly doped evidentiated the existence of three components in the decay spectra. Two of them can be explained by considering the radiative transitions from the Jahn-Teller minima on $^3T_{1u}$ and $^3A_{1u}$ APES to the ground state. The origin of third one is not completely understood: some temptative explanations invoke tunneling processes between not equivalent minima, such as tunneling either from the minima responsible for the A_T emission to A_x minima (KI and NaI) or between the minima shifted in energy by the presence of the vacancy ($KCl:Pb^{2+}$). For $KCl:Tl^+$ crystals the third component cannot be explained in the frame of the theoretical models developed up to now, because these models consider that the minima on $^3T_{1u}$ APES are equivalent (5). On the basis of the above results, new theoretical approach seems to be required.

In order to understand the origin and the nature of the third component found in other phosphors, we have undertaken measurements of the luminescence time decay of the A_x and A_T emission in KBr:Tl crystals. This phosphor was chosen because both emissions coexist in the same temperature range. Preliminary measurements show a complex signal also for A_T emission.

Moreover a parallel analysis of the time decay and of the spectral distribution of the emission excited in the A band was carried out in very diluted KCl:Pb sample. It turns out that at $T \lesssim 120°K$, where two lifetimes were found, two gaussians are responsible for the emission peak, while at higher temperatures, where a third lifetime component can be detected, also a third gaussian starts to grow on the high energy side.

1) Benci S., Fontana M.P. and Manfredi M., Solid State Commun. 18, 1423 (1976).
2) Benci S., Fontana M.P. and Manfredi M., Phys.stat.sol. (b) 81 (1977).
3) Benci S., Capelletti R., Fermi F. and Manfredi M., Journ.de Phys. Colloque C7, 138 (1976).
4) Aiello S., Benci S. and Manfredi M., Solid State Commun., in press.
5) Gerhardt V. and Gebhardt W., Phys.Status Solidi (b), 59, 187 (1973).

RESONANT RAMAN SCATTERING FROM F-CENTRES IN CsF

Giorgio Benedek and E. Mulazzi

Istituto di Fisica dell'Università di Milano and Gruppo Nazionale di Struttura della Materia del C.N.R., via Celoria 16, 20133 Milano, Italy.

Here we present the evaluations of the differential cross sections of the Raman scattering in resonance with the F-band of the F center in CsF. The selection rules for the densities of phonon states (1) prescribe that for all the incident and scattered light polarizations the Γ_1^+, Γ_3^+ and Γ_5^+ densities of phonon states are responsible of the polarized scattering processes (1). The coupling coefficients of the electron phonon interactions Γ_1^+, Γ_3^+, Γ_5^+ and the first nearest neighbors and the second nearest neighbors are determined in a consistent way from the band shape evaluated by using the theory of (1) and the resonant Raman scattering theory (1). We use the experimental value of the spin orbit interaction coupling coefficient λ (2). The lattice dynamical calculations are performed by using the breathing shell model ; the first nearest neighbor projected perturbed densities of phonon states are evaluated by using a change of the central force constant equal to -0.5; the second nearest neighbors projected densities of phonon states are unperturbed. We find that the total density of phonon states has the prominent peaks at ω=1.15 and 1.45 sec^{-1}; the total Γ_3^+ density of phonon states has the prominent peaks at ω=0.8, 1.45 and 2.6 sec^{-1}; the total Γ_5^+ density of phonon states has the prominent peaks at ω=1.45 and 2.6 sec^{-1}; the peaks at ω=2.6 sec^{-1} are the peaks in the second nearest neighbors densities of phonon states Γ_3^+ and Γ_5^+. We present the calculations of the intensity ratios of the peak at ω=2.6 sec^{-1} of the Γ_3^+ density of phonon states with respect to the same peak of the Γ_5^+ density of phonon states in the $[110] \rightarrow [1\bar{1}0]$, $[100] \rightarrow [100]$ and $[100] \rightarrow [010]$ polarized spectra and their changes with the different incident resonant light frequencies.

1) E. Mulazzi and M.F. Bishop, Jour. de Physique C7, 37, 109 (1976).
2) T.A. Fulton and D.B. Fitchen, Phys. Rev. 179, 834 (1969).

SELF-DIFFUSION AND IONIC CONDUCTIVITY IN NaI

F. BENIERE, D. KOSTOPOULOS and K. V. REDDY

Laboratoire de Physique des Matériaux

I.U.T. 22302 LANNION (France)

We present the first part of an investigation of the transport properties and lattice defects in Na I single crystals, carried out on the line of our previous analyses relative to Na Cl and KCl (1)

This includes the following experimental results :

- Self-diffusion coefficients of Na^+ in pure crystals with the radioisotope Na – 22
- Self-diffusion coefficients of I^- with the radioisotope I - 125
- Electrical conductivity in pure Na I and in crystals doped by Ca^{++} ions labelled with the radioisotope Ca - 45.

Moreover, a thorough measurement of the temperature dependence on the self-diffusion has been performed by steps of 3 Kelvins from 450 K up to only 0.5 K of the melting point. The purpose was to investigate the eventual departure from the simple exponential law of Arrhenius reported in many papers, mostly those having delt with ionic conductivity measurements at high temperature.

(1) BENIERE, M, CHEMLA, M., and BENIERE, F. *J. Phys. Chem. Solids* 37 (1976) 525.

JAHN-TELLER EFFECT IN TRIGONAL $4d^9$ CENTERS

B. D. Bhattacharyya
Physics Department, St. Xavier's College
Calcutta, India

Baranov *et al.*[1] have studied the ESR and optical spectra of paramagnetic cadmium centers in alkali halide crystals. They observed that the warming of LiCl:Cd crystals which were irradiated at 77 K leads to the appearance of a new anisotropic ESR spectrum. Morigaki[2] investigated the ESR spectra of some photosensitive centers in Ag-doped CdS and has interpreted the results in terms of no Jahn-Teller effect. The symmetry of the ESR spectra in these materials reveals unambiguously a trigonal Jahn-Teller type distortion in all cases. The present paper aims to clarify the role and nature of the Jahn-Teller distortions in the interpretation of the ESR results.

The experimental results[1,2] show that the distortions are of E symmetry and accordingly we have employed the vibronic Hamiltonian as described by Moffitt and Thorson.[3] The trigonal distortion has been found to modify the e-mode coordinates (Q_x, Q_y) and the cubic Jahn-Teller parameters V^a, V^e as follows

$$Q^+ = (\sqrt{3}Q_y + Q_x) \; ; \qquad Q^- = (\sqrt{3}Q_y - Q_x) \; ;$$

$$V^+ = \frac{1}{3}(\sqrt{2}V^a + V^e) \; ; \qquad V^- = \frac{1}{3}(\sqrt{2}V^a - V^e) \; .$$

The energy at this distortion has been lowered by the Jahn-Teller energy $\Delta E_{JT} = (V^+)^2/2\mu\omega^2$.

The vibronic wave functions were then operated on with the complete Hamiltonian and using the symmetry properties we find a splitting of the ground state vibronic triplet into a singlet Γ_1 and a doublet Γ_3. Finally employing the spin-orbit and Zeeman perturbations we obtain g values in the form

$$g\langle 111\rangle = 2+4d$$

with

$$d = R_i \zeta/\Delta' \qquad (i = \| \text{ or } \perp) \ .$$

We have also calculated the tunnel splitting parameter and estimated its value from the experimental g values.[1,2]

Comparison is made with experimental results at different temperatures.

The tunnel splitting parameter is obtained as

$\Gamma = 9\ cm^{-1}$ (at 77 K, for cadmium center) ,

$\Gamma = 2.3\ cm^{-1}$ (at 1.5 K, for photosensitive center in Ag-doped CdS) .

---

1. P. G. Baranov, R. A. Zhitnikov, and N. I. Mel'nikov, Sovt. Phys. Solid St. 15, 2353 (1974).

2. K. Morigaki, J. Phys. Soc. Japan 23, 820 (1967).

3. W. Moffitt and W. Thorson, Phys, Rev. 108, 1251 (1957).

TUNNEL-SPLITTING IN TRANSITION-METAL OXIDES AND HALIDES ON QUASI-MOLECULAR JAHN-TELLER MODEL

B. D. Bhattacharyya
Physics Department, St. Xavier's College
Calcutta, India

The variational approach[1,2] to the problem of multimode Jahn-Teller coupling of impurities in transition metal oxides and halides is extended to investigate the tunnel splitting in some tetragonal and orthorhombic states. The barriers between tetragonal and orthorhombic equivalent minima of the adiabatic potential through which tunneling of the system takes place have been obtained with relative ease by constructing a trial equilibrium density matrix of the form

$$\rho \approx \frac{\exp\ (-\beta\tilde{H}_{JT}) \cdot \exp\ (-\beta\tilde{H}_{qu\cdot ph})}{Tr\ \exp\ (-\beta\tilde{H}_{JT}) \cdot Tr\ (-\beta\tilde{H}_{qu\cdot ph})}$$

with

$$\tilde{H}_{JT} = \sum_{\Gamma\gamma} \hbar\Omega_{\Gamma} \{\frac{1}{2} (\tilde{p}^2_{\Gamma|\gamma} + \tilde{q}^2_{\Gamma|\gamma}) + K_{\Gamma}\, \tilde{q}_{\Gamma|\gamma}\, \sigma_{\Gamma\gamma}\} + \sum_{\Gamma\gamma} f_{\Gamma\gamma}\, \sigma_{\Gamma\gamma}$$

and

$$\tilde{H}_{qu\cdot ph} = \sum_{\Gamma\gamma} \sum_{j\neq 1} \hbar\Omega_{\Gamma j}\, \frac{1}{2} (\tilde{p}^2_{\Gamma j\gamma} + \tilde{q}^2_{\Gamma j\gamma})$$

Computations with experimental results are under progress and will be shortly reported.

---

1. J. R. Fletcher, J. Phys. C: Solid St. Phys. 5, 852 (1972).
2. B. Halperin and R. Englman, J. Phys. C: Solid St. Phys. 8, 3975 (1975).

MAGNETIC VIBRATIONAL RAMAN SCATTERING OF KI DOPED WITH F CENTRES

M. BILLARDON, M.F. RUSSEL
Laboratoire d'Optique Physique, ESPCI
10, rue Vauquelin, 75231 PARIS, France

and J.P. BUISSON, S. LEFRANT
Laboratoire de Physique Cristalline, Université de Paris-Sud
Bât. 490, 91405 ORSAY, France

Experimental studies of the Raman scattering by KI doped with F centres have been previously published. At 10 K the spectra show particularly a very intense and sharp line at 96 cm^{-1} which has been attributed to a Γ_1^+ resonant optical mode. In fact, the calculation predicts a strong resonant Γ_1^+ mode, but is unable to account for the 96 cm^{-1} line which appears in the Γ_3^+ and Γ_5^+ spectra. However we have recently shown that the spin-orbit interaction in the excited state could explain this feature rather satisfactorily (1). In order to check this hypothesis we have performed Raman scattering experiments under magnetic field, which turns out to be the relevant perturbation to apply for this purpose.

If the spin-orbit coupling was negligible, our experiments would only lead to the determination of Γ_5^+ modes. Actually, the Raman spectrum observed without magnetic field exhibits the 96 cm^{-1} mode and its first overtone at 193 cm^{-1}. When the magnetic field is applied, an apparent feature of the experiment turns out to be the splitting of both 96 cm^{-1} and its first overtone, into two components separated by $2g\beta H$.

This observed feature may be explained taking into account the splitting of the ^2S ground state. The magnetic field splits the 0 and 1 vibronic levels into two sub-levels possessing the magnetic quantum number $\pm$ 1/2. Then the Raman spectrum could eventually exhibit three lines. Two of them correspond to transitions involving a spin-flip and are separated by $2g\beta H$. The other one, which does not involve any spin flip, would be at the same frequency as the original one. In order to determine the selection rules we have used the Raman theory in the quasi resonant

approximation (2, 3) and we have taken into account the spin-orbit and the Zeeman interactions. We then obtain second order terms whose magnitude is proportional to $(C_i C_{so})^2$; C_i and C_{so} are the coupling constants for electron lattice and spin-orbit interactions. For a Γ_1^+ mode only both transitions involving a spin-flip can appear ; and the scattered light is then circularly polarized (σ_+ for one line and σ_- for the other). The spectra obtained for the 96 cm^{-1} line are in a good agreement with these theoretical results. On the other hand, for Γ_3^+ and Γ_5^+ modes, the three lines must appear and this has been in fact observed in other parts of the spectrum.

In conclusion, the classical selection rules are not observed when the spin-orbit interaction in the excited state is taken into account. The Raman scattering under magnetic field allowsthen a better determination of the active modes.

(1) BUISSON, J.P., SADOC, A., TAUREL, L., and BILLARDON, M., Light Scattering in Paris, Paris Flammarion 1975.

(2) HENRY, C.H., Phys. Rev. 152, 699, 1966.

(3) BUCHENAUER, C.J., Thesis, 1971.

E.N.D.O.R. OF SELF-TRAPPED EXCITON IN K Cl

D. Block, Y. Merle d'Aubigné, A. Wasiela
Laboratoire de Spectrométrie Physique
B.P. 53 - 38041 Grenoble-cédex, France

EPR in the triplet state of the self-trapped exciton (STE) was recently observed in a number of alkali halides [1]. Analysis of the hyperfine interaction with the two central halogen nuclei gives a very good confirmation of the model describing the STE as a self-trapped hole (V_K center) having trapped an electron in a more or less delocalized orbital. In order to determine the extension of this orbital we studied the electron nuclear double resonance (ENDOR) of the STE in K Cl. The same optical detection technique was used as for the observation of EPR. Two microwave frequencies (9 and 15 GHz) were used. The nuclear Zeeman effect and the existence of the two isotopes Cl^{35} and Cl^{37} allowed the assignment of the more intense linesto two non equivalent potassium nuclei and to one chlorine nucleus. Because of the small signal to noise ratio the lines could be followed only for small rotations of the magnetic field around the main axes Oz and Oy of the STE (see fig. 1). Lines due to Cl_ρ and K_β could be identified by their splitting into two components when rotating the magnetic field away from the symmetry axis. The identification of the K_β line is not completely exempt of doubt since K_π lines would split the same way. For another set of lines this angular variation could not observed so that we cannot tell if they are due to K_α or K_γ nuclei. Though the sensitivity of the apparatus was still good up to 30 MHz transitions due to the close by Cl_ρ nuclei could not be detected.

The Ayy and Azz main values of the hyperfine tensor differ by less than 1%. Neglecting the contribution of the hole their average values, represent the contact interactions of the electron with the various nuclei. In table I we also give the contact interactions of the electrons of the F and M centers in K Cl. For the STE and the M center we give the values of 2 A since they represent the electron density when the hyperfine interaction is written as $\vec{I}.\vec{A}.\vec{S}$ with S = 1. One notes that the order of magnitude of these densities are the same for the electrons of the STE and of the F and M centers. This clearly shows that the extensions of the wavefunctions are very similar. One also notes a strong desagreement with the values of the contact interactions calculated by a pseudo-potential technique [2]. Quadrupolar interaction of the two central halogen nuclei : inside the M_s = 0 state and for H along the Oz direction, the hyperfine interaction has no first order effect so that the quadrupolar interaction is directly observable. 4 lines of equal intensities were observed instead of the 2 expected for the 3/2 to 1/2 and the -3/2 to -1/2 nuclear transitions. The spectrum can be described using the standard quadrupolar hamiltonian with two equally probable constants of interaction $|P_{//}|$ = 12.2 MHz and $|P'_{//}|$ = 11.75 MHz. No good explanation was found for this peculiar effect.

References

1. A. Wasiela, G. Ascarelli and Y. Merle d'Aubigné, Phys. Rev. Let. 31, 993 (1973)
   M.J. Marrone, F.W. Patten and M.N. Kabler, Phys. Rev. Let. 31, 467 (1973)
2. A.H. Harker, S.B. Lyon and A. Wasiela, *A.E.R.E. report TP 682 (1976)*

Table I : Contact interactions of the M and F centers and S.T.E. in K Cl (in MHz)

Center / Nuclei	S.T.E. Meas. 2 Azz	S.T.E. Meas. 2 Ayy	S.T.E. Theory 2 A	F A	M 2 A
K_α	30.54	30.60	56.7	20.7	37
K_γ			2.4		21.8
K_β	24.14	24.02	5.9		20.3
Cl^{35}_ρ	10.62	10.70		6.9	

Figure 1 : S.T.E. and surrounding lattice nuclei

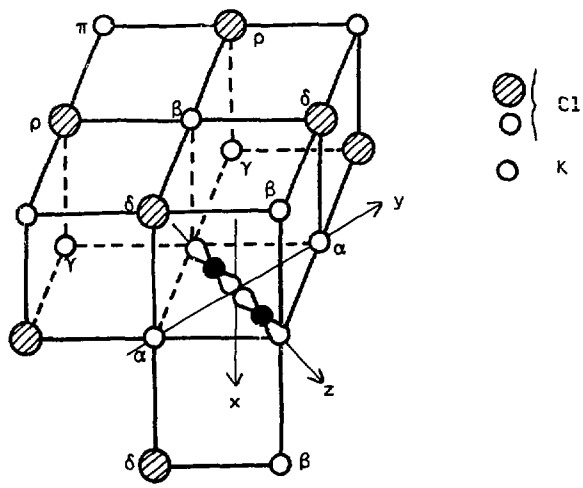

ENDOR OF V_{OD} DEFECTS IN SrO*

J. L. Boldu,** H. J. Stapleton,† Y. Chen and M. M. Abraham
Solid State Division, Oak Ridge National Laboratory
Oak Ridge, Tennessee, USA

Single crystals of SrO doped with deuterium were grown by the submerged arc fusion technique. The V_{OD} center was produced by γ-irradiation at 77 K and its identity confirmed by EPR and ENDOR measurements. The defect possesses <100> axial symmetry and can be described with the following spin-Hamiltonian parameters: $g_{\parallel} = 2.0013(2)$, $g_{\perp} = 2.0751(2)$, $A_{\parallel} = +0.396(2)$ MHz, $A_{\perp} = -0.195(2)$ MHz, and $P = +0.158(1)$ MHz. Absolute signs were assigned on the assumption that the reported positive deuterium nuclear moment requires that the anisotropic portion of the hyperfine interaction must be positive. From the hyperfine parameters, a value of 5.078 Å for the $OD^- - [Sr\ Vacancy] - O^-$ distance in this linear defect can be derived. Figure (1) is a graph of the $O^- - O^=$ distance (d) versus the lattice constant a_o for the V_{OH} and V_{OD} centers in MgO, CaO and SrO. It can be seen that if one considers V_{OD} centers in MgO and CaO, the points fall on the same straight line determined by the V_{OH} data in all three hosts

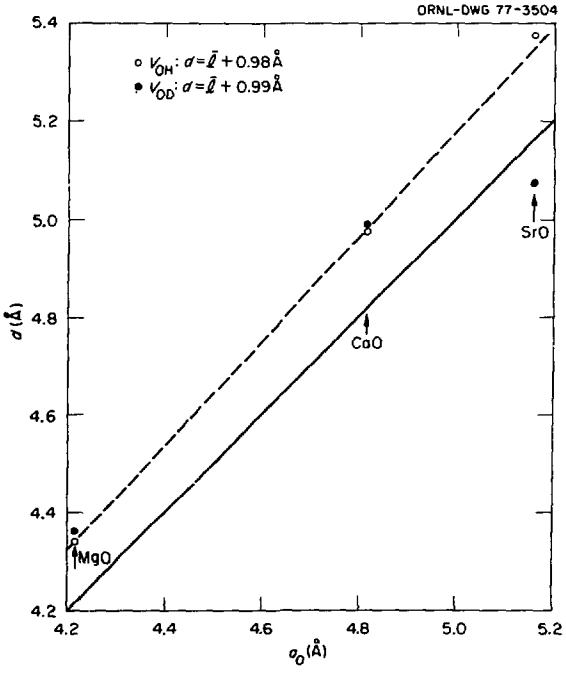

Fig. 1. Graph of $O^- - O^{2-}$ distance as a function of the lattice constant. Distances were calculated from the dipole interaction and the $OH^-(OD^-)$ bond length. The solid line represents $d = a_o$.

showing an outward relaxation of the axial oxygens. However, the V_{OD} point for SrO does not fall on that straight line and lies below the $d = a_o$ line implying an inward relaxation for the oxygens in SrO.

---

*Research sponsored by ERDA under contract with Union Carbide Corporation.

**Permanent address: Instituto de Fisica U.N.A.M., Mexico, D.F.

†On sabbatical leave from University of Illinois, Urbana-Champaign, IL.

ELECTRONIC PROPERTIES AND DEFECTS OF THE SUPERIONIC CONDUCTOR LITHIUM NITRIDE

Hermann Brendecke and Elmar Wagner

Max-Planck-Institut für Festkörperforschung
7000 Stuttgart 80, Germany

Lithium Nitride (Li_3N) has recently attracted interest for application as a highly conducting solid-state electrolyte.[1,2] We report the first measurements concerning the electronic structure of Li_3N. The optical experiments were carried out on Czochralski-grown single crystals, available now up to 2 cm^3 in size.[3] We applied absorption and photoluminescence (PL) techniques to identify intrinsic and extrinsic properties.

Absorption measurements reveal that Li_3N has an indirect band structure - in consistency with band structure calculations. The indirect and direct band gap energies are 1.5 and 2.2 eV, respectively, at 4.2 K. An impurity level 750 meV in depth could be identified from absorption measurements.

Figure 1 shows a PL spectrum of a Li_3N crystal. The emission is characterized (i) by numerous lines which are phonon replicas of 2 zero-phonon transitions (designated here by "V" at 2.066 eV and "Z" at 2.105 eV), and (ii) by a broad emission between 1.6 and 2 eV, partly caused by overlapping phonon replicas. The former are strongly sample-dependent and dis-

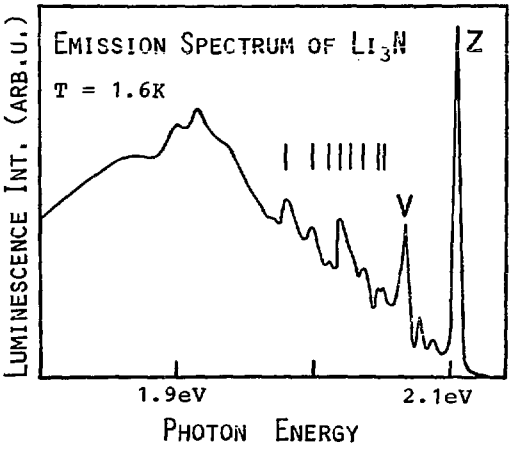

Fig. 1
PL spectrum of Li_3N at 1.6 K.
Excitation photon energy: 2.4 eV

appear completely in crystals of high perfection and purity.

Strong phonon coupling in photo-emission is demonstrated in Fig. 2 by excitation spectroscopy. The sample is excited by a tunable dye-laser with photon energies governed by the "V"-peak lineshape. As can be seen there is no thermalization, but the replicas shift in accordance with the excitation-source tuning. This suggests that the excited centers are strongly localized in the ionic crystal. The transitions "V" and "Z" most probably originate from bound (Frenkel) excitons. Isoelectronic impurities like Na or others like O, Si and Al may act as binding centers for the excitons. These elements have been identified in the samples of high PL efficiency at concentrations up to 10^{18} cm^{-3} by means of atomic absorption and microprobe analysis.

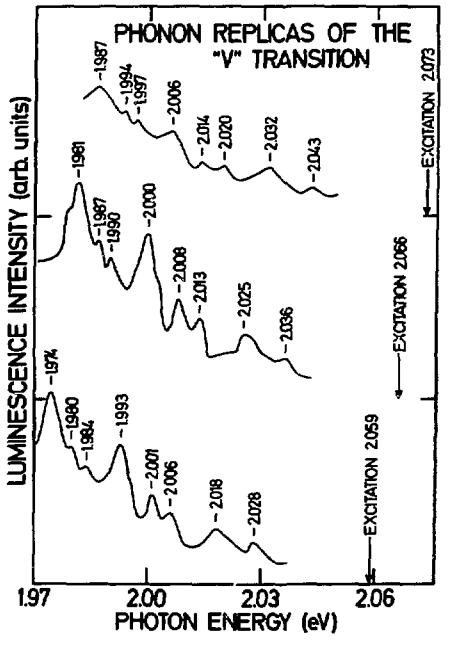

Fig. 2
PL spectrum of Li_3N at 1.6 K with varying excitation photon energy

1. U. von Alpen, A. Rabenau, G.H. Talat, APL, June 15, 1977
2. A. Rabenau, H. Schulz, J. Less-Common. Met. 50, 155 (1976)
3. Crystals have been provided by E. Schönherr and G. Müller.

SODIUM-PERTURBED F_3-CENTRES (R_A-CENTRES) IN KCl

M. Buchanan and J. Rolfe

Physics Division, National Research Council, Ottawa, Canada

When F_3-centres (R-centres) are produced in KCl crystals that contain sodium ion impurity, the low-temperature absorption spectrum contains two small zero-phonon lines on the low-energy side of the well-known R_2 zero-phonon line. The more intense of these lines occurs at 13216 cm^{-1}[2] and has a full width at half maximum (FWHM) of 8 cm^{-1}, and a weaker line can be seen at 13278 cm^{-1} with a FWHM of 11 cm^{-1}. (The R_2 zero phonon line occurs at 13471 cm^{-1} with FWHM of 6 cm^{-1}.) The relative intensity of these two lines, considered to be due to F_3 centres perturbed by sodium ions, varies from specimen to specimen, so that they cannot arise from transitions within the same centre.

To investigate the structure of these perturbed centres, we made uniaxial stress shift measurements on the lines, using a sensitive absorption apparatus. Stress was applied along the three high symmetry directions [100], [110], and [111] and the absorption was measured with light polarized parallel or perpendicular to the stress. The most conclusive measurements were made on the 13216 cm^{-1} line, as the lower intensity and the greater breadth of the 13278 cm^{-1} line made some of the stress splittings unresolvable.

The stress results showed that the 13216 cm^{-1} line must be due to a centre with a doubly degenerate ground state and trigonal symmetry, so that it has the same symmetry as the unperturbed F_3-centre. The obvious model for this centre is that a single sodium ion situated at the nearest neighbour position equidistant from all three F-centres causes the perturbation that shifts the zero-phonon line towards lower energies. In comparison with the unperturbed F_3-centre, we found that the orientational splitting constants are larger, and the electronic splitting constants are smaller.

The stress shifts observed for the 13278 cm^{-1} line are consistant with a model of a perturbed centre which also has the same symmetry as the F_3-centre, namely a trigonal symmetry centre with a doubly degenerate ground

state. Models for this centre which involve sodium ion perturbation alone are difficult to believe, since to preserve the three-fold axis there must either be three sodium ions as nearest neighbours to the three F-centres, or a single sodium ion in the fifth <111> plane away from the plane of the F_3-centre. A more likely model would invoke the presence of another negative ion impurity, possibly bromide, in the first neighbouring negative-ion <111> plane on the opposite side of the F_3-centre to a sodium ion. Experiments are under way to check this hypothesis.

FIRST-ORDER RAMAN SCATTERING INDUCED BY F CENTERS IN CsCl, CsBr, AND CsF

J.P. Buisson, S. Lefrant, M. Ghomi, L. Taurel and J.P. Chapelle

Laboratoire de Physique Cristalline - Université de Paris-Sud -
(Equipe de Recherche associée au CNRS n°13)
Bâtiment 490 - 91405 ORSAY CEDEX - FRANCE -

We present a study of first-order Raman scattering (T = 12 K) induced by F centers in cubic cesium halides in off-resonance condition of excitation and tuning the laser line in resonance with the electronic transition $\Gamma_1^+ \rightarrow \Gamma_4^-$ of the F band. In these crystals the F band shows a structure which was explained by the spin-orbit coupling of the F center in its excited state and by the electron coupling of the Γ_3^+ and Γ_5^+ Jahn-Teller active modes[1]. The off-resonance spectra taken in the polarizations of the incident and scattered light $[100] \rightarrow [\bar{1}00]$, $[100] \rightarrow [010]$, $[110] \rightarrow [1\bar{1}0]$ allow to separate the contributions of the Γ_1^+, Γ_5^+, Γ_3^+ symmetry coordinates of the ions which couple to the F center and to determine the relative values of the coefficients of the Γ_1^+, Γ_3^+, Γ_5^+ electron-phonon interactions. The spectra were calculated using phonons derived from the eleven shell model parameters which fit neutron data and assuming that the electron-phonon interaction is linear in the displacements of the first and second ion shell surrounding the F center. A softening of the longitudinal force constant between the F center and its 1 nn's (CsBr : 55 %, CsCl : 50 %, CsF : 20 %) and between its 1 nn's and its 2 nn's (CsBr : 8 %, CsCl : 13 %, CsF : 6 %) accounts for the main peaks. Raman spectra show that in the case of the F centers in CsCl and CsF the strong optical modes (CsCl : 105 $cm^{-1}(\Gamma_3^+)$; CsF : 139 $cm^{-1}(\Gamma_3^+)$, 135 $cm^{-1}(\Gamma_5^+)$) are due to the coupling of the F electron to the 2nd shell of ions. All the results confirm the previous determinations[2,3] of the relative contributions of the cubic and non cubic-modes to the second moment of the F band.

The in-resonance Raman spectra show very clearly the breakdown of the conventional selection rules. The case of F centers in CsBr is particularly discussed since in this case we have been able to study Raman spectra when exciting the whole spectral range of the F band. In this case, the Jahn-Teller active electron-phonon interactions are weaker than the Γ_1^+ electron-phonon coupling and, as for spectra of F centers in KI[4], the

depolarization of the Γ_1^+ modes is mainly due to the spin-orbit coupling of the F center in its first Γ_4^- excited state. A semi-classical theory of Raman scattering which extends Henry's calculations in the case of resonance accounts for the experimental results. It is shown particularly, as it was previously predicted[5], that Raman scattering coming from interactions of the Γ_6^- and Γ_8^- electronic states to the Γ_1^+ phonons gives rise to interference effects, and this explains the relative variations of the 55 cm^{-1} Γ_1^+ peak, as a function of the Laser line wavelength, in the spectra taken for all the polarizations of incident and scattered light.

[1] P.R. Moran - Phys. Rev. 137A, 1016 (1965)

[2] C.H. Henry, S.E. Schnatterly and C.P. Slichter - Phys. Rev. 137A, 583 (1965)

[3] T.A. Fulton and D.B. Fitchen - Phys. Rev. 179, 846 (1969)

[4] J.P. Buisson, A. Sadoc, L. Taurel and M. Billardon - Light Scattering in Solids edited by M. Balkanski, R.C.C. Leite and S.P.S. Porto - Flammarion - Paris (1975)

[5] E. Mulazzi and M.F. Bishop - Solid State Commun. 19, 39 (1976)

E.P.R. INVESTIGATIONS OF THE DISPLACIVE STRUCTURAL PHASE CHANGE IN AMF_3 CRYSTALS ON USING PARAMAGNETIC PROBES : $|F_eOF_5|^{4-}$, $|GdOF_5|^{4-}$ CLUSTERS

J.Y. Buzaré - J.J. Rousseau - J.C. Fayet
Laboratoire de Spectroscopie du Solide - E.R.A. CNRS n° 682
FACULTE DES SCIENCES - 72017 LE MANS CEDEX

$RbCaF_3$ [1], first, $RbCdF_3$ and $TlCdF_3$ [2] later, have been recognized to exhibit at low temperature, a $O_h^1 \rightarrow D_{4h}^{18}$ transition, second order or nearly second order, closely related to the examplified one, at 105 K, in $SrTiO_3$. The tetragonal distorsion consists in a rotation by $\pm \varphi$, around the (001) axis, of the ligand octahedra, otherwise of the MF or F-F bonds in the (001) plane.

A sensitive probe can be obtained by marking these bonds with a paramagnetic center responsible for E.P.R. lines which acutely depend on the angle beetween the magnetic field and the bond direction. V_K centers have been already used [3,4]. Trivalent S state ions, at M sites, compensated by O^{2-} at n.n F^- sites, are considered here.

I - Spin - hamiltonien parameters in the cubic phase :

The charge compensation by an O^{2-} substituted for F^- results in a strong axial crystal field which competes with the magnetic field to admixe $M_z = \pm \frac{1}{2}$ spin states in the two eigen states involved in the E.P.R. transition characterised by g eff $\simeq 2S + 1$, $g// \simeq 2$ (g eff = 6 for Fe^{3+}, g eff = 8 for Gd^{3+}). This rough analysis, which has been improved by a computer diagonalisation of the spin hamiltonien matrix, accounts for the sensitivity of the probes.

The contribution of the O^{2-} ligand to the axial field parameter D, is discussed in terms of overlap and covalency for Fe^{3+} and on using the superposition principle of Newman for Gd^{3+}. It appears to be the major one and accounts for the dependance of $D(Fe^{3+})$ on the host lattice parameter.

In the case of the $|F_eOF_5|^{4-}$ cluster the s.h.f. parameters have been measured for the axial and the equatorial fluorines and are compared to the corresponding parameters in cubic $|F_eF_6|^{4-}$ clusters.

II - Behaviour of the E.P.R. lines at the structural phase change :

The rotation by $\pm \varphi$ of the MF bonds in the (001) plane below T_c results in a rotation by $\pm \varphi_{loc}$ of the F_e^{3+}-O^{2-} or of the Gd^{3+}-O^{e-} bonds and in a splitting of the E.P.R. lines, which can be as large as 100 g/o. The measurements of φ_{loc} are compared to the values obtained on using other probes [3,4] and on using a model for the atomic structure of the tetragonal phase. The lines widths exhibit critical broadenings near T_c. Wefocused our attention on a particular feature which occurs in a range of few tenthsof degrees near T_c.

a) In $RbCdF_3$ (F_e^{3+}- O^{2-}) the line shape is dominated by the partially resolved s.h.f. structure due to fluorine nuclei. In a range of 0.4 K near 124 K, the line exhibits an acute transformation but always passes through at least ten fixed points. This particularity may evidence an admixture, at a variable percentage, of two components : one is cubic, one is tetragonal with a well defined value of φ_{loc}.

b) In $RbCaF_3$: (Gd^{3+} - O^{2-}), the splitted lines of the tetragonal phase, do not emerge smoothly from the cubic line but appear at neatly shifted field values where their intensity increases on few tenths of degrees, at the prejudice of the cubic line, before further splitting on cooling.

These results are consistent with a slight first order character of the transition and with other observations on using non local measurements[5]. They also may be compared with the observed assymetry of the E.P.R. line of a similar probe (F_e^{3+} - V_o) in $S_rT_iO_3$, near and below T_c.

|1| MODINE F.A., SONDER E., UNRUH W.P., BINCH C.B & WESTBROOK R.D. Phys. Rev. B10 1623 (1974).

|2| ROUSSEAU M., GESLAND J.Y., JULLIARD J., NOUET J., ZAREMBOWITCH J. & ZAREMBOWITCH A., Phys. Rev. B12, 1579 (1975).

|3| ROUSSEAU J.J., ROUSSEAU M. & FAYET J.C., Phys. Status Solidi (b) 73, 625 (1976).

|4| HALLIBURTON L.E., SONDER E., Solid State Commun 21-445 (1977)

|5| KAMITAKAHARA W.A. & ROTTER C.A., Solid State Commun. 17, 1350 (1975).

IONIC CONDUCTIVITY OF MIXED SILVER BROMIDE-SILVER CHLORIDE SINGLE CRYSTALS*

L. S. Cain, H. Manning, and L. M. Slifkin
University of North Carolina, Chapel Hill

To evaluate the effects of mixed halides on lattice defect parameters, the ionic conductivity of four mixed AgBr - AgCl single crystals, as well as the ionic conductivity of pure silver bromide and silver chloride, have been measured from 300°C to -50°C. The mixed crystals contained 20, 39, 57, and 79 mole % AgCl. All samples contained less than two parts per million divalent cation impurity, necessitating the measurements below room temperature in order to explore the extrinsic region.

In the intrinsic region, a plot of conductivity versus silver chloride composition is almost linear, decreasing from AgBr to AgCl. A preliminary analysis of the slope of the intrinsic region, which contains the enthalpies of Frenkel defect formation and interstitial migration, indicates that the slope is practically constant from AgBr to a 50-50 mole % solid solution and then increases rapidly in magnitude to the value for pure AgCl. This behavior is similar to that of the change in the bulk modulus of mixed AgBr-AgCl single crystals.[1] In fact, the dependence of the intrinsic activation energy on composition quantitatively parallels that of the product of bulk modulus with inverse dielectric constant, and hence reflects the expected dependence of defect energies on macroscopic properties.

These results are presently being subjected to a non-linear least squares computer analysis using the usual Lidiard-Debye-Hückel model. The main interest will be in determining exact values of the enthalpy of Frenkel defect formation and the enthalpy of vacancy migration as a function of AgCl concentration. These results will be presented, along with results of current experiments on mixed AgBr-AgI and AgCl-AgI crystals.

*Supported by the Materials Research Center, University of North Carolina, under Grant No. DMR-7500806 from the National Science Foundation (NSF), and by NSF Grant No. DMR72-03212-A01.

[1] L. S. Cain, J. Phys. Chem. Solids 38, 73 (1977).

ROLE OF THE ELECTRONIC EXCITED STATE OF Pb^{2+} ON THE ION REORIENTATION PROCESSES IN KCl.

R.Capelletti, F.Fermi, R.Fieschi
Istituto di Fisica dell'Università - Via d'Azeglio,85 - 43100 Parma
Gruppo Nazionale Struttura della Materia del C.N.R.

The role of the electronic configuration on the ionic motion parameters of the impurity defects, such as I.V. dipoles in ionic crystals has been recently outlined along a series of transition metals in AgCl[1].

Furthermore we have studied, for a given impurity, how different electronic configurations (for instance, the electronic excited state, e.e.s.) affect the reorientation parameters of the I.V. dipole with respect to those of the electronic ground state (e.g.s.)[2].

The system chosen is KCl:Pb, the population of the e.e.s. is obtained by shining with u.v. light absorbed in the well known spectrum induced by lead, the ITC technique is used in order to detect the reorientation phenomena in the e.e.s..

Two kinds of impurity induced defects have been studied: 1) the simple I.V. dipole and 2) the Suzuki-like phase occlusions[3]. In the latter case the "reorientation" in the e.e.s. must be regarded, more properly, such as a photostimulated diffusion of the cation vacancy. In both cases reorientation phenomena in the e.e.s. have been detected at such a low temperature at which the ionic motion in e.g.s. is hindered, even if in the latter case the effect is much more relevant.

Rate equations for the reorientation in e.e.s. have been written in the frame of diffusion model and found in satisfactory agreement with the experimental results obtained on the role of the impurity concentration, irradiation temperature, light dose and spectral distribution on the reorientation yield. Parallel e.e.s. lifetime measurements have allowed to estimate that the energy barrier for "reorientation" in e.e.s. is 1/10 of the corresponding one in e.e.s. for Suzuki-like defects.

1) A.P.Batra, J.P.Hernandez, L.M.Slifkin - Phys.Rev.Lett. 36, 876 (1976).
2) S.Benci, R.Capelletti, F.Fermi, M.Manfredi - J.Phys. 37, C7-138 (1976).
3) R.Capelletti, A.Gainotti - J.Phys. 37, C7-316 (1976).

SOLUTION AND PRECIPITATION PHENOMENA OF TRIVALENT RARE-EARTH IMPURITIES IN DIVALENT METAL FLUORIDES.

R.Capelletti, F.Fermi, E.Okuno[+]
Istituto di Fisica dell'Università - Via d'Azeglio,85 - 43100 Parma
Gruppo Nazionale di Struttura della Materia del C.N.R.
[+]Instituto de Fisica- Universidade de São Paulo, Brasil.

The study of the solution and precipitation phenomena of impurities, extensively pursued in alkali halides[1] appears rather new and promising in the field of physics of point defects in matrices with the CaF_2 structure also in view of the technological implications. In these matrices the simplest dipolar defect involving impurity (specifically trivalent rare-earth) which can be detected by means of ITC is the Rare Earth-Fluorine Interstitial (RE-FI) dipole.

In the complex ITC spectrum of CdF_2 doped with different amounts of Eu^{3+} we found that one component band can be attributed to RE-FI relaxation; each of the bands contribute to the spectrum with a weight which is function of the previous thermal history of the sample; annealings in the range $100 \leqslant Ta \leqslant 200°C$ cause a progressive growth of the RE-FI peak up to a saturation value which is increasing function of T_a (see figure). The process is ruled by a monomolecular first order kinetics consistent with the dissolution of RE-FI dipoles from aggregates.

In CaF_2 doped with different amount of Gd^{3+} and Sm^{3+} ($10^{-5} \div 10^{-2}$ m.f.) as well, the precipitation phenomena are of relevance. In fact the changes induced on ITC spectra by annealings in the range $100 \leqslant T_a \leqslant 1000°C$ suggest that ITC band peaked at ~ 200 K can be attributed, in the specific case of CaF_2, to the presence of aggregates rather than to n.n.n. RE-FI relaxation as in the case of $SrF_2:Gd^{3+}$ [2].

1) R.Capelletti - Thermal and Photostimulated Currents in Insulators - ed. D.Smyth, Lehigh Univ. Pennsylvania page 1 - 1976.
2) J.H.Crawford,Jr., G.E.Matthews - J.Phys. 37, C7-297 (1976).

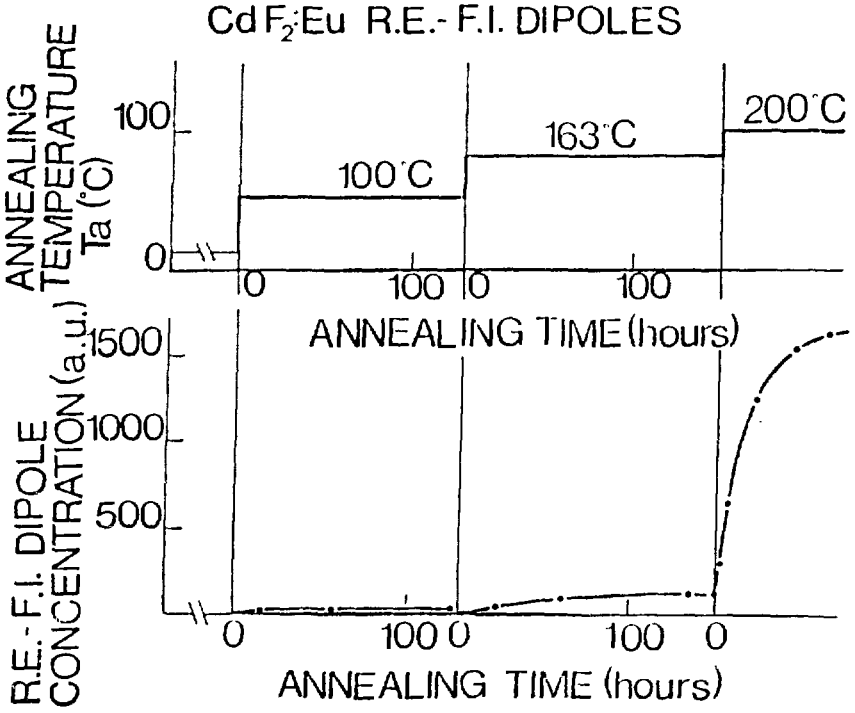
CdF2:Eu R.E.- F.I. DIPOLES
ANNEALING TEMPERATURE Ta (°C)
100
0
100°C
163°C
200°C
0
100
0
100
ANNEALING TIME (hours)
R.E.- F.I. DIPOLE CONCENTRATION (a.u.)
1500
1000
500
0
100
0
100
0
ANNEALING TIME (hours)

DISSOLUTION PROCESSES OF Be AND Mg AND MAXWELL-WAGNER RELAXATIONS STUDIED BY MEANS OF ITC IN LiF CRYSTALS.

R.Capelletti, A.Gainotti
Istituto di Fisica dell'Università - Via d'Azeglio,85 - 43100 Parma
Gruppo Nazionale di Struttura della Materia del C.N.R.

ITC technique was extensively exploited to study the relaxation processes related to simple defects (I.V. dipoles, off center ions in alkali halides and RE-FI dipoles in difluorides) and to less extent, the release of space charge[1].

Recently it has been shown that ITC can detect as well the Maxwell-Wagner interfacial relaxations which arise from the nucleation of extended Suzuki-like phase occlusions in KCl:Pb which grow at the expenses of I.V. dipoles[2].

In the present work a parallel study of the dissolution kinetics of I.V. dipoles in the range $100 \leq Ta \leq 700°C$ and of the motion parameters, as deduced from the ITC analysis, is performed in LiF:Be and Mg in order to understand the origin of the huge ITC peaks which appear in the range 30-70°C of the ITC spectrum and obey the first order reorientation kinetics. In this temperature range practically all alkali halides doped with divalent impurities exhibit huge ITC peaks, whose origin however is poorly understood.

In doped LiF a pronounced, reproducible and reversible shift of the position T_M of the huge peak towards lower temperatures is observed an increasing the annealing temperature (see figure). The rate of quenching affects as well T_M. Quenching from temperatures as high as 730°C does not succeed in suppressing the peak.

The peak turns out to be related to interfacial polarization induced by the presence of impurities, but cannot be explained in terms of Suzuki-like phase occlusions as in the case of KCl:Pb. It can be attributed to the impurity induced Cottrel atmosphere around dislocations, which is modified by annealings. Stress induced effects on ITC plot are to be taken in account as well.

1) R.Capelletti, R.Fieschi - Proceed.Intern.Sympos.Electrets and Dielectrics, Sao Carlos (Brasil) Sept. 1975, in press.
2) R.Capelletti, A.Gainotti - J.Phys. 37, C7-316 (1976).

Fig.1- ITC plot of LiF:Mg-changes induced by annealings at different temperatures T_a.

1) sample as received; 2) T_a = 100 °C ;
3) T_a = 200 °C ; 4) T_a = 300 °C.

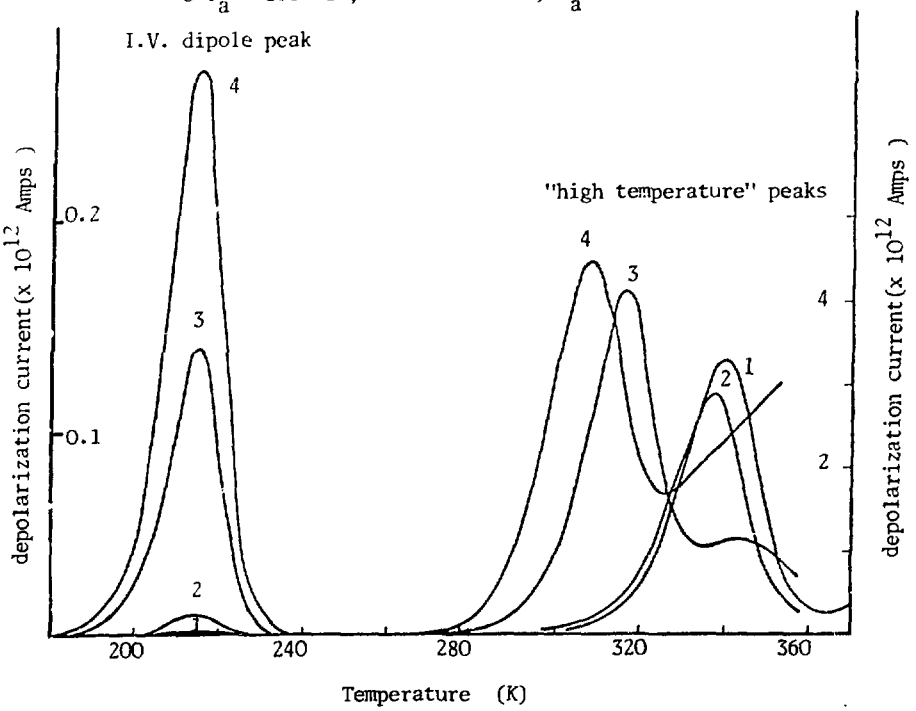

RAMAN SPECTRA IN KCl:Pb WITH SUZUKI-LIKE OCCLUSIONS.

R.Capelletti, P.P.Lottici and C.Razzetti

Istituto di Fisica dell'Università - Via d'Azeglio,85 - 43100 Parma
Gruppo Nazionale di Struttura della Materia del CNR.

The first order Raman scattering induced by the presence of divalent impurities in alkali halides has been recently investigated. In the case of KCl:Pb attention was paid in order to attribute the observed peaks to the impurity-vacancy (I.V.) dipoles, frozen in the sample by a suitable quenching from high T[1]. The effects induced on the Raman spectra by the presence of small aggregates of unknown symmetry and sizes is also reported[2].

In this work we are concerned with large aggregates (Suzuki-like phase occlusions[3] as suggested by ITC[4] and X-ray diffraction measurements[5]) built in KCl:Pb by long annealing in the range $150 \leq T_a \leq 250°C$ at the expense of I.V. dipoles. By proper choice of the annealing temperature and time[4], it is possible to select the size and the type of occlusions, and to check by means of Raman spectroscopy the change of symmetry and force constants induced by the nucleation process.

We have studied Raman spectra in parallel and perpendicular polarization for KCl:Pb ($\simeq 2 \times 10^{-4}$ m.f.) in which late stage of Suzuki-like occlusions is attained. Preliminary measurements have shown in the parallel z(yy)x polarization the occurrence of several impurity-induced peaks (62,76,84,90,102,116,151,219,246 cm^{-1}). In the z(yz)x geometry the same peaks with different relative intensities are present. A mode at 187 cm^{-1} present in z(yy)x geometry disappears in z(yz)x, where a 176 cm^{-1} mode is resolved. A scanning through the crystal with the laser beam has shown a strong spatial dependence of the Raman spectra, consistent with the inhomogeneous distribution of the occlusions themselves.
By comparing the $PbCl_2$ induced Raman spectra reported in the literature with our data, we have ruled out that the dominant spectrum could be attributed to $PbCl_2$ precipitation. Moreover it turns out that there is a

striking difference between our spectra and those reported by other authors[1,2] for I.V. dipoles or small aggregates. The crystal-like character (strong intensity, small width of the peaks) of our spectra is consistent with first order induced Raman scattering by large Suzuki-like occlusions.

The weak dependence of the spectra on the scattering geometry can be consistent with the fact that the Suzuki-like occlusions show quasi-crystalline structure with superlattice periods and are clustered together with antiphase relations among themselves[3]. The surrounding dislocations and stacking-faults patterns can be responsible as well of the unusual observed isotropy.

1. L.Marculescu, Solid State Phys. 7, 2387 (1974).
2. J.Höner zu Siederdissen, phys.stat.sol.(b) 73, 239 (1976).
3. K.Suzuki, J.Phys.Soc.Japan 10, 794 (1955).
4. R.Capelletti, A.Gainotti, J.Phys. 37, C7-316 (1976).
5. J.Z.Damm, Private Communication.

TWO PHOTON ABSORPTION OF COLOR CENTER IN NaF

M. Casalboni, G. Chiarotti*, U.M. Grassano* and A. Tanga*
Istituto di Fisica dell'Università di Roma, Roma, Italy

We report preliminary results of two photon absorption of F_3^+ and N_1 centers in NaF, measured at 1.06 μ.

The aggregate centers were obtained by u.v. irradiation of γ-rayed NaF samples. This treatment produced M, F_3^+, N_1 and N_2 centers with concentrations ranging from 10^{15} to 10^{16} cm^{-3}. The exciting light from a Q-switched Nd-Yag laser (2 kW peak power) was focussed on the sample and the absorption was monitored by synchronous detection of the emission collected at right angle and analysed by a double prism monochromator.

Laser excitation at 1.06 μ results in three broad emission bands (centered around 5750 Å, 6640 Å and 7750 Å) whose intensities increase quadratically with the laser power. The same emission bands, though with different intensities, were also detected with one photon excitation at twice the laser frequency. The excitation spectra of 5750 Å and 6640 Å bands coincide with the absorption of the F_3^+ and N_1 centers,[1,2] showing that the two photon absorption takes place in these centers. No definite interpretation has been found for the 7750 Å band.

The two photon absorption cross-section for the F_3^+ and N_1 centers are respectively: $\sigma(F_3^+)=7\cdot10^{-50}$ and $\sigma(N_1)=5\cdot10^{-49}$ cm^4 sec $photon^{-1}$ $center^{-1}$.

A broad emission was also found in the region of the laser line, both in the above NaF samples and in additively colored KCl containing only F-centers. Analogous emission has been

found in KCl and attributed to two photon absorption of F centers.[3] However the emission intensity depends linearly upon the laser power, so that we are more inclined to attribute it to luminescence coming from "hot" electrons. In this way, the process is similar to that assumed to explain the scattering background of Raman spectra in systems containing shallow electron traps.[4]

REFERENCES

* Gruppo Nazionale di Struttura della Materia del C.N.R.

1. L.F. Stiles Jr. and D.B. Fitchen, Phys. Rev. Letters 17, 689 (1966).
2. A. Chandra and D.F. Holcomb, J. Chem. Phys. 51, 1509 (1969).
3. F. De Martini, G. Giuliani and P. Mataloni, Phys. Rev. Letters 35, 1464 (1975).
4. V. Mazzacurati and G. Signorelli, Lettere al Nuovo Cimento 12, 347 (1975).

OPTICAL PROPERTIES OF NaBr:Tl^+

M. Casalboni, U.M. Grassano*, A. Scacco and A. Tanga*
Istituto di Fisica, Università di Roma, Roma, Italy

The thallium doped sodium halides have been studied much less than the analogous potassium halides and in particular the optical data on NaBr:Tl^+ are very incomplete. Therefore we have measured and analysed the absorption and emission spectra of NaBr:Tl^+ at various temperatures.

The absorption spectra at liquid helium, L He T; liquid nitrogen LNT and room temperature RT are plotted in Fig. 1. The A, B and C absorption bands are clearly visible, but no resolved structure was found in the A or C bands. The behaviour is quite analogous to that of KBr:Tl^+ as expected because of the similarity of the size of the octahedral "quasi" molecules formed by Tl^+ and its six nearest neighbours. The absorption data, and their analisys with the method of moments,[1] yield information on the parameters entering the Hamiltonian of the thallium centers. The values of the energy peaks, of ratio R of the dipole strenght of the C and A bands, of the exchange integral G, of the spin orbit splitting φ and of parameters a^2 and $2b^2+3c^2$ describing the electron-lattice coupling are summarized in Table I together with the analogous quantities for KBr taken from the literature.

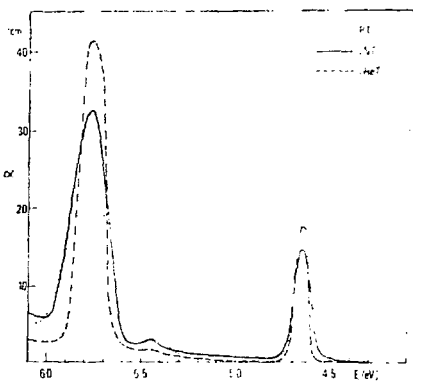

Fig. 1

The emission properties on the contrary are quite different from those of KBr:Tl^+. Two emission bands are excited with A band light. The main band, A_T, around 4.1 eV, is a resolved doublet; the smaller band, A_X, appears at 3.65 eV and does not increase with temperature as does the A_X emission in KBr. The

TABLE I

	E_A (eV)	E_B (eV)	E_C (eV)	R	G (eV)	φ (eV)	a^2 (eV)	$2b^2+3c^2$ (eV)
NaBr	4.67	5.44	5.76	3.6	0.183	0.527	0.53	3.51
KBr	4.81	5.60	5.93	4	0.197	0.551	0.25	2.45

splitting of the A_T components increases as $\sqrt{T}$ in agreement with the theory of the Jahn-Teller splitting of the emission bands.[2]

Time resolved emission spectroscopy was obtained recording the emission spectra at fixed delay times after the excitation. The spectral resolution of this emission, shown in fig. 2, is much poorer than that used in the study of the temperature splitting of the A_T band. It is however sufficient to show that both the A_T and A_X bands present "fast" emission components ($\tau_f < 1\,\mu s$), while the "slow" emission ($\tau_s \simeq 2$ ms) coincides with the high energy peak of the A_T doublet. These results, indicate the presence of a trap level under one of relaxed excited states responsible of the A_T emission.

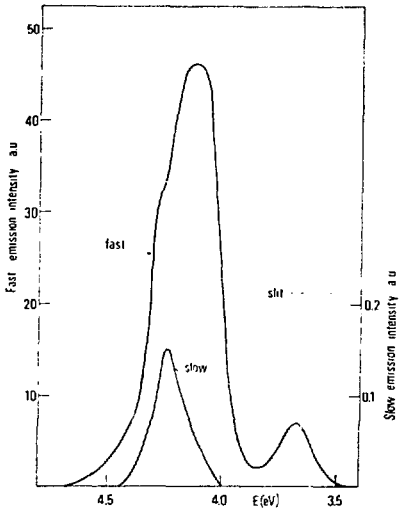

Fig. 2

REFERENCES

* Also: Gruppo Nazionale di Struttura della Materia of the C.N.R.

1. A. Honma, J. Phys. Soc. Japan 24, 1082 (1968).
2. M. Bacci, B.D. Bhattacharyya, A. Ranfagni and G. Viliani, Phys. Lett. 55A, 489 (1976).

PLASTIC DEFORMATION OF NiO SINGLE CRYSTAL IN THE VICINITY OF THE NEEL TEMPERATURE

J.CASTAING and M.SPENDEL
Laboratoire de Physique des Matériaux
C.N.R.S. Bellevue 92190 MEUDON(France)

Below 250°C, NiO shows antiferromagnetic ordering with domains appearing because of a slight rhombohedral deformation of the unit cell(1). Domain structure was observed by several techniques, including neutron topography(2).Transmission electron microscopy revealed domain wall-dislocation interactions(3). Elastic and plastic properties showed anomalous behaviour in the vicinity of the Néel temperature;a sudden increase in the hardness and,possibly,an athermal dislocation glide have been observed when the temperature is raised(4).

Plastic deformation experiments were performed on various types of crystals. The crystal perfection has been observed to greatly influence the mechanical behaviour. Dislocation microstructure observation allows to suggest a glide control mechanism.

(1) W.L. ROTH, J. Appl. Phys. 31 (1960) 2000
(2) J. BARUCHEL, M. SCHLENKER and W.L. ROTH, J. Appl. Phys. 48(1977) 5
(3) G. REMAUT, P. DELAVIGNETTE, A. LAGASSE and S. AMELINCKX, Phys. Stat. Sol. 11 (1965) 329
(4) A. DOMINGUEZ-RODRIGUEZ, J. CASTAING and J. PHILIBERT, Mat. Sci. Eng. 27 (1977) 217

PHASE TRANSITIONS IN KCN, NaCN AND RbCN CRYSTALS. THE OCN^- VIBRATIONAL SPECTRUM

J. C. Castro, H. C. Basso, M. Siu Li, and Milton de Souza
Instituto de Física e Química de São Carlos
Universidade de São Paulo
13560 - São Carlos, SP, Brasil

The cyanate ion, OCN^- occurs as a subsitutional impurity in the single crystals of the alkali cyanides grown from pro analysis salts. The vibrational spectra of the OCN^- impurity in these cyanides was used to follow the two phase transitions of the pure cyanides and of the mixed KCN-KCl and NaCN-KCN single crystals. The bending mode, degenerated in the cubic phase of these crystals, shows splittings in each of the two phases (see Fig.1). The Fermi resonance is very sensitive to the lower phase transition and insensitiv- to the ferroelastic transition.

By application of uniaxial stress during the ferroelastic phase transition approximately 95% of the CN^- ions become aligned in the orthorombic phase (see Fig.2). Differently of the polidomain orthorombic phase the visible light scattering is very low allowing optical measurments in the visible and u.v. region of the spectrum due to point defects. Studying these aligned crystals the CN^- and OCN^- alignment direction was determined to be the (110) direction of the cubic cell. The dichroic spectrum of the CN^- stretching was measured in a wide

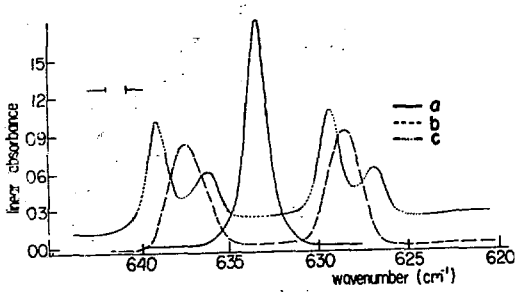

Fig.1- OCN^- bending mode spectra for the three phases of pure KCN. Curves a, b, and c were measured at R.T. (cubic phase), 90°K (orthorombic phase) and 4°K (lower temperature phase) respectively.

temperature interval without appreciable change.

The lattice distortion due to the two phase transitions was detected and found to be dependent of the alkali ion of the lattice, as shown in Fig.3. The two phase transitions were studied in the mixed crystals as a function of the CN^- concentration.

* Work supported by Fundação de Amparo à Pesquisa do Estado de São Paulo (FAPESP).

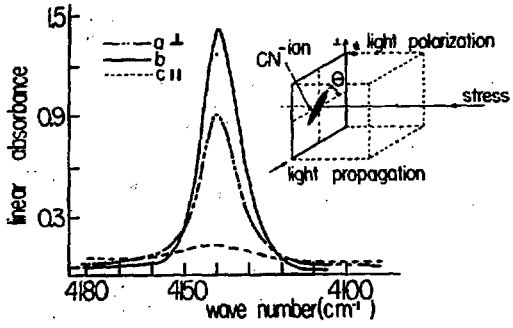

Fig.2- Dichroic spectrum of the second harmonic of the CN^- stretching vibration in aligned orthorombic phase of KCN 18% KCl single crystal. Alignment was obtained by application of uniaxial stress during the cubic to orthorombic phase transition. The OCN^- spectra also become dichroic due to the alignment of the OCN^- ion pararel to the CN^- lattice ions.

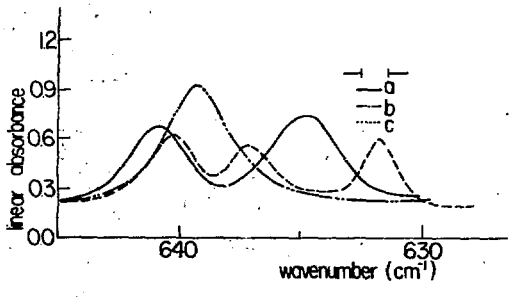

Fig.3- OCN^- bending mode spectra for the three phases of pure NaCN. Curves b, a, and c were measured at R.T. (cubic phase), 250°K (orthorombic phase) and 77°K (lower temperature phase) respectively. By application of uniaxial stress the OCN^- spectra also becomes dichroic allowing to know the OCN^- alignment direction.

A THEORETICAL STUDY OF ALKALI HALIDE CRYSTALS CONTAINING UNIVALENT IMPURITY IONS

C.R.A. Catlow, University College, London, U.K.
J. Corish, University College, Dublin, Ireland
K.M. Diller, AERE Harwell, Oxfordshire, U.K.
P.W.M. Jacobs, University of Western Ontario, London, Canada
M.J. Norgett, AERE Harwell, Oxfordshire, U.K.
B.M.C. Parker, University College, Dublin, Ireland

We have carried out an extensive theoretical study of a series of alkali halide crystals with univalent substitutional cations or anions. The systems investigated were: (a) Li^+ in the twelve alkali halides with the rock-salt structure which do not have Li^+ as the host cation; (b) $KF:Na^+$; (c) F^- in KCl, NaBr, KBr, RbBr, NaI, KI, and RbI; and (d) $KBr:Cl^-$ and $KCl:Br^-$.

We have used two sets of potential parameters both based on the shell model and determined recently for the alkali halides[1]. These potentials employ electron-gas estimates of the pairwise repulsive interactions and are fitted to represent accurately the equilibrium, elastic and dielectric properties of the crystals. The first set uses a Buckingham potential and the second a more flexible splined form which allows a coherent representation of the whole series of alkali halides. They were developed specifically to provide an interaction valid over the range of interionic separations encountered in crystals locally perturbed by lattice defects and have recently proved equal to the very demanding test of producing calculated defect formation and migration enthalpies in excellent agreement with experimental values[2,3]. We have obtained the extra potential parameters required for interactions involving the impurity ions either from a separate electron-gas calculation or by using the geometric mean rule for both repulsive and attractive parts.

We have made all calculations using the HADES package[4] which has now been applied successfully to a wide variety of defect studies. The method is that first introduced by Mott and Littleton[5]. In region 1, which includes the defect, the ions are allowed to relax to zero force. Fast matrix minimization techniques are used to obtain the equilibrium configuration. Because of the small energy changes involved in some of

these systems we have taken particular care to consider exactly the same number of ions in every calculation. By progressively increasing the number of ions which are treated explicitly in the inner region we have found the inclusion of 82 ions here to be adequate for consistent results. The remainder of the crystal is treated as a dielectric continuum. HADES gives detailed information on the energy of the system and on the positions of each ion in the equilibrium configuration. We have searched for equilibrium locations of the impurity ions along the <100>, <110> and <111> directions.

For the cation impurities we find complete agreement between our calculations and the available experimental data[6]. Our calculations also indicate that paraelectric behaviour by the Li^+ ion might be expected in some other systems. We have also investigated the effect of a contracted lattice for the KCl:Li^+ system. For the anion-impurity systems we again find good agreement between our calculations and experimental data with respect to the presence of paraelectric centres although here the calculated energies for <110> and <111> off-centre displacements in some systems are very similar.

References

1. C.R.A. Catlow, K.M. Diller and M.J. Norgett, AERE Harwell, Oxon., U.K., Report TP672, 1976.
2. C.R.A. Catlow, J. Corish, K.M. Diller, P.W.M. Jacobs and M.J. Norgett, J. Phys. (Paris) in the press.
3. C.R.A. Catlow, J. Corish, K.M. Diller, P.W.M. Jacobs and M.J. Norgett, in course of publication.
4. M.J. Norgett, AERE Harwell, Oxon., U.K., Report R7650, 1974.
5. N.F. Mott and M.J. Littleton, Trans. Far. Soc., 34, 485, 1938.
6. F. Bridges, CRC Crit. Rev. Solid State Sci., 5, 1, 1975.

DISORDER IN NON-CUBIC OXIDES

by C.R.A. Catlow and R. James,
Department of Chemistry,
University College London, U.K.

We present results of an extensive survey of defect energetics in two major types of non-cubic oxide - first rutile structured crystals, e.g. TiO_2, and secondly, crystals with the corundum structure, e.g. Al_2O_3. The results allow us to construct models of the defect structure of pure and doped crystals which will be of value in discussing transport, structural and thermodynamic data in both classes of crystal.

Our calculations use the HADES program[1] - a module of proven efficiency and reliability, which has been successfully applied to analogous investigations for cubic oxides[2]. We obtain the lattice potentials necessary for the defect simulations by fitting to empirical crystal data, including structural, elastic and dielectric properties. This fitting procedure uses a second program, PLUTO, which is briefly discussed, owing to its wide range of applications to the study of lattice potentials in non-cubic crystals.

With the aid of our calculated defect energies we discuss the following fundamental problems in the defect physics of these materials.

1. The nature of the predominant intrinsic defects, i.e. whether Frenkel or Schottky disorder dominates in the pure stoichiometric crystals.

2. The point defect structure of doped or non-stoichiometric materials.

3. The mechanisms of atomic transport, and their variation with temperature and composition. Here we use our results to discuss and analyse the available diffusion and conductivity data; related experimental observations, e.g. studies of oxide film growth are also considered.

4. The relationship between the point and extended defect structures of the rutile oxides. The observation in electron microscopy studies[3] of the extended, shear plane structures in reduced TiO_2 is a major problem in the solid state chemistry of these oxides. Results of calculations of the energies of these structures which will be reported together with our point defect energies allow us to assess the importance of a number of different factors (e.g. polarisability and relaxation effects) in stabilising extended defects.

Finally, we discuss briefly electronic defects present in non-stoichiometric crystals, e.g. TiO_{2-x}, and the interaction between these species and the atomic disorder.

References

(1) Lidiard A.B. and Norgett M.J., in Computational Solid State Physics (eds F. Herman et al., Plenum Press, New York, 1971).

(2) Catlow C.R.A. and Fender B.E.F., J. Phys. C., 8, 3267 (1975).

(3) Bursill L.A. and Hyde B.G., Prog. Solid State Chem., 7, 177 (1972).

SINGLE-CRYSTAL NEUTRON DIFFRACTION STUDY OF α-AgI BETWEEN 160° AND 300°C

R.J. Cava*, F. Reidinger**, and B.J. Wuensch*

*Department of Materials Science and Engineering, Massachusetts Institute of Technology, Cambridge, Mass.02139

**Chemistry Department, Brookhaven National Laboratory, Upton, Long Island, N.Y. 11973

Several different models have been proposed for the distribution of the conducting silver ions within the body-centered iodine ion array in the superionic conductor α-AgI (space group Im3m). These models involve either the occupancy of the 24(g) x0½ site, or distribution over the octahedrally coordinated 6(b) 0½½, tetrahedrally coordinated 12(d) ¼0½, and triangularly coordinated 24(h) 0xx sites. These models are based upon the limited number of structure factors obtainable via powder diffraction methods. Recently, Cava & Wuensch[1] successfully nucleated single crystals of the α form for an x-ray study which indicated that the bulk of the cations are confined to an anharmonic distribution around the tetrahedral site, but refinement was limited to R = 12.9%. The cation distribution in AgI is closely related to the distribution of H and D in the group VB metal hydrides which Reidinger[2] has extensively investigated through neutron diffraction.

Neutron diffraction measurements were conducted on a four-circle diffractometer at the High Flux Beam Reactor at BNL using Ge(220) - monochromated neutrons of wavelength 1.1598 Å. Single crystals of the β form, grown from solution, were transformed in situ on the diffractometer to single crystals of the α form by strongly directional heating. The crystal was studied at four temperatures: 160°, 200°, 240° and 300° C, at which, respectively, 25, 18, 21, and 19 of the 28 reflections within $2\theta<109°$ were significant (>σ). Agreement between equivalent structure factors was within 1% after standard data reduction, including correction for absorption (μR=0.06).

Refinement was carried out at BNL using Johnson's program ORSFLS, which allows incorporation and refinement of third- and fourth-order thermal tensors. Partial Fourier synthesis of the Ag scattering density

at all four temperatures studied indicate that the tetrahedrally-coordinated site at ¼¼0 is the equilibrium site for silver. The octahedral site at ½½0 is a local minimum in density. Appreciable density appears at a site near 0.39 0.39 0, a 3-coordinated bridging site which displays the characteristics of a saddle point. We attempted to quantitatively describe this complex distribution with several models. The model which gave the best agreement (R = 1.4% at 160°C) was one in which third- and fourth-order thermal tensors were applied to silver placed solely in the tetrahedral site, and a fourth-order thermal tensor was applied to the iodine ion. This model accounted completely for the observed density; difference maps were essentially featureless. This description was significantly better than the model of Bührer & Hälg[3] (R = 3.6%) or one with partial site occupancies of 12(d) and 24(h) (R = 2.7%). The fact that the octahedral site is a local minimum in density clearly rules out models which involve occupancy of that site, as proposed by Strock[4] and Burley[5].

The iodine array is greatly distorted as evidenced by large harmonic thermal parameters ($\langle \bar{u}^2 \rangle$ = 0.0999 and 0.133 $\mathring{A}^2$ at 160° and 300°C, respectively) and significant anharmonic thermal parameters (in marked contrast to the bcc metal atoms in VD_x^2). The characteristics of the silver density around the site at 0,39 0.39 0 strongly suggest that diffusion between neighboring tetrahedral sites occurs by a jump through this position. The fact that satisfactory description of the silver density requires highly significant third- and fourth-order thermal parameters to a tetrahedrally-coordinated Ag ion leads us to conclude that the motion of the silver is severely anharmonic. This questions the assumption that the diffusional and vibrational motion are independent, which has been basic in the interpretation of quasi-elastic neutron scattering data.

1. R.J. Cava & B.J. Wuensch. Superionic Conductors, p.217. G.D. Mahan & W.L. Roth, Eds. Plenum Press, N.Y., 1976(abstr.). Submitted to Acta Cryst. 2. F. Reidinger, J.J. Reilly & R.W. Stoenner. Superionic Conductors, ibid., p. 427. 3. W. Bührer & W. Hälg. Helv. Phys. Acta 47, 27(1974). 4. L.W. Strock, Z. Physik. Chem. B25, 411(1934); B31, 132(1936). 5. G. Burley. Acta Cryst. 23, 1(1967).

DEFECT CHEMISTRY OF $SrTiO_3$

N.-H. Chan and D. M. Smyth
Materials Research Center
Lehigh University
Bethlehem, Pa. 18015

The equilibrium defect chemistry of $SrTiO_3$ has previously been studied only at low oxygen partial pressures where it is an n-type semiconductor. Both the electrical conductivity, in equilibrium with H_2O/H_2 mixtures with ratios between 10^{-4} and 10^{-1} at 900-1300°C (1), and the electron concentration determined by room temperature Hall measurements made on samples quenched from equilibrium with oxygen partial pressures between 10^{-11} and 10^{-7} atm at 1200-1400°C (2), are proportional to $P_{O_2}^{-1/6}$. This suggests that the predominant defects are doubly ionized oxygen vacancies and electrons, and this model is supported by density measurements (2). The conductivity levels are similar to those reported for $BaTiO_3$ under similar conditions, and the dependencies on P_{O_2} and temperature are also similar (3, 4, 5).

The conductivity measurements have been extended to P_{O_2} = 1 atm for polycrystalline samples having controlled Sr/Ti ratios and added impurity contents. P_{O_2} was established by $Ar-O_2$, and $CO-CO_2$ mixtures, and by means of a controllable electrochemical oxygen leak and activity detector based on CaO-doped ZrO_2. As in the case of $BaTiO_3$, the conductivity for undoped and acceptor-doped material is proportional to $P_{O_2}^{1/4}$ near 1 atm., indicating p-type conduction and a stoichiometric excess of oxygen. As P_{O_2} is reduced, the conductivity passes through a minimum to an extensive region when the dependence is $P_{O_2}^{-1/4}$, before reaching $P_{O_2}^{-1/6}$ at the lowest P_{O_2} and highest temperatures. This is in agreement with a model in which the near-stoichiometric region, where the conductivity is proportional to $P_{O_2}^{\pm 1/4}$, is dominated by acceptor impurities, either accidental or added, with oxygen vacancies for charge compensation. This is to be expected in the undoped

material since acceptor type impurities, e.g. Al'_{Ti}, Fe'_{Ti}, Mg''_{Ti}, Na'_{Ba}, K'_{Ba}, etc., are naturally more abundant than donor-type impurities, e.g. $Nb^{\cdot}_{Ti}$, $Ta^{\cdot}_{Ti}$, $W^{\cdot\cdot}_{Ti}$, $La^{\cdot}_{Ba}$, $Th^{\cdot\cdot}_{Ba}$, etc.

For a sample containing an excess of added donor impurity (Nb), and a Sr/Ti ratio of unity, the conductivity is higher and has little or no dependence on P_{O_2} except at the lowest pressures, indicating that the net positive charge of the donor impurities is compensated by electrons in the near-stoichiometric region, rather than by an ionic defect. The Sr/Ti ratio has a particularly strong effect on the behavior of donor-doped samples.

(This work was supported by the Division of Materials Research of the National Science Foundation.)

REFERENCES

1. L. C. Walters and R. E. Grace, J. Phys. Chem. Solids 28, 239(1967).

2. H. Yamada and G. R. Miller, J. Solid State Chem. 6, 169(1973).

3. S. A. Long and R. N. Blumenthal, J. Amer. Ceram. Soc. 54, 515 (1971).

4. A. M. J. H. Seuter, Philips Res. Rpts., Suppl. No. 3 (1974).

5. N.-H. Chan and D. M. Smyth, J. Electrochem. Soc. 123, 1585 (1976).

Bi-EXCITON LUMINESCENCE FROM NaCl

P.J. Chandler, P.D. Townsend, and M. Aguilar*
University of Sussex, Brighton BN1 9QH England

Ukai et al [1] made the interesting suggestion that the luminescence produced in Na Cl near 500 nm during ion beam bombardment resulted from decay of a bi-exciton. Their data suggested the excited state had a long lifetime and was generated more efficiently at increasing ion beam dose rates.

To test this model we have changed flux conditions by comparing the emission induced by ion and molecular beam irradiation. The latter produces a much greater flux in a localised crystal volume without increasing the total power delivered to the crystal under steady beam conditions.

The ion beam results, together with results obtained by low energy electron simulation lead us to disagree with the Ukai model as we find no evidence that the 500 nm signal increases more than linearly with ion beam current density. However there is strong evidence that the emission efficiency changes with total accumulated dose at a different rate from that noted for the V_K emission and one must make absolute intensity measurements and not use the V_K emission as an intensity reference. Our data indicates there are changes in excited state lifetimes induced by the duty cycle of modulated beams and peak beam current. These parameters also change the emission spectra. Further, the signals are sensitive to impurities and in the case of Na Cl the emission spectrum is composed of several overlapping features. The main 500 nm emission may be a higher state transition of the normal self trapped exciton [2] and in addition we have evidence for the emission from O_2^- impurities [3] and impurity modified π state emission of excitons.

1. Ukai T., Matsunami, N. Morita K., and Itoh, N 1976 Phys. Letters 56A 127-9

2. Song, K.S., Stoneham, A.M., and Harker A.H., 1975 J. Phys. C8 1125-35

3. Rolfe, J., Lipsett, F.R. and King, W.J. 1961 Phys. Rev. 123 447-454

* Permanent address Optica y Estructura de la Materia C IV
Universidad Autonoma de Madrid
Canto Blanco, Spain

FIELD EFFECTS IN THE THERMAL DECOMPOSITION OF POTASSIUM AZIDE*

H. Chaya and B. S. H. Royce
Materials Laboratory--Princeton University
Princeton, N. J. 08540 U.S.A.

Potassium azide is a metastable solid which may thermally decompose to yield nitrogen gas and potassium metal. Application of an electric field has been shown (1) to enhance the decomposition rate at a given temperature. Experimental studies will be reported in which a surface ionization gauge and mass spectrometer were used to extend the preliminary measurements. A differentially pumped ultra high vacuum system was employed and nitrogen and potassium evolution from opposite faces of a single crystal were monitored. It was found that the presence of a field caused the potassium vapor to be evolved at a much higher rate from the negative crystal face, whereas nitrogen evolution was enhanced at both the positive and negative faces. The dependence of the steady state evolution rates on applied voltage for both potassium and nitrogen are shown in Figures 1 and 2.

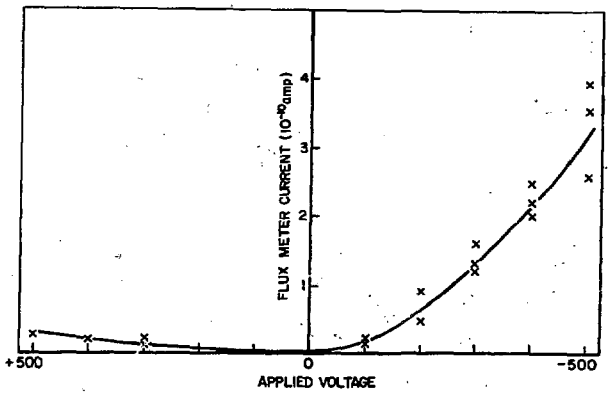

Fig. 1 Dependence of enhanced potassium evolution on applied voltage

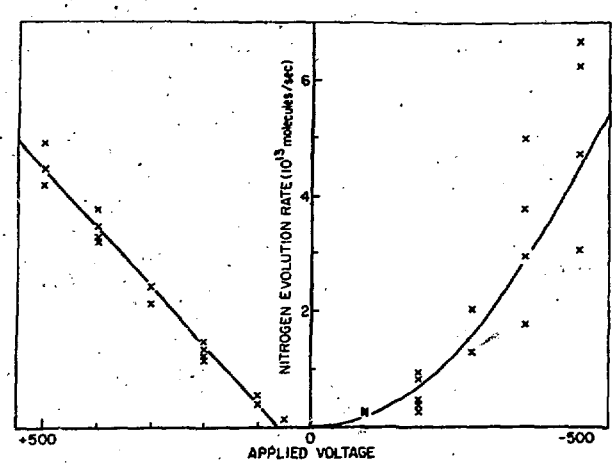

Fig. 2 Dependence of the enhanced rate of nitrogen evolution on applied voltage

The transient response of the nitrogen evolution upon the application of the field was also found to depend upon the sign of the field at the crystal surface being monitored.

The implication of these observations to proposed models for thermal decomposition will be discussed.

References

(1) A. dePanafieu, B.S.H. Royce and T. Russell J. Chem. Phys 64 (1976) 1473.

INVITED PAPER

RADIATION EFFECTS IN MgO*

Yok Chen
Solid State Division, Oak Ridge National Laboratory
Oak Ridge, Tennessee

Essential for modern energy conversion devices is the availability of materials which can withstand hostile environments, such as a radiation field. In order to understand the effects of radiation and the damage it produces in crystalline materials, it is important to identify defects produced by irradiation. Emphasis will be placed on three intrinsic defects in MgO: anion vacancies (F and F^+ centers), anion divacancies (F_2) and cation vacancies (V^- and VO). The identification of the defects,[2] using optical and magnetic resonance studies, and the description of the production mechanism occurred during electron, neutron, and ion[1] bombardment will be reviewed.

Unlike the case in alkali halides, anion vacancies and divacancies in MgO are produced primarily by a knock-on mechanism. The strong energy dependence of the production of these defects on the incident electron energy, with an observed threshold energy, demonstrates that elastic collisions are involved. In $\sim$ 2 MeV electron-irradiated crystals, primarily anion vacancies are observed. For irradiation with heavy particles, such as neutrons and ions, cluster defects are produced as evidenced by numerous optical absorption bands. Comparison of the optical absorption measurements in MgO irradiated with 14-MeV neutrons from the DT fusion source at Lawrence Livermore Laboratory with those obtained for fission neutrons (> 0.1 MeV) indicates that the defect production rate for 14-MeV neutrons is twice that for fission spectrum neutrons. Suppression of radiation damage can be attained by doping MgO with lithium.

Unlike the anion vacancy antimorph, the cation vacancy is formed by an *ionizing* process causing the displacement of hydrogen (or deuterium) from substitutional sites (V^-_{OH} center). The normally stable configuration of substitutional hydrogen and deuterium becomes highly unstable during ionizing irradiation. The cross section for displacement of hydrogen is a strong function of the irradiation temperature, being $\sim 10^8$ b at 290 K and $\sim 10^6$ b at 85 K. The displacement cross section of hydrogen at 290 K is twice that of deuterium.[2] This is the only known mechanism by which cation vacancies are formed. There is no evidence that thermal quenching or knock-on damage of hydrogen-free MgO results in the formation of stable cation vacancy. Irradiation with energetic electrons, neutrons or ions does not produce any indication of the presence of cation vacancies. Furthermore, even though plastic deformation produces anion-vacancy defects it does not produce cation vacancies.

*Research sponsored by ERDA under contract with Union Carbide Corporation.

[1] B. D. Evans, Phys. Rev. B 9, 5222 (1974).

[2] Y. Chen, M. M. Abraham and H. T. Tohver, Phys. Rev. Lett. 37, 1757 (1976).

PRODUCTION AND STABILITY OF [Li]° DEFECTS IN MgO SINGLE CRYSTALS*

Y. Chen, H. T. Tohver,† J. Narayan and M. M. Abraham
Solid State Division, Oak Ridge National Laboratory
Oak Ridge, Tennessee 37830, USA

Quenching a lithium-doped MgO crystal from high temperature, or performing a high-dose electron irradiation produces [Li]° defects.[1] In contrast to the [Li]° center formed by low-temperature γ irradiation, the hole is tightly bound to the aliovalent Li^+ ion in the quenched and electron-irradiated crystals. Investigations using EPR and ENDOR techniques at 4.2 K have established that, in both cases, the stable [Li]° centers generated have the same local electronic configuration as the unstable centers created at low temperatures. Furthermore, a motionally averaged spectrum was observed at high temperatures for the stable [Li]° system, verifying that a centrosymmetric system is indeed involved and no axial impurity charge compensation is present. An optical absorption band at 1.83 eV has been correlated with the [Li]° defect.[2]

An as-grown Li-doped crystal was used to study the thermal generation of [Li]° defects. The sample was heated isochronally for 10 minutes in air at an elevated temperature, followed by a quench into a liquid nitrogen bath. This procedure was repeated at increasing temperatures. The absorption coefficient of the 1.83 eV band after each heat treatment is plotted as a function of the annealing temperature (Fig. 1). [Li]° defects began to appear at 1300 K and rapidly increased until 1500 K; beyond this temperature saturation began to take place. The defects were generated thermally, without subsequent irradiations of any form.

In order to determine the stability of the [Li]° centers, we performed isochronal annealing on samples in which the defects were produced by the three methods. Fig. 2(a) illustrates the annealing behavoir of the [Li]° center in a crystal which was γ irradiated at 77 K. These measurements were made by EPR. Curve (b) represents the annealing data of the 1.83 eV band in a crystal which was irradiated at 290 K to a dose of $5 \times 10^{18} e/cm^2$. Curve (c) illustrates the

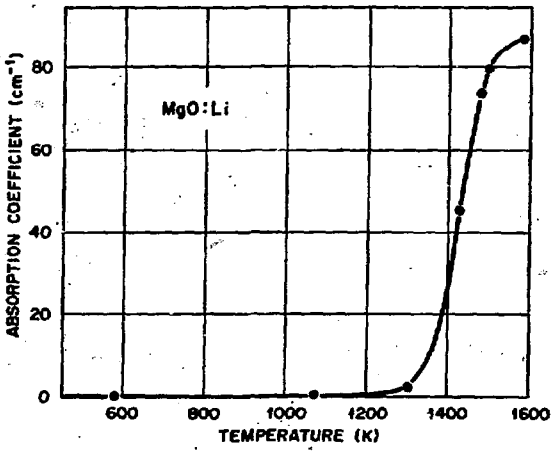

Fig. 1 Production of [Li]° Centers by Quenching

stability of [Li]° centers generated by thermal quenching from 1420 K. The temperatures at which half of the defects have been annealed out for low-temperature ionizing irradiation, high-dose electron irradiation, and thermal quenching were ∿ 210, 450 and 830 K respectively.

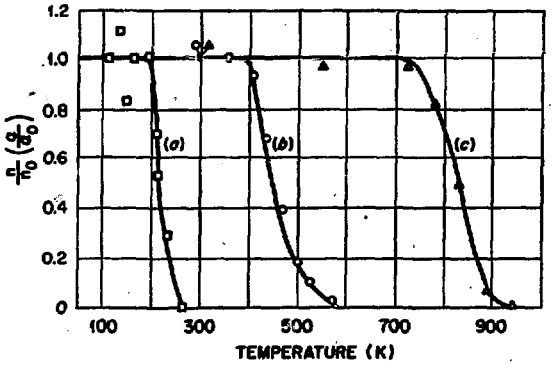

Fig. 2. Annealing of [Li]° Centers in MgO:Li Crystals

To explain the unexpected stability of the [Li]° defects, we propose that in slow-cooled (or as-grown) crystals, the lithium impurities are concentrated in precipitates. At high temperatures, each precipitate gives rise to a localized Li-rich environment surrounding the precipitate. The precipitate would, of course, diminish in size as a result. Within this "microgalaxy" of abundant substitutional Li^+ ions, charge neutrality requires that the natural state of the impurity be a Li^+ ion with a trapped hole, which is the neutral [Li]° center.

---

*Research sponsored by ERDA under contract with Union Carbide Corporation.

†On sabbatical leave from University of Alabama, Birmingham, Alabama.

[1] M. M. Abraham, Y. Chen, L. A. Boatner and R. W. Reynolds, Phys. Rev. Letters, 37, 849 (1976).

[2] F. A. Modine, Solid State Comm. 20, 1097 (1976).

OFF CENTER Cu^+ IN CsBr

B.V.R. Chowdari*
2. Physikalisches Institut, Universität Stuttgart, Germany and Department Of Physics, Indian Institute Of Technology MADRAS, INDIA
S. Radhakrishna and B. Ram Babu
Department Of Physics, Indian Institute Of Technology MADRAS, INDIA

The first indication for the possible off-center position of Cu^+ in alkali halides of NaCl type was obtained from the systematic optical absorption studies[1]. No data seem to be available regarding the location and the optical properties of Cu^+ in CsCl type crystals. In the present paper an evidence for the stabilization of Cu^+ at an off-center position displaced in ⟨111⟩ direction in CsBr crystals will be presented exclusively from the optical absorption studies.

Earlier studies of the optical absorption of Cu^+ in alkali halides of NaCl type have revealed maximum of five absorption bands. In the present studies of Cu^+ in CsBr crystals quenched from 500° C to room temperature nine absorption bands have been observed in the range of 4.87 eV and 6.15 eV. However, in the crystals annealed at 200° C only six bands are observed indicating the aggregation effects in unquenched crystals. When the impurity ion takes an off-center position, reduction of symmetry occurs which in turn lifts the degeneracy of certain otherwise degenerate levels and changes the selection rules. This results into a greater number of absorption bands than if the impurity is in on centered position.

All the observed transitions of Cu^+ should in principle be related to the electronic transitions from the ground state (^1S) arising from $3d^{10}$ configuration to the states ($^3D_{1,2,3}$ and $^1D_2$) arising from the excited $3d^9 4s$ configuration. In the crystal field of cubic symmetry, which corresponds to Cu^+ substituting Cs^+, the d^9s multiplet split into eight energy

*Alexander von Humboldt Fellow 1975-77.

levels giving rise to a maximum of only eight absorption bands. The crystals field of C_{4v} symmetry give rise to fifteen energy levels. Considering the mixing of the $^1T_{1u}$ term of the odd parity d^9p states with the d^{10} - d^9s even parity configuration as responsible for the otherwise parity forbidden transitions to become allowed, only seven transitions are expected. The substitutional impurity ion displaced along ⟨111⟩ direction give rise to a C_{3v} symmetric crystal field in which thirteen terms results out of which transitions to ten of them are allowed. Thus the crystal field of C_{3v} symmetry might nearly explain the observed number of bands of Cu^+ in CsBr.

Writing the total Hamiltonian $H=H_E + H_S$ where H_E and H_S are spin-independent and spin-orbit contributions, respectively, the matrix of $H_E + H_S$ has been calculated in SLJM representation following the procedure adopted by Knox[2] and Matsuyama et al[3] and the resulting 20x20 matrix has been diagonalized to obtain the term energies. The choice of cubic crystal field splitting parameter δ_c = -0.45 eV, and the parameter related to the additional field of C_{3v} symmetry δ_t = -0.055 eV gave good agreement between the theoretically predicted positions of the bands and the experimentally obtained ones. The accidental overlap of two of the energy states account for the observed nine bands. Thus it has been possible to show that Cu^+ in CsBr occupies an off center position in ⟨111⟩ direction.

References:

1. K. Fussganger, Phys.Stat.Sol.34,157(1969);36,645(1969)
2. R.S.Knox,J.Phys.Soc.Japan 18,Supp II,268(1963)
3. T.Matsuyama,M.Saidoh and N.Itoh,J.Phys.Soc.Japan 39,1486 (1975)

OPTICAL PROPERTIES OF COBALT CENTERS IN NH_4Cl

B.V.R. Chowdari*
2. Physikalisches Institut, Universität Stuttgart, Germany and Department Of Physics, Indian Institute Of Technology MADRAS, INDIA
S. Radhakrishna and B. Ram Babu
Department Of Physics, Indian Institute Of Technology MADRAS, INDIA

Earlier studies on transition metal-doped NH_4Cl crystals showed the possibility of different kinds of centers being stabilized depending upon the growth conditions[1-4]. It has also been shown that the phase transformation of NH_4Cl has remarkable effects on the optical properties of the substitutional and interstitial impurity ions[4]. It has been shown in the present paper that two interstitial Co^{2+} centers with different environments are stabilized in NH_4Cl depending upon the growth conditions. The values of the ligand-field splitting, electrostatic interaction and the spin-orbit coupling parameters of these two centers have been estimated.

Single crystals of NH_4Cl doped with Co^{2+} are grown from aqueous solution at about 42° C in neutral and acidic media separately[2].

The absorption spectrum of Co^{2+} consists of two groups of bands in the 16000 cm^{-1} and 19000 cm^{-1} regions. Finar details are different for differently grown crystals. The decrease in intensity of the bands as the temperature is lowered in the 300-10 K region indicates the vibrational induced nature of these transitions. Comparison of the spectra of neutral and acidic solution grown crystals shows the simultaneous existance of two different cobalt centers designated as centers I and II, the concentration of which depend upon growth conditions.

* Alexander von Humboldt Fellow 1975-1977

All the observed bands could be explained by considering the crystal field, electrostatic interaction and spin-orbit interaction. A good agreement between the experimentally observed positions and the theoretically obtained ones is found with the set of parameters D = 820 cm^{-1}, B = 880 cm^{-1}, C = 3300 cm^{-1} and S = 430 cm^{-1} for center I and D = 824 cm^{-1}, B = 900 cm^{-1}, C = 4150 cm^{-1} and S = 533 cm^{-1} for center II. In the neutral solution grown crystals where center II is predominantly present intense bands at 33886 cm^{-1} and 28169 cm^{-1} are observed and they have been assigned to charge transfer transitions.

An interstitial position of Co^{2+} in the plane of four Cl^- ions with two neutral H_2O molecules at the lattice cation sites in ⟨100⟩ direction is considered as the model for center I. Such a center will have predominantly octahedral crystal field. The difference in ionization potentials of NH_3 and H_2O explains the observation of charge transfer transitions associated with center II. In center II the H_2O molecules are replaced by NH_3 molecules.

References:

1. H.Hagen and N.J.Trappeniers, physica 31,122,251 (1965)
2. F.Boettcher and J.M.Spaeth, phys.stat.sol.61,465(1974)
3. P.A.Narayana and P.Venkateswarlu,proc.Ind.Acad.Sci 72,249(1970)
4. N.Kuroda and A.Kawarnori,J.phys. chem.solids 32,1233(1971)

THE ABSORPTION EDGE SPECTRA OF PURE AND MIXED ALKALI HALIDES BELOW AND ABOVE THE MELTING POINT

by C.D.Clark, A.H.Skull and Jenifer S. Wells
J.J.Thomson Physical Laboratory, University of Reading, U.K.

The optical absorption spectra of a number of alkali halides in the crystalline and molten states have been measured on the long wavelength side of the first exciton peak. Measurements were made in a temperature range of up to 200K below and above the melting point. The spectra are well described by the empirical Urbach Rule, $\mu(E) = \mu_0 \exp|\sigma(E-E_0)/kT|$, where μ_0, E_0 and σ are fitting parameters. Values of these parameters for pure alkali halides are given in the first table:

Substance	E_0(cryst)/eV	σ(cryst)	E_0(melt)/eV	σ(melt)
KI	5.890	0.830	4.71	0.65
KBr	6.840	0.774	5.51	0.53
KCl	7.834	0.745	6.22	0.63
NaCl	8.025	0.741	6.25	0.59
RbCl	7.51	-	6.05	0.51

The values E_0(cryst) and σ(cryst) given in the first table are those quoted by Tomiki et al (1974) with which the results of the present work generally are in good agreement. There is an abrupt reduction of E_0 of between 1.1 and 1.8eV on melting. σ is independent of the temperature in the pure alkali halides close to the melting point, with the exception of an abrupt increase in the broadening of the absorption edge on melting. The value of E_0 is assumed to correspond to the energy of the first exciton absorption line. It is suggested that the loss in long range order which occurs on melting is primarily responsible for the reduction in the energy (ΔE_0) of the first exciton peak, through the change in electrostatic energy of the system. This interpretation is in good agreement with changes in electrostatic energy predicted by computer simulations of the various molten salts.

Similar experiments have been carried out on KI doped with KBr, KCl or KF up to concentrations of 10 mol percent. In each case Urbach's rule

is followed but with different parameters μ_0', E_0' and σ' to those detailed earlier. Usually E_0' is somewhat lower than E_0 and also depends upon impurity concentration. σ (C,T) depends upon the impurity concentration C and shows a strong temperature dependence in the 200K range below the melting point. The results quoted in the second table refer to impurity concentrations of approximately 4 mol percent.

Mixture	E_0'(cryst)/eV	σ'(800K)	σ'(930K)	Melting point/K	σ'(melt)
KI:KF	$\sim$ 5.47	0.44	0.37	943	-
KI:KCl	$\sim$ 5.54	0.48	0.41	948	0.67
KI:KBr	$\sim$ 5.56	0.62	0.56	950	0.69

Notice that the broadening of the absorption edge may be greater in the crystal than it is in the melt |i.e. σ'(melt)>σ'(crystal)|. The degree of broadening in the crystalline state depends also on the mass ratio of the impurity ion and the host halide ion, the broadening being bigger the lighter the mass of the impurity ion.

It is thought that the broadening behaviour of the first exciton peak in KI is strongly influenced by the localised vibrational modes caused by the inclusion of lighter impurity ions. The impurity ion size also seems to be important for the substitution of Na^+ and Rb^+ on potassium ion sites gives results which are very similar to those observed for pure KI.

Comparison of these results with the results of computer simulation experiments will be discussed.

Tomiki,T., Miyata, R. and Tsukamoto,H., 1974, Z.Naturforsch., 29a, 145

EMISSION SPECTRA PRODUCED BY EXCITATION IN THE A, B, C AND D ABSORPTION BANDS OF KI:Sn^{2+}

Leighton L. Coatsworth, Patrick W.M. Jacobs and Yoshio Kamishina*
Department of Chemistry, University of Western Ontario
London, Ontario N6A 5B7, Canada

Most previous work on emission spectra from s^2 phosphors has concentrated on the A emission which corresponds to a transition from the relaxed excited state resulting from absorption in the A band. In the present study, experimental data on the emission spectra produced by excitation in the A, B, C and D band regions[1] of KI:Sn^{2+} in the temperature range 15 K to 300 K.

There are two strong emission bands at 2.23 eV and 2.39 eV which are produced by excitation into any of the above absorption bands at 15 K; their relative intensity depends strongly on excitation energy and also on temperature. Excitation into the lower energy (A_1) component of the A band at 3.51 eV yields maximum emission at 2.23 eV and a shoulder with a relative intensity of 0.85 at 2.39 eV. Excitation into the higher energy (A_2) component of the A band at 3.56 eV yields maximum emission at 2.39 eV and a shoulder with a relative intensity of 0.96 at 2.23 eV. On the other hand, B excitation at 3.75 eV yields an emission spectrum with two peaks of comparable intensity, at 2.26 eV and at 2.38 eV as well as extra emission bands at 1.88 eV with an intensity of 0.14 relative to the main peaks at 2.26 eV or 2.38 eV and at 3.15 eV with a relative intensity of 0.03. C_2-band excitation at 4.19 eV yields a main peak at 2.38 eV with a shoulder of 0.80 relative intensity at 2.23 eV, and extra peaks at 3.27 eV (relative intensity: 0.06), at 3.45 eV (0.06), and at 2.80 eV (0.02). C_3-band tail excitation at 4.36 eV yields a main peak at 2.37 eV with a shoulder of 0.70 relative intensity at 2.23 eV and small extra peaks at 3.03 eV (0.03), at 3.35 eV (0.02), and at 2.80 eV (0.02). D-band excitation at 4.787 eV yields a main peak at 2.24 eV with a shoulder (relative intensity: 0.68) at 2.40 eV, and extra peaks at 3.14 eV (0.10), at 2.80 eV (0.08), and at 3.66 eV (0.01).

These emission and excitation spectra are close to those measured by

---

* On leave of absence from Department of Physics, Kobe University, Kobe, Japan.

Fukuda[2]. There is one remarkable difference between them, however, and that is the extra emission peak at 1.88 eV. This band is produced by excitation in the B band but not by A or C band excitation. Though the photon energy of the emission band, 1.88 eV, is very close to half the excitation energy, 3.75 eV, this emission band is not due to second order diffraction in the grating monochrometer, but is a true emission band because the intensity of the emission changes with temperature. This emission band being the one of lowest energy so far discovered may be due to the transition $\Gamma_1^- \rightarrow \Gamma_1^+$ made allowed by mixing of Γ_1^- with Γ_3^- by lattice vibrations of E_g symmetry. As Γ_1^- does not couple with Γ_4^- this hypothesis is in agreement with the experimental observation that the 1.88 eV emission is produced by excitation in the B band but not in the A or C bands. The following table summarizes the experimental observations at 15 K.

Table 1

Relative intensity of the bands in the emission spectrum of KI:Sn^{2+} at 15 K. Symbols above the photon energies for the bands show the assignment of the relaxed excited state responsible for the emission.

	Γ_1^-?	A	A			B	C	C?	C	D
	1.88eV	2.23eV	2.39eV	2.80eV	3.03eV	3.14eV	3.25eV	3.35eV	3.45eV	3.66eV
A_1		1.0	0.85				0.03			
A_2		0.96	1.0				0.015			
B	0.14	1.0	1.0			0.025				
C_2		0.80	1.0	0.02			0.058		0.055	
C_3		0.70	1.0	0.018	0.03			0.02		
D		1.0	0.68	0.075		0.10				0.01

References

1. L. Coatsworth, P.W.M. Jacobs, Y. Kamishina and M.A. Millar, "Spectral Band Shape .... ", this conference.

2. A. Fukuda, Physics of Impurity Centres in Crystals (Acad. Sci. Estonian SSR, Tallinn 1972).

SPECTRAL BAND SHAPE FOR THE TRANSITION $a_{1g}^2 \rightarrow a_{1g}t_{1u}$ in Sn^{2+}-DOPED ALKALI HALIDE CRYSTALS

Leighton L. Coatsworth, Patrick W.M. Jacobs, Yoshio Kamishina* and Mary Anne Millar+
Department of Chemistry, University of Western Ontario
London, Ontario N6A 5B7, Canada

When an ionic impurity with the s^2 configuration in the ground state is incorporated in an alkali halide crystal three new bands designated A, B and C, which are due to the transition $a_{1g}^2 \rightarrow a_{1g}t_{1u}$, appear on the long wavelength of the intrinsic exciton absorption. When the impurity is a divalent ion the cation vacancies necessary for charge compensation may be situated near the divalent ions in a nearest neighbour (nn) or next nn position. If this is so the symmetry of the system will be lower than cubic and static splittings may occur. We are currently investigating the importance of this static splitting in the optical absorption lineshape which is governed mainly by the electron-lattice interaction (dynamical Jahn-Teller effect) in Sn^{2+}-doped alkali halide crystals.

Experimental data on the optical absorption lineshapes of the A, B and C bands in NaCl:Sn^{2+} and KI:Sn^{2+} in the temperature range ~10 K to 300 K will be presented and experimental lineshapes compared with those calculated from semiclassical theory. For the determination of parameters experimental lineshapes are resolved into the appropriate number of asymmetric Gaussian bands by using a non-linear least squares computer program. A typical computer plot of a resolved spectrum (after background subtraction) is shown in Fig. 1 for KI:Sn^{2+}.

Numerical values of energy parameters for NaCl:Sn^{2+} and KI:Sn^{2+} derived from experimental absorption spectra are given in Table 1; E_p denotes the value of the first moment of the p-band lineshape extrapolated to T = 0 K, R is the dipole strength ratio (Sugano's parameter) ζ the spin-orbit

---

* On leave of absence from Department of Physics, Kobe University, Kobe, Japan.

+ Present address: Department of Chemistry, McMaster University, Hamilton, Ontario L8S 4K1, Canada.

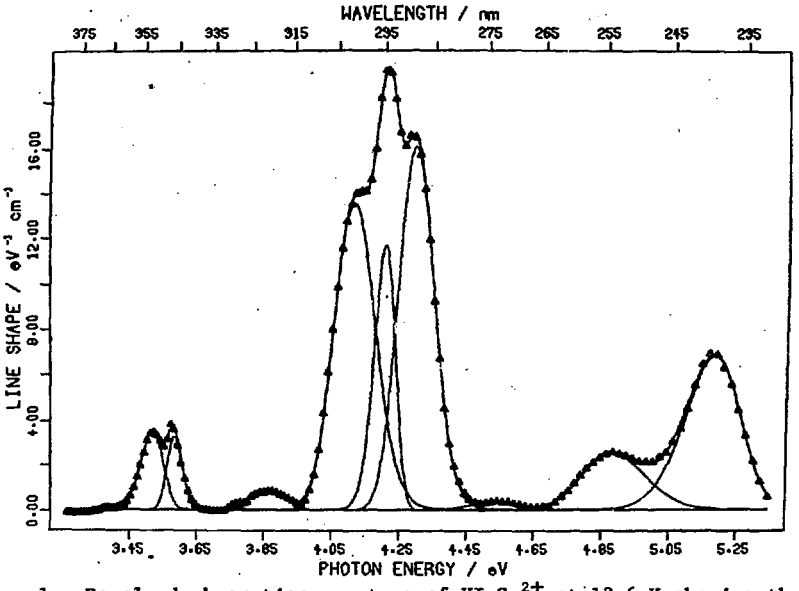

Figure 1. Resolved absorption spectrum of $KI:Sn^{2+}$ at 13.6 K showing the A, B, C and D bands.

coupling constant, G the exchange energy and λ the parameter introduced by King and Van Vleck to account for small differences between the radial functions in the singlet and triplet states.

The lineshapes of A and C bands are well accounted for by a model that allows for spin-orbit coupling and the dynamical Jahn-Teller effect in the excited states. The principal factor governing the lineshape is the coupling of the active electrons with lattice vibrations of T_{2g} symmetry but the agreement with experiment is much improved by the inclusion of coupling to lattice modes of A_{1g} symmetry, the static splitting, and the use of different (T_{2g}) force constants in the excited and ground states.

Table 1

	E_A/eV	E_B/eV	E_C/eV	R	ζ/eV	G/eV	λ
$NaCl:Sn^{2+}$	4.249	4.735	5.320	20.2	0.47	0.369	0.68
$KI:Sn^{2+}$	3.554	3.867	4.212	11.0	0.27	0.213	0.98

ELECTRON AND HOLE TRAPPING CENTERS IN IONIC OXIDES*

J. H. Crawford, Jr., K. H. Lee and G. S. White
University of North Carolina at Chapel Hill, 27514

The behavior of V- and F- type centers in Al_2O_3 and $MgAl_2O_4$ (spinel) whose binding is predominantly ionic is remarkably similar to that of their analogues in the simple cubic alkaline earth oxides, notwithstanding the considerably greater structural complexity of the former two materials. This paper discusses recent investigations involving optical absorption and emission spectra, ESR, optical bleaching and thermal stability of V- type centers in Al_2O_3 and $MgAl_2O_4$ after exposure to γ-rays. F- type centers have been similarly investigated in neutron irradiated cyrstals.

V- Type Centers: Oxygen ions adjacent to cation vacancies capture holes to form O^- ions. Optical excitation of these centers are responsible for the familiar 2.3 eV absorption band in MgO. In Al_2O_3 and $MgAl_2O_4$ these centers produce broad absorption bands at 3.0 eV[1] and 3.1 eV respectively. Partial compensation of the negative charge on the vacancy by a nearby extra positive charge (OH^- or M^{3+}) in a substitutional site only slightly perturbs the optical transition energy of the O^- but has a strong effect upon the thermal stability of the trapped hole. Evidence from infra-red spectra of OH^-[2], ESR[3], and thermoluminescence (TL) after various thermal treatments indicates the presence of three V- type centers in Al_2O_3. In order of increasing thermal stability these are the V^- (two holes trapped on the same vacancy), the V_{OH}^- (one hole trapped on a cation vacancy partially compensated by an adjacent substitutional OH^-) and the V^- (one hole trapped on a vacancy)[4]. There was no evidence for the V° three hole center even for 77K irradiations in pure Al_2O_3. Our $MgAl_2O_4$ crystals contained such a small OH^- concentration that V_{OH}^- type centers as revealed by infra-red spectra were not detectable. The TL peak associated with the thermal bleaching of the V- band complex is much broader than expected for a single trap; hence two or more V- type centers may be responsible for the 3.1 eV absorption. Although ESR spectra of the V centers in Al_2O_3 were distinct and were instrumental in the identification of the various species, such spectra

have yet to be isolated from the complex ESR data obtained on γ-irradiated spinel.

F- Type Centers: Neutron irradiated Al_2O_3 exhibits optical absorption bands at 5.4. 4.8 and 4.1 eV in addition to the well known intense band at 6.1 eV[5]. Irradiation into the 6.1 eV band enhances the other three, whereas excitation in these enhances the 6.1 eV band. On the basis of theoretical estimates, the relative oscillator strengths of the 4.8 and 6.1 eV bands and the polarization of emission upon excitation of the 4.8 eV band with polarized light; it is concluded that the 4.8 and 6.1 eV bands belong to the F^+ and F centers respectively[6]. Neutron irradiated $MgAl_2O_4$ exhibits, in addition to the V- band complex at 3.1 eV, bands at 5.4 and 6.1 eV. The 5.4 eV band is very stable being unaffected by either optical bleaching or γ-irradiation. The 6.1 eV band, however, is enhanced by optical bleaching into the V- band region and is reduced by γ-irradiation. There is some evidence for a band above 6.5 eV which is inversely related to the 6.1 eV band. Thus the 6.1 eV band is tentatively assigned to the F^+ center with the expectation that the F- center absorption lies further into the ultra violet.

1. F. T. Gamble, R. H. Bartram, C. G. Young, O. R. Gilliam, and P. W. Levy, Phys. Rev. 134, A589 (1964).
2. T. J. Turner and J. H. Crawford, Solid State Commun. 17, 107 (1975).
3. R. T. Cox, Solid State Commun. 9, 1989 (1971).
4. K. H. Lee, G. E. Holmberg, and J. H. Crawford, Jr., Phys. Stat. Sol. (a) 39, 669 (1977).
5. P. W. Levy, Phys. Rev. 123, 1226 (1961).
6. K. H. Lee and J. H. Crawford, Jr., Phys. Rev. 15, 4065 (1977).

*Supported by the Materials Research Center, UNC under Grant No. DMR 272-03024 from NSF.

JAHN-TELLER EFFECT IN THE $^3T_{1u}$ RELAXED EXCITED STATES OF Ga^+ IN KBr

Le Si Dang, R. Romestain and Y. Merle d'Aubigné
Laboratoire de Spectrométrie Physique
Boîte Postale 53 - 38041 GRENOBLE-CEDEX (France)

and A. Fukuda
Tokyo Institute of Technology
Department of Textile and Polymeric Materials
Meguro-Ku, TOKYO 152, Japan

Excitation into the A band ($^1A_{1g} \rightarrow {}^3T_{1u}$) produces two emission bands called A_T and A_X for most of Tl^+ - like ions in alkali halides [1]. In the present study we report investigations of A_T and A_X relaxed excited states (RES) of Ga^+ in KBr by means of : (i) magnetic circular polarization measurements, (ii) and microwave-optical double resonance technique.

A_T and A_X bands exhibit large magnetic circular polarization at very low temperature, and level crossing effects can be observed for appropriate orientations of the magnetic field. This provides a simple determination of the symmetry of the RES : tetragonal (along [100] directions) for A_T, and trigonal (along [111] directions) for A_X.

Electron paramagnetic resonance (EPR) spectra of both A_T and A_X RES can be described by a standard Spin Hamiltonian (S = 1, I = 3/2). It has been confirmed that A_X RES is of pure trigonal symmetry. However a small fine structure term E($\sim$ 0.1 D) is found for A_T RES, the principal axes being [100], [010] and [001].

The $^3T_{1u}$ excited states are strongly coupled to both E_g and T_{2g} modes. Assuming the existence of a quadratic orbit-lattice coupling it is shown that stable tetragonal and trigonal distortions are obtained and that they correspond to two different values of the totally symmetrical

configuration coordinate. Within this model, the temperature variation of the intensities of the A_T and A_X emission bands is well explained.

References

(1) A. Fukuda, Phys. Rev. B 1, 4161 (1970)

CATHODOLUMINESCENCE IN ZnS AND CdS CRYSTALS

S. Datta, D. B. Holt and I. M. Boswarva
Department of Metallurgy and Materials Science
Imperial College of Science and Technology, London, England

Studies of cathodoluminescence (CL) in these crystals have been carried out using a Cambridge IIA Stereoscan Scanning Electron Microscope. The associated light detector system is capable of detecting over the wavelength range 240 nm to 900 nm with a resolution of 2 nm. The response of the system varies considerably with wavelength and a computer program has been developed to obtain the corrected emission spectra from the measured data. Two modes of operation are used. With a limited area scan (of a few microns dimension) a detailed spectral analysis of the luminescence is measured.

Alternatively a larger area can be scanned and the photon counter signal passed to one of the scanned video screens to produce monochromatic or panchromatic CL micrographs.

Three aspects of these studies will be presented:-

1) Luminescence from Impurity Centres. In both cubic and hexagonal ZnS a) blue-Cu b) green-Cu c) red-Sn d) self-activated luminescence (SAL) bands have been observed. The temperature dependence in the range 78°K to 298°K and shape of the SAL band have been studied. The band is of Gaussian shape at the peak with exponential tails which become more pronounced at higher temperatures. Such a band shape is inexplicable in terms of the accepted Franck-Condon model which predicts a total single Gaussian shape at all temperatures.

2) CL Edge Emission Bands. These spectra from a) hexagonal CdS b) cubic ZnS c) hexagonal ZnS at both 78°K and 298°K have been measured. All these bands can be well described by the semi-empirical equation

$$I(E) = I(E_o)\exp[g(E-E_o)^{\beta}]$$

where E_o is the photon energy at the band maximum; g and β are shape parameters which take different values over a number of wavelength regions. In all cases on each side of the peaks the band is Gaussian but with differing values of g whilst on the low energy side two regions of exponential

dependence are observed (Urbach's Rule). The exponential region nearer the peak has been interpreted in terms of Dow and Redfield's internal electric microfields model and the second exponential region is believed to be due to donor impurity levels-to-valence band transitions.

3) CL Micrographs. In all previous work local CL variations have been attributed to i) structural changes ii) impurity segregation or iii) internal electric fields. If a series of monochromatic CL micrographs, for a number of wavelengths within the edge and impurity luminescence bands, is obtained for a selected area of a crystal the individual effects of the three influences can be deduced. In particular circumstances CL can prove to be a quick and effective method of assessing materials (e.g. phosphors, GaAs devices). For example our ZnS crystals are in the form of striated platelets containing regions of numerous polytype crystal structures. It is found that the edge emission band maximum varies with crystal structure (as identified by birefringence studies). Thus, once this relation has been determined CL can be used to quickly establish the distribution of phases in the sample.

SPIN POLARIZATION QUENCHING OF TUNNELING RECOMBINATION LUMINESCENCE BETWEEN Ag° AND V_K CENTERS*

C. J. Delbecq and P. H. Yuster
Argonne National Laboratory, Argonne, Illinois 60439

It is well known that KCl:AgCl crystals which are exposed at 77 K to ionizing radiation contain silver atoms, Ag°, and self-trapped holes, Cl_2^-.[1] Such crystals emit luminescence which can be observed for a long time after the exposure to ionizing radiation.[2] This long-lasting afterglow results from electron-hole recombination, by a tunneling process, between pairs of nearby Ag° and Cl_2^-.

In experiments at magnetic fields, $H \leq 33$ kG and $T \geq 1.5$ K, we have found that this afterglow is strongly quenched at high values of H/T and that this quenching results from an inhibition of the recombination.[3] We have been able to account for these results quantitatively by assuming: (1) the tunneling recombination is permitted only if the unpaired electron spins of the $(Ag^{\circ}\text{-}Cl_2^-)$ pair are antiparallel, (2) Boltzmann statistics are appropriate.

Recently we have extended those investigations on KCl:AgCl to higher values of H/T and have found that the experimental results deviate from the results expected on the basis of the simple model. These deviations become successively larger for the KBr:AgBr and the KI:AgI systems. If we add the assumption that a fraction, α, of the $(Ag^{\circ}\text{-}X_2^-)$ pairs with their spins parallel can undergo tunnel recombination with emission, we can fit the experimental data for values of α which increase from chloride to bromide to iodide. The parameter α can be related to the relative probability of tunneling between like pairs with spins parallel and those with spins antiparallel.

1. C. J. Delbecq, W. Hayes, M. C. M. O'Brien, and P. H. Yuster, Proc. Roy. Soc., A271, 243 (1963).
2. C. J. Delbecq, Y. Toyozawa, and P. H. Yuster, Phys. Rev. B9, 4497 (1974).
3. C. J. Delbecq and P. H. Yuster, phys. stat. sol. (b) 68, K21 (1975).

*Work performed under the auspices of the U. S. Energy Research and Development Administration.

TUNNELING RECOMBINATION LUMINESCENCE BETWEEN Ag^{++} AND Ag°.*

Charles J. Delbecq and Philip H. Yuster
Argonne National Laboratory, Argonne, Illinois 60439
and
David L. Dexter
University of Rochester, Rochester, New York 14627

After a crystal of KCl:AgCl is exposed to γ-rays at 77 K and then warmed to 280 K, the species Ag° and Ag^{++} are present. Upon cooling to 77 K and optical excitation of Ag°, a long-lived afterglow is produced. This luminescence does not arise from a thermally activated process. We believe the emission results from tunneling recombination of nearby pairs of Ag° and Ag^{++}, similar to the Ag°-Cl_2^- tunneling recombination observed previously.[1] That Ag^{++} is involved in the emission process can be shown by orienting the Ag^{++} at 5 K with polarized light and observing that the afterglow is polarized. Upon warming to 50 K, where Ag^{++} reorients, a strong reversal in the degree of polarization is observed which finally decays to zero. All of the characteristics of this luminescence can be understood if we assume: (1) a tunneling recombination mechanism in which the electric vector of the emitted radiation is dependent upon the location of the Ag° with respect to the Ag^{++} and, (2) the tunneling is anisotropic and also depends upon this location. These assumptions seem very reasonable when one considers the tetragonal (d-like) symmetry properties of the Ag^{++} complex. Good quantitative agreement between theory and experiment have been obtained on the decay kinetics, the degree of polarization, and the polarization reversal.

1. C. J. Delbecq, Y. Toyozawa, and P. H. Yuster, Phys. Rev. B 9, 4497 (1974).

*Work performed under the auspices of the U. S. Energy Research and Development Administration.

DIFFERENCES INDUCED BY ENERGETIC IONS ON THE Ag^+ LATTICE IN AgCl ACCORDING TO THEIR ENERGY .

Ch. DIAINE** J.L. GISCLON* J. DUPUY *

*Département de Physique des Matériaux LYON
**U.E.R. Pharmacie LYON

The defects induced by energetic ions in AgCl targets are essentially in the Ag^+ lattice. The perturbation induced by electronic energy losses correspond to the photolysis mechanism. The defects related to collision energy losses are Ag clusters.

We point out from Lindhard diagram the conditions necessary to realize the two types of defects ; they are related to the mass and to the ion energy. For example with RT implantations of K^+ or Rb^+ ions up to 320 keV, photolysis mechanism is not obtained, but with Na^+ ion, collisions defects can be optically observed, alone or simultaneously with ionization defects regarding to implantation energy.

The properties of Ag clusters resulting from collision energy losses will be analysed according their optical and E.P.R. properties.

OXYGEN SELF-DIFFUSION IN NiO

C. DUBOIS, S. BARBEZAT, C. MONTY

Laboratoire de PHYSIQUE DES MATERIAUX
C.N.R.S. - Bellevue - 1, place A.Briand
92190- MEUDON(France)

Self diffusion measurements are a good tool for studying point defects. In oxides, the Points Defects Populations can be connected to the deviations from stoichiometry by chemical models (Kröger & Vink), usefull when complex defects do not appear.

Cationic Self diffusion is well documented, in a great number of oxydes cations diffuse by means of predominating defects whose precise nature and charge state can be determined. Oxygen self diffusion is poorly known due to the experimental difficulties of measurements (no radioactive tracer, generaly small penetrations). Such data are of great interest in giving informations about defects of the oxygen sublattice ; only few experiments are able to investigate these defects especially in those oxides where they are minority defects.

We present here the results of measurements of oxygen self-diffusion in NiO single crystals at temperatures of 1100 to 1600°C under 150 torr oxygene pressure.

The diffusion profiles were determined by secondary Ion Emission after isotopic exchange at constant ^{18}O pressure. The obtained profiles generally

obey the analytical form :

$$erf^{-1}\left[\frac{C_S - C}{C_S - C_\infty}\right] = \frac{x}{2\sqrt{Dt}}$$

where C_S is the surface concentration, constant during the experiment. $C_\infty = 2.10^{-3}$ is the natural isotopic abundance of ^{18}O.

By plotting the first member function versus x, a linear relation is observed. On some samples we have seen anomalous profiles with two linear parts ; we shall discuss these results.

The values of the self diffusion coefficient obtained are about two orders of magnitude less than those measured by O'KEEFFE & MOORE in 1961* by the isotopic exchange method without determination of the profiles; we have obtained for example:

T ≈ 1100°C	$D \approx 5.10^{-15}$ $cm^2 sec.^{-1}$
T ≈ 1600°C	$D \approx 10^{-12}$ $cm^2 sec.^{-1}$

These values are the highest ones for the considered temperatures, taking in account the spread of the results.

* M. O'KEEFFE and W.J. MOORE J. Phys. Chem., 65 (1961) 1438
errata in " " , 65 (1961) 2277

INVITED PAPER

THE JAHN-TELLER EFFECT IN IONIC CRYSTALS : RECENT DEVELOPMENTS

J. DURAN*
Laboratoire d'Optique Physique de l'ESPCI
10, rue Vauquelin, 75231 PARIS CEDEX 05, France

A brief review will be given of our present understanding of the Jahn-Teller problem in doped crystals. Instead of trying to cover such a broad area in detail, it will be attempted to derive the essential features of the Jahn-Teller effect out of a few illustrative examples. Among them, a particular emphasis will be laid on the F:CaO (E_g coupling) and Au^-:KCl (equal E_g and T_{2g} coupling) systems, in which extensive experimental and theoretical works have allowed to get a precise description of the Jahn-Teller effect.

Most of the currently studied J.T. problems deal with excited states and have been investigated through optical experiments. It will be shown how some information on the dynamical processes occuring in the relaxed excited states (RES) can be derived from the measurement of the steady state population of the vibronic substates of the RES.

The advent of technological developments such as CW and pulsed dye lasers is also improving our knowledge of the J.T. systems. Several recent experiments using both the high spectral and time resolution of t'.ese devices will be mentioned.

* Equipe de Recherche n° 5 du C.N.R.S.

ELECTRICAL CONDUCTIVITY OF ADDITIVELY COLOURED KCl CRYSTALS. INFLUENCE OF IMPURITIES

D. DURAND - G. CHASSAGNE - J. SERUGHETTI
Département de Physique des Matériaux
Université Claude Bernard Lyon I
43, boulevard du 11 Novembre 1918
69621 Villeurbanne (France)

Electrical conductivity of additively coloured alkali halides gives informations about migration processes of F center to recover the local stoechiometry of the crystal either by colloid formation or by evaporation. Colloid formation and F center evaporation during crystal annealing are quite depending on the purity of the crystal, the electrical conductivity too. Results are numerous and frequently different, the origin of the observed conductivity and its interpretation are also largely contradictory (*).

The purpose of this paper is to present a synthesis on the electrical conductivity of additively coloured KCl crystal of various purity from the ultra pure material to deliberately Ca^{2+} doped ones or commercial KCl crystal in which anionic impurities, mainly OH^-, are also present. An either electronic or ionic conductivity is found depending on the purity of the crystal.

Space charge effects, due to non equilibrium between non stoechiometric crystal and outside potassium vapor phase are analysed and discussed. This effect, as well as dielectric loss from impurities seems to have lead to many misinterpretations of former conductivity results.

From the different results, the F center diffusion mechanism is discussed together with colloid formation process and F center evaporation. Thermoionic emission from colloids will also be discussed.

It is shown that the colloid formation needs neutral F center diffusion whereas F center evaporation can be realized at higher temperature by an ionized F center diffusion mechanism.

(*)

D. DURAND, G. CHASSAGNE, J. SERUGHETTI, J. de Phys. 34, C9, 465 (1973)

G. HEILAND, H. KELTING, Z. Physik 126, 689 (1949)
S.C. JAIN, G.D. SOOTHA, Phys. Rev. 171, 1075 and 1083 (1968)
J.N. MAYCOCK, J. Appl. Phys. 35, 1512 (1964)
Y.N. PERSHITS, M.G. PINSK, Sov. Phys. Solid State 10, 2746 (1969)
R.E. SEEVERS, A.B. SCOTT, J. Phys. Chem. Solids 31, 729 (1970)
L.M. SHAMOSKII, A. DUNINA, M.I. GOSTEVA, Sov. Phys. Solid State 2, 2252 (1960)

ELECTRON PARAMAGNETIC RESONANCE OF PHOSPHOROUS CENTERS IN PHENACITE†

R. C. DuVarney and A. K. Garrison
Emory University, Atlanta, Ga. 30322 U.S.A.

We wish to report the characterization of a radiation defect center in natural crystals of the mineral, phenacite ($2BeO \cdot SiO_2$). This study is part of a continuing EPR and ENDOR investigation of the nature and behavior of radiation defects in crystalline and ceramic BeO. One of the purposes of the study is to determine the contribution of the defects to the thermoluminescence (TL) and the thermally stimulated exoelectron emission (TSEE) in these materials. Gammage et al.[1] reported that the intensity of the TSEE in a commercial BeO ceramic, Thermalox 995, is related to the amount of SiO_2 impurity in the form of phenacite. In order to clarify the role of phenacite we began a study of x-irradiated natural phenacite crystals. Previous studies[2] found that x-irradiated phenacite gave EPR spectra with large hyperfine splittings which were attributed to PO_3^{-2} or PO_4^{-4} radicals. Our examinations of crystals from Brazil and Colorado show the reported EPR spectra in every case with intensities arising from concentration of several hundred ppm. We have made measurements of both the $\Delta m_S = 1$ $\Delta m_I = 0$ and the $\Delta m_S = 1$ $\Delta m_I = 1$ transitions. A preliminary analysis of the data gives the spin-Hamiltonian parameters, $A_{xx} = 3460.1$, $A_{yy} = 3139.2$, $A_{zz} = 3110.8$ MHz, $g_n\beta_n/h = 0.0017$ MHz (^{31}P), $g_{xx} = 2.0009$, $g_{yy} = 2.0019$ and $g_{zz} = 2.0003$. The z principal axes are along the c axis and the y axes make an angle of about 4^o with the $[1\bar{2}10]$ direction as one would expect from consideration of the pseudo-hexagonal crystalline structure. Our data also suggests that the defect is due to a phosphorous ion which substitutes for a silicon. Upon x-irradiation the P^{+5} ion which is isoelectronic with Si^{+4} traps an electron in a predominately S-type orbital to give the large, slightly anisotropic hyperfine splitting.

†Supported by N.S.F. Grant DMR 75-03281.

1. R. B. Gammage, K.W. Crase and K. Becker, Health Phys. 22, 57 (1972).
2. H. Lozykowski, R.G. Wilson, and F. Holuj, J. Chem. Phys. 51, 2309 (1969); F. Holuj, J. Chem. Phys. 54, 1430 (1971).

THERMALLY ACTIVATED ROTATION OF S^- IN KCL: A GROUND STATE JAHN-TELLER SYSTEM.

B. Eilebrecht, G. Gelfert, L. Schwan
Physikalisches Institut, Teil 2, Universität Stuttgart,
Pfaffenwaldring 57, D 7 000 Stuttgart 80

The geometric structure of the S^-centre in KCl is known by EPR and ENDOR measurements [1,2]. S^- is situated on a Cl^- site in the cubic KCl lattice (the model is shown in fig.1). The S^- has five electrons in its outer p shell. It can hence be described also by one defect electron of p type. Because of the threefold degeneracy of this p type hole the centre is distored by the Jahn-Teller effect. This distortion gives a <111> symmetry to the electronic structure of the centre which was found by EPR/ENDOR measurements. We found the absorption bands to disappear upon increasing the temperature above 20 K for ENDOR and 50 K for EPR measurements, although the S^- centre is stable up to 200 K.

We assume that the Jahn-Teller distortion is able to change its preference direction among the <111> directions by thermal activation. Increasing the frequency of this rotational hopping by increasing the temperature decreases the time the centre remains in each state being able to absorb a microwave quantum. Too less time in a state results in no absorption. Therefore, the hopping

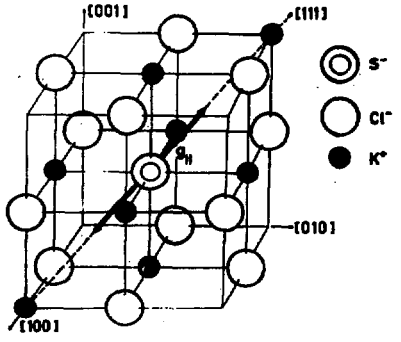

Fig.1: S^- in KCl
Lattice Surroundings of the Centre

frequency is correlated to the disappearence of absorption bands, so that the hopping frequency should be less than the measure frequency (ENDOR $\sim 10^6$ Hz, EPR $\sim 10^{10}$ Hz). In this model we are now able to estimate the activation energy for hopping (equivalent with Jahn-Teller energy) of the S^- centre.

[1] Hausmann, A., Z.Phys. 192 (1966) 313

[2] Eilebrecht, B., Schwan, L., J.d.Physique Colloq. 37 (1976) C 7

KINETICS OF THE RADIATION DEFECTS FORMATION IN ALKALI HALIDE CRYSTALS

Y.A.Ekmanis
Physics Institute, Latvian SSR Academy of Sciences, USSR

A large number of various radiation defects is produced in alkali halide crystals by radiation. Under certain external conditions (heating temperature, preradiation defects concentration, etc.) recombination of these defects, their coagulation in the crystal volume and their coagulation into larger formations occur. Under irradiation all these processes are simultaneous, nevertheless, experimentally they are treated as separate discrete phenomena which makes it difficult to represent the entire mechanism of radiolysis /1/.

Primary color and luminescence centers including their two - and three - fold aggregates have been thoroughly studied, whereas next stages of the aggregate growth require further investigation.

From our point of view analysis of the final radiolysis products formation (at room temperature and below) can be reasonably devided into the following stages: electron - hole pairs generation; point defects separation; beginning of F centers coagulation and formation of their aggregates of the nF type where $n \geq 2$; increase of the number and sizes of colloidal metal particles; stabilization of the number and sizes of colloidal particles owing to the electron and hole products interaction; destruction of the crystal due to the damage of the crystal composition stochiometry /2,3/.

Experimentally these processes have been observed qualitatively, however, a correct explanation of radiolysis requires the solution of the following problems: initial aggregate electron and hole defects localization places; sizes of the smallest stable aggregate centers and their connection

with the preradiation defects structure of the crystal; changes of the crystallographic structure of colloidal metal particles with their growth; point and aggregate defects interaction on the stages preceeding the destruction of the crystal.

Experimentally observed initial stages of the thermodynamically stable clusters and colloidal metal particles formation show the clusters consisting of several hundreds of point defects. Their formation is so fast that the smaller formations cannot be detected by usual spectroscopic and electron microscopy methods. The most probable place of their formation is the preradiation defects. The further growth of these aggregates, especially colloidal metal particles, requires phase transition of their structure observed for the particles with sizes of about 100 Å. The number of these particles reaches the order of $10^{12}cm^{-3}$ with increasing radiation dose. Then a complex equilibrium between electron and hole centers is established. Therefore, aggregates with diameter exceeding 1000 Å are formed, however, on the other hand, destruction of the larger particles to the point defects is beginning. A simultaneous formation of free halogen in the crystal volume leads to its complete destruction (with doses higher n 10^{7}Mrad).

The present consideration of the multiple experimental data on the irradiation in alkali halide crystals allows to represent the entire mechanism of radiolysis.

References

1. V.Gotlib, Ya.Kristapson, K.Shvarts, and Y.Ekmanis. Radiatsionnaya Fizika VII (Zinatne, Riga, 1973), p. 143.
2. Y.Ekmanis, E.Rosauer. - J.Appl.Phys., 46, 7, 2837, 1975.
3. L.W.Hobbs, A.E.Hughes, D.Pooley. Proc.R.Soc. London A332, 167, 1973.

THERMAL PROPERTIES AND ELECTRICAL RESISTIVITY OF OLIVINE AND PYROPHILLITE IN THE TEMPERATURE RANGE 400-2000°K

A. A. El-Sharkawy, M. A. Kenawy and S. R. Atalla
Al-Azhar University, Faculty of Science, Dept. of Physics, Cairo, Egypt

The thermal properties (specific heat, thermal diffusivity and conductivity) of olivine and pyrophillite were measured in the temperature range 400-2000°K. The theory of the method used was based on the so-called plane temperature wave method. Also the electrical conductivity of the above mentioned specimens was measured. The role of the radiative part of the thermal conductivity was investigated. The variation of the thermal conductivity with depth for the Earth's mantle was calculated.

CONCENTRATION DEPENDENT DIFFUSION IN STRONGLY IONIC CRYSTALS: A NEW METHOD OF ANALYSIS+

GENGHMUN ENG and DAVID LAZARUS
Department of Physics and
Materials Research Laboratory
University of Illinois at Urbana-Champaign

The diffusion of heterovalent ions in strongly ionic solids is characterized by a concentration dependent diffusivity, D(C), which arises primarily from the heterovalent ion augmenting (or suppressing) the normal vacancy concentration in order to maintain local charge neutrality[1]. Heterovalent ions, even as trace impurities, strongly distort penetration profiles from the gaussian profile that is characteristic of a constant diffusivity process[2].

In one rectilinear dimension, the diffusion equation is:

$$\frac{dC}{dt} = \frac{-d}{dx} D(C) \frac{dC}{dx} .$$

For the case that $D(C)=D_o(1+\underline{a}C)$, by extending the Hermite polynomial solution of the constant diffusivity case[3], we demonstrate that a complete solution to our non-linear equation can be constructed which:

1. converges
2. allows for an arbitrary 'thin source' initial state
3. is analytic for all times $t > t_{initial}$
4. exactly conserves total mass ($\int C(x,t)dx = 1$).

We furthur demonstrate that this methodology can be extended to handle any D(C) for which the series $D_o(1+\underline{a}C+\underline{b}C^2+..)$ is a good approximation. Experimental implications will be discussed.

+Supported in part by the United States E.R.D.A. under contract EY-76-C-02-1198

1. L. Girifalco, Atomic Migrations in Crystals, Gordon & Breach (1967)
2. J. L. Mitchell and D. Lazarus, Phys. Rev. B12,734(1975)
3. A. Erdelyi, Higher Transcendental Functions, McGraw-Hill (1954)

INTENSITY OF POLARIZED RAMAN SCATTERING FROM METASTABLE O_2^* IN γ-IRRADIATED SODIUM CHLORATE*

Herbert Engstrom
Brookhaven National Laboratory, Upton, N. Y. 11973

Using a combination of polarization modulation and photon counting techniques, precise measurements of the intensity of each polarization of Raman scattered light of metastable O_2^* at 1544 cm^{-1} in γ-irradiated sodium chlorate[1] as a function of the angle of polarization of the incident laser light have been made. The results were analyzed by summing the contributions to the scattering from the 12 nonequivalent orientations of the O_2^* defects. That is, if N_u is the number of photons per unit time scattered with linear polarization along a direction defined by the unit vector $\underline{u}$, one finds

$$N_u = \text{const.} \sum_{i=1}^{12} n_i \left| \underline{u} \cdot R_i A \alpha A^{-1} R_i^{-1} \underline{E}_I(\beta) \right|^2$$

where α is the diagonalized polarizability tensor for a defect of any particular orientation, A is the transformation matrix from the principal axis system of that defect to the lab coordinate system, the matrices R_i are the twelve rotation matrices of the point group T of sodium chlorate ($NaClO_3$), $\underline{E}_I$ is the electric field vector of the laser light which makes an angle β with the x-axis of the lab system, and n_i is the ground state population of the defect of orientation i. An excellent fit to the data is obtained if one assumes that the ground states of the defects are depopulated by the laser light such that these populations are proportional to

$$e^{-a \cos^2\delta}$$

where δ is the angle between $\underline{E}_I$ and the principal x-axis of the defect, and a is an adjustable parameter.

With this assumption it is found that only the α_z element of the polarizability tensor is non-zero. Thus, the number of photons scattered

with polarization along the laser direction and the number polarized at right angles to the scattering plane for all values of β and for two non-equivalent orientations of the crystal may be fit with only five parameters. These are the multiplicative constant, the absorption coefficient $a = 3.7 \pm 0.4$, and the three Euler angles defining the matrix A: $\phi = 55.8 \pm .7$, $\theta = 81.3 \pm 0.9$, and $\psi = 51.2 \pm 2.6$ degrees.

*Research supported by the U.S. Energy Research Development Administration.
+Present address: Solid State Div., ORNL, Oak Ridge, Tenn. 37830.
1. J. B. Bates and H. D. Stidham, J. Chem. Phys. 65, 3901 (1976).

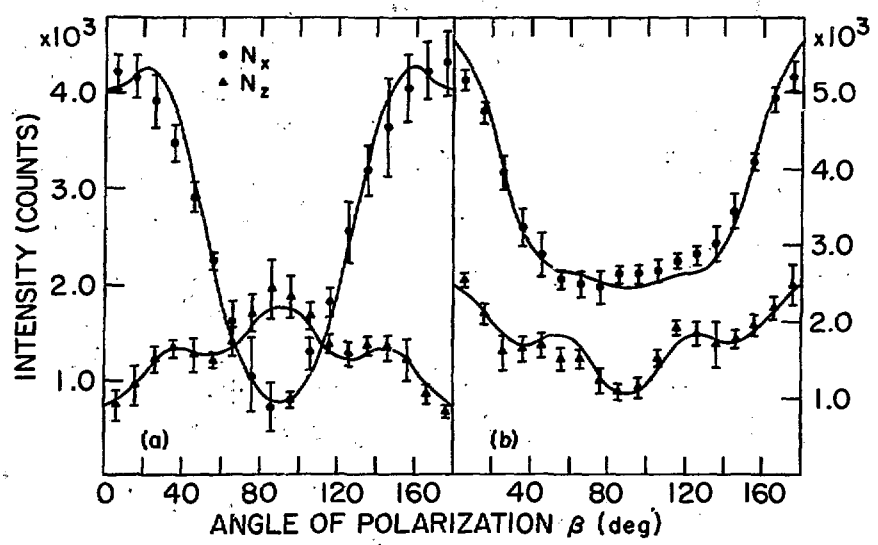

Fig. (a) N_x is the number of photons scattered with polarization along the x-axis (orthogonal to scattering plane; N_z is the number scattered with polarization along the z-axis (parallel to laser light). (b) Same as (a) but with crystal rotated about z-axis by 90°. For the calculated values the Euler angle ϕ, corresponding to rotations about z, was increased by 90°. Calculated values are shown by solid lines.

OPTICAL PROPERTIES OF DEFECTS IN HEXAGONAL BORON NITRIDE

Koh Era, Takashi Kuzuba, Toshihiko Ishii, Tadao Sato and Minoru Iwata

National Institute for Researches in Inorganic Materials
Sakura-mura, Niihari-gun, Ibaraki-ken 300-31 Japan

We report on the optical properties of carbon-related, F-like and U-like centers in hexagonal BN which is the simplest nonmetallic layer compound. Although several works have been made on these subjects.[1-5] We have intended to reveal inherent natures of defects in this unique compound.

Diffuse reflectance, luminescence, its excitation and EPR spectra were measured on powder samples prepared under various conditions. Absorption spectra were measured on single crystals grown from silicon flux.

(1) CARBON-RELATED CENTERS The figure on the next page shows typical optical spectra of carbon-treated hBN powder with our designation of grouped emission lines. The classification of the emisssion lines was made by investigating excitation characteristics of each emission line and changes of emission characteristics from sample to sample. The manner of the changes showed that a center for each emission group is different from one another. We have confirmed that incorporation of carbon in the host crystal is necessary for all the emission groups. If hydrogen is in firing atmosphere, all the emission groups appear. If not, only the α group appears. Selective coupling of an in-plane LO phonon[6] (200 meV) is seen clearly in the α and δ spectra. By close investigation of the δ, we reached the conclusion that the δ is of "hot " nature. This means that the optical transition rate is higher than the vibrational relaxation rate contrary to the usual cases in solids. An experiment using a nitrogen laser showed that response time of the δ emission was faster than 10^{-9} sec. As to the center for each emission group, we tentatively ascribe the α to carbon substituting nitrogen, the δ to carbon substituting boron (possibly associated with other imperfections), and the β and γ to some other complex carbon centers.

(2) F-LIKE CENTER Optical absorption consisiting of a line at 2.23 eV and a band extending from 2.4 eV to 3.7 eV with phonon structures have been ascribed to the F-like center in the hBN by observing a correlation between optical and EPR absorption intensities. Luminescence from this center could not be observed.

(3) U-LIKE CENTER Strong absorption at 3.39 eV can be ascribed to

an U-like center in the hBN. Characteristics of the absorption resemble well in a few point those of the U center in alkali halides.

Relations between energy bands[7] of the host crystal and the above mentioned defect states, and two-dimensional charactors of the states will be described.

1. S. Larach and R. E. Shrader, Phys. Rev. 104, 68 (1956)
2. A. W. Moore and L. S. Singer, J. Phys. Chem. Solids 33, 343 (1972)
3. A. Kazir, J. T. Suss. A. Zunger and A. Halperin, Phys. Rev. B 11, 2370 (1975)
4. A. Zunger and A. Katzir, Phys. Rev. B 11, 2378 (1975)
5. E. Y. Andrei, A. Katzir and J. T. Suss, Phys. Rev. B 13, 2831 (1976)
6. R. Geick and C. H. Perry, Phys. Rev. 146, 543 (1966)
7. A. Zunger, A. Katzir and A. Halperin, Phys. Rev. B 13, 5560 (1976)

Other works are cited in these literatures.

optical spectra at 2K of hBN powder fired at 2400K in an atmosphere containing C and H

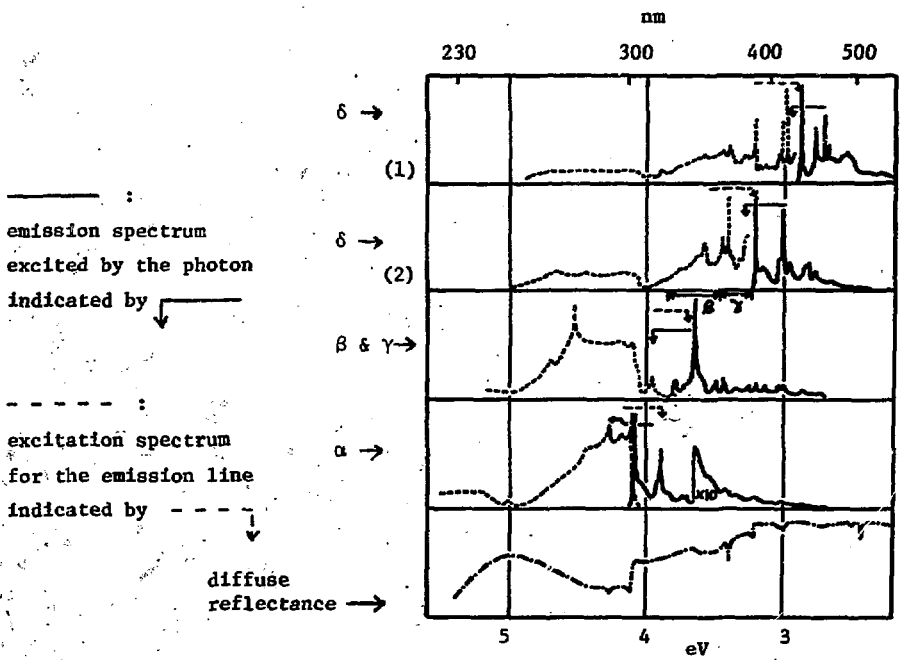

PARTICLE IRRADIATED CRYSTALLINE ALUMINA

B. D. Evans
Naval Research Laboratory
Material Sciences Division
Washington, D.C. 20375

Crystalline alumina samples bombarded with 14-MeV neutrons, 200-keV H^+, Ne^+ or Xe^+, or implanted with 200-keV Al^+ show several absorption and emission bands in the 2-to-6 eV range[1,2,3]. In particular, the neutron or proton irradiated and the aluminum implanted samples have the 4.8, 5.4 and 6 eV absorption bands well known from early electron bombardment and fission reactor exposures[4,5]. These samples luminesce at 3.8 eV when pumped at 4.8 and 5.4 eV and higher. A similar emission has been recently reported in epithermal neutron irradiated samples[6]. The quantum efficiency in the fusion-neutron irradiated samples when pumped with 4.8 eV light is near 6 % at ~10 K; at this temperature the life time is less than 10 nsec. The temperature dependence of the uv-luminescence band halfwidth follows the hyperbolic cotangent relation with an effective vibronic frequency of 393 ± 15 cm^{-1}; this is near the lowest bulk alumina modes at 400 cm^{-1}. In addition, a weak, green phosphorescence occurs near 2.5 eV when pump light at 4.1, 4.6 and 5.4 eV is used. The life time in the neutron irradiated samples at 295 K when pumped at 4.1 eV is 0.05 sec; the quantum efficiency is approximately 10^{-4}.

1. B. D. Evans and H. D. Hendricks in Ion Implantation in Semiconductors 1976, edited by F. Chernow, J. Borders and D. Brice (Plenum, New York 1977)
2. J. M. Bunch and F. W. Clinard, Jr., J. Am. Ceram. Soc. 57, 279 (1974).
3. G. W. Arnold, G. B. Krefft, and C. B. Norris, Appl. Phys. Lett. 25, 540 (1974).
4. G. W. Arnold and W. D. Compton, Phys. Rev. Lett. 4, 66 (1960).
5. P. W. Levy, Phys. Rev. 123, 1226 (1961).
6. K. H. Lee and J. H. Crawford, Jr., Phys. Rev. B15, 4065 (1977).

NEUTRON-DIFFRACTION STUDY OF STABILIZED ZrO_2: OBSERVATION OF OXYGEN SUBLATTICE SHEAR DISTORTIONS

*J. Faber, Jr., M. H. Mueller, and R. L. Hitterman**
Argonne National Laboratory, Argonne, Illinois 60439

and

T. H. Etsell
University of Alberta, Edmonton, Alberta, Canada

ABSTRACT

The superionic properties of stabilized zirconia have been studied for a number of years. The stabilizing agents (usually Ca or Y) leave the anion sublattice highly defective and the structure is taken as fluorite (Fm3m). Order-disorder phenomena occur for samples aged at ∿1275 K and relate to cation diffusion for the formation of the ordered state. Carter and Roth[1] observed forbidden reflections (under Fm3m) for samples in the ordered state but were unable to successfully analyze these results. One novel feature of their data is that the dimensions of the unit cell ($a = b = c$, $\alpha = \beta = \gamma = 90°$) appeared to remain cubic in the ordered state. Steele and Fender[2] have studied the disordered state of $Zr(Y)O_{2-x}$ but little is known of the ordered state.

We have studied the elastic scattering from $Zr(Ca)O_{2-x}$ and $Zr(Y)O_{2-x}$ single crystals with neutron diffraction techniques. Experiments were performed in both the disordered state (quenched from 1675 K) and the ordered state (aged ∿400 hours at 1250 K). In the ordered state, both Ca- and Y-doped crystals displayed forbidden Bragg reflections with mixed hkℓ indices (h, k odd and ℓ even). We note a number of striking analogies with Jahn-Teller distortions observed[3] in UO_2 (also a fluorite structure compound), and adopt a domain model to account for the forbidden (mixed hkℓ) reflections.

The application of a domain model for $Zr(Ca)O_{2-x}$ shows that (1) the domain populations are equal and (2) that for our crystal, the domains account for ∿25% of the crystal volume. The domains consist of alternate (110) oxygen sublattice planar shear deformations, where oxygen ions are displaced ∿0.23 Å from the ideal fluorite lattice sites. Only two

*Work supported by the U.S. Energy Research and Development Administration.

adjustable parameters were needed in the least-squares refinement of 25 independent mixed hkℓ reflections (residual = 0.05). The oxygen sublattice shear deformation does not require a change in the dimensions (a = b = c, $\alpha = \beta = \gamma = 90°$) of the fluorite unit cell, and is therefore an internal distortion.

The data on $Zr(Y)O_{2-x}$ (in the aged state) provide a striking confirmation of the domain model. The symmetry of the oxygen sublattice shear deformation is the same both in symmetry and magnitude with that observed in $Zr(Ca)O_{2-x}$. In addition, the domains exhibit tetragonal symmetry (c/a = 1.015) and consume ∿90% of the crystal. We find that the domain populations are not equal and obtain confirmation of the model in peak shape analysis of the parent fcc reflections of the structure. Both internal and external deformations are observed. Phonon displacement field arguments (the deformation mode is a linear combination of normal modes of the lattice: $E_u - A_{2u}$) are discussed and unify the observed behavior.

References

1. R. E. Carter and W. L. Roth, *Electromotive Force Measurements in High Temperature Systems*, ed. C. B. Alcock, pp. 125-144 (1968).
2. D. Steele and B. E. F. Fender, J. Phys. C., 7, 1 (1974).
3. J. Faber, Jr. and G. H. Lander, Phys. Rev. Letters, 35, 1770 (1975).

MAGNETO-OPTICS STUDIES OF SELF-TRAPPED EXCITON LUMINESCENCE IN CsI

L. Falco, J.P. von der Weid* and M.A. Aegerter
Institut de Physique, Université de Neuchâtel
CH 2000 NEUCHATEL, Switzerland

Self-trapped exciton (STE) luminescence in CsI occurs at 290 nm and 338 nm. We showed that the occurence of the 2 emission bands can be understood in the framework of a phenomenological theory [1], the lowest levels of both types of STE being composed of a partially allowed triplet state below a singlet state.

The validity of the model has been further tested by studying both emissions under strong magnetic field ($0 < B < 5.5$ T) down to $T \simeq 1.5$ K ($B \parallel \langle 100 \rangle$). Each triplet states split under magnetic field and both emissions detected along it should exhibit a magnetic circular dichroïsm (MCD). Experimental results confirm this point of vue. Figs. 1 and 2 show results for the 338 nm emission. The temperature and field behaviour of the MCD is more complicated than was previously shown by Kabler et al. [2]. The maximum P value foreseen by the model is -0.5. The peak observed near $B = 4.5$ T for $T < 6$ K has been attributed to the crossing of the $|{}^3\Gamma_4^-$; $\Gamma_3^-\rangle$ and $|{}^3\Gamma_4^-$; $\Gamma_5^-\rangle$ levels [1] [2] [3]. But neither its maximum value nor the particular behaviour of the MCD at low field can yet be fully explained. Fig. 3 shows results for the 290 nm emission. The maximum P value predicted is also -0.5. No change in the bands shape has been observed. We found that for the 338 nm emission the $I^+ + I^- + I$ values (normalized to 1 at $B = 0$) slightly increase with the field for $T > 10$ K but are strongly reduced for $T < 10$ K. The opposite behaviour is found for the 290 nm emission for which a slight increase is found for all temperatures.

We also measured the emissions perpendicular to the field axis. Both of them exhibit a partial horizontal polarization ($\parallel \vec{B}$); the $(I_h - I_v) / (I_h + I_v)$ values are function of temperature and field and are typically ~ 0.18 for both bands at $B = 5$ T and $T = 1.6$ K. Despite these important intensity variations the total light intensity emitted by the crystal in all directions remains constant at all temperatures for a given magnetic field, but seems to increase slightly as a function of it ($\sim 4\%$). These observations confirm the model of the transfer from the Γ_2^- STE states to Γ_4^- ones [1] and indicate that it is magnetic field dependent.

Decay time measurements and model calculation are underway in order to clarify these processes.

Research supported by the Swiss National Science Foundation.

References

* On leave of absence from Department of Physics of the Pontificia Universidade Catolica, Rio de Janeiro, Brazil.

[1] See also abstract by J.P. Pellaux, T. Iida and M.A. Aegerter
[2] M.N. Kabler, M.J. Marrone and W.B. Fowler, in Luminescence of Crystals, Molecules and Solutions, Ed. F. Williams (1973)
[3] W.B. Fowler, M.J. Marrone and M.N. Kabler, Phys. Rev. B, 8, 5909 (1973).

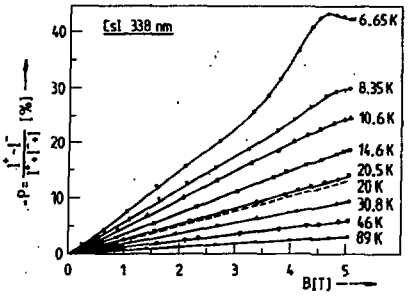

Fig. 1 : MCD of 338 nm emission for T ≥ 6.65 K. Dashed curve is from [2]

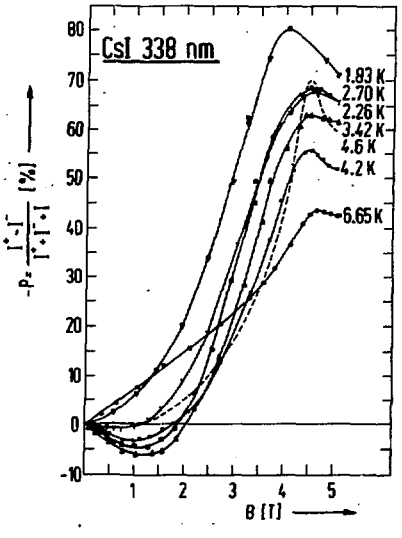

Fig. 2 : MCD of 338 nm emission for T ≤ 6.65 K. Dashed curve is from [2]

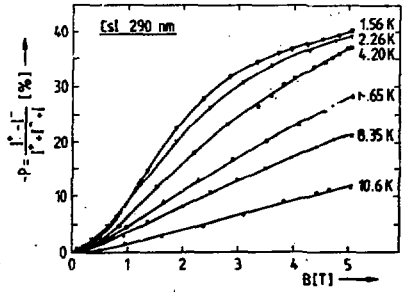

Fig. 3 : MCD of 290 nm emission

HIGH TEMPERATURE ANNEALING OF RADIATION DEFECTS IN LiF

E.E.Feldmane, A.V.Podinsh[x], K.K.Shvarts[xx]

[x]Daugavpils Pedagogical Institute, Latvian SSR, USSR

[xx]Physics Institute, Latvian SSR AS, Riga - Salaspils,USSR

LiF crystals were irradiated in atomic pile and in electronic accelerator (E = 3.5MeV) up to the dose of 2.5×10^4 Mrad. The formation of needle-like cavities and changes of optical and picnometric density by annealing at various temperatures have been studied. Measurements of the relative density changes ($-\frac{\Delta\rho}{\rho}$) of crystals irradiated with electrons with dose 2.5×10^4 Mrad (1) and with neutrons with dose 5×10^3 Mrad 1×10^{17} n/cm^2) (2) in conditions of pulse isochronous annealing are represented in fig.a, and in the conditions of isothermic annealing - in fig.b. Results show, that change of LiF crystals density is multistage process which depends on the type of irradiation. The annealing of crystals irradiated in the pile consists of the following stages: 1) 20° - 500°C (densification of the crystal up to the density before irradiation, restoration of the optical density); 2) 500° - 600°C (density does not change); 3) 600°-800°C - several tens of hours (decrease of density and cavities formation); 4) several hundreds of hours at 800°C (crystal densification and dissolution of cavities).

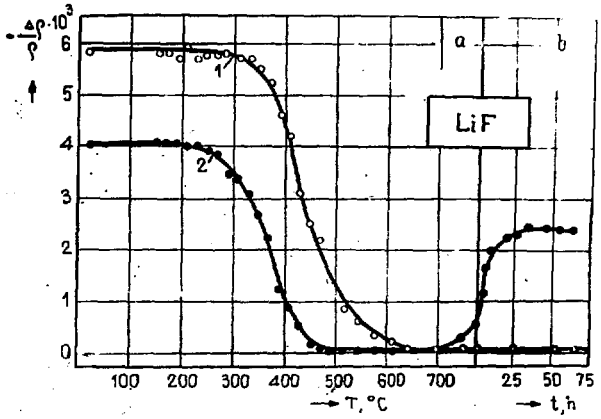

In crystals irradiated by electrons the third and the fourth stage do not take place and the cavities are not formed.

In crystals irradiated by neutrons the calculated average concentration of vacancy pairs which form cavities is approximately equal to the concentration of electron color centers. Therefore in the first stage of annealing recombination between interstitials and vacancies does not occur, and in these crystals the main process is the joining of one type of defects into formations which take the flat shape with growth only slightly distorting the lattice. In the third stage of annealing LiF radiolysis products are removed and cavities are formed of vacancies. Relative density change is equal to the cavities relative volume. In the forth stage by-vacancy dissolution of cavities and excessive vacancies diffusion on the crystal surface occur.

In the electron irradiated crystals the interstitials recombination with vacancies is the prevailing process at the end of the first stage.

The needle-like cavities distribution over crystal volume and their dependence on the dislocation concentration shows that cavities formation is connected with dislocations[1].

[1]E.E.Feldmane, K.K.Shvarts, A.V.Podinsh, Izv. AN Latvian SSR, ser. fiz.-tehn., 1973, 3, 14.

NEUTRON-INDUCED DAMAGE INVESTIGATIONS IN ALKALI HALIDE CRYSTALS WITH RADIOACTIVE RARE GASES

F.W.Felix, B. Granéli[+], M. Müller

Hahn-Meitner-Institut für Kernforschung Berlin GmbH

Glienicker Straße 100, D 1000 Berlin 39

Our systematic experimental studies of the diffusion of radioactive rare gas atoms in alkali halide crystals have shown, that the gas-atoms diffuse interstitially and that they may become trapped by lattice defects, see the review /1/. The theoretical explanation of our results (Norgett and Lidiard /2/) has confirmed that the apparent gas-diffusion coefficient D_{app} is a relevant measure for the trapping defect concentration c_T: $D_{app} \propto 1/c_T$. This simple relationship is valid under the assumption, that the equilibrium distribution of the gas atoms between their mobile and trapped states is rapidly established. By doping KCl and KBr with Sr^{2+}, it could be shown, that cation vacancies act as gas traps /3/. Further experiments demonstrated a general effect of gas-trapping due to neutron irradiation /4/.

On investigating crystals which had been exposed to high doses of neutrons, the straightforward use of Fick's 2nd law proved to be inadequate, as the evaluation would yield time-depending coefficients of diffusion. The modification of the evaluation scheme by adding adsorption and desorption terms, as proposed by Gaus /5/ and Hurst /6/, did in spite of some successes, lead to ambiguities. Recently we have been able to show qualitatively from gas-release experiments with a stepwise heating program, that the gas-trapping defects slowly anneal towards the crystal surface /7/.

+) Guest from Chalmers University of Technology, Gothenburg (Sweden)

A more direct experimental attempt can be made by determining the gas-diffusion profile corresponding to a given annealing condition by a newly developed technique of grinding after quenching the annealed crystals to room temperature. This method relies on the fact, that the gas content of the small abrazed particles is quantitatively swept out mechanically. The continuously working apparatus is described and example of the determined gas profiles and the underlying profile of the trapping defects are given.

Additional information from isochronal gas-release experiments and experiments with thermally annealed and re-irradiated crystal can be gained.

References

/1/ F.W.Felix, J.Phys. 34 (1973) C9-149

/2/ M.J.Norgett, A.B.Lidiard, Computational Solid State Physics, Eds. Hermann, Dalton & Koehler, Plenum Press, 1972, p. 385

/3/ F.W.Felix, M. Müller, Phys.Stat.Sol.(b) 46 (1971) 265

/4/ F.W.Felix, M. Müller, Indian.J.Pure Appl.Phys.14 (1976) 249

/5/ H.Gaus. Z.Naturf. 20a (1965) 1298

/6/ D.G.Hurst, AECL-1550 (1962) 40 p.

/7/ F.W.Felix, B. Granéli, M. Müller, Bulg.J.Phys. submitted

IMPURITY DIFFUSION IN POTASSIUM AZIDE - A PSEUDOHALIDE*

D. Foster** and A. L. Laskar

Department of Physics and Astronomy
Clemson University, Clemson, S. C. 29631

The alkali azides are an interesting family of compounds known as pseudo-halides due to their strong ionic nature similar to alkali halides. Recent studies[1] of the electrical conductivity and cation diffusion in KN_3 and RbN_3 indicate that like alkali halides the defect structure is Schottky type and mass and charge transport takes place by a vacancy mechanism. Earlier study[2] of K^+ in KN_3 in the extrinsic range was believed to support this view. The migration enthalpy of the cation (H_m) was estimated to be 0.8 eV. This was obtained by equating H_m to the diffusion activation enthalpy at high impurity concentration according to Lidiard's theory[3]. There is an uncertainty in this type of analysis unless it is shown experimentally that diffusivity does reach a saturation with the concentration of polyvalent impurities. To ascertain the diffusion of cations in the intrinsic range (as determined from the conductivity Arrhenius behavior) the diffusion of Na^+

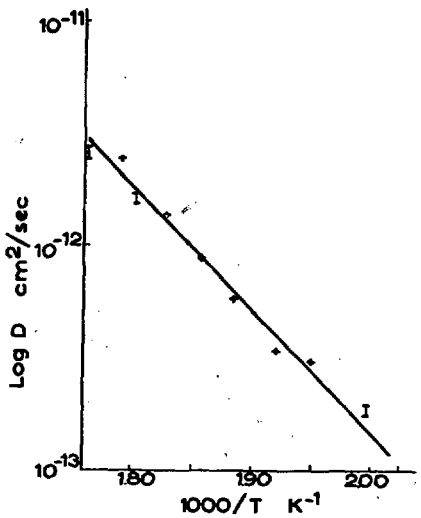

Fig. 1. Diffusion of Na^+ in KN_3.

(a homovalent alkali ion similar to K^+) was studied. The extremely short half-life of potassium isotope makes it unsuitable for long diffusion anneal required to explore the diffusivity at low temperatures.

The results of the study of the diffusion of Na^+ in KN_3 by a tracer sectioning technique are displayed in Fig. 1. The diffusivites correspond "nominally" to the c-axis. The growth direction in many of the melt-grown crystals was found to be along the c-axis[1], but it was determined later that this might vary by a few degrees. This may contribute to the scatter of the data in Fig. 1. The tracer diffusion experiments by microtome sectioning in this system proved to be somewhat exacting due to the lightness and brittle nature of KN_3. The "near surface effects" were appreciable in most of the penetration profiles. KN_3 undergoes some thermal decomposition at higher temperatures. A correction due to the moving boundary may be necessary - but was not attempted due to the lack of precise data for the involved rates.

It is seen from Fig. 1 that the diffusion of Na^+ ion in KN_3 can be adequately represented with a single activation energy over the temp. range, 200-295°C, by the following Arrhenius relation:

$$D = 11.5 \exp [-1.4 \text{ eV}/KT] \text{ cm}^2/\text{sec} \qquad (1)$$

The activation enthalpy for diffusion (1.4 eV) is in agreement with that obtained in the study[2] of conductivity in KN_3. Thus the migration enthalpy for the exchange jump of Na^+ with vacancy is the same as that of the unassociated vacancy. Also the absolute value of the diffusivities of K^+ is larger than those of Na^+ in KN_3 by about two orders. If the misfit of Na^+ (the ionic radii are 0.95 and 1.33 A° for Na^+ and K^+ respectively)[3] is a cause for this it should reflect also in their activation enthalpies for migration. The large impurity content of the specimens for K^+ diffusion can account for the higher diffusivites in that experiment. A more detailed analysis however should be based on the anisotropy of the correlation functions for a tetragonal crystal structure like KN_3 when diffusivities perpendicular to the c-axis are also known.

*Work supported by AROD grant #DA-31-126-72-G-120 and DAH co4-75-G-0130.

**Now at P. R. Mallory & Co., Inc., Burlington, Mass. 01803.

REFERENCES

1. A. L. Laskar, D. L. Foster and K. Wagner, J. de Physique 37, CF-471 (1976); and the references therein.

2. A. L. Laskar and J. Sharma, J. Phys. Chem. Solids 34, 989 (1973).

3. A. B. Lidiard, in Handbuch der Physik, edited by S. Flugge (Springer-Verlag, Berlin, 1957).

SPECTROSCOPY OF SMALL MOLECULAR IONS IN ALKALI HALIDE CRYSTALS

A.Freiberg and L.A.Rebane
Institute of Physics, Estonian SSR Academy of Sciences,
202400 Tartu, USSR

The spectra of small molecular ions O_2^-, S_2^-, NO_2^- and their analogs inserted into alkali halide crystals as anion substituents have actively been studied during a number of years. The results of our earlier investigations are summed up in [1,2]. Here are collected new data about the vibronic spectra of NO_2^- ions in the crystals with CsCl structure, and also about the details of the electron-phonon interaction and reorientation processes of molecular centers in alkali halide crystals.

1. Low-temperature spectra of NO_2^- in b.c.c. lattices of alkali halide crystals differ from the corresponding spectra in f.c.c. lattices mainly in three aspects. Firstly, if in the latter case the local dynamics of lattices is relatively weakly disturbed by the centers, then in the case of lattices with CsCl structure it is not. Besides the clear-cut vibronic spectral structure due to the excitation of high-frequency intramolecular local vibrations ν_1 and ν_2 (whose frequencies differ only slightly from those in f.c.c. matrices) the series of low-frequency local and pseudolocal vibrations induced by impurity are detected. The spectroscopic constants of NO_2^- vibrations in CsCl, CsBr and CsJ and the frequencies of impurity-induced vibrations ν_{ind} in cm^{-1} in the ground state $^1A_1$ and lower excited electronic state $^1B_2$ are determined by the vibronic spectra and summed up in the table. Secondly, the NO_2^- ion rotates nearly freely in many crystals with

Crystal	ν_1	ν_2^0		x_{11}		x_{22}	x_{12}	ν_{ind}	
	$^1B_2$	$^1A_1$	$^1B_2$	$^1B_2$	$^1A_1$	$^1B_2$	$^1B_2$	$^1A_1$	$^1B_2$
CsCl	1035	800	596	-	-0.4	-0.6	-5.1	155	155
CsBr	1016	795	591	-1.4	-0.8	0.2	-3.2	122; 150	112; 135
CsJ	984	788	621	-1.9	-0.5	-0.6	-1.8	90;127;149	88

NaCl structure (KCl, KBr, RbCl) but not in the crystals with CsCl structure. Owing to that we found partly (up to 38%) polarized luminescence of $CsBr-NO_2^-$ and $CsJ-NO_2^-$ crystals and with the help of parallel study of Raman scattering spectra of local vibrations fixed the local symmetry of the center as C_{2v}. Thirdly, the quantum efficiency of luminescence of NO_2^- within the range of a single absorption band changes both in the crystals with NaCl and CsCl structure but in the latter case the fact of the dependence of the luminescence spectrum shape on the exciting light frequency is observed.

2. The no-phonon lines of high-frequency local vibrations of molecular centers are narrow. Halfwidths from 2 to 13 cm^{-1} detected at 4.2 K are mainly due to the inhomogeneous broadening by point defects and dislocations. The corresponding homogeneous width is of the order of 0.1 cm^{-1} [3]. It is shown that owing to the low decay probability the temperature broadening of the lines of high-frequency vibrations in the region from 2 to 50 K is caused by the modulation of vibronic levels with the low-frequency (5 to 17 cm^{-1}) pseudolocal vibrations. The lines of low-frequency local vibrations in the spectra of $CsBr-NO_2^-$ are broadened both by modulation and decay mechanisms. The broadening of lines in the series of $1.\nu_2.0$ in the $KCl-NO_2^-$ spectrum can be interpreted by the decay process only.

3. It is well known that in the suitable temperature region molecular ions in crystals can reorientate between equivalent equilibrium orientations. With the help of studying time and temperature dependences of the intensity of polarized luminescence and observing the temperature alterations of the polarization degree the reorientation processes of O_2^-, S_2^- and NO_2^- ions in the ground and excited electronic states are investigated [4]. Three reorientation mechanisms, i.e. tunneling in the ground librational level, tunneling through excited librational levels and jumping over the potential barrier, are distinguished in different crystals and the reorientation parameters for the ground and excited electronic states are determined.

1. L.A.Rebane, Physics of Impurity Centres in Crystals, ed. by G.S.Zavt, Tallinn, 1972, p. 353;
2. K.K.Rebane, L.A.Rebane, J. Pure Appl. Chem., 37, 161, 1974;
3. A.Freiberg, L.A.Rebane, phys. stat. sol. (b), 81, 1, 1977;
4. L.A.Rebane, A.B.Treshchalov, J. Luminescence, 12/13, 425, 1976.

ASPECTS OF DIFFUSION IN AN ELECTRIC FIELD

Robert J. Friauf
University of Kansas, Lawrence, Kansas, U.S.A.

Since the diffusing species in ionic crystals are charged defects, it is possible to modify the diffusion behavior by imposing an external electric field [1]. It is appropriate to introduce a macroscopic tracer mobility (defined by $V = M_T E$), which is related to the tracer diffusion coefficient D_T^* by the usual Einstein relation $(D_T^*/M_T) = f(kT/q)$. The correlation factor f should have a value between 0.78 and 1 for impurity diffusion via vacancies on a fcc lattice. The macroscopic diffusion equation is then modified by including the proper term for the drift current [1].

For diffusion from a point source in an infinite medium (only one dimensional geometries are treated here), a solution can readily be obtained by using a moving coordinate system with $x' = x - Vt$. The spreading of the diffusion profile is measured by a diffusion length $d = \sqrt{4Dt}$, and the displacement is given by a drift length $s = Vt$. It is clear for this case that spreading and drift occur simultaneously and independently, i.e., the Gaussian diffusion profile for zero field is simply displaced rigidly by the drift length.

For other situations of interest (see examples below) the experimental conditions maintain a constant concentration at the surface of a semi-infinite medium. The fixed boundary in this case destroys any simple application of a moving coordinate system, but an exact analytical solution can be found for any value of the field by the method of Laplace transforms [2]. The solution is again characterized by the two lengths d and s: for a given time the length scale is established by d, and the shape of the diffusion profile is determined uniquely by the ratio $u = s/d$. The evolution of the diffusion profile in time involves a gradual spreading $(d = \sqrt{4Dt})$ and also a changing shape because drift dominates at longer times $(s = Vt)$.

Many computer generated graphs are presented to illustrate these effects. A positive field always pulls additional diffusing material into the sample from the surface, whereas a negative field inhibits penetration. A strong positive field gives essentially a step function profile of width s but rounded over a region s ± d. For negative fields at first some material enters the sample by diffusion, but at longer times a steady state exponential profile is attained.

It is also possible to integrate analytically over x to obtain the total amount of material C(t) that has entered the sample at any time. A universal function is obtained in the form $C(t) = c_0\, d(t)\, F[u(t)]$, where c_0 is the constant surface concentration. Additional graphs illustrate the general form for various cases and show the proper asymptotic behavior at long time--linear in t for positive field, $\sqrt{t}$ for zero field, and saturation for negative field.

The problem that initiated this work involves diffusion of Mn into MgO [3]. For typical values of $D_T = 10^{-10}$ cm^2/sec at 600°C and E = 1000 Volt/cm, the ratio $u = s/d = eEd/kT \approx 50$ indicates that drift should be dominant. Similar problems occur for preparation of optical waveguides by electrodiffusion of metal ions into ferroelectric crystals [4].

Thus these solutions should be of general interest. The great advantage of analytical solutions (even when complicated) is that general features, interesting trends, and asymptotic limits can be fully comprehended at a single glance. Furthermore the introduction of universal functions shows that all cases can be handled simply by using the appropriate length scale d and shape parameter u.

[1] V. C. Nelson and R. J. Friauf, J. Phys. Chem. Solids 31, 825 (1970).
[2] H. S. Carslaw and J. C. Jaeger, Conduction of Heat in Solids (Oxford Press, 1959).
[3] R. Weeks and E. Sonder, Oak Ridge Nat. Lab., private communication.
[4] T. Izawa and H. Nakagome, Appl. Phys. Lett. 21, 584 (1972).

FURTHER RESULTS FOR THE CONDUCTIVITY ANOMALY IN AgCl AND AgBr

Robert J. Friauf and Ko-Jun Kao
University of Kansas, Lawrence, Kansas, U.S.A.

AgBr shows a large and anomalous ionic conductivity at high temperatures. The value of nearly 1 ohm^{-1} cm^{-1} at the melting point is larger than for many superionic conductors, and culminates an anomalous rise of almost 100% over a 150°C range. AgCl displays similar effects on a slightly less grandiose scale. In order to study these effects closer to the melting point, previous work [1] has been extended with improved experimental techniques, and an attempt is made to apply simple empirical theories to the results.

Because the sample resistance becomes as low as 2 ohm, a four-wire method of resistance measurement, similar to that for platinum resistance thermometers, is used to compensate for lead resistances. The sample thermocouple has been recalibrated, and temperature control has been improved to 0.1°C. Attachment to a computer network facilitates acquisition and handling of data at 1°C intervals, thereby providing many more points for statistical analysis.

The observed conductivity anomaly is expressed in terms of lowering of the Frenkel formation energy, by an amount Δg which rises to over 100 meV for AgCl and 200 meV for AgBr. The new measurements provide a significantly better comparison with recent results for diffusion of Na in both AgCl and AgBr[2]; it appears that practically all of the anomaly is due to an increased concentration of defects rather than to any diminution of jump energies.

Long range Coulomb interactions, as represented by the Debye-Hückel-Lidiard theory, are important because of the large defect concentrations (over 1% in AgBr). But they can account for only one-half of the observed anomaly in AgCl and for less than one-third in AgBr. Many other effects, such as anomalous increases in lattice parameter and dielectric constant, also point to a general loosening of the lattice at high temperatures. Hence an attempt is made to include the influence of the dielectric constant on the formation energy by means of the classical continuum theory of Jost [3]. Although a plausible qualitative picture is obtained, the observed Δg rises much more rapidly at the very highest temperatures, suggesting more of a cooperative phenomenon. It may be possible to simulate such an effect by including a term in the formation energy proportional to the number of defects. But what is really needed is a much improved calculation of the formation energy for these materials!

[1] J. K. Aboagye and R. J. Friauf, Phys. Rev. B11, 1654 (1975).
[2] A. P. Batra and L. M. Slifkin, Phys. Rev. B12, 3473 (1975).
[3] W. Jost, Diffusion in Solids, Liquids, and Gases (Academic Press, 1952).

THERMALLY INCREASED RANGE AND NON-LINEAR EFFECTS IN PHOTOCONDUCTIVITY FROM F CENTERS IN KCl

Robert J. Friauf and Andrzek Radlinski*
University of Kansas, Lawrence, Kansas, U.S.A.

At 200°K the photocurrent is limited by trapping of electrons at F centers, and the photocurrent shows the expected linear dependence on light intensity and F center concentration. In the thermally increased range at 300°K the current is 10 to 100 times larger because of thermal decay of F' centers [1]. Noticeable non-linear effects are also apparent in the response to F center concentration [2], optical absorption [3], and light intensity [4].

In order to explain these effects a model is proposed involving trapping at neutral F centers, α centers formed during illumination, and additional deep traps, along with thermal decay and optical bleaching of F' centers [3,4]. For typical circumstances the conduction band electrons have a lifetime before trapping of 10^{-10} sec and a mean displacement length of 10^{-7} cm. Other characteristic times are 10^{-1} sec for decay of F' centers at 300°K and 10 sec for production of a significant number of α centers.

The theory of photoconductivity is reformulated to give an expression for the photocurrent from each volume element as proportional to the concentration of photoelectrons in that volume element at any instant of time. It is assumed that local equilibrium is attained in each volume element, i. e., that space charge effects and diffusion currents are unimportant. The total photocurrent is then found by integration over the thickness of the sample.

The rate equations for formation and destruction of photoelectrons and of F, F', and α centers contain non-linear terms for trapping of photoelectrons at α centers. Because of these terms the final steady state concentration of photoelectrons is governed by a square-root dependence on light intensity and absorption coefficient [5,6]. A very good approximate time-dependent solution can be obtained by assuming

that the concentration of photoelectrons follows quasistatically the relatively slow changes in concentration of F' and α centers. These solutions show both the gradual increase of photocurrent to the final steady state value during illumination and also the slow decay of the dark current that persists after the light is switched off.

The physical basis of the thermally increased range and non-linear effects may be understood as follows. When the light is switched on, the photoelectron concentration very quickly (10^{-10} sec) rises to an initial steady state value determined solely by trapping at F centers. This value remains constant for a very long time while the F' (and α) center concentrations gradually build up. When the decay time of F' centers is reached (10^{-1} sec), decay of these centers returns additional electrons to the conduction band, and the concentration of photoelectrons begins to rise toward the final steady state value. If trapping at α centers were negligible, the final value would be determined entirely by the additional deep traps. But because of the larger concentration of photoelectrons from F' center decay, trapping at α centers becomes significant at lower α center concentrations, and the final steady state consequently shows the square-root dependence described above. This state is attained in a characteristic time given by the geometric mean of the decay time of F' centers and build-up time of α centers (1 sec). The primary reason for the appearance of these effects in the experimental observations is that the response time of the vibrating reed electrometer used to measure the photocurrent is of the same order of magnitude (10^{-2} to 1 sec).

* Permanent address: Institute of Experimental Physics, University of Warsaw, Poland.

[1] J. J. Markham, F-Centers in Alkali Halides, (Academic Press, 1966).
[2] G. Glaser and W. Lehfeldt, Gött. Nachr. 2, 91 (1936); 3, 31 (1937).
[3] R. J. Friauf and D. R. Renneke, Bull. Am. Phys. Soc. 15, 340 (1970).
[4] H. J. Hoffmann, phys. stat. sol. (b) 57, 123 (1973).
[5] R. J. Friauf, Int. Conf. on Color Centers, Abstract 22 (1971).
[6] H. J. Hoffmann, F. Stöckmann, U. Todheide-Haupt, phys. stat. sol. (b) 56, 549 (1973).

THERMOLUMINESCENCE OF CRYSTALLINE QUARTZ*

G. E. Fuller and P. W. Levy
Department of Physics, Brookhaven National Laboratory
Upton, New York 11973

The thermoluminescence (TL) of a number of ^{60}Co gamma-ray irradiated natural crystalline quartz samples from different localities has been studied using apparatus which simultaneously measures the intensity and spectral distribution of the TL emission. Complete emission spectra from 250 nm to 800 nm are measured and recorded at closely spaced temperature intervals. These measurements are conveniently displayed as 3-D plots as shown in Fig. 1. This figure shows the results of a single TL run on a high purity single crystal sample of Brazilian hydrothermal quartz that had been exposed to 10^7 R of gamma rays. The plotted intensity is fully corrected for the phototube spectral response and is accurately proportional to the number of photons emitted per unit time and per unit energy interval.

Detailed analysis of the TL measurements are made by first fitting the corrected emission spectra for each temperature interval by one or more Gaussian bands. In nearly all the samples studied the TL emission spectra could be fitted by a single Gaussian band centered at about 2.5 eV. The band peak energy slowly increases with rising temperature, in contrast to the more often observed decrease. The band width increases with temperature as expected, but in addition it shows an abrupt jump at about 200°C. The glow curves used for kinetic analysis represent successive band area vs temperature. The glow curve shapes as seen in the 3-D plots and derived from the emission band areas vary widely and

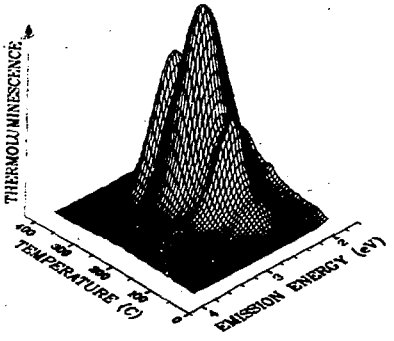

Fig. 1. Thermoluminescence of Brazilian natural quartz after gamma-ray exposure of 10^7 R. Heating rate 10.5°C min^{-1}.

*Research supported by the U.S. Energy Research and Development Admin.

depend on sample origin and radiation treatment. Three such glow curves are shown in Fig. 2. Each sample was exposed to 10^7 R of gamma rays, and the TL was recorded using identical conditions. The glow curves were analyzed by fitting first-order kinetic expressions to each glow peak. A least squares fit to the glow peaks for the TL emission from the sample described above is shown in Fig. 3. Five individual first-order peaks are shown along with their sum which passes accurately through the data points. Attempts at fitting the glow curves using second-order glow peaks are markedly less successful.

Several important observations can be made. All of the natural quartz samples studied show similar emission characteristics, with one Gaussian emission band having the same energy and width and the same temperature behavior for each sample. The glow curve shapes vary widely among the samples from different origins but are fully reproducible for similar samples. These results suggest that the luminescence center responsible for the emission is universal in all the samples, while the charge trapping centers responsible for the glow curve shapes are highly impurity dependent.

Fig. 2. Glow curves for three natural quartz samples from different origins.

Fig. 3. Glow curve and fitted glow peaks for Brazilian sample shown in Fig. 1.

INVITED PAPER

AgI-TYPE SOLID ELECTROLYTES

K. Funke, Institut für Physikalische
Chemie and Sonderforschungsbereich 126,
Göttingen, Germany.

In the first part of the talk, the following properties of AgI-type solid electrolytes are briefly reviewed:

(i) ionic conductivity
(ii) crystal structure
(iii) heat capacity
(iv) diffusion and correlation.

Ionic conductivities of AgI-type solid electrolytes are of the order of 1 $(\Omega cm)^{-1}$ and thus comparable to those of the best conducting liquid electrolytes. The ionic conduction is entirely due to the diffusive motion of the cations. Hence a "liquid-like" behavior has been ascribed to the cations since the discovery of α-AgI early in this century.

The results of structural refinements are characterized by the impossibility of assigning proper sites to the cations within the rigid framework of the anion lattice. The number of voids provided by the anions always exceeds the number of cations and the voids seem to be occupied more or less at random. The voids are interconnected by channel-like diffusion paths.

Within the cation-disordered phases, the heat capacities are found to be almost constant or even decreasing with increasing temperature. Obviously the disordering process of the cation sublattice is already completely finished at the transition into the highly conducting phase.

Comparison of tracer-diffusion coefficients and conductivity data shows that the motion of the cations in these systems is a highly correlated process. In the case of, e.g., α-AgI one has to assume a forward correlation of the jumps of different cations, see below.

In the second part of the talk, we discuss some properties of the cation motion on scales of Ångströms and picoseconds. This discussion is based on experimental results from

(v) quasielastic neutron scattering and
(vi) microwave and far-infrared spectroscopy.

Both the neutron spectra and the electromagnetic spectra are interpreted in terms of a simple model for the cation motion. At times shorter than ~1 ps, the cations essentially perform a three-dimensional liquid-like diffusion. At times longer than ~1 ps, they experience the restriction of their motion to the system of voids and channels. The cations are found to spend comparable amounts of time of the order of 10 ps resting in the voids and diffusing through the channels. In α-AgI, the radius of the local random motion within the voids and channels is estimated to be ~1 Å.

In various AgI-type solid electrolytes the process of forward correlation of diffusion steps of different ions is reflected by the microwave spectra.

References:

"Superionic Conductors: Chemistry, Physics and Applications" (G.D. Mahan and W.L. Roth eds.), Plenum Press, New York 1976

K. Funke: "AgI-Type Solid Electrolytes", Progr. Solid State Chem. 11, 345 (1976)

PHOTOINDUCED COLOR CENTER BANDS IN INSULATING CADMIUM SULPHIDE CRYSTALS

M. Georgiev, S. Kanev, K. Tsvetkova
Institute of Solid State Physics,
T. Todorov
Central Laboratory of Optical Information Storage and Processing, Bulgarian Academy of Sciences, Sofia, Bulgaria

Highly insulating CdS samples are prepared by first incorporating a stoichiometric excess of Cd from the vapor and then diffusing Cu from a cathode-sputtered layer, all at 500 ^{o}C. It is known that cadmium incorporates in the form of interstitial atoms which are doubly ionized at room temperature giving rise to n-type conductivity. On introducing copper, it compensates the electronic conductivity because of its acceptor action. Such materials are interesting to study for they imitate by composition a variety of CdS-based photo-devices.

When doubly-doped CdS crystals are illuminated with, say, white light at RT they change color and develop three new optical absorption bands: one in the visible, centered at 650 nm, and two in the near infrared, at 800 nm and 1350 nm resp. The latter IR band is well-isolated and nearly symmetric in shape while the remaining two strongly overlap. The growth kinetics of the three bands were investigated in the vicinity of RT. They reveal a thermally-activated formation rate and saturated densities that drop as the temperature is raised. The reverse process leading to saturation is found to be the thermal decomposition of the species formed. The observed growth- and thermal decay- rates of the bands strongly suggest that ionic migration is involved in the formation of the absorbing centers.

At this stage of our knowledge of the process the nature of the infrared transitions seems better understood. The longerwavelength band coincides with the well-known IR

absorption associated with substitutional copper in cadmium sulphide. The shortwavelength IR band is then due to transitions between the valence band and the Cu levels. However, it is not yet known just how this substitutional copper forms, whether during sample preparation or by photochemical reaction. The nature of the visible band seems more obscure. It is believed to arise from transitions at a complex center formed by photochemical aggregation of Cd and Cu.

A model describing the presumed photochemical reactions is proposed and compared with the experiment. Some possibilities of using the doubly-doped CdS materials for optical information storage will also be discussed.

LASER SPECTROSCOPIC EXPERIMENTS WITH COLOR CENTERS IN KCl

M. Georgiev
Institute of Solid State Physics, Bulgarian Academy of Sciences
Y. Vassilev
Faculty of Physics, University of Sofia
T. Todorov
Central Lab of Optical Information Storage and Processing
G. Todorov
Department of Physics, Medical Academy, Sofia, Bulgaria

Light pulses produced by a mode-locked Nd-glass laser either at first or at second harmonic of the generation were shone on additively colored KCl crystals at room temperature. In either case the change in transmission due to the excitation was monitored in the F' band range, at 750 nm. At second harmonic (530 nm) the excitation (near the F band peak) led to the production of thermally unstable F' centers. Shots at first harmonic (1060 nm) led to different results depending on the amount of pre-exposure of the sample to light in the F band range. Freshly-quenched samples, handled carefully in the dark prior to the shot, showed just minor signals due to transient absorption presumably resulting from two-photon (1s-2s) transitions in the F band range followed by relaxation and F' center formation as in the one-photon process. Samples in which the aggregate bands have been developed by pre-exposure exhibited higher signals due presumably to F' centers produced through photoionization of aggregate centers by the 1060 nm light followed by electron trapping at residual F centers.

Both the F' yield and decay kinetics were measured in an attempt to obtain data on the electron trapping and transition probabilities of color centers. The results are discussed in terms of pertinent models.

JAHN-TELLER INDUCED MIXING OF MAGNETICALLY PERTURBED Tl^+-TYPE ENERGY LEVELS IN POTASSIUM BROMIDE

U.Giorgianni, G.Mondio, G.Saitta and G.Vermiglio

Istituto di Fisica dell'Università di Messina, and Gruppo Nazionale di Struttura della Materia del C.N.R., Messina, Italy.

Tl^+-and In^+-doped alkali halides are characterized by three absorption bands[1] labelled A, B, and C in order of increasing energy, each of one being affected by large electron-lattice interaction which splits the energy degeneracy of the electronic states responsible of the corresponding absorption and determines their width increasing with temperature[1]. The role of the J-T effect in the excited states of this kind of phosphors has been analyzed either by normal- and modulated-spectroscopy measurements[2] which have supported the theory of magnetically induced circular dichroism, formulated by Cho[3], through the experimental evidence of a central structure in the MCD spectra of the C absorption band, as one can observe in figures 1 and 2 where we have reported dichroic line-shapes of Tl^+ and In^+-doped KBr crystals. A more interesting result has been deduced through the analysis of the experimental curves by the

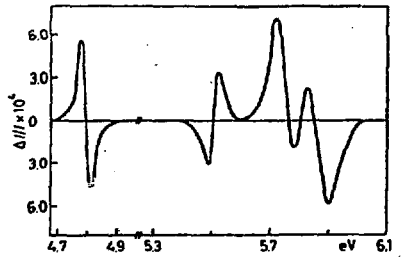

Fig. 1.

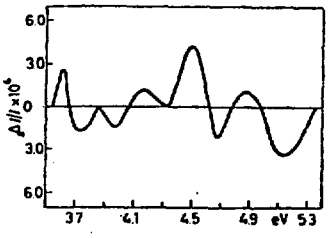

Fig. 2.

Fig. 1. – Magnetic-field-induced relative variation of the transmitted light *vs.* photon energy for KBr:Tl at liquid-nitrogen temperature.

Fig. 2. – Magnetic-field-induced relative variation of the transmitted light *vs.* photon energy for KBr-In at room temperature.

method of moments of Henry, Schnatterly and Slichter[4] (HSS) which allowed us to evaluate the effective g-factors $\tilde{g}$ of the excited states giving rise to the observed optical absorption.

The experimental values are in fact in a marked disagreement with the theoretical ones reported in the theory of Honma[5]. The discrepancy between theoretical and experimental values, tentatively attributed to the difference from unity of

the orbital g-factor, induced Honma to hypothesize the existence of two distinct orbital factors for singlet and triplet states which have different radial wave function[5]. However, on the basis of the considerations on the complete expressions of the A-, B-, and C-state eigenfunctions previously reported by us[2], we have evaluated the variations of the first order moments ΔE_R of any R absorption band related to the effective g-factors by $\Delta E_R = \mu_B g_R H$, where μ_B is the Bohr magneton and H the applied magnetic field (~4 kG). The detailed form of ΔE_R is, for the A-, B-, and C-band respectively:

$$\Delta E_A = 2\left(\mu \frac{\langle c|H_{el}|a\rangle}{E_a - E_c} - \nu\right)^2 \mu_B g_{orb} H \quad ,$$

$$\Delta E_B = 2\left(\mu \frac{\langle c|H_{el}|b\rangle}{E_b - E_c} - \nu \frac{\langle a|H_{el}|b\rangle}{E_b - E_a}\right)\left(\mu \frac{\langle b|H_{el}|c\rangle}{E_b - E_c} - \right.$$

$$\left. - \frac{\langle b|H_{el}|a\rangle}{E_b - E_a} \mu_B g_{orb} H \right) \quad ,$$

$$\Delta E_C = 2\left(\mu - \nu \frac{\langle a|H_{el}|c\rangle}{E_c - E_a}\right)^2 \mu_B g_{orb} H \quad .$$

Substituting to the various parameters their numerical values currently reported in literature, one can observe that the effective g-factors as deduced from the above expressions suffer the same variations experimentally evidenced so that the J-T effect may be invoked to explain the reduction of the A-band $\tilde{g}$ factor as arising from the electron-lattice coupling of the impurity electronic states perturbed by the external magnetic field.

References

1) - A.Fukuda, Sci. Light (Tokyo) 13, 64(1964); 27, 96 (1969).
2) - U.Giogianni, G.Mondio, G.Saitta and G.Vermiglio, Phys. Stat. Sol. (b) 74, 317 (1976).
3) - K.Cho, J. Phys. Soc. Japan 27, 646 (1969).
4) - C.H.Henry, S.E.Schnatterly and C.E.Slichter, Phys. Rev. 137, A583 (1965).
5) - A.Honma, Sci. Light (Tokyo), 16, 229 (1967); 21, 119 (1972).

THERMAL DECAY OF THE F^- CENTRE IN KCl

D. H. Goode and J. H. Simpson
Physics Division, National Research Council, Ottawa, Canada

The F^- centre plays a crucial role in the mobility of vacancy defects in coloured alkali halides at room temperature and below yet the kinetics of the formation and decay of this centre are still not well understood. We have studied both the fraction of F centres that can be converted to F^- centres by steady state illumination in the F band (F^- conversion efficiency) and the decay of the F^- centres after the irradiation ceased over the range 77 K to 230 K. F^- centres were prepared by irradiating freshly quenched, additively coloured KCl crystals with F light at 500 nm and the F and F^- populations were measured by their optical absorption.

The decay curves were analyzed with a kinetic model in which five processes were considered namely thermal excitation of electrons from the F^* and F^- levels to the conduction band, capture of conduction band electrons by F^* and F^- and decay of the F^* state to the F centre ground state. Under these conditions the decay of the F^- centre can be expressed by the equation

$$L(t) = 2 \ln \frac{f(t)}{f(0)} + F\left\{\frac{1}{f(t)} - \frac{1}{f(0)}\right\} = a\left\{\frac{t}{\tau} + \ln \frac{f(t)}{f(0)}\right\}$$

where f(0) and f(t) are the F^- centre concentrations at times 0 and t, F is concentration of F centres before any F^- centres were formed, a is the probability of an electron in the conduction band forming an F^- centre divided by the probability of the same electron forming an F centre in the ground state and τ is the lifetime of the F^- centre. Above 180 K $a \ll 2$ consequently $L(t) = at/\tau$. Plots of L(t) against time are shown in the figure. For ease of presentation the L(t) axis has been scaled by the factor X which has the values .16 at 179 K, 4.0 at 199 K and 40 at 230 K. In the range 180 K to 210 K L(t) could be accurately represented by straight lines through the origin for most of the crystals studied. This is in marked contrast to previous attempts to fit the decay[1] and is probably due to the lower concentration of colour centres in our crystals ($F < 7 \times 10^{16}$ cm^{-3}). Below 180 K, where the simple formula does not apply,

the curves are non linear near the origin but rapidly become straight lines. Above 210 K the results are not reproducible. The repeated formation and decay of F^- centres causes the F^- conversion efficiency to progressively fall and the F^- decay to become more rapid. These effects are almost certainly due to preaggregation (clustering) of the F, F^+ and F^- centres which would allow electrons to tunnel from F^- centres to nearby F^+ centres thus providing another path for the F^- centres to decay. The slope of L(t) varies exponentially with $(kT)^{-1}$ and semi log plots of these quantities gave an activation energy of 0.50 ± 0.02 eV, in good agreement with published results[1]. The analysis has assumed that the predominant process for electrons in the conduction band to reform F centres in the ground state is via capture into the F^* state consequently this activation energy represents the difference in energy between the F^* and F^- levels.

1. G. Goldberger and F. J. Owens, Phys. Rev. B, 4, 3927 (1971).

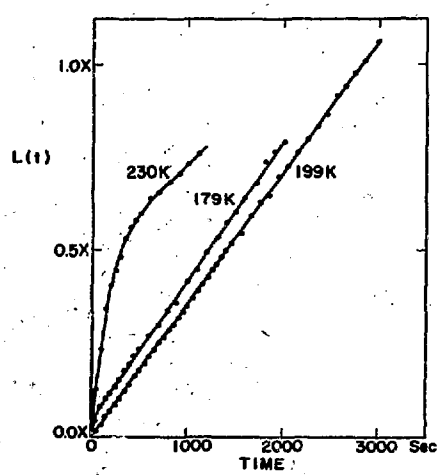

ESR STUDY OF HEAVY METAL IMPURITIES WITH p^1 CONFIGURATION IN KCl

E. Goovaerts, A. Lagendijk, D. Schoemaker

Physics Department, University of Antwerp (U.I.A.)

Tl^+, Pb^{++} and Sn^{++} impurities are known to be good electron traps in several alkali halides. A short x-irradiation at 77K produces Tl° ($6p^1$), Pb^+ ($6p^1$) and Sn^+ ($5p^1$) whose optical properties have been studied already in rather great detail. For Sn^+ ESR spectra have been detected and analysed[1]. However, the ESR spectra of Tl° and Pb^+ have escaped detection so far even after many searches.

Here we report ESR results on Tl° and Pb^+ defects which are, however, not the regular Tl° and Pb^+ species mentioned above. The Pb^+ defect is produced after a long (~ many hours) of x-irradiation at 77K while the Tl° defect is produced by x-irradiation at room temperature (where the regular Tl° is thermally unstable). These measurements were extended to KCl:In^+ and KCl:Sn^{++}. In KCl:In^+ no resonance was detected after x-irradiation at 77K, but an irradiation at room temperature yielded a strong In° ($5p^1$) resonance. In KCl:Sn^{++} a non regular Sn^+ resonance was observed too. The ESR results are summarised in the Table. These ESR data are readily explained assuming that all these metal impurities possess a p^1 configuration. The signs of the hyperfine components were obtained from a quantitative analysis.

Table. ESR data in KCl on some heavy metal ion impurities possessing p^1 configurations. The hyperfine parameters are given in gauss.

	$g_{/\!/}$ [100]	$g_\perp$	$A_{/\!/}$ [100]	$A_\perp$
In°	1.985	1.887	+387	+95
Tl°	1.7880	1.3084	+3716	-2015
Pb^+	1.6297	1.3280	+1625	-2564
Sn^+	1.9584	1.7891	-734	+622

It is believed that these metal atoms or ions are situated at positive ion sites and that they are each associated with a negative ion vacancy. Or, to put it differently, that these defects are F-centers associated with heavy metal ion impurites and that the electron is localised mostly on the heavy metal ion.

(1) C.J. DELBECQ, R. HARTFORD, D. SCHOEMAKER and P.H. YUSTER, Phys. Rev. B13, 3631 (1976).

ATOMISTIC CALCULATIONS ON DISLOCATIONS AND POINT DEFECTS IN ALKALI AND SILVER HALIDES

F. Granzer, V. Belzner, M. Bücher, P. Petrasch, and H. Potstada; Institut für Angewandte Physik der Univeristät Frankfurt am Main, Robert Mayer-Str. 2-4, D-6000 Frankfurt/M.

An account is given on atomistic calculations of dislocations and point defects in sodium and silver halide crystals. Special efforts have been made to apply realistic interaction potentials in order to distinguish properly between alkali and silver halides with respect to plastic properties and the different types of intrinsic point imperfections (Schottky or Frenkel type, respectively). For this purpose, the parameters appearing in the potentials (also three body interactions were taken into account) have been adjusted to a variety of physical properties of the crystals, e.g., elastic constants (stiffnesses) of second and third order, static and high frequency dielectric constants, several characteristic frequencies of the phonon dispersion curves, etc.

Simultaneously the elastic calculations have been supplemented with the help of second order elastic theory in order to reconcile the configuration of the atomistic treatment of the core region with that of the surrounding elastic continuum with the aim to avoid artefacts in the critical zone between.

For different slip planes, results will be given with regard to core energies, Peierls stresses, dissociations of dislocations, formation energies of point defects, and association energies between point defects and dislocations.

INTERSTITIAL STABILIZATION MECHANISM IN ALKALI HALIDES IRRADIATED AT 77 K

G. GUILLOT and A. NOUAILHAT
Laboratoire de Physique de la Matière* - Bâtiment 502
Institut National des Sciences Appliquées de Lyon
20, Avenue Albert Einstein 69621 VILLEURBANNE CEDEX -France-

The F and H centers are the primary irradiation defects in alkali halides (1). The F centers are immobile up to high temperatures, whereas H centers become mobile at quite low temperature (above 40 K in KBr). A stabilization process is necessary for the interstitial to avoid its quick recombination with F centers and to produce a stable coloration in crystals above 77 K.

We have systematically studied the growth kinetics of F centers in alkali halides irradiated with medium energy electrons as a function of various parameters (energy deposition rate, temperature, purity, crystal). The F center concentration is proportional to $t^{0.8}$ (where t is the irradiation time) up to a few $10^{19}/cm^3$ in the pure samples and to $t^{0.5}$ in doped crystals. Moreover, the dose rate dependence of the defect formation is very small at 77 K.

The set of our experimental results is not in agreement with the solution of the kinetic equations deduced from the simple models where the F center creation rate is fixed by the secondary reactions taking place after the primary Frenkel pair creation : recombination of free interstitials with F centers and trapping of interstitials by impurities (2)(3)(4).

We give a more complete model which takes into account all the experimental results. The leading process is the formation of interstitial clusters, which also have been observed by electron microscopy at 77 K (5). We show that the homogeneous stabilization (V_4 center creation by random collision of two free interstitials) is not important with an impurity concentration as small as $10^{16}/cm^3$. The cluster nucleation is inhomogeneous and takes place at the residual impurities. The V_4 center cluster originates from the interaction between a mobile H center and another one temporarily trapped by an impurity and develops then by capture of H center pairs,

the cluster acting as impurity to form the V_4 center aggregates. These ideas are in agreement with the fact that an H center trapped by a defect or by an impurity distorts the lattice and interacts very efficiently with another free one (6).

The theoretical curves obtained from the resolution of the kinetic equations are in good qualitative agreement with the experimental results if we suppose that the interstitial clusters have a capture cross section increasing with their size (up to a few hundred interstitials in ultra pure samples) (7).

---

(1) N. ITOH, J. de Physique 37, C7 (1976) 27
(2) E. SONDER, Phys.Stat.Sol. 35 (1969) 523
(3) Y FARGE, J.Phys.and Chem.Sol. 30 (1969) 1375
(4) F. AGULLO LOPEZ, F. JAQUE, J.Phys.and Chem.Sol., 34 (1973) 1949
(5) L.W. HOBBS, A.E. HUGHES, D. POOLEY, Proc.R.Soc.London A332 (1973) 167
(6) J. HOSHI, M. SAIDOH, N. ITOH, Cryst.Latt.Def., 6 (1975) 15
(7) G. GUILLOT, A. NOUAILHAT, J. de Physique, 37, C7 (1976) 611

---

* Equipe de recherche associée au C.N.R.S.

RADIATION-INDUCED OXYGEN INTERSTITIALS IN MgO*

L. E. Halliburton
Physics Department
Oklahoma State University, Stillwater, OK, USA

and

L. A. Kappers
Department of Physics and Institute of Materials Science
University of Connecticut, Storrs, CT, USA

A series of MgO single crystals have been neutron irradiated to doses from 9×10^{16} n/cm^2 to 7×10^{17} n/cm^2 while maintaining the sample temperature near 65 °C. In addition to the expected F, F^+, and V^- centers, the irradiation produced three distinct but yet very similar ESR spectra which have not been previously reported. These centers have been tentatively labeled as H_I, H_{II}, and H_{III} and their g values are given in the table. The x and z axes lie in the (010) plane but the z axis deviates from the [001] direction by the angle θ_g. The y axis is along the [010] direction.

	g_x	g_y	g_z	θ_g
H_I	2.0066	2.0014	2.0775	30.5°
H_{II}	2.0071	2.0016	2.0769	31.3°
H_{III}	2.0076	2.0019	2.0661	31.0°

These g tensors strongly suggest we have produced O_2^- molecular ions.[1] The H_{III} center exhibits a weak hyperfine coupling to a 100% abundant $I = \frac{1}{2}$ nucleus (hydrogen or fluorine) with $A_x = 8$ MHz, $A_y = 13$ MHz, $A_z = 17$ MHz, and $\theta_A = -26°$. Approximate decay temperatures for the H_I, H_{II}, and H_{III} centers are 340 °C, 290 °C, and 310 °C, respectively. As the H_{II} and H_{III} centers are thermally destroyed, the H_I center concentration

increases. It has been previously reported by Chen et al.[2] that the annealing of F-type centers in the temperature range 200-500 °C is due to interstitial-vacancy recombination.

We believe the observed H centers are the result of the stabilization in the lattice of isolated oxygen interstitials. More specifically, it is proposed that magnesium vacancies act as the stabilizing entity and that the interstitial oxygen combines with a substitutional oxygen ion adjacent to the magnesium vacancy thus forming an O_2^- molecule. This would be equivalent to having a V-type center capture an oxygen interstitial atom ($O^- + O^\circ \rightarrow O_2^-$). The three distinct H centers would then result from slight additional perturbations on the opposite side of the vacancy, i.e., the H_{III} center would be analogous to the V_{OH} or V_F center. Most likely, there will be some sharing of the unpaired electron from the molecule with one or more of the equatorial oxygen ions surrounding the magnesium vacancy.

*Research supported in part by NSF Grant DMR 73-07656-A01.

[1]T. P. P. Hall, J. Phys. C 8, 1921 (1975).

[2]Y. Chen, R. T. Williams, and W. A. Sibley, Phys. Rev. 182, 960 (1969).

LOCALIZED MODE OF LITHIUM IN AgBr-AgCl MIXED CRYSTALS

Takeshi Hattori and Akiyoshi Mitsuishi

Department of Applied Physics, Osaka University,
Suita, Osaka, Japan.

The effects of the additional halogen impurities on the Li-localized mode in AgBr are studied by the infrared absorption. When some amount of chlorine or iodine is introduced in AgBr:Li, additional new bands, resolved from the unperturbed fundamental band, are observed. Figure 1 shows the infrared absorption spectra of 'Li-localized mode' in AgBr with and without chlorine mixing. Each spectra was obtained by using the absorption coefficient of a AgBr doped with the same acount of chlorine as a reference. In the case of Fig.1, the lithium concentration in crystals was fixed nearly 10^{-3} molar fraction. In the AgBr:Li sample, the spectrum consists of two distinct peak; strong one at 205.9 cm^{-1} and a weak one at 191.8 cm^{-1} which are due to ^{6}Li and ^{7}Li localized modes, respectively.[1),2)] When the chlorine ions are added, the new bands appear and the spectrum is complicated as shown in Fig.1. Generally, the shape of the resonance type absorption band such as the localized mode shows Lorentzian-type one. Actually, in the case of the localized modes in silver halides, we have obtained the absorption bands with Lorentzian-type shape.[1)] In order to analize the obtained spectra, they were decomposed assuming the Lorenzian-type and the six bands, in which the unperturbed band was included, were obtained for the ^{6}Li-localized mode in AgBr containing chlorine ion. Each extra band observed in the samples with chlorine was assigned to the localized mode oscillator with C_{4v}, C_{3v} and C_{2v} point symmetry, respectively. Moreover, the second harmonics were also observed near 400 cm^{-1}. The shape of this absorption band is very complex, because of the overlap of the many bands. To make an analysis of the second harmonics and a detailed discussion on an anharmonic oscillator, the measurements of the Raman scattering due to the fundamental bands and the second harmonics of the Li-localized modes in AgBr:Cl are under way.

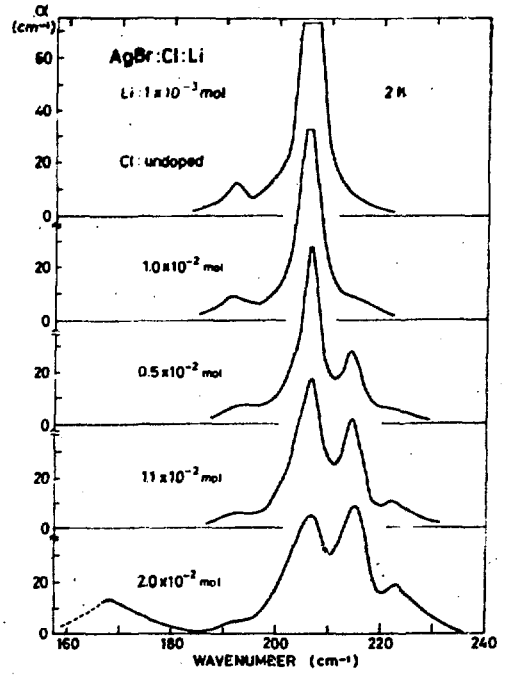

Fig.1. The absorption spectra of ^{6}Li-localized mode in AgBr doped with and without chlorine.

References

1) T.Hattori, K.Ehara, A.Mitsuishi, S.Sakuragi and H.Kanzaki: Solid State Commun., 12 545 (1973)

2) T.Hattori, K.Ehara, M.Hamasaki and A.Mitsuishi: phys. stat. sol. (b), 70 311 (1975)

LATTICE-DEFECT MODELS OF FAST ION CONDUCTORS

Y. Haven
Wake Forest University, Winston-Salem (N.C.) U.S.A.

The characteristic feature of lattice-defect models is that sites capable to receive ions are left vacant (vacancy model) or sites of second choice are partially occupied by ions (interstial(cy) model). The typical fast-ion conductor representatives in these two categories are α-AgI and β-alumina.

In this paper it will be discussed that defect models describe the transport properties of these two compounds quite well: pre-exponential factors, ratio of diffusion and ionic conductivity, infra-red properties, NMR, etc.

The fast-ion conductors distinguish themselves from regular ionic conductors by a large fraction of defects and a low value of the energy barrier. It is usually assumed that the defect mechanism in β-alumina is of the interstitial type and of α-AgI of the vacancy type. However, the transport of Ag in α-AgI is more characteristic of an interstitialcy than of a vacancy mechanism.

EDGE LUMINESCENCE AND SELF-TRAPPING OF EXCITONS IN KI AND RbI

Tetsusuke HAYASHI, Tokiko OHATA and Shigeharu KOSHINO
School of General Education, Kyoto University, Kyoto, Japan

A weak edge emission can be observed at low temperatures in alkali iodide crystals in addition to the well-known luminescence of the self-trapped exciton (STE). This emission was first observed by Kuusmann et al.[1] and was attributed to radiative decay of free excitons. We have carried out detailed investigations on the spectra and the temperature dependence of the edge emission in KI and RbI under excitation with X-rays[2] or with uv-light.

Measurements were carried out in the direction shown schematically in Fig. 1. The solid curve in Fig. 1 is the emission spectrum measured at 5 K under uv-excitation in the high energy side of the first exciton band of each crystal, while the dashed curve is that obtained under X-ray excitation. The intensity of the edge emission is 10^{-1} to 10^{-3} times as weak as that of STE emissions observed below ~4.5 eV. The peak of the uv-stimulated edge emission lies at 5.84 eV in KI and at 5.74 eV in RbI. Energy difference of the peak from the exciton absorption peak (E_{ex}) is less than 10 meV in both crystals. It seems that the X-ray induced edge emission is reabsorbed considerably by the crystal because the excitation occurs deep into the crystal compared with uv-excitation.

Figure 2 shows temperature dependence of the intensity of the edge emission obtained under uv-excitation (open circles) and X-ray excitation (closed circles), fitted with each other at 30 K. The temperature dependence is well described by the relation

$$I = I_0[\, 1 + c\cdot\exp(-\Delta E/kT)\,]^{-1}, \qquad (1)$$

which is shown by the solid curve along experimental points in Fig. 2. Here values of ΔE chosen are 18 meV in KI and 11 meV in RbI.

Let us assume that the radiative decay of free excitons with a probability $1/\tau_r$ gives rise to the edge emission, and the self-trapping of excitons occurs with a probability $1/\tau_{st}$. The efficiency of the edge

emission η_r can be given by

$$\eta_r = 1/\tau_r(\ 1/\tau_r + 1/\tau_{st})^{-1} \approx \tau_{st}/\tau_r .$$

The latter must hold because the edge emission is very weak compared with the STE luminescence. Comparing η_r with the experimental relation (1), one can express $1/\tau_{st}$ in the form

$$1/\tau_{st} = 1/\tau_{st}^{\circ} + \nu \cdot \exp(-\Delta E/kT), \quad (2)$$

on the assumption that τ_r is independent of temperature. This implies that the self-trapping of excitons occurs on the one hand with a probability $1/\tau_{st}^{\circ}$ which is independent of temperature, and on the other hand occurs thermally over a potential barrier ΔE.

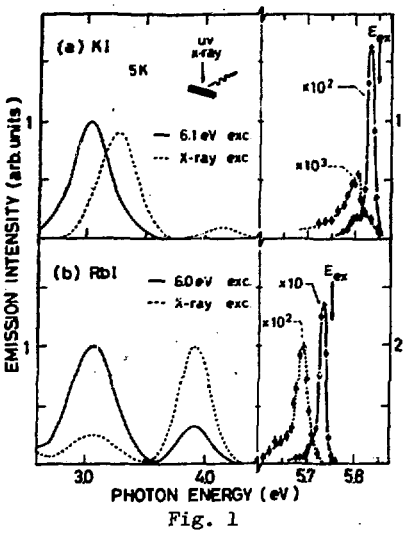

Fig. 1

The temperature dependence of the lifetime τ_{st}, which was estimated in a previous work on the quenching of the STE luminescence by coloration in KI and RbI,[3] is quite similar to that of η_r as shown by cross points in Fig. 2. Therefore, one can conclude that the efficiency of the edge emission is governed by the self-trapping probability of excitons as given by the relation (2). It is reasonable to assume that the edge emission originates from a metastable free exciton state which is separated from the STE state by an activation barrier ΔE.

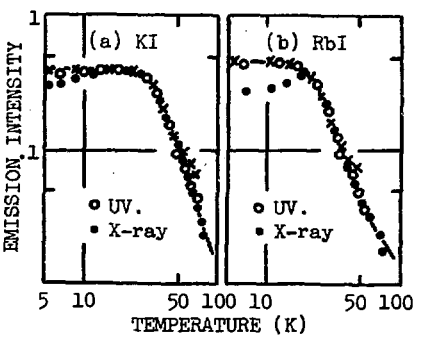

Fig. 2

References

1) I. L. Kuusmann et al.: JETP Letters 21 (1975) 72; Soviet Physics-Solid State 17 (1976) 2312.
2) T. Hayashi et al.: J. Phys. Soc. Japan 42 (1977) 1647.
3) T. Hayashi et al.: Solid State Commun. 17 (1975) 945.

FAST-ION BEHAVIOUR OF FLUORITE CRYSTALS AT HIGH TEMPERATURES

W. Hayes

Clarendon Laboratory, Oxford, U.K.

Crystals with the fluorite structure are extensively disordered above a temperature T_c which is appreciably below the melting temperature T_M (in PbF_2, for example, T_c = 705 K whereas T_M = 1128 K). The ionic conductivity in the solid above T_c is comparable with that found in the melt and is due to the cooperative generation of anion Frenkel pairs. This generation of defects occurs in a fairly diffuse manner giving rise to a specific heat maximum at T_c.

The Oxford group has carried out a detailed study of Raman and Brillouin scattering of CaF_2, SrF_2, BaF_2, $SrCl_2$ and PbF_2 at temperatures between 4 and 1500 K. Below T_c the Raman-allowed phonon shows variation in line width and peak position which can be accounted for by lattice anharmonicity. Above T_c additional scattering develops which can be explained by a theory of defect-induced scattering. The Brillouin measurements show that up to T_c the elastic constants of the crystals fall linearly with temperature, due to anharmonicity. In the region of T_c, however, a dramatic fall occurs in C_{11} whereas the shear constant C_{44} continues to show effects characteristic of anharmonicity alone. The fall in C_{11} can be accounted for by calculating effects of anion Frenkel pairs on elastic constants. Results of related measurements by the Oxford group using neutron scattering (in cooperation with M. T. Hutchings) and microwave conductivity techniques will also be reported.

Our results suggest that the number of interstitial sites occupied above T_c cannot be greatly in excess of about 20%, smaller than has usually been supposed. Work carried out in cooperation with C. R. A. Catlow shows that the cooperative interaction between defects that gives rise to the extensive disorder occurs primarily through Coulomb interaction, rather than through strain. However, at a concentration of about 20% of defects the Coulomb repulsion between like defects becomes important, inhibiting further defect generation.

INVITED PAPER

THE EXCITED STATES OF F CENTRES IN OXIDES

B. Henderson

Physical Laboratory,
Trinity College, Dublin 2,
Ireland.

In the alkaline earth oxides anion vacancies may trap two electrons, the resulting neutral F centre having a spin singlet, $^1A_{1g}$, ground state. The lowest lying excited states are then $^3T_{1u}$, $^3A_{1g}$ and $^1T_{1u}$, the proximity of which to the conduction band depend critically upon the electron-phonon coupling. Stimulated by the emerging theoretical work[1], there has developed considerable experimental interest in the electronic properties of F centres. This review will discuss some recent investigations into the nature of the excited states, in particular the optically detected resonances of F centres in both CaO and MgO. In CaO the ODMR spectrum at low temperature was used to show that the phosphorescent $^3T_{1u}$ state experiences a static Jahn-Teller distortion involving coupling mainly to phonons of E_g symmetry [2]. Measurements of the $^3T_{1u}$ ODMR at low fields (0 ~ 150G) are consistent with this interpretation [3]. Moreover, measurements of the zero field ODMR under uniaxial stress give important information concerning the dynamical properties of the centre [4]. Measurements of the temperature dependence of the $^3T_{1u} \rightarrow {}^1A_{1g}$ phosphorescence show that at high temperature population of the $^1T_{1u}$ state increases at the expense of the $^3T_{1u}$ state and results in observation of the $^1T_{1u}$ emission [1,5]. Some studies of energy transfer between F and F_A centres, measured using the $^3T_{1u} - {}^1A_{1g}$ luminescence, will be described [6].

In MgO the situation is not as clear cut. $F \rightarrow F^+$ conversion even at 1.6 K complicates observation of the F centre excited state EPR. However, when detecting using light exclusively in the F luminescence band one does detect isotropic EPR signals with $g = 2.00$ [7]. Such resonances are quite different from those observed in CaO. The significance of such a free electron g-value for differences in the electronic excited states of F centres in CaO and MgO will be discussed together with related phenomena in the photoconductivity of MgO [8].

References

1. R.F. Wood and T.M. Wilson, Sol. State Comm. 1975, 16, 545 and to be published (1977).

2. P. Edel et al. Phys. Rev. Lett. 28, 1268.

3. C.B. Haris et al. Phys. Rev. Lett, 33, 531 and B. Henderson (1977) to be published.

4. C.J. Krap, 1976, Proc. XIX Colloque Ampere, Heidelberg, 417.

5. J.B. Bates and R.F. Wood, 1975, Sol. State. Comm., 17, 201.

6. L.S. Welch et al., 1976, 2nd Europhysical Topical Conference on 'Lattice Defects in Ionic Crystals' Berlin.

7. P. Edel and B. Henderson, 1977 to be published.

8. R.W. Roberts and J.H. Crawford, 1974, J. Non Metals, 2, 133.

POINT DEFECT EQUILIBRIA IN Al_2O_3 AS DEDUCED FROM TEM STUDIES OF Ti-DOPED CRYSTALS

A. H. Heuer, T. E. Mitchell and D. S. Philips
Department of Metallurgy and Materials Science
Case Western Reserve University
Cleveland, Ohio 44106

Ti-doped Al_2O_3 single crystals, when heat-treated in oxiding atmospheres at temperatures between 1200 and 1500°C, precipitate long acicular needles of rutile, the stable form of TiO_2. These particles lie in the basal plane of the host sapphire and have a well-defined orientation relationship with the matrix. (The particles are also responsible for the asterism of gem-quality "star" sapphire.) The particle/matrix interfaces normal to the needle axes contain misfit dislocations, with a Burgers vector of the type $1/3\ \langle 10\bar{1}1\rangle$ (relative to the sapphire lattice). These dislocations are present to accommodate lattice mismatch between precipitate and host in the directions normal to the needle axis; along the needle axis, perfect coherency is maintained between sapphire and rutile.

After very long ageing times, the particles are observed to be surrounded by an array of dislocation loops (Fig.1a), which arise from the misfit dislocations acting as Bardeen-Herring sources. The climb force causing this dislocation climb in the basal plane of the sapphire is the main topic of this paper.

The incorporation of Ti^{4+} in solid solution in Al_2O_3 is written (in Kröger-Vink notation) as

$$3\ TiO_2 \xrightarrow[\longleftarrow]{Al_2O_3} 3Ti_{Al}^{\bullet} + V_{Al}^{'''} + 6\ O_O \qquad (1)$$

while the Schottky and Frenkel equilibria can be represented by

$$[V_{Al}^{'''}]^2\ [V_O^{\cdot\cdot}]^3 = K_s \qquad (2) \quad ; \quad [V_{Al}^{'''}]\ [Al_i^{\cdot\cdot\cdot}] = K_f \qquad (3)$$

The presence of a large concentration of charge-compensating aluminum vacancies due to the aleovent solute causes the equilibrium concentration of both oxygen vacancies and aluminum interstitials to

decrease, the crystal of course maintaining electrical neutrality at all times.

Equation 1 also holds for the precipitation reaction, although the arrow now points to the left. The precipitation of TiO_2 thus eliminates the excess concentration of aluminum vacancies (in essence, they are incorporated into the growing rutile needles) and neither the Schottky nor Frenkel equilibria (equations 2 and 3) are satisfied. It is an easy matter for the crystal to re-establish the Frenkel equilibria. However, re-establishment of the Schottky equilibrium requires a source of vacancies, which are provided by the misfit dislocations undergoing negative climb and emitting vacancies in stoichiometric proportions into the Al_2O_3 lattice.

We furthermore believe that these results indicate that the Schottky quintet, and not the cation Frenkel pair, must be the majority defect in Al_2O_3. Were the reverse to be true, the large number of alumimum vacancies produced to satisfy the Frenkel equilibria would also allow the Schottky equilibrium to be satisfied, thus eliminating the vacancy undersaturation.

A similar explanation is likely for the dislocation loops found by Yacaman, Hobbs, and Goringe (Phys. Stat. Sal., 39a, K85 (1977)) to surround Suzuki-phase precipitates in Mn-doped NaCl (Fig. 1b). Indeed, dislocation climb induced by vacancy undersaturation is probably a general phenomena when precipitation involving aleovalent solutes occurs in ionic crystals.

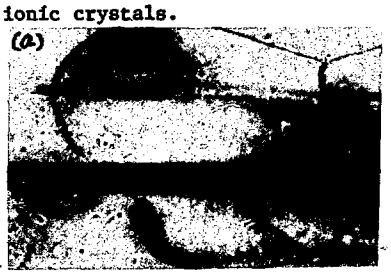

WHAT ABOUT THE Z_5 CENTER?

H.C. Hilber and H.J. Paus
Physikal. Institut Teil 2, Universität Stuttgart, Germany

During the thermal and optical F - Z_2 center conversion in KCl:Sr an absorption band, called Z_5, appears at 2.18 eV. The role of the related center in this reaction remained obscure and was simply ignored /1/. Hereafter it is called "thermal" $Z_5 = Z_5^{th}$. After a prolonged intense irradiation with F-light at +80°C the initially formed Z_2 centers are destroyed again and an absorption band at 2.13 eV grows up (hereafter called "optical Z_5" = Z_5^{opt}).

By combined optical absorption, emission, excitation and magneto-optical (MCD) experiments the following identification has been obtained (optical data collected in the table):

1) Z_5^{opt} is produced by the optical destruction of a Z_2 center. It is a paramagnetic one-electron center and exhibits a negative spin orbit splitting comparable to that of the Z_1 center. It has a broad emission band at 1.00 eV and a (110) symmetry.
2) Z_5^{th} is a second configuration of the Z_2 center, confirmed by the following facts.
   (a) Both centers have almost coinciding narrow emission bands, but can be distinguished from one another by their radiative life time:
   Z_2: $\tau \approx$ 15 ms ⟶ "slow" Z_2 center = Z_2^s
   Z_5^{th}: τ roughly 1 ms ⟶ "fast" Z_2 center = Z_2^f
   A nearly pure Z_5^{th}/Z_2^s spectrum is presented in fig. 1, curve a.
   (b) By optical irradiation Z_5^{th} can be converted into Z_2 even at liquid helium temperature (fig. 1, curve b), where the latter remains stable. Warming the crystal up to room temperature for several hours in the dark restores the spectrum (a). Z_2 center models as proposed earlier /2/ suggest a single jump of a cation vacancy for the explanation of this effect.

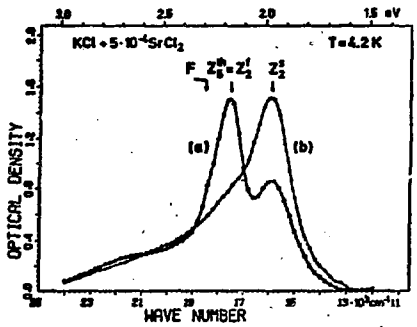

Fig. 1

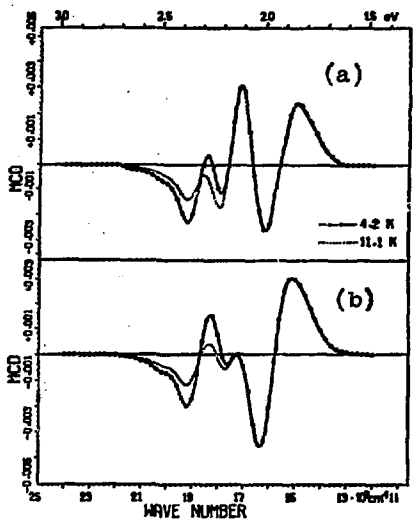

Fig. 2

(c) Z_5^{th} is diamagnetic as the Z_2^s center, as proved by its MCD measured before (fig. 1a, fig. 2a) and after (fig. 1b, fig. 2b) the Z_5 - Z_2 conversion. The spectra measured at T = 4.2 K and 11.1 K coincide perfectly in the Z_5 and Z_2 spectral region. This is merely emphasized by the small paramagnetic MCD due to few remaining F centers.

T a b l e .

	Absorption Peak/Half width (eV)	Emission Peak/Half width (eV)
Z_1	2.10 / 0.260	0.85 / 0.275
Z_5^{opt}	2.13 / 0.217	1.00 / 0.300
$Z_2 = Z_2^s$	1.97 / 0.248	1.10 / 0.135
$Z_5^{th} = Z_2^f$	2.18 / 0.240	1.13 / 0.135

/1/ See abstract by Ch. Anderson and H. J. Paus, this conference.

/2/ K.H. Umbach, H.J. Paus 1974 Int.Col.Cent.Conf. Sendai abstract 154.

VOID ANALOGUES IN IRRADIATED HALIDES

L. W. Hobbs,[1] M. Saidoh[2] and V. M. Orera[3]
Materials Development Division
A.E.R.E. Harwell, U.K.

When alkali and alkaline earth halides undergo radiolysis at temperatures at which both halogen vacancy and halogen interstitial products of radiolysis are mobile, halogen interstitials readily condense to form dislocation loops, while the complementary halogen vacancies condense to form colloidal inclusions of alkali or alkaline earth metal (4). This segregation of the products of radiolysis to separate sinks precludes efficient recombination and removes the usually-observed late-stage saturation. Instead, the concentration of stabilized radiolysis products increases linearly with dose (5) to very high concentrations (many %). Such behaviour is analogous to the void-swelling regime in metals and occurs in the same region of temperature (0.3-0.5 T_m) and dose (> 0.1 dpa). We have now studied extensively the growth kinetics, morphology and stability of these void analogues in alkali and alkaline-earth halides, irradiated up to 150 Grad with 80-120 KeV electrons, using optical absorption, small-angle thermal-neutron and X-ray scattering, and transmission electron microscopy (TEM).

Metal colloids can be followed optically by virtue of their optically-excited plasmon resonance, which provides an indication of colloid size and volume fraction. This absorption peaks at ~570 nm in NaCl, ~560 nm in CaF_2, ~600 nm in SrF_2 and ~425 nm in BaF_2 and is identified by comparison with additively-coloured crystals. A temperature of maximum colloid production efficiency exists for each halide (450 K for NaCl, 335 K for CaF_2, 488 K for SrF_2, 433 K for BaF_2) above which we suppose F centres can be re-emitted from colloids and recombination is once again more efficient. In NaCl, the colloid band is found to anneal in two stages. Extensive small-angle scattering measurements reveal scattering from inclusions whose size and evolution with dose and temperature correspond to those deduced for colloidal metal particles from optical plasmon resonance. Complementary Fresnel-contrast TEM reveals corresponding facetted inclusions, in some cases (e.g. CaF_2) in ordered arrays, as well as dense dislocation networks arising from repeated interstitial loop intersections. We presume all three techniques to be observing the same inclusions.

In each halide, several other prominent optical absorption bands from aggregates are found to grow in concert with the colloid band. Some of these bands also anneal in parallel with the colloid band, while others exhibit different thermal stability. New aggregate bands develop during annealing and are persistant to high temperatures. Since NMR studies have revealed the presence of free molecular halogen, we suggest that some of the additional bands may be associated with large halogen aggregates.

These observations in two important model systems have enormous implications for the behaviour of other ceramic solids under intense irradiation at temperatures above 0.3 T_m, some of which are now being explored (6).

Present addresses: (1) Department of Metallurgy and Materials Science, Case Western Reserve University, Cleveland, Ohio 44106, U.S.A. (2) Division of Thermonuclear Fusion Research, Japan Atomic Energy Research Institute, Tokai-mura, Japan. (3) Departamento de Fisica Fundamental, Universidad de Zaragoza,

Spain.

(4) L. W. Hobbs in 'Surface and Defect Properties of Solids,' The Chemical Society, London, Vol. 4 (1975) pp. 152-250; J. de Physique 37 (C7, 1976) 3.

(5) U. Jain and A. B. Lidiard, Phil. Mag. 35 (1977) 245.

(6) D.G. Howitt, R.S. Barnard, L.W. Hobbs and T.E. Mitchell, this conference.

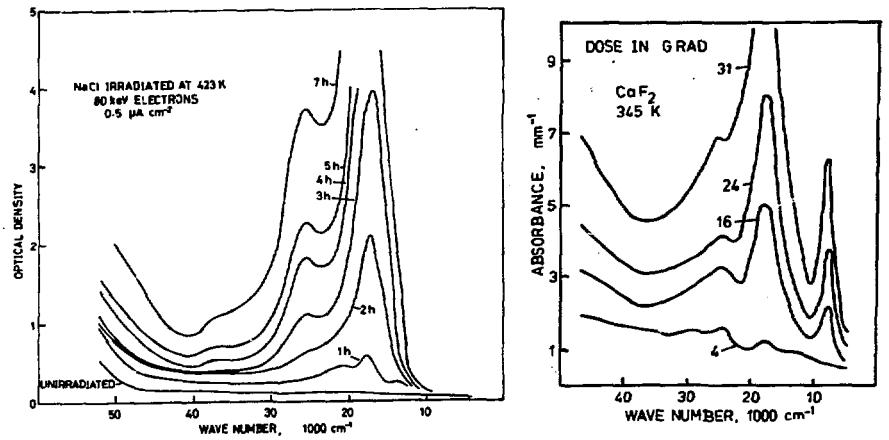

Optical absorption from heavily electron-irradiated NaCl (left) and CaF_2 (right)

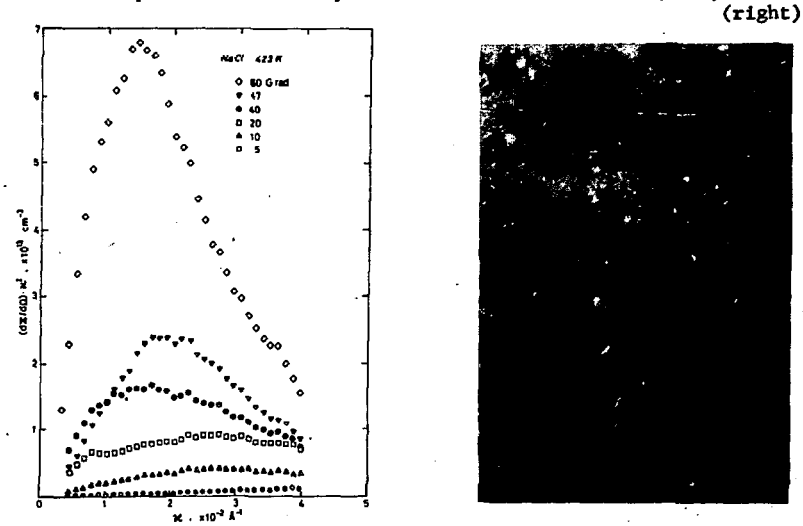

Small-angle neutron scattering (left) and TEM (right) from inclusions in heavily electron-irradiated NaCl.

THE F CENTER STABILIZATION PROCESS IN THE FIRST COLORING STAGE OF ALKALI HALIDE CRYSTALS

E. R. Hodgson, A. Delgado and J. L. Alvarez Rivas
Junta de Energía Nuclear, Madrid-3, Spain

Over the years studies have been made of the first stage F coloration of alkali halide crystals (1). From the beginning attempts were made to fit mathematically the coloring curves. However, a coherent model was lacking, particularly as to the experimental justification of the fitting parameters.

An interpretation has been presented (2), in which using a model based on interstitial trapping, a various component exponential saturating growth of the coloring curve is predicted, with the fitting parameters representing physically meaningful entities.

The work presented here is a continuation of this initial step. A coherent model has emerged in which the parameter values obtained from the fitting procedure can be independently measured experimentally.

Pure samples of NaCl (Harshaw) have been irradiated at temperatures between 15 and 85°C with bremsstrahlung gamma rays produced by stopping 1.8 MeV electrons from a HVEC Van de Graaff accelerator in a gold target. Simultaneous in beam measurements have been made of the F and M coloring curves together with the induced sample luminescence, followed immediately after irradiation by on-site measurements of thermal annealing. The experimental set-up is basically that described in Ref. 2, improved to allow the above measurements to be made. The results presented here are concerned only with the F center.

The F coloring curves have been fitted by the expression

$$n_F = a_L t + \sum_{i=1}^{n} A_i \, (1-e^{-a_i t}) \, ,$$

each exponential component representing the filling of a particular type of interstitial trap.

The number of components required has been found to be the same as the number of F annealing steps, and the partial amplitudes $A_i(1-e^{-a_i t})$,

where t is the irradiation time, are equal to the annealing step amplitudes.

The temperature dependence of the fitting components has been observed over the range 15 to 85°C. By 85°C the first component is too rapid to be measured and reaches negligible amplitude; at the same time the first annealing step and the corresponding thermoluminescence peak are no longer observed.

Comparison has been made with thermal luminescence data available for the glow peak in the 15-85°C interval (3) in which measurements have been made of the glow peak lifetime temperature dependence.

This dependence is in excellent agreement with the lifetime dependence found for the first component obtained by the fitting of the F color curves.

All these results indicate that the F center coloring process, the F center thermal annealing process and associated thermal luminescence are closely related phenomena which allow a unified treatment based on the interstitial trapping model.

The work is being extended to cover the higher temperature range, in which new phenomena, involving the F and M centers, appear.

References:

1. Sonder, E., Sibley, W. A., Defects in Solids (ed. Crawford, J. H. and Slifkin, L.) Plenum, New York, (1972).
2. Hodgson, E. R., Delgado, A. and Alvarez Rivas, J. L., Solid State Comm. 16, 785 (1975).
3. Mariani, D. F. and Alvarez Rivas, J. L., (to be published).

ENDOR STUDY OF THE VIBRATIONS OF HYDROGEN ATOMS IN KCl AND RbCl

Chr. Hoentzsch and J.M. Spaeth, Fachbereich 6,
Naturwissenschaften I, Gesamthochschule Paderborn,
479o Paderborn, W. Germany

The local mode vibrations of hydrogen atoms in alkali halides cause a substantial dynamical part in the superhyperfine (shf)-interactions. If hydrogen is replaced by deuterium, the vibrational amplitude is reduced and results in a smaller shf-interaction. Table 1 shows ENDOR results of the isotope effect

$I_{a,b,q} = 100 \left(\frac{a,b,q\ (H)}{a,b,q\ (D)} - 1 \right)$, where a is the isotropic shf constant, b the anisotropic shf constant, q the quadrupole interaction constant. Measurements were performed for interstitial (H_i^o) and substitutional hydrogen centers (H_s^o). In the H_s^o centers the hydrogen atom occupies a cation site with a Ca^{++} ion nearest in [110] (3), whereby the nearest Cl$^-$ neighbours are slightly non equivalent due to the Ca^{++}. There are three Cl$^-$ types of which two (α,β) could be analysed.

Table 1: Isotope effect for interstitial and substitutional hydrogen centers for RbCl at 55° K.

	shell	anion						cation		
		I_a		I_b		I_q		I_a	I_b	I_q
H_i^o	I	3,1 ±0,3		1,8 ±0,3		2,0 ±0,6		11,3 ±0,3	3,3 ±0,3	-2,0 ±0,6
H_i^o	II	-		-		-		2,3 ±0,4	0,6 ±0,4	5 ±3
		(α)	(β)	(α)	(β)	(α)	(β)			
H_s^o	I	6,7 ±0,2	6,2 ±0,2	3,6 ±0,2	3,6 ±0,2	-1,0 ±0,5	0 ±0,5	-	-	-

Results for KCl are very similar and not given explicitely here. The measured isotope effect can qualitatively be understood with a wave function for the hydrogen center constructed by orthogonalizing the hydrogen 1s-function to the ion cores

including first shell Cl covalency admixtures (2).

From the value of Rb^{II} in H_i^o centers is seen that the spin density at their sites is due to a transfer via the nearest Cl^- ion core. The unknown potential of the vibration can be determined from the experimental values of either I_a or I_b, assuming a harmonic potential. The two potential parameters obtained, however, differ by about a factor of two both for H_i^o and H_s^o centers.

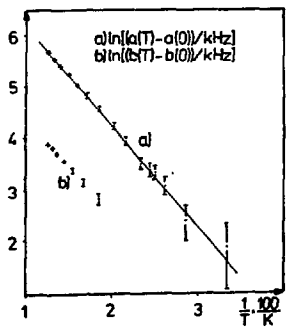

Fig. 1: Temperature dependence of H_s^o shf constants of the nearest Cl_α^I in RbCl

H_s^o centers show a relatively large temperature dependence of the shf interactions due to a slight thermal excitation of the hydrogen vibrations (see fig.1). In H_i^o centers up to the decay temperature at 100 K only zero point vibrations could be observed.

From the slope in Fig.1, activation energies of 17 ± 2 meV for RbCl and 25 ± 2 meV for KCl are obtained. Assuming a harmonic potential from the activation energies the vibrational potential can be determined independently from the isotope effect and from a theoretical model for the center wave functions. It agrees well with that obtained from I_b showing that the theoretical model works well for the anisotropic shf constant whereas the current theoretical interpretation of the isotropic constant is erroneous. Further results indicate that the isotropic halogen shf constant may be largely due to core polarization effects.

(1) J.M. Spaeth, phys.stat.sol. 34, 171 (1969)

(2) J.M. Spaeth and H. Seidel, phys.stat.sol. 46 (1971)

(3) L. Schwan, Ph.D. thesis Stuttgart 1975 (to be published)

THE EFFECT OF ANNEALING ON THE PROPERTIES OF COPPER-CALCIUM PHOSPHATE GLASSES

C. A. HOGARTH* and G.R. MORIDI+

*Department of Physics, Brunel University, Uxbridge, Middlesex, U.K.

+ Physics Department, Farah Pahlavi University, Vanak, Tehran, Iran.

Although the colouring effect of copper in glass attracted considerable attention in the past, but the other physical properties of glasses containing copper were not studied until 1969. (1) Moridi and Hogarth (2) reported that for a series of glass compositions containing 0-35 % CuO, the activation energy is dependent on both CuO content and temperature. The LnO v. 1/T curves were not linear. In the present work we report the effect of annealing on some of the Physical properties of these glasses.

The density of copper-calcuim-phosphate glasses were found to increase with annealing temprature. This presents the fact that the average inter-atomic spacing in these glasses decreases and the structure becomes compact.

Using the ESR technics, the Cu^{2+} ion concentrations in glass have been measured. It is shown that by increasing the annealing temperature, further reduction of the copper takes place and the ratio Cu^{+}/ Cu_{total} will change significantly as the annealing temperature changes.

We (3) have reported that cupric ion in the glass is in an octahedral environment with tetragonal distortion. The cuprous ion is more likely to be in a tetragonal evironment. The ESR evidence of reducing Cu^{2+} ion content as a result of an increase in the annealing temperature is consistent with the increase of density of glass with annealing temperature.

The infrared spectra of a glass annealed at different temperatures were recorded and no significant changes were observed in the absorption band positions.

The annealing temperature was found to affect both the electrical conductivity and the activation energy. As the annealing temperature increases the conductivity and activation energy decrease. Similar results were reported for iron-Phosphate glasses.[4] The electrical conductivity of these glasses were discussed [2] in terms of the theory of small polaron formation. The activation energy is ginen by $W=W_H-\exp(-\alpha R)$, where R is site spacing. Assuming that Cu-Cu spacing decreases by increasing the annealing temperature, then a decrease in the activation energy would by expected. The ESR experiments show that by increasing the annealing temperature, the Cu^+ content of glass increases. This leads to a decrease in C (1-C) in the conductivity formula. However a change in the optical phonon frequency is also expected as a result of different annealing temperature and it seems that further structural information is necessary to discuss carefully the conductivity change after annealing at different temperatures.

1) C.F. Drake, I.F. Scanlan and A. Engel, Phys. Stat. Sol; 32 (1969) 193.

2) G.R. Moridi and C.A. Hogarth, the Phys. of Non-Cryst. solid; Ed. G.H. Frischat, Trans Tech (1977).

3) G.R. Moridi and C.A. Hogarth, Int. J. Electron; 37 (1974) 141.

4) D.L. Kinser, J. Electrochem. Soc; solid state Science, 117 (1970) 546.

OFF-CENTER DEFECTS UNDER HYDROSTATIC PRESSURE: "LOCALIZED MODEL CASES" FOR DISPLACIVE FERROELECTRICS AND SUPERIONIC CONDUCTORS*

Ulrich Holland† and Fritz Luty
Physics Department, University of Utah, Salt Lake City, Utah 84112

Small point-ion off-center defects supply simple localized model-situations for two collective solid state effects of high current interest: The static off-center displacement of the isolated defect can be compared to the collective sublattice displacement in ferro-electrics (Fig. 1). In both cases ungerade (T_{1u}) electric dipole and gerade (E_g and T_{2g}) elastic distortions create a low-symmetry structure which can be aligned by electric fields or stress. Transitions between the on- and off-center defect structure correspond to displacive phase-transitions of the ferro-electric crystal (or domain).

The dynamic behavior of off-center defects (like Ag^+), on the other hand, can be regarded as a localized analogon to the motional behavior of small ions in superionic conductors (like AgI). In both systems, the lattice framework supplies a large number of voids or sites (by far exceeding the number of Ag^+), among which the ions can move along a network of paths with low potential barriers. While the motion of the Ag^+ ions through an interconnected network (in AgI) leads to superionic conductivity the spatially restricted motion of the isolated Ag^+ in the multi-well off-center potential leads only to "local superionic conductivity" = large dielectric polarization. The same small-size ions (Ag^+, Cu^+, Li^+, Na^+, F^-) give rise to off-center and superionic conduction behavior.

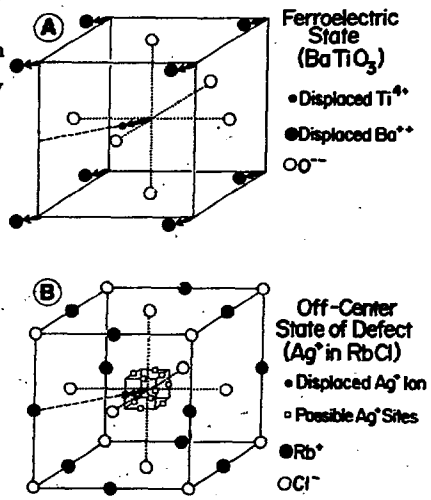

These parallels and model-aspects can be particularly explored, when off-center defects are studied

under hydrostatic pressure; the increase of Born-Mayer repulsion by the pressure offsets the delicate energy balance producing the off-center potential, makes it more shallow and tunes it eventually into an on-center potential. We have studied various Ag^+, Cu^+, and Li^+ off-center systems at low temperatures under hydrostatic pressure using optical and dielectric techniques. Dramatic changes in the motional behavior of the ions are observed under pressure, with thermally activated Arrhenius motion tuned through steadily decreasing activation energies into a phonon-assisted tunneling behavior. Similar to superionic conductors, which require for optimum diffusion a critical match between ion-size and cross-section of the paths, the optimum low temperature ionic motion occurs in shallow off-center potentials with small size-mismatch, tuneable by the pressure.

At a critical pressure, characteristic for each off-center defect system, the displacement dipole collapses rather abruptly (Fig. 2) -- similar to the pressure-induced disappearance of the displacive phase in ferro-electrics. The question, if this off- to on-center transition is of first or second order, will be discussed in connection with recent theoretical work which showed the importance of the electronic (d-s) quadrupolar deformability of the Ag^+ ion for off-center effect, pressure-induced phase-transition and for superionic conductivity.[1]

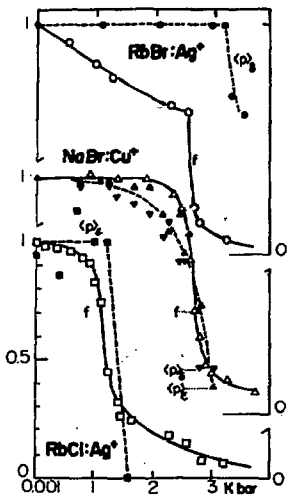

*Supported by NSF grant #DMR-74-13870-A02.

†Present address: Max Planck Institut for Solid State Research, Stuttgart.

[1]W. G. Kleppmann, J. Phys. C 9, 2285 (1976).

EPR AND OPTICAL STUDIES OF γ-IRRADIATED MgO:Ga*

G. E. Holmberg, K. H. Lee and J. H. Crawford, Jr.
University of North Carolina at Chapel Hill

Four new EPR lines appear between 5.3 and 11 kG at X-band when MgO:Ga is subjected to gamma-irradiation. These lines have been identified as due to Ga^{2+} and can be fit by the spin Hamiltonian

$$H = g\beta\vec{H}\cdot\vec{S} + g_n\beta_n\vec{H}\cdot\vec{I} + A\vec{I}\cdot\vec{S}$$

with g = 2.000 ± 0.001 and A = 8.563 ± 0.005 GHz for ^{69}Ga at 77 K. For both ^{69}Ga and ^{71}Ga the 4s electron of Ga^{2+} has a strong hyperfine interaction with the I = 3/2 nucleus. Two lines are observed for each isotope, corresponding to the transitions from ($F = 1, M_F = -1$) to ($F = 2, M_F = -2$) and ($F = 2, M_F = -2$) to ($F = 2, M_F = -1$). The Ga^{2+} spectrum observed here is analagous to that reported by Raüber and Schneider[1] for photo-induced Ga^{2+} in ZnS. They reported g = 1.9974 ± 0.005 and A = 6.072 ± 0.003 GHz.

The lines are isotropic within experimental error and possess satellites. The line width of the central transition from ($F = 2, M_F = -2$) to ($F = 2, M_F = -1$) is about 1 G and the outer satellites for this line show some angular dependence. It is believed that the majority of the Ga^{2+} ions created by gamma-irradiation are in cubic sites, but some sites are apparently slightly perturbed.

The number of Ga^{2+} centers produced saturates at about $5 \times 10^{18}/cm^3$ after a dose of 3×10^4 rad.

Optical absorption measurements were also made after irradiation and after subsequent bleaching. Two bands were observed at 300 nm and 370 nm. The intensities of the absorption bands and Ga^{2+} EPR signal decay when the sample is held at room temperature and reach saturation in about 48 hours. Optical bleaching in 300 nm band partially restores the amplitude of 370 nm band and the Ga^{2+} EPR signal as well. The 300 nm band partially restores and 370 nm band and the Ga^{2+} EPR signal are partially eliminated

if the bleached sample is held at room temperature for period of 24 hours. Hence, we attribute the 370 nm band to Ga^{2+} and the 300 nm band to Ga^{1+}.

[1] A. Rauber and J. Schneider, Phys. Sat. Sol. 18, 125 (1966).

*Supported by the Materials Research Center, UNC under Grant No. DMR272-03024 from NSF.

DOUBLE QUANTUM EPR TRANSITION IN AgCl:Ni*

G. E. Holmberg and L. M. Slifkin
University of North Carolina at Chapel Hill
and
J. C. Hempel
University of North Carolina at Greensboro

Ni^{2+} enters the AgCl lattice in a substitutional cation site. At low temperatures the nickel ion is usually charge-compensated by a nearest or next-nearest cation vacancy. However, some nickel sites have no nearby charge compensation and have octahedral symmetry, giving rise to an isotropic EPR line at $g = 2.276 \pm 0.004$.[1] Nickel has a spin triplet ground state; D-term broadening causes the width of this isotropic line to be about 110 G at 4.2 K. At high microwave powers at 4.2 K a narrow line, superimposed at the same g value as the octahedral center, appears and increases rapidly in amplitude with microwave power. This line has been identified as a double quantum transition between $M_S = \pm 1$ levels, and is analogous to the double quantum transition observed by Orton, Auzins, and Wertz for nickel in an octahedral site in MgO:Ni.[2] However in the case of AgCl:Ni, where the nearest neighbors are chlorine ions which possess nuclear moments, resolved superhyperfine structure is observed and can be fit by the spin Hamiltonian:

$$H = g\,\vec{H}\cdot\vec{S} + \sum_{n=1}^{6} (AI_z^n S_z + B(I_x^n S_x + I_y^n S_y) - g_N^n \beta_N^n \vec{H}\cdot\vec{I}^n)$$

Where $A = 7.35 \pm 0.1$ G and $B = 2.40 \pm 0.1$ G. A data analysis based on the independent bonding model is being performed. Comparison with previously reported values of spin transfer coefficients, f_s anf f_p, for NiF_6^{4-} complexes[3] shows f_s to be similar and f_p to be larger in the case of AgCl:Ni, as expected.

[1] M. Hohne, M. Stasiw, and A. Watterich, Phys. Stat. Solidi 34, 319 (1969).
[2] J. W. Orton, P. Auzins, and J. E. Wertz, Phys. Rev. Letters 4, 128 (1960).
[3] J. Owen and J. H. M. Thornley, Rep. Prog. Phys. 29, 675 (1966).
*Supported by the Materials Research Center, UNC, under Grant No. DMR-7500806 from the NSF, and by NSF Grant No. DMR72-03212-A01.

EFFECTS OF OSCILLATING DISLOCATIONS ON THE DISTRIBUTION OF SOLUTES IN AgBr*

S. E. Horan and L. M. Slifkin
Department of Physics and Astronomy, University of North Carolina
Chapel Hill, N. C. 27514

The dislocation—defect interactions in single crystal silver bromide doped with small, precise amounts of cadmium and strontium are being studied using internal friction techniques at 35 kHz. The response of these crystals to small harmonic stresses is systematically investigated for limited ranges of temperature (37° - 175° C) and impurity concentration (75 ppm and less). Unprecedented discontinuities in the internal friction and modulus defect versus strain amplitude can be induced reproducibly in some samples by controlled changes of applied harmonic stresses.

Furthermore, samples annealed for long times (3 months) at room temperature exhibit decrements and modulus defects which decrease markedly with increasing harmonic strain, for low strains and temperatures. Subsequent high temperature anneals remove these low strain peaks. We suggest that this effect is associated with stages of solute aggregation. This interpretation is consistent with the observed effects of room-temperature aging on the ionic conductivity of AgBr:Sr. Moreover, long-term monitoring of the strain-independent internal friction shows an increase in Δ_I over time at all temperatures, in spite of intermittent annealing which lowers the total dislocation density of the specimen. These data are also consistent with formation of Sr aggregates.

Superimposed on this background are at least two phases of equilibrium dislocation-pin structure, each of which is stable over a characteristic stress-temperature range, thus giving rise to the discontinuity mentioned above. Extensive data on the temperature, stress, frequency and hysteresis characteristics of this effect, indicating discontinuous change in the distribution and a simultaneous reduction in the number of pins along the dislocation core, are consistent with a model predicting a critical stress-temperature combination for pin aggregation.

It is thus postulated that strontium-containing pins which segregate to dislocations form multiple-defect pinning centers under the influence of the oscillating loops.

*Supported by NSF Grant No. DMR72-03212-A01 and by the Materials Research Center, University of North Carolina, under Grant No. DMR-7500806 from the National Science Foundation.

CONF-771002--1

DEFECT AGGREGATION IN IRRADIATED OXIDES

D. G. Howitt, R. S. Barnard, L. W. Hobbs and T. E. Mitchell
Department of Metallurgy and Materials Science
Case Western Reserve University
Cleveland, Ohio 44106 U. S. A.

Ionic displacements in the oxides MgO and Al_2O_3 can be produced by collisions with energetic incident particles. The 650keV electrons of the CWRU High Voltage electron microscope have been used to provide direct lattice displacements and to observe the resulting defect aggregation at high temperatures.

While the individual anion vacancies (in the form of F+ or F centres) have been identified in MgO(1) and Al_2O_3(2) and the cation vacancy in MgO(3), the fate of the displaced interstitial ions has escaped spectroscopical identification. We have shown that, as in the alkali halides(4), the interstitials aggregate to nucleate interstitial dislocation loops at temperatures where the interstitials have sufficient mobility.

In Al_2O_3, irradiation of $\langle 10\bar{1}0\rangle$ foils at 700°C produces dislocation loops on basal planes (figure 1) while irradiations above 800°C also produce such loops on prismatic $\{10\bar{1}0\}$ planes (figure 2). These loops are all pure edge type and interstitial in character with respective Burgers vectors of 1/3 [0001] and 1/3 $\langle 10\bar{1}0\rangle$. Such defects involve the insertion of two additional oxygen layers and their associated cations into either the basal or prismatic planes. These dislocation loops therefore fault only the cation sublattice and maintain the hexagonal close-packing of the oxygen sublattice.

In MgO, unfaulted interstitial dislocation loops, with Burgers vectors 1/2 $\langle 110\rangle$, form on {110} planes at temperatures above 500°C (figure 3). With extended irradiation above 800°C these loops assume an elongated growth mode along $\langle 001\rangle$ and eventually intersect to form dense dislocation networks (figure 4).

This research was supported by the Energy Research and Development Administration under Contract No. AT(11-1)2119.

(1) A. E. Hughes and B. Henderson, in 'Points Defects in Solids', ed. J. H. Crawford and L. M. Slifkin, Plenum Press (1972), pp. 381-490.

(2) K. H. Lee and J. H. Crawford Jr., Phys. Rev. B 15 4065 (1977).

(3) A. J. Tench and M. J. Duck, J. Phys. C 6 (1973) 1134-48.

(4) L. W. Hobbs in 'Surface and Defect Properties of Solids', The Chemical Society, London, Vol. 4 (1975) pp. 152-250.

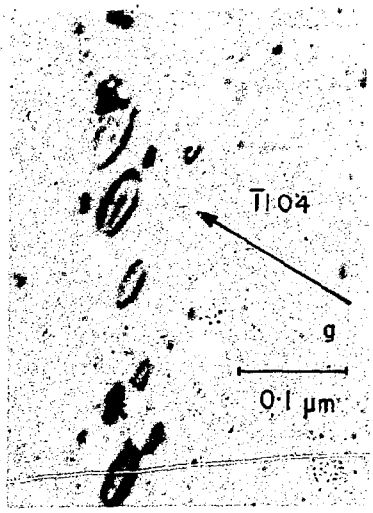

Figure I. Basal dislocation loops in Al_2O_3 irradiated at 700°C.

Figure 2. Basal and prismatic loops in Al_2O_3 showing stacking fault contrast.

Figure 3. Dark field of perfect {110} dislocation loops in MgO irradiated at 800°C.

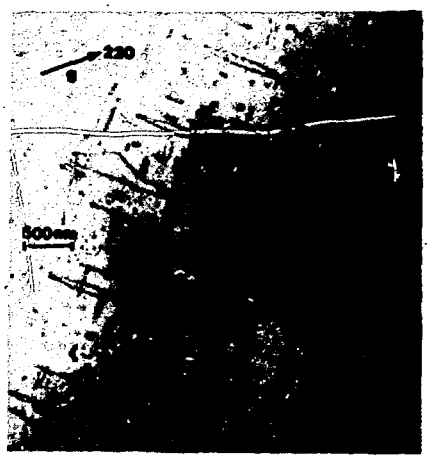

Figure 4. Elongated dislocation loops in MgO after extended irradiation.

VIBRONIC THEORY OF THE MAGNETIC PROPERTIES OF THE RELAXED EXCITED STATE OF THE F CENTERS

Takeshi IIDA*), Koichi IMANAKA, and Hiroshi OHKURA

*) Department of Physics and Department of Applied Physics
Osaka City University, Sumiyoshi-ku, Osaka , JAPAN 558

Although the nature of the relaxed excited state (RES) of the F centers has been progressively understood through the vibronic study of the Stark effects in F center emission[1], the study of the magnetic properties has still remained unexplored. Some of the experimental quantities to reveal the magnetic nature of the RES have been observed; they are the g-factor g or the g-shift $\Delta g (=g-g_f)$[2,3], where g_f is for the free electron, and both dia- and para-magnetic circular polarization (MCP) of emission[4,5] which are denoted as Δ_d and Δ_p, respectively. When the magnetic field H_0 is applied to the z-direction, the Zeeman interaction is given by $H_z = \beta H_0 (g_{orb} \ell_z + g_f s_z)$, where g_{orb} is the p-orbital g-factor. The spin-orbit interaction $H_{so} = \lambda_p \vec{\ell}\cdot\vec{s}$ plays an important role in the RES[6], where λ_p is the spin-orbit interaction constant of p-orbitals.

On the basis of the Kayanuma and Toyozawa's vibronic theory[7], we have derived the expressions of Δ_d and Δg. Here, we treated H_z and H_{so} as a small perturbation and solely took into account of the interaction with the T_{1u}-mode phonons where the coupling constant is denoted as S_1. Now,

$$(1) \quad \Delta_d = -2\, g_{orb} (\beta H_0 / \hbar\omega) \sum_n \{[b_0^1(n)]^2/[(\Delta+n) - E_0^1]\} / N^2,$$

$$(2) \quad \Delta g = -(4/3) (\lambda_p / \hbar\omega) g_{orb} \sum_n \{[b_0^1(n)]^2/[(\Delta+n) - E_0^1]\} ,$$

where notations of Δ , n, $b_0^1(n)$, N^2, and E_0^1 are given in refs. 1 and 7; $\hbar\omega$ is the LO phonon energy. The quantities in the brace can be computed when the parameters Δ and S_1 are known; they are determined from the Stark effects[1]. Thus, the values of [g_{orb}, λ_p(meV)] are determined as follows: [0.43, 3.5] for KF; [0.56, 12] for KCl; [0.83, 66] for KBr and [0.99, 331] for KI, respectively. Comparison of λ_p-values with $\hbar\omega$ and S_1-values [see ref.1] implies that H_{so} cannot be treated as a small perturbation for whole crystals.

As a next step, we set up a new scheme in which the total Hamiltonian

$H = H_{vib} + H_{so}$ is diagonalized. The total angular momentum $\vec{K} = \vec{J} + \vec{S}$ satisfies $[H, \vec{K}^2]=0$ and $[H, K_z]=0$, so that the eigenstates of H are classified by the quantum numbers K and K_z together with the parity P; the i-th lowest state of (K,K_z,P) is written as $\phi_i(K^P,K_z)$. The matrix element of H_z obeys the selection rules $\Delta K=0$ or 1, $\Delta K_z=0$, and $\Delta P=0$. Then, to the first order of H_0, the perturbed lowest RES $\Psi_\pm(H_0)$ is written by the linear combination of $\phi_1(1/2^+,\pm1/2)$, $\phi_i(1/2^+,\pm1/2)$ and $\phi_j(3/2^+,\pm1/2)$. The emission intensities for the left-(σ^+) and right-(σ^-) circular polarization along the magnetic field are given as $I^H_{\sigma\pm}(\pm)=I^0_{\sigma\pm}(\pm)+\delta I_{\sigma\pm}(\pm)$, where $I^0_{\sigma\pm}(\pm)$ are magnetic independent part and (±) stands for the transition from $\Psi_\pm(H_0)$. According to the time reversal symmetry, $I^0_{\sigma^+}(+)=I^0_{\sigma^-}(-)$, $I^0_{\sigma^-}(+)=I^0_{\sigma^+}(-)$, $\delta I_{\sigma^+}(+)=-\delta I_{\sigma^-}(-)$, and $\delta I_{\sigma^-}(+)=-\delta I_{\sigma^+}(-)$, respectively. Using these relations, the total magnetic circular polarization is represented as,

$$(3) \qquad \Delta = [I_+ - I_-]/[I_+ + I_-] = \Delta_p + \Delta_d \quad , \text{ where}$$

$$\Delta_p = P^* \cdot [I^0_+(-) - I^0_-(-)]/[I^0_+(-) + I^0_-(-)] = P^* \cdot F_p \ ,$$

and $\Delta_d = \Delta_{sz} + \Delta_{LZ}$ with $\Delta_{sz} = g_f \beta H_0 \cdot F_{sz}$ and $\Delta_{LZ} = g_{orb} \beta H_0 \cdot F_{LZ}$, where P^* is a spin polarization in the RES. The g-factor of the lowest RES is then given as,

$$(4) \quad g = 2 \langle \phi_1(1/2^+,1/2) | H_z | \phi_1(1/2^+,1/2) \rangle / \beta H_0 = g_f G_s + g_{orb} G_L \ .$$

Here, F_p, F_{sz}, and F_{LZ} in eq.(3) and G_s and G_L in eq.(4) are the function of (Δ,S_1,λ_p). Using experimental data of ESR[2,3] and MCP[4,5] together with the temperature dependence of the Stark polarization and radiative life time[1], one can determine four parameters Δ, S_1, g_{orb}, and λ_p, simultaneously. With this result, both electric and magnetic effects in the RES can be consistently understood. Computations are on progress. The results will be presented in this conference.

References: (1) K.Imanaka, T.Iida, and H.Ohkura, 1977, in this conference; submited to J.Phys.Soc.Japan. (2) Y.Ruedin et al.: Phys.Status solidi (b) 54 565 (1972). (3) L.F.Mollenauer and S.Pan:Phys.Rev. B6 772 (1972). (4) M.P.Fontana and D.B.Fitchen: Phys.Rev.Letters 23 1497 (1969). (5) G.Baldacchini et al.: preprint (1977). (6) H.Ohkura et al.:J.Phys.Soc. Japan 41 2137 (1976). (7) Y.Kayanuma and Y.Toyozawa:ibid. 40 355 (1976).

DATING WITH LATTICE DEFECTS INDUCED BY NATURAL RADIATION: ESR AND THERMOLUMINESCENCE DATING OF CAVE DEPOSITS

By Motoji IKEYA and Toshikatsu MIKI

II.Physikalisches Institut,Universität Stuttgart BRD and Technical College, Yamaguchi University, Ube 755, Japan

Some defects produced by natural radiation in minerals, rocks and archaeological materials are stabilized and stored for more than a million years at room temperature. Dating of such materials is possible by estimating the total dose of natural radiation from the content of the radiation-induced defects. The purpose of this paper is to show that the physics on defects can be extended to the chronology more convenient and simpler than C-14 or other isotope methods.

1) ESR and TL of Cave Deposits: Defects in $CaCO_3$

ESR measurements of stalactite, stalagmite, flow stones, and cave pearls indicate the presence of ESR signal with g= 2.003 in addition to that of Mn^{++} and other impurities[1]. The signal intensity decays with thermoluminescence (TL) by raising the temperature and is enhanced by an artificial γ-ray irradiation. The intensity of the signal increases from the surface to the inside as shown in Fig.1: the old inside has higher defect concentration than the young growing surface. It was suggested that the defect is CO_3^{---} radicals associated with charge compensating trivalent cation impurities from the thermal stability and the g value.

TL measurements of cavern deposits indicate the thermal glow at 500 K. The glow peak height is enhanced by an artificial γ-irradiation following the creation of a new glow peak at 400 K. The latter center has a poor stability. The ESR intensity and the peak height at 500 K is correlated. Thus, the peak height at 500 K was used for TL dating. The total

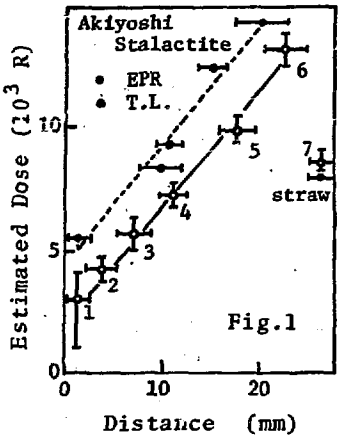

Table I. The age and growth rate of cave deposits at different caves.

Material		Age (yr)	Growth rate* (μm/yr)
Akiyoshi Stalact.	A	3.5×10^5	0.35(recent) 0.035(old)
	B	7.0×10^4	0.40(recent)
Cave Pearl	A	1.2×10^5	0.40
	B	7.5×10^4	0.04
Okinawa Stalact.		2.5×10^4	2.0
Petralona Stalagmite		2.5×10^5	0.18

* Radial growth rate is tabulated.

dose of the exposure was estimated by studying the enhancement of the ESR signal or the peak height by γ-irradiation.

2) Annual Radiation Dose : Age and Growth Velocity

The annual radiation dose must be determined to convert the total dose of natural radiation obtained above into the real age. The contents of radioactive elements(^{238}U- and ^{232}Th-series and ^{40}K) have been determined with γ-ray spectroscopy of cave deposits. Defects produced by α-rays are generally dense along its track so that the recombination rate is high. Only 10% of the energies is assumed to contribute to the formation of stable defects for α rays. The dose rates are 0.15-0.25 R/yr depending on the samples at different caves[2].

The age at different positions in a sliced stalactite or stalagmite gives an average growth velocity as shown in Table I. The work is further extended to date materials found in Greece Petralona cave, where a skull and tools of old human being are discovered by anthropoligists during the excavation.[3]

1) M.Ikeya, NATURE 255 (1975) 48.
2) M.Ikeya, Health Physics 31 (1976) 76.
3) A.Poulianos, ANTHROPOS, 3 (1976) 195.

TUNNELLING RECOMBINATION IN LiH IRRADIATED AT LOW TEMPERATURE

By Motoji IKEYA and Toshikatsu MIKI

II.Physikalisches Institut, Universität Stuttgart, BRD and Technical College, Yamaguchi University, Ube 755, Japan

Since the anion sublattice of the simplest ionic crystal, LiH, consists of the lightest hydrogen, some defect may show the properties of a quantum defect; the migration of which is dominated by the tunnelling rather than the thermally activated processes. In this paper, we present the phonon assisted tunnelling thermoluminescence (TL) and ESR of LiH irradiated at low temperature.

Fig.1 shows TL glow curve of LiH irradiated at 8K. The characteristic features are the linear increase of the TL intensity and the exponential fall off ($50 \lesssim T \lesssim 150$ K) in contrast with the ordinary shape of thermal glow with an exponential rise and an abrupt fall off. The temperature dependence of the afterglow also shows that the decay between 50 K and 150 K is temperature independent. The recombination rate obtained from the glow curve analysis is proportional to T ($T \lesssim 50$ K) similarly to the reorientation rate of OH^- dipole by one phonon assisted tunnelling. Temperature independent region proceeds between 50 K and 150 K for LiH in stead of the T^4-dependence for the multiphonon assisted tunnelling rotation of OH^- dipoles in alkali halides. Generally, the tunnelling rate may be expressed as $1/\tau = \Sigma f(n)/\tau_n$, where f(n) is the fraction of the center at the n phonon state and τ_n is the tunnelling time from such a state. Two level scheme rather than the multilevel scheme may be more appropriate for an anharmonic crystal of LiH where the tunnelling time from the high energy state is considerably short. The tunnelling rate may be expressed as $1/\tau \approx n \cdot \exp(-\Delta E/kT)/(1 + n \cdot \exp(-\Delta E/kT)) \times 1/\tau_1$ since the high energy states are close to the one phonon state. Similar recombination rate for ^6LiD indicates that the

the defect is strongly coupled with the lattice.

The TL spectrum is quite similar to that of the intrinsic luminescence observed by UV- or X-ray stimulation[1,2]. The thermally stimulated current (TSC) measurements indicate that the moving entity responcible for TL is neutral in charge.

ESR measurements of LiH irradiated at 4 K indicate the formation of a broad V type center before F centers are created at the late stage. The angular dependence can be analyzed with a zero field splitting (DS_z^2 term) for S=1 with a rough axis of [100]. It is suggested that an interstitial hydrogen atom is in exchange coulped state with a nerby F center.

The energy levels of an interstitial hydrogen atom in LiH was calculated theoretically using the computer for U_2 in alkali halides. The lattice of 2×2×2 and 4×4×4 of LiH were employed using the calculated overlaps. The level of H^0 comes about 1 ev above the valence band. The broad absorption found from the absorption edge to about 1 ev after the irradiation may be associated with the transitions of H^0 from the valence band of H^- ions to H^0. The presence of F center nearby would also contribute to the broadening. F and V bands are formed at the latter stage of X-irradiation. This may be associated with the formation of diinterstitial (H_2 molecule) which stabilizes F centers. Only F centers have been observed by UV-irradiation presumably because of the high local density of defects.

1) M.Ikeya, Solid State Commun. 17 (1975) 1235.
2) T.Miki, M.Ikeya, Physics Letter __ (1977)

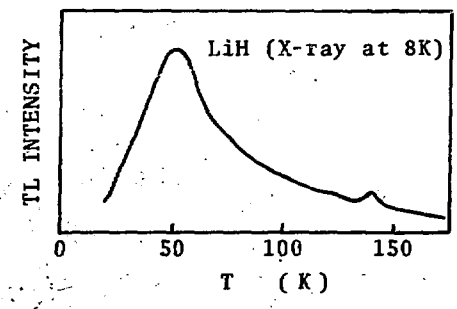

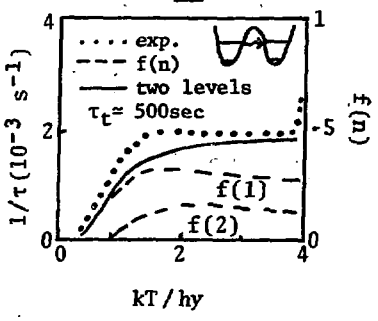

VIBRONIC THEORY OF THE STARK EFFECTS IN F CENTER EMISSION

Koichi IMANAKA, Takeshi IIDA*), and Hiroshi OHKURA
Department of Applied Physics, and *) Department of Physics,
Osaka City University, Sumiyoshi-ku, Osaka JAPAN 558

The Stark effects in F center emission have been observed by Bogan and Fitchen[1] for six alkali halides, and by us[2] for KBr, KI, RbBr, and RbI. Bogan and Fitchen derived a form of the temperature dependence of the Stark polarization P(T). By thoretical curve-fitting of experimental data, they determined two important parameters to describe their proposed model for the relaxed excited state (RES). Application of Bogan and Fitchen's form of P(T) for KI and RbI, however, gives unreasonably large 2p fraction in the lowest RES[2]; the fact is inconsistent with their model.

Ham and Grevsmühl have developed the vibronic theory, in which they show that the interaction with the T_{1u}-mode phonon in the RES is so weak that both P(T) and the temperature dependence of radiative life time of the RES $\tau(T)$ have the same temperature dependence.[3] No experimental data of P(T) and $\tau(T)$ are available to be consistently fit for their prediction.[2] Kayanuma and Toyozawa have developed the vibronic theory which includes the intermediate coupling case[4]. We derived P(T) as the extension of their theory[5]. We diagonalized a perturbed Hamiltonian due to the electric field effects with vibronic system which had been provided in ref.4. Here, the T_{1u}-mode coupling was solely taken into. The forms of P(T) and $\tau(T)$ are described in terms of the zeroth moments calculated by using the diagonalized eigenfunctions[5] which are represented by the total angular momentum $\vec{J}$, its z-component M, phonon number n, and the parity P, respectively. P(T) and $\tau(T)$ are calculated by taking into phonon levels up to ten levels. They are described by two parameters, namely, 2s-2p electronic energy separation Δ, and coupling constant with the T_{1u}-mode phonon S_1, respectively; both parameters have been proposed by Kayanuma and Toyozawa[4].

When the lowest RES consists of the 2p-like state $[J^P=1^-]$, computed $\tau(T)$ is independent of temperature up to about 100 K, while P(T) decreases rapidly with increasing temperature. No experimental data of P(T) and $\tau(T)$ which are fit for these theoretical predictions have been

observed. Thus, this case is ruled out as the model of the RES. When the lowest RES consists of the 2s-like state [$J^P=0^+$], theoretical forms of P(T) and τ(T) are derived as follows,

$$P(T)/P(0) = \sum_{J,\lambda} K_J^{\lambda} \exp(-\delta E_J^{\lambda}/kT) \;/\; \sum_{J,\lambda} (2J+1)\, R_J^{\lambda} \exp(-\delta E_J^{\lambda}/kT) \qquad (1)$$

$$\tau(T)/\tau(0) = \sum_{J,\lambda} (2J+1) \exp(-\delta E_J^{\lambda}/kT) \;/\; \sum_{J,\lambda} (2J+1)\, R_J^{\lambda} \exp(-\delta E_J^{\lambda}/kT) \qquad (2)$$

with $\delta E_J^{\lambda} = E_J^{\lambda} - E_0^{\lambda}$; $K_J^{\lambda} = \sum_M [\, I_{\eta}^F(J,M,\lambda) - I_{\perp}^F(J,M,\lambda)]/[\, I_{\eta}^0(0,0,1) - I_{\perp}^0(0,0,1)]$,

and $R_J^{\lambda} = (2J+1)^{-1} \sum_M [\, I_{\eta}^0(J,M,\lambda) + I_{\perp}^0(J,M,\lambda)]/[\, I_{\eta}^0(0,0,1) + I_{\perp}^0(0,0,1)]$,

where $I_{\eta}^F(J,M,\lambda)$ is the zeroth moment of emission polarized to η-direction at the lowest λ-th level in the (J,M) state under application of electric field F. Numerical computation shows that both different forms of P(T) derived in refs.1 and 3 are included in eq.(1) as the limiting cases[5].

From the theoretical curve-fitting of eqs.(1) and (2) with experimental data of P(T)/P(0) and τ(T)/τ(0), the values of Δ and S_1 are determined[5]. They are tabulated in the following Table: both values are normalized by the dispersionless LO phonon energies $\hbar\omega$. When (Δ,S_1) are determined, the 2p-fraction in the lowest RES N^2; the energy separation between the first excited and lowest RES δE_1^1 ; the ratio of 2p-fractions between both levels R_1^1 ; and the dipole moment μ; can be estimated and are listed in the Table for whole available crystals. [Here,(Δ,S_1) values for *-marked crystals are determined only from P(T).].

	(Δ , S_1)	$\hbar\omega$ (meV)	N^2	R_1^1	δE_1^1 (meV)	K_1^1	μ (A)
KF	(0.0 , 0.5)	41.4	0.37	1.61	13.1	-0.95	2.9
KCl	(1.25, 0.35)	26.8	0.15	2.04	16.3	-0.34	3.1
KBr	(1.50, 0.25)	21.0	0.10	2.43	14.9	+0.10	4.3
KI *	(2.3 , 0.2)	17.9	0.05	2.34	14.8	+1.20	2.5
RbCl	(1.5 , 0.3)	22.3	0.12	2.20	15.0	-0.01	2.0
RbBr*	(2.0 , 0.2)	16.1	0.06	2.46	12.9	+0.91	3.2
RbI *	(2.5 , 0.2)	13.3	0.05	2.28	11.2	+1.37	2.8

References: (1) L.D.Bogan and D.B.Fitchen:Phys.Rev.B1 4122 (1970). (2) H.Ohkura et al. J.Phys.Soc.Japan 42 1942 (1977). (3) F.S.Ham and U.Grevsmühl: Phys.Rev. B8 2945 (1973). (4) Y.Kayanuma and Y.Toyozawa: J.Phys.Soc. Japan 40 355 (1976). (5) K.Imanaka et al.J.Phys.Soc.Japan 43 519 (1977).

ELECTROLYTIC COLOURATION OF KCl:Tl^+ CRYSTALS

A. Ioan
Physics Department
University of Bucharest
Romania

V. Topa
Institute of Physics and
Technology of Materials,
Bucharest, Romania

The electrolysis of KCl:Tl^+ crystals (200°C - 560°C and 100 - 6000 V/cm) transforms all Tl^+-ions in that part of the crystal, where the colouration takes place.

This process can be followed easily by the modification of the absorption and luminescence spectra.

After electrolytical colouration the characteristic bands of the Tl^+-ion disappear and a well shaped absorption band peaking at 3.5 eV appears, with about the same intensity as that of the faded away A-absorption band of Tl^+ ions. We attribute the band at 3 5 eV to Tl^- complex centres.

By migration of the F centres in electric field at the temperature of colouration, the band at 3.5 eV is transformed too, and a structured large band (1.5 eV half width) with two peaks at 4.15 eV and 5.08 eV comes out. The last absorption is associated with colloids of Tl^0.

A strong argument in favour of the Tl^--complex centre model is the fact that the annealing at about 560°C, in H_2 of crystals with this kind of centres brings about the evanescence of the band at 3.5 eV with concomitant formation of the H^--centre band (with an intensity proportional to the initial Tl^+ concentration) and without re-formation of the Tl^+-ions. In the samples previously subjected to migration

in electric field a similar heat treatment do not induce the appearance of the H^--centre.

Other arguments for the Tl^- complex centre model are :

- the stability of the band at 3.5 eV under optical irradiation
- its thermal stability till to 350°C
- the fact that the annealing above 350°C for a short time destroys the Tl^--complex centres, forming F-centres and, probably, Tl^0 interstitials (by a process similar to that put in evidence by Fischer et al. [1], leading to the creation of F-centres on the account of H^--ions)
- the fact that the annealing at 600°C transforms the Tl^--complex centres in colloids, as in the case of Ag-doped crystals [2].

[1] F. Fischer, H. Gründig and R. Hilsch - Z.Phys., 189, 79 (1966)

[2] V. Topa - Thesis, Bucharest (1967)
V. Topa - Rev.Roum.Phys., 12, 781 (1967)

NEW CENTRES IN KCl:Tl^+ + Ca^{2+} AND KCl:Tl^+ + Sr^{2+} CRYSTALS

A. Ioan
Physics Department
University of Bucharest
Romania

V. Topa
Institute of Physics and
Technology of Materials,
Bucharest, Romania

After electrolytical colouration in special conditions (200°C, 6000 V) of (Tl^+ + Ca^{2+}) and (Tl^+ + Sr^{2+}) doped KCl crystals, three new bands have been found in the optical absorption spectrum (see table 1).

Table 1

Absorption peak position ($\mathcal{E}_{max}$) and half width (H) in eV (at 300 K)

KCl:Tl^+ + Ca^{2+}	$\mathcal{E}_{max}$	3.23	2.56	1.7
	H	0.6	0.4	0.5
KCl:Tl^+ + Sr^{2+}	$\mathcal{E}_{max}$	2.8	2.1	1.5
	H	0.35	0.25	0.3

In these conditions of colouring one obtained also the absorption band peaking at 3.5 eV, which appears in KCl:Tl^+ crystals, and that we attributed [1] to Tl^--complex centres. It is to be noted that two of the three new bands are superimposed upon the absorption band of the Tl^- complex centres.

There exists a strong dependence of the new bands on temperature, voltage and time of electrolytical colouration, and concentration of Tl ions.

The KCl crystals doped with the same concentration of Ca^{2+} or Sr^{2+}-ions, but without Tl^{+}, do not present any absorption band after electrolytical colouration.

By decreasing the temperature of absorption measurements, the intensities of the three new bands grow, their half widths decrease and the peaks shift towards longer wavelengths.

The best conditions concerning the concentrations of Tl^{+} and Ca^{2+}, or Tl^{+} and Sr^{2+}, are given for the appearance of the new bands.

A heat treatment above 350°C destroys the corresponding centres.

Based on these results and on the strong dependence of the positions of ε_{max} for the three new bands upon the nature of the divalent impurity, we conclude that the corresponding centres contain a divalent ion and a Tl^{-} - complex.

[1] A. Ioan and V. Topa - Rev.Roum.Phys., in press

EPR STUDY OF V^{2+}-VACANCY DIPOLES IN ALKALI HALIDES

Takeo IRI and Takao ITO
The University of Electro-communications,
Chofu-shi, Tokyo 182, JAPAN

The electronic states of V^{2+}-vacancy dipoles in LiCl, NaCl and KCl have been studied by EPR method. Crystals were grown from the melt of those alkali halides which were mixed with VCl_2. When the vanadium trichlorides were sealed into quartz ampoule together with the appropriate amount of the powder of metalic vanadium and were heated for two days at 600°C, the vanadium dichlorides were obtained through reducing reaction.

Divalent ions in alkali halides have long been a subject of study by EPR method, but have been restricted tc S-state ions. The ground state of V^{2+} in Oh-site is $^4A_2$ and the excited state $^4T_2$ of the same spin multiplicity is mixed into it in first order through spin orbit interaction. We can visualize the symmetries and lower fields in the dipoles through fine structure in EPR spectra. The spin Hamiltonian parameters were determined, and the results are summarized in Table I.

Table I. Spin Hamiltonian Parameters at 77°K

	nn dipole			nnn dipole		
	LiCl	NaCl	KCl	LiCl	NaCl	KCl
g	1.956 ±0.002	1.952 ±0.002		1.962 ±0.002	1.957 ±0.002	1.958 ±0.002
A [$\times 10^{-4}$ cm^{-1}]	76.5 ±2.0	79.7 ±2.0		78.5 ±2.0	76.9 ±2.5	80.8 ±3.0
D [$\times 10^{-4}$ cm^{-1}]	101.0 ±1.0	22.2 ±1.0		278.0 ±2.0	534.0 ±3.0	726.6 ±3.0
E [$\times 10^{-4}$ cm^{-1}]	300.0 ±2.0	409.0 ±2.0		~0	~0	~0

In NaCl:V^{2+} the investigation has also been performed concerning the establishment of equilibrium of population distribution between nearest and next nearest neighbour V^{2+}-vacancy dipoles. The process of mutual exchange of these two dipoles was only taken into account, since there has

not been detected any trace of the dipole aggregation below room temperature. The kinetic rate equations for these systems have been given by Symmons[1]. The rate W_3 at which nn dipoles change to nnn dipoles and the rate W_4 of the inverse process to that of W_3 have been determined in the temperature range (-150 to 20°C). This was accomplished by measuring the ratio R(t) of the number N_1, the total number of nn dipoles in the crystal at time t, and N_2, that of nnn dipoles, and by the aid of two relations: $R(\infty)=2W_3/W_4$ and

$$\frac{R(0)-R(\infty)}{R(t)-R(\infty)} + \frac{R(0)-R(\infty)}{1+R(\infty)} = \frac{1+R(0)}{1+R(\infty)}\exp[2(W_4+2W_3)t]. \qquad (1)$$

The logarithm of the quantity on the left of eq.(1) as calculated from experimental data is plotted against t in Fig.1. Expressing W_3 and W_4 in the Arrhenius form $W_j=A_j\exp(-E_j/kT)$ there result the values: $A_3\simeq 4.4\times10^{15}\ s^{-1}$, $E_3=0.68\pm0.02$ eV, $A_4\simeq 1.6\times10^{16}\ s^{-1}$ and $E_4=0.70\pm0.02$ eV.

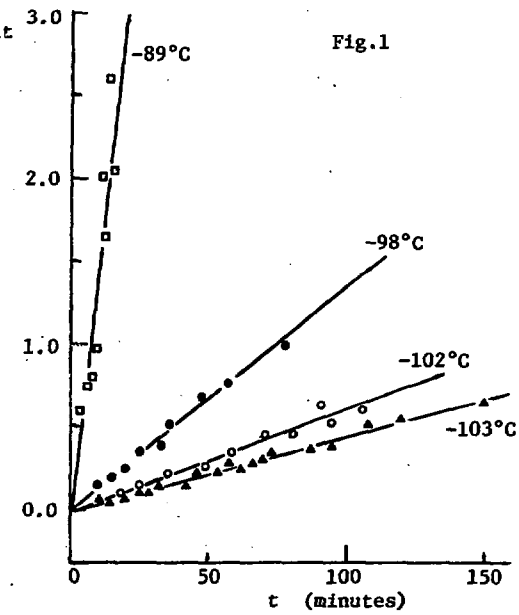

Fig.1

1) H. F. Symmons: J. Phys. C 3(1970)1846.

THE INITIAL PRODUCTION OF DEFECTS IN ALKALI HALIDES: F AND H CENTER PRODUCTION BY NON-RADIATIVE DECAY OF THE SELF-TRAPPED EXCITON

N. Itoh*, A. M. Stoneham and A. H. Harker
Theoretical Physics Division, AERE Harwell, Oxfordshire, UK.

Radiation damage in KCl can be produced by the decay of a self-trapped exciton into an F and an H center. We present calculation of energies of the states involved for various stages in the evolution of the damage. The calculation uses a self-consistent semi-empirical molecular-orbital method, here the CNDO method as implemented in Harwell MOSES code. This method meets our need to obtain the total energies for open-shell systems involving a relatively large number of atoms.

The molecular orbital parameters for alkali and halogen were chosen so that they reproduced observed properties (notably potential energy curves) of KCl molecules and of Cl_2^- molecular ions. A large cluster of ions is used (either 42 or 57 ions) in the CNDO claculation. Since there are long-range Coulomb interactions with ions outside the cluster, we have included proper Madelung corrections. The calculated band structure of the KCl crystal was in very acceptable agreement with experiment, verifying that one-electron excitations will be predicated well. It is very important to use the correct geometry near any defect. For the local lattice distortion around the self-trapped exciton as it evolved into an H center and an F-H pair we used results obtained with the HADES program, developed by Norgett. The distortion around an F center in its ground state was disregarded. Explicit basis orbitals for the F center were included in some cases to give an appropriate 1s - 2p transition energy. The effect of these F-center orbitals on the binding energy was found to be negligible.

The binding energy of an F center and an H center was calculated by taking the difference between the formation energy of the F-H pair and of a separated pair of F- and H-centers. One particularly striking feature of the result is the repulsive F-H interaction at the nearest-neighbor spacing,

* Permanent address: Department of Crystalline Materials Science, Faculty of Engineering, Nagoya University, Nagoya, Japan

compared with attractive interaction at the larger spacings. The energy difference between the ground state (best described as an α-Cl_2^- pair) and the first excited state (best described as an F-H pair) for the nearest neighbor spacing was about 1.5 eV, whereas that for the next nearest neighbor was much smaller. The latter result suggests the possibility of tunneling annihilation of the F-H pairs at the short separations.

The present method was employed to calculate the energies of the several excited states of the isolated self-trapped exciton. The calculated recombination energy of the self-trapped exciton and the absorption energy from the lowest self-trapped exciton state agree with the experimental results and with previous theoretical work by other methods. The energy of the lowest self-trapped exciton state was found to be slightly smaller than the energy of the distant F-H pair: this result accounts for the occurence of the π-emission seen in the F-H recombination.

The energies of various stages in the evolution of a self-trapped exciton displaced along a <110> direction were calculated both for the ground state and for the excited state of the self-trapped hole. For the hole in its lowest state the ground state and the σ- and π-emissive states were found to be stable against the <110> deviation of Cl_2^- as a whole. The other electron-excited states were also found not be evolve to the F and H centers.

Calculation of the energies of several hole excited states were tried. It was hard to enforce convergence on such states because of the presence of others with the same symmetry and nearly the same energy. The excited state we have obtained corresponds to the hole in an excited π-state and the electron in a higher σ state. The interesting feature was that the energy surface for the excited state is flat against the <110> evolution into a nearest F-H pair. This result strongly support the model proposed by Itoh and Saidoh that damage proceeds through an excited hole state.

Ag^{o}-V_k TUNNELING RECOMBINATION IN ALKALI HALIDES

Noriaki Itoh, Shigeru Takeuchi, Takashi Tashiro and M. Saidoh

Department of Crystalline Materials Science, Faculty of Engineering,
Nagoya University, Nagoya, Japan

It is known that tunneling recombination between the Ag^{o} and V_k centers in alkali Halides produces prominent emission bands. In the present paper, we report the dynamic of Ag^{o}-V_k tunneling in KCl and NaCl between the time interval of 10^{-7} s and 10 s and between 80 K and 570 K. Significant differrences in the decays of tunneling luminescence of KCl and NaCl and in their temperature dependence are demonstrated and ascribed to the difference in the anisotropic nature of the tunneling.

Specimens of NaCl and KCl doped with Ag^{+} at a concentration of about 0.1 mol% were irradiated with 2 MeV pulsed electron beams from a Febetron accelerater. In order to increase the dynamic range, light output was fed into two photomultipliers, the output of which was measured with two oscilloscopes set at two different time ranges.

First we show a remarkable difference in the time dependence of the tunneling luminescence in KCl and NaCl. In KCl the luminescence intensity was nearly proportional to $t^{-0.77}$, whereas in NaCl it was proportional to t^{-1}. A t^{-1}-dependence in KCl has been obtained by Delbecq et al.[1] for t>10 s. The tunneling rate w of a pair separated by a distance r is given by $w(r)=w_o\exp(-r/r_o)$, where w_o and r_o are constants. Thus the intensity of I(t) of luminescence at time t is given by

$$I(t) = \int_0^\infty n(r)w(r)\exp(-w(r)t)dr,$$

where n(r)dr is the number of pairs separated by a distance r. A numerical integration gives $I(t) \propto t^{-0.88}$, if $n(r) = 4\pi r^2$, and it is easily shown that $I(t) = t^{-1}$ if n(r) = const. Delbecq et al. have assumed a $4\pi r^2$-distribution and a movement of the recombination front to explain the t^{-1}-dependence.

Temperature dependence of the decay of tunneling luminescence was measured. If $n(r) = 4\pi r^2$, the isotropic annihilation is responsible for the

luminescence, and a diffusion-controlled annihilation scheme is held. Then the decay rate is expected to be enhanced with increasing temperature. This was indeed observed for KCl in t<1 s, where the $t^{-0.77}$-dependence was observed. In NaCl, however, the decay rate was found to be even reduced with increasing temperature, as shown in Fig. 1. This result indicates clearly that the simple diffusion-controlled annihilation is not effective in NaCl, in which the t^{-1}-dependence was observed.

The following model is invoked to explain the t^{-1}-dependence: Only the V_k center lying on six <110> rows passing through the neighboring sites of Ag^0 causes tunneling luminescence. It is clear that this model, in which n(r)=const, accounts for the t^{-1}-dependence. Furthermore the temperature dependence of the decay is explained as follows: A few jumps of the V_k centers put some of them on the line feasible to emit luminescence. Thus an enhancement of luminescence at given t occurs as long as new V_k centers reach the line within time t. A Monte Carlo calculation was made, the result of which was consistent with the result shown in Fig. 1.

The present model is consistent with Delbecq's observation that the luminescence in KCl for t>10 s, where the t^{-1}-dependence was observed, is polarized along the axis of the V_k center. The difference between the decay of NaCl and KCl for t<1 s, may be accounted for by the largeness of the anisotropy around the V_k center in NaCl than in KCl. ENDOR experiments by Mieher shows that anisotropy is larger in LiF than in NaF. The anisotropy may be smeared out for large r even in KCl.

The result of the present investigation indicates that an aligned Ag^0-V_k pair separated at a certain distance emit luminescence at a given time interval. A time-resolved EPR study may reveal the electronic interaction of such a pair.

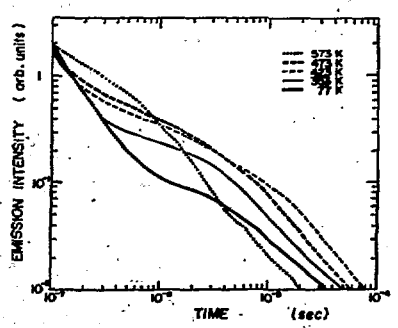

Fig. 1.

1) C. J. Delbecq, Y. Toyozawa and P. H. Yuster, Phys. Rev. B 9, 4497 (1974)

THEORETICAL INVESTIGATION OF THE HYPERFINE-STRUCTURE CONSTANTS OF THE H-CENTER USING A VALENCE-BOND WAVE FUNCTION FOR THE HALOGEN-MOLECULE

A. N. Jette and F. J. Adrian
Applied Physics Laboratory
The Johns Hopkins University
Laurel, Maryland 20810

The valence-bond (VB) theory previously used to investigate the polarization and band intensities of the optical transitions[1] and the hyperfine structure constants[2] (hfc) of the V_K center has been extended to interpret the hfc of the H-center in KCl and KBr and the $H_A(Na^+)$-center in LiF. A semi-empirical VB wave function is constructed of the form

$$\Psi = N\{[\varepsilon A\Phi_A(p_z)\Phi_B^- \Phi_C^- \Phi_D^- + A\Phi_A^- \Phi_B(p_z) \Phi_C^- \Phi_D^-]$$

$$+ \sqrt{1-\varepsilon^2}\,[A\Phi_A^- \Phi_B^- \Phi_C(p_z) \Phi_D^- + A\Phi_A^- \Phi_B^- \Phi_C^- \Phi_D(p_z)]\}$$

where $\Phi_N(\mu)$ (Φ_N^-) is a product of atomic (ionic) Hartree Fock SCF functions centered on the Nth nucleus while μ is the neutral atomic orbital (AO) occupied by the unpaired electron in a particular structure. Here N is a normalization constant, A, is the antisymmetrization operator and ε is a factor that weighs the diatomic molecule structure involving A and B with the molecular binding to the ligand ions C and D. Thus, this wave function permits the unpaired electron to spend a portion of the time on the ligand ions as indicated by the experimental hfc data.

Intra-atomic electron correlation is treated by using ionic AO's in the product Φ_N^- and halogen atom AO's in the product $\Phi_N(\mu)$. Interatomic electron correlation is treated by a perturbation theory calculation of the polarization of the orbitals $\Phi_N(\mu)$ by the crystal field. Interatomic polarization and the requirement that orbitals on different atoms be orthogonal are the important factors in the isotropic hfc. It is also important to consider both valence and inner shell excitations.

With the spin-correlated VB wave function, the isotropic hyperfine constant A_0 was calculated as a function of internuclear distance R_{AB} and structure factor ε for the molecular nuclei (A and B). The ligand ions (C and D) were constrained to lie on perfect lattice sites. The values of R_{AB} and ε were determined as those giving the best fit between calculated and experimental A_0 values. The anisotropic coupling constants $B_{||}$ for the molecular and ligand nuclei were than calculated

and compared with the corresponding experimental quantities. The experimental value for $B_{||}$ of the molecular nuclei was corrected for the contribution arising from spin-orbit mixing of ground and excited states which can be related to the electronic g-factor data. The results appear in Table I.

Table I

Comparison of Experimental and Theoretical Hyperfine Coupling Constants for the H-Center

	KCl Cl^{35}		K Br Br^{81}		LiF ($H_A(Na^+)$) F^{19}	
	Theory	Exp.	Theory	Exp.	Theory	Exp.
A_A(MHz)	129	129[3]	532	538[4]	744	744[6]
A_C(MHz)	6	12[3]	45	56[5]*	127	130[5]
R_{AB}(a.u.)	4.62	---	5.30	---	3.32	---
ϵ	0.990	---	0.990	---	0.985	---
B_A(MHz)	171	177[3]	830	894[4]	1722	1959[6]
B_C(MHz)	8.5	8.7[3]	52	111[5]*	125	121[5]

*The experimental perpendicular component of the ligand hyperfine tensor is not known. These values were derived by assuming it to be zero.

1. F. J. Adrian and A. N. Jette, Phys. Rev. B 9, 3587 (1974).
2. A. N. Jette and F. J. Adrian, Phys. Rev. B 14, 3672 (1976).
3. D. Schoemaker, Phys. Rev. B3, 3516 (1971).
4. D. Schoemaker and A. Lagendijk, to be published.
5. W. Känzig and T. O. Woodruff, J. Phys. Chem. Solids 9, 70 (1958).
6. M. L. Dakss and R. L. Mieher, Phys. Rev. 187, 1053 (1969).

THERMOLUMINESCENCE IN KCl X-IRRADIATED AT 80K

M. Jiménez de Castro and J.L. Alvarez Rivas
Junta de Energía Nuclear, Madrid, Spain

The thermoluminescence up to room temperature of pure KCl single crystals x-irradiated at 80K has been studied. At a heating rate of 8.3K/min., the thermoluminescence spectrum exhibits nine glow peaks whose maxima are respectively at 98, 120, 150, 166, 195, 219, 238, 267 and 304 K. It has been possible to obtain the shape of most of these glow peaks. By irradiating at temperatures above 80K no additional glow peaks appear, but the relative intensity of those glow peaks above the irradiation temperature varies.

The spectrum of the emitted light has been measured at several temperatures. It shows three main emission bands peaked around 310, 490 and 630 nm. Their relative intensities change with temperature and around 290K an emission band peaked at about 435 nm becomes predominant (1).

The dependence of the emission spectrum on the temperature makes it difficult to obtain reliable values of the activation energy and the pre-exponential factor of the thermoluminescent processes from the resolved shapes of the corresponding glow peaks. The isothermal method has been used to obtain these parameters. The analysis of isothermal light decay curves between 80K and room temperature has shown that there are nine first order thermoluminescent processes operative in this temperature range. The pre-exponential factors of some of these thermoluminescent processes are very low compared with the values usually assigned to them.

The photo-stimulated thermoluminescence of samples x-irradiated at room temperature and then bleached with F light at 80K has also been studied to detect the electron traps in these samples. The luminescence measured in this case is that of the F^* centers. This thermoluminescence spectrum shows six glow peaks around 100, 112, 155, 170, 207 and 250 K, and there is not any correspondence among these and the glow peaks observed in samples x-irradiated at 80K. It is concluded that no glow peak in the irradiated samples can be attributed to electron untrapping.

To clarify the nature of the carriers in the thermoluminescent processes occurring in the irradiated samples, the thermally stimulated currents have been measured after x-irradiation at 80K. The glow current spectrum shows only a large peak at 195K which agrees with a glow peak of the thermoluminescence spectrum. The initial rise method yields an activation energy of 0.43 eV for this current peak. The samples photostimulated at 80K do not show this current peak but several peaks at the temperatures of the glow peaks observed in their thermoluminescence spectrum.

The thermal stability of the F centers induced by x-irradiation at 80K has been studied. The F-center annealing curve in samples heated at 8.3 K/min presents a step at the temperature of each glow peak in the thermoluminescence spectrum, except at 195K. The analysis of the isothermal F-center decays shows that there are first order annealing processes whose activation energies correspond to those of the thermoluminescent processes, except for that at 195K.

It is concluded that all the glow peaks, except that at 195K, are due to the recombination of thermally released chlorine atoms (interstitials) with F-centers (1). The glow peak at 195K is likely induced by the recombination of thermally released holes with electrons at impurities.

References:

1. Ausín, V. and Alvarez Rivas, J. L., J. Phys. C. 5, 82 (1972).

LUMINESCENT CENTERS IN THALLIUM-DOPED ALKALI HALIDES

R. V. Joshi, L. H. H. Prasad, and P. W. Deshpande
M.S. University of Baroda, Baroda, India

Much experimental and theoretical work has been reported on the optical absorption and luminescence of alkali halides containing thallous ion impurity. To explain the optical processes in these systems, Seitz[1] proposed a model in which activator ions enter the lattice substitutionally at cation sites. The isolated substitutional Tl^+ ion model of Seitz was reinforced by the quasi-theoretical treatment of Williams and his co-workers.[2-5] Subsequent experimental work however, showed that the apparent simplicity of the thallium-doped alkali halide system was an illusion and that a more complex problem was involved.[6-8] For instance, it was observed that in alkali halides that were not lightly doped with thallium, the intensity of the emission in the visible region increased faster than linearly with thallium concentration. This emission was therefore suggested to be associated with Tl^+ ions in pairs (dimers) occupying nearest neighbor cation positions in the lattice.

On the basis of the study of the heavily doped KCl:Tl phosphors carried out in the present work, it is believed that the centers primarily responsible for luminescence in these phosphors are Tl^+ ions in the disturbed regions of the lattice which get bonded with the neighboring Cl^- ions. In such cases the luminescent centers could either be TlCl molecules or charged complex ions of the type $(TlCl_n)^-$. The results obtained further suggest that in heavily doped KCl:Tl, where TlCl can precipitate out as a separate phase, K^+ ions replacing Tl^+ ions in TlCl lattice (TlCl:K) also play a role in the formation of the luminescent centers.

Thallium-activated alkali halides that have been investigated in more detail in regard to their luminescent behavior are KCl:Tl, KBr:Tl, and KI:Tl. It is generally presumed that Tl^+ ions will not behave substitutionally differently in other alkali halide crystals. Detailed measurements on the luminescence of NaCl:Tl phosphors undertaken in the present work however, reveal that the state of perfection of the crystal has an important bearing on the nature of the luminescent centers. The Tl^+ ion

is comparable in size with a K^+ ion but large relative to an Na^+ ion. As in KCl:Tl, NaCl:Tl does not show a concentration dependent increase in the visible emission attributable to the dimers. The luminescence centers formed by the association of Tl^+ ions with Cl^- ions in the strained regions of the lattice are predominantly favored in NaCl:Tl phosphors at all concentrations of Tl^+.

References:

1. F. Seitz, J. Chem. Phys. 6, 150 (1938).
2. F. E. Williams, J. Chem. Phys. 19, 457 (1951).
3. P. D. Johnson and F. E. Williams, J. Chem. Phys. 20, 124 (1952).
4. P. D. Johnson and F. E. Williams, J. Chem. Phys. 21, 125 (1953).
5. F. E. Williams and P. D. Johnson, Phys. Rev. 113, 92 (1959).
6. R. S. Knox and D. L. Dexter, Phys. Rev. 104, 1245 (1956).
7. D. A. Patterson and C. C. Klick, Phys. Rev. 105, 401 (1957).
8. J. Ewles and R. V. Joshi, Proc. Roy. Soc. A 254, 358 (1960).

EVOLUTION OF MOLECULAR ORDER AND PHASE TRANSITIONS IN MIXED ALKALI-HALIDE-CYANIDE CRYSTALS

I. INFRARED ABSORPTION, DOMAIN SCATTERING AND CHRISTIANSEN EFFECT

Michael D. Julian and Fritz Luty
Department of Physics, University of Utah, Salt Lake City, Utah 84112

The availability of high quality alkali-halide-cyanide single crystals, like $(KCN)_x:(KCl)_{1-x}$, over the whole range of mixture ($0 \leq x \leq 1$), has opened up the possibility of studying the orientational motion and ordering processes of the CN^- dipoles under gradually increasing interaction. The starting-point is the dilute dipole system ($x < 10^{-3}$), with its well studied and understood paraelectric and paraelastic behavior. The end-point is the pure alkali-cyanide crystal ($x = 1$), which transforms from the orientationally disordered pseudo-cubic high-temperature phase via a sharp first-order transition (T_c = 168K for KCN) into an orthorhombic structure, in which the cyanide molecules are parallel (ferroelastically) ordered. Studies between these two extremes should reveal the evolution of collective order and phase-transitions from single defect and defect-cluster behavior.

In this part, the optical properties of this mixed system, built from spherical ions and optically anisotropic molecules, are discussed:

(1) The substitution of CN^- molecules introduces into the transparent infrared region of the crystal a strong absorption band (at ~5μ) and a ~200 times weaker band (at ~2.5μ), which are due to the fundamental and second harmonic CN^- stretching vibrations. Measurements of these bands in mixtures of KCN with KCl, KBr, and KI, and in pure NaCN -- in connection with chemical CN^- analysis -- show approximately linear scaling of the integrated strengths of these bands with the CN^- content, indicating additivity of the vibrational oscillator-strength and a constant anharmonicity throughout the mixtures.

(2) One of the important experimental manifestations of the first-order ferroelastic phase transition is the abrupt appearance of domain structure at the transition-temperature T_c, (with the orthorhombic domain

axes along the six equivalent <110> direction. The parallel order of the optically anisotropic CN^- molecules in each domain produces strong birefringence, so that light is scattered due to the refractive index mismatch between differently oriented domains. The temperature of appearance (T_c), strength, and spectral shape of this scattering effect was measured -- starting from pure KCN -- into the mixtures of KCl, KBr, and KI. In all these cases, T_c shifts gradually with decreasing CN^- content to lower temperatures, while parallel to this the strength of the scattering decreases rapidly. At a critical CN^- concentration x_c (which is x_c = 0.55, 0.80, and 0.90 for the KBr, KCl and KI mixture, respectively) the light scattering from domains (i.e. the manifestation of spontaneous ferroelastic order) disappears completely. A wave-optical model, based on phase-retardation and diffraction effects due to the birefringent domain structure, can be fitted to the IR data, explaining the observed λ^{-2} dependence of the scattering strength and allowing estimates on the domain sizes.

(3) Within the IR attenuation spectra from domain-scattering, a sharp transmission spike was observed to appear close to the high-energy side of the CN^- stretching band. At the wavenumber of this spike ($\nu_s \approx 2088\ cm^{-1}$ for KCN) the otherwise opaque and completely light-depolarizing crystal is nearly perfectly transparent and non-depolarizing. This amazing optical phenomenon can be quantitatively understood as a particular and novel form of the "Christiansen-filter effect". Due to the fact that the anisotropic polarizability of the CN^- consists of a high-frequency electronic and a low-frequency vibrational part, their combined $n(\lambda)$ curve must cross the $n = 0$ line at some intermediate frequency in the anomalous vibrational dispersion region. At this wavelength of crossing (which is predictable from the optical and Kerr effect data to lie closely to the observed λ_s) the CN^- molecule has a completely isotropic polarizability, so that clusters or domains of any orientation behave optically isotropic, and light scattering and depolarization disappears. Polarized measurements in this narrow "transmission window" at λ_s reveal a detailed structure, which can be related to the optical properties of the domains.

VACANCY-INTERSTITIAL PAIR PRODUCTION BY ELECTRON-HOLE RECOMBINATION IN HALIDES

M.N. Kabler and R.T. Williams
Naval Research Laboratory
Washington, D.C. 20375

The nature of the electronic states through which band-to-band excitations or excitons evolve into F-H pairs is a question central to an understanding of the defect production process. The choice of models has been narrowed considerably by various experiments, particularly pulsed electron and laser excitation measurements which have shown that the process can occur in 10 picoseconds with a quantum efficiency approaching unity and have located an intermediate state of the self-trapped exciton (STE) which is a precursor of the F-H pair. The present paper develops a recent empirical model[1] in which an excited STE becomes an F-H pair through a relaxation process that preserves the σ bond between the two halide ions of the X_2^-. This process is in general accord with available experimental data.

The figure shows energy levels of the e-h system in KCl for three lattice configurations: perfect crystal, STE, and F-H pair. These levels were obtained and characterized using a wide range of experimental and theoretical data and are designated by conventional notation. Some of the observed optical transitions are also shown. A STE state at P has been identified as an effective precursor to F(1s) + H(σ_u).[2]

The potential surfaces which govern motion from one configuration to another have been investigated in terms of correlation rules, using the diabatic approximation.[3] The dashed lines in the figure represent several of the correlations obtained. These resemble the potentials suggested by Toyozawa,[4] although the present treatment differs from his. It has been found that F(1s) + H(σ_u) correlates with a higher

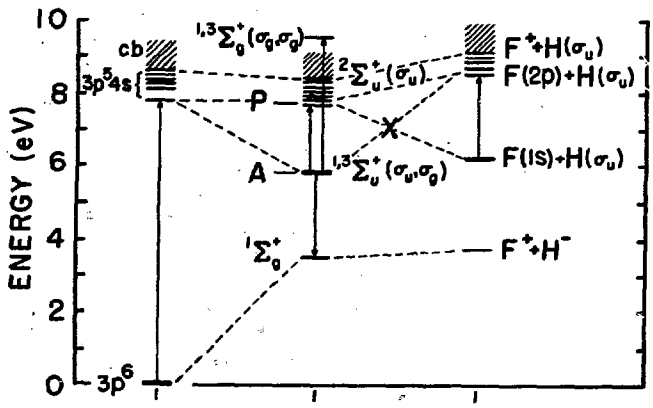

STE state involving a σ_u hole orbital and a σ electron orbital to which 3d orbitals on the halogens contribute. We identify this STE state with the precursor P.

The initial ionic motion between P and F(1s) + $H(\sigma_u)$ is not necessarily confined to a close-packed direction in alkali halides. The near F-H pairs observed in alkaline earth fluorides are cited as examples of initial vacancy formation involving rotation as well as translation of an excited halide-ion pair. Conditions relating to the required crossing of potential surfaces at X in the figure are considered.

1. M.N. Kabler, in Proceedings of the NATO Advanced Study Institute on Radiation Damage Processes in Materials, Corsica, 1973, ed. by C.H.S. Dupuy (Noordhoff International, Leyden, 1975), p. 171.
2. R.T. Williams, Phys. Rev. Letters 36, 529(1976).
3. M. Barat and W. Lichten, Phys. Rev. A6, 211(1972).
4. Y. Toyozawa, in Proceedings of the IV International Conference on Vacuum Ultraviolet Radiation Physics, Hamburg, 1974, ed. by E.E. Koch, R. Haensel, and C. Kunz (Pergamon Vieweg, Braunschweig, 1974), p. 317.

REORIENTATIONAL DISORDER OF NO_3^- IN $CsNO_3$

R. Kamel, Y. A. Badr, and Z. I. Badawy
Physics Department, Faculty of Science, University of Cairo

The totally symmetric stretching mode of vibration, ν_1, of NO_3^- ions in some nitrates showed a multistructural nature characterized by a weak low frequency band beside the main peak. In the present work, the polarized I.R. spectrum of $CsNO_3$ in the region of the stretching mode was considered in the temperature range -100 to 170°C. A computer program was used for the resolution of the complex contours into its constituents. Fig. 1 shows the I.R. absorption spectrum of $CsNO_3$ at low temperatures. The low frequency component at 1047 cm^{-1} completely disappeared at a temperature less than -60°C. The intensity of this component increased rapidly on heating while the intensity of the main component decreased until the transition point where the two intensities equalized.

In a previous work by the authors[1] it was assumed that the low frequency component was due to the disordered distribution of the NO_3^- in the lattice. The distinguishable alternate structures that the molecules can take are clusters with argonite or calcite coordination of the anions and cations. These different types of orientation differ by rotation of the NO_3^- ion by an angle of 30° about the axis normal to its plane. To a first degree of approximation, we assume that the intensities of the two components corresponding to ordered and disordered orientations of the nitrate groups are proportional to the populations of these states, which are determined by the difference in the interaction energy U of the nitrate group with the rest of the crystal in the alternative positions.

The temperature dependence of the half-band widths, $\Delta\nu_1$ and $\Delta\nu_1'$, of the main and the low frequency component is shown in Fig. 2. It is here thought that the observed band width is formed of a temperature dependent part characterizing the reorientational process of the NO_3^- between the two alternative positions, and the own band width related to the relaxation process of the intermolecular vibration. It was found that near T_c the broadening of the bands occurred more rapidly than exponentially. It was thus thought that the cooperative phenomena near T_c might be much stronger. Since a general theory for the temperature dependence of the band width in solids is absent, we adopt the theory of rotatory diffusion in liquids.[2] Hence, the average life-time, τ, between two consecutive reorientations is related to the band width $\Delta\nu$ cm^{-1} by the relation: $\Delta\nu = 1/\pi c\tau$, c being the velocity of light. The temperature dependence of the life periods related to the band widths $\Delta\nu_1$ and $\Delta\nu_1'$ of the main and low frequency components are shown in Fig. 3.

The height of the potential barrier, ΔU, which must be crossed during the reorientational process showed a remarkable decrease with temperature (see Fig. 4), indicating that the interaction between the neighboring NO_3^- groups considerably changed as a result of increased reorientations.

We conclude that, beside the ordered positions of the NO_3^- ions in the lattice, there also exist alternative orientations produced by rotation of

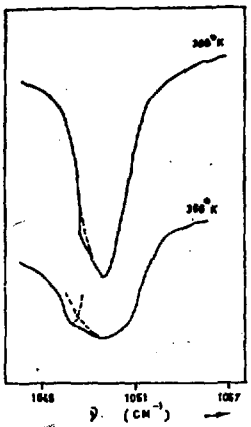

Fig. 1

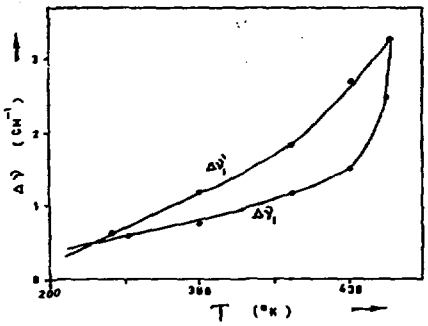

Fig. 2

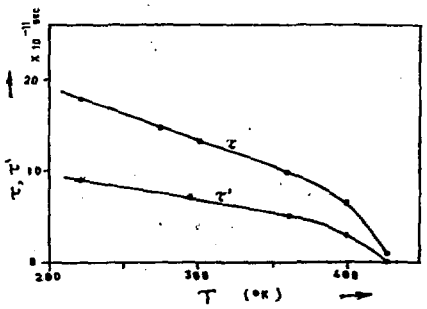

Fig. 3

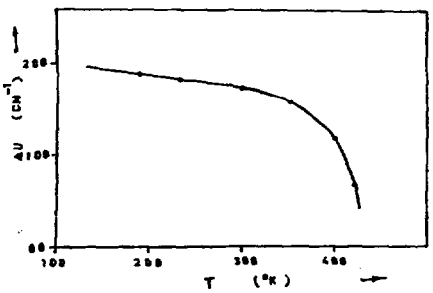

Fig. 4

the NO_3^- groups by an angle 30° around the triagonal axis. These orientations are separated by a potential barrier of about 0.07 eV with an activation energy of about 0.1 eV. Increasing the temperature increases the thermal population of the alternate orientations. The partial disordering near T_c decreases the energy of the alternative orientations leading finally to an equalization with the energy of the main basic orientations at the critical temperature.

1. B. Subrahmanyan and G. J. Janz, J. Chem. Phys. 51, 4084 (1972); Y. A. Badr and R. Kamel, Third Crystallographic Meeting, Zurich, (1976).

2. E. N. da C. Andrade et al, phys. stat. sol. 61, 471 (1974).

ESR STUDY ON PHASE TRANSFORMATION OF LI METALS IN LIF

T. Kamikawa and S. Nagasaka,
Faculty of Science, Yamagata University, Yamagata 990, Japan

It has been confirmed that a heavy neutron irradiation above 10^{19} nvt produces precipitates of Li metals in LiF crystals. We observed ESR absorption due to Li metals in LiF crystals irradiated with neutrons to a dose of 2×10^{19} nvt and annealed at 320 °C. We report here a temperature behavior of this ESR signal above room temperature.

(1) Below melting temperature of Li metals (180 °C) peak to peak width of the ESR absorption derivative decreases monotonically with increasing crystal temperature. At 180 °C it shows a discontinuous decrease. Above 180 °C it increases with increasing temperature at a slower rate than below 180 °C.

(2) Absorption intensity expressed in peak to peak amplitude increases with increasing temperature. At 180 °C it jumps to a somewhat higher value and steadily increases above 180 °C.

(3) At around 180 °C more detailed studyies are performed on temperature variation of width and intensity. The temperatures at which intensity and width of the ESR absorption line change discontinuously, are 181 °C and 176 °C upon warming and cooling, respectively.

Melting point of lithium metal is reported to be 181 °C.[1] A jump in width and intensity upon warming occurs at the temperature, but that upon cooling corresponds to a lower temperature than m.p..

Observed undercooling is a measure of purity or size of lithium precipitates.[2] Study on growth of Li metals in LiF neutron-irradiated and annealed may be possible by the undercooling measurements.

1) T.B.Douglas, L.F.Epstein, J.L.Dever and W.H.Holland, J. Am. Chem. Soc. 77, 2144 (1955).

2) D.Turnbull, Solid State Phys. 3, 225 (1956).

DIRECT OBSERVATION OF THE TRACE OF ULTRASOUND PROPAGATION IN AgCl CRYSTALS BY THE 'PRINT-OUT EFFECT'

Takuji Kaneda*
Solid State Division, Oak Ridge National Laboratory†
Oak Ridge, Tennessee 37830 USA

The effect of ultrasounds on the "print-out effect" in AgCl crystals is studied at room temperature. Figure 1 is a schematic circuit diagram of the equipment used to generate repetitive synchronized pulses of electric field, light and ultrasound. When pulses of the electric field and the light are applied concurrently to the annealed crystals in which longitudinal standing waves exist, darkening is observed. A typical result is shown in Fig. 2. There are three kinds of darkening. One of them is effected by stationary longitudinal ultrasounds. (Others are not effected by ultrasounds). The darkening is composed of many black planes. They are located perpendicularly to the direction of the wave propagation. The interdistance of the black planes roughly equals a half-wavelength of the ultrasound. They are arranged in nodal planes. It is concluded that these planes are the result of a print-out effect due to fresh dislocations moved by the shear stress of the standing waves.

The trace of the ultrasound propagation is directly observed by the darkening, which is the first direct observation of the wave propagation trace in solids. When a quartz transducer of diameter 6 mm is used, it is revealed that 5 MHz longitudinal ultrasounds radially propagate in the [100] direction of AgCl crystals within an angle of about 8° from the normal to the transducer.

---

*On leave from Research Laboratories, Fuji Photo Film Co., Ltd., Asaka, Saitama 351, Japan.

†Operated by Union Carbide Corporation under contract with the ERDA.

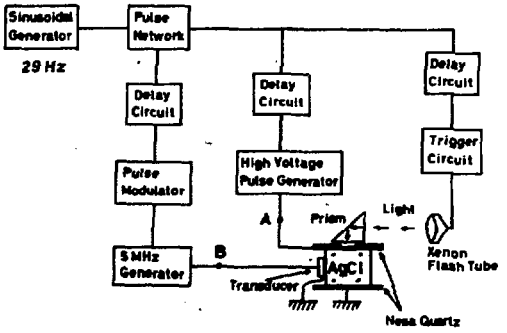

Fig. 1. Schematic diagram of equipment used to generate repetitive synchronized pulses of electric field, light and ultrasound.

Fig. 2. Darkening in an annealed crystal produced by synchronized application of pulses of electric field, light and ultrasound.

LUMINESCENCE FROM KCl:I AT LOW TEMPERATURES

Ken-ichi KAN'NO, Minoru ITOH, Eiji YOSHIKAWA, and Yoshio NAKAI
Department of Physics, Kyoto University, Kyoto 606, Japan

Photo-excitation at LNT in KCl:I has been known to give rise to two well-defined main emission bands; the one at 2.70 eV (Blue Green emission) is attributed to the decay of excitons localized at isolated iodine ions,[1] and the other at 4.65 eV (Ultra Violet emission) is due to the iodine pairs.[2] An additional new emission band was found to appear on the higher energy side of the UV emission by lowering temperature down to 10 K. We believe that this new emission band is due to de-excitation from a higher relaxed state of excitons localized at isolated iodine impurities, i.e. [ICl^- + electron].

I) Figure 1 shows emission spectra (10 K) of KCl crystals doped with iodine ions of 10^{-2} mole fraction under excitation at 6.73 and 7.73 eV. These excitation energies are at the first and the third absorption peaks due to iodine ions in KCl:I.[3, 4] In addition to the BG and UV emissions, a new emission band of a Gaussian shape is observed at 5.76 eV with the half-width of 0.295 eV.

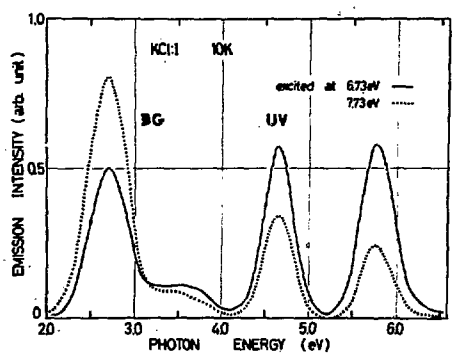

Fig. 1

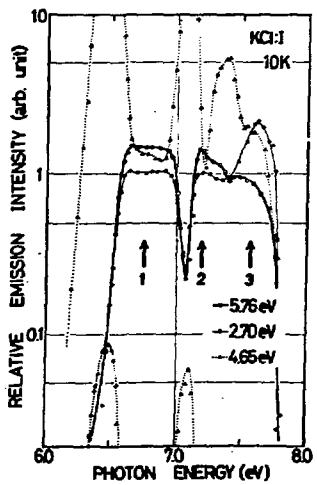

Fig. 2

II) In Fig. 2 are drawn the excitation spectra (10 K) for the new emission (thick curve with open circles) and the BG emission (thin curve with closed circles). That for the UV emission (dotted curve) is also shown for comparison. Positions of three absorption maxima due to isolated I^- ions are indicated by thick arrows. The excitation spectra for the 5.76 eV and 2.70 eV (BG) emissions are similar to each other. In fact, two curves are almost parallel in the region of the 1st and 2nd absorption bands. But in the 3rd peak region (~7.7 eV), where the BG emission is stimulated very well, the intensity of the new emission is somewhat depressed.

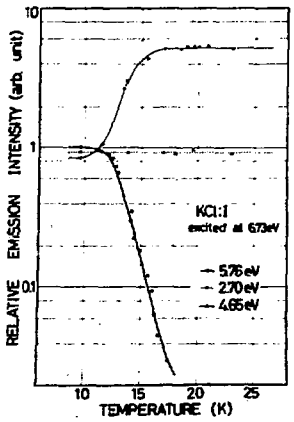

Fig. 3

III) As shown in Fig. 3, the intensity of the 5.76 eV emission decreases abruptly above 12 K with the activation energy of 15 meV, with complementary enhancement of the BG emission, whereas intensity of the UV emission does not change up to 200 K.

IV) Two-photon excitation ($2h\nu$ = 7.35 eV) into the impurity absorption was found to be possible by using an N_2 laser to stimulate the similar emission spectrum. The decay time of the 5.76 eV emission is ~400 ns at 10 K and decreases above 12 K, while that of the BG emission (~200 μs) scarcely changes.

All results mentioned above offer close connection of the new emission band with the BG emission. Investigation of recombination luminescence in colored crystals is under progress with the aim to confirm whether the new emission still occurs together with the BG emission or not.

1) H. Mahr: Phys. Rev. 130 (1963) 2257.
2) K. Toyoda, K. Nakamura and Y. Nakai: J. Phys. Soc. Japan 39 (1975) 994.
3) K. Nakamura, K. Fukuda, R. Kato, A. Matsui and Y. Uchida: J. Phys. Soc. Japan 16 (1961) 1262.
4) N. Nagasawa: J. Phys. Soc. Japan 27 (1969) 1535.

INVITED PAPER

ELECTRON-PHONON INTERACTION IN ALKALI AND SILVER HALIDES

H.Kanzaki

Institute for Solid State Physics
The University of Tokyo, Japan

A basic understanding of the defect-related properties of non-metallic crystals is dependent on knowledge of the electron lattice interaction of the host material. We will describe various aspects of the electron-phonon interaction in alkali and silver halides, with emphasis on the recent developments.

Charge carriers

Two types of carriers exist in ionic crystals: one is nearly free and the other is self-trapped. Transport of free carriers is well described in terms of interaction with longitudinal optical phonons, free polaron state. The self-trapping of charge carriers, on the other hand, is caused essentially due to short-range interaction with acoustic phonons.

In alkali halides, the hole is self-trapped forming the X_2^- molecular ion, with a possible exception of CsF in which FCsF center is observed. In AgCl, the self-trapped hole is of one center type forming Ag^{2+}. In AgBr, the stable hole state is a free polaron, and the anomalous temperature dependence of hole mobility is ascribed to the existence of a metastable self-trapping state above it.

Excitons

Intrinsic luminescence of insulators can be classified into two categories: the radiative decay of free and self-trapped excitons. In alkali halides, the structure of self-trapped exciton (X_2^- + e) has been studied in detail. The exciton self-trapping is entirely determined by the hole self-trapping in this case.

In silver halides, a conversion of the free exciton luminescence in AgBr to the self-trapped exciton luminescence in AgCl has been observed in the mixed crystals $AgBr_{1-x}Cl_x$ and explained in relation to the Urbach-Martienssen rule. Another specific feature in silver halides is an appreciable delayed luminescence due to the distant pair recombination between localized electrons and holes.

Bound polarons

Polaron in a Coulomb potential has been of much theoretical interest for some time. Recent observation of transient absorption spectra of shallow localized electrons revealed new features related to an electron-phonon coupling in the higher excited states, and opened up a new aspect of the bound polaron problems.

In silver halides, the intrinsic shallow electron center is identified as an electron bound at a silver interstitial ion. The one-LO phonon sideband in the absortion spectra exhibits a splitting into three peaks which can be explained in terms of vibronic interaction in the excited state.

In alkali halides, absorption spectra from the RES of F-center also show a similar behavior, indicating a significant coupling of phonons with the HES of F-center.

Formation of lattice defects

The formation of Frenkel defects in alkali halides is now accepted as another decay channel of the electronic excited state interacting strongly with the lattice. In silver halides, behaviors of the intrinsic electron center are entirely different between AgBr and AgCl , and it is suggested that the Frenkel defect pair is produced during band-to-band excitation of AgCl at low temperature.

HYDROGEN IMPURITY MODES IN MONODOMAIN $SrTiO_3$ SINGLE CRYSTALS

S. KAPPHAN and J. KOPPITZ
FB 4, University of Osnabrück
45 Osnabrück, W-Germany

Hydrogen impurities in strontium titanate give rise to an absorption band at about 3500 cm^{-1} associated with an O-H stretching vibration[1]. The temperature dependence of the position of this absorption band shows a splitting into three components at the temperature (T_o about 105 ^oK) of the structural phase transition from cubic to tetragonal symmetry[2]. High resolution measurements (res. < 0.2 cm^{-1}) performed with a Fourier IR-spectrometer (Bruker IFS 113 CV) reveal the existence of several sidebands with analogous splitting pattern (Fig. 1). The concentration dependence of these absorption bands, their structure and band shape under the influence of electric field and uniaxial stress have been studied in detail.

For the first time, a strong polarization dependence of the absorption bands in the tetragonal low temperature phase could be observed (Fig. 2) under [110] stress. The [110] stress applied here is well below the critical one where other phase transitions in $SrTiO_3$ may occur, and is of a magnitude known[3] to render the crystals essentially monodomain with the c-axis in the [001] direction. The main absorption band at 3515 cm^{-1} (for $T \approx 77$ ^oK) and the sidebands at 3523 cm^{-1} and 3537 cm^{-1} vanish for light polarized perpendicular to the applied [110] stress and therefore have to be assigned to vibrational modes in the a-b plane of the crystal. Thus the polarization of the modes and their behavior under the influence of electric field and uniaxial stress yield detailed information on a microscopic scale about the energetically different positions of the hydrogen impurity in the tetragonal perovskite structure of $SrTiO_3$.

References:

(1) F.G. Wakim, J. Chem. Phys., 49, 3738 (1968)

(2) A.F. Klukhuhn, J. Bruining, B. Klootwijk and J. van der Elsken, Phys. Rev. Lett. 25, 380 (1970)

(3) K.A. Müller, W. Berlinger, M. Capizzi and H. Gränicher, Sol. State Comm. 8, 549 (1970)

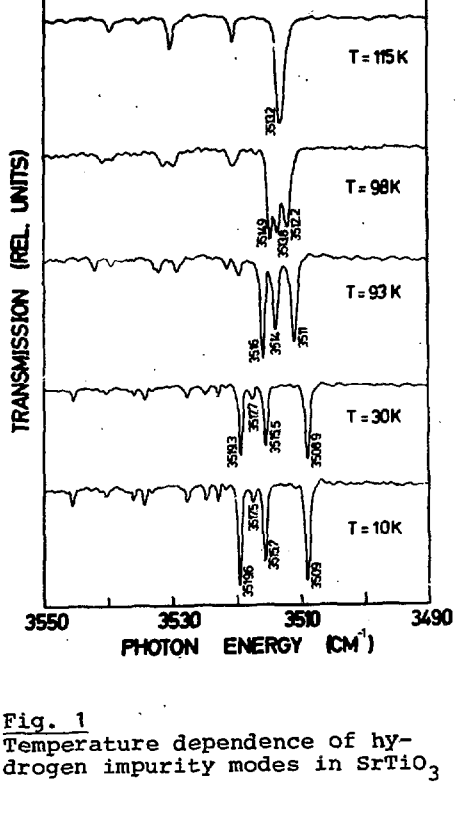

Fig. 1
Temperature dependence of hydrogen impurity modes in $SrTiO_3$

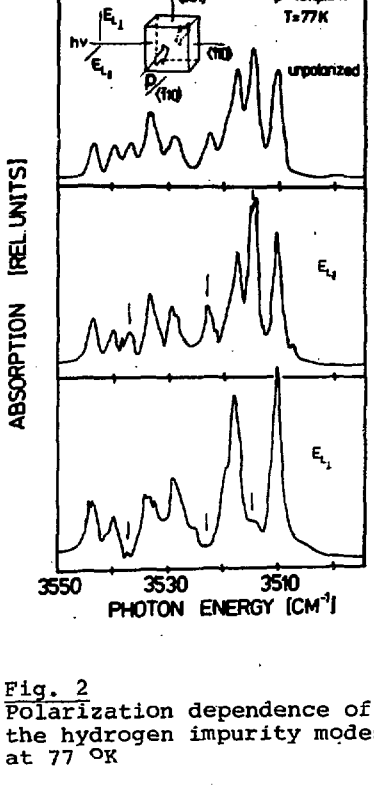

Fig. 2
Polarization dependence of the hydrogen impurity modes at 77 °K

VUV- AND NIR-ABSORPTION OF OH^--IMPURITIES IN ALKALI FLUORIDES

S. KAPPHAN and J. KOPPITZ
FB 4, University of Osnabrück
45 Osnabrück, W-Germany

In the alkali fluoride crystals, substitutional OH^--impurities replace a F^--ion of somewhat smaller ionic radius. We report here measurements to check whether OH^--centers (produced by doping in the melt) in these crystals can be oriented by an electric field at low temperatures, similar to the well known paraelectric behavior in other alkali halide host materials[1]. We measured the optical absorption properties of OH^--centers in LiF, NaF and CsF in the electronic transitions in the vacuum ultraviolett (in NaF and CsF) and in the O-H stretching vibration bands at about 2.7μ. The spectral band shape and the temperature dependence of the integral absorption show a marked difference in comparison to OH^--centers in KCl and KBr for instance. A sideband structure in the electronic transitions similar to the one in NaF : OH^- (Fig. 1) had been previously observed only in CsBr : OH [1].

No electro-optical effects due to reorientation under high electric fields ($> 10^5$ V/cm) in $\langle 100 \rangle$ and $\langle 111 \rangle$ directions could be observed at 1.6 °K (with the samples immersed in suprafluid helium), neither in the VUV-bands nor in the NIR-absorption bands of OH^--centers in the above fluorides.

Thus our experimental results do not agree with the tunneling reorientation behavior deduced previously by Guckelsberger et.al.[2] from thermal conductivity measurement on LiF crystals, which had been heated in water vapour to produce (presumably) OH^--centers. Our measurements rather, indicate that a reorientation of the OH^--centers in alkali fluorides under applied electric fields at 1.6 °K is not possible.

References:

(1) S. Kapphan and F. Lüty,
J. Phys. Chem. Solids, 34, 969 (1973)

(2) K Guckelsberger, K. Neumaier and H.R. Zelsmann,
Phys. Lett., 31A, 397 (1970)

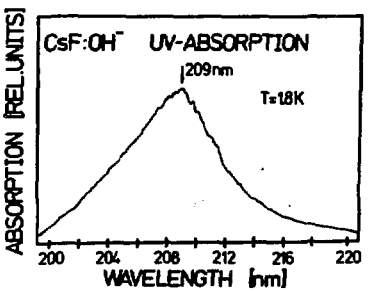

Fig.1 UV absorption spectrum of OH^-centers in CsF

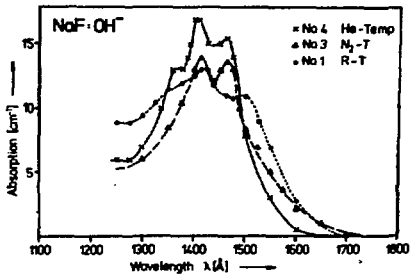

Fig. 2 UV absorption spectrum of OH^-centers in NaF

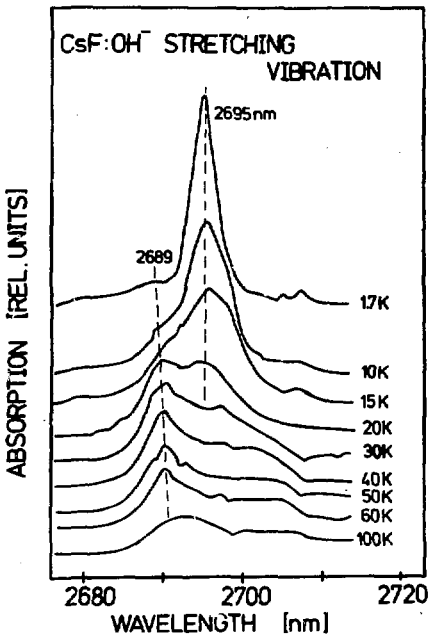

Fig. 3 Stretching vibration of OH^-centers in CsF

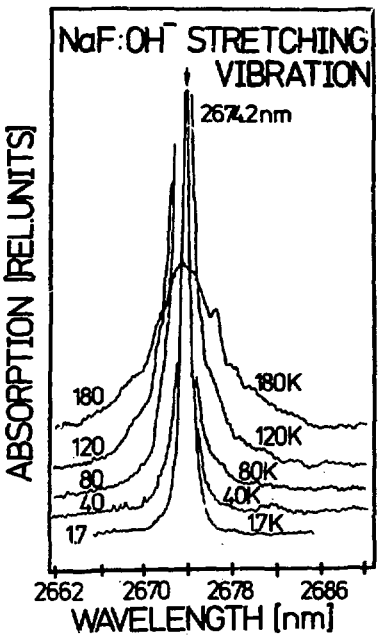

Fig. 4 Stretching vibration of OH^-centers in NaF

ESR OF OFF CENTERED Eu^{2+} IN KCl:Eu CRYSTALS

K.KAWANO, R.NAKATA, M.SUMITA, E.HIGUCHI

UNIVERSITY OF ELECTRO-COMMUNICATIONS
CHOFUSHI, TOKYO, JAPAN

Recently, there was reported an ESR study of Eu^{2+}-vacancy complexes, whose Eu^{2+} ion shifted along the [111] directions by a small amount from its normal lattice sites in host RbCl crystals. A brief comment was given there on the off-centered Eu^{2+} ions in KCl crystals.[1] In this report, there are shown detaied results of them and also presented some other features related to their origin.

Fig.1 shows a part of typical x-band spectra of the off-centered Eu^{2+}-vacancy pairs. Those spectra have characteristic features different from those for ordinary Eu^{2+}-vacancy pairs as follows: (1) Each fine structure is composed with three groups of hfs lines, whose intensity ratio is approximately 1 :2:1. (2) For the static magnetic field directing toward the [100] direction, those groups of hfs lines are coincident each other at the lower magnetic field, as in the case of ordinary Eu^{2+}-vacancy pairs, while they are split at the higher magnetic field. Those spectra can be described by using the following spin Hamiltonian as;

$$\mathcal{H}=g\beta HS+AIS+\Sigma B_n^m O_n^m+[u\beta[S_x^3H_x+S_y^3H_y+S_z^3H_z-\frac{1}{5}SH(3S(S+1)-1)]+U[S_x^3I_x+S_y^3I_y+S_z^3I_z-\frac{1}{5}SI(3S(S+1)-1)]]$$

, where the first three terms represent Zeeman, hf interaction and crystalline field terms, respectively, while the last term is introduced to account for the splitting at the higher magnetic field. Table 1 gives Hamiltonian parameters obtained by computer-simulating the angular dependence of fs spectra. The simulated curves fit within an accuracy of 10 gauss even at the higher magnetic field with the experimental results.

The origin of those spectra is attributed to the shift of

the Eu^{2+} ion from the normal lattice site substituted for K^+ ions to an off-centered site along the [111] direction. The typical result, as shown in Fig.1, suggests the shift by an amount of 0.07a, which is maximum in our measurements. The shift is stable around the room temperature, but its amount depends upon the concentration of Eu^{2+} ions. It is negligible at the lower concentration than 0.01 mole %, and it increases with concentrations to the maximum as stated above at abou 0.05 mole % and decreases again at the higher concentration. Similar effects are observed in RbCl:Eu crystals. Such a fact suggests presence of forces acting on Eu^{2+}-vacancy pairs such as interaction between the pairs, or between pairs and isolated Eu^{2+} ions, to establish the stabilized off-centered Eu^{2+} ions.

References: (1)K.Kawano et al.:J.Phys.Soc.Japan 41(1976)72

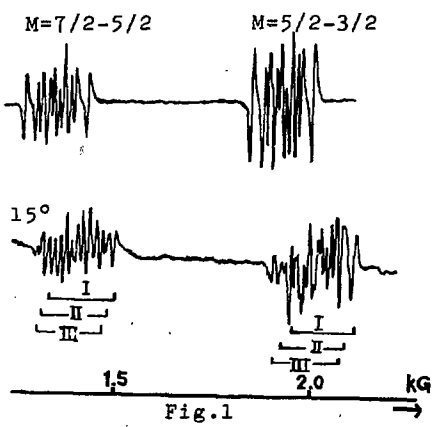

Fig.1

(angles from the [100] direction in the (100) plane)

	g	1.9944 ± 0.0003	
	b_2^0	346.6 ± 2.0	
	b_2^2	91.4 ± 4.0	
b_4^0	-5.0 ± 0.2	b_6^0	0.0
b_4^2	9.4	b_6^4	4.6
b_4^4	28.0	$b_6^2+b_6^6$	7.0
	A^{151}	-31.3 ± 0.2	
	A^{153}	-14.0 ± 0.2	

	I	II	III
u	-0.2	+0.2	+0.5
U	--	--	-0.05

Table 1

(in $10^{-4}cm^{-1}$, besides g factor)

AN APPROACH TO THE PROBLEM OF BOUND POLARON

Y.Kayanuma and Y.Kondo

Institute for Solid State Physics
University of Tokyo, Japan

Recent advances of experimental techniques have revealed interesting features of excited states of bound polaron.[1] The attention of the theoretical studies, however, has been focused on the ground state in most cases, and general ways of analyzing the properties of the excited states are practically not yet known.

Putting stress on the spherical symmetry of the system, we developed a new apprach to such a problem. We start from the general expression of the Hamiltonian for bound polaron, that is, an electron bound in a spherically symmetric potential and interacting with dipersionless LO phonons through Fröhlich interaction H_I. Expanding H_I by the eigenfunctions $\psi_{n,l,m}$ of the electron Hamiltonian, where n, l and m are the principal, azimuthal and magnetic quantum numbers, respectively, and paying attention on the symmetry properties, we can rewrite H_I as

$$H_I = \sum_{n,n'} \sum_{l,l'} \sum_{J} \gamma_J(nl,n'l') \sum_{M} (-1)^M \rho_{J,M}^{(nl,n'l')} \{ b_{J,-M}^{(nl,n'l')\dagger} + (-1)^M b_{J,M}^{(nl,n'l')} \}.$$

We have defined operators and coupling constants for the electron and phonons as

$$\rho_{J,M}^{(nl,n'l')} = \sum_{m,m'} (l,m;l',m'|J,M)(-1)^{m'} a^{\dagger}_{n,l,m} a_{n',l',-m'},$$

$$\gamma_{J,M}(nl,n'l') b_{J,M}^{(nl,n'l')} = \sum_{m,m'} \sum_{k} (-1)^{m'} (l,m;l',m'|J,M) \times \{ \int \psi^*_{n,l,m}(r) V_k(r) \psi_{n',l',-m'}(r) d^3r \} b_k,$$

where a and $a^{\dagger}$ are creation and annihilation operators for the electron, b_k is the annihilation operator for the phonon of wave vector k and $V_k(r)$ is the Fröhlich coupling coefficient.

The operator $b_{J,M}^{(nl,n'l')}$ thus introduced represents the phonon mode of angular momentum (J,M) connecting (n,l) and (n',l') electronic states with the coupling constant $\gamma_J(nl,n'l')$, which is, on the other hand, determined from the normalization condition for $b_{J,M}^{(nl,n'l')}$. This is a generalization of the concept of the interaction modes[2] which enables us to select minimum number of modes relevant for the interaction out of tremendous number of degrees of freedom. Note that there appear only those modes that satisfy the conditions, $|l-l'| \leq J \leq |l+l'|$ and $l+l'+J$ = even.

Approximating the electron wave functions by hydrogenic ones, we applied our formula to the analysis of HES of F-center and investigated the features of vibronic interactions in detail. For example, the values of the coupling constants for typical modes relevant for HES are given in dimensionless form as $\gamma_1(3s,3p)^2 = 0.00705\times S$, $\gamma_2(3p,3p)^2 = 0.00432\times S$, ..., where S is given in terms of static and optical dielectric constants ε_s, ε_∞, the Bohr radius a, the charge of the electron e and the energy of LO phonon $\hbar\omega$ as

$$S = (1/\varepsilon_\infty - 1/\varepsilon_s)e^2/a\hbar\omega,$$

and is estimated to be 10~20 for F-center in alkali halides. Generally speaking, $\gamma_J(nl,n'l')$ becomes smaller as n or n' (or both) becomes larger, and detailed investigation showes that we can reasonably confine ourselves to the subspace n = 3 in analyzing HES of the group of KCl as a first approximation.

References

1) For example, Y.Kondo and H.Kanzaki, Phys.Rev.Letters 34 (1975) 664.
2) Y.Toyozawa and M.Inoue, J.Phys.Soc.Japan 21 (1966) 1663.

SURFACE CONDUCTANCE OF NH_4CL CAUSED BY AN AMMONIUM ATMOSPHERE

A. Kessler and E. Betz

2. Institute of Physics, University Stuttgart, W.Germany

Several attempts have been made in the past to supply experimental evidence for the theoretically expected enhanced mobility of lattice defects on crystal surfaces. The experiments concerned with ionic crystals were based for the most part on an investigation of samples consisting of microcrystalites[1]. By changing e.g. the size of the crystalites a variation of the area, on which surface conduction is assumed to take place, can be realized. The experiments have shown in fact, that the transport of ions and of charge carriers respectively is enhanced if the surface area is "increased".

An alternative experimental approach, which is expected to provide a reasonable assesment of the mobility, has become feasible of late, by the discovery that under the influence of a NH_3-atmosphere defects are formed on the surface of NH_4Cl[2]. Experiments conceived on this phenomenon have yielded a measurable effect , as ilustrated e.g. in Fig.1. The built-up of a NH_3-pressure is accompanied by an increase of the current caused by a constant voltage drop on the sample. Because the arrangement of sample and electrodes secured an acces of NH_3 exclusively to the sample surfaces parallel to the electric field the measured current increase ΔI is, no doubt, caused by the formation and transport of charge carriers on the crystal surface in question.

ΔI is made up of a nearly instantaneous and of a delayed component. In consequence ΔI depends as well on the time as on the "history" of the exposure to NH_3. The instantaneous component is connected with the formation of an equilibrium concentration of defects on the surface, the delayed component with a penetration of defects into the bulk of the sample. If a crystal is

exposed long enough to a given NH_3-pressure an overall saturation is reached[2]. The magnitude of ΔI depends further on the NH_3-pressure p and on the temperature T. In a narrow temperature range ΔI is strictly proportional to p and to an exponential of -1/T. At higher temperatures it falls increasingly behind this. There are reasons to assume, that this is caused by the decrease of the NH_3adsorption with an increasing T. At lower temperatures there is a minimum of ΔI, followed by a steep increasse with a still further decreasing T. It is believed that this increase indicates the formation of a continuous layer of NH_3 with a different type of conduction.

If the specific surface conductivity is calculated from the obtained data of ΔI and compared with the specific bulk-conductivity of samples saturated at the same pressure one gets e.g.for 25 C and 100 torr for the former $2.5 \times 10^{-11} \Omega^{-1}$, for the latter $1.2 \times 10^{-9} \Omega^{-1} cm^{-1}$. Even if it is assumed that the "surface conductance" is not realized literally on the surface but in a surface layer, it still cannot be explained merely by the increase of the number of defects. One arrives in consequence at the conclusion that the mobility on the surface is enhanced by several orders of magnitude.

1. J.F.Laurent, J.Bénard, C.R.Acad.Sci.Paris,241,1204 (1955); J.Shapiro, I.M.Kolthoff, J.Chem.Phys., 15, 41 (1947).
2. P.Berteit, A.Kessler, T.List, Z.Phys.B 24, 15 (1976)

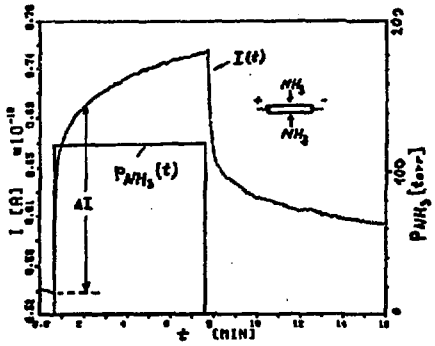

Fig.1.Current versus time plot at a constant voltage drop of a NH_4Cl sample exposed 7.5 minutes to 120 torr of NH_3.

IONIC TRANSPORT IN Na BETA-ALUMINA SINGLE CRYSTALS*

K. K. Kim, J. N. Mundy, and W. K. Chen
Materials Science Division, Argonne National Laboratory, Argonne, Il. 60439

Accurate methods for measuring conductivity and diffusivity in well characterized Na beta-alumina single crystals have been developed. The experimental techniques have been applied to the study of the ionic transport mechanism in this highly defective material. The ionic conductivity measurements have been made with a two-probe method using molten sodium electrodes. The electrode area was precisely defined by locating a rectangular parallelepiped sample between two sodium reservoirs in a tunnel made up of a stack of alpha-alumina masks with rectangular bore. The d.c. conductivity was the same as the a.c. conductivity (1-20 kHz), within the accuracy of the bridge used, in the temperature region 150-450°C. The measured values of conductivity, with reproducibility of better than $\pm$ 1% and data scatter of less than $\pm$ 1%, follow an Arrhenius relation $\sigma T = C \exp(-E/kT)$ with $C = (2370 \pm 20)\ \Omega^{-1}cm^{-1}\ K$ and $E = (3.28 \pm 0.01)$ kcal mol^{-1}. The measured conductivity tends to decrease with decrease in cross-sectional area as shown in Fig. 1. The values of activation energy for large crystals converge to (3.28 ± 0.01) kcal mol^{-1}, while that for small samples appears to be higher. Samples taken from the end of a boule, in which solidification occurred last during crystal growth, appear to show a two stage conductivity plot, exhibiting a lower activation energy below 300°C, in a manner similar to that reported by Allen et al.[1]

Diffusivity was measured by cation exchange in a molten salt bath and by a nondestructive method based on positron annihilation techniques.[2] Our results will be compared with predictions derived from various theoretical models. Transport mechanisms compatible with our results and with currently available information on defect structure will be discussed.

*Work supported by the U.S. Energy Research and Development Administration.

1 S. J. Allen, Jr., A. S. Cooper, F. DeRosa, J. P. Remeika, and S. K. Ulasi, Bull. Am. Phys. Soc. 22 (3), 370 (1977).

2 K. K. Kim, J. N. Mundy, and S. M. Puri, to be published in Rev. Sci. Inst.

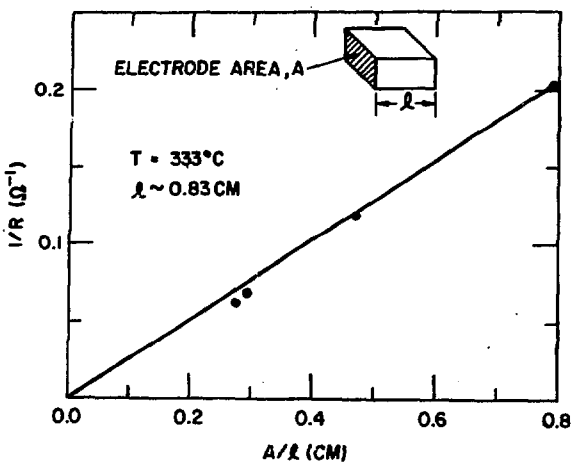

Fig. 1. Plot of conductance vs. sample cross-sectional area

EFFECT OF Fe IONS ON THE EARLY STAGE COLORATION OF MgF_2*

K.K. Kim+ and A.S. Nowick
Henry Krumb School of Mines, Columbia University, New York, NY 10027

and

R.S. Title
IBM Research Center, Yorktown Heights, NY 10598

A comparative study of the early stage F-band growth following γ-ray irradiation and subsequent bleaching has been made for MgF_2 single crystals that contain varying amounts of Fe^{2+} (0 - 110 ppma) and/or Li^+ (0 - 115 ppma) impurity ions, as well as high purity material. Irradiation was carried out with ^{60}Co at a dose rate of 1.5×10^6 R/h. The only appreciable absorption band observed was the F-center band at 257 nm.[1]

It was found that the early stage F-center production is enhanced predominantly and systematically by the presence of Fe^{2+}, becoming saturated after 1 h of irradiation (Fig. 1). The following features due to Fe ions are observed: (1) The early stage growth curves obey the saturating exponential $\alpha(t) = A[1 - \exp(-ft)]$, where $\alpha(t)$ is the absorption coefficient, t is the time, A is the saturation level, and f is the rate constant. (2) The initial slope, C, is independent of [Fe], and thus $A = C/f$. (3) The quantity A depends on the Fe concentration [Fe] as $A = C/\{D + E/[Fe]\}$, where D and E are constants. The F-band growth curves for crystals that contain only Li^+ impurity exhibit no saturation in the dose range investigated (10 h irradiation). The difference in the roles played by the Li^+ and Fe^{2+} ions is also demonstrated in isochronal annealing, as shown in Fig. 2. Samples that contain appreciable Fe show a distinct annealing stage near 100°C, whereas samples that contain Li ions bleach continuously over the temperature range 100-350°C. ESR studies reveal that iron is present in the Fe^{3+} state only after irradiation. Isochronal annealing shows that the Fe^{3+} ESR signal strength first increases between 20° and 100°C, and then sharply decreases before 150°C. An appreciable Fe^{3+} concentration remains, however.

The striking enhancement of the early stage of coloration by the presence of Fe is ascribed to a process in which Fe^{2+} ions capture holes, thus enabling precursor vacancies to capture electrons and become F-centers. On the other hand, Li ions are believed to contribute to F-center production only via a radiolysis process.

*This work was supported in part by the National Science Foundation under grants GH-34269 and DMR 75-09603.
+Present address: Materials Science Division, Argonne National Laboratory, Argonne, Illinois 60439.

REFERENCES

[1]W.A. Sibley and O.E. Facey, Phys. Rev. 174 (1968) 1076.

Table 1. Fe and Li content (ppma)

Sample	Fe	Li
J2T	112	18
J2B	45	<9
J3T	34	45
J3B	11	<9
J3M	9	9
J1T, J1B	6	ND*
H1	<1	ND
H1, Li-diffused	<1	115

*ND ≡ None Detected

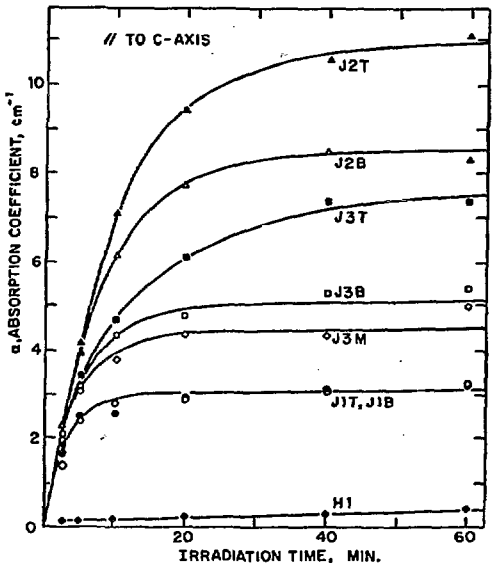

Fig. 1 F-band height vs. irradiation time. Samples are identified in Table 1.

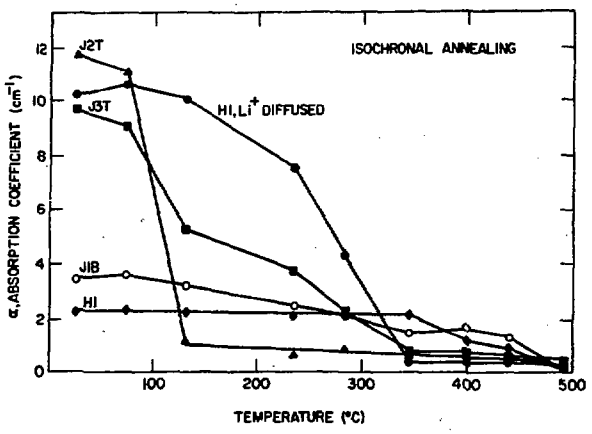

Fig. 2 Bleaching of F-centers in isochronal annealing. Heating time was 20 min.

INVITED PAPER

SEGREGATION PHENOMENA IN MAGNESIUM OXIDE

W. D. Kingery

Ceramics Division, Department of Materials Science & Engineering
Massachusetts Institute of Technology, Cambridge, Massachusetts 02139

In recent work done with Christian Bertholet, Anders Henriksen, Joe Driear, John Black and other students we have investigated segregation phenomena adjacent to surfaces and grain boundaries in magnesium oxide.

One process leading to segregation is the easy nucleation of a second phase at a surface or boundary without the limitations of strain energy restraints. In studies of magnesium oxide containing 90ppm Al_2O_3 we have found that there is a very great difference between quenched and slowly-cooled samples. In slowly-cooled samples there is a wide segregation region, a micron or more, adjacent to surfaces of boundaries resulting from easy nucleation and resulting precipitation of spinel, $MgAl_2O_4$. This is probably the most common cause of "segregation" which has been reported in the literature. Recent studies of phase equilibria data for SiO_2 and ZrO_2 in MgO indicate that their solubility is very small; precipitation phenomena are to be expected.

Samples were also studied by heating in a transmission electron microscope. Under these conditions surface precipitation was observed at a temperature of about 750°C. That is, when a sample of initially uniform composition is heated to this temperature range, segregation phenomena begin to occur. Clearly the heat treatment and its influence on defect distribution and structure are an essential specification for any experimental work in this area.

A second factor leading to segregation at a boundary is the strain energy associated with solid solution.

A third sort of segregation has been more difficult to measure and calculate, in part because it depends on the total defect population. If we consider a solution of iron in a magnesium oxide single crystal, for example, many different defects may be present. We have developed an iterative computer program to calculate defect equilibria and defect

concentrations from a series of non-linear equations in which the equilibrium constant for each process is considered, along with the overall charge balance, cation and anion site balance, and overall solute mass balance. Some defects increase in concentration while others decrease as the temperature level is changed.

One of the consequences of charged defects is the development of a boundary charge which depends on the ease of formation of vacancies and also on the concentration of defects in extrinsic crystals. We can consider for the boundary generation process the following equations:

$$Mg_{Mg} = Mg^{\bullet\bullet}_{Boundary} + V''_{Mg}$$

$$O_o = O''_{Boundary} + V^{\bullet\bullet}_{o}$$

clearly, if the cation vacancy concentration is increased, the magnesium concentration on the boundary is decreased at equilibrium and a negative boundary charge should result.

Studies of the segregation of iron in MgO to the surface region have been carried out in both reducing and oxidizing atmospheres using an ion mass spectrometer to determine the concentration profile near the surface. In the reduced state no segregation is observed. In contrast, ferric iron shows a significant segregation in an area about 200-300 Å thick adjacent to the surface. This segregation corresponds to the space cloud balancing the surface charge. The interpretation of this segregation and its influence on properties will be discussed.

RADIATION-INDUCED CONDUCTIVITY OF Al_2O_3: THEORY AND EXPERIMENT*

R. W. Klaffky, B. H. Rose and G. J. Dienes
Brookhaven National Laboratory
Upton, New York 11973

The defect properties of Al_2O_3 have received a great deal of attention recently because of its potential as laser or solar cell windows and as an electrical insulator for components of MFE devices. In the latter application the insulating properties of Al_2O_3 in the presence of ionizing radiation are of interest because a background dose rate up to 10^4 rad/sec has been estimated to result from the neutron activation of reactor structural materials. The effect of this ionizing radiation is to generate electron-hole pairs within Al_2O_3 leading to a radiation-induced electrical conductivity. We performed steady-state a.c. electrical conductivity measurements on single-crystal Al_2O_3 samples during continuous irradiation with 1.5 MeV electrons at dose rates up to 2×10^5 rad/sec. The radiation-induced conductivity is extremely sensitive to carrier trapping by impurities and defects as is apparent from a comparison of the conductivities of undoped Linde and Meller samples, Linde samples doped with 0.004, 0.028 and 0.0[illegible] wt. % Cr_2O_3, and undoped Linde samples exposed to a fluence of 4.7×10^{16} n/cm^2 of 14-MeV neutrons at the LLL Rotating Target Neutron Source and to fluences of 1×10^{17} n/cm^2 to 3×10^{20} n/cm^2 at the BNL High Flux Beam Reactor.

A theoretical model has been developed which describes the observed dose-rate and temperature dependence of the radiation-induced conductivity. The model assumes that electrons are the dominant charge carriers and attributes the increases in the radiation-induced conductivity as the temperature varies from 20°C to 1000°C to the thermal release of electrons from a shallow and a deep electron trap. Decreases in the conductivity are attributed to the thermal release of trapped holes and the subsequent recombination of these holes with electrons at the shallow electron traps.

In the case of undoped Linde and Meller samples, where the shallow trap concentration is high compared to that of the deep trap, the conductivity increases near room temperature as the shallow electron traps empty and then decreases as holes are released at higher temperatures. Finally, at high temperature, the deep electron trap empties causing the conductivity to increase again. In the doped and heavily neutron-irradiated samples (annealed at 1100°C for one hour before measurement) the concentration of deep electron traps is much larger than that of the shallow traps. The low temperature induced conductivity is thereby greatly suppressed by trapping. The conductivity decreases with increasing temperature until the temperature is reached where the electrons released from these deep traps lead to a final increase in the conductivity.

The results of EPR and TSC measurements will be discussed with reference to the identity and concentration of the major electron and hole traps.

*Research supported by the U.S. Energy Research Development Administration.

RES ABSORPTION SPECTRA OF F CENTER IN ALKALI HALIDES

Y.Kondo, Y.Kayanuma and H.Kanzaki

The Institute for Solid State Physics
University of Tokyo, Japan

Electrons in RES and HES (higher excited state) of F center have small binding energies in contrast with its ground state. These shallow electron systems, RES and HES, are very interesting in view of that they correspond to an intermediate case between bound electron and bound polaron systems.

Infrared absorption spectra due to the transition from RES to HES of F center (F^* absorption spectra) in K-halides were first reported by us[1]. Recently, we have extended the similar experiment to other alkali halides. Moreover, we successfully analyzed the observed spectral feature using the vibronic Hamiltonian developed by Kayanuma.

Figure 1 shows the F^* absorption spectra in RbCl and NaCl. The features in RbCl are very similar to those in K-halides, but show striking contrast with those in NaCl as shown in Fig.1. On the other hand, both spectra show common features that a sharp peak appear at E_o below thermal ionization energy ΔE_T,

Fig. 1.

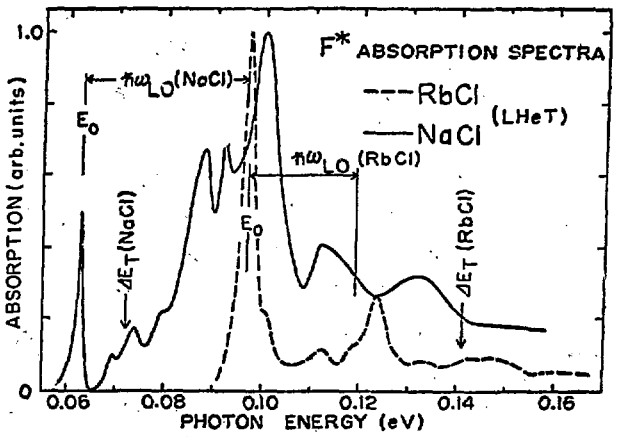

and three peaks appear at about $\hbar\omega_{LO}$ higher than the E_o peak.

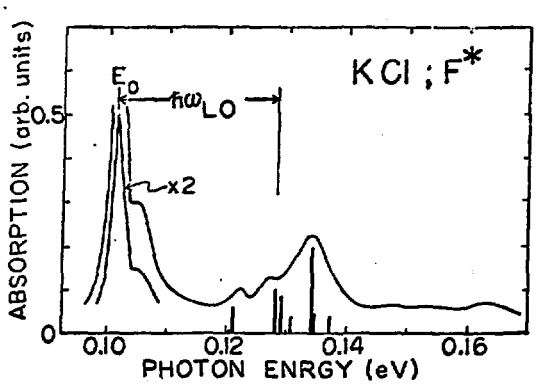

Fig. 2.

Since RES is totally S-like and is an admixture of 2s and 2p states interacting with each other via P-like phonon[2,3], HES responsible for F^* absorption spectra must be totally P-like and will be composed of 3s, 3p and 3d states interacting weakly with each other via S, P, D, F and G-like phonon modes. Using hydrogenic wave functions and Fröhlich Hamiltonian, and considering only nearly degenerate 3s, 3p and 3d states (up to two phonon states), the relative energies and absorption intensities were calculated. In Fig.2, calculated energies and intensities of absorption bands normalized with the lowest peak at E_o are indicated by vertical lines for KCl as an example. They agree well with those of observed spectrum. Thus the E_o peak and the three peaks can be assigned as the transitions from RES to 3p and one-phonon states, respectively, perturbed through vibronic interaction. It should be noted that our model can account for both RES properties[3] and F^* absorption spectra.

In NaCl, the intensity of E_o band is considerably weaker than one-phonon bands. This may be partly due to the strong mixing of 2s and 2p states in RES and partly correlated to the fact that binding energy of HES is smaller than $\hbar\omega_{LO}$.

1) Y.Kondo and H.Kanzaki, Phys.Rev.Letters 34 (1975) 664.
2) F.S.Ham and U.Grevsmühl, Phys.Rev. B8 (1973) 2945.
3) Y.Kayanuma and Y.Toyozawa, J.Phys.Soc.Japan 40 (1976) 355; Y.Kayanuma, J.Phys.Soc.Japan, 40 (1976) 363.

UV RADIATION INDUCED ABSORPTION IN LITHIUM FLUORIDE

H.-J. Kos and R. Nink
Physikalisch-Technische Bundesanstalt, Institut Berlin
Abbestraße 2-12, 1000 Berlin 10

UV radiation in the F band region reduces the thermoluminescence (TL) of LiF if it acts on the irradiated crystal before TL read out. However, if the crystal is exposed to F radiation after the first read out, TL can be observed a second time. This phenomenon called "UV induced" TL is very important from the dosimetric point of view because there is the possibility to determine a dose twice after one exposure to ionizing radiation. Both bleaching effects are well known in literature but the physical mechanism is not yet clear. For this we have studied the effect of F band radiation on the optical absorption of non-thermoluminescent LiF doped with Mg and of thermoluminescent LiF doped with Mg and Ti either directly after exposure to X-rays or after exposure and subsequent thermal annealing. All absorption curves underwent a computer analysis in order to get datas about the amount of concentration of the different absorption centers. The results of the analysis show that in LiF : Mg and LiF : Mg, Ti without additional thermal annealing Z_1 centers are formed which do not give rise to TL. The energetic position of the Z_1 center absorption band is E = 4.5 eV, the halfwidth Δ E = 0.72 eV. With additional thermal annealing in LiF : Mg, Ti there is not only the formation of Z_1 centers but also the formation of centers creating the Z_2 band and the 3.3 eV band. The formation of Z_2 centers is believed to be due to a conversion of F centers into Z_2 centers as it is known in other alkali halides. A qualitative comparison of the absorption results with F band radiation induced TL shows that the Z_2 and 3.3 eV induced absorption bands are responsible for the restored TL.

TWO MODELS FOR EVALUTION OF TEMPERATURE DEPENDENCE OF F CENTRE ACCUMULATION EFFICIENCY IN DOPED ALKALI HALIDES.

E.KOTOMIN[+], I.TĀLE[+] and I.FABRIKANT[++]

[+]Latvian State Universuty, Rainis 19, Rīga, USSR

[++]The Institute of Physics, Salaspils, USSR

It has been observed [1] that if temperature rises between liquid nitrogen temperature (LNT) and room temperature (RT), the F centre accumulation efficiency (FCAE) in doped alkali halides increases several times. The fate of the Frenkel (genetic) pairs- F and H centres -is believed to affect the FCAE. The above-mentioned temperature dependence, being due to the probability for a diffusing H centre to leave its genetic F centre, cannot be caused by instant annihilation (occuring with $\tau \leq 10^{-13}$s.) but must be attributable to some inertial (as compared to the diffusion time) recombination mechanism.

Two such mechanisms, well-established in alkali halides, are (i) a tunneling recombination (TR) of spatially separated electron-hole defect pairs, (ii) annihilation stimulated by elastic interaction of defects via a lattice deformation. The later interaction holds if a crystal and/or one of defects are anisotropic. This interaction is attractive in certain directions and repulsive in others. However, on the average, it stimulates annihilation because a mobile defect avoids the repulsive part of the potential.

We have considered two models for the diffusion-controlled FCAE in doped alkali halides [2]. It is assumed that (i) an genetic pairs occur in the primary process and are described by the initial distribution function $\varphi(r,T)$. In the course of secondary reactions mobile centres (ii) interact with their F centres in accordance with the above-mentioned mechanisms or (iii) are trapped by pre-existing defects. Defects do not affect the F-H correlated annealing but prevent blurring

of different genetic pairs (with is the case for early stages of F centre accumulation).

The model based on TR indicates an increase of the FCAE starting from LNT with further saturation below RT (e.g.220 K in KBr). If $\varphi(r,T)$ decreases exponentially with r, the FCAE is aptly described by the Arrhenius relation with the effective energy $E^{*}=E_a r_0/r'$, where E_a is the diffusion activation energy of an H centre, r' half the average distance within a Frenkel pair and r_0 half the Bohr radius of F centre. In this model the different values of E^{*}, observed for KCl and KBr having close E_a values, are due to the difference in r_0/r'. If $\varphi \propto \delta(r-\ell)$, E^{*} slowly decreases, being of the order of $E_a/4$. The theoretically predicted decrease of primary seperation ℓ with the temperature does not appreciably affect this result, i.e. the secondary reactions are desisive for the temperature dependence in question. This model provides E^{*} estimates close to steady-state experiment, but cannot explain the pulse data because TR occurs with times exceeding 10^{-7} s.

The analysis of the second model, presented first by Sonder [1], shows that for $\varphi \propto \delta(r-\ell)$ the FCAE also increases above LNT and the Arrhenius relation holds for $E^{*}=\eta A/\ell^{3}$, where A is the interaction strength, η depends on the angular behaviour of the elastic potential. One estimates the $E^{*} \simeq 0{,}04$ eV in KBr with is close to the experiment only for the nearest F-H pairs. This model- contrary to the TR one -predicts a rapid E^{*} decrease with ℓ and its independence on E_a. Unfortunately, the choise between the two models as well as the E^{*} interpretation, are complicated by the unknown initial spatial distribution, within a genetic pair and a rather approximate estimate of the elastic interaction energy.

REFERENCES

1 . Sonder E., J.Physique, 1973, 34 C-9, 483-7; Phys.Rev., 1975, B12, 1516-25.

2 . Kotomin E., Fabrikant I., Tāle I., J.Phys.C: Solid State Phys., 1977, 10 (in press).

F-CENTER FORMATION IN ION BOMBARDED MgO*

G. B. Krefft and K. L. Brower
Sandia Laboratories, Albuquerque, New Mexico 87115

The optical absorption near 250 nm was measured for hydrogen and argon implanted single crystals of MgO (Tateho Chemical Industries, Japan) for ion fluences from 10^{15} to 10^{17} ions/cm^2. Two absorption bands in this region of the spectrum have been attributed to two different charge states of an oxygen vacancy, the F^o and the F^+ center.[1] However, EPR measurements have not consistently supported this interpretation. In an earlier investigation[2] of ion-bombardment-induced volume changes in MgO, expansion of the implanted surface layer was observed for 500 keV A^+ bombardment; surprisingly, volume compaction was observed for subsequent H^+ bombardment of the A^+ implanted layer. This compaction was attributed to ionization-stimulated annealing of the argon-induced damage. It was speculated that defects with different charge states account for these positive or negative volume changes and that the energy partitioning of the incident ion into atomic and electronic processes plays a key role in determining the charge states of the resulting defects. This model seems to be substantiated by the fact that distinct absorption bands are produced by hydrogen and argon bombardment which we tentatively attributed to F^+ and F^o centers, respectively, i.e., an oxygen vacancy with either one or two trapped electrons.

EPR measurements have now been performed on the same samples. A weak EPR spectrum with a g-value of 2.0024 ±0.0003 and a ^{25}Mg hyperfine splitting, corresponding to the F^+ spectrum previously reported by Wertz, et al,[3]

*This work was supported by the United States Energy Research and Development Administration (ERDA) under Contract AT(29-1)789.

was observed after ion implantation. In hydrogen implanted samples, the intensity of the F^+ EPR spectrum increases rapidly with fluence from 10^{15} to 10^{17} H^+/cm^2. The rate of increase of the F^+ center measured by EPR is very similar to the rate of increase of the optical absorption band at 250 nm. On the other hand, argon implanted samples also exhibit an F^+ signal in EPR measurements; however, the intensity of this spectrum is nearly constant for the fluence range from 10^{15} to 10^{17} A^+/cm^2 investigated. Again, a similar weak fluence dependence is observed for the intensity of the optical absorption band centered about 245 nm. This saturation is also similar to the stress saturation observed earlier[2] for argon fluences greater than 10^{15} A^+/cm^2.

In addition to the ion-implantation-induced changes in the F^+ centers, the EPR measurements also revealed ion-implantation-induced changes in the Fe^{3+} impurity centers. The EPR and optical measurements will be discussed and correlated with the volume change measurements.

[1]L. A. Kappus, R. L. Kroes, and E. B. Hensley, Phys. Rev. B1 (10), 4151 (1970).
[2]G. B. Krefft, J. Vac. Sci. Technol. 14 (1), 533 (1977).
[3]J. Wertz, P. Auzius, R. Weeks, and E. Silsbee, Phys. Rev. 107, 1535 (1957).

FORMATION OF HOLE CENTERS IN BaF_2 BY NON-IONIZING RADIATION, AND ANNIHILATION OF THESE CENTERS

N. KRISTIANPOLLER, B. TRIEMAN AND Y. KIRSH

DEPT. OF PHYSICS AND ASTRONOMY,
TEL AVIV UNIVERSITY, TEL AVIV, ISRAEL

The production of point defects in SrF_2 by vacuum uv irradiation (vuv) has recently been investigated in our laboratory[1]. The results indicated that hole centers were induced by the vuv irradiation at 80°K in both pure and RE doped samples, via the creation of excitons. These studies have been extended to other alkaline-earth-flourides and we report here on recent results obtained for Tb doped BaF_2.

Irradiation at 80°K with monochromatic light in the range 110-180 nm, caused no detectable changes in the absorption spectrum. However, a strong TL and TSC could be measured during the heating of the crystal to RT. The main glow peaks appeared essentially at the same temperatures (120, 140, 170, 235°K) as in x irradiated samples. These glow peaks are attributed to the thermal decay of V_K, V_H and V_{KA} centers. This is supported by the analysis of the thermal activation energies of the TL peaks. We found that in the doped crystals, TL could also be excited by uv irradiation of lower energies up to about 250 nm. Again the same glow peaks appeared as after vuv and x irradiation. The excitation spectra of the TL in this region showed an excitation maximum at 223 nm. It is assumed that the non-ionizing uv irradiation causes a transfer of electrons, from flourine ions to nearby impurity ions which form local energy levels within the forbidden band. The hole is trapped by nearby fluorine ions, forming a V_K center. Calculations of the photon energies, required for such a process, give values which are in agreement with the experimental results. It is assumed that the uv irradiation at 80°K causes simultaneously the reduction of Tb^{3+} ions to Tb^{2+}. Thermally released holes may then recombine with the Tb^{2+} ions to form Tb^{3+} in an excited state; upon their decay to the ground state TL

is emitted. The measured spectral composition of the LNT phosphorescence and TL emission consisted of sharp bands at 385, 415, 440, 490, 530 and 610 nm. These spectral bands fit the transitions, $^5D \rightarrow ^7F$ of an excited Tb^{3+} ion.

Effects of optical bleaching at 80°K with visible light on the uv excited crystals have also been investigated. The intensities of all glow peaks were found to decrease exponentially with the dose of the bleaching light when illuminated with wavelengths $550 < \lambda < 600$ nm. However, uv excited samples, which were heated to above the 120°K glow peak, recooled to 80°K and then illuminated with visible light, showed no bleaching of the higher temperature glow peaks. V_K centers in BaF_2 decay by heating to above 120°K, and are partly transferred to other hole centers (V_H etc.) which are stable at higher temperatures[2]. The illumination with the visible light appears to bleach the V_K centers only and therefore does not affect the other hole centers, when the V_K centers were annealed thermally.

References:

1. Y. Kirsh and N. Kristianpoller, J. of Lum. 15 (1977), 35.

2. J. H. Beaumont, W. Hayes, D. L. Kirk and G. P. Summers, Proc. Roy. Soc. A 315 (1970) 69.

PROPOSED CATALYTIC RECOMBINATION OF CLOSED CHARGED FRENKEL PAIRS IN ALKALI HALIDES

V. Krumins
Latvian State University, Riga, USSR

The decay and growth of optical absorption in the spectral range 1.8–6.5 eV have been studied in KBr-Na (60 ppm) X-rayed at 85 K by F-F' light exposure and/or by pulse annealing. The interaction efficiency of the H centres with F', F, V_K and α centres during thermal annealing of H_A centres are estimated.

The parallel decay of H_A and V_K centres observed by Schoemaker[1] is shown due to recombination of V_K centres with the F' electrons. At the same time the number of stable V_K centres produced by reaction $H+\alpha \rightarrow V_K$ is one tenth as much as the number of decayed α centres. Moreover as the H_A centres decay a large part of the I_A centres decays too(Fig.1).The remainder I_A centres decay above 200 K. It is found that the number of decayed H_A centres n_{H_A} almost twice as small as the sum of decayed F and α centres $\Delta n_F+\Delta n_\alpha$ after warming to 120 K (Fig.1,b). Besides, some H centres are lost by reason of the V_4 centres production, etc. In such a case we have: $n_{H_A} < \Delta n_F+\Delta n_\alpha+2\Delta n_{V_4}+\ldots$ Therefore it is reasonable to suppose that the mobile H centres cause the catalytic recombination of closed charged $\{\alpha-I_A\}$ pairs: $H + \{\alpha-I_A\} \rightarrow \{V_K-I_A\} \rightarrow H_A+h\nu)_{ex,Na} \rightarrow H$. An intermediate $\{V_K-I_A\}$ pair is unstable because the V_K centre moves to the I_A centre due to thermal energy released by reaction $H+\alpha \rightarrow V_K$. The recombination is accompanied by exciton-like luminescence ($h\nu$)~2.7 eV). When Na^+ concentration is higher then 100 ppm the H_{AA} and $H_{A'A}$ centres annealing is observed at 140 and 165 K respectively and the same catalytic recombination of closed $\{\alpha-I_A\}$ and/or $\{\alpha-I_{AA}\}$ pairs takes place.

The mobile holes e^+ can initiate the catalytic recombination of closed cation $\{v_c^- - i_c^+\}$ Frenkel pairs if they are produced[2] during irradiation: $e^+ + \{v_c^- - i_c^+\} \rightarrow \{V_F - i_c^+\} \rightarrow e^+$.

A mobile hole e^+ is captured by a cation vacancy v_c^- and the V_F centre is formed. It makes the way for returning the interstitial cation i_c^+ into the cation vacancy near-by.

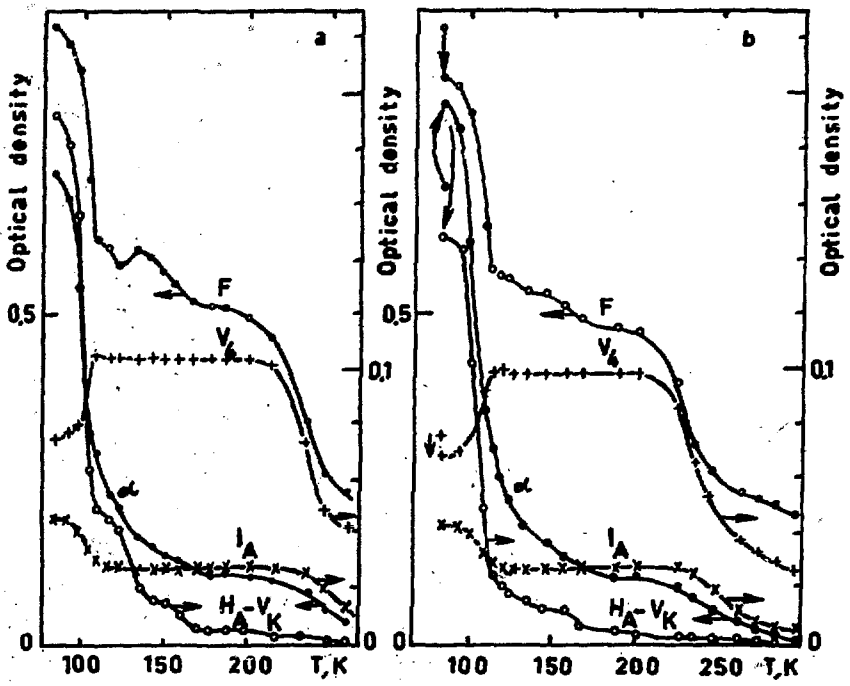

Fig.1. Absorption changes of the F, H_A-V_K, V_4, I_A and α bands in pulse annealing. KBr-Na (60 ppm) crystal X-rayed for 3 hrs at 85 K. The sample was kept for 2 min at each temperature and then cooled again to 85 K for measurements: a/ just after irradiation, b/ after 1 min bleaching with F-F' light, the absorption changes are showed by vertical arrows.

1. D.Schoemaker, Phys. Rev., B3, 3516 (1971).
2. Ch.B.Lushchik, R.I.Gindina, H.V.Jogi, L.A.Ploom, L.A.Pung et.al., Tr. Inst. Fiz. Akad. Nauk Est.SSR, 43, 7 (1975).

EFFECT OF IMPURITY DOPING ON THE HIGH TEMPERATURE TRANSITION IN $(M_xV_{1-x})_2O_3$ ALLOYS*

H. Kuwamoto, W. R. Robinson, and J. M. Honig
Department of Chemistry, Purdue University
West Lafayette, IN 47907 USA

The electrical resistivity of $(M_xV_{1-x})_2O_3$ has been measured for alloys in which M = Aℓ, Cr, Fe, Ga, Rh, Ti and x = 0.01 (as well as for 0.05, 0.06, 0.20 for certain of the alloys). Lattice parameters have also been determined for these materials at room temperature. Whereas the lattice parameters for all $(M_{0.01}V_{0.99})_2O_3$ alloys are nearly identical only Aℓ- and Cr-doped V_2O_3 exhibit the high temperature transition. The latter transitions are marked by enormous hysteresis and by domain effects. These findings strongly indicate that the lattice plays a very important role and that the high temperature transition is not dominated exclusively by electron correlation effects.

*Supported by NSF-MRL Grant No. DMR 76-00889

NONLINEAR ARRHENIUS PLOTS IN IONIC TRANSPORT STUDIES IN SILVER HALIDES

A. L. Laskar, W. Mealing and D. Foster*
Department of Physics & Astronomy
Clemson University, Clemson, S.C. 29631

Diffusion coefficients in solids are traditionally represented by an Arrhenius law, $D(T) = D_o \exp(-H/KT)$, where both H, the activation enthalpy of diffusion, and D_o, the pre-exponential factor, are taken as temperature independent. For most of the solid systems some deviations from the linear Arrhenius plots are observed. Extensive studies of homovalent and polyvalent ions in silver halides[1-2] however provide one of the most interesting spectrum of nonlinear Arrhenius plots (Table I.).

TABLE I. Nonlinearity in Arrhenius Plots in AgCl & AgBr

Diffusant in AgCl	Diffusant in AgBr	Nature of Arrhenius plot	Possible Explanation	Reference[1]
Cd^{2+}	Cd^{2+}	Decrease of slope at low temp.	Polyvalent impurities in tracer & specimens	Reade & Martin; Hanlon
Cd^{2+}		Same	Interstitial diffusion at low temperature	Sawyer & Laskar
Mn^{2+}	Mn^{2+}	Same	Polyvalent impurities in tracer	Laskar & Slifkin; Suptitz et al.
Cu^{+}	Cu^{+}	Increase of slope at low temp.	Impurities in the specimens	Suptitz
Au^{+}		Same	Ambient chlorine gas causing deviation from stochiometry	Batra, Laskar and Slifkin
Ag^{+}	Ag^{+}	Continuous curvature	Direct & indirect interstitialcy mechanisms	Compton & Maurer; Friauf
Br^{-}, Cl^{-}, I^{-}		Same	Anion single vacancy & vacancy pairs	Tannhauser; Batra & Slifkin

An "inherent curvature" in the Arrhenius plot is indeed expected in silver halides due to the temperature dependence of the defect formation energy. Aboagye and Friauf[1] have shown that the appreciable curvature in the conductivity Arrhenius plots, starting from about 300°C and leading to an anomalous rise of conductivity by 250% at high temperature, is due to this temperature dependence. Recent study of Na^{+} diffusion in AgCl by Batra and Slifkin leads to an excellent quantitative agreement with the above hypothesis.

This expected "inherent curvature" in Arrhenius plots is however conspicuous by its absence from the diffusion of other impurity ions in silver halides. A typical example is the temperature dependence of the diffusivity of Fe^{2+} in AgCl and AgBr, recently studied in our laboratory.[2,3] It is now believed that a large number of factors can contribute to this non-observance of inherent curvature. H, the activation enthalpy of diffusion, in general can be written as

$$H = [H_f - \Delta H_f(T)]/2 + H_m - H_a + H_{cf}(T) + H_\gamma(T) \qquad (1)$$

where subscripts m, a, cf, and γ refer to the migration of vacancy or interstitial, vacancy-impurity association, correlation effects, activation coefficient in LDH theory to take care of defect-defect interaction, respectively. In addition, the anion vacancy pairs seen in the study of anion diffusion may indicate the possibility of cation vacancy pairs and thus introduce additional terms in Eq.(1). It is to be noted that both H_m and H_a may decrease with temperature due to the sharp drop of the elastic constants at high temperatures.[1]

A linear Arrhenius plot is not surprising due to the possible cancellation effects of the various contributions. However, precise interpretation of the activation enthalpy of diffusion remains to be a non-trivial exercise. In case of impurity diffusion by vacancy mechanism, H_{cf} is taken to be zero, as is often justified to consider that solute-vacancy exchange jump to be much smaller compared to the other jumps involved. One can then proceed to evaluate H_m of the diffusant by calculating the various terms in Eq.(1) from LDH-Friauf theory if and only if the impurity concentration in the crystal and H_a, impurity vacancy association enthalpy, is precisely known. The latter is known only in a few cases. Uncertainty of the impurity concentration and H_a make these analysis approximate. Finally, even with the great refinement of the present day tracer diffusion techniques, a delicate balancing is needed to extract true D values from the penetration profiles which are unavoidably perturbed due to the evaporation and solubility of the isotope used and the inadvertent presence of trace impurities. The distribution coefficient of impurities in silver halide crystals grown by Bridgman method, may cause an additional perturbation since D will be then concentration dependent.

*Now at P. R. Mallory & Co., Inc., Burlington, Mass. 01803

REFERENCES

1. A. P. Batra and L. M. Slifkin, J. Phys. C.: SSP 9, 947 (1976), and 8, 2911 (1975), J. Phys. Chem. Solids 37, 967 (1976); E. W. Sawyer and A. L. Laskar, J. Phys. Chem. Solids 33, 1149 (1972) and the references in these.
2. D. L. Foster and A. L. Laskar, Phys. Stat. Sol. (a) 29, 1967 (1975).
3. W. Mealing and A. L. Laskar, Bull. Am. Phys. Soc. 19, 272 (1974).

LUMINESCENCE IN MgO : EVIDENCE FOR ELECTRON HOLE RECOMBINATION AT A MAGNESIUM ION VACANCY*

K. H. Lee and J. H. Crawford, Jr.
University of North Carolina at Chapel Hill

Two luminescence bands appear at 4.95 eV and 3.2 eV when high purity MgO is excited by x-rays at 90°K. The 3.2 eV band has been studied in the past[1]. The intensity of the 4.95 eV band is enhanced by about a factor of three if the sample is previously exposed to 5×10^6R γ irradiation. The enhanced intensity decays upon standing at room temperature. The 3.2 eV band is unaffected by γ irradiation. ESR data show very low concentration of Mn, Cr, Fe impurities in our sample. MgO samples doped with various impurities (Cr, Cu, Fe, Ni, Mn, Ga) have been studied in order to determine whether impurities are responsible for the luminescence bands. In MgO:Ni^{2+}, the $^1T_{2g} \rightarrow {}^3A_{2g}$ luminescence band (2.5 eV)[2] of Ni^{2+} has been observed but the 4.95 eV and 3.2 eV bands were missing. For Fe doping no detectable luminescence band can be observed even at the 100 ppm doping level. No correlation between the impurities and the 4.95 eV and 3.2 eV bands can be found which suggests that intrinsic defects may be responsible for these luminescence bands. The magnesium vacancy is a major intrinsic defect in our MgO sample. The effect of irradiation on and thermal stability of the 4.95 eV band parallels the V- type centers; therefore, we tentatively assign the 4.95 eV band to the recombination luminescence of the V- type centers,

$$O^-\square + e \rightarrow (O^{=}\square)^* \rightarrow O^{=}\square + 4.95 \text{ eV} .$$

Additional evidence for this assignment is:

1. Room temperature annealing shows that the 4.95 eV band has several annealing stages indicating that it is a composite band similar to that associated with the V- type centers in MgO. One of the components with an eight hour half life at room temperature is partially eliminated by high temperature (1200°C) oxidation for 72 hours. It is believed that this component is due to V_{OH} center.[3]

2. A 210°K thermoluminescence band is observed when the high purity sample is warmed after irradiation with x-rays at 90°K. The

EXPERIMENTAL AND THEORETICAL STUDY OF F CENTRES IN $SrCl_2$, BaClF AND SrClF

S. Lefrant[a], A.H. Harker[b] and L. Taurel[a]

a) Laboratoire de Physique Cristalline - Université de Paris-Sud -
(Equipe de Recherche associée au CNRS n°13)
Bâtiment 490 - 91405 ORSAY CEDEX - FRANCE -

b) Theoretical Physics Division, AERE Harwell,
OXFORDSHIRE - OX11 ORA - ENGLAND -

Theoretical models of F centres have given very good results in the past in the case of alkali halides. The most successful are the Point-Ion model developped by Gourary and Adrian[1] and the Ion Size approximation of Bartram et al.[2]. We have used these two methods for F centres in alkaline-earth halides of lower symmetry, such as $SrCl_2$, BaClF and SrClF.

In $SrCl_2$, the site symmetry of the F centre in the fluorite lattice is T_d and the F band is attributed to an $A_1 \rightarrow T_2$ transition. We have made both Point-Ion and Ion-Size variationnel calculations and, in a first-approximation, only the spherical part of the potential was retained. The use of s and p functions leads to results in good agreement with the experiments for the absorption peak and the isotropic constant for the first shell of chlorines. On the other hand, the g orbital factor, found experimentally zero, need to be interpreted a (p + d) mixture for the first excited state while the fundamental one is described by a (s + f) mixture. This model was already introduced for the fluorides[3] and a recent determination of g_{orb} in CaF_2[4] confirms this description.

In the mixed crystals BaClF and SrClF, the anion vacancies are of two types, fluoride and chloride, giving two types of F centres : an F centre in fluoride site with D_{2d} symmetry and an F centre in chloride site with C_{4v} symmetry. In these conditions, the F centre excited state will be split into a doublet and a singlet. Four bands are observed experimentally, two polarized parallel to and two perpendicular to the four-fold axis of the crystal. The centres are labelled I and J and their associated bands I_1, I_2, J_1 and J_2. In BaClF, the two bands are respectively at 2.83 eV ($\vec{E}//\vec{c}$) and 2.25 eV ($\vec{E}\perp\vec{c}$) and for the J centre 2.33 eV ($\vec{E}//\vec{c}$) and 2.82 eV ($\vec{E}\perp\vec{c}$). We have applied the Point-Ion model to calculate the energy levels of these centres in order to determine which centre is the F centre

4.95 eV light is observed but not the blue light (3.2 eV). Blue thermoluminescence observed above room temperature has been attributed[4] to the capture of holes thermally released from V- type centers by impurities, presumably iron. Absence of the blue thermoluminescence in the 210°K peak indicates that holes are not involved. Therefore, it is suggested that the 4.95 eV emission is due to electrons released from shallow traps and captured by V- type centers. However, we have no suggestion to make for the origin of 3.2 eV emission excited by x-rays at 90°K.

1. J. E. Wertz, L. C. Hall, J. Helgeson, C. C. Chao and W. S. Dykoski, in Interaction of Radiation with Solids, edited by A. Bishay (Plenum Press, Inc., New York, 1967), p. 617.
2. W. E. Vehse, K. H. Lee, S. I. Yun, and W. A. Sibley, J. of Luminescence, 10, 149 (1975).
3. E. F. Harris and J. H. Crawford, Jr., Phys. Stat. Sol. (a) 35, 667 (1976).
4. W. A. Sibley, J. L. Kolopus, and W. C. Mallard, Phys. Stat. Sol. 31, 223 (1969).

*Supported by the Materials Research Center, University of North Carolina under Grant No. DMR, 72-03024 from NSF.

in fluoride or chloride site. For the $F(F^-)$ centre, its D_{2d} symmetry allows transitions $A_1 \rightarrow B_2$ ($\vec{E} // \vec{c}$) and $A_1 \rightarrow E$ ($\vec{E} \perp \vec{c}$) and so, the wave-function used are s for A_1, p_z for B and p_x, p_y for E levels.

The $F(Cl^-)$ centre with C_{4v} symmetry allows $A_1 \rightarrow A_1'$ ($\vec{E} // \vec{c}$) and $A_1 \rightarrow E$ ($\vec{E} \perp \vec{c}$) transitions. We have used wave functions $(s + p_z)$ for the A_1 and A_1' and p_x, p_y for the E levels. The results are indicated in the table 1 and lead to the conclusion that the I centre is the $F(Cl^-)$ centre while the J centre is the $F(F^-)$ centre.

		$F(F^-)$ Calcul.	J centre Exp	$F(Cl^-)$ Calcul.	I centre Exp.
BaClF	$\vec{E} // \vec{c}$	$A_1 \rightarrow B_2$ 2.13	2.33	$A_1 \rightarrow A_1'$ 2.70	2.83
	$\vec{E} \perp \vec{c}$	$A_1 \rightarrow E$ 3.076	2.82	$A_1 \rightarrow E$ 2.04	2.25

Table 1. Calculated and experimental transition energies (in eV) of F centres at F^- and Cl^- sites in BaClF

In the case of the $F(Cl^-)$ centre, another set of calculations, which does not take account of the small axial field mixing the s and p_z components gives results quite similar for the transition energies. Nevertheless, recent endor experiments[5] on this centre show an anisotropy in the hyperfine interactions as already observed in the alkaline-earth fluorides[3]. Therefore the $(s + p_z)$ mixing seems to be more appropriate, even if the point-ion model always overestimates the contribution of higher angular momentum terms[6].

1 Gourary B.S. and Adrian F.J. Phys. rev. 105, 1180-92 (1957)

2 Bartram R.H., Stoneham A.M. and Gash P. Phys. Rev. 176, 1014-24 (1968)

3 Bartram R.H., Harmer A.L. and Hayes W. J. Phys. C:Solid St. Phys. 4 (1971)

4 Roger J.P., S. Lefrant, L. Taurel and M. Billardon Sol. St. Com. 18 (1976)

5 M. Yuste - Private communication -

6 Harker A.H. D. Phil. Thesis University of Oxford (1973)

VIBRONIC MODEL FOR AN ns^2 SYSTEM : KCl:Au^-

D. LEMOYNE, J. DURAN and J. BADOZ
Laboratoire d'Optique Physique de l'ESPCI
10, rue Vauquelin, 75231 PARIS CEDEX 05, France

The Au^- centre in KCl is isoelectronic to the Tl^+-like ions. We have performed various experiments on the $^3P_1$ state (1). Three different ways for ascertaining a vibronic model have been used which involve polarization measurements under various perturbations in absorption and emission in the zero-phonon line and in the broad band. The striking result of this study is the equality of the three different sets of parameters thus obtained by using a single vibronic model.

At liquid helium temperature some quenching effects due to relaxation processes occur in the emission measurements.

Broad band experiments. Following a classical procedure (2), one may extract the Huang and Rhys factor S_Γ and the corresponding mean phonon frequencies $\hbar\omega_\Gamma$ from the perturbative measurements performed on the broad band. Experimentally, we found :

$$S_{A_1} = 3.8 \pm 0.4, \quad S_E = S_{T_2} = 0.72 \pm 0.08$$

$$\hbar\omega_{A_1} = 65 \pm 7 \text{ cm}^{-1}, \quad \hbar\omega_E = \hbar\omega_{T_2} = 160 \pm 16 \text{ cm}^{-1}$$

The emerging feature of this result consists in the equality of the coupling to the E_g and T_{2g} modes. The corresponding theoretical problem (the so-called D-mode model) has received much attention these last years and exact solutions have been derived for the diagonalization of the total hamiltonian at least for the lowest vibronic eigenstate. According to O'Brien's calculations (3) the expected values for $K(T_1)$ and $K(E) = K(T_2)$ are 0.26 and 0.56 respectively.

Combined zero-phonon line and broad band experiments. The quenching factors may be directly measured from the comparison of the first-moment change in the zero-phonon line and in the broad band when an external

(1) LEMOYNE, D., DURAN, J., BILLARDON, M., LE SI DANG, Phys. Rev. B14 (1976) 747.

perturbation is applied. $K(T_1)$, $K(E)$ and $K(T_2)$ are associated respectively to the magnetic, stress along <001> and stress along <110>.

Experimentally, we obtained :

$$K(T_1) = 0.24 \pm 0.04 \; ; \; K(E) = 0.58 \pm 0.08 \; ; \; K(T_2) = 0.53 \pm 0.08$$

The remarkable agreement of the two sets of quenching factors values obtained by two independent methods shows the high consistency of the D-mode model applied to the $KCl:Au^-$ system. In turn, this model may be used in the interpretation of our fluorescence experiments.

Fluorescence experiments. In the case of the D-mode model, Romestain and Merle d'Aubigné (4) have calculated the exact vibronic wave-functions of the relaxed excited state. The knowledge of these wave-functions makes possible the calculation of the selection rules for polarized light emitted from the relaxed excited state sublevels split by an external perturbation. These selection rules are simple functions of the $K_1 = K(T_1)$ and $K_2 = K(E) = K(T_2)$ factors. Thus, the measurements of the polarization degrees lead us to another determination of K_1 and K_2 :

$$K_1 = 0.25 \quad 0.03 \; ; \; K_2 = 0.56 \quad 0.06$$

values which are in complete agreement with those previously obtained.

Relaxation process. Some quenching occurs in the measured polarization degrees as soon as temperature is decreased below 4.2 K. At first, this fact may be related to two essential features : (i) The random internal strains which mix the vibronic eigenstates of the applied perturbation. Taking into account the bandwidth of the zero-phonon line, the existing internal stresses cannot explain the relatively large observed reductions. (ii) The relaxation processes which may be too slow to feed the split sublevels.

It can be shown that the polarization degrees are functions of the relaxation time. We have thus been able to show that τ_R deduced from our experimental results follows a T^{-1} law in the temperature range 1.1-4.2K. This result indicates that a classical one-phonon process is active.

(2) HENRY, C., SLICHTER, C.P., in Physics of Color Centers (New-York: Academic Press) 1968.
(3) O'BRIEN, M.C.M., J. Phys. C:Solid State Physics 4 (1971) 2524.
(4) ROMESTAIN, R., MERLE D'AUBIGNE, Y., Phys. Rev. B4 (1971) 4611.

FORMATION OF M^{++}-VACANCY DEFECTS IN ALKALI HALIDE CRYSTALS

E.Lilley and J.E.Strutt*
Materials Science Division, School of Engineering and Applied Sciences,
University of Sussex, Brighton, U.K.

In the various studies of clustering of divalent cation vacancy pairs, pioneered by J.S.Dryden and co-workers, there is strong evidence for third order kinetics indicating that trimers $[M V]_3$ are being formed [1]. If equilibrium is established between pairs and trimers then the mass action equation is

$$\frac{C - x_p}{3x_t^3} = z \exp \frac{-\Delta G_t}{kT}$$

where C is the divalent ion concentration existing as pairs and trimers, x_p is the pair concentration, x_t is the trimer concentration, ΔG_t is the trimer free energy of formation, z is the geometric entropy, k is the Boltzmann constant and T the absolute temperature. The difficulty in applying this equation to ageing studies in which the associated pair concentration is measured as a function of time is that equilibrium is rarely established. Normally the plateau region, representing a pseudo equilibrium between pairs and trimers, is far from horizontal in the kinetic plot due to the fact that the trimers continue to grow to larger aggregates. It is our view that in the second stage of clustering precipitate particles are being formed rather than stable higher order clusters [2,3]. In our studies of Mg^{++} doped LiF we have found a way to avoid this problem. This involves solution heat treating at 400°C followed by a quench to room temperature, as is usual, then ageing between 100 and 170°C. At these ageing temperatures which are much higher than those used in most previous studies, the driving force for precipitation is reduced since the undercooling is less. (Typically the solubility limit of an 88 ppm Mg^{+} doped crystal is 227°C.) Consequently very long times are needed to initiate precipitation and long horizontal plateaux are found in the kinetic plots which are ideal for determining the equilibrium concentrations. The $Mg^{++}V$ pair concentrations are in fact calculated from dielectric loss measurements. The Arrhenius plot for these equilibrium concentrations yields a trimer bonding energy of 0.95 ± 0.05 eV.

* Now at the Cranfield Institute of Technology, Cranfield, Beds., U.K.

Next consider the bonding energy of divalent cation vacancy pairs. Such values have invariably been determined from ionic conductivity-temperature plots. The precise analysis even with the aid of computer fitting is difficult because there are so many parameters. Recently we have made measurements of conductivity and capacitance over a frequency range which allows us to determine both the free vacancy and $M^{++}V$ pair concentration at various temperatures. From the appropriate mass action equation we can then calculate the binding energy of these pairs. Results covering several divalent impurities will be presented.

References

1. J.S.Dryden, Conf. Crystal Lattice Dfects, Kyoto, paper IIc-6 (1962).
2. J.E.Strutt and E.Lilley, Phys.Stat.Solidi (a), 33 229 (1976).
3. M.H.Bradbury and E.Lilley, J.Phys.D. (1977), to be published.

GRAIN BOUNDARY CONDUCTIVITY IN BETA ALUMINA

E.Lilley and J.E.Strutt*
Materials Science Division, School of Engineering and Applied Sciences,
University of Sussex, Brighton, U.K.

A detailed electrical study has been made of polycrystalline beta alumina containing 20% β'' phase using blocking Al electrodes. Conductivity and capacitance were measured over the frequency range 10 to 10^7 Hz and the temperature range -135 to 400°C. These measurements were plotted in the form of a complex impedance plot which exhibits two semicircles and a spur. The first semicircle (at high frequencies) arises from the bulk impedance, the second semicircle from the grain boundary impedance and the spur from the double layer capacitance at the interface. An Arrhenius plot of the values of the bulk and grain boundary conductivities extracted from these complex plane plots is shown in figure 1. ▲ points represent the bulk conductivity and the ● points the grain boundary conductivity. The bulk conductivity is linear over four decades and has an activation energy of 0.18 eV. The grain boundary conductivity has the same activation energy at low temperatures. At high temperatures the two lines intersect and above this point the grain boundary resistance becomes negligible. Fortunately this intersection occurs below the operating temperature (350°C) of the Na/S battery.

The low temperature linear region of the grain boundary data is interpreted as being due to the passage of Na^+ ions through easy paths across the grain boundary, i.e. at some points where the Na^+ ions can pass through unimpeded, with the same activation energy as the bulk. This leads to a constrictive resistance model from which we can calculate that on average for each fast conducting plane in a grain of beta alumina only one intersection with the fast planes of an adjacent grain will be an easy path, i.e. about one in a thousand.

* Now at the Cranfield Institute of Technology, Cranfield, Beds., U.K.

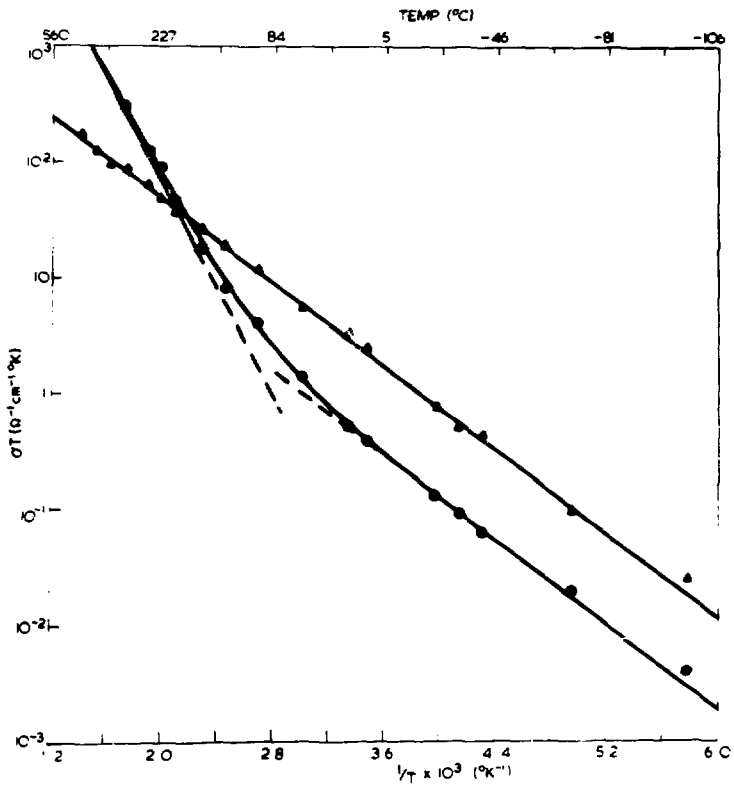

Fig.1 Conductivity plot of the 20% β'' sample of beta alumina. The Δ represent the conductivity of the grains and o represent the conductivity of the bulk.

STUDY OF INTERSTITIALS CLUSTERS IN γ-IRRADIATED HIGH PURITY AND Mg DOPED LiF SINGLE CRYSTALS, BY THERMAL CONDUCTIVITY MEASUREMENTS BETWEEN 0.05 AND 70 K

M. LOCATELLI
Centre d'Etudes Nucléaires de Grenoble
Service des Basses Températures
85 X
38041 GRENOBLE-CEDEX (France)

In a previous work K. Guckelsberger and K. Neumaier [1] have detected clusters in γ-irradiated LiF by thermal conductivity measurements at low temperatures (1 to 50 K).

They were able to show the presence of small lithium aggregates (1 nm diameter) in addition to F-centers and dislocations ; the concentration of these defects was increasing with the irradiation dose in agreement with the results of Cagnon [2].

But they could not conclude on the nature of the nucleation centers (impurities, dislocations ...).

The purpose of this work was to look for more information about this question. We have measured the thermal conductivity of a LiF crystal of higher purity and also an Mg-doped LiF crystal (75 ppm), in the temperature range 0.05 to 70 K, after γ-irradiations of different doses.

For the pure sample two results have been obtained.

Firstly, in addition to the presence of the small clusters, large defects of about 50 nm are observed event at low irradiation doses. Their number increases with the irradiation dose. These defects cannot ben spherical, since the total estimated number of interstitials uniformly distributed in these defects supposed spherical, would lead to an internal density of interstitials too low to be detected. The possibility of platelets will be tested by electron microscopy.

Secondly the number of small clusters (1 nm) is apparently less than in the less pure samples previously studied [1]. On the other hand, in the Mg-doped LiF we detect a greater number of large and small clusters than in the pure samples for the low irradiation dose, therefore we can conclude in favour ot the role of the impurities as nucleation

centers.

Finally for the highest irradiation doses, approximatively the same number of clusters is obtained in all cases.

REFENCES -

[1] K. GUCKELSBERGER and K. NEUMAIER
J. Phys.Chem.Solids 36, pp 1353-1363 (1975)

[2] M. CAGNON
Xe Colloque de Métallurgie, p 79 - Presses Universitaires de Paris (1966)

THERMOLUMINESCENCE AND ELECTRON SPIN RESONANCE AFTER X-RAY IRRADIATION OF NaCl:Mn^{++}

F.J. López, F. Jaque, A.J. Fort and F. Agulló-López
Sección de Optica y Estructura del Sólido
Instituto de Física del Estado Sólido (C.S.I.C.)
Universidad Autónoma de Madrid
Cantoblanco, Madrid (SPAIN)

A parallel investigation of thermoluminescence (TL), electron spin resonance (ESR) and optical absorption on both room temperature (RT) and liquid nitrogen temperature (LNT) X-irradiated NaCl:Mn^{++} has been performed. TL spectra from RT to 300°C consist of five glow peaks, numbered from I to V, whose maximum heights are at 314, 341, 391, 425 and 489 K respectively. The wavelength spectrum for all peaks consists of two bands at 595 and 400 nm. The 595 nm emission is attributed to hole capture by Mn^{+} and subsequent desexcitation of Mn^{++}. The 400 nm band is attributed to hole -F center recombination.

TL spectra from LNT to RT consist of four glow peaks numbered from i to iv, with maximum heights at 108, 170, 182 and 221 K. The wavelength spectrum consists on the 595 nm emission band and on other bands, differents for each peak.

The correlation of TL glow peaks to various defects and to the aggregation state of the impurity has been investigated. Peak II is clearly related to Mn^{++} - vacancy dipoles and peak I can be roughly associated to free cation vacancies. Peak V is intrinsic and not related to impurities, whereas peaks iii and IV appear to be relate to large Mn - Aggregates.

On the other hand ESR and optical absorption data indicate that each glow peak in the 595 nm emission is associated to the annihilation of a given Mn - center. For example:

peaks ii and iv to Mn° - B, peaks I and II to Mn° - C, peaks II and III to Mn^{+} and peaks IV and V to Mn° - D. The figure displays two TL spectra at low and high temperature, showing the annihilation of some Mn^{-} centers.

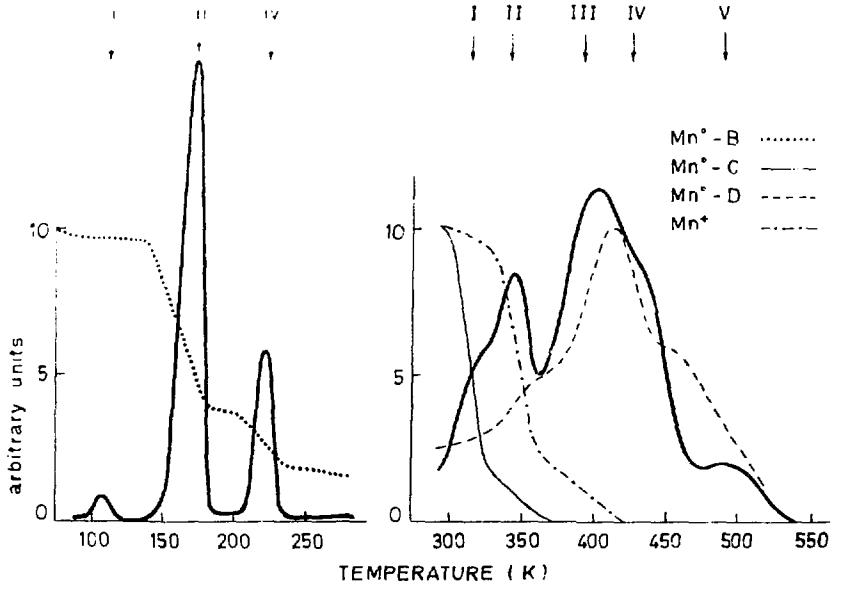

This work has been partially supported by the Instituto de Estudios Nucleares (J.E.N.).

POSITIVE-ION BOMBARDMENT OF KCl: THE ROLE OF PARTICLE INFRATRACKS*

M. Luntz, P. E. Thompson and R. B. Murray
Physics Department, University of Delaware
Newark, Delaware, U.S.A. 19711

Single crystals of KCl at room temperature were bombarded by H^+ and He^+ ions in the MeV region. Combining the results of a photomicrographic procedure with measurements of crystal optical density, profiles yielding F centers/cm^3 versus depth are obtained. It is found that the F-center concentration does not follow dE/dx as a function of depth. Profile shapes and magnitudes are accounted for in terms of the positive-ion infratrack, a cylindrical region of direct interaction of the positive ion with atoms of the host crystal. The concept of ion infratrack has been previously utilized in studies of radiation biology[1,2]. Analysis of data shows that the infratrack dominates F-center production and reasonably accounts for the observed F-center profiles and high saturation concentration of F centers ($\sim 2 \times 10^{19}$ cm^{-3}).

The interpretation given predicts that the projectile velocity is a key parameter, as the infratrack radius is proportional to the ion velocity. This prediction is confirmed by comparison of F-center profiles for He^+ and H^+ ions. It is also observed that the suppression of F-center production by impurities, a well-known effect for gamma or electron irradiation, is greatly reduced for positive ion irradiation. Very similar results are obtained for ions having the same initial velocity. These observations are consistent with the dominant role of the infratrack in F-center production.

---

*Work supported by the National Science Foundation.

(1) A. Mozumder, Advances in Radiation Chemistry, edited by M. Burton and J. L. Magee (John Wiley & Sons, New York, 1969).

(2) W. Brandt and R. H. Ritchie, U.S.A.E.C. CONF 721001, edited by R. D. Cooper and R. W. Wood (1974).

MECHANISMS OF CATION DEFECTS CREATION IN ALKALI HALIDES

Ch.B.Lushchik, A.A.Elango, R.I.Gindina, A.Ch.Lushchik,
A.A.Maaroos, T.N.Nurakhmetov, L.A.Ploom, L.A.Pung,
J.V.Põllusaar, H.A.Soovik and N.A.Jaanson
Institute of Physics, Tartu, 202400, USSR

Radiation damages in alkali halides arise due to the decay of self-trapped excitons into F and H centres [1,2]. The stabilization of mobile centres can occure in the temperature range 60÷100 K either as a result of the formation of cation defects by the interaction of two H centres [3,4] or due to the interaction of H centres with cation vacancies caused by the decay of anion or cation excitons [5,6].

We shall denote anion and cation vacancies v_a^+ and v_c^-, interstitial of an halide or alkali ions and atoms i_a^-, i_a^o, i_c^+ and i_c^o and electrons, holes and excitons e^-, e^+ and e^o. In principle the following reactions are possible:

$e^o \rightarrow v_a^+ e^- + i_a^o$ (1); $e^o \rightarrow v_a^+ + i_a^-$ (2);

$e^o \rightarrow v_c^- e^+ + i_c^o$ (3); $e^o \rightarrow v_c^- + i_c^+$ (4);

$v_c^- + e^+ \rightarrow v_c^- e^+$ (5); $v_c^- + i_a^o \rightarrow v_c^- e^+ + i_a^-$ (6);

$v_c^- + e^+ + i_a^o \rightarrow v_c^- e^+ i_a^o$ (7); $v_c^- + i_a^o + i_a^o \rightarrow v_c^- e^+ i_a^o + i_a^-$ (8);

$e^+ + i_a^o \rightarrow v_c^- e^+ i_a^o + i_c^+$ (9); $i_a^o + i_a^o \rightarrow v_c^- e^+ i_a^o + i_c^+ i_a^-$ (10);

$i_c^+ + v_a^+ e^- e^- \rightarrow v_a^+ i_c^-$ (11); $e^o v_a^+ \rightarrow v_a^+ v_c^- + i_c^+$ (12).

For middle doses of X-rays (10 Mrad) due to these reactions immobile associations of $i_a^- i_c^+$, $v_a^+ v_c^-$, v_c^-, e^+, i_a^o and others can be created. In KCl and KBr with the impurity concentration less than 10^{16} cm^{-3}, color centres of the type $v_c^- e^+ i_a^o$ (partially with closely situated i_a^-, i_c^+, $i_a^- i_c^+$) are produced at the temperatures where H centres are mobile. The absorption spectra of $v_c^- e^+ i_a^o$(5.3 eV in KCl; 4.5÷4.6 eV in KBr0 are close to the absorption spectra of X_3^- molecules. The X_3^- centres occupying one cation and two anion sites, are oriented along the <100> axes.

After the photodissociation of X_3^- centres e^+ (V_k), $v_c^-e^+$ (V_F) and i_a^o (H) are created. After an irradiation of KCl at 80, 200 and 300 K an associative ionic conductivity increases in the temperature range 300÷450 K. The irradiation produces the divacancies $v_a^+v_c^-$. There also arise anty-Schottky pairs $i_a^-i_c^+$ (absorption at 6.4 eV). After an irradiation KCl at 4 K ionic conductivity increases at 300-400 K (probably the number of v_c^- increases). In KCl-NO_2 and KBr-NO_2, where e^- and possibly i_c^+ are trapped by NO_2 ions, V_k centres are effectively accumulated and reactions (7) and (9) are possibly with the creation of $v_c^-e^+i_a^o$ centres oriented along the <100> axes. In KBr-Sr a reaction similar to (8) takes place [4].

Direct manifestations of reaction (10) in regular regions of the crystals KCl and KBr have not yet been detected. One can conclude from [7] that reaction (10) is not realized in CsBr. In NaBr reactions (1), (10) are of low effeciency and reaction (4) is predominent [8].

An hypothesis about the decay of excitons upon the Frenkel defects as a result of the transformation of the one-halide excitons (X^oe^-) to the dihalide excitons ($X_2^-e^-$) is discussed [2,8].

1. E.Sonder, W.Sibley, in "Point Defects in Solids", Ed. J.Crawford, L.Slifkin, New York - London, Plenum Press, v. 1, 1972, p. 201.
2. Ch.Lushchik, I.Vitol, M.Elango, Uspekhi fiz. nauk, 122, 223, 1977.
3. L.Hobbs, A.Hughes, D.Pooley, Proc.Roy.Soc., A332, 267, 1973.
4. A.Elango, T.Nurakhmetov, Phys.Stat.Sol. (b), 78, 529, 1976.
5. Ch.Lushchik, I.Vitol, M.Elango, Fiz. Tverd. Tela, 10, 2753, 1968.
6. Ch.Lushchik et.al., Izv. AN SSSR, ser.fiz., 38, 1219, 1974.
7. B.Chowdari, N.Itoh, J.Phys.Chem.Solids, 33, 1773, 1972.
8. V.Denks et al., Fiz. Tverd. Tela, 18, 2151, 1976.

THE ODD-PARITY JAHN-TELLER EFFECT FOR IMPURITY IONS IN ALKALI EARTH OXIDES

N.B. Manson

Department of Solid State Physics
Research School of Physical Sciences
Australian National University
Canberra, A.C.T.

The fine structure of the vibronic lines in the optical absorption of Ni^{2+} impurities in single crystals of CaO[1,2] and MgO [3] has been shown to be due to the coupling with odd parity vibrations.

The Ni^{2+} ion has an appreciably smaller radius than Ca^{2+}. Consequently, when it is substituted for Ca^{2+} in CaO it is only loosely bound and is associated with a low frequency localised vibration of T_{1u} symmetry. Electronic transitions between states coupled to this localised vibration give sharp lines in the low temperature optical absorption. When the excited electronic state is non-degenerate the associated optical absorption has only one line. However, when the excited state is degenerate, the absorption has fine structure arising from the splitting of the excited vibronic multiplet by the interaction between the electron and the odd-vibration. For example the multiplet formed by the T_{1g} spin-orbit component of the $^3T_{1g}{}^a$ state coupled to the T_{1u} localised vibration is split by ~30 cm^{-1} by the terms in the electron vibration interaction with E_g symmetry [2]. The effect of uniaxial stress on those vibronic lines has been studied and this data will be presented. In the case of the $T_{1g} \times T_{1u}$ multiplet it is found that both the vibronic lines are split by stress along the <001> direction and the components are strongly σ/π polarised. When the stress splitting is less than the vibronic splitting this can be explained by considering an interaction due to the stress of $E_g\theta$ symmetry in addition to the vibronic interaction which as $(E_g\theta + E_g\varepsilon)$ symmetry.

A comparison will be made between vibronic splitting of the above type associated with odd parity modes and the closely related Jahn-Teller effect associated with even parity modes. In the case of the Jahn-Teller effect the linear term in the electron-vibration interaction is dominant. For odd-parity modes the linear term gives no contribution so that higher order terms, in particular the quadratic terms, must be involved. The effects of coupling to odd parity modes are consequently much weaker than for even-parity modes, and in the systems studied give splittings of similar magnitude to those of weak or dynamic Jahn-Teller effects. Even so, splittings are large as 60 cm^{-1} have been observed, showing that these interactions give larger effects than has previously been recognised.

[1] N.B. Manson and K.Y. Wong (1975) Observation of the Splitting of the Vibronic Levels of CaO:Ni^{2+} by Electron-odd vibration Interaction. J. Phys.C: Solid St. Phys. 8, L73-76.

[2] N.B. Manson and K.Y. Wong (1976) Vibronic Splitting in the $^3T_{1g}{}^a$ Crystal Field Level of CaO:Ni^{2+}. J. Phys. C: Solid St. Phys. 9, 611-626.

[3] N.B. Manson (1976) Electron-vibration Splitting of the Vibronic Levels of the $^1T_{2g}$ State of MgO:Ni^{2+}. Solid State Comm. 18, 257-260.

DISPERSION AND FARADAY ROTATION ASSOCIATED WITH POINT-IMPERFECTIONS

J.J. Markham* and K. N. Vasudevan
Physics Department
Illinois Institute of Technology
Chicago Ill. 60616

Here we consider dispersion and Faraday rotation arising from "transitions" of electrons associated with point-imperfections in polar solids. The general case is extremely involved especially if effects of phonons are included. It, therefore, seems worthwhile to consider a simple but realistic case where the point symmetry is O_h, the electron's spacial ground state is a Γ_1^+ function and its excited states are Γ_4^- functions. The phonons which interact with the electron will have Γ_1^+ symmetry and a single frequency.

We need to know:

1) Equations for the dispersion of linearly, right-circularly and left-circularly polarized light.

2) How to expand these equations so that one may obtain "simple" expressions for the Verdet constant.

3) What occurs when phonon effects are explicitly considered.

4) Finally how to cast the relations in a manner that they will be experimentally useful.

In the literature our problem has been handled essentially classically (Becquerel equation) even though quantum mechanical operators appear. The object here is to obtain quantum mechanical expressions and thus to include effects which traditionally are not associated with Becquerel's equation. Also we have avoided the use of the Kramess-Krönig relations so as to gain further insight into the problem. The basic approach used here is that due to Born and Jordan[1] whose considerations on atoms apply to our case.

..../..

We have obtained expressions for the polarization of our center by linear, right and left polarized light as well as expressions for the Verdet constants. Some results are:

(1) Operators have been obtained (i.e. expressions corresponding to X for electric dipole transition) associated with dispersion produced by right-and left-circularly polarized light. These are compared with those associated with absorption and emission.

(2) Using the "exact" expression for the Verdet constant we have obtained expansions depending on the frequency of the electro-magnetic wave as well as other parameters. These expansions show the nature of the approximations made in the literature.

(3) The equation for dispersion has an overlap integral of the vibrational eigenfunctions identical to the absorption case. Hence the phonon effects can be included easily. If one is at $0^{O}K$, they are nondegenerate and have Γ_1^+ symmetry-no Jahn-Teller effect. Detailed calculations have been made on various possible situations. Some curves will be shown.

The calculations indicate that the phonon dispersion is extremely important in these calculations. We suggest a simple but only approximate way to take care of the spread of phonon frequencies into account.

REFERENCES

*. On sabbatical leave at J.J. Thomson Physical Laboratory , University of Reading, Reading, England.

1) M Born and P Jordan, Elementare Quantenmechanik (Verlag-Berlin, 1930) p.267.

2) Since the paper was completed, the authors have seen the paper by A.S. Davydov [JETP 24, 197 (1953)] . It suggests the presence of the overlap integral in dispersion.

ELECTRON SPIN RESONANCE ABSORPTION SPECTROSCOPY INVESTIGATION OF MAGNETIC ION IMPURITIES IN SINGLE CRYSTAL YTTRIUM ALUMINUM GARNET*

S. A. Marshall

Argonne National Laboratory, Argonne, Illinois 60439

T. Marshall

Suffolk University, Boston, Massachusetts 02114

R. A. Serway

Clarkson University, Potsdam, New York 13676

The electron spin resonance absorption spectra of octahedral iron, tetrahedral iron, octahedral chromium, and dodecahedral gadolinium in single crystals of yttrium aluminum garnet have been reinvestigated at both X-band and Q-band wavelengths. Fine structure spectral parameters deduced from spectral observation made at Q-band wavelengths, satisfactorily predict spectra at both X- and Q-band wavelengths. Spectral lines due to dodecahedral gadolinium are found to be sufficiently narrow to permit partial resolution of hyperfine structure arising from the isotope Gd(157). This hyperfine structure is orthorhombic and its Fermi contact term suggests that a significant fraction of the electronic spin density is removed from the parent ion.

A crystal mosaic structure study conducted through the spectra of these four crystal-ion systems indicates that, in addition to the background crystal mosaic, there exists what appears to be a mosaic structure characteristic of each crystal-ion. This structure, characterized by a mosaic angle $\Delta\theta$, varies from $\Delta\theta = 0.11$ deg for dodecahedral gadolinium to $\Delta\theta = 0.50$ deg for tetrahedral iron.

*Work performed under the auspices of the U. S. Energy Research and Development Administration.

ANOMALOUS RELAXATION PROCESS OF THE OFF-CENTER Li^+ IONS IN KCl:Li AT ZERO ELECTRIC FIELD.

Masao MATSUOKA, Yuzo MORI, and Hiroshi OHKURA

Department of Applied Physics, Osaka City University, Osaka, Japan 558

The tunneling structure of the ground state of the off-center impurity Li^+ ions in KCl has been well studied.[1] The tunneling splitting of Δ is estimated as 23.1 GHz at zero electric field.[2] Paraelectric resonance (PER) is the study of cw microwave absorption of a dipole p_∞=5.3D[2,3] in the tunneling system; the PER studies, the ion-lattice relaxation time T_i is estimated as less than 10^{-9} sec.[4] We have tried a pulse PER method on lithium-doped KCl crystals.[5] Intense microwave pulse with electric field component $\vec{E}_1$ is applied on a sample which is sited at a place where E_1 is maximum in a TE_{101} cavity, and then, after termination of pulse, a transient recovery signal is observed at 9.4 GHz cw microwave with reduced power level by 47 dB from pulse power. The recovery signal shows a simple exponential curve with recovery time T_1 of 0.2 msec at 4.2 K depending on the sample size. Neither pure KCl nor lithium-doped KBr have shown similar recovery signal as are described here.

We have analyzed recovery signal on the basis of the electric analogy of the BPP scheme which had been successfully applied for the spin system[6]. Initial intensity of recovery signal $S(\tau)$, which is observed just after the termination of microwave pulse of width τ, is proportional to $[n_0-n(\tau)]$, where n_0 and $n(\tau)$ are the population differences of the tunneling states at the equilibrium and at the burnt state by pulse of duration time τ, respectively. When a value of $S(\tau)$ is plotted as a function of τ, for several microwave powers, it is found that $S(\tau)$ is saturated at longer pulse width; the saturated intensity is denoted as $S(\infty)$. A simple calculation based on BPP scheme shows that

$$S(\infty) - S(\tau) \propto \exp(-\tau/T_1 Z), \qquad (1)$$

where Z is a saturation factor defined as $Z^{-1} = 1+(2\pi/\hbar^2)(\vec{p}\cdot\vec{E}_1)^2 T_1 \rho_t$; T_1 is a relaxation time, and ρ_t is a state density of the final state for microwave transition. When $[S(\infty)-S(\tau)]$ is plotted as a function of τ, for several powers, it is found that eq.(1) well satisfied; this leads to

determining the values of T_1 and $(p^2\rho_t)$. It is found that the value of T_1 is the same as the recovery time T_1; this confirms the validity of our assumption. The value of $(p^2\rho_t)$ is 2.5×10^{-30} [(e·m)^{2}sec]; this value cannot be explained in terms of quantities obtained from the PER.[2,3]

Study of T_1 is on progress. Some of the preliminary results are as follows; (1) the temperature dependence. $(T_1)^{-1}$ as well as $(p^2\rho_t)$ are increased with decreasing temperatures. This dependence is similar to temperature dependence of phonon scattering probability obtained from thermal conductivity,[7] but it is absolutely contrary to that of T_i.[4] (2) the size effect. T_1 increases with increasing square cross sections of samples. This implies that a one-phonon, which is emitted in T_i at a microwave-excited Li^+ ion, will propagate through a sample until scattered at surface boundary; this process dominates the relaxation time. (3) the concentration dependence. T_1 values for samples of same size are constant in various concentration from 1×10^{17} to 1×10^{19} Li^+ ions/cm^3. This implies that a dipole-packet, which lies nearly off-resonance position in the PER line is quite independent each other and is well-localized.

References: (1) V.Narayanamurti and R.O.Pohl: Rev.mod.Phys. 42 201 (1970). (2) R.A.Herendeen and R.H.Silsbee: Phys.Rev. 188 645 (1969). (3) M.F.Deigen and M.D.Glinchuk: Sov.Phys.Usp. 17 691 (1975). (4) R.Osswald and H.C.Wolf: Phys.Status solidi b50 K93 (1972). (5) M.Matsuoka et al.: J.Phys.Soc.Japan 43 713 (1977). (6) N.Bloembergen, E.M.Purcell, and P.V.Pound: Phys.Rev. 73 679 (1948). (7) D.P.Pressini, J.P.Harrison, and R.O.Pohl: Phys.Rev. 180 926 (1969).

RELAXED EXCITED STATES OF $(Tl^+)_2$-TYPE CENTERS IN ALKALI HALIDES

Akira Matsushima and Atsuo Fukuda

Nagasaki University, Faculty of Liberal Arts, Japan 852

Tokyo Institute of Technology, Japan 152

There is a general belief that the interaction between the paired ions in $(Tl^+)_2$-type centers is directly reflected in the polarization characteristics of the luminescence. In Tl^+-type centers, on the other hand, the polarization characteristics are determined by the Jahn-Teller effect (JTE). For the purpose of understanding the relaxed excited states (RES's) responsible for the luminescence in $(Tl^+)_2$- as well as Tl^+-type centers, we have investigated its spectral and polarization characteristics at 4.2 K in KI:$(Ga^+)_2$, KI:$(In^+)_2$, and KI:$(Tl^+)_2$, and concluded that some of the RES's are principally determined by the JTE even in $(Tl^+)_2$-type centers; these RES's are localized in either of the paired ions.

In all the investigated emission bands, summarized in Table I, the degree of polarization (DP) as a function of azimuthal angle in the (001) plane is zero in the <110> direction and its absolute value is maximum in the <100> direction. Therefore, contrary to the conclusion made by previous investigators, the direction connecting the paired ions is <100>. Table I shows that the emission bands excitable by the A_Σ and A_Π absorption bands in the paired-ion center are located (1) close to the A_T emission band in the corresponding single-ion center (KI:$(Ga^+)_2$, KI:$(In^+)_2$), (2) close to the A_X emission band (KI:$(Tl^+)_2$), or (3) in the region where the corresponding single-ion center shows no emission band (KCl:$(Tl^+)_2$).

Since the interaction between the paired ions is small in the triplet excited states, the interaction can be regarded as a perturbation to the

RES's responsible for the A_T and A_X emission bands. The A_T RES corresponds to the three equivalent tetragonal minima on the $\Gamma_4^-(A)$ adiabatic potential energy surface (APES). The perturbation destroys the equivalence of the three distortions; one of them becomes slightly different from the other two. Thus the $A_{T\Sigma}$ and $A_{T\Pi}$ emission bands are observed separately as in $KI:(Ga^+)_2$. Although these two bands could not be separated in $KI:(In^+)_2$, the polarization characteristics observed indicate that the 2.76 eV emission band consists of at least two component bands, $A_{T\Sigma}$ and $A_{T\Pi}$. Since the A_X RES corresponds to the four equivalent trigonal minima on the $\Gamma_4^-(A)$ APES, the perturbation does not destroy the equivalence but causes the mixing of wavefunctions; the 3.00 emission band in $KI:(Tl^+)_2$ is single and does not consist of Σ and Π components. Even at 4.2 K no emission band was observed near the A_T emission band; the perturbation must stabilize the trigonal minima in $KI:(Tl^+)_2$. Thus the 2.61 emission band in $KCl:(Tl^+)_2$ can also be assigned to the A_X emission band perturbed by the interaction between the paired ions, though in $KCl:Tl^+$ the A_X emission band itself has not been observed.

Table I

	absorption			emission			
	A_Σ	A_Π	C_Σ	A_X	$A_{T\Sigma}$	$A_{T\Pi}$	C_Σ
$KI:(Ga^+)_2$	-	-	4.51	-	2.32,	2.40	3.14
$KI:(In^+)_2$	3.75		4.25	-	2.76		-
$KI:(Tl^+)_2$	4.24,	4.29	4.97	3.00	-	-	-
$KCl:(Tl^+)_2$	4.88		-	2.61	-	-	-

THE PART OF V_K CENTERS IN THE EQUILIBRIA BETWEEN CENTERS CREATED BY ELECTRON IRRADIATION AT LIQUID HELIUM TEMPERATURE IN KBr

E. MERCIER, A. NOUAILHAT and G. GUILLOT
Laboratoire de Physique de la Matière* - Bâtiment 502
Institut National des Sciences Appliquées de Lyon
20, Avenue Albert Einstein 69621 VILLEURBANNE CEDEX -France-

In KBr irradiated at 4 K, the primary centers, F and H centers, are stable, but the charged centers, F^+ and I centers (1), which are created by a poorly known secondary reaction (2), are more numerous. The growth kinetics have been described by several models (3). Experimental results have shown the existence of V_k centers in pure crystals (4), but their influence on the kinetics have never been studied.

In KBr, the V_k and H centers both have their absorption band peaking at 380 nm, which creates an experimental difficulty, so a global analysis of all the phenomena is necessary. We have systematically studied the growth kinetics of the F, F^+, I and 380 nm bands with an apparatus (5) allowing us to measure the simultaneous growth of several centers under irradiation up to very high concentration ($\sim 5.10^{19} cm^{-3}$) as well as their behaviour when the irradiation is switched off. The various related emissions of the crystal (luminescence and phosphorescence) are measured simultaneously and analysed. Our results have shown that the slow evolution (time scale of a few minutes) of the populations of centers, as well as the related emission which take place after the cut of the irradiation are due to the tunneling of the electrons of the F-centers to V_k centers, according to the pair reaction $F + V_k \rightarrow F^+ + h\nu_e$.

The theoretical analysis of the tunneling kinetics gives a good account for the experimental data, and the distribution of the pairs number versus the partner distance can be said to be constant. In the same manner, we have studied the tunneling $F^* + V_k$ by stimulating the F-centers in their absorption band.

The presence of V_k centers under irradiation is due to the charge compensation of the electrons trapped on F^+ centers. Their number has been

studied as a function of various parameters : energy deposition rate $\dot{\varepsilon}$, F^+ centers concentration, F^+/F ratio, and the results have been interpreted theoretically considering the dynamical equilibrium between their creation rate and their destruction rate related to their recombination with either free electrons or F-centers electrons.

The importance of the number of the V_k centers (concentrations higher than $1.14\ 10^{18} cm^{-3}$ are reached for $F \approx 2.78\ 10^{18} cm^{-3}$) and their part under electron irradiation at LHeT are thus clearly pointed out, as well as the necessity of taking them into account when analysing the defect growth kinetics.

---

(1) V.H. RITZ, Phys.Rev. 142 (1966) 505
J.D. COMINS, Phys.Stat.Sol. 33 (1969) 445
(2) N. ITOH, Journal de Physique C7, 12 (1976) 27
(3) G.J. DIENES, Journal of Nonmetals 1 (1973) 1965
I. TALE, D. MILLERS and E. KOTOMIN, J.Phys.C,Sol.Stat.Phys. 8 (1975)2366
(4) T.M. SRINIVASAN and W.D. COMPTON, Phys.Rev. 137 A (1965) 264
(5) E. MERCIER, G. GUILLOT and A. NOUAILHAT, Rev.Phys.Appl.12 (1977) 61

---

* Equipe de recherche associée au C.N.R.S.

RADIATION DEFECT BLEACHING IN ALKALI HALIDES AT HIGH TEMPERATURE AFTER PULSED ELECTRON BEAM IRRADIATION

D.K.Millers, E.A.Baumanis, A.E.Plaudis, J.J.Ābolipš
P.Stučhka Latvian State University, U.S.S.R.

The decay of radiation defects, such as F, H and V_4 centers in KBr and KCl after irradiation in the temperature range from 300 K to 900 K has been studied. Irradiation was achieved with a pulsed electron beam of a duration shorter than 20 ns, 300 amperes in peak current, about 0,3 MeV in energy. Absorption spectra were mesuared from 200 nm to 2100 nm.

The F, H and V_4 band decay rates strongly depends on temperature. The F band decay shows that more than two first order processes are going on in the temperature range from 300 K to ~ 500 K. This is in agreement with the results obtained by Ueta [1]. In the temperature range from ~ 500 K to 900 K one or more processes are responsible for the F band decay. The Arhenius plot of the F band lifetime dependence on temperature is linear for each process and gives the activation energies close to that of H center migration energy and $0,39\pm0,05$ eV and $0,23\pm0,04$ eV in the temperature range from 300 to ~500 K for KBr and KCl respectively.

Decay processes of the H and V_4 bands are similar to those the F band and the activation energies for the V_4 band decay are $0,40\pm0,05$ eV and $0,28\pm0,05$ eV for KBr and KCl respectively. It should be mentioned that we have not observed an H center decay process which could be responsible for the creation of V_4 center, probably because such a process is very fast [2].

Thus, it is concluded the main radiation defect bleaching process is the recombination of electron centers with interstitial halide centers in the temperature range from 300 K to ~ 500 K.

The F band decay processes gives the activation energies $1,12 \pm 0,03$ eV and $1,43 \pm 0,03$ eV in the temperature range from ~ 500 K to 900 K for KBr and KCl respectively. In this temperature range activation energies for H and V_4 bands decay are different to that of F band. By varying of the heating rate and heating time of the crystal at the irradiation temperature, it was estimated that in the temperature region from ~ 500 K to 900 K a considerable part of F centers interacted with thermally generated lattice defects, probably anionic vacancies. This process leads to formation of F_2^+ and / or other aggregate electron centers. The next step of radiation defect bleaching at these temperatures is recombination of electron centers with halide interstitial centers. This point of view is supported by a rise and decay of absorption bands observed in the infrared region of spectrum.

References

1. M.Ueta, J.Phys.Soc Japan, 23,(1967), 1265.
2. M.Saidoh, J.Hoshi, N.Itoh, Solid State Commun,, 13 (1973), 431.

OPTICAL DICHROISMS OF [Li]° DEFECTS IN MgO[1]

F. A. Modine
Solid State Division, Oak Ridge National Laboratory
Oak Ridge, Tennessee 37830

Stable [Li]° centers (i.e., electron holes trapped at substitutional Li^+ ions) were produced in MgO by quenching MgO:Li from high temperatures. The stress- and magnetically-induced optical dichroisms of the centers were measured and analyzed to obtain a large amount of information on the properties, structure and local environment of the centers. This information has significant implications for models of alkaline-earth-oxide V-type centers.

The magnetic circular dichroism (MCD) spectrum has a nearly absorption-derivative-like shape and a temperature-dependent intensity which imply that the MCD derives from the combination of a magnetically-induced spin polarization in the ground state and a strong spin-orbit coupling in the excited state.[2] The ground-state paramagnetic resonance spectrum of the [Li]° center can be detected as a reduction in the intensity of the MCD. This confirms that [Li]° centers produce the observed optical spectra; and, it also substantiates the origin suggested for the magneto-optical phenomena. The ion model of Bartram et al.,[3] which considers the optical transitions to be between the Stark-split 2p levels of a single O^- ion, gives a qualitative explanation of the MCD. This conclusion is contrary to that of Izen et al.,[4] and it advances the ion model and also the mixed-ion-polaron model, proposed by Norgett et al.[5] Schirmer et al.[6] have proposed the polaron model in which optical transitions are between the vibronic potential wells that correspond to hole localization in the σ orbitals of different O^{2-} ions. In the mixed-ion-polaron interpretation, both the ion- and polaron-model transitions contribute to the optical band. A polaron-model explanation of the MCD appears untenable unless the model is modified by assuming significant π-orbital contributions to the excited-state wave functions. If configurational and magnetic-field-induced admixtures of π-orbitals are included, a qualitative interpretation of the MCD spectrum can be obtained. A quantitative explanation of the MCD based upon any of the proposed models appears to require stronger magnetic interactions than are expected for O^- ions.

The stress-induced linear dichroism has a temperature-dependent intensity and a mixed absorption-like and absorption-derivative-like shape which reveal that it results predominantly from a stress-induced alignment of inherently anisotropic $[Li]^{\circ}$ defects. The low-temperature behavior of the dichroism reveals that the defect alignment is not controlled by stress and temperature alone. Apparently, there are internally-generated stresses or electric fields in the crystals that tend to pin the centers into random orientations. The higher- and lower-energy portions of the absorption band respectively derive from states predominantly of A_1 and E symmetry. The ion model consequently gives an incomplete description of the defect, unless an A_1 symmetry component is included in the excited state. An interpretation of the defect anisotropy, based upon Henderson's value[7] for the elastic moment gives a ratio of transition-dipole strengths, $D_{\parallel}/D_{\perp} \simeq 2.2$ and an energy splitting, $E_{\parallel}-E_{\perp} \simeq 0.37$ eV, for light polarized parallel ($\parallel$) and perpendicular ($\perp$) to the defect symmetry axis. These values are well explained by the polaron model, and there is no evidence for an ion-model contribution to the optical band. The low-temperature stress-induced alignment of the defects is hindered by random crystal fields which can be described by an effective temperature, $T_c \simeq 11$ K. The fields can be attributed to a distribution of charged point defects, but they cannot be attributed to F^+ centers.

---

1. Research sponsored by the Energy Research and Development Administration under contract with Union Carbide Corporation.

2. F. A. Modine, Solid State Commun. 20, 1097 (1976).

3. R. H. Bartram, C. E. Swenberg and J. T. Fournier, Phys. Rev. 139, A 941 (1965).

4. E. H. Izen, R. M. Mazo and J. C. Kemp, J. Phys. Chem. Solids 34, 1431 (1973).

5. M. J. Norgett, A. M. Stoneham and A. P. Pathak, J. Phys. C 10, 555 (1977).

6. O. F. Schirmer, P. Koidl and H. G. Reik, Phys. Status Solidi (b) 62, 385 (1974).

7. B. Henderson, J. Phys. C 9 L579 (1976) and private communication.

INVITED PAPER

BROADLY TUNABLE LASERS USING COLOR CENTERS IN THE ALKALI HALIDES

L. F. Mollenauer
Bell Telephone Laboratories
Holmdel, New Jersey 07733

ABSTRACT

Certain color centers in the alkali halides can be used to make efficient, optically pumped, broadly tunable ("dye-like") lasers. To date, successful cw laser action has been obtained in the color center types $F_A(II)$[1], $F_B(II)$[2], and F_2^+[3]. With these three types of center, the net tuning range is $0.9 \lesssim \lambda \lesssim 3.2$ μm at least. This entire range is of importance to molecular spectroscopy, laser-induced chemical reactions, and pollution detection. The wavelengths $\gtrsim 2.2$ μm are of especial importance, since they correspond to the fundamental resonance of most hydrogen bonds. Accordingly, commercial production of the longer-wavelength color center lasers can be expected soon. The shorter wavelengths ($0.9 \lesssim \lambda \lesssim 1.4$ μm) correspond to the optimal transmission range for fiber-optic communications. And, finally, the entire range is of interest to the physics of semiconductors.

High-powered pulsed operation of the type II centers has also been achieved[4], with peak output powers on the order of 10 kW, again (as in the case of cw operation) with no bleaching or aging effects, as long as the crystals were properly cooled. One can easily project from this result that oscillator-amplifier combinations capable of ~100 kW or greater peak output powers should be possible. Such a source would be of great interest for non-linear studies. Also, by using the stimulated Raman effect, the

output of such a pulsed color-center laser could be translated down, in a single step, to just about any other frequency of interest to molecular physics.

Frequency definition of the color center lasers is excellent, with performance in this respect exceeding that obtained with the best dye lasers. In cw operation, bandwidths of less than 200 kHz have been reported.[5] In high-powered pulsed operation, it should be possible to make a source whose frequency width is essentially Fourier-transform limited. Such frequency definition would represent many orders of magnitude improvement over the best performance attainable from the only other high-power tunable sources in the infrared, the parametric oscillators.

The usefulness of color centers to quantum electronics has been further enhanced through the recent discovery that U to F center conversion can be initiated by a two-photon absorption of a high-powered, UV laser beam.[6] By interfering the UV laser beam with itself, one can write thick gratings of any desired period greater than half the UV wavelength. Gratings of F_A(II) centers written in that manner have already been used to make successful distributed feedback lasers.[4] In a more general sense, the two-photon coloration process should allow the creation of a host of integrated optics devices.

REFERENCES

1. L. F. Mollenauer and D. H. Olson, J. Appl. Phys. 46, 3109 (1975).
2. G. Litfin et al, submitted to Appl. Phys. Letters.
3. L. F. Mollenauer, submitted to Optics Letters.
4. G. C. Bjorklund, L. F. Mollenauer, and W. J. Tomlinson, Appl. Phys. Letters 29, 116 (1976).
5. R. Beigang et al, submitted to Optics Comm.
6. L. F. Mollenauer, G. C. Bjorklund, and W. J. Tomlinson, Phys. Rev. Letters 35, 1662 (1975).

THERMAL CONDUCTIVITY OF DAMAGED MgO*

A. R. Moodenbaugh, C. L. Tsai, H. Weinstock, IIT, Chicago, IL 60616
and Yok Chen, ORNL, Oak Ridge, TN 37830

Low temperature (0.4 K to 80 K) thermal conductivity studies of fast-neutron irradiated[1] and deformed[2] MgO crystals are analyzed with a Debye model as modified by Callaway,[3] and utilizing a contribution to scattering from density variations as proposed by Walton.[4] Additional measurements on irradiated samples of two doses (2×10^{18} n·cm^{-2} and 2×10^{19} n·cm^{-2}) and a deformed sample (compressed approximately 2%) have been made both prior to and after annealing to 750°C.

Callaway's[3] modification of the Debye theory gives for thermal conductivity,

$$K(T) = \frac{k_B}{2\pi^2 v_s}\left(\frac{k_B T}{\hbar}\right)^3 \int_0^{\frac{\theta_D}{T}} dx\, \frac{x^4 e^x}{(e^x-1)^2}\, \tau(1+\beta\tau_n^{-1})$$

where k_B is Boltzmann's constant, v_s the sound velocity, T the temperature, θ_D = 945 K (Debye temperature) $x = \hbar\omega/k_B T$ (ω, the phonon frequency). β is itself an integral expression to take into account the effect of the three normal phonon process,[5] $\tau_n^{-1} = H_n \times T^5$ (due to normal processes) and τ is defined by

$$\tau^{-1} = \tau_B^{-1} + \tau_{imp}^{-1} + \tau_n^{-1} + \tau_u^{-1} + \tau_p^{-1}.$$

where $\tau_B^{-1} = B$, $\tau_{imp}^{-1} = Cx^4T^4$, $\tau_u^{-1} = Fx\cdot\exp(-\theta_D/GT)$, and $\tau_p^{-1} = Rx^4T^4$ for $x < \hbar\omega_o/k_B T$ and a constant for $x > \hbar\omega_o/k_B T$. The terms are due to boundary scattering, impurities, and density variations, respectively.

Values obtained for B, C, and R are listed below:

Sample	B(sec^{-1})	C(sec^{-1} K^{-4})	R(sec^{-1} K^{-4})
Pure	3.15×10^6	1.6	0.0
Deformed	7.86 "	3.0	4.0
Deformed, annealed	3.15 "	3.0	6.5
n-irrad. (2×10^{18}n cm^{-2})	83.9 "	10.0	250
n-irrad. anneal (2×10^{18})	57.2 "	2.0	10
n-irrad. (2×10^{19}n cm^{-2})	14.5 "	10.0	4000

Some general observations concerning the variation of these coefficients can be made. First, a comparison of the boundary terms indicates that the original single crystal MgO samples have internal crystal boundaries introduced by deformation and irradiation. The term C shows that deformed and irradiated samples both have point defects introduced which are for the most part removed on annealing. The most interesting effect is evident in the coefficient R associated with plateau scattering. This term was originally proposed to account for the thermal conductivity of disordered materials, many having a plateau region for which thermal conductivity does not vary much with temperature near 10-20 K. The physical origin of this scattering is a density variation in the material — long wavelength phonons will see just the average density while shorter wavelength phonons ($\leq$ 10 Å) will be mostly Rayleigh scattered. It is understandable that this source of scattering appears in n-irradiated samples, since the relatively high energy neutrons can, on impact, move around a significant number of Mg and O atoms to provide the needed density variations. The annealing process gives ambiguous results in the case of the deformed sample, since R rises after annealing. However, the fitted curves are probably not sensitive enough for such a small variation in R to be significant. Annealing of the n-irradiated (2×10^{18} n·cm^{-2}) sample seems to reduce this source of scattering significantly.

---

*Supported by U. S. Energy Research and Development Administration.

1. D. S. Kupperman, G. Kurz and H. Weinstock, J. Low Temp. Phys. 10, 193 (1973).

2. J. B. Hartmann, H. Weinstock and Y. Chen, Phonon Scattering in Solids, L. J. Challis, V. W. Rampton, and A. F. G. Wyatt, eds. (Plenum Press, New York 1976) p. 190.

3. J. Callaway, Phys. Rev. 113, 1046 (1959); J. Callaway, Phys. Rev. 122, 787 (1961).

4. D. Walton, Solid State Commun. 14, 335 (1974).

5. I. S. Ciccarello and K. Dransfeld, Phys. Rev. 134, A1517 (1964).

6. P. G. Klemens in: Solid State Physics, ed. by F. Seitz and D. Turnbull (Academic Press, New York, 1958) V. 7, p. 87.

DEVELOPMENT OF HYDROGEN DOPED CRYSTALS FOR FAST NEUTRON DETECTION*

S. P. Morato, B. M. Rzyski and K. S. V. Nambi**
Instituto de Energia Atomica - CPRD AMD
Caixo Postal 11049, São Paulo, SP - Brazil

The state-of-the-art of accomplishing fast neutron detection using luminescent crystals has remained far from satisfactory. The most significant attempts so far have been the employment of proton recoil techniques by mixing thermoluminescent crystal powder with hydrogen rich materials. These methods have had limited success so far largely because of the inefficiency of the mixture geometry and the operational problems involved when using this mixture for routine dosimetry.

This work describes a different and successful attempt to improve the neutron detection efficiency that consisted of the utilization of a system such as CaF_2:RE:H^- luminescent crystal. We studied the thermally activated luminescence of CaF_2 crystals doped with rare earths before and after the diffusion of hydrogen for various exposures to fast neutrons from an Am-Be source or a van de Graaff accelerator. Definite increases in the ratio of the neutron to gamma sensitivity of the hydrogenated samples were obtained. This fractional gain reached a factor of 80 for CaF_2:Dy:H^-.

*Supported by CNEN and FAPESP

**Present Address: Health Physics Division, Bhabha Atomic Research Centre.

ANISOTROPIC ELECTRIC FIELD EFFECTS ON THE SPIN RELAXATIONS OF THE F_A(Li) CENTERS IN KCl.

Yuzo MORI, Tohru WATANABE, and Hiroshi OHKURA

Department of Applied Physics, Osaka City University, Osaka, Japan 558

Electric field effects on the longitudinal and transverse spin relaxation times, T_1 and T_2, of the F_A(Li) centers in KCl were studied at 1.5 K and at the magnetic field of about 3340 Oe by means of saturation recovery and microwave-saturation methods of ESR signals, respectively. A saturation recovery signal was shown by a sum of two exponential curves. Electric field effects were solely found in the slow component which we denoted as T_1. T_2 was determined by theoretical curve-fitting of modified Castner's form with observed saturation curve.[1)]

Both T_1 and T_2 are increased with increasing the electric field when the field is applied in the plane perpendicular to the center symmetry axis of the optically aligned F_A centers; the characteristics are more remarkable in the case when the field is applied to <110> direction than the case applied to <100> as shown in Figs.1 and 2. No change in T_1 and T_2 was observed when the field is applied parallel to the symmetry axis. In addition to these field effects, the following four facts were observed in the temperature region from 1.5 to 4.2 K. (1) absolute value; $T_1=7.8\times10^{-3}$ sec and $T_2=2.0\times10^{-8}$sec at 4.2 K for the $F_A(^7Li)$ center. (2) slight temperature dependence of T_1 and T_2^{-1} which is parallel manner with each other. (3) isotope effect of the Li^+ ion; $T_1(^7Li)=1.3T_1(^6Li)$. (4) isotropic T_1 and T_2 with respect to the magnetic field and the symmetry axis.

Theoretical forms of the field dependence of T_1 and T_2 were obtained through the Redfield theory[2)] on the basis of the idea that both relaxations are caused by an interaction with a tunneling system of the Li^+ ion. Solid lines in Figs.1 and 2 are theoretical plots with the fitting parameters at zero electric field, rms of fluctuating magnetic field $H_f=4$ Oe with correlation time $\tau_0=2.4\times10^{-9}$ sec, and tunneling splitting $\Delta^7=2\times10^{-4}$ eV and an induced electric dipole moment $p_\infty=0.55$ eA of the Li^+ ion; facts (1) and (2) can be consistently explained in terms of the forms with these values. The values are compared with already known values of $\Delta^7=1.0\times10^{-4}$ eV[3)] and the ion-lattice relaxation time $T_i\sim10^{-9}$ sec of the isolated

impurity Li^+ ion in KCl and a classical electric dipole moment p_∞=1.0 eA of the F_A(Li) center[5] which have been obtained by the PER and the Stark effect measurements, respectively. To solve the discrepancies found in Δ^7 and p_∞ is a future problem in our research.

The amount of H_f can be estimated as rms value of fluctuating hyperfine field at hf-coupled surrounding ions. In this argument, a tunneling motion of the Li^+ ion is approximated by a fluctuating motion of an electric dipole which produces electric field at the ions, so that the hf-field is fluctuatingly modulated. Judging from the electric-field induced shift of ENDOR frequency of the ^{39}K nucleus in the first shell,[6] it is shown that electric field of 2×10^6 V/cm induces H_f of 4 Oe; this field strength is reasonably caused by a dipole moment of 0.2 eA separated by the interionic distance. The fact (4) can be explained on the basis of this argument.

The fact (3) implies that a coupling Hamiltonian between the spin and the tunneling systems is inversely proportional to the mass of the Li^+ ion; detailed mechanism has not been clarified yet.

Fig. 1

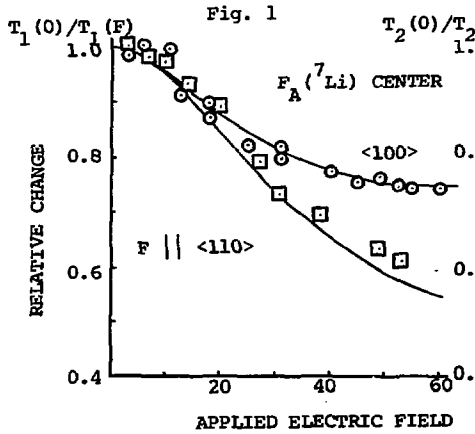

Fig. 2

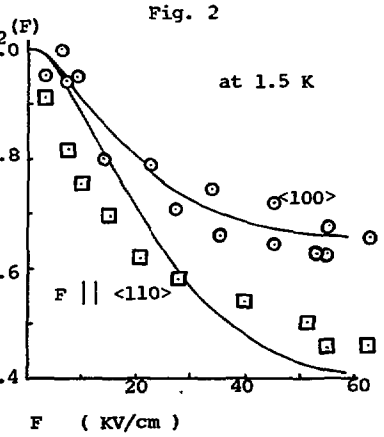

References: (1)H.Ohkura et al.:J.Phys.Soc.Japan 41(1976)707. (2)C.P. Slichter: Principles of Magnetic Resonance (Harper and Row, N.Y.,1963)p.153. (3)R.A.Herendeen and R.H.Silsbee:Phys.Rev. 188(1969)645. (4)R.Osswald and H.C.Wolf:Phys.Stat.Sol. (b)50(1972)K93. (5)F.Rosenberger and F.Lüty:Solid State Comm. 7(1969)983. (6)V.G.Grachev and Yu.V.Fedotov:Soviet Phys.-Solid State 16(1975)1717.

THERMALLY STIMULATED DEPOLARIZATION CURRENTS IN THORIUM DIOXIDE*

R. Muccillo and L. L. Campos
CPRD-AMD, Instituto de Energia Atômica, S. Paulo, Brazil

Thermally Stimulated Depolarization Currents (TSDC) have been measured in Thorium Dioxide ceramic discs in the temperature range 100 K-350 K. The induced polarization is found to be due to grain boundary-enhanced migration of charge carriers in the bulk of the specimen with trapping at grain boundaries. The thermal activation energy for releasing charge carriers from trapping sites upon heating up the pre-biased specimen is determined to be ~ 0.3 eV, suggesting that the mobile charge carriers are O^{2-} ions. It is also found that the higher the sintering temperature of cold-pressed ThO_2 discs, the lower the integrated TSDC spectrum, showing that pores and/or grain boundaries are acting as trapping sites. The integrated TSDC spectrum could then be used for the study of grain growths in the bulk of ceramics and consequently for the determination of the average grain size attained in the kinetics of grain growth.

*Research work supported by Comissão Nacional de Energia Nuclear.

VIBRATIONAL RAMAN SCATTERING INDUCED BY JAHN-TELLER SYSTEMS IN POLAR CRYSTALS

E. Mulazzi and N. Terzi
Istituto di Fisica dell'Università di Milano and Gruppo Nazionale di Struttura della Materia del C.N.R., via Celoria 16, 20133 Milano, Italy.

Recently particular attention has been paid to the Raman scattering induced by Jahn Teller impurities in polar crystals (1,2). In these Raman spectra it is possible to observe the vibronic levels structure in the low frequency region and vibrational structure due to the first order contribution of the phonon densities of states transforming according to the irreducible representations of the point group of the impurity site symmetry in the rigid lattice.

Here we present only the study of the vibrational part of the Raman scattering due to Jahn-Teller impurities in cubic and tetragonal symmetry site. We evaluate the first order Raman cross section in different polarization geometries taking into account the properties of (i) the ground degenerate electronic state and of (ii) the electric dipole moment for the virtual electronic transition, and of (iii) the electron-phonon interactions in the ground and all the excited electronic states.

Through the study of (i) and (ii) one can determine the selection rules for the densities of phonon states determining the polarized scattering spectra, through the (iii) one can determine the weight of the densities of phonon states in the polarized spectra. We find that the selection rules for the densities of phonon states depend on the degeneracy of the ground electronic state, then the selection rules determined for a degenerate ground state are <u>always</u> different from those determined for a singlet ground electronic state. The case of a Γ_3^+ electronic doublet ground state at a cubic crystal site is treated in detail, by considering all the excited states transforming following Γ_4^- and Γ_5^-.

1) S. Guha and L.L. Chase, Phys. Rev. B <u>12</u>, 1658 (1975).
2) L.L. Chase and C.H. Hao, Phys. Rev. B <u>12</u>, 5990 (1975).

COMPUTER SIMULATION OF CORRELATION EFFECTS IN SUPERIONIC CONDUCTIVITY AND DIFFUSION*

G. E. MURCH AND R. J. THORN
Chemistry Division, Argonne National Laboratory,
Argonne, Illinois 60439

It is generally acknowledged that the lattice gas model provides a useful basis for developing at least a conceptual understanding of superionic conductivity and diffusivity [1]. In such a lattice gas model one treats the conduction plane as a one component system consisting of, for example, nearest neighbor repelling particles (ions) and vacant sites. If all sites are equivalent a priori then the lattice gas is an important analogue of the Ising anti-ferromagnet in an external field.

Correlation between successive jumps of the ions is an important contributor to the ionic conductivity and tracer diffusion but it has not been possible to assess such effects rigorously in analytical treatments [2,3]. We have used computer simulation to calculate both charge carrier and tracer correlation factors, f_c and f_t, in sodium β"-alumina. Firstly, a lattice in thermodynamic equilibrium was constructed. Cooperative diffusion was then simulated by modifying the jump frequency according to the local environment. The paths of all the ions were followed for 50-100 jumps per ion and f_t in the $\hat{x}$ direction was calculated from:

$$f_{x,t} = \frac{\langle X2 \rangle}{n_x \lambda_x^2} , \qquad (1)$$

where $\underline{X}$ is the vector displacement, n_x is the number of jumps, λ_x is the component of the jump distance and <> denotes a statistically weighted average over all possible paths.

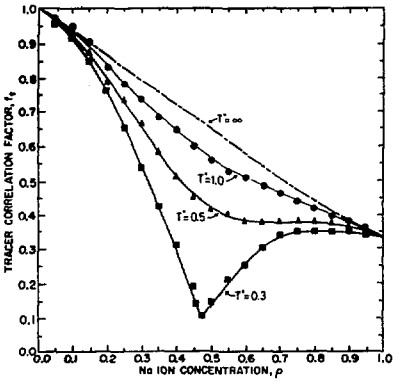

Fig. 1. The tracer correlation factor at T* = 0.3, 0.5, 1.0 and ∞ as a function of concentration.

The results for f_t as an average of $\hat{x}$ and $\hat{y}$ directions are shown in Fig. 1 at 4 values of $T^*(\equiv|kT/\varepsilon|$, ε = interaction energy). The ions execute a random walk near ρ = 0.0 and diffuse by the vacancy mechanism near ρ = 1.0. As $T^* \to 0$ f_t drops, particularly so near ρ = 0.5. The ordered region is centered around ρ = 0.5 and has an order/disorder temperature at

$T^* = 0.38$. In an ordered environment an ion which makes a disordering-like jump will tend next to make a reordering-like jump and $f_t \to 0$.

The charge carrier correlation factor, f_c includes only the non-random motion of *indistinguishable* particles and *cannot* be calculated from eq. (1). We have deduced an indirect method of calculating f_c by simulating ionic conductivity and determining the average drift of the ions <X> in an electric field, E. f_c is then given by:

$$f_{x,c} = \frac{2kT\langle X\rangle}{qE_x n_x \lambda_x^2}, \qquad (2)$$

where q is the charge.

The results for f_c are shown in fig. 2. The analytical treatment of Sato and Kikuchi [2] predicted that $f_c = 1$ in β"-alumina. Clearly this is not correct at all. There is a temperature dependence of f_c for similar reasons as for f_t. The link between the tracer diffusivity and the ionic mobility is made through the generalized Nernst-Einstein relation:

$$D_t/u = kTH_R/q, \quad H_R = f_t/f_c$$

The Haven ratio, H_R, is plotted in fig. 3 at $T^* = 0.5$ (results for the other temperatures are very similar). The minima in f_t and f_c cancel almost completely and H_R remains between the geometrically dependent limiting values of unity and 1/3.

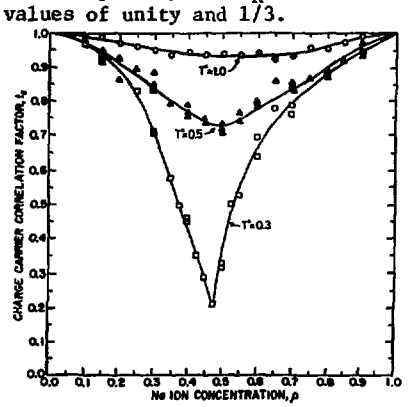

Fig. 2. f_c at $T^* = 0.3, 0.5, 1.0$

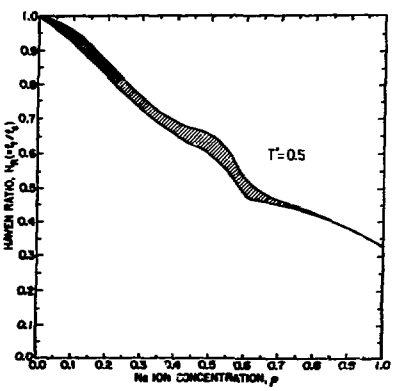

Fig. 3. H_R at $T^* = 0.5$.

References

*Work performed under the auspices of the USERDA.

1. G. D. Mahan and W. L. Roth, *Superionic Conductors*, (N.Y.: Plenum 1976).
2. H. Sato and R. Kikuchi, J. Chem. Phys. 55, 677, 702 (1971).
3. G. E. Murch and R. J. Thorn, Phil. Mag. 35, 493 (1977).

POSITIVE ION DAMAGE AND RADIATION ANNEALING IN MAGNESIUM OXIDE*

R. B. Murray, F. S. Uralil, C. M. Fou and W. T. Franz
Physics Department, University of Delaware
Newark, Delaware, U.S.A. 19711

The number of anion-vacancy defects produced in MgO single crystals at room temperature by MeV H^+, He^+ and N^+ ions was obtained from the optical absorption spectrum of the F and F^+ bands at 250 nm. These data, and earlier results on Ne^+ bombardment of MgO from another laboratory, were compared with calculated values based on the Kinchin and Pease theory for elastic collision cascades. The calculated values are considerably higher than those observed, and the ratio of calculated to observed defect concentrations depends on the mass of the projectile, as seen in the table below:

	Anion Vacancy Defects per Projectile		
Projectile	(Calculated)	(Observed)	Ratio(calc/observed)
0.5 MeV H^+	3.0	0.8	4
2.0 MeV H^+	4.8	1.0	5
0.5 MeV He^+	28	2.5	11
2.0 MeV He^+	32	3.0	11
0.5 MeV N^+	279	~13	21
3.0 MeV Ne^+	600	31[1]	20

The fact that fewer defects are observed than calculated is customarily attributed to the recombination of close vacancy-interstitial pairs, and is described as "radiation annealing". We have examined the above results on the basis of two models of vacancy-interstitial recombination: (1) an athermal, spontaneous recombination for pairs separated by a distance less than a critical separation distance R_c, a property of the host lattice, and (2) a thermal spike mechanism in which local heating by a recoil atom promotes interstitial diffusion. The data are not consistent with model (1) as R_c is found to depend on the identity of the projectile, and the calculated dependence of defect concentration on radiation fluence is in disagreement with experiment. Data are reasonably

consistent with the thermal spike model of Altovskii.[2]

---

*Work supported by the National Science Foundation.

(1) B. D. Evans, Phys. Rev. B9, 5222 (1974).

(2) I. V. Altovskii, Rad. Eff. 17, 275 (1973).

STUDIES ON C CENTER COLLOIDS AND ANNEALING OF RADIATION DAMAGE IN NaCl CRYSTALS

Y. V. G. S. Murti and N. Sucheta
Department of Physics, Indian Institute of Technology,
Madras 600036, India

Studies on photo-induced F⇌C transformations in γ-irradiated and X-irradiated crystals of NaCl have led to the first proposal of a model of the C center: an aggregate of four Na atoms formed near dislocations. We measured the changes in the electrical conductivity accompanying the evolution of the colloids from F centers and their subsequent annihilation. Coloration suppresses the usually dominant cation vacancies. In crystals containing F centers, the conductivity is electronic with an activation energy of 2.6 eV representing the thermal ionization energy of F centers, the dissociation occurring in the presence of a nearly fixed number of anion vacancies. The magnitude of the conductivity corresponds to a low level of ionization. The coagulation apparently involves migration of F centers by an α-center mechanism.

The conductivity of crystals exclusively containing C centers shows activation energies of 1.06 eV and 0.78 eV during heating and cooling runs, respectively. The conductivity σ(t) shows a maximum on standing at temperatures where C centers decay. These results are interpreted in terms of trapping of cation vacancies by halogen interstitials, the thermal release of which governs the recovery process. C center annihilation follows first order kinetics with activation energy 1.9 eV. Studies on thermoluminescence and isothermal decay of luminescence lend support to the interpretation. The glow curves observed in crystals containing F centers or C centers are similar, and neither are amenable to analysis in terms of conventional models based on electron untrapping. The isothermal decay reveals several stages of decay, one having an activation energy of 1.8 eV. Theoretical calculations made on the energies of halogen interstitials show that the thermal dissocation of the chlorine atom from vacancy traps and its migration via a direct interstitial mechanism provide the controlling step in the annealing of radiation-induced defects in NaCl.

RELAXED EXCITONIC STATES IN $CdBr_2$ AND $CdBr_2$:I

H. NAKAGAWA, K. HAYASHI and H. MATSUMOTO
Department of Electronics, Fukui University, Fukui, Japan

Cadmium bromide is an ionic crystal of layer structure. The luminescence intensity, life time and linear polarization have been measured in $CdBr_2$ and $CdBr_2$:I as a function of temperature to investigate the relaxed excitonic states in cadmium halide crystals.

Under excitation with UV-light in the regions of intrinsic excitonic absorption or of localized excitonic absorption due to doped I^--ions[1], two prominent emission bands appear as shown in Fig. 1, the UV- (3.30 eV) and the Y- (2.15 eV) emission bands in $CdBr_2$ and the UV- (3.35 eV) and the G- (2.52 eV) emission bands in $CdBr_2$:I[2]. As the temperature T rises, the UV-emission changes into the Y- or the G-emission around 60K.

Values of degree of polarization $P = (I_\perp - I_{//})/(I_\perp + I_{//})$ obtained at LHeT or LNT are also shown in Fig. 1 for each emission band, where $I_\perp$ and $I_{//}$ are intensities of polarized luminescence, perpendicular and parallel to the crystallographic c-axis, respectively. The values of P of the UV-emission decrease from high to low energy sides and, as shown in Fig.2, the ratio $I_{//}/I_\perp$ decreases exponentially with $1/T$. This indicates that for the UV-emission are responsible two close excited states which exchange popu-

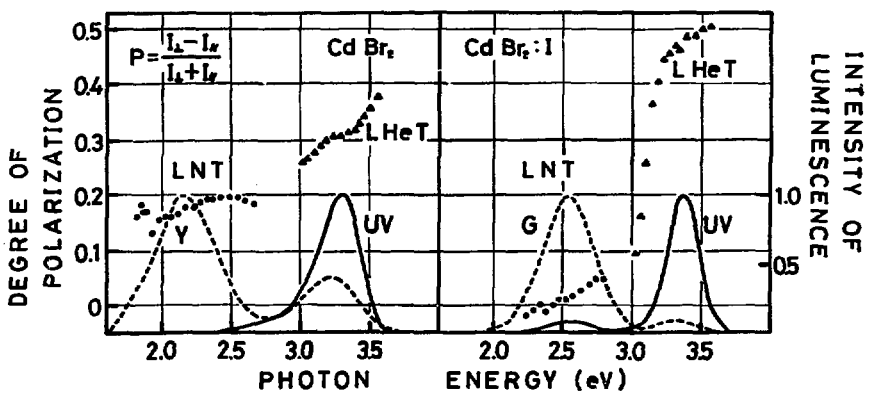

Fig. 1

lation by thermal activation processes. The values of P of the Y- and the G-emission are 0.2 and zero independently of T.

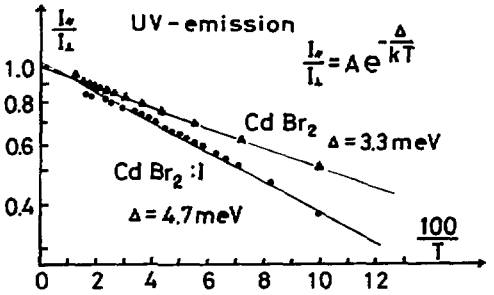

Fig. 2

The life time (0.6 μs in $CdBr_2$ and 0.3 μs in $CdBr_2$:I) and intensity of the UV-emission are independent of T below 50 K and decrease rapidly above 50 K by thermal activation. This suggests that the UV-emission should be related to a parity allowed transition. Since the life time of the Y-emission consists of two components of 1 and 20 μs at LNT and their values decrease gradually with increasing T, the Y-emission may be associated with parity forbidden transitions, for which forbiddenness is partially broken by lattice vibrations of odd parity. The G-emission in $CdBr_2$:I , the life time of which is 3.5 μs independently of T, is also associated with parity forbidden transitions which are supposed to be partially allowed by the static deformation caused by the presence of I^--ions.

Experimental results described above are explained on a supposition that the relaxed excitonic states are approximated by the excited states of the $[Cd^{2+}X_6^-]^{4-}$-complex molecular ion ($X^- = Br^-, I^-$) of D_{3d} symmetry. Taking the electrostatic and spin-orbit interactions into consideration, the energy levels of this complex molecular ion will be discussed in detail in connection with the behaviors of the UV-, Y- and G-emission.

Validity of the model for the relaxed excitons will be also examined by the data on polarization correlation of luminescence with exciting light and the experimental results of the same kind in the $CdCl_2$-systems.

References

1) H. Nakagawa, T. Abe and H. Matsumoto: J. Phys. Soc. Japan 40 (1976) 1363.

2) H. Matsumoto and H. Nakagawa: J. Luminescence 12 (1976) 403.

TRANSMISSION ELECTRON MICROSCOPE STUDIES OF Li-DOPED MgO*

J. Narayan, M. M. Abraham, Y. Chen and H. T. Tohver†
Solid State Division, Oak Ridge National Laboratory
Oak Ridge, Tennessee 37830, USA

A recent study has shown that thermal quenching from high temperatures, or a high dose electron irradiation at ambient temperature, of lithium-doped MgO crystals results in substitutional lithium ions, each with a tightly bound hole, forming the stable [Li]° defects.[1] The stability of these [Li]° defects is an anomaly and appears to be inconsistent with previously held concepts of production and stability of the entire class of hole defects in the oxides. It has been speculated[2] that there exist in these crystals precipitates containing lithium, that substitutional Li^+ ions form a localized lithium-rich environment surrounding these precipitates, and that these ions trap holes to form the [Li]° centers. We report here the results of transmission electron microscopy studies on as-grown MgO: Li crystals in which Li_2O precipitates are observed, and the effects of high-temperature quenching and ionizing radiation on these precipitates.

Figure 1a shows an electron micrograph of an as-grown MgO:Li crystal. The black spots are precipitates, with average precipitate size 220 Å and the density 2.5 x $10^{13}cm^{-3}$. From stereomicroscopy and tilting experiments, the shape of these precipitates was determined to be octahedral. Detailed microdiffraction studies made on individual precipitates clearly identified them as Li_2O having the fluorite structure. On annealing the same microscope sample for 12 minutes in air and quenching from 1200°C, the average size of the precipitate was reduced to 150 Å, while the cluster density remained approximately the same (Fig. 1b). The effect of e^- irradiation was studied by irradiating the as-grown thin samples in-situ in a 200 keV electron microscope (flux $\simeq$ 2 x $10^{18}e^-/cm^2$). A reduction in precipitate size of about 15% was observed after an estimated electron dose of 5 x $10^{20}e^-/cm^2$. From this result the effective cross section was

*Research sponsored by ERDA under contract with Union Carbide Corporation.
†On Sabbatical leave from University of Alabama, Birmingham, Alabama.

estimated $\sim 10^3$ barns. These studies suggest that precipitates act as a source for the formation of the stable [Li]° centers.

1. M. M. Abraham, Y. Chen, L. A. Boatner and R. W. Reynolds, Phys. Rev. Letters, 37, 849 (1976).
2. Y. Chen, H. T. Tohver, J. Narayan and M. M. Abraham, "Production and Stability of [Li]° Defects in MgO Single Crystals" (this proceeding).

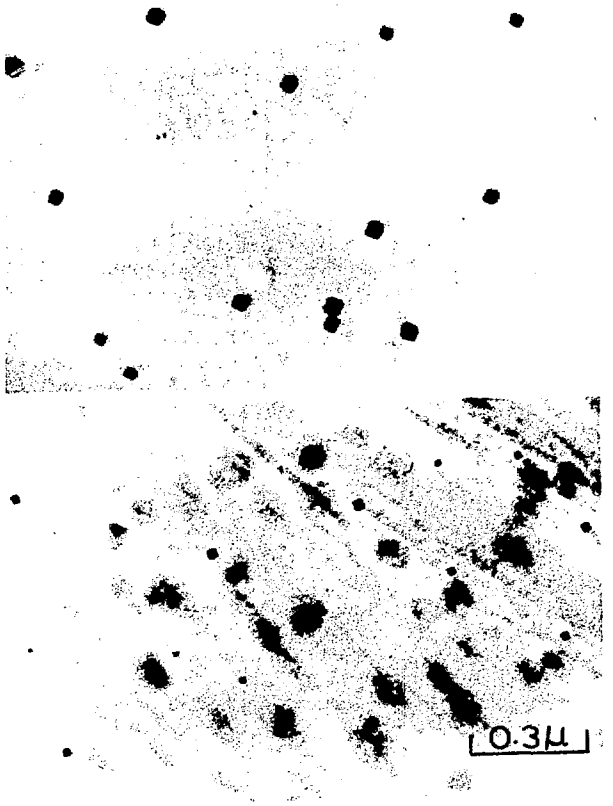

Fig. 1. Bright field electron micrographs under kinematical diffraction conditions: a) Li_2O precipitates in as-grown MgO:Li, b) Li_2O precipitates after quenching from high temperature (the same microscope sample as Fig. 1a, but not the same area).

ELECTRICAL-CONDUCTION-INDUCED AGGREGATION OF DEFECTS AND THERMAL BREAKDOWN IN MgO*

J. Narayan, R. A. Weeks and E. Sonder
Solid State Division
Oak Ridge National Laboratory
Oak Ridge, Tennessee 37830

Recently it was reported that when MgO single crystals (sources: Norton Company and ORNL) were subjected to a DC electric field (~1000 v/cm) at high temperatures for extended periods of time (>100 hours), the electrical current passing through the specimens increased with time by several orders of magnitude until catastrophic breakdown occurred.[1] Here we report on the results of transmission electron microscopy studies made on the samples that had been electric field treated at 1200°C till just before the breakdown. These specimens were cooled to room temperature with the field applied and then thinned by chemical polishing for electron microscopy.

This investigation revealed the presence of a type of dislocation loop, not previously observed in this material, with a<100> Burgers vectors lying in {001} planes. Fig. 1a, b and c show the presence of these loops in large grains enclosed by subboundaries, near a dislocation and at a subboundary respectively. There are two types of loops in Fig. 1a, denoted as α and β. It has been shown from the contrast analysis that the α loop has a[001] Burgers vector and lies in (001) plane, the β loop has a[010] Burgers vector and lies in (010) plane. Most of the observed loops in Fig. 1b and c are the α type loops, except for a few loops denoted as γ which have a/2[101] Burgers vector. a/2<101> type of loops are commonly observed in this material. The above loop substructure was found to have two characteristics; firstly the development of the substructure was a function of elapsed time of electric field treatment, secondly this substructure could be annealed out by heating the specimens at high temperature (>1300°C) thereby also recovering the electrical properties of virgin specimens.

A possibility is being considered that the a<100> dislocations in MgO introduce energy levels in the energy gap between the valence and conduction band. These levels may be similar to energy levels associated with dislocations in Ge and Si[2] and could provide a mechanism for electronic conduction, leading to the large currents which are observed. The joule heating due to large currents leads ultimately to the breakdown of the material.

REFERENCES

1. R. A. Weeks, E. Sonder, J. Narayan, K. F. Kelton and J. C. Pigg, Proceedings Conf. on High Temp. MHD Systems, April 4-6, 1977, Argonne National Laboratory.

2. R. Labusch and W. Schröter in Lattice Defects in Semiconductors, The Institute of Physics, London (1975), p. 56.

*Operated by Union Carbide Corporation for the ERDA.

FIGURE CAPTIONS

Fig. 1a Bright field electron micrograph under kinematical diffraction conditions (w = 0.6) showing α and β loops. The arrow indicates the direction of diffraction vector ($\bar{g}$) [200], and it is 0.3μ long.

Fig. 1b Bright field electron micrograph (w = 0.6) showing α type loops near a dislocation. The loop denoted γ has a/2[101] Burgers vector. The arrow shows the direction of $\bar{g}$ [200].

Fig. 1c Bright field electron micrograph (w = 0.6) showing α type loops near a subboundary. The arrow shows the direction of $\bar{g}$ [200].

LATTICE RELAXATION IN JAHN-TELLER SYSTEM AND POLARIZATION CORRELATION BETWEEN PHOTO-ABSORPTION AND LUMINESCENCE

Keiichiro NASU and Tadanobu KOJIMA

Second Department of Physics, Faculty of Science

Tohoku University, Sendai 980, Japan

A theory of the polarization correlation between the photo-absorption and the luminescence of the Jahn-Teller system is formulated on the basis of the theory of the resonant photon scattering[1] including the lattice relaxation. The case of the A_1-E transition of a localized electron ccupled with phonons of b_1 and b_2 symmetries in a C_{4v} crystal field is worked out as an example.

In treating the lattice relaxation process, we use three kinds of models:the first is the so-called dynamical model used in the case of weak electron-phonon coupling. In this model the relaxation is described as a time damping of the phonon correlation function due to dispersion. The optical response function of the resonant photon scattering is casted into a form of the cumulant expansion with respect to the correlation function. The second is the so-called stochastic model used in the case of the moderate or strong coupling. In this model only a pair of localized phonons is assumed to couple with the electron. The relaxation of these phonons is brought about through their weak interaction with a heat reservoir by making use of conventional stochastic approximations. In order to express the relaxation in an intuitively clear way connecting with the semi-classical theory,[2] we used the adiabatic approximation in the third model, in which the depolarization mechanism of the absorbed photon is described as a nonradiative transtion of the electron from one adiabatic potential energy surface to the other.

By combining results obtained under these models, we could clarify how the polarization memory of the exciting photon dissipates during the lattice relaxation as a function of the exciting frequency and the electron-phonon coupling constants.

Detailed results were published in ref. 3.

1) Y. Toyozawa, J. Phys. Soc. Japan 41(1976),400.
2) Y. Toyozawa and M. Inoue, J. Phys. Soc. Japan 21 (1966),1663.
3) K. Nasu, Prog. Theor. Phys. 57(1977),361.

THE TEMPERATURE DEPENDENCE OF PHONON-DEFECT MODE HYBRIDIZATION IN KCl(CN)*

R. M. Nicklow and W. P. Crummett†
Solid State Division, Oak Ridge National Laboratory
Oak Ridge, Tennessee 37830

The hybridization of phonons with the internal modes of CN^- impurities in KCl has been studied by inelastic neutron scattering as a function of temperature in the range 5-120 K. The hybridization near 0.5 THz observed previously[1] at 5 K shows a strong dependence on temperature, essentially disappearing above 40 K. This result is consistent with theoretical predictions and with the observed behavior of the elastic constants.[2] A resonant-like frequency shift is also observed just below 1.0 THz in the E_g[110] branch up to 120 K, suggesting the existence of additional phonon defect interactions not previously observed.

*Research sponsored by the Energy Research and Development Administration under contract with Union Carbide Corporation.

†Oak Ridge Associated Universities Graduate Laboratory Participant from West Virginia University, Morgantown, West Virginia.

[1]D. Walton, H. A. Mook and R. M. Nicklow, Phys. Rev. Lett. 33, 412 (1974).

[2]N. E. Byer and H. S. Sack, Phys. Stat. Sol. 30, 569 (1968).

ENDOR INVESTIGATION OF F CENTRES IN BaClF

J.R. Niklas, G. Heder, M. Yuste and J.M. Spaeth,
Fachbereich 6, Naturwissenschaften I, Gesamthochschule Paderborn, 4790 Paderborn, W.Germany

As illustrated in fig.1 in the crystal structure of BaClF(D_{4h}^7) two types of F centres can be produced: $F(F^-)$ at a fluoride site and $F(Cl^-)$ at a chloride site (1). Both F centres give rise to two optical absorption bandseach labeled I_1, I_2 and J_1, J_2. From ESR studies it has been concluded that the I_1, I_2 bands are due to $F(Cl^-)$ centres and the J_1, J_2 bands to the $F(F^-)$ centres (2).

In order to verify the site of the F centre unambiguously and to determine the superhyperfine interactions with the lattice nuclei we have performed ENDOR experiments on BaClF crystals showing the I_1, I_2 bands. Fig.2 shows the angular dependence of the nearest neighbour fluorine ENDOR lines for a rotation of the magnetic field $\vec{B}_o$ in a $\vec{c}$-$\vec{a}$ plane from $\vec{B}_o \parallel \vec{c}$ (0^o) to $\vec{B}_o \parallel \vec{a}$ (90^o).

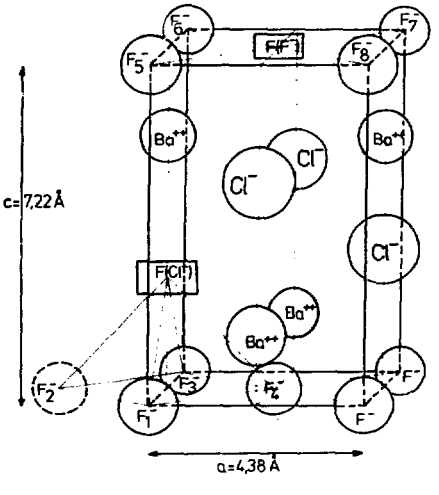

Fig.1: Unit cell of BaClF showing the position of the $F(F^-)$ and $F(Cl^-)$ sites.

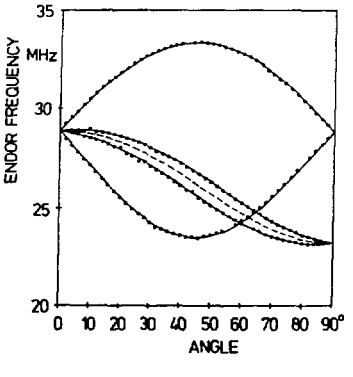

Fig.2: Angular dependence of ENDOR frequencies for the nearest F^- neighbours of the $F(Cl^-)$ centre. (m_s=-1/2). The lines are calculated from the Spin Hamiltonian.

This dependence shows clearly that the F centre investigated is on a Cl^- site, since on a F^- site for $\vec{B}_0 \parallel \vec{a}$ (90^o) only one ENDOR transition for $m_s = -1/2$ would appear because of the equivalence of the 4 nearest F^- nuclei. The crystal is tilted by 6^o showing up in a small splitting of the central ENDOR line. The dotted line would be observed without tilting. The solid lines are calculated by fitting the shf constants for the nearest F^- neighbours. The shf constants for three further shells of F^- neighbours could be determined, too. The results are shown in table 1.

Table 1: shf constants of F^- neighbours of the $F(Cl^-)$-centre in BaClF (in MHz)

F^--shell	distance(Å)	a/h	b/h	b'/h	γ	α	β
1	3,36	25.65	6.21	-0.31	45^o	0^o	0^o
2	5.17	1.96	0.14	-1.00	5^o	0^o	0^o
3	5.52	6.70	1.23	0.25	57^o	18^o	-8.5^o
4	6.77	0.84	0.35	-0.03	46^o	26.5^o	0^o

α,β,γ are the Euler angles between the shf principal axes system and the crystal axes, γ is the angle between Z_{shf} and $\vec{c}$. For the definition of a,b,b' see e.g. (4).

The isotropic shf constant a for the nearest F^- neighbours is an order of magnitude smaller than that calculated on the basis of a point ion lattice model (3) which yields 237 MHz. Furthermore the values of the anisotropic shf constants b relative to a are much higher than e.g. in alkali halide F-centres. An astonishing result is also that the 3rd nearest F^- neighbours have a considerable larger interaction than the second nearest F^- neighbours. The results show that the electron distribution strongly deviates from spherical symmetry and that the present theory must be considerably revised.

Further ENDOR experiments including $F(F^-)$ centres are in progress.

(1) E. Nicklaus and F. Fischer, phys.stat.sol.(b) 52, 453 (1972)
(2) M. Yuste, L. Taurel, M. Rahmani and D.Lemoyne J.Phys.Chem.Sol. 37, 961 (1976)
(3) S. Lefrant and A.H. Harker, Solid State Comm., 19, 853 (1970)
(4) J.M.Spaeth and M. Sturm, phys.stat.sol. 42, 739 (1970)

ESR MEASUREMENTS ON Pb^{3+} - CENTER IN CUBIC PbF_2 CRYSTAL

Masato NISHI, Hideo HARA, Yoshifumi UEDA and Yukio KAZUMATA[+]

Department of Applied Physics, Faculty of Engineering, Hiroshima University, Hiroshima, Japan

[+]Japan Atomic Energy Research Institute, Tokai-mura, Naka-gun Ibaraki-ken, Japan

We have studied on the electron spin resonance (ESR) due to the Pb^{3+}- center produced in the cubic PbF_2 crystal by the irradiation with γ-rays and neutrons at low temperatures. The ESR-spectra in the x band are composed of three groups of lines, centered (a) at about free electron resonance field, (b) at ~5600 G and (c) at ~8700 G, respectively. The intensity of the lines in group (a) is about 20 times as strong as that of the lines in other groups. The line group (a) originates from the even isotopes (^{204}Pb, ^{206}Pb and ^{208}Pb) which together are 79 % abundant and which have no nuclear spins, while the other two groups (b) and (c) are caused by the ^{207}Pb isotope (natural abundance 21 %) with nuclear spin I=1/2 and nuclear moment $\mu_N=0.5837\ \mu_k$, which has a large Fermi-contact interaction between 6s-electron and the nuclear moment. All the central resonance field of each group does not depend on the orientation of the crystal, indicating that the hyperfine (hf-) splitting constant and the g value are isotropic. From the Breit-Rabi formula the hf-splitting constant A(^{207}Pb) and g value can be determined.

The superhyperfine (shf-) structure consists of nine groups, each group with several lines. The splitting of each group is due to the interactions with eight F nuclei in the first shell, whereas that of the satellite line in each group is attributed to the interaction with several ^{207}Pb nuclei in the second shell. The observed central resonance fields of these nine groups can be fitted to the result solved by means of the second order perturbation theory;[1] thus, the shf-constant $A(F)_{//}$ and $A(F)_{\perp}$ can be obtained. The angular dependences of the satellite lines are all shown by the equi-distant curves, which means the isotropic splitting originated

by the interaction with the ^{207}Pb nuclei in the second shell; so the isotropic shf-constant of ^{207}Pb nucleus, $a(^{207}Pb)$ is given. These values are listed in Table 1.

In interpreting hf- and shf- data the covalent bonding had often to be considered; this is usually with the covalency parameter[2]. The reduction in the observed $A(^{207}Pb)$ from the value of free ion means that about 40 % of the unpaired electron of the Pb^{3+}- center occupy ligand orbitals, that is the ESR spectra of Pb^{3+}- center also indicate an intensive covalency in the electronic structure of the ground state. A simple model[3] was used, in which the overlap of orbitals was neglected. The wave function

$$|\psi> = N\,(\,|6s> - \lambda_{2s}|\chi_{2s}> - \lambda_{2p\sigma}|\chi_{2p\sigma}> - \lambda_{6s}|\chi_{6s}>\,)$$

can be determined by fitting N to the measured hf-constant $A(^{207}Pb)$ and the covalency parameters λ_{2s}, $\lambda_{2p\sigma}$ and λ_{6p} to the shf-constants $A(F)\parallel$, $A(F)\perp$ and $a(^{207}Pb)$. $|\chi_{2s}>$, $|\chi_{2p\sigma}>$ and $|\chi_{6s}>$ are molecular orbital (MO) functions which are linear combination of the 2s, 2pσ and 6s orbitals of the outermost fully occupied shell of the eight F-ligands and twelve Pb^{2+} ions in the next nearest neighbour, respectively.

Table 1.

g	$A(^{207}Pb)$ (cm^{-1})	$A(F)\parallel$ (G)	$A(F)\perp$ (G)	$a(^{207}Pb)$ (G)	λ_{2s}	$\lambda_{2p\sigma}$	λ_{6s}
2.007	47.1	171.5	37.5	78.0	0.24	0.96	0.22

The results show clearly the importance of the covalent 2pσ admixture; this means that the ESR spectrum originates from a $(PbF_8)^{-5}$ complex ion.

1) D.Schoemaker, Phys. Rev. 149, 693 (1966)
2) W.Frey, R.Huss, H.Seidel and E.Werkmann, Phys. stat. sol. (b) 68, 257 (1975)
3) W.Dreybrodt and D.Silber, Phys. stat. sol. 20, 337 (1967)

DIFFUSION OF FREE EXCITONS IN KI

A. NOUAILHAT, E. MERCIER and G. GUILLOT
Laboratoire de Physique de la Matière* - Bâtiment 502
Institut National des Sciences Appliquées de Lyon
20, Avenue Albert Einstein 69621 VILLEURBANNE CEDEX -France-

The problem of energy transfer by diffusion of free excitons in alkali halides at low temperature has been much investigated and discussed. Great strides have been made with the recent work by Tomura's team on the iodides (1). In KI, they have studied the behaviour of the exciton as a function of its formation energy in crystals doped with ns^2 luminescent ions, and they have interpreted the results by exciton diffusion before its relaxation. The analysis is made difficult by the presence of the D absorption band of the luminescent centers which partially overlaps the intrinsic one and can give rise to resonance transfer. Thus, we have approached the question using the properties of excitonic luminescence quenching of some defects created by electron irradiation (2) and pointed out the increase of the interaction between the defect and the exciton created by UV excitation at 205 nm when the temperature decreases from 77 K down to 4 K (3).

We have gone further into this study analyzing the evolution of both π emissions at 3.01 eV (410 nm) and 3.31 eV (380 nm) versus the conditions of excitation in the first excitonic peak (200 - 220 nm), the temperature and the defect concentration.

We have shown that the emission at 410 nm, excited at 215 nm is specially sensitive to the presence of defects. The decrease of its intensity versus the concentration N of defects created by irradiation is quicker than the 380 nm's one and can be represented by a law like $(1 + \alpha N)^{-1}$ where α depends on temperature. On the other hand, this kind of law is different from the one which describes the exciton defect interaction without diffusion, where the luminescence intensity decreases according to $\exp -\beta N$, β being the interaction volume (2).

The set of experimental results can be correctly interpreted with the help of a mechanism of diffusion of the exciton in its free state, according to Tomura on the origin of both emissions at 3.01 eV and 3.31 eV (1) : the exciton is created by a first exciton peak excitation in a bound free non relaxed state, from which it can either go by temperature independent tunneling into the state responsible for the 410 nm emission, or go by a thermally activated process into the state responsible for the 380 nm emission, or diffuse to impurities (which are here radiation created defects) with a probability equal to $4 \pi a ND$, where D is the temperature dependent diffusion coefficient and a is the exciton defect collision diameter.

We have deduced from the study versus temperature and excitation energy that the diffusion coefficient of the free exciton is a decreasing function of temperature between 4 K and 90 K.

We have been able to conclude definitely that in KI energy transfer takes place from free excitons according to the "wave packet" transport mode.

---

(1) Essentially, *papers* by M.TOMURA'S team. For the case of exciton diffusion in KI, H. NISHIMURA and M. TOMURA, J. of the Phys.Soc.of Japan 39 (1975) 390.

(2) G. GUILLOT, A. NOUAILHAT, E. MERCIER and P. PINARD, J. of Lumin. 12/13 (1976) 1327.

(3) A. NOUAILHAT, E. MERCIER and G. GUILLOT, J.de Physique 12, C7 (1976) 492.

---

* Equipe de recherche associée au C.N.R.S.

DEFECT INTERACTIONS IN CaO- AND Y_2O_3-DOPED CeO_2

A.S. Nowick, D.S. Park+, J. Griffith and M.P. Anderson
Henry Krumb School of Mines, Columbia University
New York, New York 10027

Ceria (CeO_2 fluorite structure) doped with di- or tri-valent cations has been shown to be a fast-ion conductor, due to the oxygen vacancies (V_O) which compensate for the lower valent cation.[1] The present study is directed toward determining key kinetic parameters and the nature of the defect interactions in these materials, by utilizing ac ionic conductivity, dielectric relaxation (the ITC method[2]), and anelastic relaxation measurements.

In the case of CaO-doped CeO_2, it had earlier been deduced[3] that the basic defect formed in dilute solutions at low temperatures is the Ca^{2+}-V_O pair in the nearest-neighbor configuration (along <111>). Such pairs give rise both to dielectric and anelastic relaxation. Analysis of conductivity curves (log σT vs 1/T) shows[4] that below about 700°C, the results fall into stage III, in which the pairs are primarily associated, i.e. $[V_O] \ll C_O$ (the total dopant concentration), and the apparent activation enthalpy is given by $H_m + \frac{1}{2}H_A$, where H_m is the oxygen-vacancy migration energy and H_A the pair association energy. As shown in Fig. 1, the conductivity at any one temperature increases monotonically as a function of C_O out to 15% CaO. At the same time, the activation enthalpy remains almost constant, at 0.92 eV, over the entire composition range (see Fig. 2). The above interpretation of the conductivity curves is supported by dielectric relaxation measurements, which show that virtually all of the Ca^{2+} in the sample is present as bound pairs. The single Debye peak, with H_R = 0.74 eV observed for 1% CaO gradually changes to a peak showing considerable broadening toward lower temperatures for concentrations greater than $\sim$ 2% CaO. This broadening is a sensitive measure of higher order defect interactions which are not apparent from the conductivity measurements.

The study of Y_2O_3-doped CeO_2 shows very different results. First, the conductivity as a function of dopant concentration goes through a sharp maximum, while the activation enthalpy rises sharply above $\sim$ 4% Y_2O_3 (see Figs. 1 and 2). Here the basic defect complex is not known, though it seems clear that one V_O is introduced for every two Y^{3+} ions. The dielectric relaxation for dilute solutions shows a double peak corresponding to enthalpies H_R of 0.55 and 0.64 eV, respectively. The relative heights of these two peaks changes with Y_2O_3 concentration, indicating that they originate in two different defect species. Only a single peak, corresponding to the higher H_R value has been found in anelastic relaxation, however. By analysis of these and further results, it is intended to present a model for the defect structure of Y^{3+}-doped CeO_2.

Acknowledgement--This work was supported by the NSF under grants DMR 74-23877 and DMR 76-80157.

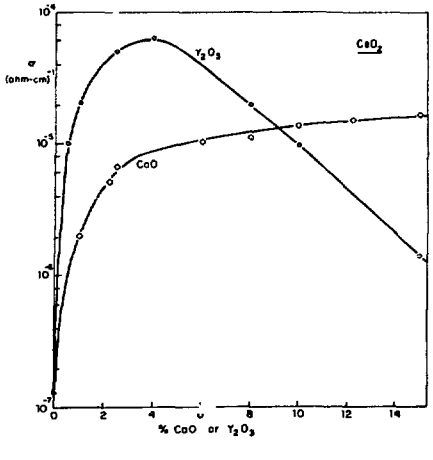

Figure 1

Conductivity of doped CeO_2 at 280°C as a function of CaO or Y_2O_3 concentration.

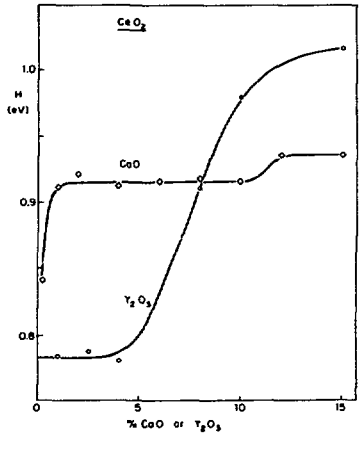

Figure 2

Activation enthalpy, H, from the conductivity of doped CeO_2 as a function of CaO or Y_2O_3 concentration.

+Dr. D.S. Park is now at General Electric Research and Development Center, Schenectady, New York 12301.

REFERENCES

1. H.L. Tuller and A.S. Nowick, J. Electrochem. Soc. 122 (1975) 255.
2. C. Bucci, R. Fieschi and G. Guidi, Phys. Rev. 148 (1966) 816.
3. J.B. Wachtman, Phys. Rev. 131 (1963) 517; K.W. Lay and D.H. Whitmore, Phys. Stat. Sol. (b) 43 (1971) 175.
4. A.S. Nowick and D.S. Park, in Superionic Conductors, ed. G. Mahan and W. Roth, Plenum Press, N.Y. 1976, p. 395.

THE INFLUENCE OF IRRADIATION TEMPERATURE ON THE FORMATION OF F-AGGREGATE CENTERS IN LiF CRYSTALS

MORITAMI OKADA, KOZO ATOBE and MASUO NAKAGAWA

Research Reactor Institute, Kyoto University,
Kumatori-cho, Sennan-gun, Osaka, 590-04, Japan

In the optical absorption spectra at 77 K of undoped LiF crystal irradiated at 20 K, F, F_2 (=M), F_2^+ and V_k bands are observed. During the thermal annealing of the specimens, the F_3^+, F_3 (=R), F_4 (=N) 560 nm and more higher F-aggregate bands are produced in addition to the above bands. In the temperature region between 305 and 450 K, the absorption band at 560 nm appears with decreasing the F and F_3^+ bands. The intensity of the 560 nm band reaches its maximum at about 370 K. In this temperature region, the thermal behaviors of the F, F_2, F_3^+ and 560 nm bands are shown in Fig. 1. In this figure, the peak height, D_o, is normarized to the maximum values of each bands, D. As seen in the figure, the F_2 band is excepted from the components to produce the 560 nm band. Therefore, it is concluded that the 560 nm band is responsible for the F_4^+ center which is formed by the aggregation with the F_3^+ and F centers ($F_3^+ + F \longrightarrow F_4^+$).

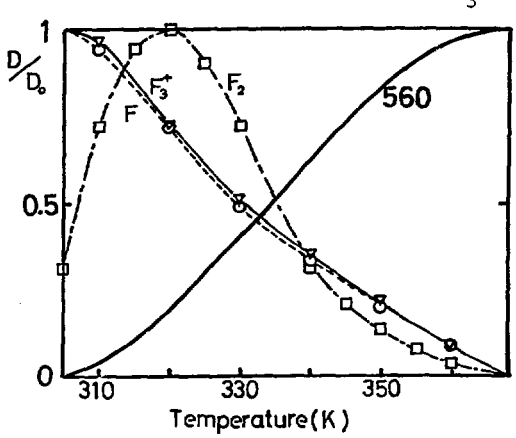

Fig. 1 The thermal behaviors of F, F_2, F_3^+ and 560 nm bands. Peak height, D_o, is normarized to the maximum value.

On the other hand, in the specimens after the irradiation at pile temperature (about 370 K), the F, F_2, F_3, F_4 and 542 nm (=I) bands are already produced. In this case, the ionized F-aggregate bands such as the F_2^+, F_3^+ and 560 nm bands are not produced. In the annealing temperature region from 480 to 630 K, a band at 500 nm enhances with the decrease of the F, F_2, F_3 and F_4 bands. The intensity

of the 500 nm band reaches its maximum at about 565 K and then disappears at about 630 K. This behavior is quite similar to the formation processes of the F-aggregate centers such as the F_2, F_3 and F_4 centers, i. e. $F + F \longrightarrow F_2$, $F_2 + F \longrightarrow F_3$ and $F_3 + F \longrightarrow F_4$[1]. The thermal behaviors of the F, F_2, F_3, F_4 and 500 nm bands are shown in Fig. 2. From this figure, it is concluded that the 500 nm band is responsible for the F_5 center formed by the aggregation with the F_2 and F_3 centers.

In view of the above experimental results, the ionized F-aggregate centers are induced during the thermal annealing in the specimens irradiated at low temperature, whereas these are not induced in the specimens irradiated by reactor neutrons at pile temperature. The formation mechanisms of the F-aggregate centers in LiF crystals irradiated at pile temperature are quite different from that irradiated at 20 K.

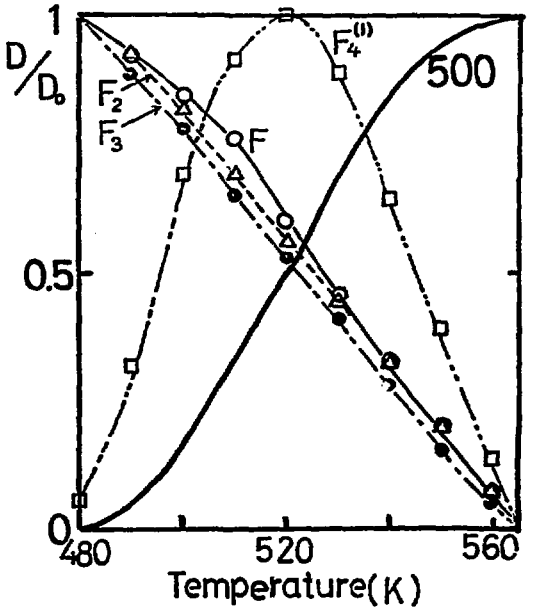

Fig. 2 The thermal behaviors of F, F_2, F_3, F_4 and 500 nm bands. Peak height, D_0, is normalized to the maximum value.

1) W. D. Compton and H. Rabin, in Solid State Physics, Vol. 16, Ed. by F. Seitz and D. Turnbull (Academic Press, New York, 1964).

SPECTRAL DISTRIBUTION OF THE TRIPLET TO SINGLET LUMINESCENCE OF F_2 CENTER IN KCl, KBr and KI

J.M. ORTEGA
Laboratoire de Physique des Solides
Université Paris-Sud
91405 ORSAY (France)

The spectral distribution of luminescence corresponding to the transition between the triplet singlet ground states of the F_2 center has been measured in KCl, KBr and KI by using a tunable infra-red filter operating at liquid helium temperature. The observed spectra exhibit a zero-phonon line respectively located at 0.202, 0.194 and 0.161 (± 0.01) eV in KBr, KCl and KI. In addition both Huang-Rhys parameters and related phonon frequencies have been estimated for the associated structured broad bands.

RADIATIVE DECAY OF THE TRIPLET STATE OF THE F_2 CENTER IN KCl and KBr

J.M. ORTEGA[+], Y. FARGE[+], R.H. SILSBEE[++]

[+] Laboratoire de Physique des Solides
Université Paris-Sud
91405 ORSAY (France)

[++] LASSP - Clark Hall - Cornell University
ITHACA, N.Y. 14850 (USA)

The decay of the triplet state of the F_2 center in KCl and KBr has been shown to be mostly radiative (1) at low temperature. A phenomenological model (2) of a spin-orbit induced electric dipolar triplet to singlet transition is firstly developed. The predictions of this model are well verified by triplet-lifetime measurements under magnetic field, for different orientations of the field versus the axis of the defect, between 1,8 and 4,2 K. Secondly (3), a quantitative model of the spin-orbit mixing between singlet and triplet states is presented. Numerical calculations of the triplet lifetimes using the ENDOR (4) data of the F_2 centers lead to a satisfactory agreement with the experimental data.

(1) J.M. ORTEGA - to be published.

(2) J.M. ORTEGA - to be published.

(3) R.H. SILSBEE, Y. FARGE, J.M. ORTEGA - to be published.

(4) H. SEIDEL, H.C. WOLF in "Physics of color centers", W.B. Fowler, Ed. (Academic Press, New York, 1968), Ch. 8.

OPTICAL ABSORPTION, PHOSPHORESCENCE, PHOTOLUMINESCENCE AND THERMOLUMINESCENCE CORRELATION STUDIES IN CALCIUM FLUORIDE CRYSTALS DOPED WITH LANTHANIDES*

Choyu Otani and R. Muccillo
CPRD-AMD, Instituto de Energia Atômica, S. Paulo, Brazil

and

K. S. V. Nambi and S. M. D. Rao
H. P. D., Bhabha Atomic Research Centre, Bombay, India

CaF_2:RE (RE: Lanthanide Rare Earth) crystals find uses in thermoluminescence dosimetry as efficient phosphor-detectors and also as laser materials. It is generally believed that $RE^{3+} \rightleftharpoons RE^{2+}$ valence reduction-oxidation plays a key role during excitation and stimulated emission. In the present investigations attempts have been made to verify the extent of these valence changes for as many rare earth dopants as possible after X-irradiation, as well as after various thermal anneals, by correlating their optical absorption, phosphorescence, photoluminescence and thermoluminescence characteristics.

There are interesting results such as i) in the case of the Eu dopant the TL emission corresponds to Eu^{2+} fluorescence and is unaccompanied by radiation/thermal induced valence changes; ii) in the case of Sm dopant the TL emission seems to be due to the fluorescence of both 3^+ and 2^+ ions.

*Research work supported by Comissão Nacional de Energia Nuclear.

PARAMAGNETIC DEFECTS AS PROBES OF STRUCTURAL PHASE TRANSITIONS

F. J. Owens
Energetic Materials Laboratory, ARRADCOM, Dover, N.J.

It is possible to obtain information about the static and the dynamic properties of a structural phase transition by monitoring the EPR of a paramagnetic defect as the lattice changes phase. The defect may be radiation induced or doped into the lattice. Particularly in the case of a defect with $S > 1/2$, the EPR spectra will be sensitive to changes in symmetry. The zero field splitting depends on the order parameter as Φ^N where N is 1 or 2 depending on the absence or presence of inversion symmetry and thus its temperature dependence can be used to measure the temperature dependence of the order parameter near T_c. Deviations from mean field temperature dependence associated with critical behavior can be detected in certain cases. If ϕ_1^m is the appropriate component of the soft mode, the second moment of the line $\langle \delta H^2 \rangle$ will depend on $\left\langle (\phi_1^m)^2 \right\rangle$. The fluctuations of the order parameter near T_c will then be manifested as a divergence of line width. In the case of a ferroelectric phase transition where there is a softening polar mode, the fluctuation in the polarization may cause the line width anomaly and then $\Delta H = \sqrt{\langle P^2 \rangle}$ and thus $\Delta H = (T_c - T)^{1/2}$ for the mean field approximation. A number of recent studies will be discussed which illustrate the manner in which this kind of information can be deduced from the EPR data. The use of the AsO_4^{-4} defect in KDP and ADP will be discussed.[1,2] Some examples of transition metal ion defect probes will be considered. Typical are the Fe^{3+} - vacancy center in $SrTiO_3$ and the Mn^{2+} - vacancy center in NaN_3 as well as Cr^{3+} in triglycine sulphate and in some of the alums.[3-7]

1. R. Bline, P. Cevc, and M. Scharra, Phys. Rev. 159, 411 (1967).
2. F. J. Owens, J. Mag. Resonance 20, 130 (1975),
3. K. A. Muller and Th. Von Waldkirch in Local Properties of Phase Transitions (North Holland Publishing Co., Amsterdam, 1976).
4. F. J. Owens, Chem. Phys. Letters 35, 269 (1975).
5. K. Nishimura and T. Hashimote, J. Phys. Soc. Japan 35, 1699 (1973).
6. F. J. Owens, J. Phys. Chem. Solids (in press).
7. F. J. Owens, Chem. Phys. Letters 46, 380 (1977).

A NEW F-AGGREGATE CENTER: THE (F + U) - CENTER PAIR

David S. Pan and Fritz Luty
Physics Department, University of Utah, Salt Lake City, Utah 84112

The four types of primary F-aggregate centers in alkali-halides are formed by attaching an F center either to an alkali-defect (F_A), to another F center (F_2), to a divalent cation vacancy complex (F_Z), or to a defect substituted for a halide ion (F_H). While the first three types of F-aggregates have been produced and studied in most alkali-halides, the only F_H center identified so far has been an F center Cl^-defect pair in CsBr:Cl (which -- due to the bcc structure -- has <100> symmetry). In none of the NaCl-structure crystals has an F_H center (expected to have <110> symmetry) been found so far.

Particularly interesting should be an $F_H(H^-)$ center, the combination of the simplest prototype electronic defect (F) with the prototype local mode defect (U): The electronic structure and transitions of this pair should approximately consist of the sum of the properties of both constituents (U and F center), each somewhat perturbed by the presence of the <110> defect neighbor. The threefold degenerate local mode ν_0 of the U center should split into three components which -- due to the interaction of the H^- vibrating dipole with the induced F center dipole moment -- are expected to be shifted to lower energies from ν_0.

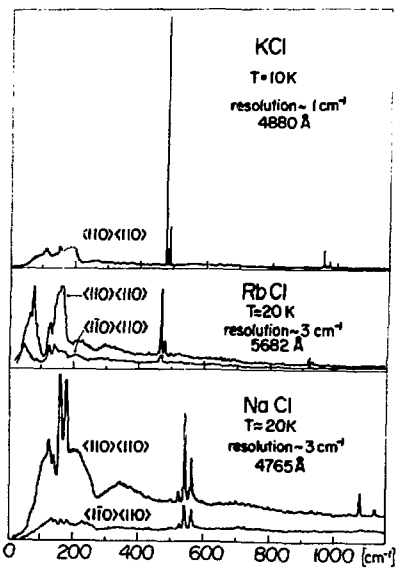

We have produced -- by laser-light-induced F center aggregation in NaCl, KCl and RbCl crystals of high U center concentrations -- these $F_H(H^-)$ centers, and have identified them by the appearance of a triplet of sharp H^- local mode lines in the resonance Raman spectrum of the F center (Fig. 1) after

their aggregation to U centers. The three local modes ν_a, ν_b, and ν_c, and the selection rules for their appearance under excitation of the F electron in the three Raman scattering geometries A_{1g}, E_g, and T_{2g} are illustrated in Fig. 2. This predicted Raman behavior for the <110> F + U pair is exactly observed, allowing the identification of the three measured lines with the ν_a, ν_b, and ν_c modes. Under tuning with different laser excitations, the large variation of the Raman intensity (due to resonance enhancement in the F-band) is found to be similar for the normal F center Raman and the $F_H(H^-)$ local-mode spectrum. This shows that the electronic absorption of the $F_H(H^-)$ center in the visible coincides with that of the normal F center. The second harmonic of the local mode spectrum was also detected and studied with Raman techniques, and was found to consist essentially out of combinations of $(\nu_a + \nu_a)$ and $(\nu_b + \nu_c)$.

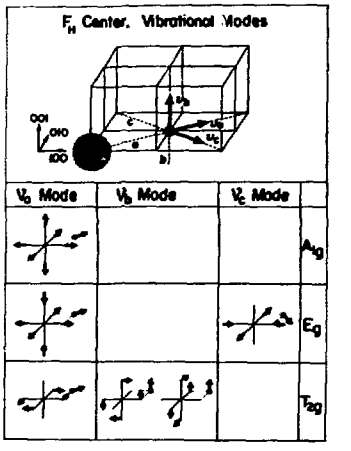

The exchange of one of the twelve Cl^- neighbors of the F center by a H^- local-mode-oscillator should have various interesting consequences: First, a vibronic substructure due to the coupling of the F-electron to the high frequency H^- oscillator, may appear in the absorption and emission of the $F_H(H^-)$ center. In the relaxed excited state (RES), the large amplitude H^- vibration should introduce extra strong mixing of the 2s and 2p states, thus changing the optical emission properties. Due to the much stronger (s-p) polarizability of the F center in the RES, the interaction energy between vibrating H^- and induced F center dipole moment will be much larger than in the ground state, so that the frequencies ν_a, ν_b, and ν_c should be appreciably shifted to lower energies in the RES. Experiments directed towards the observation of part of these properties are under way.

*Supported by NSF grant #DMR-74-13870-A02.

F-CENTERS WITHOUT RELAXED EXCITED STATES?

I) ABSORPTION AND DOUBLE-LASER-BEAM RAMAN STUDIES OF F- AND F' CENTERS IN NaI

David S. Pan and Fritz Luty
Physics Department, University of Utah, Salt Lake City, Utah 84112

According to a model, frequently used and discussed (by Seitz, Klick et al and recently by Bartram and Stoneham[1]), electronic excitations with very strong phonon-coupling and sufficiently large relaxation energies $S\,E_{phonon}$, may not achieve relaxation in the excited state and therefore will not exhibit luminescence. Arguments for this behavior are based on a simple configurational coordinate diagram model, in which for $S\,E_{phonon} > \frac{1}{4}\,E_{absorption}$ the crossing-point between ground and excited state curves lies below the unrelaxed excited state, so that during relaxation the system should make a radiationless cross-over transition into the ground state curve. Among alkali-halides with F-centers, NaI and NaBr quality for this criterion -- and indeed, no F-center luminescence has been found so far in these materials. In view of the significance as model-case for other strongly phonon-coupled non-luminescent electronic excitations (and in view of a general lack of reliable F center work in these materials) we undertook a systematic study.

F-centers were produced in highly zone-refined NaI by UV or x-ray conversion of U centers. For the following, it is important to realize that in crystals from non-purified material (or in samples close to air-exposed surfaces) perturbed F centers are formed, characterized by a considerably broadened absorption band and by photo-chemical and emission behavior very different from pure F centers.

Pure F-centers (characterized by an F-band at 2.086 eV of 0.21 eV low-temperature width) exhibit under F-light excitation a reversible conversion into a slightly wider (0.34 eV) band at higher photon-energies (2.43 eV), with the following behavior:

a) F center systems of low concentration show a thermally activated-optical conversion, yielding an activation energy of 0.04 eV.

b) F center systems of high concentration show an essentially temperature-independent high efficiency conversion.

c) Back-conversion (by optical excitation into the high energy band) occurs in all cases temperature independent with high efficiency.

d) Comparison to the F → F' conversion rates in KBr show, that in the above processes the maximum efficiency corresponds to the destruction (or recreation) of two F centers per absorbed photon.

The above results necessitate an interpretation of the high energy band as the F' band in NaI. Like in other alkali-halides, the F → F' electron transfer occurs either by thermally activated ionization in the optical cycle (low F concentration), or by direct temperature-independent tunneling of the excited electron into a neighboring F center. Unlike other alkali-halides, the optically induced electron tunneling leads in NaI to a completely stable F' center (and not to a tunneling back-process into the original vacancy). This is surely related to the most striking feature of this system, namely that in NaI the F' band is located at higher energies compared to the F band. Arguments for the existence of an abnormally low lying F' ground state (and the possible existence of a bound excited F' state) will be discussed.

Extended off-and on-resonance Raman scattering studies were performed on F-center systems in NaI. Under variation of the laser excitation energy, different dynamical equilibria of F and F' centers can give rise to a complicated superposition of F and F' Raman spectra. In order to separate these out, a double beam technique with two exactly superimposed focussed laser beams was developed, in which one strong pump-beam determines and shifts the F/F' equilibrium, while a weaker probe-beam measures the Raman effect at a different laser frequency. By this method, the Raman response of the system could be separated for all symmetries A_{1g}, E_g and T_{2g} into the isolated F and F' spectrum. Both Raman spectra consist mainly of a sharp line of A_{1g} symmetry (at 113 cm^{-1} for F and at 121 cm^{-1} for F'), with the F' line exhibiting considerably more thermal broadening under temperature increase.

[1] R. H. Bartram and A. M. Stoneham, Sol. State Comm. 17, 1593 (1975).

OPTICAL SPECTROSCOPY OF LEAD IN ALKALI HALIDE CRYSTALS. EFFECT OF X-IRRADIATION

J.L. Pascual

F.E.M.S.A. Hermanos García Noblejas 19. Madrid 17. Spain

L. Arizmendi, F. Jaque and F. Agulló-López

Dpto. de Optica y Estructura de la Materia

Facultad de Ciencias. Universidad Autónoma de Madrid

Cartoblanco, Madrid. Spain

A comparative investigation of the absorption and luminescence spectra of lead ions in NaCl, KCl, KBr and KI has been performed. Special attention has been paid to the role of lead concentration and prior thermal treatments under various atmospheres. At very low concentration (< 10 ppm), one single emission band is observed which is essentially independent of the excitation wavelength within the A-absorption band. At higher concentrations, and even after quenching, this (main) band shifts according to the excitation wavelength, suggesting that various centers under the A band are contributing to the emission. Moreover, another emission is then observed at the low energy side of the main band. This additional band is relatively very small, except for NaCl where it becomes comparable with the main band for lead concentrations $\gtrsim$ 100 ppm. The behavior for KI is quite peculiar, the emission spectra being drastically dependent on thermal quenching. Therefore, it is not completely clear how it can be correlated with that corresponding to the other alkali halides. Other emission bands are also observed in heavily doped samples, which are markedly dependent on the thermal history. Evidence has been found for the ocurrence of $PbCl_2$ in NaCl and $PbBr_2$ in KBr.

The emission spectra of lead doped alkali halides after X-irradiations shows a number of new features. In particular, the relative height of the low energy band is

markedly enhanced by the irradiation.

The creation of F centers has been studied in NaCl and KCl as a function of concentration and state of aggregation of lead, during the first-stage of the room temperature X irradiation. The rate of coloring increases with concentration for very low concentrations and saturates at $\sim$ 10 ppm. In both systems, the initial stage of dipole aggregation does not apparently influences the efficiency of F coloring although we have found appreciable differences between as received and quenched samples.

Table I

Crystal Band	NaCl	KCl	KBr	KI
Main band	320 mμ	346 mμ	365 mμ	397mμ
Low Energy	380 mμ	416 mμ	467 mμ	(456mμ)

Work partially supported by the Instituto de Estudios Nucleares (J.E.N.).

THERMOLUMINESCENCE OF ORDERED AND DISORDERED $NaAlSi_3O_8$*

E. S. Pasternack and A. M. Gaines+
Department of Geology, University of Pennsylvania
Philadelphia, Pennsylvania 19104

P. W. Levy
Department of Physics, Brookhaven National Laboratory
Upton, New York 11973

The defect structure of ordered and disordered $NaAlSi_3O_8$ is being investigated with the apparatus which records thermoluminescence (TL) emission spectra at closely spaced temperatures. $NaAlSi_3O_8$ (albite) is a corner member of the very common naturally occurring feldspar ternary system $NaAlSi_3O_8$ - $CaAl_2Si_2O_8$ - $KAlSi_3O_8$.

Like most feldspars, $NaAlSi_3O_8$ exhibits Al-Si disordering which can be characterized by x-ray measurements, most often by a determination of $\Delta 131 = 2\theta(131)-2\theta(1\bar{3}1)$ using CuK_α radiation. After exposure to ^{60}Co irradiation ordered $NaAlSi_3O_8$ ($\Delta 131 = 1.088 \pm .025$) exhibits a strong Gaussian-shaped TL emission band centered at 4.4 eV and weaker Gaussian bands at 3.08 and 2.22 eV (shown not to be second order 4.4 eV band

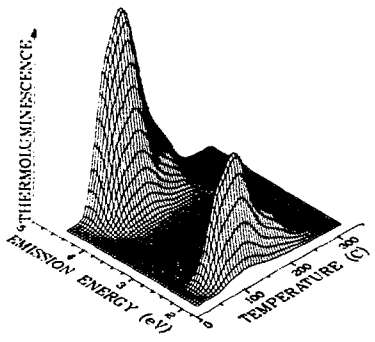

Thermoluminescence of ordered $NaAlSi_3O_8$ prior to heating but exposed to a 10^6 rad ^{60}Co gamma-ray irradiation.
Maximum intensity = 3.8×10^4.

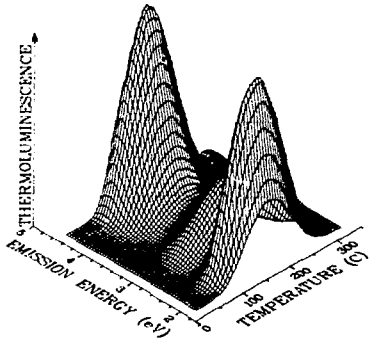

Thermoluminescence of $NaAlSi_3O_8$ disordered by heating at 1060 C for 499.3 hours and after exposure to a 10^6 rad ^{60}Co gamma-ray irradiation.
Maximum intensity 9.0×10^3.

*Research supported by the U.S. Energy Research and Development Admin.
+Now at the National Science Foundation.

diffraction). The 4.4 eV emission band exhibits three obvious glow peaks in the 75-105, 140 and 200 C regions (heating rate 10 C min^{-1}). Glow curves constructed from the individual emission spectra are poorly fitted by first-order TL kinetics in comparison with excellent fits obtained from second-order kinetics. In addition, as shown by the following table, first-order kinetics provide unreasonable parameters.

	First-Order Kinetics		Second-Order Kinetics	
Peak,C	s,sec^{-1}	E, eV	$sn_o/N,sec^{-1}$	E, eV
75-105	$7.0x10^5$	0.54	$2.6x10^8$	0.71
140	$6.3x10^2$	0.41	$4.1x10^6$	0.71
200	$4.7x10^1$	0.37	$1.5x10^{11}$	1.24

Other measurements, e.g. decay following irradiation, also suggest second-order kinetics.

Prolonged heating of $NaAlSi_3O_8$ at 1060 C induces Al-Si disordering; $\Delta 131$ changes to $1.94 \pm .05$ for complete disorder. The disordering is accompanied by large changes in radiation induced TL properties. As the disorder increases the 3.08 eV band shifts to 2.93 eV and increases markedly in intensity, the 4.4 eV band shifts to 4.3 eV and decreases in intensity and the 2.22 eV band shifts to 2.19 eV and increases. The kinetics are largely unaffected by disordering but any subtle changes would be obscured by the intensity changes.

These observations on the TL of ordered and disordered $NaAlSi_3O_8$ provide a number of important results. Of 40 or more individual glow peaks studied with the "3-D" intensity vs wavelength and temperature apparatus the albite glow curves are the first encountered which are not readily describable by first-order kinetics. The observed second-order kinetics occurs when retrapping is appreciable, a situation quite consistent with the large defect concentrations which would be expected in a material which can be thermally disordered. Lastly, the degree of disorder can be correlated with the TL properties.

PROTON-INDUCED X-RAY MEASUREMENTS IN ION IMPLANTED MgO*

P. S. Peercy
Sandia Laboratories, Albuquerque, New Mexico 87115

The atomic displacement damage produced in MgO by ion implantation has been investigated using channeled proton-induced x-ray techniques (CPIX). Measurements of the channeling yield versus fluence were made for A, Ne, He and H implantations to investigate the different mechanisms for defect formation in insulators. The implant energy was chosen such that the atomic damage peak occurred at the same depth for each ion to permit direct comparisons of the atomic displacement damage versus the ratio of energy deposited into electronic and atomic processes as this ratio was varied from 2.8 to 70. Measurements of the channeling yield after 500 keV $^{40}Ar^{+}$ implantations are found to correlate well with the volume changes measured under similar conditions,[1] and the atomic displacement damage is found to scale as energy deposited into atomic processes. However, results for light ion bombardment ($^{1}H^{+}$ and $^{4}He^{+}$), where most of the energy is deposited into ionization processes, are anomalous in that the rate of displacement damage production is greater than would be expected from considerations of energy deposited into atomic processes alone. These results indicate that the atomic displacement damage is assisted by the energy deposited in electronic processes for highly ionizing particles. This result is closely related to our observations of ion track effects for displacement damage for low fluence H^{+} and H_2^{+} implantation in which the rate of displacement damage per incident atom is found to be higher for H_2^{+} implantation than for the corresponding H^{+} implantation.

*This work was supported by the United States Energy Research and Development Administration (ERDA) under Contract AT(29-1)789.

[1]G. R. Krefft, J. Vac. Sci. Technol. 14, 533 (1977).

STUDIES OF SELF-TRAPPED EXCITON LUMINESCENCE IN CsI

J.P. Pellaux, T. Iida* and M.A. Aegerter
Institut de Physique, Université de Neuchâtel
CH 2000 NEUCHATEL, Switzerland

Self-trapped exciton (STE) luminescence is observed in all pure alkali halides exposed to X-ray or UV excitation and the occurence of these emissions when V_K centers and electrons recombine led to the identification of the $(V_K + e^-)$ center as the STE. In CsI two emissions are observed peaking at 290 nm and 338 nm. At low temperature both bands have a complex behaviour but appear as concurrent, the sum of their intensities being constant.

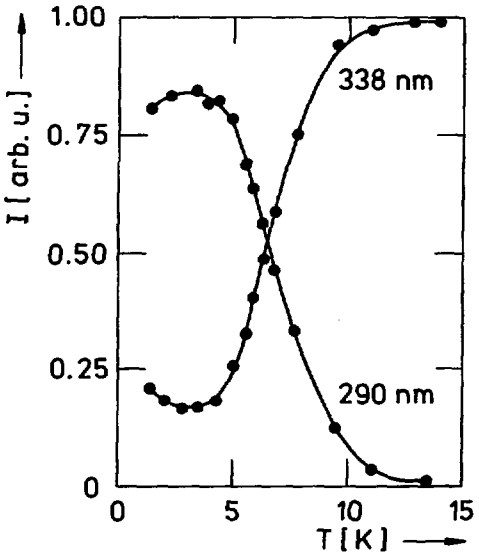

Fig. 1
Temperature variation of the normalized intensities of the 290 nm and 338 nm emission of STE in CsI.

A theoretical model for the relaxed STE in CsCl structure has been worked out by considering the electronic states of a cluster composed of an anionic diatomic molecule X_2^{--} surrounded by 12 alkali ions in a D_{4h} symmetry. Excitation of this cluster leaves an electron in a Γ_1^+ or Γ_3^+ state with a hole in a Γ_2^- or Γ_5^- state. Assuming that relaxation processes do not change the overall D_{4h} symmetry and taking into account the spin-orbit interaction up to 2nd order perturbation the various excitonic states can be constructed. Two kinds of STE state manifold are obtained. Both of them are composed of a partially allowed triplet state below a singlet one. (Fig. 2)

On the basis of experimental results we have attributed the Γ_2^- manifold to the 290 nm emission ($\pi + \sigma$ polarized) and the Γ_4^- manifold to the 338 nm emission (only π polarized). A thermal and athermal process connecting both kinds of STE states can account for the temperature behaviour of both emissions. Other experiments have been done in order to test the model [1] : optical, ESR and theoretical investigations show that V_K centers

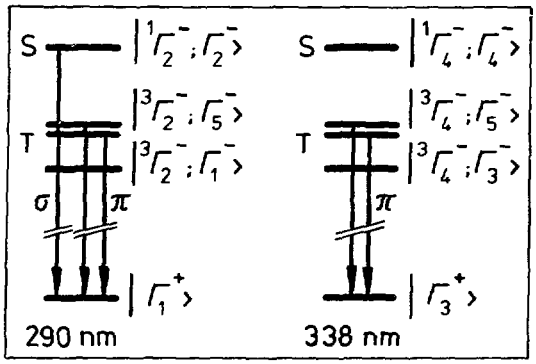

Fig. 2
The lowest levels and the allowed transitions of the two types of STE in CsI. The symmetry of the levels are labelled as |orbital function; total function>.

can be almost completely aligned for T < 60 K in a [100] direction by optical excitation in their $^2\Sigma_u^+ \rightarrow {}^2\Sigma_g^+$ UV transition (410 nm). The (V_K-e^-) recombination should then appear linearly polarized.

Experimental results confirm it only partially. The 338 nm emission polarization is independent of temperature as it should be but its value is only 26% instead of 100% as foreseen. The 290 nm emission polarization decreases as the temperature increases due to thermal population transfer to the singlet state but its maximum value at LHeT is only 18%. We therefore postulate that an athermal reorientation process of the bound e^--hole pair occurs during their relaxation in higher excited states of the STE. In our case 45% of the exciton created with a fully aligned V_K center system reorient along the two other <100> directions. This is in agreement with recent observations of STE emission in KCl by Purdy et al. [2] and Williams [3]. Using reasonable values for the other parameters we shall show that it is possible to fit the experimental data including the temperature dependence of intensities, linear polarizations and decay times of both emissions.

This research was supported by the Swiss National Science Foundation.

References

* Now at Osaka City University, Sumiyoshi-ku, Osaka, Japan.

[1] See also other abstract by L. Falco, J.P. von der Weid and M.A. Aegerter
[2] A.E. Purdy, R.B. Murray, K.S. Song and M.A. Stoneham, Phys. Rev. 15, 2170 (1977)
[3] R.T. Williams, Phys. Rev. Lett. 36, 529 (1976).

HIGH TEMPERATURE ELECTRICAL CONDUCTIVITY AND DEFECT CHEMISTRY OF IRON DOPED ALUMINA

T. M. Pollak, H. K. Bowen and H. L. Tuller

Department of Materials Science and Engineering
Massachusetts Institute of Technology
Cambridge, Massachusetts 02139

The excellent insulating property of alumina (Al_2O_3) at elevated temperatures is known to be very sensitive to additions of transition metal impurities for levels as small as 10 ppm. In this study the electrical conductivity of alumina doped with 0.08, 0.5 and 4.4 percent iron was investigated as a function of temperature (1000 - 1600°C) and oxygen partial pressure ($1 - 10^{-9}$atm). Electrical characterization of more heavily doped alumina was expected to aid in clarifying the defect structure of this sytem as well as predicting the electrical properties of alumina in contact with iron rich electrodes operating at high temperatures.

The magnitude of the electrical conductivity was found to vary from $\sim 10^{-5} - 10^{-2}(\text{ohm-cm})^{-1}$ over the temperature range from 1400 - 1600°C; while the observed activation energy in pure oxygen was 3.9 ($\pm$0.2)eV. This energy can be attributed to contributions from defect formation and ionization.

The operative conduction mechanisms were found to change both with variations in the iron content as well as the P_{O_2}. For low dopant levels ($\leq$0.5%) the conductivity decreased upon initial reduction (from 1 atm) following a $P_{O_2}^{0.15}$ dependence to approximately 10^{-5}atm where upon further reduction σ increased as $P_{O_2}^{-0.15}$. The position of the minima in σ observed at $\sim 10^{-5}$atm appeared to remain independent of temperature and dopant level for dopant levels $\leq$0.5 mol%.

For large dopant levels, on the other hand, the conductivity increased immediately upon reduction with $\sigma \propto P_{O_2}^{-0.18}$, reached a maxima at $\sim 10^{-3}$atm and decreased with further reductions in P_{O_2}. The reductions in σ at low P_{O_2}'s will be shown to be due to the onset of second phase segregation at these P_{O_2}'s. Defect reactions will be presented which

help to explain the shift in mechanism at high P_{O_2}'s from "p" type conductivity in the systems with low iron content to "n" type conductivity in the alumina system doped with 4.4 mol% Fe.

MOLECULAR CHROMATE CENTERS IN CESIUM IODIDE

S. Radhakrishna, K. Hariharan and S. Haridoss
Department of Physics, I. I. T. Madras-600036, India

Single crystals of cesium iodide doped with CrO_4^{2-} ions were grown by the Bridgman technique. The crystals obtained were yellow in color. The optical, vibrational and ITC spectra of these crystals were studied.

Optical absorption spectra of the crystal were recorded in the temperature range 80-300°K; Fig. 1 shows the spectrum recorded at 80°K. The structure observed is characteristic of the impurity ion CrO_4^{2-} and is interpreted in terms of vibronic transitions.[1,2] The separation between the lines in the spectrum is of the order of 760 cm^{-1}.

The infrared absorption spectrum of the crystal shows seven lines. An anion vacancy present in any of the six equivalent nearest neighbor positions compensates for the extra negative charge of the CrO_4^{2-}. This vacancy influences the ligands in such a manner that the symmetry around the chromate ion is reduced from T_d to C_{2v} symmetry. As a consequence of this, the triply degenerate mode T_2 splits into three modes, and the totally symmetric mode A_1 becomes IR allowed. A small number of CrO_4^{2-} ions which do not have charge compensating defects in the immediate neighborhood continue to have local T_d symmetry and a line characteristic of the unsplit T_2 mode is also observed. On the other hand, if the crystal contains background divalent cations, e.g. Ca^{2+}, the charge of the CrO_4^{2-} ion is compensated by the divalent impurity. The surrounding symmetry of the chromate ion is now reduced to C_{3v} which splits tha T_2 mode into a doublet and a singlet. This will result in the appearance of two more IR lines. Thus the seven lines are accounted for.

The CrO_4^{2-} impurity with the charge compensating vacancy bound to it form an impurity vacancy (I.V.) dipole. The relaxation of this dipole was studied using the ionic thermo-current technique (I.T.C.).[3] A prominent peak at ∿228°K was obtained. The initial rise analysis of this ITC peak gives a value for the activation energy for reorientation of the I.V. dipole to be ∿0.33 eV. The full mathematical analysis of the curve together with the discussion of the possible orientation mechanism has also been

undertaken.

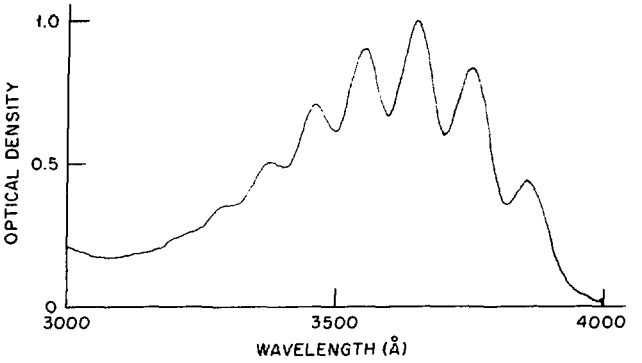

Fig. 1. CsI:CrO_4^{2-} at 80°K.

References:

1. C. J. Ballhausen and H. B. Gray, Molecular Orbital Theory (Benjamin, New York, 1964).

2. S. C. Jain, A.V.R. Warrier and S. K. Agrawal, Chemical Physics Letters 14, 211, 1972.

3. C. Bucci, R. Fieschi and G. Guidi, Phys. Rev. 148, 816 (1966).

A-P-E-S OF THE $|A_z>$ STATE OF Pb^{2+} IN CsBr

S. Radhakrishna and V. S. Sivasankar
Department of Physics, Indian Institute of Technology,
Madras 600036, India

In order to explain the appearance of two emission bands[1] (A_T and A_X) in Pb^{2+} doped CsBr crystals, and the variation of their relative intensities with temperature, the adiabatic potential energy surfaces[2] (APES) of the $|A_z>$ state of Pb^{2+} ion in CsBr have been calculated. Appropriate values for the exchange (G) and spin-orbit (ζ) parameters have been evaluated using the optical absorption data.[3,4] Also, the electron-lattice interaction constant (b) has been calculated by the method of moments analysis.[5,6] The van Vleck parameter[4] (λ) is assumed to be unity. With the values of G, ζ, b, and λ so prescribed, the resulting APES in the E_g space shows two kinds (T_X and T_Z^*) of (tetragonal) minima. Fig. 1 shows the contours of the reduced energy[7] of the $|A_z>$ state in E_g space. The deeper (T_X) minimum is 1.16ζ = 0.62 eV below the shallower (T_Z^*) minimum. The minimum barrier height for $T_Z \rightarrow T_X$ is 0.36ζ = 0.19 eV, while for $T_X \rightarrow T_Z$ it is 1.52ζ = 0.81 eV. Apparently, the initial relaxation following the absorption process is to the T_Z^* minimum. Hence, at very low temperatures (4.2 K) there is only one emission band (A_T). As the temperature is raised, the electrons escape from the T_Z^* minimum and are trapped in the deeper T_X minimum. Thus the temperature variation of the intensities of A_T and A_X bands can be explained. Probably at temperatures much above room temperature, the $T_X \rightarrow T_Z$ process becomes operative, once again giving rise to two bands in the spectrum. The experimental difference between the peak positions of the A_X and A_T bands is 1.56 eV which compares less favorably with the theoretical value of 0.62 eV for the difference in the depths of the T_X and T_Z^* minima. This quantitative discrepancy may be traced back to the limited accuracy of the values used for G and ζ.

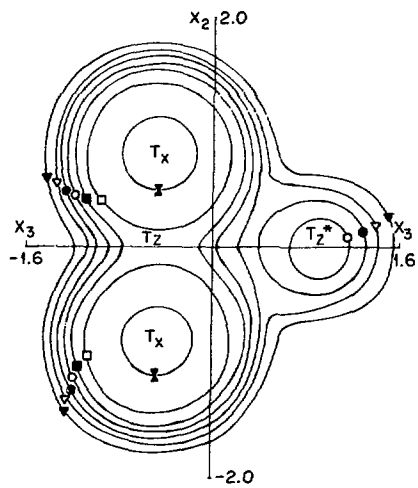

Fig. 1. Contours of reduced energy of $|A_z>$ state in E_g space: g = 0.6, and A = 2.1. (y+g) values are: ▲ - 0.0, △ - 0.3, ● - 0.5, o - 0.7, ■ - 0.9, □ - 1.2, ⧗ - 1.8.

References:

1. Radhakrishna, S., J. Lum 12/13, 409 (1976).
2. Fukuda, A., Phys. Rev. B 10, 4161 (1970).
3. Radhakrishna, S. and Pandey, K. P., Phys. Rev. B7, 424 (1973).
4. Fukuda, A., Sci. Light Tokyo 13, 64 (1964).
5. Henry, C. H. and Slichter, C. P., 'Physics of Color Centers,' Chapter 6, Ed: Fowler, W. B., Academic: N.Y., 1968.
6. Bimberg, D., Dultz, W., Fussganger, K., and Gebhardt, W., Z. Phys. 224, 364 (1969).
7. Jacobs, P. W. M. and Thorsley, S. A., J. Lum. 8, 391 (1973).

AN EPR STUDY OF PALLADIUM AND PLATINUM GROUP IMPURITIES IN MgO AND CaO

A. Raizman and J. T. Suss

Solid State Physics Dept., Soreq Nuclear Research Centre, Yavne, Israel

The results of a continuing systematic study of the electron paramagnetic resonance (EPR) of palladium (4d) and platinum (5d) group impurities in single crystals of MgO and CaO are reported. We grew the MgO crystals by the flux evaporation method[1] using a PbF_2 flux. The CaO crystals were grown for us by W. & C. Spicer Ltd., in an electric arc furnace. In both cases the dopants were added before melting either as metal powder or as a salt. So far we have studied the following ions:

a. In MgO: Ru^{3+}, Rh^{4+}, Rh^{2+}, Pd^{3+}, Ir^{4+}, Ir^{2+}, Pt^{3+}.

b. In CaO: Ru^{3+}, Rh^{2+}, Pd^{3+}, Ir^{4+}, Ir^{2+}.

All the ions are strong field (low spin) cases and belong either to a d^5 or to a d^7 electronic configuration.

d^5 ions. The ground state in a strong octahedral crystal field is the orbital triplet $^2T_{2g}(t_{2g}^5)$. The spectra of Ru^{3+} in MgO[2] and CaO[3] and Rh^{4+} in MgO[4] are isotropic. Two types of spectra were observed for Ir^{4+}: an isotropic one in MgO[5] and CaO[6] and two anisotropic spectra of tetragonal symmetry in both crystals[6]. The models proposed for these tetragonal centers are: Ir^{4+}-O^{2-}-$\boxplus$ and Ir^{4+}-O^{2-}-$\boxplus$-O^{2-}-M^+, lying along the [100], [010] or [001] axis. Here $\boxplus$ designates a Mg^{2+} (or Ca^{2+}) vacancy and M^+ is a diamagnetic cation having a charge greater than 2. Investigation of the tetragonal spectra provides interesting information on the hyperfine and quadrupole parameters, as well as on the magnitude and sign of the tetragonal field splitting in both hosts.

d^7 ions. The ground state is the orbital doublet $^2E_g(t_{2g}^6e_g)$ undergoing a Jahn-Teller (JT) effect. The electric field gradient required for the quadrupole interaction (QI) of Ir^{2+}[7] is caused in our case by the JT distortion. The QI of Ir^{2+} in MgO was found to be larger than the hyperfine interaction. The study of the transferred superhyperfine interaction between the Ir^{2+} JT ion and a next nearest neighbor ^{25}Mg ion

via an O^{2-} ion in MgO shows that this interaction is strongest along the JT distortion axis[8], and presents direct evidence of strong covalent bonding. The investigation of the oxygen-17 superhyperfine structure of Rh^{2+} JT ions in MgO[9] provided information on the covalency parameters of the Rh-O bond. A transition from a dynamic to a static JT effect (increasing $\bar{\delta}/3\Gamma$) occures in MgO, going from the $3d^7$ configuration (Ni^{3+})[10] through the intermediate cases of the $4d^7$ configuration (Pd^{3+} [11,12], Rh^{2+} [12]) to the static effect in $5d^7$ ions (Ir^{2+} [7], Pt^{3+} [13]). In CaO the investigated d^7 ions (Rh^{2+} [3], Pd^{3+}, Ir^{2+} [7]) exhibited a static JT effect. These results are consistent with those reported for Ag^{2+} in SrO, CaO and MgO[14].

References:

1. F. W. Webster and E. A. D. White, J. Crystal Growth 5, 167 (1969).
2. A. Raizman, J. T. Suss and S. Szapiro, Solid State Commun. 9, 1799 (1971).
3. A. Raizman and J. T. Suss, Proc. 18th AMPERE Congress on Magnetic Resonance and Related Phenomena, Nottingham 1974 (Edited by P. S. Allen, E. R. Andrew and C. A. Bates), Vol. I, p. 121.
4. A. Raizman, J. T. Suss and S. Szapiro, Phys. Letters 32A, 30 (1970).
5. J. T. Suss, W. Low and M. Foguel, Phys. Letters 33A, 14 (1970).
6. A. Raizman and J. T. Suss, to be published.
7. A. Raizman, J. T. Suss and W. Low, Phys. Rev. B, in press (1977).
8. A. Raizman, J. T. Suss and W. Low, Physica 86-88 B, 1229 (1977).
9. Z. Luz, A. Raizman and J. T. Suss, Solid State Commun. 21, 849 (1977).
10. A. Schoenberg, J. T. Suss, Z. Luz and W. Low, Phys. Rev. B 9, 2047 (1974).
11. B. Barnett, A. Raizman and J. T. Suss, Bull. Israel Phys. Soc. 22, 26 (1976).
12. B. Barnett, A. Raizman and J. T. Suss, to be published.
13. A. Raizman, A. Schoenberg, J. T. Suss and S. Szapiro, Bull. Israel Phys. Soc. 20, 64 (1974), and detailed paper to be published.
14. L. A. Boatner, R. W. Reynolds, M. M. Abraham and Y. Chen, Phys. Rev. Letters 31, 7 (1973).

POINT DEFECT PARAMETERS IN $NaNO_3$ CRYSTALS

C. Ramasastry and Y. S. Rao
Department of Physics, Indian Institute of Technology
Madras-600036, India

The d.c. electrical conductivity of $NaNO_3$ crystals grown from the melt of the E. Merck 'Suprapure' material as well as those doped with sodium sulphate and calcium nitrate is reported. The intrinsic defects are of the Frenkel type consisting of cation vacancies and cation interstitials. Both of them are found to contribute to the electrical conductivity. The activation energy in the intrinsic region is 3.8 eV.

The conductivity of the crystals with low SO_4^{2-} content was found, compared to that of the Suprapure crystals, to be lower in the extrinsic range but higher in the higher temperature region. It appears that the interstitials are more mobile than the vacancies, at least in the high temperature region. The activation energy in SO_4^{2-} doped crystals was found to decrease from 1.15 eV to 1.05 eV with increasing impurity content, indicating the need of the Debye-HUckel corrections. This activation energy includes half the enthalpy of association between SO_4^{2-} and Na^+ interstitial.

Addition of calcium impurity increased the conductivity. The enthalpy of migration of the cation vacancies is $h_{1J} = 0.65 \pm 0.05$ eV and the enthalpy of association of vacancies with impurities is $h_{1a} = 0.50 \pm 0.05$ eV. Precipitation effects were noticed in crystals containing more than 20 ppm of calcium. The enthalpy of precipitation is estimated to be 0.5 ± 0.05 eV (see figure).

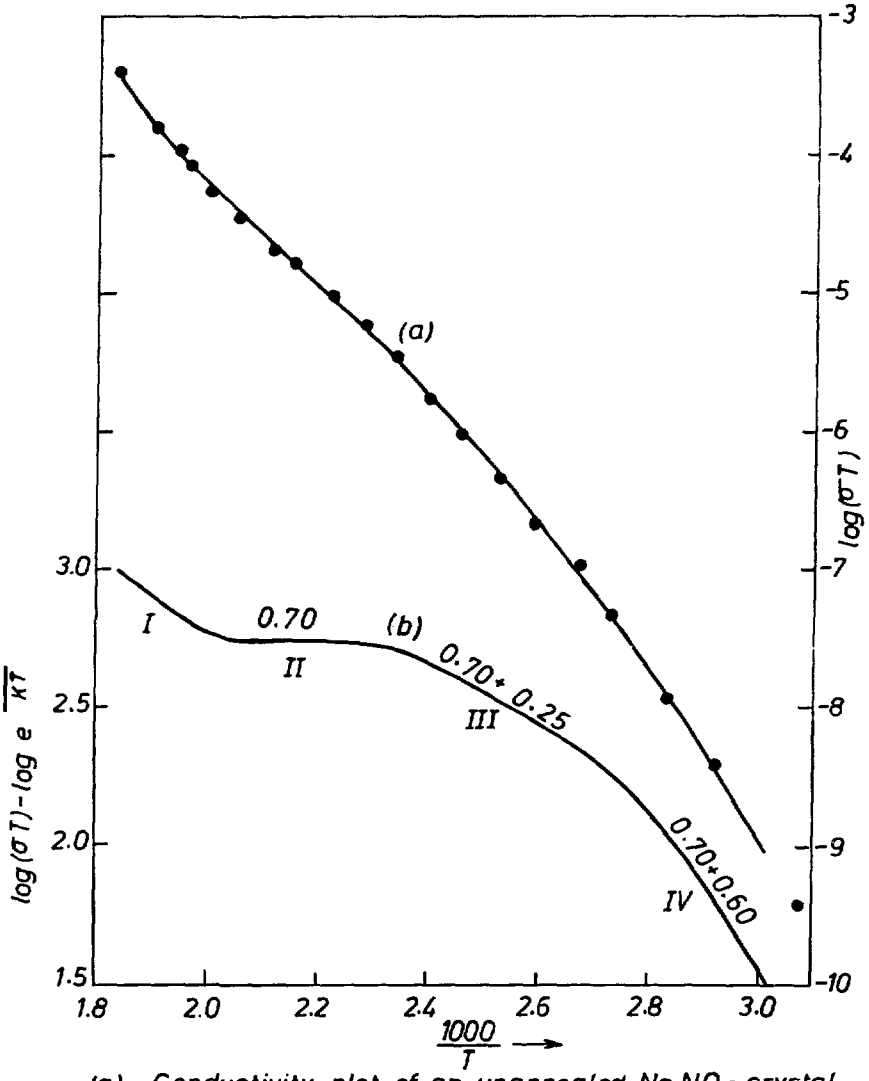

(a) Conductivity plot of an unannealed $NaNO_3$ crystal containing more than 20 ppm of Ca^{2+} impurity.

(b) Relative variation of cation vacancy concentration

NON RADIATIVE TRANSITIONS IN ALKALI-HALIDE PHOSPORS

A.Ranfagni, G.Viliani*, M.Cetica**, G.Molesini***
Istituto di Ricerca sulle Onde Elettromagnetiche del CNR
Firenze, Italy

Non radiative transitions occurring in impurity centers are studied by the WKB approximation; in particular the temperature dependence of the A_T and A_X emission-intensities in Tl^+-centers is fairly well accounted for within a non-phenomenological model.

Fukuda's original model of Tl^+-luminescence has been largely modified and put on firmer theoretical grounds in a series of papers by our group.[1,2] This model is based on the coexistence of two kinds of minima in the adiabatic potential-energy surfaces in the space of the normal coordinates. The coexistence of two kinds of minima is due either to the quadratic Jahn-Teller effect (QJTE),[2] or to strong spin-orbit mixing between triplet and singlet states:[1] in particular, the level scheme resulting from spin-orbit mixing (T^* and X minima) appears to be particularly suited to explain Tl^+ emission, while QJTE seems the most likely agent to produce coexistence in lighter impurities such as Ga^+ and In^+. Recent experimental results are in agreement with the overall model;[3,4] in some cases a proof of the coexistence of tetragonal and trigonal minima was found.[5,6]

Fig.1 shows a cross-section of the potential surface $^3T_{1u}$ along the classical trajectory connecting T^* and X minima: the high-energy A_T and low-energy A_X emissions are attributed to transitions from these minima to the ground state. After optical excitation in the A band the system relaxes most probably into the T^* minimum, the lower-lying X minimum being populated only by non-radiative transitions from T^*. As the temperature is raised the $T^* \rightarrow X$ transition probability increases, changing the intensity balance of the two emissions. The non-radiative transition probability has been evaluated in the WKB approximation by computing the transmission coefficient for each vibrational level. The results for the intensities in the case of KI:Tl^+ are reported in Fig.2 where the circles represents experimental data. The overall fitting is quite satisfying especially in view of the simple unidimensional model we have employed.

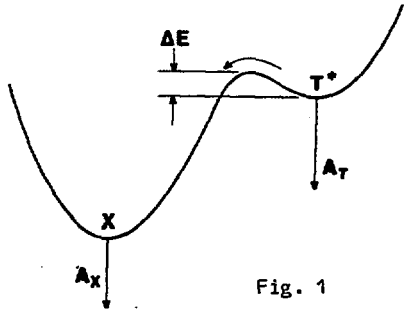

Fig. 1

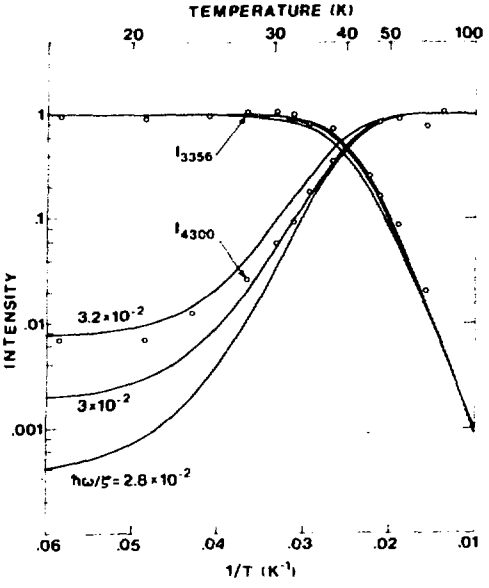

Fig.2
Temperature dependence of the intensities of A_T(3356 Å) and A_X(4300 Å) emission of KI:Tl. Circles: experimental data of Illingworth (Phys.Rev. 136 A508 (1964)); full lines: WKB computations.

1. A.Ranfagni, Phys.Rev.Letters 28, 743 (1972).
2. M.Bacci, A.Ranfagni, M.P.Fontana, G.Viliani, Phys.Rev. B11, 3052 (1975) and references therein.
3. W.D.Drotning and H.G.Drickamer, Phys.Rev. B13, 4576 (1976).
4. A.Fukuda,A.Matsushima, and S.Masunaga,J.Luminescence 12,13,139 (1976).
5. M.F.Trinkler and J.S.Solovkina, Izv.Akad.Nauk. SSR 40, 1939 (1976); phys.stat.sol.(b) 79 49 (1977).
6. Le Si Dang, private communication.

* *Facoltà di Scienze dell'Università di Trento, Trento, Italy*
** *Istituto di Elettronica, Facoltà di Ingegneria dell'Università di Firenze, Firenze, Italy*
*** *Istituto Nazionale di Ottica, Firenze, Italy*

EPR OBSERVATION OF SIZE EFFECTS IN SMALL DIELECTRIC PARTICLES OF $SrCl_2:Gd^{3+}$

M. Rappaz, C. Solliard, L. A. Boatner and A. Châtelain
Ecole Polytechnique Fédérale de Lausanne, Laboratoire de Physique Expérimentale, CH-1007 Lausanne, Switzerland

Previous experiments using x-ray or electron diffraction and electron microscopy have indicated that very small particles are characterized by an increased defect density and that a lattice contraction or dilatation is associated with a diminution in particle diameter below 200 Å. The present work shows that it is also possible to use EPR techniques to study size effects in small dielectric particles[1] with the ultimate goal of determining whether the observed change in the lattice constant is due to the effect of surface tension or to increased defect density.

Small particles (∿100 Å in diameter) of Gd^{3+}-doped $SrCl_2$ were prepared by evaporating a single crystal in a low-pressure argon flow and were examined with an X-band EPR spectrometer without intervening exposure to air. A "bulk" reference sample was prepared by mechanically grinding a doped single crystal. The size of the small-particle sample was determined by electron microscopy. The EPR results are shown in the Figure. For the small-particle sample, the observed Gd^{3+} spectrum exhibits an increase in both the magnetic field separation and the line width of the EPR transitions relative to the "bulk" powder spectrum. The observed shift ΔH (see Fig.II) of the transition $-3/2 \rightarrow -1/2$ ($\vec{H}||\langle 100\rangle$) corresponds to an increase in the cubic crystal-field parameter $|b_4|$ of 1.6 %. By fitting this line with a Lorentzian line shape, the full width at half maximum has been found to be 20 gauss. Annealing the small-particle sample at 400 °C for 1 min. coagulates the small particles and the line width reduces to 7.8 gauss. The parameter b_4 is then equal to that of the "bulk" reference sample. Using the results of Hurren et al[2], we have assumed that b_4 varies with the nn distance r as: $b_4 \propto r^{-6}$. Accordingly, the observed increase in $|b_4|$ corresponds to a lattice-parameter contraction of 0.27 %. This lattice contraction has been confirmed by high-resolution electron diffraction measurements from which lattice contractions of 0.25 % and 0.30 % were

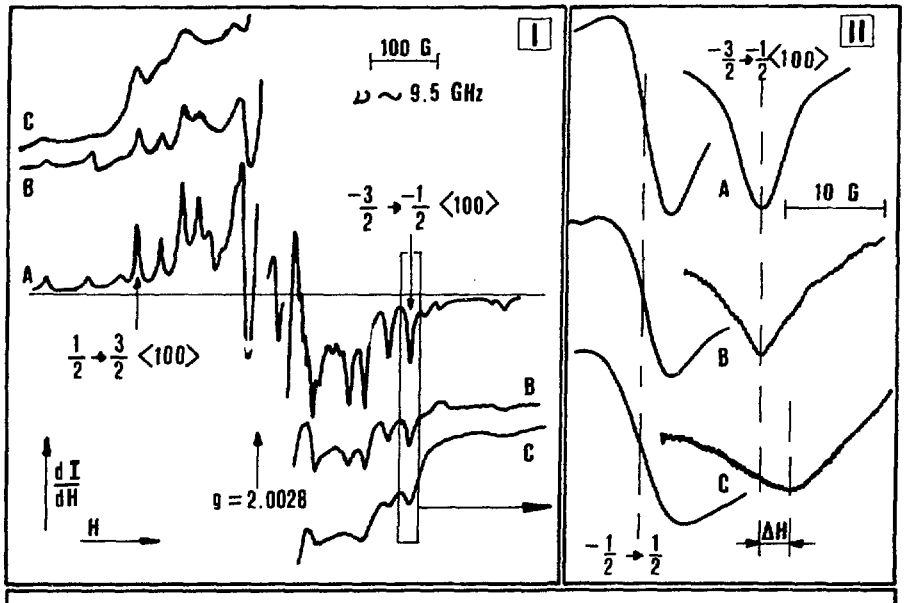

FIGURE: (I)- $SrCl_2:Gd^{3+}$ EPR powder spectrum of: A. a "bulk" reference sample, C. a small-particle sample (d ~ 100 Å), and B. the small-particle sample following a short anneal at 400 °C. (II)- Details of the -1/2 → +1/2 and -3/2 → -1/2 ($\vec{H}||<100>$) transitions showing the relative shift ΔH observed for the small-particle sample.

determined for the (4,0,0) and (4,2,2) Debye-Scherrer rings respectively. The line broadening observed for the small-particle sample can be used to calculate the distribution in b_4 due to the increased defect density if the sample consists of an ensemble of well-defined particles of uniform diameter. With the present samples, however, it is possible that the size distribution also contributes to the line width.

1. M. Rappaz, A. Châtelain and L.A. Boatner, Journal de Physique, To be published.

2. W. R. Hurren, H. M. Nelson, E. G. Larson, and J. H. Gardner, Phys. Rev. 185, 624 (1969).

RADIATION-INDUCED MICROSTRUCTURAL CHANGES IN YTTRIUM OXIDE AND ALUMINUM OXIDE*

M. D. Rechtin, H. Wiedersich, and A. Taylor
Materials Science Division
Argonne National Laboratory
Argonne, Illinois 60439

The displacement-induced, high-temperature radiation-damage microstructure of Y_2O_3 and Al_2O_3 has been investigated by transmission-electron microscopy. Irradiations were performed at temperatures of 1000-1300 K with 2-MeV oxygen ions and/or 0.6-MeV helium ions. The defect structures of these two refractory insulators were substantially different, which may be related to their different crystal structures. Yttrium oxide has a cubic CaF_2 structure in which the difference in stoichiometry is accommodated by vacant sites on the oxygen sublattice. Aluminum oxide is a hexagonal structure, with c/a = 2.73, in which the oxygen ions form a close-packed sublattice.

The defect microstructure of yttrium oxide irradiated with 2-MeV oxygen ions at 1000 K was composed of interstitial Frank loops on the {111} planes with a density of $\sim 10^{16}/cm^3$ for dosages of 3-6 displacements per atom (dpa). Figure 1 shows a typical microstructure with some loops on edge and some inclined loops, which show moire fringe contrast indicative of another phase of yttrium oxide. Precipitate spots were observed in the diffraction patterns, and these spots could be indexed on the basis of the high-temperature hexagonal-close-packed phase, normally stable from 2500 K to the melting point of 2700 K. A dark-field image formed from one of these precipitate spots is shown in Fig. 2. This micrograph is an on-edge view of the precipitate and shows the variation in thickness of the precipitate present on the stacking-fault loop. A postirradiation anneal at 1000 K for 1 h resulted in the disappearance of the unstable hexagonal-close-packed phase with no noticeable change in loop density or size. Subsequent annealing at 1300 K resulted in changes in the loop size and density. A discussion of the kinetics of loop growth and shrinkage will be presented.

In aluminum oxide, the irradiations with oxygen and oxygen plus helium resulted in a variety of defect structures. Specimens subjected to oxygen bombardment at the 1-3 dpa level exhibited a high density ($\sim 10^{16}/cm^3$) of loops with an average diameter of $\sim$400 Å that were lying on both the basal and the prismatic planes. Furthermore, line dislocations were observed with a Burgers vector along the $\vec{a}$ axis and a density of $\sim 10^{10}/cm^2$. If several thousand ppm of helium are injected at room temperature into the damage range of oxygen and then irradiated with oxygen, virtually all the loops are formed on the basal plane. The presence of helium during irradiation seems to affect the kinetics of loop formation and may be a manifestation of helium trapping at radiation-induced defect sites with subsequent retardation of diffusion, as predicted by Welch et al.[1] A portion of the injected helium was present as small bubbles ($\sim$30 Å diameter) aligned along the c axis (Fig. 3). Postirradiation annealing at 1300 K

*Work supported by the U.S. Energy Research and Development Administration.

resulted in the increase of loop size and reduction in density. For oxygen plus helium bombarded specimens, the helium bubbles migrated to dislocations and coarsened to an average diameter of ∿100 Å, as can be seen in Fig. 4.

Reference

1. D. O. Welch, O. Lazareth, G. J. Dienes, and R. D. Hatcher, Theory of Helium Migration and Trapping in α-Al_2O_3, to be published in Radiation Effects.

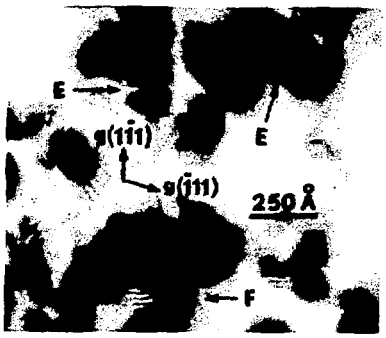

Fig. 1. Micrograph of Y_2O_3 Showing On-edge Loops E and Inclined Loops with Moire Fringes F.

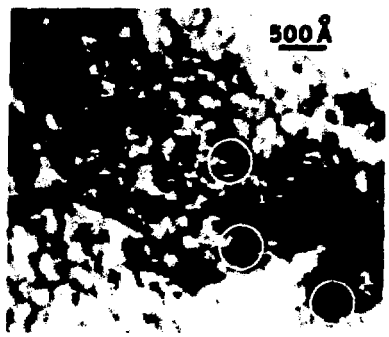

Fig. 2. Dark-field Micrograph of Y_2O_3 with Loops Nearly On Edge. The loops indicated by arrows have several precipitate clusters.

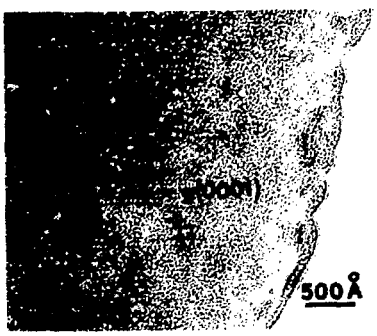

Fig. 3. Underfocused Micrograph of Irradiated Sapphire Showing Strings of Helium Bubbles along the c Axis.

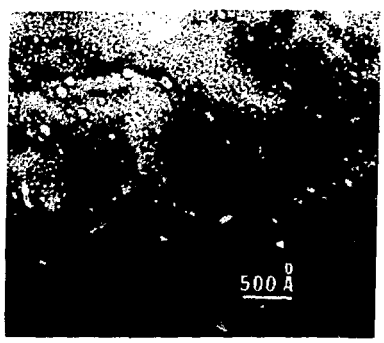

Fig. 4. Irradiated Sapphire Annealed at 1300 K for 1 h Showing Coarsened Helium Bubbles Lying on Dislocation Lines.

RADIATION EFFECTS IN $A\ell_2O_3$

A. Rehavi and N. Kristianpoller
Department of Physics and Astronomy
Tel Aviv University, Ramat Aviv, Israel

Effects of monochromatic uv radiation on nominally pure sapphire were investigated. uv induced thermoluminescence (TL) was compared to that obtained after x-irradiation. Essentially the same glow peaks appeared after irradiation with uv light of wavelengths shorter than 150 nm, as after x-irradiation. uv excitation spectra of the 250, 310 and 450K glow peaks were measured in the vacuum uv range (110-160 nm), and showed a maximum at 138 nm, which coincides with the onset of the band-to-band transition. A shoulder appears at 134 nm. A sharp drop appearing at 122 nm does not necessarily indicate that the transfer of excitation from the lattice is inefficient, but may be due to a strong absorption peak. An additional excitation maximum appears at 145 nm for the 310K glow peak only. This glow peak showed also an emission band at about 610 nm, which did not appear in the emission of the other glow peaks. The TL emission spectra of the glow peaks are given in figure 1. The 250K glow peak showed a broad, probably composed, emission band in the near uv. Weak uv emission bands appear also at the other glow peaks. The main emmission bands of the 310 and 450K glow peaks appear at about 700 nm.

Some of the x-irradiated samples were heated to about 550K, recooled to 80K and illuminated with monochromatic near uv and visible light. TL peaks appeared as result of this photostimulation at the same temperatures as in the x-or vuv excited samples. However, in the TL emission spectra, recorded after this procedure, only the 700 and 610 nm could be detected.

The emission at 700 nm is obviously due to the R-line of Cr^{3+}. It is assumed that during the vuv excitation in the range of the fundamental absorption, as during x-irradiation, a Cr^{3+} impurity ion is reduced to Cr^{2+}, while the hole is trapped at an existing $A\ell$-vacancy. The R emission at the 450K glow peak is attributed to the capture of a thermally released hole by a Cr^{2+} ion and the relaxation of the Cr^{3+} from the excited to the ground state. This is supported by the fact that the excitation spectrum of the photostimulation of the 450K peak had a maximum at about 400 nm, which coincides with a known V-absorption band. A similar R-emission band has recently been found also on γ-induced TL of $A\ell_2O_3$ at 420 and 550K[1]. We recorded the same R-emission at the 310K glow peak. This glow peak appears to be due to a different process; possibly to the thermal release of trapped electrons, which recombine with a Cr^{4+} impurity forming, again, Cr^{3+} in excited state. This is supported by the fact that the excitation spectrum of the photostimulation of this peak had a single maximum at 227 nm which has previously been attributed to an electron trap[2]. In the present work additional emission bands were recorded; the uv emission bands may be due to an iron impurity[3].

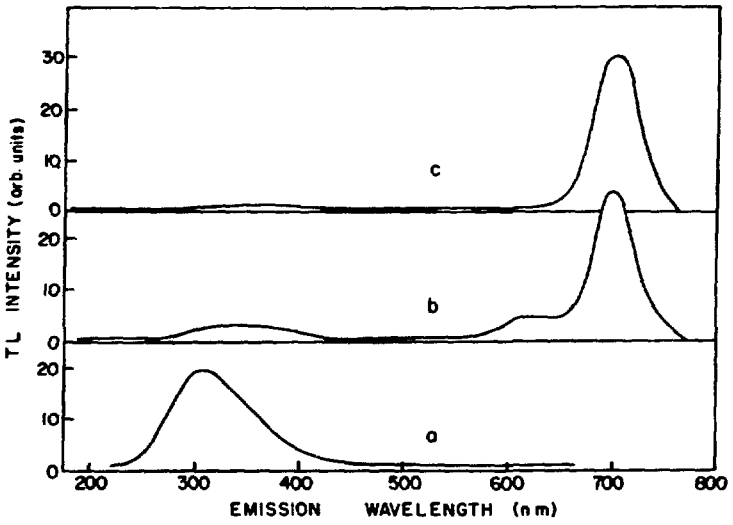

Figure 1: TL emission spectra of the main glow peaks recorded at (a) 240K (b) 290K (c) 440K. (The intensities were not corrected for the spectral response of the EMI 9558Q photomultiflier).

References:

(1) K. H. Lee, G. E. Holmberg and J. H. Crawford,Jr. Phys. Stat. Sol. (a) 39, 669 (1977).

(2) S. Govinda, Phys. Stat. Sol. (a) 32, K95 (1975).

(3) W. A. Runciman, Solid State Com. 6, 537 (1968).

ABSORPTION SPECTRA OF O_2^- IN ALKALI HALIDE CRYSTALS

John Rolfe

Physics Division, National Research Council, Ottawa, Canada

The emission spectra of O_2^- ions in alkali halide crystals give a great deal of information about the ground state of the O_2^- ion, because a large number of sharp zero-phonon lines are visible. The regular spacing of these lines is the separation between vibrational levels of the O_2^- ion in the ground state, and from accurate wavelength determinations a complete anharmonic potential energy curve of the ground state of the O_2^- ion can be calculated. The transitions that give rise to the zero-phonon lines originate from the $v' \approx 0$ vibrational level of the excited state and terminate on various levels $v'' > 0$ of the ground state. The 0 - 0 transition cannot be observed because of lack of intensity, but the frequency of this transition, ν_{00}, can be calculated.

The absorption spectra are quite different. Even at low temperatures, using conventional equipment, no zero-phonon lines can be seen, only a very broad band with a full width at half maximum (FWHM) of about 6000 cm^{-1}, which varies little with temperature. With the aid of a sensitive absorption apparatus, recently extended into the ultraviolet wavelength range, we have been able to detect zero-phonon absorption lines of O_2^- in some alkali halides. These lines appear most clearly in NaCl : O_2^- and accurate wavelength measurements were possible for eight such lines. No isotope lines were observed, so the excited state quantum numbers v' of the lines could not be calculated, but, on the assumption that the origin (ν_{00}) of the absorption and emission spectra were the same, the spectroscopic constants $\nu_{00} = 27\ 312 \pm 4\ cm^{-1}$, $\omega_0' = 596 \pm 1\ cm^{-1}$ and $\omega_0' x_0' = 6.24 \pm 0.07\ cm^{-1}$ were calculated. Since the value of ν_{00} calculated from emission is $27\ 305 \pm 2\ cm^{-1}$, this assumption is almost certain to be correct.

A potential energy curve of O_2^- in NaCl was constructed with both the ground state and the excited state completely characterised. The shift in equilibrium internuclear distance in the excited state was determined from the most intense transitions in absorption and emission, i.e. the vertical transitions from $v' = 0$ and from $v'' = 0$. However, there remain some unex-

plained phenomena in the absorption spectra. First of all, of six alkali halide host crystals investigated, the expected zero-phonon lines were only observed in NaCl. Secondly, even in NaCl, these lines were unexpectedly broad, and increased in width as the vibrational quantum number v' increased. Thus, at v' = 3 the FWHM was 20 cm^{-1} and at v' = 11 the FWHM was more than 60 cm^{-1}. Finally in two crystals, KBr and RbBr, some very sharp zero-phonon lines were observed with vibrational separations similar to the 600 cm^{-1} separations found in NaCl : O_2^-, but since these lines occurred at energies lower than ν_{00} for O_2^- in emission, they cannot be due to the same O_2^- species that gives rise to the emission spectra.

RADIATION INDUCED DEFECTS IN THE OCTAHEDRAL COORDINATION SPHERE OF A_2MX_6-COMPOUNDS

K. Rössler and L. Pross

Institut für Chemie der Kernforschungsanlage Jülich GmbH
Institut 1 : Nuklearchemie
D-5170 Jülich 1, FRG

Radiation induced defects in the octahedral ligand shell of hexahalometallates A_2MX_6 (O_h^5-Fm3m) were investigated by means of optical spectroscopy at low temperatures. Single crystal plates and polycrystalline layers of K_2SnCl_6, K_2ReCl_6 and K_2ReBr_6 were irradiated with 3 MeV-electrons or 30 to 130 keV Ar^+- and Kr^+-ions. The experiments were carried out in a new cryostat system [1] which enabled the detachment of the samples from the beam line and transport to the spectrometer under continuous vacuum and liquid He cooling. The electronic spectra were recorded in the region from 300 to 1400 nm in transmission (single crystals) and diffuse reflectance (polycrystalline layers), cf. [2].

The irradiation created new, additional bands in the region from 270 to 600 nm (K_2SnCl_6) and from 500 to 800 nm (K_2ReX_6), respectively. The lack of colouring in K_2SnCl_6 as well as that of thermal annealing effects excludes colour centres. The new peaks can rather be attributed to ligand field bands of halogen deficient complexes: $[MX_5\square]^-$ or $[MX_4\square_2]$. Since especially the quartet -dublet transition bands remain the same before and after irradiation, macroscopic changes of the samples seem not to occur, i.e. the new peaks are due to species with low concentration but high extinction The assignment of the bands is based on a treatment of the reduction of ligand field strength and symmetry in the damaged units. The remaining ligands most probably relax to square pyramidal ($MX_5\square^-$) and tetrahedral ($MX_4\square_2$) arrangements,

respectively. The shrinking of metal-halogen bond lengths in these defect species is taken into account.

The results from the optical methods agree well with those from preceding radiochemical studies [3] and dielectric measurements of defect molecular units in A_2MX_6 [4]. The concentrations of radiation induced defects are estimated via computer simulation of collision cascades [5] and extinction coefficients in the order of $\varepsilon \approx 10^3 l \cdot Mol^{-1} cm^{-1}$ can be evaluated for the ligand deficient species.

[1] L. Pross, J. Hemmerich and K. Rössler, Rev.Sci.Instr. 47, 353 (1976)

[2] L. Pross, K. Rössler and H.J. Schenk, J.inorg.nucl.Chem. 36, 317 (1974)

[3] K. Rössler, J. Otterbach and G. Stöcklin, J.Phys.Chem. 76, 2499 (1972)

[4] J. Winter and K. Rössler, J.Physique 37, C7-265 (1976)

[5] K. Rössler and M.T. Robinson in Atomic Collisions in Solids, ed. Datz, Appleton and Moak, Plenum Publ. Corp. New York, 1975, Vol. 1, p. 237

DIELECTRIC MEASUREMENTS OF FRENKEL PAIRS IN K_2SnCl_6

K. Rössler and J. Winter[+]

Institut für Chemie der Kernforschungsanlage Jülich GmbH
Institut 1 : Nuklearchemie
D-5170 Jülich, FRG

The most frequent radiation defect in hexahalometallates A_2MX_6 is a Frenkel pair formed by a vacancy in the octahedral MX_6^{2-}-ligand shell and an interstitial halide ion: $MX_5\square^- - X^-$ [1,2]. In K_2SnCl_6 ppm-concentrations of these defects can be created by a mild irradation with thermal neutrons ($D \approx 4 \cdot 10^{15} cm^{-2} s^{-1}$) via the (n,γ)-recoil of halogen ligands. Dielectric properties were measured in ⟨1,1,1⟩-direction of single crystal plates of K_2SnCl_6, cut parallel to the natural (1,1,1)-surfaces. D.C. conductivitiy (DC), ionic thermo current (ITC) and phase transition induced dipolar relaxation (TIDR) methods were applied [3,4].

Both components of this Frenkel pair could be identified and their annealing reactions followed independently. The vacancies in the ligand shell were monitored via the TIDR-peak intensity making use of the stimulation of the $MX_5\square^-$-rotary movements at the 252 K and 262 K structural phase transitions of K_2SnCl_6. They were stable up to 340 K at which temperature the annealing started. A saturation value of 60% annealing was reached at 400 K. The motion of the halides was measured by DC and ITC. The chloride ions were found to be trapped on interstitial sites near impurities. They become mobile with an effective activation energy of $E_A \approx 1.1$ eV. A strong correlation between the decrease of $SnCl_5\square^-$ and Cl^- was observed. The results agree well with those obtained from radiochemical experiments of ^{38}Cl-recoil in the isostructural K_2ReCl_6.

In non-irradiated K_2SnCl_6 in thermal equilibrium, the most frequent defect type was the cationic Frenkel pair. The ionic conductivity was predominantly caused by the migration of K^+-interstitials or the corresponding vacancies. The energy of formation of cationic Frenkel pairs was evaluated from DC to E_F = 0.9 eV, whereas the energy of migration amounted to E_M = 0.4 eV. Despite the low concentration in the 10 ppb-range the thermal formation of $SnCl_5\square^-$-Cl^- pairs could be measured in pure K_2SnCl_6 and single crystals doped with about 0.1 Mol% of K_2SnCl_5X (X= F,Br,I).

[1] R. Bell, K. Rössler, G. Stöcklin and S.R. Upadhyay, J.inorg.nucl.Chem. 34, 461 (1972)

[2] M.T. Robinson, K. Rössler and I.M. Torrens, J.Chem. Phys. 60, 680 (1974)

[3] J. Winter and K. Rössler, J.Physique 37, C7-265 (1976)

[4] J. Winter, Report-Jül-1419-May 1977 (Thesis RWTH Aachen)

THE SIDE-BANDS IN ABSORPTION AND LUMINESCENCE EXCITATION SPECTRA OF KBr:Tl.

M. ROTH and A. HALPERIN
THE RACAH INSTITUTE OF PHYSICS, THE HEBREW UNIVERSITY, JERUSALEM, ISRAEL.

It is well known that thallium-(or other heavy metal) doped alkali halides show several absorption bands in the uv, known as the A, B and C bands. Absorption in these bands results in characteristic luminescence. The absorption and excitation spectra for luminescence often show, especially in highly doped crystals, various side bands. The origin of these satellite-bands is not quite clear. Some authors[1] attribute them to complex thallium centers and assign the various bands to thallium dimer-, trimer-, and tetramer-centers. Other authors[2] claim that the satellite band near the A band should be associated with direct excitation up to the normally forbidden ^3P_o metastable energy level of the monomer thallium center.

In the present work we show that at least part of these satellite-bands arise from complex centers which include various impurities present in small concentrations in practically all crystals. Thus, we were able to enhance these bands by doping the crystals with proper impurities. Figure 1 shows a few examples. Curve a in this figure shows the A-Absorption region in an undoped KBr:Tl crystal at 9°K. The thallium concentration in this case was nearly 10^{-4} mole/mole. Under such high concentrations of thallium, the absorption spectrum shows clearly in addition to the main A-band at 4.80 eV an additional band at 4.68 eV (2650A) with a shoulder at 4.64eV (2670A). Both the additional bands were ascribed by Tsuboi[1] to the thallium dimer center. In curve b of Figure 1 we show the prominent enhancement of the 2650A band by doping a crystal containing practically the same concentration of thallium by about 1% of KI (introduced in the powder used for growing the crystal). This band is thus shown definitely to be associated with the presence of an iodine ion in the vicinity of the thallium ion in the crystal. Curve c shows the absorption

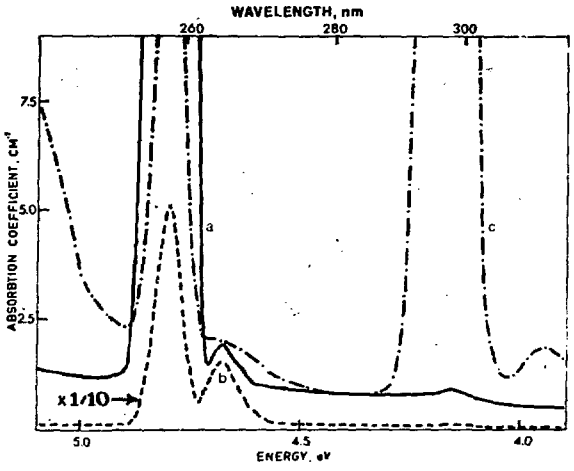

Figure 1

obtained by the addition of about 10^{-4} mole/mole of lead to a crystal containing only 5 X 10^{-6} mole/mole of thallium. The absorption spectrum shows now a weak absorption at the long wavelength side of the A-band which appears as a band peaking at 2670A in the excitation spectrum. The bands at longer wavelengths in Curve c are due to the KBr:Pb^{++} center.

Other side-bands including those near the B- and C-bands were also found to belong to complex centers introduced by various impurities.

Various complex bands in absorption and excitation spectra and the luminescence spectra obtained by excitation in these bands will be described and discussed.

1. T. Tsuboi, J. Phys. Soc. Japan, 29, 5 (1970).
T. Tsuboi, Can. J. Phys. 54, 1772 (1976).
2. A. Ranfagni et al, Phys. Rev. Letters 28, 1035 (1972).

RECOMBINATION LUMINESCENCE BETWEEN TRAPPED ELECTRONS AND SELF-TRAPPED HOLES IN $SrCl_2$ DOPED WITH ALKALI CATIONS AFTER X-IRRADIATION

E. Rzepka, L. Taurel and J.P. Chapelle

Laboratoire de Physique Cristalline - Université de Paris-Sud -
(Equipe de Recherche associée au CNRS n°13)
Bâtiment 490 - 91405 ORSAY CEDEX - FRANCE -

After X-irradiation in the range 10-145 K, $SrCl_2$ doped with M^+ ions ($M^+ = Na^+, K^+, Rb^+$) gives rise to a post-luminescence whose spectrum, independent of the M^+ cation nature, is formed principally of a broad band at 500 nm. The hyperbolic law of isothermal decay of post-luminescence ($I_t = C N_0/t$ where N_0 is the initial number of V_k centres) suggests that this emission is due to a tunnelling recombination between V_k and perturbed F centres. While between 10 and 38 K the coefficient C does not depend on T, at higher temperatures the value of C is very sensitive to the X-irradiation temperature. In particular in the range 35-100 K the behaviour of the coefficient C is well explained by the motion of V_k centres viewed as small polarons.

The glow peaks at 45 and 100 K observed by warming the X-irradiated crystals at 10 K arise from V_k centres which become mobile with respectily 180° and 90° jumps and come into the neighbourhood of F centres.

E. Rzepka, S. Lefrant, L. Taurel and J.P. Chapelle
J. Phys. C. : Solid State Phys. 10, 1 (1977)

FURTHER EVIDENCE FOR THE DI-INTERSTITIAL MODEL FOR THE V_4 CENTRE

M. Saidoh* and P.D. Townsend
University of Sussex, Brighton BN1 9QH, U.K.

The observed concentration of single and multiple point defects is a function of their rate of production as well as the total irradiation dose and, for example, flux effects are well known in establishing an equilibrium between F and M centres. Similarly flux changes may be used to test the di-interstitial model of the V_4 centre in alkali halides [1]. We have made major changes in the flux conditions without altering the power dissipation in the sample by forming the colour centres by ion implantation with either separate ions or with molecules. In the latter case the dissociation of the molecule at the surface generates two simultaneous ion tracks which originate at the same point on the surface. By adjusting the ion current and energy one may thus deliver the same power over approximately a constant projected range into the crystal for ions derived from the molecule as for ions which were directly implanted. The volume of excited material is larger than that excited by the ions because of the exciton diffusion. Either from arguments of atomic displacement or exciton/Pooley type F and H centre formation we expect to produce a central core which is vacancy rich surrounded by an annulus containing interstitials. Therefore molecular ion bombardment should generate a higher concentration of multiple defects (e.g. M, R, V_4) than a comparable energy deposition from an ion beam. The results obtained in KBr clearly follow this pattern and give strong evidence that the V_4 band in the 4.5 eV region is indeed a multiple interstitial centre [2].

1. Itoh, N., Kawamata, T., Hirao, T. and Kanzaki, H. 1967 J. Phys. Soc. Japan 23 453

2. Saidoh, M., Townsend, P.D., 1977 J. Phys. C. 10 1541-48

* Present address Division of Thermonuclear Fusion Research
Tokai Jaeri,
Jokai-Mura,
Naka-Gun,
Ibaragi-Ken,
Japan.

DYNAMIC JAHN-TELLER VIBRONIC COUPLING IN $T \times \tau_2$

N. Sakamoto and S. Muramatsu

Department of Electronic Engineering, Utsunomiya, University, Utsunomiya, Japan

The problem of vibronic solution in the Jahn-Teller coupling has been one of the important problems in the theory of the Jahn-Teller effect. The objective of this work is a further challenge from a different approach to the fundamental problem ($T \times \tau_2$) first analysed numerically by Caner and Englman.[1]

Our method is a direct application of recent numerical analysis for diagonalization of a sparse matrix. We have found that the Lanczos method[2] can be applied effectively to the Hamiltonian matrix with which we are concerned, even if the order of its matrix is very large. This method has the advantage of easy inclusion of the higher vibrational states, since we have no need to construct the symmetry adopted basis functions,[1] and can avoid the tedious calculation of the matrix elements. There is, however, a weak point inhering in the Lanczos method. We can remove this weakness by taking steps of reorthogonality of column vectors of the transformation matrix by the use of which we transform the Hamiltonian matrix into a tridiagonal one.

Figs. 1 and 2 show part of our results of the calculation which takes into account up to vibrational excited states corresponding to the phonon number 16. The parameter S' in Fig. 1 is such that exp(-S') is the fraction of the total intensity in the zero-phonon line of a transition from an electronic A state. Our result of S' for $k^2 \leq 0.3$ coincides precisely with that given by the approximate expression in weak coupling derived by Nasu,[3] $S' = k^2(1-k^2/8)/(1+k^2/4)^2$. The relation among Ham's reduction factors, $K(E)$, $K(T_1)$ and $K(T_2)$ has been recently investigated by Leung and Kleiner,[4] their result being

$$K(E) + \frac{3}{2}[K(T_2) - K(T_1)] = 1 - 3f(T_1).$$

Fig. 2 is a plot of the factor, $3f(T_1)$. As seen from this figure, the magnitude of this factor is so small even in the strong coupling that we can regard that the relation, $K(E) = 1 - 3[K(T_2) - K(T_1)]/2$ is a good approximation under general vibronic coupling.

An extension of this work to the general problem of $T \times (\tau_2 + e)$ is now under way.

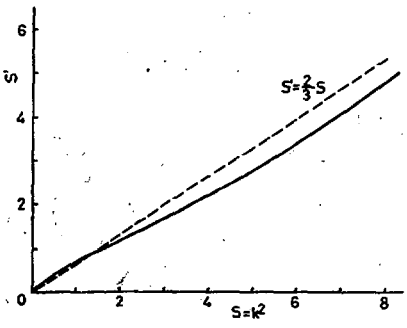

Fig. 1. A plot of S' against the square of the coupling constant k.

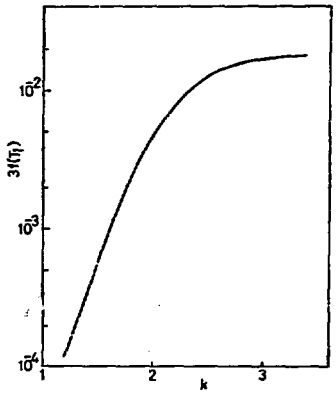

Fig. 2. The factor $3f(T_1)$ is plotted as a function of k.

1. M. Caner and R. Englman, J. Chem. Phys. 44, 4954 (1966).
2. C. Lanczos, J. Res. Nat. Bur. Stand. 45, 255 (1950).
3. K. Nasu, Z. Naturforsh 30, 1060 (1975).
4. C. H. Leung and W. H. Kleiner, Phys. Rev. B10, 4434 (1974).

OPTICAL AND ELECTRICAL PROPERTIES OF RbI:Pb

S. B. S. Sastry and K. Balasubramanyam
Department of Physic, I.I.T., Madras-600036, India

Heavy ions like In^+, Tl^+, Pb^{2+} etc., with ns^2 configuration, when doped in alkali halides are known to show absorption bands due to intra-ionic transitions $(ns^2) \rightarrow (ns)(np)$ in the otherwise transparent region of the host crystals designated as A, B, and C bands. They are due to $^1S_o(A_{1g}) \rightarrow {}^3P_1(T_{1u})$ (spin orbit allowed), $^1S_o \rightarrow {}^3P_2(T_{2u} + E_u)$ (vibration induced) and $^1S_o \rightarrow {}^1P_1(^1T_{1u})$ (dipolar) transitions respectively. Fukuda[1] made a systematic study of these absorption bands. In some cases A and C bands showed doublet and triplet structure respectively. Sastry et al[2] observed structure in A and B bands of Pb^{2+} doped in NaCl and tentatively gave dynamical Jahn Teller (DJT) effect as one of the probable causes for the observed splitting. Jacobs et al[3] studied the line shapes of A, B and C bands and also concluded that the DJT effect is responsible for the splitting of A and C bands in the case of tin-doped alkali halides. In this paper we report a triplet splitting observed in the C-band of Pb^{2+} doped with RbI. The observed shape of the C band is remarkable and is very close to that predicted theoretically by Inoue and Toyozawa.[4] The shape of the C band and the possible origin of D' band observed are discussed.

It is known that the dielectric loss in alkali halides doped with aliovalent cations, when plotted against frequency on a log-log scale, shows peaks which can be related to the jump processes or orientation of dipoles formed by the impurity-vacancy (charge compensating) pairs. Here we report the results of dielectric loss and d.c. conductivity measurements on RbI doped with Pb^{2+} ions. Two loss peaks are observed, their positions being shifted to higher frequencies with increasing temperature. The data could be fitted to an exponential equation $f=f_o\exp(-E/kT)$. The activation energy E is estimated to be 0.54 ev for the first peak and 0.51 ev for the second peak which is more intense. The d.c. conductivity measurements gave an activation energy of 1.41 ev in the intrinsic region and an activation energy of 0.76 ev in the association region. All these data

are correlated and discussed. From the relative sizes of the lead and rubidium ions, relative intensities of the loss peaks and the ratio of the pre-exponential factors, it is concluded the lead ion and nn vacancy exchange places to give the first loss peak and the rubidium ion exchanges with the nnn vacancy to give the second loss peak. Assuming the value of the association energy of the impurity-vacancy pair, calculated by Rao and Rao[5] the energy of formation of a schottky pair in RbI is estimated from the present conductivity data and is found to be in agreement with the theoretically estimated value.[5]

References:

1. A. Fukuda, Science of Light (Tokyo) 13, 64 (1964).
2. S.B.S. Sastry, V. Viswanathan and C. Ramasastry, Phys. Stat. Solidi 55, K21 (1973).
3. P.W.M. Jacobs et al, Canad. J. Phys. 53, 192 (1975); J. Phys. C: Solid State Phys. 7, 221 (1974); J. Phys. Chem. Solids 36, 1383 (1975).
4. Y. Toyozawa and M. Inoue, J. Phys. Soc. Japan 21, 1663 (1966).
5. K. J. Rao and C.N.R. Rao, Phys. Stat. Solidi 28, 157 (1968).

OPTICAL AND THERMOLUMINESCENCE PROPERTIES OF UNDOPED AND TIN DOPED RbCl

S. B. S. Sastry and K. Balasubramanyam
Department of Physics, I. I. T., Madras-600036, India

It is well known that the presence of impurity ions induces new bands in the optical absorption spectrum of alkali halides and also affects their electrical and thermoluminescence (TL) properties. Here our studies on TL and optical properties of undoped and tin-doped RbCl crystals are reported and probable radiative recombination processes suggested to correlate various emission bands observed at different temperatures. This throws some light on the nature of the actual recombination centers that are responsible for the emission.

The optical absorption spectrum of melt grown undoped RbCl crystal shows a weak band at 5.04 ev(246 nm), a shoulder at around 5.52 ev(225 nm) and a sharply rising absorption peaking at 6.25 ev(197 nm) at room temperature. They are thought to be due to the presence of some hydrogen and OH^- centers[1] stabilized probably in the presence of trace impurities like magnesium. The effects of radiation damage on these crystals are discussed.

Irradiation with low doses of x-rays produces Sn^+ centers along with V centers in the tin-doped crystals. To have an idea about these tin centers without the interference of V centers, absorption spectra of additively and electrolytically colored undoped and tin-doped samples are studied. The bands observed at 3.55, 4.1 and 5.9 ev are attributed to Sn^o and Sn^+ centers. The bands observed at 2.45 and 3.1 ev in electrolytically colored tin-doped crystals are attributed to Sn^- centers.

TL glow curve of tin-doped RbCl crystal under low dose of irradiation shows three prominent peaks. Optical bleaching of such crystals reduces the glow and found to produce a new glow peak at higher temperature indicating that electrons released during optical bleaching are trapped at a deeper trap which releases the electrons at a higher temperature, an interesting phenomenon of transfer of energy from one center to another by optical means. The emission region of these x-irradiated crystals, as observed by means of different filters, is the same in all cases indicating

that the recombination center may be the same in all cases. The emission region for an optically bleached crystal is different from that of an unbleached crystal.

On the basis of the TL glow and emission results on moderately irradiated (with γ-rays 5×10^6R) undoped and tin-doped crystals, an energy level diagram for the TL processes is proposed choosing the band gap of RbCl[2] to be around 7.6 ev.

References:

1. J. Rolfe, Phys. Rev. Letters. 1, 56 (1958).
2. J. E. Eby, K. J. Teegarden and D. B. Dutton, Phys. Rev. 116, 1099 (1959).

THERMOLUMINESCENCE AND OTHER PROPERTIES OF UNDOPED AND TIN DOPED RbI CRYSTALS

S. B. S. Sastry and K. Balasubramanyam
Department of Physics, I. I. T., Madras-36, India

The optical absorption of alkali halides containing heavy metal ions like Tl^+, In^+, Pb^{2+}, Sn^{2+}, etc. has been widely studied.[1,2] Here we report the results of optical absorption, thermoluminescence (TL) glow and emission and esr measurements made on undoped and tin-doped rubidium iodide crystals after γ-irradiation. It is found that tin enhances the TL glow compared to undoped crystals. The TL emission seems to have got shifted to longer wavelengths as compared to undoped crystals. The emission due to the prominant glow peak in the tin-doped crystals is around 2.4 ev. The emission obtained at different temperatures indicates that there is a common recombination center. In these tin-doped crystals the F center concentration is more than that in the undoped crystal for the same radiation dose (in contrast to tin-doped RbCl) indicating the formation of Sn^{3+} after γ-irradiation. This is further confirmed by esr spectra also. From the known values of the band gap energy of RbI[2,3] and other absorption energies, an energy level scheme explaining various TL processes is proposed on similar lines as is done in the case of NaCl: Pb.[4] It is concluded that Sn^{2+} enhances the TL output contributing an electron during irradiation to form more F centers and the resulting Sn^{3+} ion acting as a recombination center to emit photons.

References:

1. A. Fukuda, Sci. of Light (Tokyo) 13, 64 (1964); J. Phys. Soc. Japan 27, 96 (1969).

2. K. Inohara, Sci. of Light (Tokyo) 14, 92 (1965).

3. G. R. Huggett and K. Teegarden, Phys. Rev. 141, 797 (1966).

4. S. B. S. Sastry and K. Balasubramanyam, J. Lum. (1977).

ESR, OPTICAL ABSORPTION AND THERMOLUMINESCENCE STUDIES ON IRRADIATED NaCl:Ni

S. B. S. Sastry and C. N. Subbanna
Department of Physics, I. I. T., Madras-600036, India

and

A. Scharmann
I. Physics Institute, Justus Liebig University, Giessen,
Federal Republic of Germany

The ESR spectrum of NaCl:Ni observed at 77 K after x-irradiation at room temperature (this is done to avoid the formation of V_k centers) and optical bleaching (to remove F-center ESR) consists of two groups of lines and a broad isotropic line at g = 2.418. The Ni^{2+} ion has a $3d^8$ configuration and on trapping an electron becomes Ni^+. Since the irradiation is done at room temperature, all the Ni^{2+} ions are not likely to be associated with their charge compensating vacancy and these Ni^+ centers are likely to have a symmetric configuration giving rise to the single isotropic ESR line as observed. The two groups of lines observed may be the same as reported earlier by Kuwabara,[1] which are described as due to shf interaction of the four and two chlorine nuclei ($\perp$ and $\parallel$) surrounding the Ni^+ ion in the compressed tetragonal symmetry. The g-values estimated for the two patterns are $g_\perp = 2.295$ and $g_\parallel = 2.059$.

The optical absorption spectrum of NaCl:Ni showed the characteristic bands[2] of Ni^{2+} at 5.0 and 6.4 ev. On irradiation with x-rays the absorption increased in the 5-6 ev (V-bands) region and in the 2-3 ev (F-band) region. There is an effective reduction in the 5.0 ev band and increased absorption in the 3.5-4.5 ev region indicating some changes in Ni^{2+} centers, like formation of Ni^+ centers etc. Bleaching with F-light removes the F-band completely but not the V-bands, which means that some V centers are still present. The new bands observed at 4.5, 4.0 and 3.7 ev are attributed to nickel centers (eg. Ni^+, Ni^o etc.). The Ni^+ center is considered to be stable if the lattice around the ion relaxes.[3]

The thermoluminescence glow curve of a γ-irradiated NaCl:Ni sample showed three prominent peaks at 340, 405 and 470 K. The emission due to these three glow peaks was recorded keeping the sample at constant temper-

ature slightly below the peak value. The emission spectra recorded at 310 and 360 K show bands at 1.97, 2.61 and 3.46 ev (three) and at 1.98 and 3.49 ev (two) respectively. The emission at 420 K showed four bands at 3.44, 2.85, 2.61 and 1.97 ev.

The mechanisms involved in the TL processes are discussed in the light of these emission and optical absorption bands and an energy level diagram, very similar to that suggested in the case of NaCl:Pb,[4] is proposed.

References:

1. Goro Kuwabara, J. Phys. Soc. Japan 31, 1074 (1971).
2. K. Polak, Z. Phys. 223, 338 (1969).
3. K. Polak and J. Malek, Cryst. Latt. Defects 6, 239 (1976).
4. S. B. S. Sastry and K. Balasubramanyam, J. Lumin., to be published (1977).

MICROSYNTACTIC INTERGROWTH AND DEFECTS OF β-ALUMINA TYPE COMPOUNDS

H. Sato, Y. Hirotsu and Y. Tang
School of Materials Engineering
W. Lafayette, IN 47906

Structural characteristics and defects of β-alumina type compounds are investigated by means of the lattice imagining technique of transmission electron microscopy. The data shown are specifically for Mg-doped β-alumina[1] and Ba-ferrites.[2] In both cases, the crystalline repeat distance in the c-direction is not uniform but is a random mixture of unit cells of different sizes. The variation of the size of unit cells can be understood if these unit cells are built up by a stacking in the c-direction of a number of structural subunit blocks and if these subunit blocks behave independently. Details of structural defects like dislocations can also be understood on this basis. Implications of such characteristics in connection with superionic β-alumina compounds will be discussed.

1. H. Sato and Y. Hirotsu, Materials Research Bulletin 11 1307 (1976).
2. Y. Hirotsu and H. Sato, American Ceramic Society Bulletin 56 298 (1977).

PULSE RADIOLYSIS STUDIES OF DEFECT FORMATION IN ALKALI HALIDES AT HIGH TEMPERATURES

R. D. Saxena, K. Tanimura and N. Itoh

Department of Crystalline Materials Science, Faculty of Engineering.
Nagoya University, Nagoya, Japan

It is known that the pulse radiolysis studies of alkali-halides have already contributed a great deal in understanding the primary processes of defect production at low temperatures. Recently much attention has been paid on the defect production at high temperatures of the secondary reactions of primary defects. Since some of these reactions are expected to occur in a very short time, the technique of the pulse radiolysis appears to be very useful in order to clarify the mechanisms of these reactions. The purpose of present paper is to describe the pulse radiolysis studies of KBr in the temperature range of 200 K to 500 K. It is shown that the V_4 centers which are produced simultaneously with the quick formation of the F centers at 200 K are transformed to other interstitial defects within a time period of 20 nsec at higher temperatures. Some properties of the transformed defects are described.

The specimens of KBr obtained from Harshaw were irradiated with 1 MeV, 20 ns pulse electron beams from a Febetron accelerater and transient change of optical absorption coefficient was measured in the wavelength range of 270 nm to 900 nm. The production of the F center followed quickly the electron pulse irradiation and a comparatively slow decay was accompained. Figure 1 shows the temperature dependence of the yield of the quickly formed F centers. It is to be noted that the yield is independent of temperature. On the other hand the formation yield has been shown decreasing with increasing temperature above 200 K when continuous irradiation is employed.[1)] The difference between two results can be ascribed to the back reaction of the defects produced by irradiation.

The complementary defects to the F centers produced quickly at 200 K has been known to be the V_4 centers or the di-H centers, which can be created

by the interaction of dynamic interstitials with other H centers. It was found that as the temperature increases, the concentration of the quickly formed V_4 centers decreases prominently. The decrease of the production efficiency of the V_4 center without any loss of the F center production indicates that the V_4 center is transformed to some other interstitial defects rather than to be decomposed. This quick transformation can be assumed to be the formation of the dislocation loops as observed by Hobbs using electron microscopic technique.[2)]

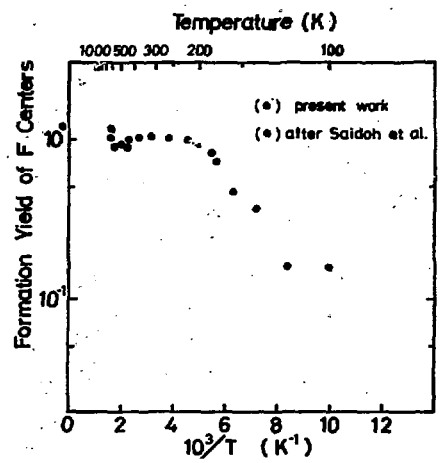

Fig. 1

The decay curves of the F center between 370 K and 500 K can be divided into two exponentials. The rate of the first exponential decay was found to follow an Arrehenius equation with an activation energy of 0.25 eV. This activation energy appears to represent the releasing process of the interstitials from the transformed defects. The second exponentials have a decay of a rate between 10^{-3} and 10^{-4} $s,^{-1}$ which increases with increasing temperature. The amount of the F center which annihilates at the second exponentials may correspond to the concentration of the interstitials stabilized in the transformed defects (e.g. dislocation loops) and the decay may be ascribed to the F-center migration.

1) E. Sonder and W. A. Silbley: Point Defects in Solids vol. 1. ed. J. H. Crawford, Jr and L. M. Slifkin (Plenum, New York, 1972) p. 201
2) L. W. Hobbs, A. E. Hughes and D. Pooley: Phys Rev. Letters 28, 234 (1972)

EVOLUTION OF MOLECULAR ORDER AND PHASE-TRANSITIONS IN MIXED ALKALI-HALIDE-CYANIDE CRYSTALS

II. DEVELOPMENT OF FERROELASTICITY FROM PARAELASTIC DEFECT BEHAVIOR

Luiz Carlos Scavarda do Carmo* and Fritz Luty
Department of Physics, University of Utah, Salt Lake City, Utah 84112

Dilute CN^- defects in potassium-halides reorient by quantum-mechanical tunneling between eight <111> minima of a very shallow rotational potential. From the measured size of the isolated CN^- electric and elastic dipole moment, it is evident that the elastic dipole interaction is much stronger compared to the electric one. In agreement with this, the high-temperature disorder-order phase-transition of pure KCN is essentially an elastic one (parallel order of the CN^- elastic dipoles in a <110> direction), while electric dipole-order occurs only at much lower temperature. Using stress-optical measurements on the mixed system KCl:KCN, we address ourselves to the question of how paraelastic alignment of individual non-interacting elastic dipoles changes under progression to dipole-pairs, -triples ... and larger clusters, and how eventually spontaneous collective elastic dipole ordering (ferroelasticity) evolves in the mixed system.

Under applied uniaxial stress of different symmetry, the achieved alignment of the CN^- system was detected by the stress-induced dichroism of the second harmonic CN^- vibrational absorption at 2.5 μ, measured parallel (∥) and perpendicular (⊥) to the stress. While <100> stress reveals the E_g, and <111> stress the T_{2g} elastic dipole part, experiments under <110> stress allow to measure the alignment effects from both symmetry parts.

Extended experimental results covering these symmetries, the whole KCl:KCN mixture, and the temperature range between He- and room temperature, will be presented and discussed. Only a few basic trends and outstanding results can be indicated here. Starting from the Curie-law (T^{-1}) behavior of the isolated dipoles ($x<10^{-3}$), the low-temperature alignment ($T<40K$) disappears very quickly with increasing dipole concentration, while alignment effects appear at higher temperatures. Consequences of these results

for the possible symmetry of the smallest cluster, the elastic dipole pair, will be discussed and compared to Raman-results and to the expected pair-symmetries.

While in the middle of the mixture (x≈0.5) the stress-alignment response has nearly disappeared, it starts to build up again when x approaches the critical concentration x_c (mentioned in Part I). For $x \approx 0.76$ (just below x_c), stress-alignment is possible above 70K, has maximum efficiency around 85K, and decreases toward higher temperatures. This broadly temperature dependent stress-alignment effect is reversible in the high-temperature and irreversible in the low temperature range. For slightly higher CN^- concentration ($x \approx 0.8$, just above x_c) where domain scattering starts out, the irreversible (ferro-elastic) stress-alignment response becomes huge, so that already a very small stress (~30 atm) achieves nearly complete dichroism and a strong reduction of light-scattering and depolarization. This general behavior persists from x_c upward to pure KCN, for which we could achieve a stress dichroism of $K(\perp):K(\parallel) \approx 10$ and a good optical transparency. In all these cases above x_c, ferro-elastic stress-alignment is possible between T_c and a temperature in the 50-85K range, where the alignment rate becomes time-dependent and eventually freezes in.

These measurements confirm that above x_c the crystal consists of domains of parallel ordered CN^- molecular dipoles. These domains, which can be regarded as "giant elastic dipoles", are oriented at random in the six <110> orientation. Both E_g and T_{2g} stress can achieve alignment of these domains, removing the light scattering, and introducing irreversible and oriented ferroelasticity into the crystal.

The consequences of the results of Part I and II will be comprehensively discussed, particularly the problem of a critical concentration x_c in the mixtures, at which domain-formation and collective ferroelastic order appears abruptly, and the problem of the variation of the x_c value in the KCl, KBr, and KI mixtures.

*On leave from Pontificia Universidade Catolica (PUC) de Rio de Janeiro, and supported by a fellowship from PUC and CNPq (Brazil).

MODULATED ABSORPTION OF Z_2(Eu) CENTERS IN KCl.

W. Scheu and H.J. Paus
Physikal. Institut Teil 2, Universität Stuttgart, Germany

ESR experiments /1/ of the paramagnetic Eu^{++}-ions in Z_2(Eu) require a strict (100) axial symmetry of this center and lead to a first idea of its atomistic model. On the other hand, optical excitation experiments show that two different configurations can be distinguished by their radiative lifetimes /2/. Polarized measurements reveal a (110) symmetry for the "fast" Z_2^f center ($\tau \ll 1$ ms), whereas no symmetry information is obtainable for the "slow" Z_2^s center ($\tau \approx 1$ ms).

Modulated absorption spectroscopy (temporary bleaching) - especially suitable for centers with long radiative lifetimes - should be able to eliminate the discrepancy between the reported ESR and optical findings.

As an example the figure shows the modulated absorption spectrum of Z_2(Eu) centers for a bleaching light of E ≈ 2 eV

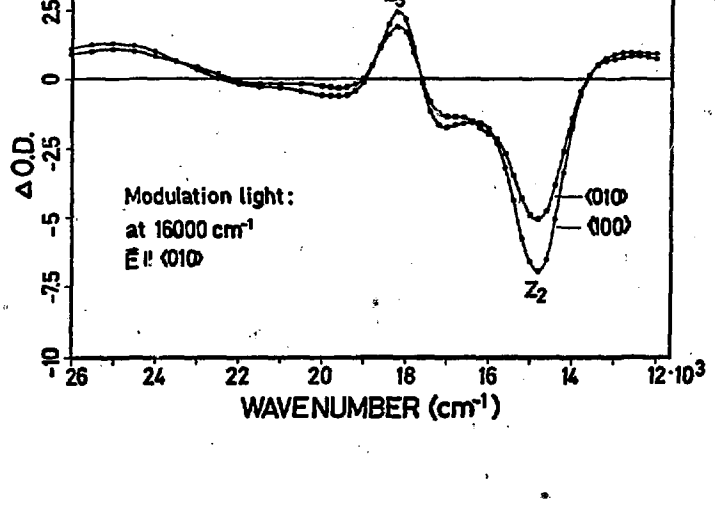

polarized along (010). The following informations can be drawn from this spectrum:

1) As stated from excitation experiments the absorption band at 1.84 eV is due to Z_2^S(Eu) centers. Further, but smaller bands at higher energies, presumably in the 2 eV-region must also be attributed to this center /2/.

2) As in the case of Z_2(Sr) and Z_2(Ca) a broad F'-like band underlies the spectrum. The explanation of this band is still speculative.

3) A Z_3 or Z_3-like center(E = 2.26 eV and 2 - 2.1 eV)is formed by the high intensity excitation. Unlike the "normal" case of Z_3(Sr) or Z_3(Ca) the Z_3(Eu) absorption is thus completely hidden under the F band (2.3 eV) explaining the "impossibility" of a direct Z_3 center formation by ionization of Z_2 centers.

4) A (100) dichroism (but no (110)-dichroism within experimental error) by polarized bleaching has been obtained, revealing that the Z_2^S(Eu) center has a (100) symmetry as found by the paramagnetic resonance experiments.

/1/G.Kenntner and H.J.Paus Z.Physik B 25, 219 (1976)
/2/K.H.Umbach and H.J.Paus 1974 Int.Col.Center Conf. Sendai, abstract 154

SMALL POLARON VERSUS CRYSTAL FIELD TRANSITIONS IN A DEEP OXIDE ACCEPTOR

O.F. Schirmer

Institut für Angewandte Festkörperphysik
der Fraunhofer-Gesellschaft, D-7800 Freiburg

Small polaron (SP) optical transfer between equivalent sites dominates /1, 2/ the optical absorption of trapped holes in oxide materials, previously assigned to O^- crystal field (CF) transitions. The first identification of such a CF transition, reported here, shows that CF absorption is weak compared to SP absorption.

Both were studied with the system BeO: $[Li]^0$. The hole is preferentially localized along c by the polar crystal field. The absorption mechanisms are indicated in Fig. 1. The SP absorption is π- and σ-polarized; CF only σ. A Pseudo-Jahn-Teller treatment /2/ led to the following SP absorptions (up to frequency independent factors):

$$\alpha_\pi^{SP}(\omega) = \hbar\omega \cdot \exp\left(-w\left(\hbar\omega - 8/3\, E_{JT} + 2J\right)^2\right)$$

$$\alpha_\sigma^{SP}(\omega) = \hbar\omega \cdot \exp\left(-w\left(\hbar\omega - 8/3\, E_{JT} - J\right)^2\right)$$

(E_{JT} hole stabilisation energy, J resonance integral between orbitals $|\beta_i\rangle$, $w^{-1} = 16/3 \cdot E_{JT} \cdot \hbar\omega_o$, $\hbar\omega_o$ representative vibration frequency of the LiO_4 tetrahedron.) The π-absorption (Fig. 2) can be fitted with $E_{JT} = 1.08$ eV, $\hbar\omega_o = 0.11$ eV and $J \approx 0.2$ eV. With respect to the dicrepancy at high energy see /1, 2/.

The σ-absorption is a superposition of two bands:

$$\alpha_\sigma(\omega) = C_1 \cdot \alpha_\sigma^{SP}(\omega) + C_2 \cdot \alpha_\sigma^{CF}(\omega)$$

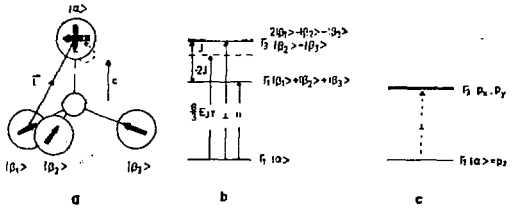

1a: Arrangement of O^{2-} p_z orb. in BeO:Li. At low T, only $|\alpha\rangle$ is populated. $\vec{l}$: dipole arm for SP transition. 1b: Level scheme for SP transitions. 1c: Level scheme for CF transitions.

with $\alpha_\sigma^{CF} = \hbar\omega \exp(-u(\hbar\omega - E_{CF})^2)$. A fit of the σ-absorption is obtained with the above SP parameters and $u = 2.49\ eV^{-2}$, $E_{CF} = 2.10$ eV. C_1 and C_2 correspond to a SP oscillator strength 7.6 times higher than that of the CF absorption $\alpha_\sigma^{CF}(\omega)$.

The CF assignment is based on these features: 1) σ-polarization as predicted. 2) E_{CF} is comparable with the CF splitting determined from ESR, 1.75 eV /3/. 3) The CF transition is Laporte forbidden to a large extent. The band is therefore weaker than the polaron bands, which are genuinely electric dipole allowed. 4) The CF band is more narrow, since in contrast to the SP absorption not all the band energy is expended to the lattice, but leads to an orbital promotion. - - The short bond distances in BeO favor the appearance of a CF band because of the concomitant s-p-hybridisation. CF transitions are therefore weaker in most other oxide materials. The electric field induced dichroism in MgO:V^- /4/ can be explained /1/ by SP absorption only.

/1/ O.F. Schirmer, Z. Physik B 24, 235 (1976)
/2/ O.F. Schirmer, R. Schnadt, Solid State Comm. 18, 1345 (1976)
/3/ O.F. Schirmer, J. Phys. Chem. Solids 29, 1407 (1968)
/4/ B.H. Rose, D.L. Cowan, Solid State Comm. 15, 775 (1974)

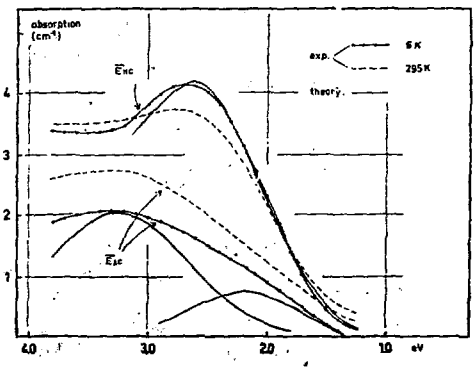

2: Absorption of BeO: $[Li]^0$ and analysis with the described model.

TRANSIENT ABSORPTION FROM THE RELAXED EXCITED STATE OF THE F CENTER IN KF

Irwin Schneider
Naval Research Laboratory
Washington, D.C. 20375

It has recently been reported[1] that absorption from the relaxed excited state (RES) of the F center in KCl, KBr and KI lies at roughly 0.1 eV and exhibits structure which is attributed to transitions to 3p, 3d and 4p levels. These assignments, however, apparently contradict those of Ham and Grevsmühl[2] who interpreted earlier data by Park and Faust[3] in terms of a predominant 2s-2p transition. In particular, Ham and Grevsmühl predict a 2s-2p electronic energy difference of about 0.09 and 0.15 eV for KCl and KF, respectively. It is worth noting that this value for KCl agrees well in energy with Kondo and Kanzaki's[1] assigned 2s-3p zero-phonon line at 0.106 eV.

The transient spectrum from the RES now measured in KF near 4K has as its most striking feature a relatively large absorption consisting of a shoulder component peaking at roughly 0.139 eV and a broad, intense band peaking at 0.148 eV, labeled Eo and Eo′ in Table I, respectively. Table I compares these and several weaker absorptions appearing at higher energies with the corresponding peaks found by Kondo and Kanzaki in other alkali halides. To within experimental error, transient absorption was not detected from the low energy shoulder of Eo down to about 0.083 eV. Furthermore, if one compares the energy spacing of Eo, Eó and several of the higher energy peaks with the KF LO-phonon energy of about 41.4 meV then one might reasonably expect that the higher peaks be attributed to multivibronic structure associated with the transitions Eo and Eó (See Table I).

These assignments are quite tentative particularly in view of the fact that the spin-orbit splitting of several of the states involved is still unknown.

There is considerable agreement that the RES is 2s-like, but some uncertainty regarding the specific identify of the absorptions arising from the RES. Aside from spin-orbit splitting, part of this uncertainty concerns whether Eo and Eó are transitions to 3p and 3d states or to 2p, 3p states. The peak energy of Eo and Eó in KCl and now KF agree well with Ham and Grevsmuhl's predicted values for 2s-2p. The situation, however, is somewhat clouded by the results of Imanaka, Iida and Ohkura[4] who conclude from Stark Effect measurements that the 2s-2p electronic energy difference is very much smaller than 0.08 eV, particularly in KF.

1. Y. Kondo and H. Kanzaki, Phys. Rev. Letters 34, 664 (1975).
2. F.S. Ham and U. Grevsmuhl, Phys. Rev. B8, 2945 (1973).
3. K. Park and W. Faust, Phys. Rev. Letters 17, 137 (1966).
4. K. Imanaka, T. Iida and H. Ohkura (to be published).

TABLE I

	KF (eV)	KCl (eV)	KBr (eV)	KI (eV)
E_o	0.139	0.106	0.087	0.078
Eó	0.148	0.111	0.092	-----
E_1	0.171	0.139	0.111	0.097
E_1'	0.192	-----	-----	-----
E_2	0.207	0.167	0.133	0.113
E_2'	0.232	-----	-----	-----

A FREELY LIBRATING ELASTIC DIPOLE IN KCl

Dirk Schoemaker and Ad Lagendijk
Physics Department, University of Antwerp (U.I.A.)
2610-Wilrijk, Belgium

When they exhibit motions, atomic or molecular defects in solids generally jump between equivalent orientations, spending negligeable time in between. If these are phonon assisted tunneling motions or motions characterised by a very low activation energy they can be studied with uniaxial stress at low temperature.

The interstitial type Cl_2^- molecular defect known as the $H_A(Li^+)$ center in KCl:Li^+, exhibits a large-angle librational motion with respect to a {110} plane. This motion is unique in the fact that all positions along the librational path are equally probably. This was demonstrated by an ESR study at low temperature using uniaxial stress. An initial ESR analysis placed the Cl_2^-, which occupies a single negative ion site, statically in a {110} plane and making a 26° angle with <100> (Fig. 1). Uniaxial stress along [001] at 4.2K pushes the Cl_2^- out of its {110} plane and with increasing stress the Cl_2^- describes an octant of a cone around [100]. At high stresses the Cl_2^- approaches the (001) plane perpendicular to the stress direction. A further important observation is that increasing the temperature above 4.2K undoes the effect of the uniaxial stress: the Cl_2^- returns to its {110} plane where it arrives at about 50K.

These experiments can be understood if one introduces the concept of a freely librating elastic dipole in a stress field. In this model the Cl_2^- librates freely over an almost quadrant of a cone around [100] and all positions along the librational path are equally probable. The librational frequency is sufficiently fast so that in ESR one observes the Cl_2^- in its average orientation, i.e., in a {110} plane. Applying [100] uniaxial stress changes the average Cl_2^- orientation. The statistics of these elastic dipoles in a stress field are readily calculated. One obtains a Langevin-type curve relating the average orientation characterised by a $\langle\cos^2\theta\rangle$ to the variable σ/T. The experimental data are plotted in Fig. 2 and yield a linear stress coupling coefficient $\beta = 7 \times 10^{-24}$ cm^3. From

uniaxial stress measurements along <110> one obtains two differential stress coupling coefficients. This permits a determination of the elastic dipole tensor of the $H_A(Li^+)$ center. One axis is in the neighborhood of <111> and probably coincides with the Li^+-interstitial Cl direction which is expected to induce the major part of the elastic dipole.

An accurate quantitative analysis of the ESR spectra without stress fully confirms the existence of this large angle librational motion.

D. SCHOEMAKER and A. LAGENDIJK, Phys. Rev. B15, 115 (1977)

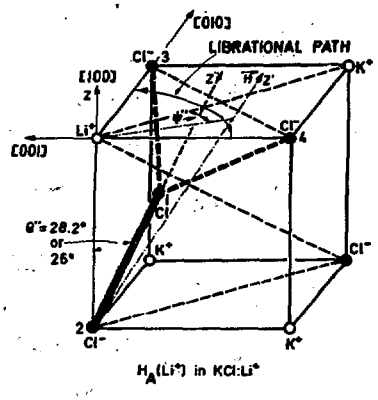

Fig. 1. Very schematic representation of the $H_A(Li^+)$ center. The librational path is indicated.

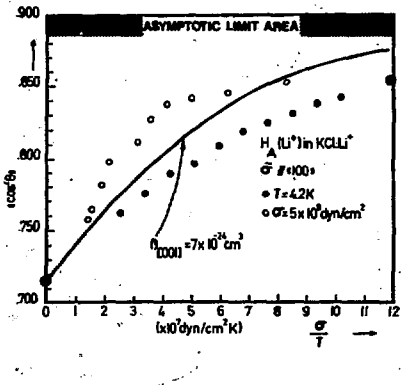

Fig. 2. Langevin-type plot of the $\vec{\sigma} \parallel [001]$ uniaxial stress data.

DEFECTS AND PHOTOREFRACTION PROCESSES IN $LiNbO_3$ CRYSTALS

K.K.Shvarts, P.A.Augustov, A.O.Ozols
Physics Institute, Latvian SSR AS, Riga - Salaspils, USSR

Photorefraction - optically induced refractive index change - was found in ferroelectrics by A.Ashkin et al. /1/. Lately it has been used for the recording of phase holograms (see Rev. /2,3/). The first theoretical model of photorefraction was proposed by F.Chen (/4.31/ in /2/) and developed by A.M.Glass et al. /3/. According to these conceptions photorefraction is due to the internal electrooptical effect.

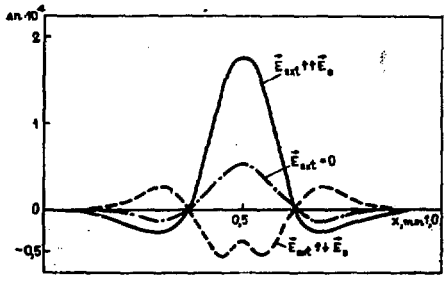

Fig. 1

The influence of the internal electric field on birefrigence $\Delta n = \Delta(n_e - n_o)$ (fig. 1) has been studied by means of the polarization interference methods (/4.43/ in /2/). The magnitude of the compensating electric field under focused illumination from He - Ne laser with intensity 30 W/cm^2 in $LiNbO_3$ crystal is equal to 11 kV/cm.

The influence of $\vec{E}_{ext}$ on photorefraction in $LiNbO_3$ - Fe crystals (0,1 weight % Fe) is weaker than in the undoped crystals. This is explained by a considerably larger light induced change of the internal electric field. In $LiNbO_3$ - Fe crystals the jump - like decrease of the light induced refractive index change - quasi-breakdown - is experimentally found (fig. 2). The volume charge field forming $\Delta n_o = 1,7 \cdot 10^{-3}$ at

the moment of breakdown and determined from the experimental data gave value 200 kV/cm.

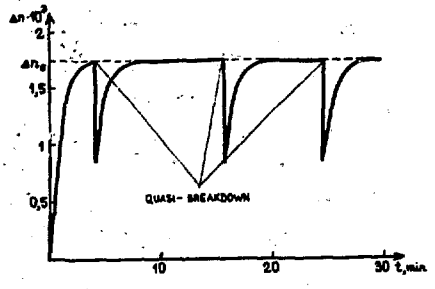

Fig. 2

Photorefraction in $LiNbO_3$ - Fe was also studied by holographic and optical methods. The anisotropy of centres responsible for photorefraction Fe^{+2} is caused by light polarized normally to the optical axis of the crystal ($\Delta n_{e\perp}/\Delta n_{e\parallel} \approx 1{,}4$; $\Delta n_{e\perp}/\Delta n_{e\parallel} \approx 1{,}4$) with the unusual refractive index changing to a greater extent ($\Delta n_e/\Delta n_o \approx 2{,}5$). This is evidently connected with Fe^{+2} centres dichroism ($\varkappa_\perp/\varkappa_\parallel \approx 2$).

References

1. Ashkin A., Boyd G.D., Dzicdzic J.M., Smith R.G., Ballman A., Levinstein J.J., Nassau K. - Appl. Phys. Lett., 1966, vol. 9, No. 1, pp. 72 -74.
2. Shvarts K.K., Gotlib V.I., Kristapson J.Z. Optical Recording Materials (in Russian), published by "Zinatne", Riga, 1976, p. 184.
3. Glass A.M., Linde D. von der, Auston D.H., Negran T.J. - J. Electr. Mater., 1975, vol. 4, No.5, pp. 915 - 943.

INVITED PAPER

THE ROLE OF FUNDAMENTAL RESEARCH IN DEVICE DEVELOPMENT

W. A. Sibley
Physics Department
Oklahoma State University
Stillwater, Oklahoma

Systems engineering has proven to be the accepted method for attacking the immediate technical problems in the fields of energy, space and information devices. The foundation of the system approach is the mass of fundamental information that has been accumulated over many years of research. Because of the deadlines imposed on developmental tasks and the necessity for reliability, systems engineers feel it is imperative that only thoroughly researched materials be considered. However, the present emphasis by some on immediate application of research results has tended to dilute the information base available on new materials and defects. Therefore, it is important that the scientists at this conference be able to bridge the gap between fundamental research on materials (including the development of new materials) and the application of this research to devices and the needs of society. This talk will survey a few device applications in which defects are important and illustrate how fundamental research contributes to the solutions of our device needs.[1]

The effect of defects on reactor materials, whether fission or fusion, on electronic devices such as solar cells and metal-oxide-silicon field effect transistors (MOSFETS) and on reflection coating are considerable. The type of research considered at this conference provides a firm base for advances in these areas. Moreover, ion implantation is important in the fabrication of some types of MOS devices and radiation annealing and aggregation studies aid our understanding of this process considerably. However, since 80% of information transfer in our society occurs by optical means, optical devices will be emphasized in this presentation.

Radiation dosimetry plays an important role in society. With the advent of deep tumor diagnosis and treatment by accelerators and the use of high energy electrons for welding the need for better dosimeters is obvious. Since human cell damage by radiation is due to ionization and is proportional to the energy absorbed (1 rad = 10mJ/kg), dosimeters should be made of materials with $Z \simeq 8$. Thus, most effective dosimeter materials are oxides

and fluorides. In fact LiF has long been a favorite dosimeter material for radiation, but it is known that certain impurities, (Mg and Ti) must be present to obtain an acceptable thermoluminescence response with dose.[1,2,3] Recently there has been interest in fast neutron dosimeters. Oxide systems such as MgO and CaO have been investigated for this purpose using both the optical absorption and emission of F type centers as the radiation monitor.[4]

Information storage and display are basic to communication networks today, and defect research provides ideas for new systems and the needed fundamental information for the development of devices. Luminescence from defects or impurities are used in bright screen display systems, whereas color centers or the quenching of emission by radiation defects can be used in dark screen devices. Electron beam irradiation of a phosphor (KI:Tl) can be used to produce an information storage system with read, write and erase capability and a memory of about 10^8-10^9 bits.[1]

Infrared to visible light conversion (up-conversion) involves the absorption of infrared photons and the combination of these individual photons with energy hν in twos or threes to produce photons with energies of 2hν and 3hν.[5,6] Such a system gives visible images from infrared light and can be used for infrared microscopes, heat scanners, etc. However, since two infrared photons must be added to give one visible photon the quantum efficiency is not more than 50%, and the lifetime and oscillator strengths of the excited states strongly affect the process. Energy transfer is necessary for some devices and this leads to a number of interesting problems. A reduction of activator ion site symmetry can usually increase the efficiency of the system. Thus, radiation damage techniques should enhance the efficiency of the up-conversion process through site symmetry reduction and exchange effects.[7]

1. A. E. Hughes and D. Pooley, Real Solids and Radiation Wykeham Publications (London 1975) p. 168-190.
2. M. C. Wintersgill, P. D. Townsend and F. Cusso-Perez, J. de Physique 37 C7-123 (1976).
3. R. Nink and H. J. Kos, J. de Physique 37 C7-127 (1976).
4. G. P. Pells and A. E. Hughes, Harwell AERE Report R8686 (1977).
5. F. E. Auzel Proc. IEEE 61, 758 (1973).
6. G. F. J. Garlick, Contemp. Phys. 17, 127 (1976).
7. K. H. Lee and W. A. Sibley, Phys. Rev. B12 3392 (1975).

NON-RADIATIVE DECAY OF THE TRIPLET-SINGLET OF THE F_2 CENTER IN KCl and KBr

R.H. SILSBEE[+], Y. FARGE[++], J.M. ORTEGA[++]

[+] LASSP - Clark Hall - Cornell University
ITHACA, N.Y. 14850 (USA)

[++] Laboratoire de Physique des Solides
Université Paris-Sud
91405 ORSAY (France)

At low temperature, the triplet to singlet transition arises mainly from a radiative mechanism (1). Triplet lifetime measurements versus applied strain and temperature ($4\ K < T < 200\ K$) indicate that a non-radiative component appears and becomes predominant when the temperature increases. We have been able to apply to the F_2 center case the general theory of non-radiative transitions (2) and obtained numerical estimations of both non-radiative decay probability and its behaviour with temperature which are in satisfactory agreement with the experimental data.

(1) J.M. ORTEGA - to be published.

(2) J. JORTNER, S.A. RICE and R.M. HOCHSTRASSER - Advan. Photochem., I, 149, (1969).

SYSTEMATICS OF ENERGY LEVELS OF IONS IN HOST CRYSTALS

John Simonetti and Donald S. McClure
Department of Chemistry, Princeton University
Princeton, N.J. 08540

Vacuum UV measurements have been made of the charge transfer absorption band energies of the first row divalent transition ions in LiCl host crystal. These energies decrease linearly with increasing atomic number from Mn to Cu, an effect long ascribed to the linear increase of the second ionization potential in this series.[1] With the complete set of data available, deviations from this proportionality are examined and other spectral details are considered. It is also shown that a semi-classical calculation can give the correct average energy of the charge-transfer band system. A similar calculation gives the energy of chemical reduction of the divalent ion to the monovalent state and the position of the monovalent ion relative to the conduction band, and thus the internal photoionization energy. This latter is the reverse of the charge transfer process except for the presence of the compensating metal-ion vacancy in the stable form of the doped crystals.

In the case of V^{++} in LiCl, the spectrum is not due to charge transfer, but instead we find that 3d→4s, and possibly 3d→4p occurs. This result can be predicted from the charge transfer bands of the heavier metals, and from the d→s [2] and d→p [3] band positions in the fluoride host crystals.

The study of Cu^{+} in LiCl has begun our work on the monovalent ions. We observe only the well known 3d→4s band, and the newly discovered 3d→4p band.[3] The absorption from the metastable excited triplet of Cu^{+} to higher states will be shown to give some new information on the d^9p configuration in solids and on the potential surfaces of the states derived from d^9s and d^9p.

On the basis of such data and by using semiclassical calculations, the energy level schemes of transition metal ions in host crystals can be related to each other and to the energy levels of the host crystal.

An important part of the picture is the mode and extent of relaxation of different ion-host crystal combinations. This aspect is less clear to us, but some examples will be given, and possible ways to generalize from the examples will be discussed.

1. C. K. Jorgensen, Electron Transfer Spectra, Progress in Inorganic Chemistry, vol. 12, pp. 101-158, Wiley-Interscience, New York (1970).

2. J. F. Sabatini, A. E. Salwin and D. S. McClure, Phys. Rev. B11, 3832 (1975).

D. B. Chase and D. S. McClure, J. Chem. Phys., 64, 74 (1976).

3. J. Simonetti and D. S. McClure, Phys. Rev. (to be published).

INVITED PAPER

ION TRANSPORT IN SIMPLE IONIC CRYSTALS*

L. Slifkin, University of North Carolina at Chapel Hill

Our understanding of point defects in such relatively simple ionic crystals as the alkali and silver halides has by now reached the point that one can profitably examine some of the finer details of mass transport processes. One of these questions deals with the analysis of the conductivity Arrhenius plot. It has become clear that even the refined computer analysis, introduced in 1966 by Beaumont and Jacobs[1], is not adequate to provide unambiguous experimental values for enthalpies and entropies of defect formation and migration, as recently emphasized by Murthy and Pratt[2]. Instead, one must combine these conductivity data with detailed tracer diffusivities, as has been done, for example, by the Bénière's and Chemla[3].

In the case of the alkali halides, one result that has been emerging, both from experiment and from a theoretical analysis by the Harwell group[4], is that the migration energies for the halide and the alkali ions are really not very different - a conclusion which now makes difficult the understanding of the curvature of the intrinsic region of the Arrhenius plot. Perhaps additional mechanisms (interstitial?) (trivacancy?) come into play as one approaches the melting point. An alternative possibility, however, is suggested by recent work on AgCl and AgBr.

In the silver halides, the conductivity Arrhenius plot is even more strongly curved at high temperatures than is the case for alkali halides. The effect is twice as large as can be explained by the Lidiard-Debye-Hückel screening. Aboagye and Friauf[5] have recently analyzed this conductivity anomaly in terms of a decrease at higher temperatures of the Frenkel defect formation energy, and subsequent experiments by Batra[6] on the diffusion of Na^+ in AgX have quantitatively corroborated this interpretation. One is thus led to wonder whether a similar, although smaller, effect might not be involved in the alkali halides.

A second problem concerns the rôle of the properties of a substitutionally dissolved foreign ion in determining its activation energy for exchange with a vacancy. Recent research has begun to reveal two aspects of this question: the effect of the radius of the solute ion[7], and the influence of the crystal field for those ions with partially filled d-shells[8].

The recent controversy over the kinetics of aggregation of solute-vacancy complexes to form dimers and/or trimers will also be discussed. There is evidence now[9,10] that one can observe <u>either</u> second- or third-order kinetics, depending on the initial supersaturation of the complex. Detailed calculations of energies and rate constants would be quite useful here. Further, there have been a number of indications

that along dislocations, the aggregation processes can be quite different, especially at low solute concentrations, for which little aggregation is to be expected in the bulk. This will be illustrated by some recent internal friction studies on AgBr:Sr, performed by Horan[11].

Finally, some remarks will be made concerning several other unsolved problems, such as (a) the effects of ionic space charge on defect distribution near interfaces and dislocations, and (b) diffusion in crystals other than univalent halides.

References:

(1) J. Beaumont & P. Jacobs, J. Chem. Phys. 45, 1496 (1966).
(2) C. Murthy and P. Pratt, J. Physique Coll. 37, C7-307 (1976).
(3) M. Bénière, M. Chemla, & F. Bénière, J. Phys. Chem. Sol. 37, 525 (1976).
(4) C. Catlow, J. Corish, K. Diller, P. Jacobs, & M. Norgett, J. Physique Coll. 37, C7-253 (1976).
(5) J. Aboagye & R. Friauf, Phys. Rev. B 11, 1654 (1975).
(6) A. Batra & L. Slifkin, ibid 12, 3473 (1975); J. Physique Coll. 37, C7-396 (1976).
(7) M. Bénière, F. Bénière, C. Catlow, A. Shukla, & C. Rao, J. Phys. Chem. Sol. 38, 521 (1977).
(8) A. Batra, J. Hernandez, & L. Slifkin, Phys. Rev. Lett. 36, 876 (1976).
(9) J. Strutt & E. Lilley, Phys. Stat. Sol. A 33, 229 (1976).
(10) D. Golopentia, Ph.D. Thesis, Univ. of N. C., 1975; J. Dutta, Ph.D. Thesis, Univ. of N. C., 1975.
(11) S. Horan, Ph.D. Thesis, Univ. of N. C., 1977.

*Supported by NSF Grant No. DMR 76-18862

FINITE-ENERGY SUM RULES FOR INFRARED REFLECTION SPECTROSCOPY: APPLICATION TO IONIC CRYSTALS AND SOLAR HEAT MIRRORS*

David Y. Smith

Argonne National Laboratory, Argonne, Illinois 60439

and

Corinne A. Monague

Mount Holyoke College, South Hadley, Massachusetts 01075

Many new sum rules for the optical constants of matter have been reported[1,2] in the last few years. These, like the famous f sum rule, apply directly to the complex dielectric response function, $\tilde{\epsilon}(\omega)$, its inverse and the complex refractive index, $\tilde{n}(\omega)$. In general, similar rules do not hold for the reflectivity spectra because of the particular mathematical structure of this quantity.[3] However, in the special case in which low-energy absorptions may be considered to be superimposed on a real dielectric background, ϵ_∞, arising from electronic transitions at higher energies, finite-energy sum rules applicable to the low-energy reflectivity spectra hold. A classic example of such a system is the infrared absorption of lattice or defect modes in an alkali halide. The reflectivity rules may be derived by standard techniques of complex analysis; they are exact in the limit in which there is no dispersion in the high-energy background, a good assumption for most insulators and wide-bandgap semiconductors.

Two examples of rules for the normal amplitude reflection coefficient,

$$r(\omega)e^{i\theta(\omega)} = \frac{\tilde{n}(\omega) - 1}{\tilde{n}(\omega) + 1} \quad ,$$

of a system with refractive index $\tilde{n}(\omega)$ are:

- The zeroth-moment reflectivity rule,

$$\int_0^\infty \ln\left[\frac{r(\omega)}{r_\infty}\right] d\omega = 0,$$

where $r_\infty = (\epsilon_\infty^{1/2} - 1)/(\epsilon_\infty^{1/2} + 1)$. Qualitatively, this is a reflectivity conservation rule: to each energy region with reflectivity which exceeds the background reflectivity, r_∞, there exists a corresponding region with $r < r_\infty$.

- The phase f sum rule,

$$\int_0^\infty \omega\, \theta(\omega)\, d\omega = \frac{\pi\, \omega_p^2}{2\varepsilon_\infty^{1/2}(\varepsilon_\infty - 1)} ,$$

where ω_p is the "plasma frequency" associated with the infrared absorption. This allows a direct calculation of the infrared oscillator strength from the phase without the necessity of an intermediate calculation of the refractive index and the dielectric function. These and other rules and their application to the *Reststrahl* reflection of the alkali halides and to transparent heat mirrors for solar applications will be discussed.

---

*Work performed under the auspices of the U. S. Energy Research and Development Administration.

1. M. Altarelli, D. L. Dexter, H. M. Nussenzveig, and D. Y. Smith, Phys. Rev. B 6, 4502 (1972).
2. M. Altarelli and D. Y. Smith, Phys. Rev. B 9, 1290 (1974).
3. D. Y. Smith, J. Opt. Soc. Am. 67, 570 (1977).

DETERMINATION OF THE Fe^{2+} AND Fe^{3+} CONCENTRATION IN MgO*

E. Sonder, F. A. Modine and R. A. Weeks
Solid State Division, Oak Ridge National Laboratory
Oak Ridge, Tennessee 37830 USA

Crystals of MgO containing 140 ppm iron were reduced in CO or oxidized in air at 1150°C and the iron concentration in different valences was determined by optical and magnetic techniques. Optical density, electron spin resonance and magnetic circular dichroism measurements gave self-consistent results that yield calibration constants for determining the Fe^{2+} and Fe^{3+} concentrations by optical means. These constants, which may be used in general to extract Fe^{2+} and Fe^{3+} concentrations from measured values of optical density or magnetic circular dichroism, are given in Table 1. Oscillator strengths of the absorption bands at 1000 *nm* and 285 *nm* were calculated from the iron concentrations in the 2+ and 3+ valence states. They are compared with previously determined values in Table 2. Furthermore the results indicate that at these relatively low concentrations more than 90% of the iron is unassociated, Fe^{2+} or Fe^{3+}. Alternate oxidation with air and reduction with CO converted 80% of this iron between 2+ and 3+ valence states, while the other 20% remained as Fe^{2+}.

Table 1. Proportionality constants for calculating MgO Fe^{2+} and Fe^{3+} concentrations from optical measurements. The constants are appropriate for low temperature. Dichroism constants are scaled to saturation, but may be scaled to any temperature with the appropriate Brillouin function.

Valence	Measurement Wavelength (nm)	Dichroism^{-1} (wt. ppm/cm^{-1})	Absorption^{-1} (wt. ppm/cm^{-1})
Fe^{2+}	1000	$(9.1 \pm 1.5) \times 10^3$	$(4.8 \pm 0.6) \times 10^3$
Fe^{3+}	285	15 ± 2	2.0 ± 0.3

*Research sponsored by the Energy Research and Development Administration under contract with Union Carbide Corporation.

Table 2. Oscillator strengths of MgO iron bands.

Optical Band	Oscillator Strength	Source
Fe^{2+} : 1000 nm	7.3×10^{-6}	This work
	$(3 - 5) \times 10^{-5}$	Manson, et al.[1]
	5×10^{-6}	Hjortsberg[2]
Fe^{3+} : 285 nm	3.8×10^{-2}	This work
	4.1×10^{-2}	Davidge[3]
	1.4×10^{-2}	Sibley, et al.[4]

1. N. B. Manson, J. T. Gourley, E. R. Vance, D. Sengupta and G. Smith, J. Phys. Chem. Solids 37, 1145 (1976).

2. A. Hjortsberg, Thesis, Chalmers University of Technology, Goteborg (1975); Bull. Amer. Phys. Soc. 21, 421 (1976).

3. R. A. Davidge, J. Mat. Science 2, 339 (1967).

4. W. A. Sibley, J. L. Kolopus and W. C. Mallard, Phys. Stat. Sol. 31, 223 (1969); Y. Chen and W. A. Sibley, Phys. Rev. 154, 842 (1967).

OPTICAL PROPERTIES OF ADDITIVELY COLORED α-Al_2O_3 CRYSTALS.

M.Springis, J.Valbis.
Latvian State University, Riga, USSR.

Additive coloration in reducing atmosphere is a well-known method of producing F centers in alkali earth oxides (1). Electrical measurements indicate that under similar treatment some sort of donor centers (probably interstitial cations) are created also in α-Al_2O_3 crystals (2,3). In the present investigation we have studied the optical properties of these centers.

Nominally pure α-Al_2O_3 crystals were treated for several hours at $1950 \pm 50^{\circ}C$ in different reducing atmospheres providing oxygen partial pressures from 10^{-10} to 10^{-20} atm. After such treatment the main absorption bands could be observed at 4.5, 6.1 and 7.0 eV as well as some increase in absorption in the 7.5 -9.0 region. The additional absoption was stronger in crystals treated at lower oxygen partial pressures. The crystals had a dominating luminescence band at 2.9 eV which could be excited by irradiation in the additional absorption bands and also by X-rays and cathode-rays. Such luminescence has been previosly observed in UV-irradiated (4) and neutron-bombarded crystals (5).

The additional absorption and luminescence exibited considerable anisotrophy. It was impossible to determine the exact value of dichroism in the 4.5 eV absorption band because of overlapping with some other bands, but it can be stated that $\alpha_{\parallel c} < \alpha_{\perp c}$. The luminescence in the 2.9 eV band was also polarized (including the case of excitation by ionizing radiation) with $\frac{I_{\parallel c}}{I_{\perp c}} = 0{,}35 \pm 0{,}05$.

The experimental results seem to lend support to the

view, that interstitial aluminium ions are created during the reducing treatment (2). These interstitials evidently occupy part of the octahedral sites normally free in stoichiometric α-Al_2O_3 crystals. The equilibrium charge state of the interstitial ions depends on the Fermi level position which, in turn, is determined by the degree of deviation from stoichiometry and heterovalent impurity concentration.

Some of the observed additional absorption bands correspond quite well to the transition energies 4,65 eV (^1S-^3P) and 7,4 eV (^1S -^1P) in free Al^+ ions indicating, that the interstitials may be Al_i^+. Al^+ is isoelectronic with the S^2 ions Tl^+, In^+, Ga^+ widely studied in different host crystals and giving rise to luminescence in the visible and near UV region. The 2,9 eV luminescence band seems to be related to the transition between states ^3E_u and ^1A_g formed from the states ^3P and ^1S of free Al^+ ion in the crystalline field of C_{3i} symmetry. This transition is multiplicity-forbidden, thus accounting for the long radiative lifetime (40 ms (4)). The transition ^3E_u - ^1A_g provides also reasonable explanation to the observed polarization of the luminescence.

The existence of other states of the interstitial ions (Al_i^{3+}, Al_i^{2+}, Al_i°) is also possible expecially if Al_i is situated in the vicinity of heterovalent impurities (e.g. Mg^{2+}, Si^{4+}). Under ionizing radiation transitions between different charge states, involving electron and hole captures and radiative recombination, evidently take place.

1) E.B.Hensley, W.C.Ward, B.P.Johnson, R.L.Kroes, Phys.Rev. 175, 1227 (1968).

2) R.Brook, J.Yee, F.Kröger, J.Am.Ceramic Soc. 54, 444 (1971).

3) K.Kitazawa, R.Coble, J.Am.Ceramic Soc. 57, 245 (1974).

4) H.W.Lehmann, Hs.H.Gunthard, J.Phys.Chem.Sol., 25, 941, (1964).

5) Sh.A.Vakhidov, D.R.Khatamov, M.Yangibaev, Izv.AN Uzb.SSR, N 4, 65 (1976).

DIRECT-FORBIDDEN EXCITONS IN TETRAGONAL GeO_2

M. Stapelbroek* and B. D. Evans
Naval Research Laboratory
Material Sciences Division
Washington, D.C. 20375

The intrinsic, polarized uv-absorption edges in single crystals of tetragonal GeO_2 (rutile structure, space group D_{4h}^{14}) have been examined at room temperature, 77 K, and approximately 10 K using both flux- and hydrothermally-grown samples. The salient features of the edge absorption are: (1) a pronounced dichroism with the $\vec{E} \perp \vec{c}$ edge occurring at lower energy and having a much steeper slope than the $\vec{E} \parallel \vec{c}$ edge at all three temperatures; (2) at absorption coefficients of 100 cm^{-1}, a shift between room temperature and 77 K of ~0.2 eV and ~0.08 eV in the edge absorption for $\vec{E} \parallel \vec{c}$ and $\vec{E} \perp \vec{c}$ respectively, and only a small ~0.0035 eV shift for both polarizations between 77K and 10 K; and (3) sharp-line structure (FWHM $\approx$ 0.0035 eV) strongly polarized $\vec{E} \perp \vec{c}$ at 77 K and 10 K. These features are remarkably similar to those reported[1-4] for edge absorption in the isomorphic material SnO_2.

Based on the SnO_2 analogy and the observation that the integrated absorption coefficient of these lines is the same within experimental error in both flux- and hydrothermally-grown samples, the low-temperature sharp-line structure, shown in Fig. 1, is attributed to intrinsic excitons associated wi direct-forbidden band-to-band transition.[3,5] Exciton properties and ir implications for the band structure of tetragonal GeO_2 will be discussed; these differ with the results of previous work on tetragonal GeO_2.[6]

* NRC-NRL Resident Research Associate.

1. R. Summitt and N. F. Borrelli, J. Appl. Phys. 37, 2200 (1966).
2. M. Nagasawa and S. Shionoya, Solid State Comm. 7, 1731 (1969).
3. M. Nagasawa and S. Shionoya, J. Phys. Soc. Japan 30, 158 (1971).
4. V. T. Agekyan, I. P. Shiryapov, and L. V. Oreshnikova, Fiz. Tverd. Tela. 16, 2473 (1974) [Sov. Phys.-Solid State 16, 1613 (1975)].
5. R. J. Elliott, in Polarons and Excitons, ed. by C. G. Kuper and G. D. Whitfield (Plenum, New York, 1962).
6. F. J. Arlinghaus, W.A.Albers, Jr., J.Phys.Chem.Solids 32, 1455 (1971).

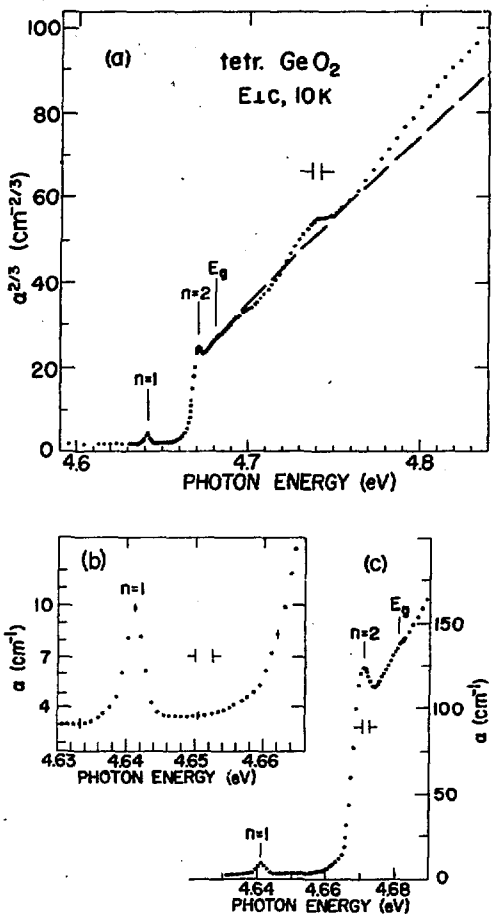

Figure 1. Polarized edge absorption in tetragonal GeO_2 near 10 K. (a) Photon energy vs. $\alpha^{2/3}$; the dashed curve normalized at $E = E_g$ represents a theoretical expression due to Elliott[5] for the continuum absorption with exciton effects included but without phonon effects considered. (b) and (c) Linear plots of α vs. E showing the relative intensity of the dipole-forbidden n = 1 line at 4.641 eV and the allowed n = 2 line at 4.671 eV.

THE CALCULATION OF SURFACE AND BULK LATTICE DEFECTS IN ALKALINE-EARTH OXIDES AND NiO

R F STEWART AND W C MACKRODT
ICI Corporate Laboratory, PO Box 11, The Heath
Runcorn, Cheshire WA7 4QE, UK

In this paper we report calculations of surface and bulk lattice defects in alkaline-earth oxides and NiO using extensions to the HADES method, previously described (1, 2). For MgO a comprehensive list of defects is examined, including the formation energy of intrinsic defects, lattice substitution and migration by iso- and aliovalent cations, surface and bulk OH formation and migration, the solubility of the simple transition-metal oxides and the lattice energy of a variety of colour centres. In addition we contrast the formation of the F-Centre in MgO with the corresponding process in CdO and show that for the latter, reduction to Cd^{o} and an anion vacancy is energetically more favourable. As a pointer to future calculations, defect energies derived from a non-empirical potential, based on a modified form of the 'electron gas' model (3), are compared with those derived from the empirical potential of Catlow et al (4), and the former are shown to be the more consistent set of results.

Next, we present the calculated intrinsic defects in CaO, SrO and BaO, the principle finding being that despite a rapid fall in the Frenkel formation energy on going from MgO to BaO, Schottky defects dominate the series. The calculated Schottky energies are shown to vary linearly with the melting point and as previously reported (2), the formation and binding energies of the neutral divacancy vary smoothly with the static dielectric constant. It is shown that the most probable mode for ionic diffusion is by a vacancy mechanism; however, in view of the high values for the Schottky energy, extrinsic control by impurities such as Si^{4+} would seem to be necessary. On this basis, the overall agreement with experiment is good. Calculations show a systematic decrease in the hole formation energy on going from MgO to BaO and that the formation energy at both the (001) and (110)

surfaces is less than in the bulk. We suggest that electron donation from O^{2-} at low co-ordination sites seem a likely possibility in catalytic reactions such as N_2O and NO decomposition and O_2 exchange over these oxides.

Finally, we report the results of surface defect calculations on the doping of NiO by Ga^{3+} and Li^+. For Ga^{3+} doping both in the bulk and at the (001) surface the preferred mode of solution is by lattice substitution compensated by cation vacancy formation. For Li^+ doping on the other hand there are two possibilities. In the presence of excess oxygen Li^+ substitutes the cation sublattice and is compensated by Ni^{3+} both in the bulk and at the (001) surface. In the absence of oxygen we show that the formation of the $Li^+ - Li^+$ (111) 'dumb-bell' at cation sites is favoured over Li^+ substitution and anion vacancy formation. The (111) dumb-bell has not been suggested previously for Li_2O/NiO, though it has recently been observed by Kim and Nowick for Li^+ doped Mg F_2 (5). The observed oxygen desorption is discussed in terms of these defects and the two are shown to be entirely consistent.

References

1 W C Mackrodt and R F Stewart, J Phys C : Solid State Physics, 10, 1431, (1977).

2 R F Stewart and W C Mackrodt, J de Physique, Colloque, C-7, (1976).

3 W C Mackrodt and R F Stewart. To be published.

4 C R A Catlow, I D Faux and M J Norgett, J Phys C : Solid State Physics, 9, 419, (1976).

5 K K Kim and A S Nowick, J Phys C : Solid State Physics, 10, 509, (1977).

DIFFUSE X-RAY SCATTERING FROM NEUTRON IRRADIATED MgO

J.P. Stott, D. Grasse, B. von Guérard and J. Peisl
Sektion Physik, Universität München, 8 München 22, W. Germany

Diffuse X-ray scattering resulting from the displacements of the lattice atoms around a defect provides information about the strength, sign and symmetry of the displacement field, and thus of the defect configuration. The technique is particularly useful for the study of interstitials and their clusters.

MgO samples, from W. & C. Spicer, Ltd., with (100) (cleaved) and (110) (sawed and polished) faces were used. They were etched in hot orthophosphoric acid and annealed in vacuum at 1200C before irradiation. It was found that, without the etching, the sawed samples had a poor Bragg peak and strong diffuse scattering. The samples were exposed to a neutron dose of $2 \times 10^{18} n.cm^{-2}$ (E>0.1MeV) at 70C. The diffuse scattering, at 20K, and the optical absorption due to the F^+ centre were measured after the irradiation and at various stages of thermal annealing up to 1200C.

The results for the samples as irradiated show that the centres produced are sources of dilation and that the average volume change per defect $\frac{\Delta v}{v} = 6$, in good agreement with the results of lattice parameter change measurements by Henderson and Bowen. This suggests that the scattering is due to cation and anion interstitials, isolated or in small clusters. The observed symmetry is consistent with cube centre sites, although a [100] oriented dumbell could produce results within the error limits. The observation of such high symmetry is good evidence that both anion and cation interstitials lie on sites of the same symmetry.

The annealing results show that the optical absorption anneals below 500C, before the diffuse scattering, in agreement with the flow stress measurements of McGowan and Sibley.

Interpretation of the diffuse scattering data is complicated by the intensity enhancement which occurs when defects cluster and which may mask any decrease in their number, however the symmetry of the displacement field does not change during annealing and the asymptotic scattering typical of clusters is not observed. This suggests that clustering does not dominate the scattering during annealing.

Measurements on samples irradiated at liquid helium temperature and more detailed annealing measurements are at present being made and will be reported.

B. Henderson and D.H. Bowen, J. Phys. C, 4, 1487, (1971)
W.C. McGowan and W.A. Sibley, Phil. Mag., 19, 967, (1969)

PARAMAGNETIC RESONANCE OF THE OPTICALLY EXCITED TRIPLET STATE of Z_2(Sr) in KCl.

K. Strohm, L. Schwan and H.J. Paus
Physikal. Institut Teil 2, Universität Stuttgart, Germany

By intense optical excitation Z_2 centers can be transferred from their usual singlet ground state into a metastable triplet state suitable for ESR experiments. For Z_2(Sr) in KCl a four-line spectrum showing a characteristic (100) axial symmetry has been reported /1/.

Sensitive experiments using a double modulation (field and light) technique and a conventional X-band spectrometer gave new surprising results. A multiline spectrum for Z_2 centers in KCl:Sr ($4 \cdot 10^{-3}$ mole fraction of $SrCl_2$ in the melt) has been found. All lines are inhomogeneously broadened with a peak-to-peak width of 50 Gauss. Their angular dependence for a crystal rotation around (100) is shown in fig. 1. The corresponding optical absorption and excitation spectra coincide with those given in the literature /1/.

By variation of the light modulation frequency the spectrum can be subdivided into two parts:

a) modulation with about 10-15 Hz gives a spectrum(unconnected points in fig. 1), which is not yet analysed in full detail.
b) modulation with 1.5 Hz displays an additional spectrum (full lines in fig. 1) which is due to a center with $S = 1$ and $g = 1.97 \pm 0.01$. Its fine structure data obtained by direct diagonalization are $D/g\beta = (2720 \pm 40)$ Gauss, $E/g\beta = (410 \pm 20)$ Gauss. The symmetry axes of the center are (100), (011) and $(01\bar{1})$.

The unusual high life time of this center of about 1 s exceeds all values known for Z_2 centers from optical experiments. The large D-parameter points towards some sort of F'-triplet center. Qualitative understanding of this center is possible within the framework of proposed Z_2 center models /2/.

/1/W.Adlhart, G.Gehrer, E.Lüscher phys.stat.sol.(b)66,517(1974)
/2/K.H.Umbach, G. Kenntner, H.J.Paus J.Phys.suppl.11-12,C9-107 (1973)

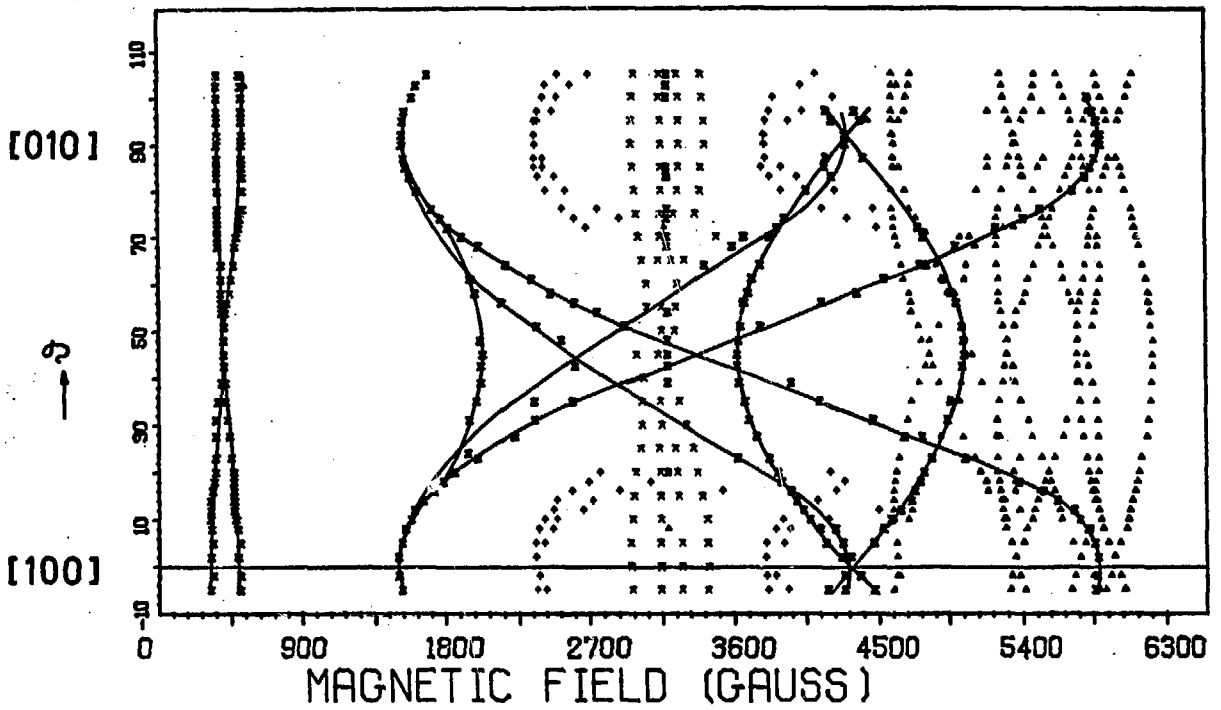
[010]
[100]
φ
110
90
70
50
30
10
-10
0
900
1800
2700
3600
4500
5400
6300
MAGNETIC FIELD (GAUSS)

Fig. 1

CONTROLLED CRYSTAL GROWTH OF YTTRIA AND THE RARE EARTH SESQUIOXIDES*

Sherman Susman and David Hinks

Argonne National Laboratory, Argonne, Illinois 60439

The cubic, rare-earth sesquioxides are a class of refractory compounds with unusual physical and chemical properties. Y_2O_3, the parent of these bixbyite-structured oxides, evidences numerous properties that are of practical importance to MHD, CTR and energy storage technologies. Y_2O_3 is a crystallographically complex system possessing two cation site symmetries, anion diffusion channels and several distortions while retaining the simplicity of a defect fluorite structure. ^{89}Y is 100% abundant, has a nuclear spin of 1/2 and is not paramagnetic. The compound undergoes no polymorphic transformations below 2250°C and displays remarkable resistance to corrosion by molten alkali metals and to damage by neutron irradiation. It is a proven electronic (not ionic) conductor at elevated temperatures.

Single-crystal specimens with controlled physical and chemical properties are required for basic transport-property or defect-production studies. Conventional flux-grown or Verneuil-grown crystals are either of low purity or poor physical perfection. Monocrystals of undoped Y_2O_3 and the heavy rare-earth sesquioxides have been grown from the melt by a containerless, plasma-beam, float-zone procedure. The precipitated oxalate salt is calcined, isostatically pressed into rod-form, sintered and diamond-ground to precise dimensions. Sources of contamination have been identified and subsequently eliminated through the use of laminar-flow or controlled-gas environments. The rods serve as the "feed" for crystal growth from a vertical, molten floating zone in an oxygen plasma. The oxygen partial pressure in the plasma is adjusted to minimize dissociation of the sesquioxide. Control of stoichiometry is achieved through optical methods. The substoichiometric oxide takes on a rich, dark color characteristic of the electron excess centers in the particular matrix: purple in Er_2O_3, green in Y_2O_3, brown in Yb_2O_3, etc.

The purification attendant to crystal growth has been documented and is largely correlated to the partial pressures of the impurity-oxides at the melting point of Y_2O_3 (2420°C).

Post-growth cracking of the boules along <111> is a common occurrence. This is expected with bixbyites as a consequence of alternate {111} cation planes without intervening oxygen ions. Methods for minimizing the problem have been devised based on modifying radiative and losses and reducing the thermal gradients. Shaped cathode inserts and both active and passive "afterburners" have proven effective. The physical perfection has been assessed by x-ray analyses and by dislocation counts on etched surfaces. The monocrystal specimens prove markedly superior to Verneuil-grown samples.

Oriented, monocrystalline specimens are currently the subject of ESR, transport-property and defect-production studies.

*Work performed under the auspices of the U. S. Energy Research and Development Administration.

F CENTER FORMATION IN PICO SECOND RANGE IN KI

Yoshiro SUZUKI and Masamitsu HIRAI
Department of Physics, Tohoku University,
Sendai, Japan

It has been confirmed that the F centers in KI crystals grow with time constants of 11±9psec, 120±25psec, 140±25psec and 190±40psec at 295K, 240K, 200K and 140K, respectively. The crystal was excited through the two photon absorption process of the second harmonics(347nm,3.75eV) from a mode locked ruby laser, and the F band growth was monitored by the fundamental light(694nm,1.785eV). The experimental arrangement of the optical system and the handling of the data were almost the same as done by Bradford et al.[1] A typical result at 295K is shown by closed circles in Fig.1. Short bars are the experimental error obtained by the root mean square method on 4~11 data at a given time. The data could be followed by an equation,

$$\frac{OD_2(t)}{OD_3} = \frac{1}{OD_3}\int I(t')\left\{1-e^{-(t-t')/\tau_1}\right\}e^{-(t-t')/\tau_2}\,dt' + \frac{1}{OD_3}\int I(t')\left\{1-e^{-(t-t')/\tau_3}\right\}dt', \qquad (1)$$

where, $OD_2(t)$ is the optical density at a time t after the 347nm light illumination and OD_3 is that at about 10nsec, where the absorption of the F band reaches to an almost constant value.

The first term with τ_1=10±10psec and τ_2=10±5psec and the second term with τ_3=11±9psec are shown by the chain and the thin broken curves. The total of them is presented by the solid curves. The width between solid curves shows the range arising from the variation of ±9psec in τ_3. Since the F center has a very long decay time,[2] the component shown by the thin broken curve should reflect the formation of the F

centers.

Under the two photon excitation of KI by the 347nm light, I^{o} will be produced mainly. I^{o} relaxes to form I_2^{-}, and successively captures an electron to form I_2^{--*} at a shallow electronic level. The electron cascades down to the $2p_z$ state by emitting phonons and tunnels to the 1s state on the way of the V_k type relaxation.[3] From this point I_2^{--*} starts to move progressively into the <110> direction of the crystal, leaving an electron at a negative ion site to form an F center. If these processes are acceptable, the present result suggests that τ_3=11±9psec corresponds to the time required for these processes.

Fig.1

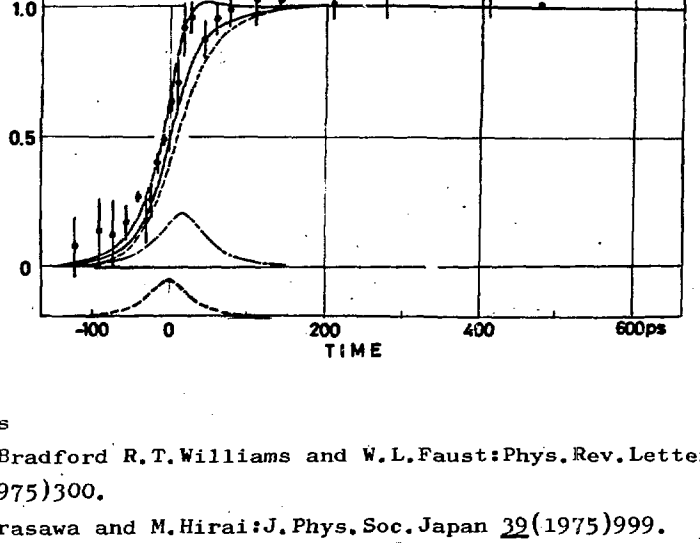

References

1) J.N.Bradford R.T.Williams and W.L.Faust:Phys.Rev.Letters 35(1975)300.

2) T.Karasawa and M.Hirai:J.Phys.Soc.Japan 39(1975)999.

3) Y.Toyozawa:"International Conference on Color Centers in Ionic Crystals" Sendai, 1974, D43.

FORMATION OF SELF TRAPPED EXCITON IN PICO SECOND RANGE IN KI

Yoshiro SUZUKI and Masamitsu HIRAI
Department of Physics, Tohoku University,
Sendai, Japan

By using a mode locked ruby laser, it has been confirmed that the self trapped excitons(STE) in KI crystals grow with time constants of 210±15psec at LHeT and 190±40psec at LNT. Experimental procedures and handling of the data are described in the abstract on the F center formation in KI in this abstract booklet. A typical result at LHeT is shown in Fig.1.

Under the pulsed electron beam irradiation near LHeT, two transient absorption bands are reported to occur at 742nm (1.67eV) and 1050nm(0.95eV) in KI.[1,2] These bands arise from the STE at $A0_g1s:{}^3\sum_u^+$ state. In the present experiment, since KI is excited by the second harmonics (347nm, 3.57eV) and since the variation of the absorption is monitored by using the fundamental light (694nm, 1.785eV) of the laser, the result in Fig.1 shows the growth of the 742nm band, though the tail of the 1050nm band overlaps very slightly at 694nm. It has been reported that the 742nm band grows with a time constant faster than 10nsec and decays with ~6μsec.[1,2] Therefore, the component growing with time constant τ_3=210±15psec shown by the thin broken curve in the figure appears to present the growth of the 742nm band. A tentative formation process of the STE will be discussed below.

The intensity of the intrinsic luminescence is nearly 10^5 times intense than that of the edge luminescence under the band to band excitation.[3] Therefore, most I^o created by this excitation will relax to form I_2^- and successively capture an electron to form I_2^{--*}. The electron captured at shallow levels of I_2^{--*} cascades down to the $2p_z$ state in a fairly short time by emitting phonons. The radiative transition of $2p_z \rightarrow$

1s would take time more than 10^{-8}sec, which is too longer than 210±15psec. Another possible relaxation of the electron is the tunneling process from $2p_z$ to 1s on the way of the V_k type relaxation as suggested by Toyozawa.[4] Then the electron relaxes down to the bottom of the 1s state to form the STE at $A\Gamma_g 1s: {}^3\Sigma_u^+$. The present τ_3=210±15psec may correspond to the relaxation time of these kinds, i.e. the V_k type relaxation of I^0 to form I_2^- and the relaxation of the electron to form I_2^{--*} at $A\Gamma_g 1s: {}^3\Sigma_u^+$.

The fast growing and decaying component with τ_1 and τ_2 (the chain curve) suggests the temporal formation of an incomplete F center perturbed by I_2^- which is going to escape from a negative ion site but comes back again to the original site. However, we need to study further details for the above conjecture.

Fig.1

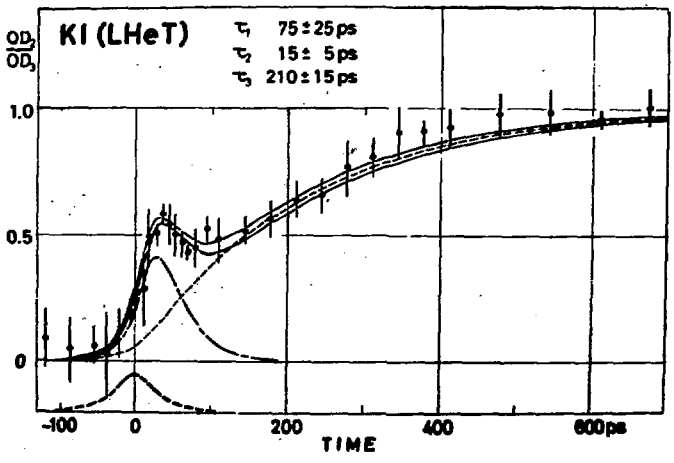

References

1) R.T.Williams and M.N.Kabler: Phys.Rev.B9(1974)1897.
2) T.Karasawa and M.Hirai: J.Phys.Soc.Japan 39(1975)999.
3) I.L.Kuusman et al.: Sov.Phys.Solid State 17(1975)2312.
4) Y.Toyozawa: "International Conference on Color Centers in Ionic Crystals" Sendai, 1974, D43.

LUMINESCENCE OF THE F CENTERS IN LiCl

Ken TAKIYAMA, Toshiaki FUJITA, Atsuhiro FUJII[+] and Masato NISHI

Department of Applied Physics, Faculty of Engineering, Hiroshima University, Hiroshima, Japan

[+]Department of Physics, Faculty of Science, Kumamoto University, Kumamoto, Japan

A model has been used by Bartram and Stoneham[1] to explain the occurence or non-occurence of F-center luminescence in ionic crystals, in terms of a simple two-state configuration coordinate diagram. In this model, the criterion for the occurence of luminescence is expressed as $\Lambda<1/4$, where Λ (=excited-state lattice relaxation energy/ optical-absorption energy) is a parameter, related to the relative displacement of the ground and excited state curves.

Bosi[2] has recently observed the low intensity photoconductivity from F center in NaBr ($\Lambda=0.375$), although he could not detect its luminescence. From the data on the photoconductivity he obtained the values of an activation energy and the photoconductive life time, whose values are typical of F centers in alkali halides. Therefore he suggested the possibility of occurence of F-center luminescence in NaBr. At that time the hygroscopic samples with $\Lambda>1/4$ as NaBr, NaI and Li-halides except LiF are not studied because of its difficulties of the coloration and of the handling.

We tried to detect luminescence from F centers in LiCl whose Λ is 0.371, and then could observe the F-luminescence contrary to Bartram's forecast.

The crystals used in this investigation were grown with the Bridgeman method after the zone-refinement of the extra-pure LiCl powder (99.999 %). Coloration was done by the irradiation with 25 MeV electrons at LNT. The cureves (a), (b) and (c) in Fig. 1 show the optical absorption, emission and excitation spectra measured at LHeT, respectively. The emission curve (b) with a peak at 1.56 eV was found by the F-light excitation; its half width was estimated as 0.43 eV at LHeT. The F-band region of the excitation

curve (c) shows a good agreement with the absorption curve (a). Further, the weak excitation bands observed in the higher energy region seem to correspond to L bands observed by Klick[3], since L_1- and L_2- light excitation resulted in the same emission as that observed by the F-light excitation. These facts mean that the emission band peaked at 1.56 eV is attributed to the F electrons.

This emission band did not show the polarization by the excitation with the light polarized along [100] and [110] directions.

The decay time of this emission band was measured and found to be 1.9 μ sec at LHeT; its temperature dependence was very similar to the F centers as shown in Fig. 2. Moreover, since the emission decay curve was a single exponential curve, this emission mechanism is one process.

In conclusion, this 1.56 eV-emission may occur from the relaxed excited state of the F center in LiCl.

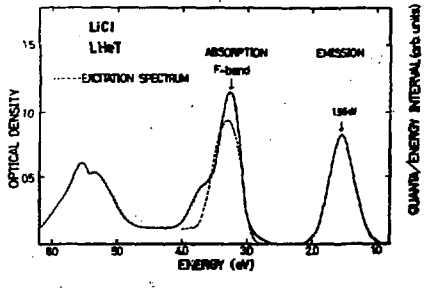

Fig.1

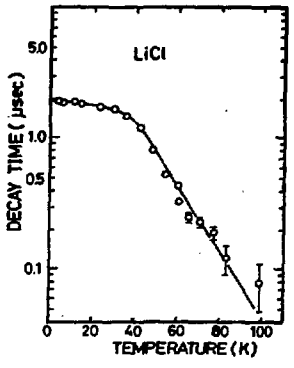

Fig.2

1) R.H.Bartram and A.M.Stoneham, Solid State Commun. 17,1593 (1975)
2) L.Bosi. Phys. state. sol. (b) 75, K 163 (1976)
3) C.C.Klick. Phys. Rev. 137, A 1814 (1965)

THERMAL ANNEALING OF F AND V_2 CENTRES IN KCl CRYSTALS

I.TALE and A.NAGORNYI.

Latvian State University,Rainis 19,Riga,USSR

It is now believed that there is one efficient primary process responsible for production of Frenkel defects in alkali halides at all temperatures.In pure KCl crystals above LNT irradiation produces mainly F and V_2 centres (molecule X_3 placed in one cation and two anion sites)[1,2].Simultaneous thermal annealing of F and V_2 centres occurs in the temperature range of 350-450 K and is accompanied by luminescence peaking at 2.9 eV.

We have exsamined the thermal annealing of F and V_2 centres by fractional glow technique [3],which permits to estimate the thermal activation energies even when the annealing process is complex.This method is characterised by a high resolving power and great accuracy.

The samples of KCl crystal,purified by zone melting 60-times,were irradiated by X-rays at various temperatures and for varying periods of time (0.1-11 hours).Temperature oscillations of value $\Delta T=0.03\cdot T_m$ were performed,where T_m is the maximum temperature of the sample for a given oscillation.Additionaly the T_m was raised for each successive oscillation by the value of $T_m-T_{m-1}=0.005\cdot T_{m-1}$.The partial light sum emitted during each temperature cycle and proportional to the glow intensity was recorded and from the slopes of the heating and cooling curves in Arrhenius plots the activation energy of the annealing process was evaluted.No thermal quenching of luminescence in the temperature range 300-480 K was observed.

The glow curve caused by annealing of the F and V_2 centres depends on irradiation conditions: the maximum of the glow curve shifts to high temperature when the irradiation temperature and/or the irradiation time rises (see fig.,a),the total light sum being proportional to the number of annealed F centre.In the course of annealing of the F and V_2 centres the activation energy is not constant (see fig.,b). Changes in the temperature dependence of the activation energy E(T) under different irradiation conditions are also observed,which show that there are two independent mechanisms for annealing. The first of them prevails in the temperature range of about 340 to 420 K with activation energy E of 0.9 to 1.24 eV and effective frequency factor ω' of the order of $10^{12}-10^{13}\ s^{-1}$.There is reason to suppose this mechanism to be the reaction of close defect pairs (F and V_2 centres;V_2 centre and another radiation defect - the intersitials or vacancies),since a preliminary heating of the irradiated sample to the maximum temperature of

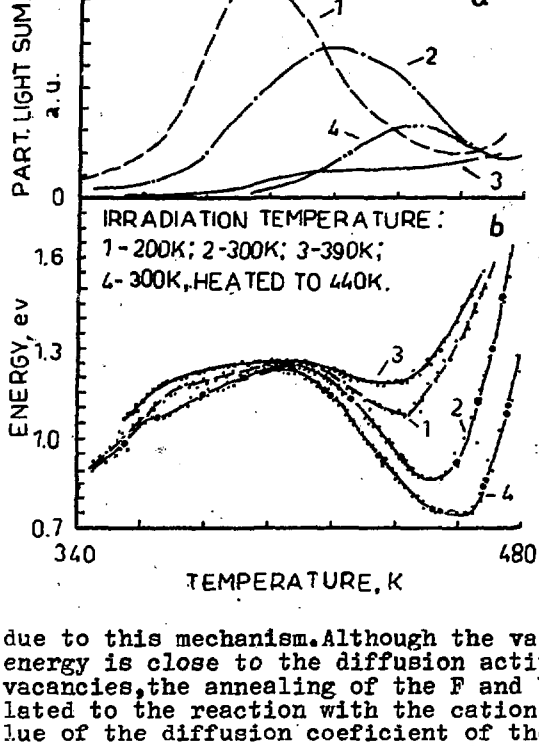

the glow curve decreases the part of the F and V_2 centres annealed by this mechanism (the maximum of the glow curve shifts to high temperatures). Moreover, the E(T) below 420 K depends slightly on the irradiation conditions. Another likely mechanism might be that of thermal dissociation of V_2 centres, but it does not seems to be the case, since then all of them would be anneald by such a mechanism.

For second annealing mechanism the value of the activations energy is $E \leq 0.74$ eV and the effective frequency factor of the order of $10^5 - 10^6\ s^{-1}$. Only about 10 per cent of the total light sum is emitted due to this mechanism. Although the value of the activation energy is close to the diffusion activation energy of cation vacancies, the annealing of the F and V_2 centres cannot be related to the reaction with the cation vacancies, since the value of the diffusion coeficient of the latter is too high in the temperature range under consideration. The low value of the effective frequency factor suggests that the annealing of the F and V_2 centres here may by caused by the diffusion of one of the above-mentioned defects, most likely V_2 centres.

R E F E R E N C E S

1. Winter E.M., Wolfe D.R. and Christy R.W., Phys.Rev. 1969, 186, 949-52.
2. Jaanson N., Gindina R. and Lushchik Ch., Fiz.tverd.Tela, 1974, 16, 379-83.
Lushchik Ch., Gindina R., Pung L., Tyisler E., Elango A., Jaanson N., Izv.Akad.Nauk SSSR, ser.fiz., 1974, 38, 1219-22.
Elango A. and Nurakhmetov T., phys.stat.sol.(b), 1976, 78, 529-36.
3. Gobrecht H. and Hofmann D., J.Phys.Chem.Solids, 1966, 27, 509-22.

ENERGY TRANSFER BY THE PRECURSOR OF FRENKEL PAIRS IN ALKALI HALIDES

K.Tanimura

Department of Nuclear Engineering, Osaka University, Yamada-kami, Suita 565 Japan

One of the most important problems in color center formation in alkali halides concerns the nature of the precursor of Frenkel pairs. In this paper, we will show that the precursor is mobile and transfers its energy to an alkali impurity to form the relaxed exciton associated with the impurity $(V_K e)_A$, in some alkali halides at low temperature.

The effects of the addition of alkali impurities on the defect formation yield and on the population rates of radiative exciton states were studied for several KBr:Na-type systems.[1] Population rates of the states responsible for intrinsic σ and π emissions are conserved irrespective of the presence of the alkali impurity. On the other hand, the formation yield of the F center η_F in KBr and KCl is reduced. The reduction is found to be compensated by the enhancement of the formation yield η_A, of $(V_K e)_A$ which causes the π_A emission: The η_F and η_A can be described, as a function of the impurity concentration C_A, as

$$\eta_F = (\eta_F)_o - \eta_A ,$$
$$\eta_A = (\eta_F)_o V^* C_A ,$$

where $(\eta_F)_o$ is the F-center formation yield in pure salts, and V^* is constant. From the complementary behaviour between η_F and η_A, the origin of the reduction of η_F is attributed to the de-excitation of the precursor of F-H pairs in terms of π_A emission through the selective interaction with the impurity to form $(V_K e)_A$. It is, therefore, concluded that the energy transfer from the host to the impurity is caused by the exciton state which is responsible for F-H pair formation. Then, V^* may represent the rate of the energy transfer.

In Fig.1, $\eta_F/(\eta_F)_o$ is plotted against C_A to obtain V^* in several systems. V^* in KBr:Li is about two times larger than that in KBr:Na. The difference between these two may reflect the difference in mismatching in the lattice which the impurities introduce. On the other hand, the smaller value of V^* in KCl:Na than that in KBr:Na may come from differences in some

properties of the exciton, since the Na^+ ion in KCl and KBr is considered to give similar perturbation to the hosts.[2] The Li^+ ions in NaCl do not cause the suppression of the F-center formation, nor the change in population rates of states which results in σ and π emissions. Then, the NaCl:Li system is the special case where V* is zero. Thus, V* depends not only on the kind of impurity, but the host itself, which may indicate that V* involves two factors; the cross section of the impurity for capturing the exciton, and the mean free length of the exciton motion, the later of which depends considerably on the kind of alkali halides.

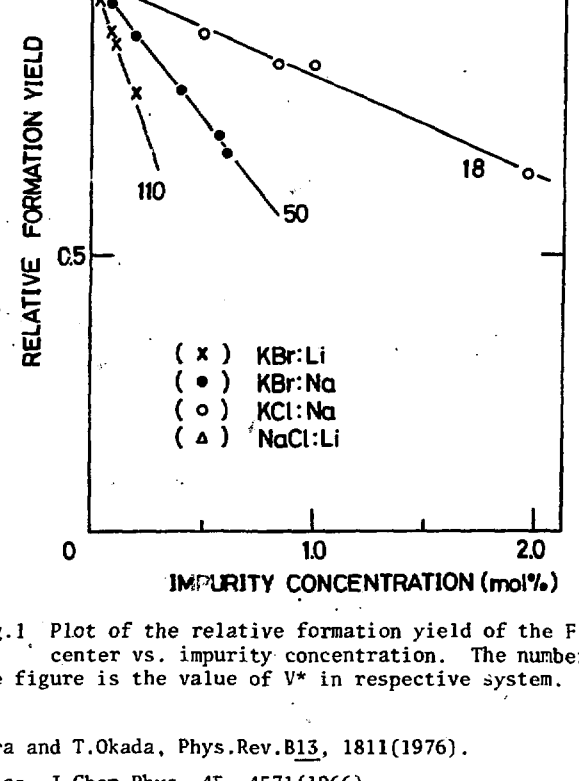

Fig.1 Plot of the relative formation yield of the F center vs. impurity concentration. The number in the figure is the value of V* in respective system.

References

1) K.Tanimura and T.Okada, Phys.Rev.B13, 1811(1976).

2) T.B.Douglas, J.Chem.Phys. 45, 4571(1966).

NON-RADIATIVE RECOMBINATION PROCESS OF THE SELF-TRAPPED EXCITON IN ALKALI HALIDES

K.Tanimura

Department of Nuclear Engineering, Osaka University, Yamada-kami, Suita 565 Japan

One of the crucial problems in current research on the exciton in alkali halides concerns the non-radiative recombination. This process has been considered to take place through electron-phonon interaction;[1] nevertheless, few clear experimental works on the mechanism of non-radiative transition of the self-trapped exciton ($V_K e$), has not been performed. In this paper, we reveal that the internal mode of vibration of the molecular ion in the form of $(MX)_2$ compound(where M and X stand for the alkali and halogen, respectively) is responsible for the radiationless transition of the exciton, through the study of the perturbation of ($V_K e$) by nearest-neighbor alkali impurities in KBr.

Electronic structure and transitions concerned with the relaxed exciton associated with the nearest-neighbor foreign alkali ion ($V_K e$)$_A$ were studied extensively, using pulse electron irradiation as well as x-ray excitation. The nature of the initial state of the π-polarized emission from ($V_K e$)$_A$, the π_A emission, was un-ambiguously assigned to be the lowest triplet state of the exciton associated with alkali impurities. The transition energies of absorption and emission, the lifetime. and the frequency ν_e, which describes the temperature-dependent broadening of the halfwidth of the π_A emissions for ($V_K e$)$_A$ are shown in Table 1.

The association of the foreign alkali ion with the exciton causes significant change in non-radiative transition probability. In Fig.1 is shown the temperature dependence of the decay time of the π_{Na} and π_{Li} emissions. Thermal quenching of the decay time is described adequately in terms of two competitive processes; the radiative decay with a probability of $1/\tau_o$ and non-radiative transition with a temperature-dependent probability of $\nu_q \exp(-E_q/kT)$. The values of ν_q and E_q are also shown in Table.1. The most striking features are seen for the frequency factor, ν_q: As seen from the table, ν_q is strongly dependent on the nearest neighboring alkali ion, which is very much in contrast to the fact that ν_e is not affected by the associa-

Table 1. Peak energies of absorption E_a and emission E_e, halfwidth of π_A emission band W, and activation energy of quenching of decay time E_q, are given in units of eV. Lifetime τ_o, and frequency factors for quenching of decay time ν_q and for broadening ν_e, are given in units of sec and sec^{-1}, respectively.

	E_a		E_e	W	τ_o ($X10^{-5}$)	E_q	ν_q	ν_e ($X10^{12}$)
$(V_Ke)_{Li}$	1.6	1.75	2.75	0.47	1.5	0.048	4.7×10^6	2.3
$(V_Ke)_{Na}$	1.5	1.65	2.90	0.49	2.5	0.075	3.2×10^9	2.3
(V_Ke)	1.58	1.77[a]	2.27[b]	0.40[b]	10^c	0.050[c]	1.3×10^{11}	—

a) From ref.2. b) From ref.3. c) From ref.4.

tion with the alkali impurity. The strong dependence of ν_q indicates that the transition rate near the cross point between the lowest excited state and the ground state in configuration coordinate diagram is sensitive to the neighboring alkali ion. The remarkable amount of reduction of ν_q by association with alkali impurities in the order of Na and Li suggests the larger contribution of the difference in mass of nearest neighboring alkali ion of (V_Ke) to ν_q. Therefore, it is concluded that the internal mode of vibration in the form of $(MX)_2$ conpound is important in the non-radiative decay of the self-trapped exciton.

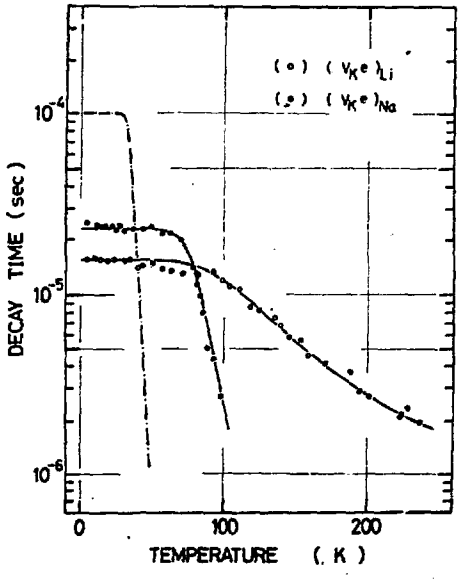

Fig.1 Temperature dependence of decay time of π_A emissions. The chain curve represents that of π emission(ref.4).

References

1) D.Pooley, Proc.Phys.Soc., 87, 245(1966).

2) R.T.Williams and M.N.Kabler, Phys.Rev.B9, 1897(1974).

3) M.N.Kabler, Phys.Rev. 136 A1296(1964).

4) T.Karasawa and M.Hirai, J.Phys. Soc.Japan, 40, 128(1976).

THE ELASTIC INTERACTION OF THE H CENTER WITH A Rb^+ ION DURING THE DYNAMIC MOTION AND THERMAL MIGRATION IN KBr

K.Tanimura

Department of Nuclear Engineering, Osaka University, Yamada-kami, Suita 565, Japan

The secondary reactions of interstitial halogen atom(X_i^o) created by irradiation are dominant in color-center formation process at higher temperatures. Two different modes of motions of X_i^o have been shown to exist; one is the dynamic replacement collision sequence(RCS), the other thermal motion(TM).[1] In this paper, we point out that the difference in modes of the motion causes, in some cases, the essentially different effects in the elastic interaction of X_i^o with other imperfections, through the study on defect formation and thermal annealing of F and H centers in KBr doped with Rb^+ ions at low temperature.

A new optical absorption band peaked at 3.19 eV is formed only during thermal annealing of KBr:Rb irradiated at 6 K. This band is attributed to be due to the H center trapped by a Rb^+ ion based on following observations;

1) The formation efficiency of this band by thermal annealing increases with increasing Rb^+ concentration, while thermal annihilation of the F center is suppressed by the presence of Rb^+ ion.

2) The 3.19-eV band decays thermally at 55 K in parrallel to the annihilation of the F center.

The fact that this 3.19-eV band is not formed by x-ray irradiation at 6 K indicates that the attractive interaction between H centers with Rb^+ ions does not take place at the temperature.

Coloration at 6 K is found to be suppressed by the addition of Rb^+ ions: formation yields of color centers, typically F and H centers, decreases linearly with the increase of Rb^+ concentration. The emission spectra and intensities of x-ray excited luminescence in KBr:Rb are found to be essentially the same as those in pure KBr. No additional emission bands, such as the π_A-emission band in KBr:Na,[2] are observed, which may show that no interaction between the exciton and a Rb^+ ion takes place. Thus, the suppression of colorability in the present case is considered to be not due to the exciton-impurity interaction, but to be caused by interaction events between RCS of Br_i^o and Rb^+ ions.

In order to deepen understandings of above-mentioned features, we make calculation of the elastic interaction energy(E_{int}) between the H center and a Rb^+ ion, using formulas developed by Shuey and Beyelar.[3] For three types of orientations between the H center oriented along [110] and a Rb^+ ion with connection lines along [001], [110], and [1$\bar{1}$0] directions, which are of primary importance to discuss the interaction concerned, E_{int} are $-0.022/r^3$, $0.0082/r^3$, and $0.014/r^3$, respectively, where r is the distance between two defects with the unit of a half of the lattice constant. These results of calculation show that the interaction along <110> is repulsive, whereas that along <001> attractive.

The prominent mode of motions of Br_i^o during irradiation at 6 K is RCS. In this mode, Br_i^o may approach the Rb^+ ion only along a <110> direction, since the motion is considered to be restricted to one dimention along the direction. This type of approach of the crowdion toward a Rb^+ may be interrupted, because the interaction is always repulsive. Then, the atom may not be able to arrive at a Rb^+-ion site to form the $H_A(Rb^+)$ center. In the case where the repulsive potential is high enough. RCS cannot sufficiently separate to form the stable F-H pair from the initial position where an F center is formed, which may result in the prompt recombination between created F-H pairs. Thus, the suppression of colorability may result. On the other hand, TM of the H center is supposed to be the sequence of random walk with free re-orientation. Then, the H center may reorient to reduce the interaction energy, and approach along <001> directions may be possible. Thus, the $H_A(Rb^+)$ center is formed because of the attractive interaction along <001> direction only during thermal annealing. Therefore, the difference in modes of motions of X_i^o results in the significant differences in the elastic interaction with other defects.

References

1) N.Itoh, Cryst. Lattice Defects. 3. 115(1972).

2) K.Tanimura and T.Okada, Phys.Rev.B13, 1811(1976).

3) R.T.Shuey and H.U.Beyeler, Z.Angew.Math. und Phys. 19, 274(1968).

DISLOCATION INTERATION WITH RADIATION-INDUCED SINGLE HALOGEN INTERSTITIALS IN KBr

K.Tanimura, T.Hagihara, T.Okada, and M.Fujiwara

Department of Nuclear Engineering, Osaka University, Yamada-kami, Suita 565 Japan

The crucial question in radiation hardening phenomena concerns the nature of the interaction of dislocations with radiation-induced defects. Although several works have suggested the importance of interstitials in these hardening phenomena, clear informations on the role of interstitials have not yet been presented.[1] In this paper, we will make clear the nature of single halogen interstitials as the hardening agent, through comprehensive studies based on both macroscopical approach in terms of thermal activation mechanism of dislocation dynamics and microscopical one, including theoretical calculation, on the structure of defects and their interaction with dislocations. The most important finding is that the single interstitial ion is the more resistant to dislocation movements than the atom, and that the origin comes from the stronger elastic interaction force of the ion with dislocations.

All experiments were performed for the system including single interstitials stabilized by alkali impurities (H_A and I_A centers), in order to avoid practical difficulties in performing mechanical tests at low temperature where samples becomes too brittle.

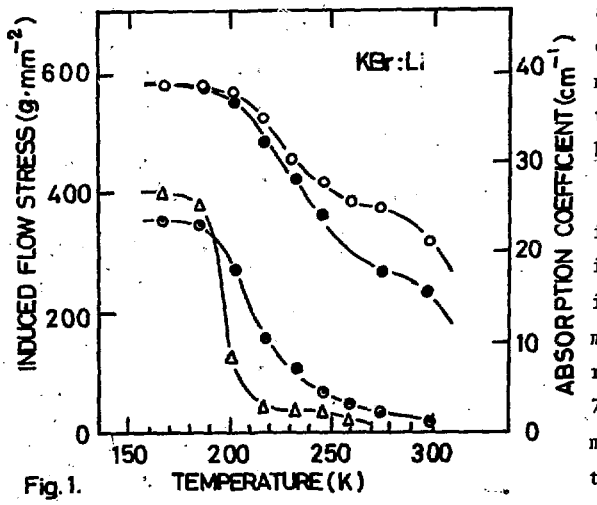

Fig.1.

In Fig.1, we show the isochronal pulse annealing curves of radiation induced flow stress increment ($\Delta\tau$) of KBr:Li irradiated with γ rays at 77 K. Considerable amount of $\Delta\tau$ is reduced at the stage around 230 K

where both H_A and I_A centers decay thermally. The similar curve of $\Delta\tau$ of the specimens illuminated by visible light at 77 K after γ irradiation is also shown. By the optical illumination at 77 K, complete bleaching of the H_A center and the increase in the concentration of the I_A center by about 40% were induced. One can see in Fig.1 that the recovered amount of $\Delta\tau$ at the stage in optically bleached specimens is larger by about 40% than that in as-irradiated one, irrespective of complete bleaching of the H_A centers in the former. Thus, it is evident that the I_A center is mainly responsible for $\Delta\tau$ at the stage which clearly indicates that the interstitial ions interrupt dislocation movements more strongly than the atom.

The interaction of dislocation with the I_A center was found to involve the thermal activation process, which indicates that the interaction is short-range. Then, the maximum interaction force F_{max} can be evaluated to be 1.6 X 10^{-4}dyne, using the formula: $F_{max} = b^2\tau_0(2C_{IA})^{-1/2}$, where τ_0 is the flow stress at 0 K and C_{IA} is the concentration of the I_A center, both of which can be determined experimentally.

Table 1. Maximum Interaction Forces (X10^{-4}dyne)

	Edge	Screw
I center	1.1 ; 0.94	0.22 ; 0.21
H center	0.51	0.088

In order to know the origin of greater obstruction of dislocation movement by the interstitial ions, we carried out the calculation of elastic interaction force between primary interstitials and dislocations, based on the original procedure,[2] utilizing the double force tensor of H and I centers.[3] Calculated F_{max} is listed in Table 1. The results indicate that F_{max} for the I center is about two times stronger than that for H center, irrespective of the difference in types of dislocations. Moreover, it should be pointed out that F_{max} evaluated experimentally is roughly equivalent to that obtained from the calculation of the elastic interaction of the I center with edge dislocation. Thus, it is concluded that greater obstruction of moving dislocations by the ion is mainly due to the stronger elastic interaction between the ion and dislocations.

References

1) J.S.Nadeau, Can.J.Phys. 45, 827(1967).
2) A.W.Cochardt, G.Schoek, and H.Wiedersich, Acta. Met. 3, 533(1955).
3) K.Bachmann and H.Peisl, J.Phys.Chem.Solids, 31, 1525(1970); and R.Balzer, H.Peisl, H.Peters, and W.Waidelich, J.dePhys. Suppl. C9-273(1973).

THE EFFECT OF HEATING RATE ON THE THERMOLUMINESCENCE SENSITIVITY OF LiF (TLD-100)

G.C.Taylor and E.Lilley
Materials Science Division, School of Engineering and Applied Sciences, University of Sussex, Brighton, U.K.

Themoluminescence studies in the past have often ignored the fact that the heating rate may itself be an experimental variable giving different glow peak intensities at different heating rates. Booth et al [1] recognized that such effects could be important in studies on TLD-100 crystals.

Studies on crystals of LiF:Mg, Ti (TLD-100) aged after irradiation have shown that significant changes occur in the intensities of the glow peaks 2 to 5 [1] [2] . Peaks 2 and 3 are seen to decrease, and peaks 4 and 5 increase in the initial stages of annealing above room temperature. Peaks 2 and 3 have been associated with Mg^{2+} cation vacancy pairs and peaks 4 and 5 with higher order clusters, possibly trimers [3][4] The ageing study results suggest that defect reactions are occurring in which Mg^{2+} cation vacancy pairs are diffusing to form trimers. On the basis of these experiments similar effects are expected to occur during the readout of crystals and be sensitive to the heating rate.

Experiments have been carried out at heating rates from 0.016 to 30°C/sec following a rapid quench from 400°C and irradiation. The results for the intensity of peaks 2 and 5 as a function of heating rate are shown in figure 1.

All peaks show a decrease with decreasing heating rate due to the precipitating of Mg^{2+} ions [4] [5] . Peak 5 is seen to decrease at rapid heating rates whilst peak 2 is still increasing. The results may be explained as follows. Rapid quenching will produce mainly Mg^{2+} cation vacancy pairs, trimers having had little time to form. At fast heating rates there will be insufficient time for the $Mg^{2+}V^{-}$ pairs to diffuse and form clusters during readout. Peaks 2 and 3 are then expected to increase to a constant value with increased heating rate corresponding to a maximum freezing in of the $Mg^{2+}V^{-}$ pairs. Peak 5 correlated with trimers will be reduced at high heating rates since the clusters have not had time to form. This is consistent with our measurements.

The decrease in peak 5 intensity at fast heating rates is not only due to thermal quenching [6] but is predominantly due to clustering reactions occurring during readout. The results suggest that for rapidly quenched crystals a rapid heating rate during readout is necessary to avoid clustering during readout, and the corresponding changes in intensity of the glow peaks.

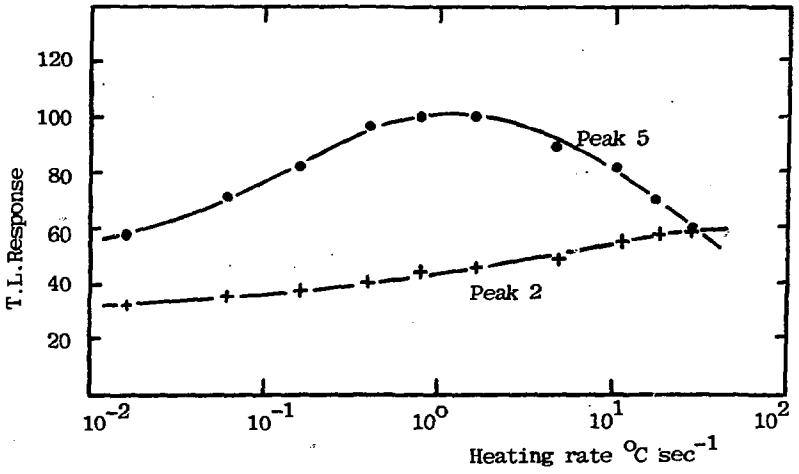

Figure 1: The variation in intensity of peaks 2 and 5 as a function of heating rate.

References

1. L.F.Booth, T.L.Johnson, F.H.Attix, Health Phys., 23, 137 (1972).
2. J.S.Dryden, B.Shuter, J.Phys.D:Appl.Phys., 6, 123 (1973).
3. A.M.Harris, J.H.Jackson, Brit.J.Appl.Phys. (J.Phys.D), 2, 1667 (1969).
4. M.H.Bradbury, B.C.E.Nwosu, E.Lilley, J.Phys.D., 9, 1009 (1976).
5. M.H.Bradbury and E.Lilley, J.Phys.D., 1977, to be published.
6. S.G.Gorbics, A.E.Nash, F.H.Attix, Int.J.Appl.Radiation Isotopes, 20, 829 (1969).

ORDERING OF DEFECTS IN TiO_x

H. Terauchi and J. B. Cohen
Department of Materials Science and Engineering
The Technological Institute
Northwestern University
Evanston, IL 60201
U.S.A.

In the monoxides of the first transition series, the defects appear to be non-random even at high temperatures. The interaction Hamiltonian in the system may be given in terms of a direct pair coupling of the deviation operator σ_i from the average defect concentration at the i'th site and a defect-electron coupling as follows:

$$H_{int} = \frac{1}{2} \sum_{ij} J_{ij}\sigma_i\sigma_j + \frac{1}{\sqrt{N}} \sum_{iq} G_q\sigma_i\rho_q e^{iq\cdot r_i} \qquad (1)$$

where J_{ij} represents the configurational energy between the i and j'th site of defects, and G_q the coupling energy of σ_i and the charge density wave ρ_q. As a result of screening of the density wave, the free energy of the defect system is written by:

$$F = \frac{1}{2}\sum_q J_{eff}(q)\langle\sigma_q\rangle^2 + \text{entropy term} \qquad (2)$$

where $J_{eff}(q)$ represents the Fourier transform of an effective potential which includes J_{ij} and G_q. Then X-ray scattering intensity employing the random phase approximation can be written as:

$$I_d = N\,|\Delta F|^2\,(1 + J_{eff}(q)/kT)^{-1} \qquad (3)$$

in the disordered phase, and the equilibrium condition $\partial F/\partial\langle\sigma_q\rangle$ gives the superlattice intensity as:

$$I_s = N^2 |\Delta F|^2 \langle \sigma_q \rangle^2 \qquad (4)$$

in the ordered phase, where $|\Delta F|^2$ represents the total scattering minus fundamental Bragg scattering.

Absolute X-ray intensity measurements for TiO_x were made with single crystals with both quenched specimens and specimens at high temperatures above and below the ordering reaction temperature T_c. Comparing the measured intensities with Eq. (3), it is found that there are strong defect-defect interactions in the fifth and sixth neighbor shells around a vacancy and also there is evidence for scattering due to the Fermi surface which arises from defect-electron interactions above T_c. The results of this study on the location of some of the diffuse scattering above T_c, all of which are consistent with the electron diffraction study[1], are given in Table I. This table reveals the location in reciprocal space of diffuse maxima for two compositions and also the requirements imposed on $J_{eff}(q)$ due to these intensity maxima. The ordered phase of TiO_x at several compositions (x) will be discussed.

Table I

Type of Interaction	$TiO_{1.01}$		$TiO_{1.25}$	
	q	$J_{eff}(q)$	q	$J_{eff}(q)$
defect-defect	(110)	at a minimum	not detected	not at a minimum
	(2/300)	at a minimum	not detected	not at a minimum
defect-electron	(100)	at a minimum	near (5/600)	at a minimum

This research was supported by the U.S. Army Research Office.

Reference

(1) J. R. Castle, J. M. Cowley and A. E. C. Spargo: Acta Cryst., A27 (1971) 376.

DEFECT CREATION AND PRECIPITATION IN IMPLANTED MgO

P. THEVENARD, A. CACHARD, J.P. DUPIN, M. MARICHY
et M. GUERMAZI
Département de Physique des Matériaux
Université Claude Bernard Lyon I
43 boulevard du 11 Novembre 1918
69621 Villeurbanne (France)

Magnesium oxyde is implanted with various ions : Mg, Ni, Li, Na, K, Rb, Ne, Ar. The ion energy varies in the range from 30 keV to 24 MeV. During the implantations at 77, 300 or 700K the defect production is studied with optical absorption measurements. The kinetics of intrinsic defects like F and F^+ centers can be explained taking into account nuclear collisions of the particles in small volumes surrounding the particle trajectories.

The amplitude of the 575 nm absorption band depends on the implanted ions : V^- (Li) and V^- (Na) can be created in MgO with implantation. In the case of magnesium, the stability of the 575 nm band with temperature, implies that interstitial centers created by irradiation interact with implanted magnesium.

Colloid absorption bands due to plasma oscillations of small metallic aggregates of implanted particles appear at different temperatures with an isochronal thermal treatment after irradiation. The observation of potassium aggregates in implanted MgO by electron microscopy (1, 2) let to confirm the formation of colloids. In the case of high concentration of implanted Na, K, Rb, Mg a satellite absorption band is observed and can be associated with surface plasma oscillations in platelets or infinite aggregates (percolation process).

Laboratoire Associé au CNRS n° 172

(1) M. TREILLEUX, P. THEVENARD, G. CHASSAGNE et L.W. HOBBS
Physic Letters (to be published)

(2) M. TREILLEUX et G. CHASSAGNE , International Conference on Defects in Insulating Crystals - Gatlinburg October 1977

HYDROSTATIC PRESSURE TUNING OF MOLECULAR DEFECT ROTATION IN ALKALI-HALIDES

Klaus Thörmer and Fritz Luty

Physics Department, University of Utah, Salt Lake City, Utah 84112

Molecular defects (like OH^-, CN^-, NO_2^-...), substituted in dilute form into alkali-halides, perform -- more or less hindered -- rotational motions within the angular multi-well potential of the cubic crystal field. Mechanism and rates for the reorientation among the minima of this potential depend essentially on

a) the moment of inertia of the reorienting molecule
b) the symmetry and strength of the hindering potential, i.e. the width and barrier heights separating the energy minima
c) the non-cubic (T_{1u}, E_g and T_{2g}) lattice distortions, (due to electric and elastic polarization of the surrounding lattice), "dressing" the defect and often strongly hindering its motion.

Both b) and c) vary -- for a given defect -- often strongly with the host, producing drastic variations in the reorientation behavior (ranging from rapid tunneling to thermally activated motion over sizeable barriers). As these variations are theoretically rather poorly understood, we have started a study on the reorientation behavior under hydrostatic pressure, using dielectric techniques. This should yield information on how a tuneable change in lattice-parameter (increase of Born-Mayer repulsion) affects the reorientation potential (and possibly the dressing) of the molecular defect.

As first examples we have studied OH^- defects in KI and KBr, two systems which have very different static and dynamic behavior: While OH^- in KI moves in an extremely shallow potential with twelve <110> minima at extremely high rates ($\tau^{-1} > 10^9$ sec^{-1} at 1.5 K) and gives rise to interesting sharp paraelectric resonance effects, OH^- in KBr moves in a deeper potential with six <100> minima with slower rates (~$2 \cdot 10^5$ sec^{-1} at 1.5 K). We find completely different pressure effects for both systems:

A) KI:OH^- shows for atmospheric pressure, as expected, a dielectric response which is loss-free (in the used $3 \cdot 10^2$ - 10^5 Hz range), and

shows a Curie law T^{-1} dipolar dielectric constant contribution to lowest temperatures. Increase of pressure, while keeping the dipole-moment essentially constant, changes drastically the relaxation behavior: At 1.5 Kbar, a drop in dielectric constant and a loss-peak appears at the lowest accessible temperature (1.3K), which both are tuned with increasing pressure to increasingly higher temperatures (at 6.4 Kbar they reach 8K, and continue to shift). The loss-peaks are Debye-shaped and can be well-fitted with Arrhenius expressions. Such a fit yields activation energy values ΔE, which are tuned from unmeasurable small values at 1 Kbar to a value of $\Delta E = 110K \approx 10^{-2}$eV at 6 Kbar. Parallel to this, the pre-exponential factor increases under pressure by several orders of magnitude.

B) KBr:OH^- shows in drastic contrast to this essentially no pressure effect, with its dielectric loss peak shifting less than 0.2K over the whole pressure range.

The two observed effects are amazing in their contrast: While in KBr the effective reorientation-potential for the OH^- is basically invariant against small (<1%) compression of the lattice, the situation in KI:OH^- appears to be extremely unstable under small (<1.5%) lattice parameter reduction. The observation that the electric dipole moment changes little under pressure, excludes the possibility of major pressure-induced changes in the dressing or in possible off-center effects of the OH^- in KI. The observed relaxation tuning must therefore most likely be attributed to an amazingly large variation of the crystal potential, produced by very small lattice compression. Possible origins for the contrasting behavior A and B (like the different <110> and <100> symmetry in the two cases) will be discussed.

Several other OH^- systems with large and small tunneling splitting of <100> symmetry (KBr, NaCl, RbCl, RbBr, RbI) and of <110> symmetry (NaBr) are under similar study, to obtain a better statistics on the conditions and system-parameters, which lead to behavior A or B. Results of this study will be reported.

Work supported by NSF grant #DMR-74-03870-A02.

EXCITON DIFFUSION AND DEFECT FORMATION IN Na Cl

P D Townsend and M C Wintersgill
University of Sussex Brighton BN1 9QH England

It is generally accepted that defect formation in the halogen sub-lattice of alkali halides proceeds by a Pooley-Hersh type mechanism. Refinements to the model and more data have only modified the details rather than the basic idea.[1, 2] To obtain direct evidence for the halogen replacement collision sequences we have used low energy electron irradiation to form the defects, stimulate luminescence and eject atoms from the surface. The ejection patterns confirm the halogens motion by halogen-halogen collisions whereas the metal atoms merely evaporate in random directions. One result of variations in the electron beam energy and frequency modulation of the excitation has been to reveal evidence for different modes of decay for exciton states in the surface and bulk regions. For example the surface exciton is strongly stimulated by an electron energy corresponding to the K_α X-ray level of the alkali ion.[3]

These results have lead to a reinterpretation[4] of the Saidoh et al[5] concept of an interaction volume between H centres and the lattice. In this alternative model, three dimensional exciton diffusion is the major contributor to the volume and the replacement collision sequence is limited to at most four to five steps.

1. ITOH N and SAIDOH M 1973 J. de Physique 34 C-9 101-5
2. SAIDOH M and TOWNSEND P D 1975 Rad. Effects 27 1-12
3. TOWNSEND P D, BROWNING R, GARLANT D J, KELLY J C, MAHJOOBI A, MICHAEL A J and SAIDOH M, 1976 Rad. Effects 30 55-60
4. TOWNSEND P D 1976 J. Phys. C 9 1871-77
5. SAIDOH M, HOSHI J and ITOH N 1975 J. Phys. Soc. Japan 39 155-61

LUMINESCENCE FROM SELF-TRAPPED EXCITONS IN KBr:Na

Koichi TOYODA,* Kaizo NAKAMURA+ and Yoshio NAKAI+

* Department of Physics, Osaka Dental College, Japan
\+ Department of Physics, Kyoto University, Japan

Ultraviolet excitation of KBr containing Na ion produces characteristic luminescence related to Na^+ in addition to the intrinsic luminescence. The Na luminescence consists of two emission bands peaking at 2.72 eV and at 2.90 eV. Together with results on recombination luminescence in X-rayed crystals, they are confirmed to result from the STE with different types of V_{KA} centers shown in Fig. 1.[1] In the figure, letters A, B and C represent possible positions occupied by an Na ion.

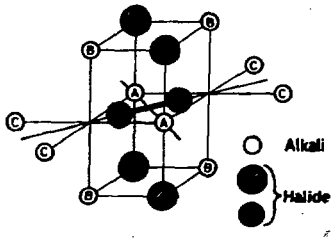

Fig. 1

Behavior of the Na luminescence depends strongly on the exciting photon energy. Spectral shape of the Na luminescence changes clearly according as the exciting energy is below or above the first exciton peak at 6.85 eV. Excitation spectra of the Na luminescence and the σ luminescence for various Na concentrations are shown in Fig. 2. It is seen that three excitation spectra (curves (1), (2) and (3)) are distinctly more crowded in the energy region below 6.85 eV (E_l) than above (E_h).

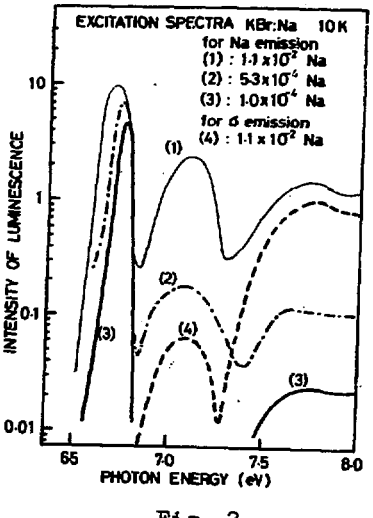

Fig. 2

In the emission spectra obtained by stimulating in the E_h region,

intensity of the 2.72 eV component is comparable to that of the 2.90 eV component and the ratio of the total Na luminescence to the σ luminescence increases linearly with the Na content over nearly 3 orders of magnitude. Open circles in Fig. 3 show the intensity ratio of the Na luminescence to the σ luminescence both excited at 7.7 eV. Most part of the change is ascribed to that of the Na emission itself since the intensity of the σ luminescence is found to change only a little in the concentration range studied.

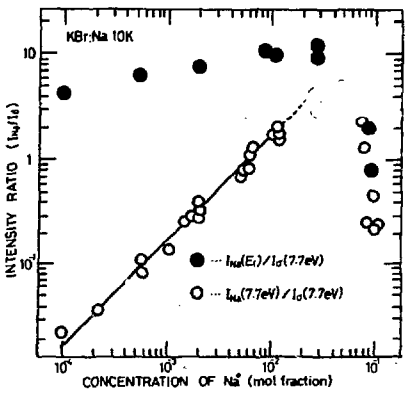

Fig. 3

For the excitation in the E_1 region, on the other hand, the 2.90 eV component surpasses the 2.72 eV component. As shown by solid circles in Fig. 3, relative intensity of the Na luminescence to that of the σ luminescence which is excited at 7.7 eV is fairly large and increases only by a factor of 3 for the increase of the Na concentration over 3 orders of magnitude.

Large yield of the Na luminescence in the E_1 region even for very low concentration of Na (1×10^{-4} mol fraction) suggests that the exciton created in this region has a long lifetime before self-trapping, and at the same time that the Na ion has a large cross section to trap excitons resulting in the 2.90 eV emission band.

1) K. Toyoda, K. Nakamura and Y. Nakai: J. Phys. Soc. Japan 41 (1976) 1981.

ANNEALING STUDIES IN ERBIUM DOPED ALKALINE EARTH FLUORIDES*

DONALD TREACY and JOHN FONTANELLA, U. S. Naval Academy, Annapolis, Md.
CARL ANDEEN, Case Western Reserve University, Cleveland, Ohio

Samples of CaF_2:Er, SrF_2:Er, and BaF_2:Er having nominal concentrations of 0.01, 0.1, and 1.0 mol-% were annealed in vacuum at 1120K and quenched by withdrawing the annealing tube from the furnace. (An additional sample of 0.3 mol-% CaF_2:Er was also studied.) The vacuum was of the order of 10^{-6} Torr. The samples remained clear after this treatment. The crystals were examined before and after treatment using optical and dielectric spectroscopy. The optical spectra were taken on a Cary 17 recording spectrophotometer and the dielectric data were obtained using apparatus described elsewhere.[1]

Five relaxations were studied in CaF_2:Er. The lowest temperature, 0.03 ev, relaxation, which grows monotonically with concentration and is thought to be cluster-associated, was observed to decrease when the samples were annealed and quenched. In the 0.3 mol-% sample, for example, the 0.03 ev relaxation decreased by a factor of three. The 0.15 ev relaxation, on the other hand, grew by a factor of ten and the 0.4 and 0.55 ev relaxations each grew by a factor of three. The optical absorption bands recently associated with clustered rare-earth ions[2] showed a decrease. An increase in absorption bands associated with relaxations having tetragonal symmetry[3] was observed. The magnitude of the increase in the tetragonal absorption bands was close to three.

In the SrF_2:Er where the low temperature dielectric relaxation is not observed until higher concentrations than in the CaF_2:Er the samples show little change upon annealing and quenching at concentrations less than 1.0 mol-%. The 1.0 mol-% samples show a decrease in the low temperature relaxation upon annealing and quenching. Some growth has been observed at intermediate temperatures. No substantial change in the principal relaxation was observed. The D.C. conductivity was significantly enhanced at high temperatures. The optical absorption spectra showed a substantial decrease in spectral regions similar to the CaF_2:Er. No growth in absorption was observed.

In the BaF_2:Er samples, where no low temperature, cluster-associated relaxation is observed up to concentrations of 1.0 mol-%, the dielectric spectrum showed no significant changes other than an increased D.C. conductivity. The optical spectra, on the other hand, showed a decrease in absorption similar to that observed for CaF_2:Er and SrF_2:Er. No increase in absorption was observed.

Further experiments were conducted to attempt to restore the samples to their original state. Samples of CaF_2:Er having concentrations of 0.3 mol-% and 1.0 mol-% were annealed in vacuum at temperatures of 620K, 645K, 670K, and 695K for 15 minutes and quenched in the same manner as the original quenching. In the 0.3 mol-% sample, the changes in the optical spectrum were found to be reversible. The dielectric spectra, however, showed no changes in the three peaks which grew after the original annealing and quenching.

The general conclusion of this set of experiments is that the optical and dielectric spectra are only weakly correlated.

1. J. Fontanella and C. Andeen, J. Phys. C.: Solid St. Phys. 9, 1055 (1976).
2. D. Tallant and J. Wright, J. Chem. Phys., 63, 2074 (1975).
3. C. Rector, B. Pandey, and H. Moos, J. Chem. Phys. 45, 171 (1966).

*Work supported by the Naval Academy Research Council.

OBSERVATION OF EXTRINSIC COLLOIDS OF POTASSIUM IMPLANTED IN MgO SINGLE CRYSTAL

M. TREILLEUX, G. CHASSAGNE*
Dept. Physique des Matériaux*
Université Claude Bernard - LYON (F)

MgO crystals (3N purity), cleaved along (100) have been implanted with potassium ions (10^{17} cm^{-2}) at 77 K. After a thermal treatment (1073 K - 1 h), the optical absorption spectra exhibit a band located at 900 nm and attributed to small clusters of potassium (plasma oscillations). The sizes of these clusters can be deduced from the half width of absorption bands (1).

By transmission electron microscopy (100 keV), small potassium precipitates ($\sim$ 50 Å diameter) have been precedently identified (2).

New observations reveal beside these small precipitates, the existence of large precipitates (up to 2500 Å). The images are disturbed by the presence of dislocation networks produced by irradiation, principally in the (100) plane of the sample. These observations give informations about the nature of the colloidal precipitates : they are found to be b.c.c. potassium. The colloids are revealed by absorption contrast and with the help of their diffraction spots ; they are not coherent precipitates and lie in several orientations with respect to the host matrix. Large colloids can be molten in situ ($\sim$ 333 K) and cristallized again with the same orientation.

From the size distribution observed by high voltage microscopy on large areas, it is possible to suggest a growth process of these extrinsic colloids.

(1) P. Thévenard, J. de Phys. C_7 - 526.530 (1976).

(2) M. Treilleux, P. Thévenard, G. Chassagne, L.W. Hobbs.
Physics Letters - to appear (1977).

* associé au C.N.R.S. : LA 172.

IONIC AND ELECTRONIC CONDUCTION IN THORIA OXIDE ELECTROLYTES

Harry L. Tuller

Department of Materials Science and Engineering
Massachusetts Institute of Technology
Cambridge, Massachusetts 02139

A number of oxides with fluorite or related structures, Thoria (ThO_2) among them, can be made to act as good oxygen ion conductors by heavily doping them with appropriate lower valent cation impurities. At elevated temperatures, under sufficiently reducing or oxidizing conditions, electrons and electron holes are generated making the oxide a mixed ionic and electronic conductor and thereby limiting its usefulness as a solid electrolyte. The region in P_{O_2}, T space for which the conductivity is almost exclusively ionic is called the electrolytic domain. To characterize fully the transition from strictly ionic to mixed ionic and electronic conduction in these solids one needs to determine the position of these electrolytic domain boundaries as a function of the type as well as the concentration of dopant impurities. In the past this has only been done on a limited basis for ThO_2 electrolytes.[1]

Recent data by Lasker and Rapp[2] on $ThO_2 + Y_2O_3$ and Maiti and Subbarao[3] on $ThO_2 + CaO$ have been used by the author to extend this form of analysis to a much wider group of thoria electrolytes. The P_{O_2} dependence of the total conductivity of each of the yttria and calcia doped electrolytes was used to separate out their ionic and electronic components and thereby enable the construction of the electrolytic domain boundaries for each of these systems.

One of the most striking results of this analysis is that the conductivity of these electrolytes is found to become increasingly ionic with increasing temperature (under oxidizing conditions) in contrast to what is usually expected. Examination of the domain boundary equation shows that this may be expected if the activation energy for ionic conduction is greater than that for electronic conduction. This is in fact the case for most of the thoria solid solutions studied here.

The electron hole conductivity in both the yttria and calcia doped

systems can be characterized by an equation of the form $\sigma_h = B_h/T \exp(-\Delta H_h/kT) P_{O_2}^{1/4}$ where $B_h \sim 5 \times 10^4$ K atm$^{-1/4}(\Omega\text{-cm})^{-1}$ (B_h tends to increase with impurity level) and $\Delta H_h \sim 1.1$eV. The activation energy of conduction as well as the energy associated with electron hole formation appear to be insensitive both to the type and concentration of impurity as might well be expected for hole conduction in the oxygen 2p valence band. Estimates of hole mobilities of the order of 100cm^2/v-sec leads to hole concentrations at 1000°C and 1 atm of oxygen pressure of $\sim 10^{14}$cm^{-3}.

Ionic conduction on the other hand appears to depend sensitively on the type of impurity incorporated into the lattice. Ion mobilities of the order of 1.5×10^{-5}cm^2/v-sec were obtained at 1000°C for yttria doped specimens while Ca doped specimens exhibited mobilities about 1/5 as large. Although both systems exhibited activation energies associated with ionic motion of $\sim 1.1 - 1.2$eV at sufficiently high temperature, the Ca doped system showed much steeper activation energies at intermediate temperatures which Maiti and Subbarao suggest are due to impurity - vacancy interactions.

Comparisons of electrolytic domain diagrams of the yttria and calcia doped systems show that yttria doped thoria electrolytes generally exhibit markedly larger electrolytic domains than thoria electrolytes doped with the same concentration of calcia. One also finds that for a given dopant type, the electrolytic domain tends to increase with increasing dopant level.

1) J. B. Hardaway III, S. W. Patterson, D. R. Wilder and J. D. Schieltz, J. Am. Ceram. Soc. 54, 94 (1971).

2) M. F. Lasker and R. A. Rapp, Z. Phys. Chem. N. F. 49, 198 (1966).

3) H. S. Maiti and E. C. Subbarao, J. Electrochem. Soc. 123, 1713 (1976).

LUMINESCENCE IN MgO: TIME-RESOLVED SPECTROSCOPY WITH ELECTRON-PULSE EXCITATION

Thomas J. Turner
Wake Forest University, Winston-Salem, N. C. 27109

K. H. Lee
University of North Carolina, Chapel Hill, N. C. 27514

Richard T. Williams
Naval Research Laboratory, Washington, D. C. 20375

Time-resolved measurements of optical emission from relatively pure and doped MgO crystals have been made in the range from nanoseconds to milliseconds at liquid nitrogen and at liquid helium temperatures. Electron pulses of 5 nanosecond duration and 500-keV mean electron energy were used to excite the crystals.[1]

In pure MgO at liquid nitrogen temperature two composite bands occur whose shape and apparent peak energy change as a function of time after excitation. The first of these bands peaks at 3.8-eV, 10 μsec after excitation and at 3.4-eV, 1.6 msec after excitation. Subtraction of spectra corresponding to different times is used to resolve the bands into components according to their life times. For example the spectrum at 50 μsec subtracted from the spectrum at 10 μsec yields a gaussian peak at 3.95-eV. The second composite peak appears at 4.95-eV with its maximum essentially unchanged in position as a function of time. However, it is clear from oscilloscope photographs made at different times after excitation that the band is composite in nature. At 5.2-eV the intensity can be fit with a sum of four exponentials with decay times of 3.0 μsec, 46 μsec, 350 μsec and 1.66 msec. In a crystal doped with 100 ppm iron the 4.95-eV band is absent but a composite band appears at approximately 3.6-eV.

Others[2,3] have observed multiband spectra in MgO by means of X-ray luminescence. By exciting into the V-band at 2.3 eV Eisenstein[2] has demonstrated that a phosphorescent band at 3.5-eV results from recombination upon release of holes. A portion of what we have observed in

the region of 3.6 eV probably arises from the same effect. In addition, our first composite band probably includes components due to transition elements such as Ni and Fe as well as F^+ centers produced by the electron irradiation.

As suggested in the preceding abstract by Lee and Crawford the 4.95-eV band has characteristics that we associate with electron-hole recombination at various V centers, such as V^-, V_{OH}, and $V_{A\ell}$. If indeed, this assignment is correct it is interesting to note that these bands, which absorb at essentially the same energy (2.3-eV), have lifetimes varying over several orders of magnitude.

In addition to a significant part of the 4.95 eV, several components of the lower energy composite band have decay times of the order of milliseconds. We will discuss various explanations for these long-lived components including recombination of the electron-hole pair in a triplet state and charge transport phenomena.

1. Williams, R.T. and Kabler, M. N., Phys. Rev. B9, 1897, (1974).
2. Eisenstein, A. S., Phys. Rev. 93, 1017, (1954).
3. Wertz, J. E.; Hall, L. C.; Helgeson, J.; Chao, C. C., and Dykoski, W.S., in Interaction of Radiation with Solids, edited by A. Bishay (Plenum Press, Inc., New York, 1967), p. 617.

PROBLEMS IN THE THEORY OF F- AND F_A- CENTRE STATES IN ALKALI HALIDES

John M. Vail
Department of Physics,
University of Manitoba,
Winnipeg, Manitoba, R3T 2N2, Canada.

A critical survey is given of some outstanding problems in the theory of energy levels and wave functions of F- and F_A- centres in alkali halides, and recent results of the author and co-workers are described.

F - Centres

Although the theory of F-centre absorption has been fairly successful, the ENDOR results of Kersten (1) for the ground state have not been fully reproduced by a self-consistent theory. The same is true for the results of Mollenauer and Baldacchini (2) for the relaxed excited state in KI . The radial dependence of trial wave functions for these states is discussed. The role of dynamic lattice screening in determining the localization of F-centre states, particularly the relaxed excited state, remains in doubt despite Fowler's analysis (3). An effective hamiltonian which includes this effect is presented. The emission process is known to involve parity mixing in KCℓ, but the results of a static lattice analysis for a variety of alkali halides has only been carried out previously by Wood and Joy. (4). Results of a more complete survey by C.K. Ong are presented. These results focus attention on the ion-size effect as a crucial difficulty in the theory.

F_A- Centres

Results are reported from a survey by C.K. Ong of F_A- centre absorption splitting in a number of alkali halides. The role of the ion-size effect in this process is emphasized. Progress by A. Kung in establishing an empirical criterion for type II behaviour is described, as well as his "molecular model" estimate of F_A(II) emission energies. Since Ong's detailed theoretical treatment of these topics for KCℓ was largely unsuccessful (5), and Kung's approach cannot be extended,

we discuss a project in which lattice distortion is only treated in lowest order, but in which the fairly flexible trial wave functions of A.H. Harker's PRISM program (6) are used. The objective is to establish first estimates of the energies and wave functions for vacancy and saddle-point states of F_A-centres based on a consistent rigorous analysis of a fairly realistic model.

References

(1) R. Kersten, phys. stat. sol. 29, 575 (1968)

(2) L.F. Mollenauer and G. Baldacchini, Phys. Rev. Lett. 29, 465 (1972).

(3) W.B. Fowler, Phys. Rev. 135, A1725 (1964).

(4) R.F. Wood and H.F. Joy, Phys. Rev. 136, A451 (1964).

(5) C.K. Ong and J.M. Vail, Phys. Rev. B8, 1636 (1973).

(6) A.H. Harker, Report No. AERE-M2775, AERE Harwell, 1976, unpublished; sec. 4.3.

ABOUT RADIATION DAMAGE IN α-QUARTZ*

VAN DEN BOSCH A.

Materials Science Department, S.C.K./C.E.N., B-2400 MOL (Belgium)

Radiation effects in geologic formations is of interest at high-level radioactive waste disposal. Jenks [1] recommended certain radiation experiments on rock-forming minerals with gamma-ray doses up to ~ 2×10^{10} rads and fast neutron fluences of ~ 1×10^{17} neutrons, of an energy > 0.3 MeV, per cm^2; the radiation which will prevail in rock immediately adjacent to buried waste. Reported here is an experiment on α-quartz, one of the most stable of the minerals. Single crystals have been irradiated near spent fuel elements of the BR2 reactor, at temperatures just above room temperature, for doses up to 1×10^{11} rads. The paramagnetic part of the static susceptibility, which obeys the Curie law, has been measured following the Faraday method. The paramagnetism became detectable, > 3.σ, in the sample irradiated to the highest γ-ray dose considered. Although the energy deposition per unit mass in the γ-irradiated sample was estimated to be two orders in magnitude larger than that in a reference crystal which was irradiated with fast neutrons to 4×10^{17} n/cm^2 (E > 0.3 MeV), its Curie-paramagnetism was five times smaller than that in the reference. The behaviour is explained by assuming two types of damage processes to occur in quartz: 1 - the production of Frenkel pairs with a rather large auto-annihilation; and 2 - the creation of more stable defect centres which produce the amorphous transformation. The efficienty for creating the latter centres then is larger for neutrons than for gammas. The neutron irradiation resulted in the reference sample in a relative density decrease of 0.035 %.

[1] G.H. Jenks, ORNL-TM-4827 (1975)

*Work performed under the auspices of the Association R.U.C.A. - S.C.K./C.E.N.

ESR STUDY OF Sn^- DEFECTS IN ALKALI HALIDES

F. Van Steen, A. Lagerdijk, D. Schoemaker
Physics Department, University of Antwerp (U.I.A.)
2610-Wilrijk, Belgium

Sn^{++} impurities and their associated vacancies trap electrons and form Sn^+ centers when KCl:Sn^{++} crystal are x-irradiated at 77K[1]. Irradiation at this and higher temperatures produces three other tin defects which we have identified from their ESR spectra as being essentially Sn^- ($5p^3$, $^4S_{3/2}$) ions.

The first Sn^- defect exhibits an isotropic ESR line with g = 1.970. It is produced strongly by a rather short x-irradiation at room temperature and has been found in NaCl, KCl, RbCl, RbBr, KBr and KI. The linewidths scale with the F-center or V_K-center ESR linewidths in these crystals, indicating that the species is on a negative ion site. The ^{119}Sn hyperfine interaction is 101 gauss in KCl. This defect is ascribed to a Sn^- ion in the perfect octahedral symmetry of a negative ion site, not perturbed by the presence of a vacancy.

The second Sn^- defect possesses tetragonal symmetry around <100>. It is produced in KCl by x-irradiation at 230K or, more strongly, by a short x-irradiation at room temperature followed by an x-irradiation at 77K.

The ESR spectrum is described by a spin hamiltonian of the type $DS_z^2 + g\mu_B\vec{H}.\vec{S}$ with $S = \frac{3}{2}$, $D \gg g\mu_B H$. One finds g = 1.976. The observed effective g-factors in the ESR spectrum are: $g_{//}$ = 1.981 and $g_{\perp}$ = 3.931. A likely model for this defect is a Sn^- on a negative ion site perturbed by a positive ion vacancy along <100> immediately adjoining the Sn^-.

The third Sn^- defect possesses orthorombic symmetry and is produced by x-irradiation at room temperature. The ESR spectrum is described by $DS_z^2 + E(S_x^2 - S_y^2) = g\mu_B\vec{H}.\vec{S}$ with $S = \frac{3}{2}$ and $D > E \gg g\mu_B H$. The analysis yields g = 1.981, E/D = 0.15 and the z axis makes a small (2.1°) angle with <100> in a {100} plane. Here the Sn^- is believed to be perturbed by two vacancies, a cation and an anion vacancy.

The production mechanism of these defects is still a matter of conjecture. From the fact that the Sn^- defects are produced quite rapidly (< 30 min. x-irradiation for maximum intensity) it is thought that the excitation energy moves quickly to the Sn^{++} impurities and that defect formation takes place in the immediate neighborhood of the Sn^{++}. The creation of a negative ion vacancy, the trapping of electrons, and the transfer of the tin to the negative ion site, could then occur rather quickly explaining the rapid formation of the Sn^- defects.

(1) C.J. DELBECQ, R. HARTFORD, D. SCHOEMAKER, P.H. YUSTER, Phys. Rev. B13, 3631 (1976).

THE KINETICS OF BARIUM PRECIPITATION AT DISLOCATIONS IN NaCl MONOCRYSTALS

G. Vlasák and M. Hartmanová
Institute of Physics, Slovak Academy of Sciences,
Dúbravská cesta, 899 30 Bratislava, Czechoslovakia

The kinetics of barium precipitation at dislocations in NaCl monocrystals has been studied in thermally and mechanically treated NaCl 4 ppm $BaCl_2$ samples by investigating the isothermic change of ionic conductivity as a function of time. The results obtained show that the impurity precipitation in this system takes place at dislocations located at grain boundaries. According to Cottrell and Bilby [1] and to Harper [2], supposing that the precipitation rate decreases proportionally with the volume of precipitated phase, it is

$$\frac{N(t)}{N(0)} = 1 - \exp\left[-\alpha G\left(\frac{ADt}{kT}\right)^{2/3}\right]$$

The dependence $\ln\left[1 - \frac{N(t)}{N(0)}\right]$ vs $t^{2/3}$ obtained by applying this relation for experimental data is shown in Fig. 1. As can be seen, the course of precipitation may be divided into three regions.

The presence of region 1 is due to diffusion of the impurity ions to the dislocation core where only after sufficient increase of impurity concentration, nucleation and precipitation may occur. Thus, region 1 is an "incubation" time necessary for nucleation.

During ageing time some dislocations were ordered to the grain boundaries. The higher number of dislocations occurring in this crystal already before annealing ($\sim 5 \times 10^7/cm^2$) was demonstrated by a substantial increase of the number of dislocations at grain boundaries before measurement and a large decrease in the region 2. Interactions between dislocations that lead to their annihilation or formation of grain boundaries are stronger than the pinning of dislocations by impurities. The dislocations move faster than is the rate of Cottrell atmosphere formation so that agglomeration of impurities around dislocations, nucleation and precipitation begin after the pinning of dislocations at grain boundaries. Thus, one may say that the precipitation in region 2 takes place at dislocations occurring at grain boundaries already before the measurement.

In region 3 the precipitation is further caused also by dislocations that formed new boundaries or climbed to already existing boundaries during measurement, respectively.

Between regions 2 and 3 an "inflexion point" is observable. This effect can be explained qualitatively on the base of Cahn theory [3]. It is the case when the nucleus at dislocation grows and its free energy reaches a local minimum at value r_0. At a suitable ratio of the number of dislocations to the free impurity concentration after a certain time the precipitation slows down or even interrupts due to the creation of a local

minimum of the free energy of nucleation. In NaCl - $BaCl_2$ the interruption occurs - if the conditions for minimum creation are fulfilled - at the radius of nuclei being $r_o = 6.925 \times 10^{-8}$ cm.

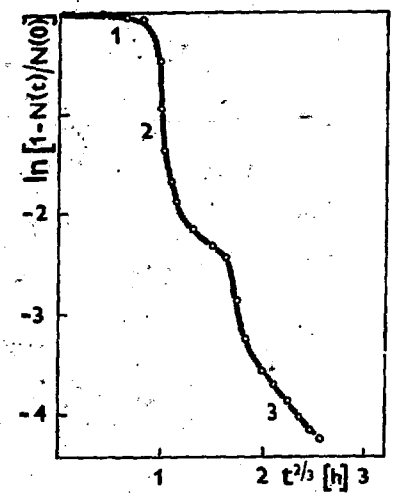

Fig. 1

References:

1. Cottrell, A. H. and Bilby, B. A., Proc. Phys. Soc. A62, 49 (1949).
2. Harper, S., Phys. Rev. 83, 709 (1951).
3. Cahn, J. W., Acta Met. 5, 169 (1957).

F CENTERS PROPERTIES AND PHASE TRANSITIONS : KCN AND NaCN

J.-P. von der Weid † and M.A. Aegerter
Institut de Physique, Université de Neuchâtel,
CH - 2000 Neuchâtel, Switzerland

KCN and NaCN crystals show many interesting properties which arise from the molecular character of the CN^- ion group. From temperatures just below the melting point down to a critical temperature T_1 (168 K for KCN and 288 K for NaCN) these crystals have the NaCl structure, with rapid reorientation of the CN^- group in the cubic crystalline field. A structural phase transition occurs at T_1, with ferroelastic ordering of the CN^- ions. The crystal symmetry point group changes from cubic (O_h) to orthorhombic (D_{2h}). At a second critical temperature T_2 (83 K for KCN and 172 K for NaCN) the electric dipoles of the CN^- ions become oriented in an antiparallel way, leaving the crystal in an antiferroelectric state.

The optical properties of F centers in KCN and NaCN were measured in the temperature range from 300 K down to 4.2 K. The single gaussian shaped absorption band in the cubic phase splits into three components at the temperature T_1, but no change in the first moment of the whole band was observed within our experimental errors. Between T_1 and T_2 the F band remains nearly unchanged. Below T_2, a marked blue shift of the low energy component was observed, whereas the other two remained nearly unchanged. Also a small absorption band in the near infrared appeared below T_2. The position of the observed absorption bands are shown in the Table.

The luminescence of F centers in KCN was also measured. The lifetime of the relaxed excited state in KCN is 21.5 ± 2 nsec at 4.2 K, its value decreasing with the increasing temperature. No luminescence from F centers in NaCN crystals was detected.

The overall behavior of the F band is explained by the symmetry change of the crystalline structure at T_1 and by the local electric field which appears below T_2. The spontaneous deformation ΔQ of the cubic cell at T_1 can be decomposed in the cubic symmetry in two deformations ΔQ_{31} and ΔQ_{53} which transforms respectively like the basis functions $(2z^2 - x^2 - y^2)$ and

(xy) of the Γ_3^+ and Γ_5^+ irreductible representations of the cubic group [1]. In KCN, for example, $\Delta Q_{31} \simeq 0{,}04\ a$ and $\Delta Q_{53} \simeq 0{,}03\ a$, where a is the cubic lattice parameter. To the first order in ΔQ the strain Hamiltonian of the F center predicts a splitting of the Γ_4^- excited state as shown in the figure, with no change in the first moment of the whole F band.

Below T_2, the local electric field which appears along the z axis will only mix the 2s (Γ_1^+) and $2p_z$ (Γ_3^-) states leaving unperturbed the $2p_x$ (Γ_4^-) and $2p_y$ (Γ_2^-) states. The small band which grows below T_2 can be assigned to the 1s → 2s transition, which becomes partially allowed by the field mixing. Assuming the same dipole matrix element $\langle 2s|z|2p_z\rangle$ of F centers in KCN and KBr [2], the local field in KCN can be estimated as $\sim 10^7$ V/cm.

Uniaxial stress experiments in order to induce a single domain crystal are under way so that more information can be obtained from polarisation measurements.

Research supported by the Swiss National Science Foundation.

†On leave from the Physics Department of the Pontificia Universidade católica, Rio de Janeiro, Brazil.

[1] C.H. Henry and C.P. Slichter, in "Physics of Colour Centers" Ed. W.B. Fowler, Academic Press, N.Y. (1968).

[2] U.M. Grassano, G. Margaritomdo and R. Rosei, Phys. Rev. B2, 8, 3319 (1970).

	KCN	NaCN
ε_z (Γ_1)	$2{,}09_7$	$2{,}13_1$
ε_y (Γ_2)	$2{,}20_3$	$2{,}34_0$
ε_x (Γ_4)	$2{,}35_0$	$2{,}54_0$
$\varepsilon_{2s}(\Gamma_1)$	$1{,}5_1$	—

TABLE

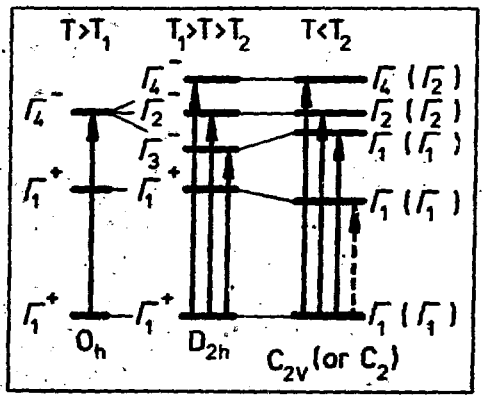

DIELECTRIC STUDY OF MOBILE IONS IN A SUPERIONIC CONDUCTOR

J. Wahl, U. Holland and E.S. Koteles
Max-Planck-Institut für Festkörperforschung, 7 Stuttgart 80, Germany

A fundamental characteristic of superionic conductors is the existence of a large number of possible sites for the mobile ion. When ions occupy many of these positions, displacement dipole moments result. The static and dynamic properties of these ions can be studied directly by measuring dipole alignment and reorientation with dielectric techniques at low temperatures where the dc conductivity is negligible. We report the first such measurements on superionic conductors which provide information on the locations of the available sites, the jump rates and possibly the jump paths of the mobile ions. Results are presented for Li_3N which has recently been shown to be an excellent Li superionic conductor[1].

Li_3N is a hexagonal crystal with Li_2N layers normal to the c-axis, connected by Li ions[2]. Large, high quality single crystals were grown by the Czochralski technique[3]. Li ionic conductivity values of 10^{-3} $(\Omega cm)^{-1}$ were obtained perpendicular to the c-axis at room temperatures[1].

The dielectric constant and loss were measured over the temperature range 4K to 80K as a function of frequency ($10-10^5$ Hz). As the temperature was decreased, the dielectric constant for $E \perp c$ was observed to increase while that for $E \parallel c$ remained constant. For $E \perp c$ the observed behavior between 80K and 60K obeyed a Langevin Debye 1/T law but in the range 60K to 40K, the rate of dielectric constant increase was reduced. Below 40K a frequency dependent decrease of the dielectric constant was measured. Simultaneously, strong dielectric loss was observed, as expected from dipole dispersion. In Fig.1 the dielectric loss ($E \perp c$) is plotted as a function of frequency at several temperatures. (The loss for $E \parallel c$ was smaller by a factor of 100).The large magnitude of the loss eliminates paraelectric impurities as a possible source. Contrary to the predictions of a Langevin Debye law, the die-

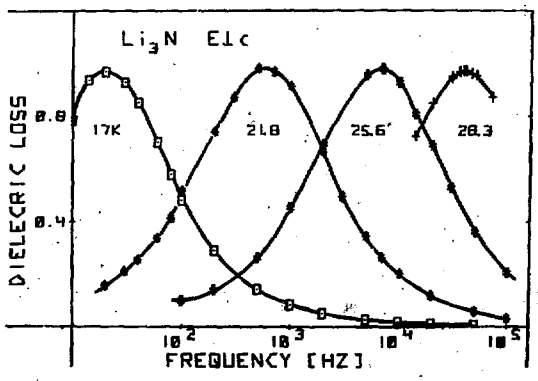

Fig.1

lectric loss does not increase as the temperature is lowered. This is consistent with the deviation observed in the rate of dielectric constant increase in the range 60K to 40K. In Fig.2 the relaxation rate for dipole reorientation as given by the peak frequency of the dielectric loss curve is plotted as a function of inverse temperature. The curve has been fitted by two Arrhenius laws as shown.

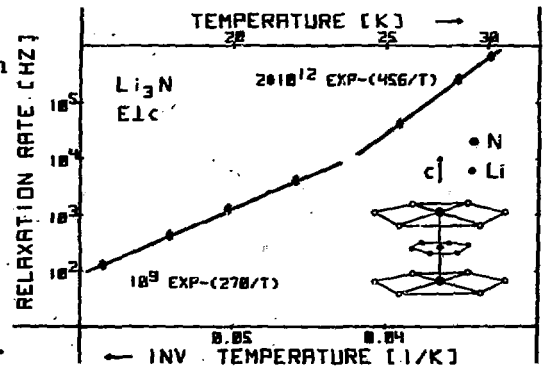

Fig.2

We propose a simple model to explain these observations. From room temperature x-ray studies[2] the interplanar Li ions are known to reside in the middle between the N ions with large vibrational amplitudes perpendicular to the c-axis. The low temperature anisotropic paraelectric properties could be due to the interplanar displacement of these Li ions away from this middle position as illustrated in the insert in Fig.2. The activation energy can then be related to Li ion jumps between equivalent off-center sites. The change in activation energy as a function of temperature might be due to a change in jump path. More measurements are needed to confirm this model and to explain the deviation from paraelectric behavior at low temperatures. Thermally stimulated current measurements and dielectric measurements under bias field and hydrostatic pressure are now in progress.

(1) U. von Alpen, A. Rabenau and G.H. Talat, Appl. Phys. Lett., in press
(2) A. Rabenau and H. Schulz, J. Less Common Metals, 50, 155 (1976).
(3) E. Schönherr and G. Müller, to be published.

LOCATIONS OF THE CONDUCTING-ION SITE NEAR THE MID-OXYGEN POSITION IN BETA-ALUMINAS

J. C. Wang

Solid State Division, Oak Ridge National Laboratory[*]
Oak Ridge, Tennessee 37830

The conducting-ion (CI) site near the mid-oxygen (MO) position in the mirror plane has been observed for beta-aluminas from crystal structure studies.[1-5] The location of this site is not exactly at the MO position and is different in each material. In particular, deviations of 0.38, 0.50, and 0.63 Å from the MO position toward the anti-Beevers-Ross (ABR) site have been reported for Na, K, and Rb beta-aluminas, respectively.[2-4] These systematic deviations of the CI site toward the ABR site are very peculiar, since larger ions are expected to be more difficult to move toward the ABR site.

The values of the lattice constant c are reported to be 22.53, 22.722, and 22.87 Å for Na, K, and Rb beta-aluminas, respectively.[2-4] It is interesting to note that the plot of the deviation of the CI site versus c is very close to a straight line. This suggests that the deviation of the CI site may also be related to the repulsive potentials produced by the conducting ions.

In a previous study[6] it was demonstrated that, in the ideal structure of beta-aluminas, $M_2O \cdot 11Al_2O_3$, all M^+ ions should sit near Beevers-Ross (BR) sites. The three ABR sites next to a BR site have a potential at least 2 Volts higher than that of the BR site. However, because of the excess M^+ ions compared to the ideal structure, some of the conducting ions must form pairs to share BR sites. A pair of M^+ ions sharing one site will, because of the Coulombic and short-range repulsive potentials, repel each other and locate near the MO positions. In this work it is intended to use this idea to explain the systematic deviations of the CI site in different materials. It will be shown that larger paired ions, due to their larger radii, will move closer to the ABR sites.

---

[*]Operated by Union Carbide Corporation for the ERDA.

REFERENCES

1. W. L. Roth, J. Solid State Chem. 4, 60 (1972).
2. C. R. Peters, M. Bettman, J. W. Moore and M. D. Glick, Acta Cryst. B27, 1826 (1971).
3. P. D. Dernier and J. P. Remeika, J. Solid State Chem. 17, 245 (1976).
4. T. Kodama and G. Muto, J. Solid State Chem. 19, 35 (1976).
5. T. Kodama and G. Muto, J. Solid State Chem. 17, 61 (1976).
6. J. C. Wang, M. Gaffari and Sang-il Choi, J. Chem. Phys. 63, 772 (1975).

FIRST-SHELL ENDOR AND SPIN RELAXATION OF THE F_A(Li) CENTERS IN KBr AT LHeT

Tohru WATANABE, Yuzo MORI, and Hiroshi OHKURA

Department of Applied Physics, Osaka City University, Osaka, Japan 558

Although the ENDOR signal of the F_A(Li) centers in KCl disappears at LHeT, the first-shell ENDOR of the F_A(Li) centers in KBr has been observed even at LHeT[1]. The angular dependence of the quadrupole-splitted ENDOR spectrum on the magnetic field direction is well described by using a form $W_{HFS} = a + b(3\cos^2\theta - 1)$, in which a and b are isotropic and anisotropic hyperfine (hf) interaction constant. This implies that the Li^+ ion is sited on the center symmetry axis at LHeT. The values of a and b at the K nuclei are different depending on the nuclear sites parallel or perpendicular to the symmetry axis. These values at LHeT are quite the same as those observed by Mieher at 90 K[2]. The a-value at the Li^+ ion (6.93 MHz at 1.8 K) is larger than that of 6.80 MHz at 90 K[2]. The q-value is 0.17 MHz for $^{39}K^+$ ion on the symmetry axis. The detailed analysis are described as follows.

(1) In order to explain the inequality relationships found in the a- and b-values, together with consistently explaining the red-shift of the F_{A2} optical absorption band[3], an off density-center wave function is proposed by modifying the GA function as[4]

$$\Psi(|\vec{r}|) = A' \exp\left[-\xi' |(\vec{r}-\delta\vec{r})|/c\right], \qquad (1)$$

where $\vec{r}$ is an electron coordinate, $\delta\vec{r}$ is the displacement of the density-center toward the Li^+ ion; both are measured from the center of the anion vacancy, ξ' and $\delta r/c$ for the F_A(Li) centers in KCl(77K) and KBr(1.8K) are determined as 2.03 and 2.08, and -0.003 and -0.015, respectively. It shows that the sign of δr is negative in the F_A(Li) centers; the fact is quite contrary to the F_A(Na) center.[4] The fact that the value of δr in KCl is less than that in KBr may be relevant to the tunneling motion of the Li^+ ion in KCl.[3]

(2) Temperature dependence of the hf interaction constant at the Li^+ ion, a_{Li}, has been described by using the Doyle and Wolbarst's form which has been proposed for the F centers[5]: This shows that

$$a(T) = a(0) - B_1 \coth(C_1/T) + B_2 \coth(C_2/T), \qquad (2)$$

with $B_1=(da/dp)(\gamma N_0/2)h\nu_0$, $B_2=(h\nu_\ell/K)[-(3g/2K)(da/dr)_{r_0}+(1/4)(d^2a/dr^2)_{r_0}]$, $C_1=(h\nu_0/2k)$, and $C_2=(h\nu_\ell/2k)$, respectively, where γ is the Grüneisen constant, K and g are harmonic and anharmonic constant, ν_0 and ν_ℓ are bulk and localized phonons frequency. Computor fitting of eq.(2) with experimental data above 77 K by Fedotov et al.[5] and below 77 K by us for KCl and KBr gives best-fitting parameters for [KCl;KBr] as ν_0(1/sec)=[4.0×10^{12};2.3×10^{12}], ν_ℓ(1/sec)=[15.4×10^{12};11.2×10^{12}], g/K(1/cm)=[6×10^{9};4×10^{9}], da/dp (Hz/bar)=[130;543], and da/dT(Hz/T)=[10.9×10^{3};10.7×10^{3}], respectively. Comparison of these values with those of the F center shows remarkable differences;[4] (1)g/K values are 100 times as large (2) da/dp value for KBr is 4.6 times as large (3) da/dt values for both crystals are 10 times as large as those of the F centers, respectively.

(3) When temperature is decreased from 77 K to LHeT, microwave-saturation curves of the ESR signal for the F_A(Li) centers in KCl and KBr have shown marked drooping at higher microwave power region[7]. Theoretical curve-fitting for KCl, based on a usual T_1-T_2 model, gives values of T_1 and T_2 as 8 msec and 2×10^{-8} sec, respectively. The latter value is anomalously shorter than that for the F center and F_A(Li) centers at 77 K. Since the ENDOR measurement is relevant to the hole-burning of a spin packet, the width of which is determined by $(1/T_2)$, disappearance of the ENDOR in KCl at LHeT is interpreted in terms of shortened T_2. In case of KBr, theoretical curve fitting of microwave-saturation curve needs one more relaxation process associated with another heat reservoir. The values of T_1' and T_2' associated with this new reservoir are determined as 2 msec and 6 μsec, respectively, at 1.7 K. Based on this fact, one may suggest that the ENDOR is observed through the hole-burning of the T_2' packet.

References: (1) T.Watanabe et al.: J.Phys.Soc.Japan 42 (1977) 1787. (2) R.L.Mieher: Compt.rend. 11 Colloque Ampere (1962) p.699. (3) F.Lüty: "Physics of Color Centers" ed.W.B.Fowler (Acad. Press, N.Y., 1968)chapt.3. (4) H.Ohkura et al.: J.Phys.Soc.Japan 27 (1969) 790. (5) W.T.Doyle and A.B.Wolbarst: J.Phys.Chem.Solids 36 (1975) 549. (6) Yu.V.Fedotov: Sov.Phys. -Solid State 18 (1976) 154. (7) H.Ohkura et al.: J.Phys.Soc.Japan 41 (1976) 707.

ELECTRIC FIELD INDUCED CHANGES IN CONDUCTIVITY OF MgO AT HIGH TEMPERATURE*

R. A. Weeks, E. Sonder, J. C. Pigg and K. F. Kelton
Solid State Division, Oak Ridge National Laboratory
Oak Ridge, Tennessee 37830 USA

Changes in the electrical conductivity of single crystals of MgO, over the temperature range 1000-1400°K due to extended treatment with moderate (1000 V cm^{-1}) electric fields have been measured. Although different samples of MgO have different initial conductivities, the changes produced by the electric fields and resulting currents are qualitatively similar. Treatments for relatively short times, for example, 25 h at 1473°K, causes the temperature dependence to change slightly and the conductivity to decrease either a small amount or as much as a factor of four, depending upon the sample. Results for one sample are shown in Fig. 1 where the heavy solid line represents the initial temperature dependence of the conductivity and where the heavy dashed line represents the conductivity after treatment of anywhere between 20 and approximately 100 h It is very probable that this decrease in conductivity is related to the reduction of trivalent impurities that occurs in comparable times and has been reported previously.[1] If the electric field treatment is continued beyond 100 h the samples become

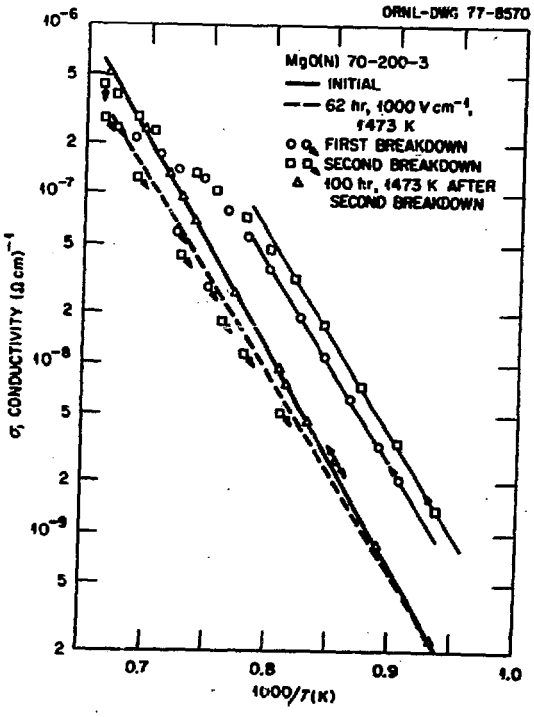

progressively more conducting until catastrophic failure occurs. The electric current passed by such a sample during treatment is often more than two orders of magnitude greater than at the beginning of treatment. If after such a lengthy treatment, but before breakdown has occurred, the sample temperature is lowered and the conductivity is measured during a subsequent increase of temperature, curves as indicated in Fig. 1 by the circles and squares are obtained. It is clear that the electric field treatment has caused changes in the sample that cause its conductivity to be much greater than before treatment. However, the slope of the $\ln \sigma$ vs T^{-1} remains the same, suggesting that the mechanism of current flow is the same after extended treatment as after short treatment (dashed line). As the temperature is raised to within about 150 degrees of the treatment temperature, the conductivity changes anneal out and the conductivity closely approximates that of the sample after short treatment. To regain the conductivity of the virgin sample a rather lengthy anne ' is necessary. As the triangles indicate, a 100 h anneal causes the conductivity of the sample to return to that measured before any electric field treatments were made.

---

*Research sponsored by the Energy Research and Development Administration under contract with Union Carbide Corporation.

1. R. A. Weeks, E. Sonder, J. C. Pigg and K. F. Kelton, J. de Physique 37, Suppl. C7, 411 (1976).

INVITED PAPER

DISLOCATIONS AND MECHANICAL PROPERTIES OF IONIC CRYSTALS

R.W.Whitworth, Department of Physics, University of Birmingham, U.K.

The theme of this review paper will be the importance of the dislocation core.

The flow stress of most simple ionic crystals rises, often steeply, with decreasing temperature and is dependent on the concentration and state of dispersion of small quantities of aleovalent impurities. Related behaviour is observed in measurements of dislocation velocities. At least at low temperatures, dislocation movement seems to be limited by the interaction of dislocations with point obstacles related to the impurities or associated vacancies. There is no evidence that the motion of dislocations unimpeded by impurities has yet been observed.

The theory of dislocation movement through a random array of point obstacles is fairly well established. Subject to certain important assumptions, especially that a single type of point obstacle is dominant, all mechanical experiments lead in principle to a relation between the force which the dislocation exerts on an obstacle and the energy barrier still to be overcome thermally for the dislocation to get past that obstacle. This relation can be compared with theoretical predictions of the shape of the force - distance curve, but such comparisons do not constitute a very critical test of the models. A commonly used model is based on the interaction of a tetragonal defect (e.g. an impurity - vacancy pair) with the elastic field of the dislocation. Unfortunately the strongest part of the interaction occurs at such small distances that the defect should be considered as within the dislocation core where the elastic calculation will break down. In many cases the dislocation will actually shear the impurity - vacancy pair in half, and an edge dislocation can even carry the vacancy away with it.

The theory of crystal defects based on interionic potentials has developed greatly in recent years. Such calculations give the positions of ions in the core and suggest that the Peierls stress is small. It is possible to calculate the binding energies of point defects to sites in the core, and, looking to the future, we can hope for calculations of force - distance curves suitable for comparison with results of mechanical experiments. Will such results be available? Careful experiments are required on ultra-pure crystals doped with the appropriate impurity at $\sim$ 10 ppm levels (to avoid excessive aggregation) and tested right down to liquid helium temperature.

A different way of studying the core of an edge dislocation is by observing its charge. In some structures such as ZnS edge dislocations are inherently charged, dislocations of opposite charge moving in opposite directions under stress. They transport charge during deformation, and deformation is strongly influenced by an applied electric field. In the NaCl structure the usual dislocations on {110} planes are inherently uncharged but may acquire a charge due to jogs or the binding of point defects. As dislocations moving in opposite directions now carry the same sign of charge, the effects are smaller than in ZnS but they can still give useful information.

Experiments involving the oscillation of dislocations at high frequencies can in principle be used to determine the equilibrium charge, and, in suitable cases, could lead to values of the binding energy of a vacancy to the core. Experiments involving motion over larger distances show that edge dislocations can sweep up the vacancies from impurity - vacancy pairs. They can acquire rather high limiting charges, which will surely modify the point-obstacle interaction used to interpret mechanical experiments. The problem is more complex than we often imagine, and is primarily concerned with the structure of the dislocation core.

PRODUCTION OF COLLOIDAL LEAD AND N_2 BY IRRADIATION OF $Pb(N_3)_2$

D.A. Wiegand and W.L. Garrett
Energetic Materials Division, ARRADCOM, Dover, N.J.

$Pb(N_3)_2$ single crystals were subjected to visible, ultraviolet and x-ray irradiation and colloidal Pb formation and N_2 evolution were studied as a function of exposure time, intensity, and temperature. Colloidal Pb was detected by optical extinction[1] and N_2 evolution was monitored by mass spectrometric techniques in high vacuum.[2][3] N_2 evolution was followed continuously during and after irradiation and optical density measurements were made on the same samples in situ between exposures. For most of the conditions of these experiments the only significant types of disorder produced were colloidal Pb and N_2. Because of this simplicity, $Pb(N_3)_2$ is a rather ideal material for the study of the mechanisms of defect production. The results indicate that the formation of colloidal Pb and N_2 are intimately related and part of the same process. Following the initial stage of irradiation in which N_2 is trapped in the lattice, the rate of Pb colloidal formation is proportional to the rate of N_2 evolution. Kinetic studies as a function of wave length and intensity indicate that the rate of defect production is simply related to the rate of energy absorption and the amount of disorder produced. For weakly absorbed radiation (low disorder) the mechanisms of decomposition can be described in terms of simple monomolecular processes. For large amounts of damage the processes may be more complex and optical measurements indicate the presence of metallic Pb.

While the efficiencies of colloidal Pb production and N_2 evolution decrease with decreasing temperature, studies of colloidal Pb production at very low temperatures (~12°K) indicate that this process is not diffusion limited. Thermal stability of the disorder was also investigated and optical bleaching effects were observed.

When samples which have been irradiated in high vacuum are exposed to air there is a very marked decrease in the optical extinction due to Pb colloids, thus indicating a high reactivity of this form of Pb. Optical measurements as a function of polarization for orthorhombic $Pb(N_3)_2$ indicate that the optical extinction is primarily due to absorption.

REFERENCES

1. D.A. Wiegand Phys. Rev. 10, 1244 (1974)
2. W.L. Garrett, Ph.D. Thesis, University of Delaware (1972)
3. W.L. Garrett, P.L. Marinkas, F.J. Owens and D.A. Wiegand "Energetic Materials", Vol. 1, "Physics and Chemistry of Inorganic Azides, Chapter 7, H.D. Fair and R.F. Walker, Editors, Plenum Press, New York (1977)

INVITED PAPER

PHOTOCHEMISTRY OF F-CENTER FORMATION IN SIMPLE HALIDE CRYSTALS

R.T. Williams
Naval Research Laboratory
Washington, D.C. 20375

A review of experimental and theoretical progress on the question of how electronic excitation of halide crystals leads to the formation of F centers will be given, with emphasis on developments since about 1973. Several related mechanisms wherein the higher electronic states of self-trapped excitons are unstable against F-H pair formation (without direct involvement of the repulsive STE ground state) were first presented in 1973-74. These models are becoming rather widely accepted now as containing at least the general outline of the defect formation process. Even so, questions as fundamental as the identities of the "defect-forming" exciton states remain unresolved. The array of problems associated with understanding the relaxation dynamics and in detailing specific paths taken among the reaction coordinates makes this area both challenging and timely with regard to current activity in solid-state and molecular photochemistry. The same basic mechanism of defect formation seems likely to be operative in alkaline earth halides as well as in the alkali halides, and quite probably in still other materials.

Experiments in the picosecond time range will be discussed, as will other recent results with nanosecond excitation by laser and/or electron pulse. Data to be reviewed will include primary defect yields, temperature dependence, and limits on formation times. Experiments in

excited-state EPR which bear on defect formation processes will be reviewed. Concepts of level correlations, relaxation rates, and the adiabatic approximation are to be addressed briefly with regard to F-center formation. Recent calculations and refinements of the models will be discussed.

SHORT-PULSE LASER STUDIES OF EXCITON RELAXATION AND F-CENTER PRODUCTION IN ALKALI HALIDES

R. T. Williams, J. N. Bradford, and W. L. Faust
Naval Research Laboratory
Washington, D. C. 20375

Laser pulses of about 30 picoseconds duration have been employed to generate electron-hole pairs in KCl and to probe the resulting onset of F-center absorption.[1] The present paper will address refinements in techniques of picosecond spectroscopy of defects in solids and the extension of these experiments to other electronic systems in alkali halides.

The time required to populate the lowest triplet level of the self-trapped exciton in NaCl after electron-hole pair generation at T ≈ 15 K is found to be less than 10 psec. This is despite a 2-eV energy gap between the first and second STE excited states in NaCl. The fraction of initially produced electron-hole pairs reaching the lowest STE triplet state is about 0.19 in NaCl as measured by optical absorption.

Apparatus has been developed for measuring absolute yields of absorbing centers very shortly (e.g. 30 psec) after e-h pair generation. In this way we are fairly assured of counting most primary products prior to back-reactions even at high temperature. In the accompanying figure, the number of F centers produced per electron-hole pair excited in KCl is plotted versus temperature from 12 to 880 K, where the F absorption is measured about 46 psec after e-h pair generation. Experimental tests show that pre-existing vacancies make a negligible contribution (in fact a slight negative contribution!) to the early F-center absorption in measurements under these conditions. The quantum yield increases with temperature, reaching about 0.8 F centers per e-h pair at 880 K, and apparently extrapolating toward unity near the melting point of KCl.

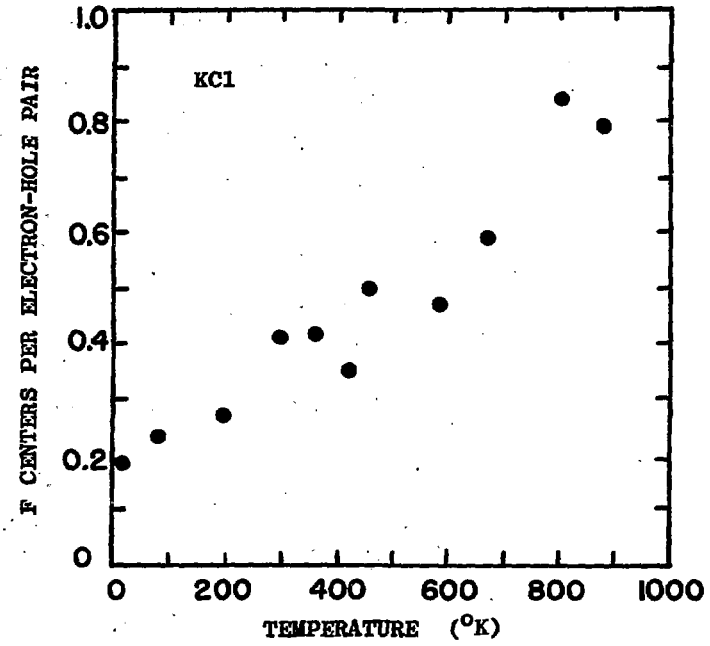

As a natural extension of these experiments we have heated KCl beyond its melting point and looked for uv-induced absorption of green light in liquid KCl. Fairly strong transient absorption of 532-nm light following uv excitation of the molten KCl was found. Spectral characteristics of this absorption are not yet known, but it is intriguing to speculate on the possibility that local sites resembling F centers for times of at least 100 picoseconds may be photoinduced in normally-transparent KCl liquid by "band-gap" excitation.

1. J. N. Bradford, R. T. Williams, and W. L. Faust, Phys. Rev. Letters 35, 300 (1975).

A SEARCH FOR INFRARED ABSORPTION BY SELF-TRAPPED EXCITONS IN SODIUM CHLORIDE

R. T. Williams, M. N. Kabler, and I. Schneider
Naval Research Laboratory
Washington, D. C. 20375

Transient absorption spectroscopy has provided detailed information concerning optical transitions originating in the lowest triplet state of the self-trapped exciton (STE) in alkali halides. The lowest-energy transitions were described as a Rydberg-like sequence of electron excitations terminating in the conduction band, with the main peak for most alkali halides occurring at an energy roughly 1/2 eV below that of the F band.[1] Prompted by recent theoretical work, we have extended our earlier measurements on NaCl farther into the infrared. We find no additional transitions between 0.1 eV and the onset of the 2.0-eV band. Thus the original concept of Rydberg-like states remains reasonable and the theoretical prediction[2] of a lower energy transition is not borne out.

A double-beam transient absorption spectrometer was used to compare simultaneously absorption in the range 0.1 - 2.1 eV with absorption in the 2.0-eV STE band following electron pulse excitation. The figure shows the spectrum just after the pulse, where the points were measured using InSb and Ge:Hg infrared detectors and the solid curve was measured in Ref. 1 by photoelectric scanning. The experiment was capable of detecting transient absorption as small as 2 % of that at 2.0 eV throughout the 1 - 12 μm spectrum, and within this limit there is no STE transition at lower energy than the 2.0-eV band. The weak band at 0.32 eV has the wrong lifetime to be a transition originating in the STE triplet, and is probably due to a triplet state of the F' center.

The first theoretical calculations of STE energy levels were carried out by Stoneham and others,[2,3] treating hole

excitations by the Hartree-Fock approximation and electron excitations by a pseudopotential method. While these calculations gave several transitions in the observed range, they predicted the lowest $\sigma_g \rightarrow \sigma_u$ excitation ($A_{1g} \rightarrow B_{3u}$ in the notation of Ref. 2) to be at significantly lower energy than the observed transitions. In NaCl the calculation placed this transition in the 0.7 - 1.1 eV range, whereas the earlier measurements had found no absorption in the range from 0.5 eV (the measurement limit) to the onset of the 2-eV band.[1] The present data reinforce the earlier measurements and effectively rule out such a transition. It seems reasonable to conclude that the calculated 0.7 - 1.1 eV transition actually falls within the strong 2.0-eV band. Polarization data have indicated that $\sigma_g \rightarrow \pi_u$ electron excitations also contribute to this band.[4] Thus the absorption below 2.8 eV is complex, with σ and π transitions evidently overlapping.

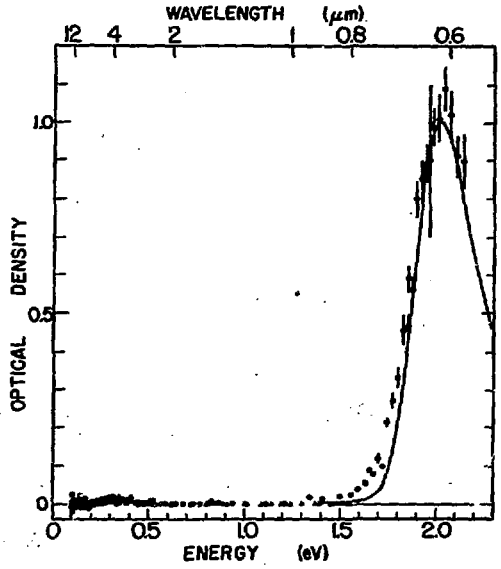

1. R. T. Williams and M. N. Kabler, Phys. Rev. B9, 1897 (1974).
2. K. S. Song, A. M. Stoneham, and A. H. Harker, J. Phys. C 8, 1125 (1975).
3. A. M. Stoneham, J. Phys. C 7, 2476 (1974).
4. R. T. Williams, Phys. Rev. Lett. 36, 529 (1976).

ELECTRON PULSE RADIOLYSIS OF MAGNESIUM FLUORIDE

R.T. Williams, C.L. Marquardt
J.W. Williams, and M.N. Kabler
Naval Research Laboratory
Washington, D.C. 20375

Time-resolved measurements of optical absorption and emission in pure MgF_2 have been made using electron pulse excitation. At 10 K an absorption band having its peak at 275 nm is produced by the electron pulse and subsequently decays with time constants of 6.4 and 0.75 msec. Both the 275-nm absorption and a luminescence band at 385 nm are attributed to self-trapped excitons. Approximately one STE with assumed unit oscillator strength is formed per 28 eV deposited by the electron pulse. Thermal quenching of both the 275-nm absorption and 385-nm luminescence becomes significant above 60 K, and transient absorption with a spectrum more nearly resembling the F band becomes dominant at temperatures above 170K. This component of the absorption grows stronger and decays faster as temperature is raised, but there is no corresponding luminescence. It is attributed to F centers, most of which apparently are annihilated by the ejected interstitial fluorine atoms within a few hundred microseconds. The initial transient absorption (represented by points) and stable F-center absorption (continuous curve) are compared in Fig. 1 at three temperatures on a normalized optical density scale.

It is interesting to compare STE and F-center transition energies in CaF_2, SrF_2, and BaF_2[1] with the corresponding transition energies in MgF_2. Figure 2 plots energies of the band peaks as a function of (crystal volume per atom)$^{1/3}$ or of average nearest-neighbor distance ($\overline{R_{nn}}$). Both parameters

are uniquely related to the lattice constant in the fluorites, but there is some ambiguity in placing MgF_2 on this plot, as represented by the uncertainty bars. The symbols correspond to electron (●) and hole (○) transitions of the STE, and to transitions of stable F (▲), H(△), and V_k (□) centers. Extrapolation from the fluorites suggests that in MgF_2 the principal electron and hole transitions effectively coincide for the STE and also for F, H, and V_k centers.

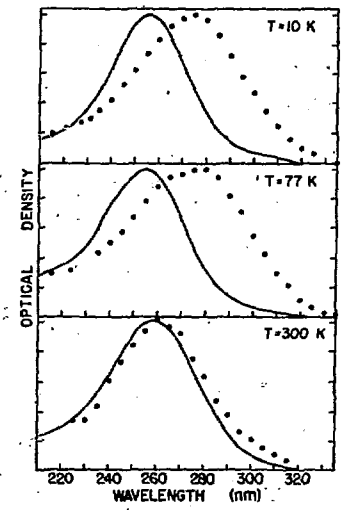

Fig. 1

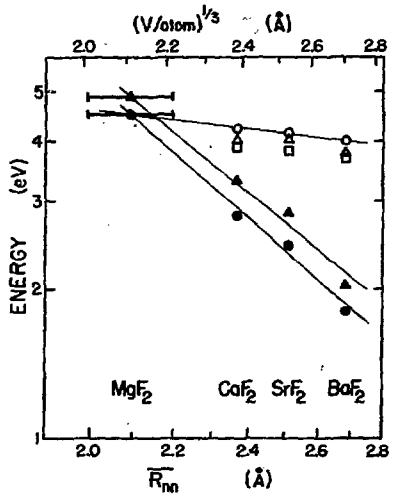

Fig. 2

1. R.T. Williams, M.N. Kabler, W. Hayes, and J.P. Stott, Phys. Rev. B14, 725 (1976).

ELECTRONIC STRUCTURE OF THE F^+ CENTER IN ALKALINE EARTH OXIDES*

T. M. Wilson† and R. F. Wood
Solid State Division, Oak Ridge National Laboratory
Oak Ridge, Tennessee 37830, U.S.A.

We have calculated the absorption and emission states of the F^+ center in MgO, CaO and SrO within the framework of a model developed previously for F and U centers in the alkali halides and subsequently modified for the F center in the alkaline earth oxides. The model emphasizes the importance of (a) electronic structure on the ions neighboring the defect, (b) electronic and ionic polarization of the lattice, and (c) lattice distortion and its effects on the energy levels and wave functions of the defect. When an electron of the center is at a large distance from the negative ion vacancy, the model Hamiltonian goes over into an effective-mass form. The energy at the bottom of the conduction band of the perfect crystal then enters into the problem. This energy is composed of two terms one of which represents the energy ϵ_{HF} of the bottom of the conduction band in the Hartree-Fock approximation and the other of which gives a polarization-correlation contribution to the energy. In the absence of reliable band calculations, ϵ_{HF} may be taken as an adjustable parameter. However, in the alkaline earth oxides it seems reasonable to require that ϵ_{HF} be the same for both the F and F^+ centers. We have found that straightforward application of our model to the F^+ center using the values of ϵ_{HF} found for the F center gives absorption energies which are too high by approximately 2 eV in MgO, CaO and SrO. Our analysis of this difficulty has convinced us that the basic assumptions of the model are inadequate for the F^+ center in the alkaline earth oxides. More specifically, it is the description of the hole left behind during the electronic transition that is at fault. The model assumes that the electronic polarization of the lattice due to the vacancy can be formulated in terms of the induced dipole moments on the neighboring ions. We believe that this assumption breaks down in the case of the F^+ center and that one must go to a molecular orbital description of the hole created during the electronic transition.

Although we now believe our original model to be too inflexible to describe all aspects of the F^+ center, it is still possible to reformulate it in such a way that useful information can be extracted from it. This involves redefining ϵ_{HF} in such a manner that it includes approximately the energy gained in the formation of the molecular orbital. Results of calculations with this modification of the model will be given and compared to the appropriate experimental data. Progress in the incorporation of a molecular-orbital description of the hole into the model will be described.

---

*Research sponsored by ERDA under contract with Union Carbide Corporation.

†Oklahoma State University, Stillwater, Oklahoma 74074.

EXCITON RELAXATION IN AgBr STUDIED BY RESONANT RAMAN SCATTERING

J. Windscheif, H. Stolz and W. von der Osten,
Fachbereich Naturwissenschaften I, Experimentalphysik,
Gesamthochschule Paderborn, W.Germany

Laser excitation in the vicinity of the indirect Γ-L_3' exciton absorption at low temperature was recently found to lead to selectively enhanced narrow multiphonon Raman scattering [1]. The strongest resonant phonons are TO- and LA-pairs with opposite wavevectors near the L-point of the Brillouin zone. In particular, the temperature dependence of the scattered intensity was qualitatively interpreted assuming damping by long wavelength acoustic phonons.

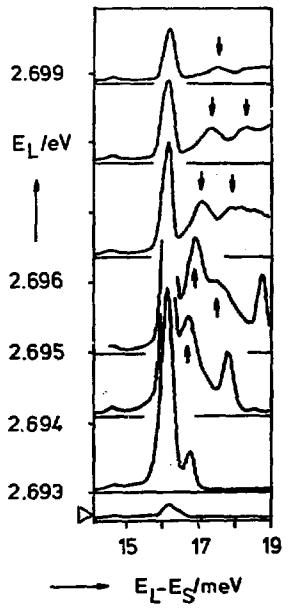

Fig. 1 Resonant Raman spectra of AgBr at 1.8K for different incident laser energies E_L. The intensity is plotted vs. the Raman energy shift $E_L - E_S$. The baseline of each spectrum is arranged along the ordinate corresponding to different incident laser energies E_L. The strongest line at 16,2 meV corresponds to the 2 TO(L) process (see text).

Using a tunable dye laser we measured the Raman spectra for different incident photon energies

E_L in the region of the indirect absorption. Besides the two-phonon modes a number of additional scattering peaks were found. They are due to various relaxation processes of the 1s exciton acting as intermediate state of the two-phonon process [2]. From analyzing the Raman energy shifts and intensities the different exciton relaxation processes are found to have a twofold influence on the Raman spectra:

1. They give rise to additional multiphonon scattering peaks that are observed in the spectra.
2. Through different exciton-phonon interactions they determine the lifetime of the 1s exciton, i.e. the intensity of the scattering lines.

As one example, in fig.1 dispersive phonon modes are shown (arrows) that occur besides the 2TO(L) line, with their Raman energy shifts (E_L-E_S) depending on E_L. These are attributed to relaxation processes involving LA phonons near the zone center. The quantitative analysis of these spectra enables us to obtain directly the average effective mass of the 1s indirect exciton to be 1.5 m_o (m_o = electron mass).

For higher excitation energies the exciton lifetime is predominantly determined by intraband scattering via LO phonons, as seen by dramatic changes in line shape for the free exciton emission as function of E_L. Finally, the energy dependence of the 2 TO(L) scattered intensity (see fig.1) suggests reduction of the exciton lifetime by another effective scattering mechanism the nature of which is still under study.

[1] VON DER OSTEN, W., WEBER, J., and SCHAACK, G., Solid State Commun. 15, 1561 (1974)

[2] WEBER, J., and VON DER OSTEN, W., Z.Physik B 24, 343 (1976)

LUMINESCENCE SITES FOR LiF DOSIMETRY

M C Wintersgill and P D Townsend
University of Sussex Brighton BN1 9QH England

LiF:Mg:Ti forms the basis of the familiar radiation dosimeter material but it is clear that the system is complex with a wide range of alternative impurity and intrinsic defect complexes.[1] In particular the titanium (Ti^{4+}) site requires stabilization.

Oxygen substituted on halogen lattice sites has been suggested [2] as the most likely impurity and this has been confirmed by chemically "clean" doping using an ion accelarator.[3] Changes in the emission spectrum and radiation efficiency are in accord with a titanium-oxygen complex as the luminescence site. The spectra of LiF samples from different suppliers are not the same even though the Mg and Ti doping levels are similar. Some of the material shows a thermoluminescence response which is sensitive to the radiation flux (i.e. LET) and in extreme cases a sensitization of a factor of 10^3 has been recorded. A model for this effect will be discussed.

1. Fairchild, R.G., Mattern, P.L., Lengweiler, K., and Levy, P.W. 1974 IEEE trans. Nucl. Sci. 21 366-372

2. Davies, J.J., 1974 J. Phys. C 7 599

3. Wintersgill, M.C., Townsend, P.D., and Cusso-Perez, F., 1977 J. de Physique C-7 123-126

LATTICE DEFECT EQUILIBRIUM IN KCl:Eu

J. B. Wolfenstine and T. G. Stoebe
University of Washington, Seattle

Several studies in KCl:Eu have indicated the presence of Eu^{+}, Eu^{++} and Eu^{+++} ions in this material, with predominant specie at room temperature being Eu^{++} present in the form of Eu^{++}-vacancy dipoles. Eu^{++} may be investigated using its characteristic ultraviolet absorption bands occurring near 330 nm and 240 nm. At low temperatures these absorption bands may be resolved into a series of lines, the most intense being at 343 and 243 nm. Equilibrium lattice defect configurations and divalent (or trivalent) ion concentrations may also be investigated using ionic conductivity measurements.

A study of lattice defect equilibria in Harshaw-grown KCl:Eu was undertaken using the techniques noted above. Polarographic analysis of Eu impurity content was obtained from a variety of samples near the cone and near the heel of a large KCl:Eu single crystal ingot (1). Optical absorption and ionic conductivity samples were taken immediately adjacent to these polarographic analysis samples for comparative purposes.

Ionic conductivity was determined using an A.C. method with a Wayne-Kerr bridge on 5 samples each taken from 4 different regions containing Eu impurity contents between 30 and 60 ppm. Intrinsic ionic conductivity plots were also determined using pure Harshaw material. Eu-ion concentrations, interpreted as Eu^{++}, were then determined from the position of the "knee" in the conductivity plots. Optical absorption measurements were undertaken using a Cary 14 spectrometer at room temperature using another 5 samples from the same 4 regions of the original crystal. The optical absorption coefficients, α, were determined at 343 and 243 nm and compared with the Eu^{++} contents determined using ionic conductivity. These results indicate a linear relationship between these two measurements such that

$$\text{Mole \% } Eu^{++} = 4.4 \times 10^{-4}\ \alpha. \qquad (1)$$

This result may be compared to the polarographic analyses of adjacent samples. The comparison agrees to within about ±10% in three of the locations measured but varies by 25% at the fourth. The reasons for this discrepancy are not clear. This result may also be compared to results of Sill and Martin (2) who used atomic absorption spectroscopy to measure Eu impurity content. Compared to the optical absorption coefficient of the 243 nm band, Sill and Martin obtained a proportionality factor that was a factor of 4 higher than that in eq. (1). This may indicate the presence of additional Eu in the crystals, present in a state of agglomeration, which would not be measured using ionic conduction. This possibility is being investigated further using other lattice defect investigative techniques.

1) Honeywell, Inc., Monthly Progress Report No. 8, AFML Contract No. F33615-75-C-5110, Sept. 10, 1975.

2) E. L. Sill and J. J. Martin, Mat. Res. Bull. 12, 127 (1977).

TEMPERATURE AND RADIATION INDUCED PROCESSES IN SULPHATE DOPED ALKALI HALIDES

V.P.Zeikats
Latvian State University, Riga, USSR

Defect complexes consisting of the divalent anion SO_4^{2-} associated with a net charge compensating interstitial Ag_{int}^{+}[1] or Pb^{2+} on cation site[2] in KCl and KBr crystals are treated under X-rays and temperature by means of infrared and UV absorption.

If crystals containing such defects are subjected to radiation at room temperature the following processes occur:

1. Complexes $SO_4^{2-} \cdot Ag_{int}^{+}$ as well as $SO_4^{2-} \cdot Pb^{2+}$ add an extra electron and reduce the charge state of the metal to that of Ag° or Pb^{+} respectively. This removes the splitting of degenerate stretching mode of the sulphate[3]. Immediately after irradiation infrared spectrum exibits one peak associated with the absorption of sulphate anion bound to a Ag_{int}° or Pb^{+}. This peak is shifted from the corresponding band for the "free" (unassociated) ion SO_4^{2-} on T_d symmetry.

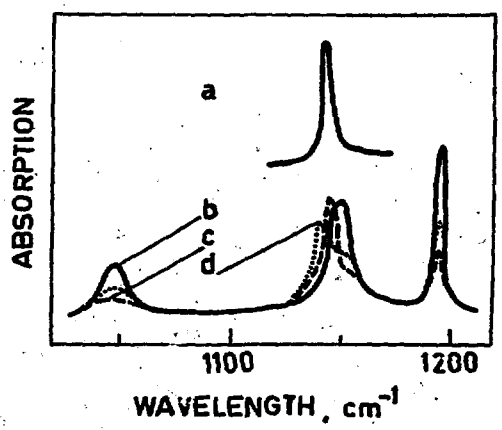

Figure 1 shows infrared absorption spectra of doped KCl crystal at RT:

a) —— unassociated sulphate in T_d symmetry;
b) —— complex $SO_4^{2-} \cdot Pb^{2+}$
c) – – after 20 min irradiation of b);
d) ····· after 24 h annealing of c).

2. During subsequent annealing of the X-irradiated crystals two processes are involved: a) the releasing extra electron from the complexes $SO_4^{2-} \cdot Ag^{\circ}_{int}$ or $SO_4^{2-} \cdot Pb^{+}$ and b) dissociation of these complexes giving rise to unassociated SO_4^{2-}. On further annealing (or heating) the crystals, dissociated complexes recover again as $SO_4^{2-} \cdot Ag^{+}_{int}$ and $SO_4^{2-} \cdot Pb^{2+}$.

3. Prolonged irradiation ($t_{irr} > 3$ h) leads to another complex - $SO_4^{2-} \cdot V_a^{+}$ formation. Detailed experiments on the mechanism and kinetics of the latest species are still in progress.

References

1. J.R.Zakis, I.K.Schmit, Sov.Phys.Sol., 17, 950 (1975).
2. J.C.Decius, E.H.Coker and G.L.Brenna, Spectrochim. Acta, 19, 1281 (1963).
3. J.R.Zakis and V.P.Zeikats, in "Colour centres in Ionic Crystals", Reading, England, H160 (1971).

DIFFUSION OF IMPURITIES IN KI 1% KCl SINGLE CRYSTALS*

S.C.Zilio, D.G.Pinatti, M.Siu Li, and Milton de Souza

Instituto de Física e Química de S.Carlos,
Universidade de São Paulo
Caixa Postal - 369
13560 - São Carlos, SP, Brasil

The dielectric relaxation due to impurities that give rise to defects with electric dipole moment, can be conveniently measured by the ITC technique. The impurities studied in KI and KI 1% KCl crystals were Ca^{++}, Cu^{+} and Eu^{++}. In KI one single relaxation peak was found for all three impurities. In the KI 1% KCl crystals two well defined peaks were found at distinct temperatures. Figure 1 illustrates this behavior for KI 1% KCl doped with Cu^{+}. The same general features are found in KI 1% KCl doped with Ca^{++} as figure 2 shows. The ITC spectra of figures 1 and 2 were taken after quenching of samples from temperatures near the fusion point. The lower temperature peak is attributed to an impurity ion having one Cl^{-} in its closest neighborhood. The higher temperature peak is due to the reorientation of impurity dipole having only I^{-} in its neighborhood but with a smaller lattice parameter than pure KI. In the case of divalent impurity this effect has already been observed (1). With the Cu^{+} impurity the smaller lattice parameter of KI 1% KCl crystals

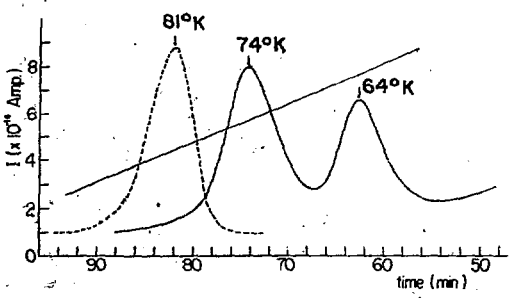

Fig.1- Single relaxation ITC peaks due to Ca^{++} ion in KI:KCl single crystals. The area of the two peaks are in 1 to 1 proportion.

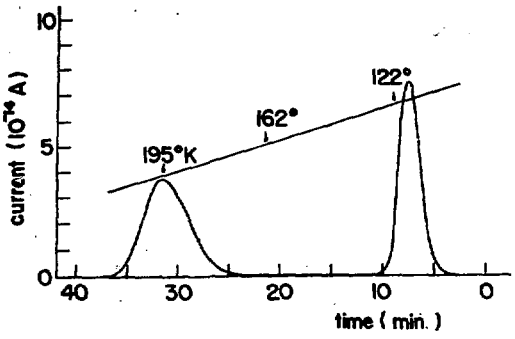

Fig.2- Full line- Depolarization of KI 1% KCl Cu^+ crystal. Dotted curve - Depolarization with same temperature rate of KI:Cu^+ sample. Both polarizations were done in order to have full saturation. Straight line is the sample temperature.

compared with that of the pure KI (a long range effect of the Cl^- ions) causes a decrease in the activation energy for the Cu^+ ion to jump between its off center positions. The lower temperature peak in both cases was found to be in a proportion higher than expected from a random distribution of the impurities in the high temperature of the quenching process. This suggests that Cl^- ions act as capture centers for those ions that diffuse through the crystal. The misfit in radius of the Cl^- ion relative to the I^- ion generates a driving force for diffusion of elastic nature. The aggregation of the impurities was followed and found to be strongly affected by the presence of the Cl^- ion in KI. In a first stage both peaks decrease as a function of the time in a fixed temperature , the lower temperature one decreasing faster. In a second stage the lower temperature peak increases and the other decreases. In a third stage both peaks decrease. The aggregation kinetics of the Ca^{++} ion was found to be the same in KCl 2% KI as in pure KCl.

* Work supported by Fundação de Amparo à Pesquisa do Estado de São Paulo (FAPESP).

CALCULATED PRESSURE SHIFTS OF F-CENTER HYPERFINE INTERACTION PARAMETERS IN ALKALI CHLORIDES

R.D. Zwicker
Department of Physics,
University of the Witwatersrand,
Johannesburg, South Africa.

We have calculated the change in the F-center shell I hyperfine interaction (hfi) constants with pressure of KCℓ, NaCℓ and LiCℓ. The calculation was based on a pseudopotential model[1] similar to that of Bartram, Stoneham and Gash[2], but modified for compatability with a variational solution and expanded to include interactions of the F-electron with ionic p-states. Electronic polarization was included by means of an r-dependent polarization potential suggested by Fowler[3] and used with modifications by Opik and Wood[4].

The results are expressed in terms of the dimensionless quantity

$$\theta = -\frac{a}{3\rho_I}\frac{d\rho_I}{da} = \frac{B}{a_I}\frac{da_I}{dP}$$

where a is the lattice spacing, ρ_I is the shell I spin density, P is pressure, a_I is the contact hfi parameter, and the effective local modulus B is approximated by half the bulk modulus for these materials. We obtained for θ values of 0.69, 0.47, and -0.17 for KCℓ, NaCℓ and LiCℓ, respectively. Experimental values[5] are available for KCℓ (0.54) and LiCℓ (-0.06) only.

Our results are interpreted in terms of the increasing importance of the indirect overlap terms[6] with increasing ion-size ratio R-/R+. These terms result from the requirement of orthogonality of core states on neighbouring ions, and their importance in interpreting experimental hfi data was first pointed out by Wood[6]. The results obtained here verify our previous conclusion[7] that the indirect overlap terms can actually dominate the hfi pressure shifts, as in the case of LiCℓ.

References

1. R.D. Zwicker, Phys. Rev. B15 (To be published)

2. R.H. Bartram, A.M. Stoneham, and Philip Gash, Phys. Rev. 176, 1014 (1968).

3. W.B. Fowler, Phys. Rev. 151, 657 (1966).

4. U. Opik and R.F. Wood, Phys. Rev. 179, 772 (1969) ; R.F. Wood and U. Opik, Phys. Rev. 179, 783 (1969).

5. A.B. Wolbarst, J. Phys. Chem. Solids 33, 2013 (1972).

6. R.F. Wood, Phys. Status Solidi 42, 849 (1970).

7. A.B. Wolbarst and R.D. Zwicker, Phys. Rev. Lett. 37, 1487 (1976).

AUTHOR INDEX

Ābolinš, J. J., 286
Abraham, M. M., 48, 86, 306
Adler, D., 1
Adrian, F. J., 207
Aegerter, M. A., 126, 336, 455
Aguilar, M., 3, 81
Agulló-López, F., 3, 270, 331
Akhvlediani, Z. G., 5
Albuquerque, A. R., 7
Alcalá, R., 8
Al-Chalabi, A. O. H., 10
Alexopoulos, K., 11
Alvarez Rivas, J. L., 174, 209
Andeen, C., 13, 440
Anderson, Ch., 15
Anderson, M. P., 319
Arizmendi, L., 331
Arnold, G. W., 17
Asami, K., 19
Atalla, S. R., 117
Atobe, K., 21, 321
d'Aubigné, Y. M., 46, 100
Augustov, P. A., 389

Badawy, Z. I., 217
Badoz, J., 262
Badr, Y. A., 217
Balasubramanyam, K., 369, 371, 373
Baldacchini, G., 23, 25
Barbezat, S., 107
Barklie, R. C., 27
Barnard, R. S., 187
Bartram, R. H., 28
Basso, H. C., 71
Bates, J. B., 30, 32
Batygov, S. Kh., 34
Baumanis, E. A., 286
Beamonte, J., 8
Beigang, R., 35
Belzner, V., 155
Benci, S., 37
Benedek, G., 39
Bénière, F., 40
Betz, E., 234
Bhattacharyya, B. D., 41, 43
Billardon, M., 44
Block, D., 46
Boatner, L. A., 350
Boldu, J. L., 48
Boswarva, I. M., 102
Bowen, H. K., 338
Bradford, J. N., 471
Brendecke, H., 50
Brower, K. L., 249
Buchanan, M., 52
Bücher, M., 155
Buisson, J. P., 44, 54
Buzaré, J. Y., 56

Cachard, A., 434
Cain, L. S., 58
Campos, L. L., 297
Capelletti, R., 59, 60, 62, 64
Casalboni, M., 66, 68
Castaing, J., 70
Castro, J. C., 71
Catlow, C. R. A., 73, 75
Cava, R. J., 77
Cetica, M., 348
Chan, N.-H., 79
Chandler, P. J., 81
Chapelle, J. P., 54, 364
Chassagne, G., 110, 442
Châtelain, A., 350
Chaya, H., 83
Chen, W. K., 236
Chen, Y., 48, 85, 86, 292, 306
Chiarotti, G., 66
Chowdari, B. V. R., 88, 90
Clark, C. D., 92
Coatsworth, L. L., 94, 96
Cohen, J. B., 432
Corish, J., 73
Crawford, J. H., Jr., 98, 182, 258
Crummett, W. P., 312

Dang, Le Si, 100
Datta, S., 102
Dekle, J. M., 28
Delbecq, C. J., 104, 105
Delgado, A., 174
Deshpande, P. W., 211

Dexter, D. L., 105
Diaine, Ch., 106
Dienes, G. J., 242
Diller, K. M., 73
Dubois, C., 107
Dupin, J. P., 434
Dupuy, J., 106
Duran, J., 109, 262
Durand, D., 110
DuVarney, R. C., 112

Eilebrecht, B., 113
Ekmanis, Y. A., 115
Elango, A. A., 273
El-Sharkawy, A. A., 117
Eng, G., 118
Engstrom, H., 119
Era, K., 121
Etsell, T. H., 124
Evans, B. D., 123, 404

Faber, J., Jr., 124
Fabrikant, I., 247
Falco, L., 126
Farge, Y., 324, 393
Faust, W. L., 471
Fayet, J. C., 56
Feldmane, E. E., 128
Felix, F. W., 130
Fermi, F., 59, 60
Fieschi, R., 59
Fontanella, J., 13, 440
Fort, A. J., 270
Foster, D., 132, 256
Fou, C. M., 301
Franz, W. T., 301
Freiberg, A., 134
Friauf, R. J., 136, 138, 140
Fujii, A., 418
Fujita, T., 418
Fujiwara, M., 428
Fukuda, A., 100, 282
Fuller, G. E., 142
Funke, K., 144

Gaines, A. M., 333
Gainotti, A., 62
Garrett, W. L., 467
Garrison, A. K., 112
Gelfert, G., 113
Georgiev, M., 146, 148
Ghomi, M., 54
Gindina, R. I., 273
Giorgianni, U., 149
Gisclon, J. L., 106
Goode, D. H., 151
Goovaerts, E., 153
Granéli, B., 130
Granzer, F., 155
Grassano, U. M., 23, 66, 68
Grasse, D., 408
Griffith, J., 319
Guermazi, M., 434
Guillot, G., 156, 284, 317

Hagihara, T., 428
Halliburton, L. E., 158
Halperin, A., 362
Hara, H., 315
Haridoss, S., 340
Hariharan, K., 340
Harker, A. H., 203, 260
Hartmanová, M., 453
Hattori, T., 160
Haven, Y., 162
Hayashi, K., 304
Hayashi, T., 163
Hayes, W., 165
Heder, G., 313
Hempel, J. C., 184
Henderson, B., 27, 166
Heuer, A. H., 168
Higuchi, E., 230
Hilber, H. C., 170
Hinks, D., 412
Hirai, M., 414, 416
Hirotsu, Y., 376
Hitterman, R. L., 124
Hobbs, L. W., 172, 187
Hodgson, E. R., 174
Hoentzsch, Chr., 176
Hogarth, C. A., 178
Holland, U., 180, 457
Holmberg, G. E., 182, 184
Holt, D. B., 102
Honig, J. M., 255

Horan, S. E., 185
Howitt, D. G., 187

Iida, T., 189, 195, 336
Ikeya, M., 191, 193
Imanaka, K., 189, 195
Ioan, A., 197, 199
Iri, T., 201
Ishiguro, M., 19
Ishii, T., 121
Isotani, S., 7
Ito, T., 201
Itoh, M., 222
Itoh, N., 203, 205, 377
Iwata, M., 121

Jaanson, N. A., 273
Jacobs, P. W. M., 73, 94, 96
James, R., 75
Jaque, F., 3, 270, 331
Jette, A. N., 207
Jiménez de Castro, M., 209
Johnston, R. L., 13
Joshi, R. V., 211
Julian, M. D., 213

Kabler, M. N., 215, 473, 475
Kamel, R., 217
Kamikawa, T., 219
Kamishina, Y., 94, 96
Kaneda, T., 220
Kanev, S., 146
Kan'no, K., 222
Kanzaki, H., 224, 244
Kao, K.-J., 138
Kappers, L. A., 158
Kapphan, S., 226, 228
Kawano, K., 230
Kayanuma, Y., 232, 244
Kazumata, Y., 315
Kelton, K. F., 463
Kenawy, M. A., 117
Kessler, A., 234
Kim, K. K., 236, 238
Kingery, W. D., 240
Kirsh, Y., 251
Klaffky, R. W., 242
Kojima, T., 310
Kondo, Y., 232, 244
Koppitz, J., 226, 228
Kos, H.-J., 246
Koshino, S., 163
Kostopoulos, D., 40
Koteles, E. S., 457
Kotomin, E., 247
Krefft, G. B., 249
Kristianpoller, N., 251, 354
Krumins, V., 253
Kuwamoto, H., 255
Kuzuba, T., 121

Lagendijk, A., 153, 387, 451
Laskar, A. L., 132, 256
Lazarus, D., 118
Lee, K. H., 98, 182, 258, 446
Lefrant, S., 44, 54, 260
Lemoyne, D., 262
Levy, P. W., 142, 333
Lilley, E., 264, 266, 430
Litfin, G., 35
Locatelli, M., 268
López, F. J., 270
Lottici, P. P., 64
Luntz, M., 272
Lushchik, A. Ch., 273
Lushchik, Ch. B., 273
Lüty, F., 25, 180, 213, 327, 329, 379, 435

Maaroos, A. A., 273
Mackrodt, W. C., 406
Manfredi, M., 37
Manning, H., 58
Manson, N. B., 275
Marichy, M., 434
Markham, J. J. 277
Marquardt, C. L., 475
Marshall, S. A., 279
Marshall, T., 279
Masunaga, S., 19
Matsumoto, H., 304
Matsuoka, M., 280
Matsushima, A., 282
McClure, D. S., 394
Mealing, W., 256
Mercier, E., 284, 317

Miki, T., 191, 193
Millar, M. A., 96
Millers, D. K., 286
Mitchell, T. E., 168, 187
Mitsuishi, A., 160
Modine, F. A., 288, 400
Molesini, G., 348
Mollenauer, L. F., 290
Monague, C. A., 398
Mondio, G., 149
Monty, C., 107
Moodenbaugh, A. R., 292
Morato, S. P., 294
Mori, Y., 280, 295, 461
Moridi, G. R., 178
Muccillo, R., 297, 325
Mueller, M. H., 124
Mulazzi, E., 39, 298
Müller, M., 130
Mundy, J. N., 236
Muramatsu, S., 367
Murch, G. E., 299
Murray, R. B., 272, 301
Murti, Y. V. G. S., 303
Myzina, V. A., 34

Nagasaka, S., 219
Nagornyi, A., 420
Nakagawa, H., 304
Nakagawa, M., 21, 321
Nakai, Y., 222, 438
Nakamura, K., 438
Nakata, R., 230
Nambi, K. S. V., 294, 325
Narayan, J., 86, 306, 308
Nasu, K., 310
Nicklow, R. M., 312
Niklas, J. R., 313
Nink, R., 246
Nishi, M., 315, 418
Norgett, M. J., 73
Nouailhat, A., 156, 284, 317
Nowick, A. S., 238, 319
Nurakhmetov, T. N., 273

O'Donnell, K. P., 27
Ohata, T., 163
Ohkura, H., 189, 195, 280, 295, 461
Okada, M., 21, 321
Okada, T., 428
Okuno, E., 60
Orera, V. M., 8, 172
Ortega, J. M., 323, 324, 393
Osiko, V. V., 34
Otani, C., 325
Owens, F. J., 326
Ozols, A. O., 389

Pan, D. S., 327, 329
Park, D. S., 319
Parker, B. M. C., 73
Pascual, J. L., 331
Pasternack, E. S., 333
Paus, H. J., 15, 170, 381, 410
Peercy, P. S., 335
Peisl, J., 408
Pellaux, J. P., 336
Petrasch, P., 155
Philips, D. S., 168
Pigg, J. C., 463
Pinatti, D. G., 486
Plaudis, A. E., 286
Ploom, L. A., 273
Podinsh, A. V., 128
Pollak, T. M., 338
Põllusaar, J. V., 273
Potstada, H., 155
Prasad, L. H. H., 211
Pross, L., 358
Pung, L. A., 273

Radhakrishna, S., 88, 90, 340, 342
Radlinski, A., 140
Raizman, A., 344
Ramasastry, C., 346
Ram Babu, B., 88, 90
Ranfagni, A., 348
Rao, S. M. D., 325
Rao, Y. S., 346
Rappaz, M., 350
Razzetti, C., 64
Rebane, L. A., 134
Rechtin, M. D., 352
Reddy, K. V., 40
Rehavi, A., 354

Reidinger, F., 77
Robinson, W. R., 255
Rolfe, J., 52, 356
Romestain, R., 100
Rose, B. H., 242
Rössler, K., 358, 360
Roth, M., 362
Rousseau, J. J., 56
Royce, B. S. H., 83
Russel, M. F., 44
Rzepka, E., 364
Rzyski, B. M., 294

Saidoh, M., 172, 205, 365
Saitta, G., 149
Sakamoto, N., 367
Sastry, S. B. S., 369, 371, 373, 374
Sato, H., 376
Sato, T., 121
Saxena, R. D., 377
Scacco, A., 68
Scavarda do Carmo, L. C., 379
Scharmann, A., 374
Scheu, W., 381
Schirmer, O. F., 383
Schneider, I., 385, 473
Schoemaker, D., 153, 387, 451
Schuele, D., 13
Schwan, L., 113, 410
Serughetti, J., 110
Serway, R. A., 279
Shvarts, K. K., 128, 389
Sibley, W. A., 391
Silsbee, R. H., 324, 393
Simonetti, J., 394
Simpson, J. H., 151
Siu Li, M., 71, 486
Sivasankar, V. S., 342
Skull, A. H., 92
Slifkin, L. M., 58, 184, 185, 396
Smith, D. Y., 398
Smyth, D. M., 79
Solliard, C., 350
Sonder, E., 308, 400, 463
Soovik, H. A., 273
de Souza, M., 71, 486
Spaeth, J. M., 176, 313
Spendel, M., 70
Springis, M., 402
Stapelbroek, M., 404
Stapleton, H. J., 48
Stewart, R. F., 406
Stoebe, T. G., 482
Stolz, H., 479
Stoneham, A. M., 203
Stott, J. P., 408
Strohm, K., 410
Strutt, J. E., 264, 266
Stuchka, P., 286
Subbanna, C. N., 374
Sucheta, N., 303
Sumita, M., 230
Susman, S., 412
Süss, J. T., 344
Suzuki, Y., 414, 416

Takeuchi, S., 205
Takiyama, K., 418
Tāle, I., 247, 420
Tang, Y., 376
Tanga, A., 23, 66, 68
Tanimura, K., 377
Tanimura, K., 422, 424, 426, 428
Tashiro, T., 205
Taurel, L., 54, 260, 364
Taylor, A., 352
Taylor, G. C., 430
Terauchi, H., 432
Terzi, N., 298
Thévenard, P., 434
Thompson, P. E., 272
Thörmer, K., 435
Thorn, R. J., 299
Title, R. S., 238
Todorov, G., 148
Todorov, T., 146, 148
Tohver, H. T., 86, 306
Topa, V., 197, 199
Townsend, P. D., 81, 365, 437, 481
Toyoda, K., 438
Treacy, D., 13, 440
Treilleux, M., 442
Trieman, B., 251
Tsai, C. L., 292
Tsvetkova, K., 146
Tuller, H. L., 338, 444

Turner, T. J., 446

Ueda, Y., 315
Uralif, F. S., 301

Vail, J. M., 448
Valbis, J., 402
Van den Bosch, A., 450
Van Steen, F., 451
Varotsos, P., 11
Vassilev, Y., 148
Vasudevan, K. N., 277
Vermiglio, G., 149
Viliani, G., 348
Vlasák, G., 453
von der Osten, W., 479
von der Weid, J.-P., 126, 455
von Guérard, B., 408

Wagner, E., 50
Wahl, J., 457
Wang, J. C., 459
Wasiela, A., 46
Watanabe, S., 7
Watanabe, T., 295, 461
Weeks, R. A., 308, 400, 463
Weinstock, H., 292
Welling, H., 35
Wells, J. S., 92
White, G. S., 98
Whitworth, R. W., 465
Wiedersich, H., 352
Wiegand, D. A., 467
Williams, J. W., 475
Williams, R. T., 215, 446, 469, 471, 473, 475
Wilson, T. M., 477
Windscheif, J., 479
Winter, J., 360
Wintersgill, M. C., 437, 481
Wolfenstine, J. B., 482
Wood, R. F., 32, 477
Wuensch, B. J., 77

Yoshikawa, E., 222
Yuste, M., 313
Yuster, P. H., 104, 105

Zeikats, V. P., 484
Zilio, S. C., 486
Zwicker, R. D., 488